Gold(I)-Catalyzed Transformations with Bifunctional Ligands and the Synthesis of Daucane Natural Products

Àlex Martí Zaragoza

UNIVERSITAT ROVIRA i VIRGILI

ICIQ Institut Català d'Investigació Química

Gold(I)-Catalyzed Transformations with Bifunctional Ligands and the Synthesis of Daucane Natural Products

Àlex Martí Zaragoza

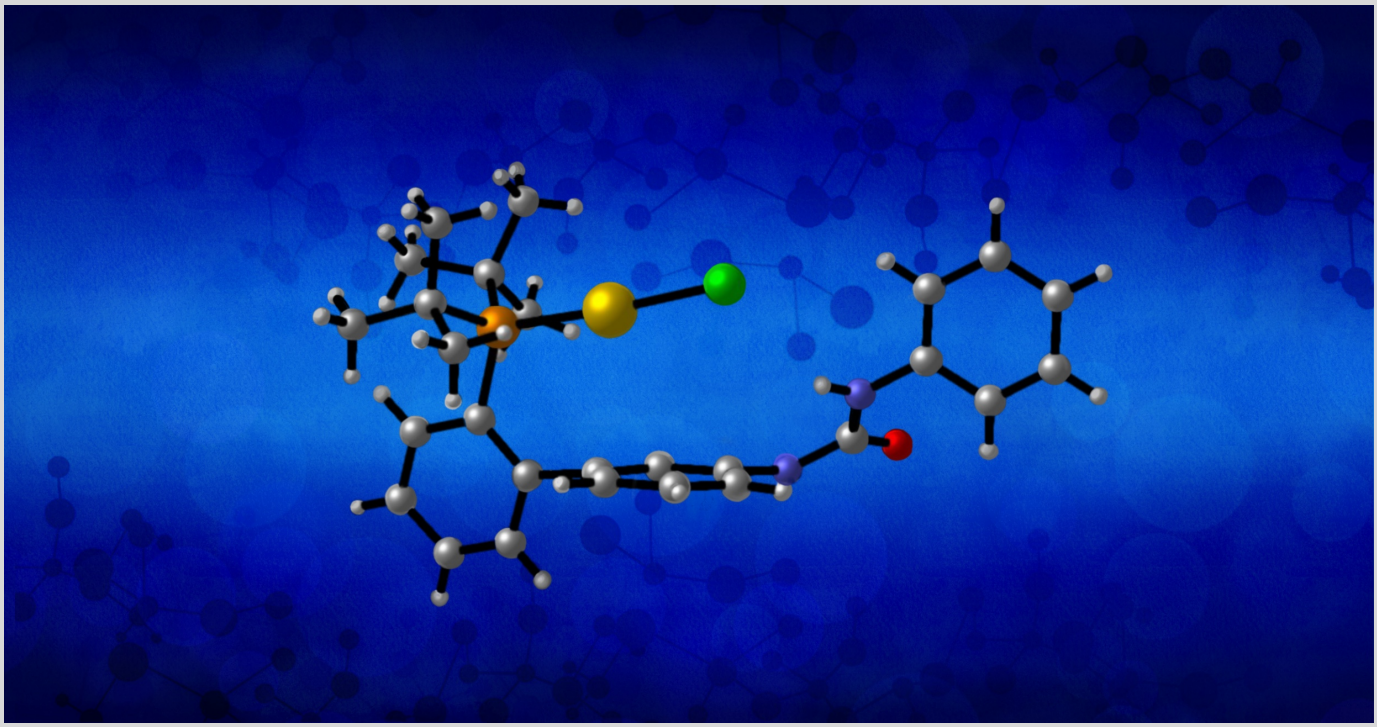

DOCTORAL THESIS
2024

Àlex Martí Zaragoza

Gold(I)-Catalyzed Transformations with Bifunctional Ligands and the Synthesis of Daucane Natural Products

Doctoral Thesis

Supervised by Prof. Antonio M. Echavarren

Institut Català d'Investigació Química (ICIQ)

Tarragona 2024

Institut Català d'Investigació Química

UNIVERSITAT ROVIRA i VIRGILI

I STATE that the present study, entitled "**Gold(I)-Catalyzed Transformations with Bifunctional Ligands and the Synthesis of Daucane Natural Products** ", presented by Àlex Martí Zaragoza to award the degree of Doctor, has been carried out under my supervision at the Institut Català d´Investigació Química (ICIQ).

Tarragona, November 27th, 2024

Prof. Antonio M. Echavarren

Doctoral Thesis Supervisor

A mis padres y abuelos

Real knowledge is to know the extent of one's ignorance.

Confucius

Ackowledgements

Quiero empezar dando las gracias al director de mi tesis, el Prof. Antonio M. Echavarren por abrirme las puertas a su laboratorio durante mi Summer Fellow y por darme la oportunidad de quedarme para el Máster y Tesis Doctoral. Gracias por todo lo que me has enseñado a nivel de química y a nivel personal. Aunque no compartamos las mismas ideas, siempre he disfrutado de tus charlas sobre aves y política.

També m'agradaria agrair a dos persones molt importants per a tots els membres del grup Echavarren, a Sònia Gavaldà i la Dra. Imma Escofet. Moltes gràcies per tot el vostre suport i ajuda. Realment, el grup sense vosaltres, no podria funcionar igual.

I would like to thank Prof. John F. Hartwig for the opportunity of joining his group during my stay at UC Berkeley. Additionally, I want to thank the people who made me feel at home: Isaac Yu, Christina Pierson, Nicholas Hadler, John Brun, Jeremy Nicolai and Dr. Kyan D'Angelo. I also want to thank the friends with whom I had the pleasure to discover the US: Kiko y Elena (y Mateo aunque no nos conocemos aún), Dani, Esther, Julie, Jessie, Teresa and Marc.

I also want to thank ICIQ's Research Support Area units for their help during these years: NMR, X-Ray Diffraction, High Resolution Mass Spectrometry, CHROMTAE and CRTU.

I would like to continue by thanking all the current and former members of the Echavarren group, for the moments we shared in the lab, the interesting chemical discussions, and the continuous learning. Especially I want to thank those people with whom I had the pleasure to collaborate with: Dr. Marc Montesinos, Dr. Allegra Franchino, Dr. Stefano Nejroti, Gala Ogalla, Miquel Àngel Pérez, Dr. Helena Armengol and Dr. Anna Sadurní.

Me gustaría agradecer a los compañeros del laboratorio que han hecho este viaje mucho más ameno:

Gala Ogalla, nos conocimos en el máster y nos hicimos amigos enseguida. Muchas gracias por estar allí en las buenas y en las malas y por todos esos momentos que hemos vivido en estos 5 años.

Tania Medina, no podría haber pedido una mejor compañera de viajes y de dramas. Por todos esas bromas y risas que nos hemos echado, muchas gracias por todo. Ah y gracias por ser mi secretaria, para ser que no cobrabas no lo hiciste nada mal.

Pablo Mora y David Balcells, mis compañeros de piso, por esas partidas por la noche de Fortnite, gracias por volver siempre a recuperar mi tarjeta, y por esas cenas y películas. Joan Guillem gracias por invitarme a vuestras cenas y por esas charlas random y filosóficas. Eric Palomo por tus imitaciones y por esa salchicha en el pasillo, siempre habrá un poquito de ti en nuestro piso.

Dr. Eduardo García por esos momentos en los que nos sacabas unas risas a todos solo siendo tú mismo, Dra. Isabel Arranz por siempre tener una sonrisa en la cara, Dra. Alba Helena por siempre tener un refrán debajo la manga y Dr. David Nieto por no aprenderte en 4 años que soy de Camarles no Sant Carles de la Ràpita, Dra. Ana Arroyo y Dr. Andrea Cataffo, por ese día random en el que terminamos viendo un documental de cefalópodos después de un deprimente sábado en el lab, muchas gracias chicos. Dra. Elena Borrego, Dra. Inma Martin y Laura Lerena, las chicas del sur, gracias por todo lo que nos hemos reído y por los buenos momentos vividos dentro y fuera del lab. Dr. Nicolas Fincias, gracias por esos postres, por esas discusiones tan interesantes y por despertarme por las mañanas en el lab poniendo heavy metal a primera hora de la mañana. To the new incorporations in the lab Anna Arnanz and Luyu Cai, and to Xiaoqing Shao and Arnau Sugranyes I wish you all the best in the future.

Als meus amics de tota la vida, Laura, Pau, Miriam, Josep, Eva, Jaume i Imma, moltes gràcies per donar-me suport i per animar-me quan estava aclaparat, per ajudar-me a dissociar i a distreure'm quan algunes coses no anaven gaire bé.

Per acabar m'agradaria agrair a tota la meva família pel seu suport. En especial als meus pares, moltes gràcies per tot el suport que meu donat, per estar sempre al meu costat, per ensenyar-me que tot esforç te la seva recompensa i per ser els meus models a seguir, aquesta tesis es tan meva com vostra.

This work was carried out with the support of the Ministerio de Ciencia e Innovación (PID2022-136623NB-I00/MICIU/AEI/10.13039/501100011033/ FEDER, UE) and FPU for my predoctoral fellowship from 2020 to 2024 (FPU20/02555) as well as financing a 6-months mobility fellowship (EST23/00730), the AGAUR (2021 SGR 001256 and a FI predoctoral fellowship to A.M.Z from 2019 to 2020), the CERCA Program/Generalitat de Catalunya and the ICIQ foundation for financial support.

At the time of the writing of this Doctoral Thesis, part of the results have been reported in the following publications:

- Franchino, A.; Martí, À.; Nejrotti, S.; Echavarren, A. M. Silver-Free Au(I) Catalysis Enabled by Bifunctional Urea- and Squaramide-Phosphine Ligands via H-Bonding. *Chem. Eur. J.* **2021**, *27*, 11989–11996.
- Franchino, A.; Martí, À.; Echavarren, A. M. H-Bonded Counterion-Directed Enantioselective Au(I) Catalysis. *J. Am. Chem. Soc.* **2022**, *144*, 3497–3509.
- Martí, À.; Montesinos-Magraner, M.; Echavarren, A. M.; Franchino, A. H-Bonded Counterion-Directed Catalysis: Enantioselective Gold(I)-Catalyzed Addition to Alkynyl Enones as a Case Study. *Eur. J. Org. Chem.* **2022**,-e202200518.
- Martí, À.; Ogalla, G.; Echavarren, A. M. Hydrogen-Bonded Matched Ion Pair Gold(I) Catalysis. *ACS Catal.* **2023**, *15*, 10217–10223

Table of Contents

Prologue

The manuscript of this Doctoral Thesis has been divided into four main parts: a general introduction on gold(I) catalysis and three main research Chapters. These Chapters are preceded by the abstract and general objectives and followed by the overall conclusions. Each Chapter contains five sections including a specific introduction on the topic, the objectives, the discussion of the results, the conclusions and, finally, the experimental section. The numbering of compounds, schemes, figures, tables and references is organized by Chapters.

The **General Introduction** covers the basic principles of homogeneous gold(I) catalysis and gives an overview on the cycloisomerization of 1,*n*-enynes, the challenges faced when performing enantioselective gold(I) catalysis and some examples of the application of gold(I) in the total synthesis of natural products.

Chapter 1 presents a new design of gold(I) catalysts embedded with (thio)urea/squaramide motifs and its application on the silver-free activation of alkynes. Mechanistic studies were performed on the cycloisomerization of *N*-propargylbenzamide evidencing the participation of the H-bond donor in the activation of the Au–Cl bond. Part of the results presented were done in collaboration with Dr. Allegra Franchino and Dr. Stefano Nejrotti and have been published in *Chem. Eur. J.* **2021,** *27*, 11989–11996.

Chapter 2 introduces the combination of chiral counterions with (a)chiral gold(I)-catalysts, bearing dual H-bond donors for the gold(I)-catalyzed enantioselective cyclization of 1,*n*-enynes. Mechanistic studies on this novel approach for asymmetric gold-catalysis demonstrated the role of the H-bond donor in anchoring the chiral counterion close to the reaction center. Part of the results presented were done in collaboration with Dr. Allegra Franchino, Dr. Marc Montesinos and Gala Ogalla and have been published in *J. Am. Chem. Soc.* **2022**, *144*, 8, 3497–3509; *Eur. J. Org. Chem.* **2022**, e202200518 and *ACS Catal.* **2023**, *13*, 10217−10223.

Chapter 3 summarizes our efforts towards the total synthesis of three members of the daucane family of natural products. The synthetic strategy is based on a previously developed gold(I)-catalyzed reaction by our group. Part of the results presented were done in collaboration with Dr. Anna Sadurní, Dr. Helena Armengol and Miquel Àngel Pérez. These results have not been published to the date of the writing of this manuscript.

Finally, at the end of this Doctoral Thesis, final remarks on the results obtained thorough the manuscript are disclosed in the **General Conclusions**.

Abbreviations and Acronyms

In this manuscript, the abbreviations and acronyms most commonly used in organic and organometallic chemistry have been used following the recommendations of "Guidelines for authors" published in the Journal of Organic Chemistry.

Additional abbreviations and acronyms are listed below:

ACDC	Asymmetric Counterion-Directed Catalysis
APCI	Atmospheric Pressure Chemical Ionization
APPI	Atmospheric Pressure Photoionization Ionization
$BAr^F{}_4^-$	Tetrakis[3,5-bis(trifluoromethyl)phenyl]borate
dr	Diastereomeric ratio
DCE	1,2-dichloroethane
ee	Enantiomeric Excess
er	Enantiomeric Ratio
ESI	Electrospray Ionization
HB	Hydrogen Bond
HCDC	Hydrogen-Bonded Counterion-Directed Catalysis
HRMS	High Resolution Mass Spectrometry
Int	Intermediate
IPr	1,3-Bis(2,6-diisopropylphenyl)imidazole-2-ylidene
JohnPhos	(2-Biphenyl)di-*tert*-butylphoshpine
L	Ligand
MALDI	Matrix Assisted Laser Desorption Ionization
*m*CPBA	*meta*-chloroperbenzoic acid
Mes	2,4,6-Trimethylphenyl
MW	Microwave Irradiation
NTf_2^-	Bis(trifluoromethyl)imidate
OTf^-	Trifluoromethanesulfonate
*t*BuXPhos	2-(Di-*tert*-butylphosphino)-2',4',6'-triisopropyl-1,1'-biphenyl
TFA	Trifluoroacetic acid
TRIP	3,3′-Bis(2,4,6-triisopropylphenyl)-1,1′-binaphthyl-2,2′-diyl hydrogenphosphate
TS	Transition State

Abstract

Homogenous gold(I) catalysis has become a powerful tool for the rapid buildup of molecular complexity from relatively simple starting materials. In the last two decades, the potential of gold(I) catalysis has been evidenced by its application in the synthesis of numerous natural products due to its high chemoselectivity towards the activation of alkynes. Usually, gold(I) is prepared as a stable gold(I)-chloride precatalyst, which requires activation to be catalytically active. This is usually performed by adding exogenous chloride scavengers, such as silver salts, which can also exhibit catalytic activity and give rise to side reactions, a phenomenon generally known as the "silver effect". To eliminate the need for such additives, new designs for silver-free gold(I) catalysis have been developed over the past decade. Despite the exponential development observed in gold(I) catalysis, the enantioselective versions of this class of transformations remain underdeveloped, mainly due to the linear dicoordination of gold(I) complexes, which places the chiral information on the direct opposite site of the reactive center. The activation of alkynes, which are not prochiral, and the outer-sphere mechanism of gold(I)-mediated reactions further complicate the development of effective catalytic enantioselective processes.

In this Doctoral Thesis we have addressed these problems by strategically introducing hydrogen bond donors into the ligand scaffold to allow the removal of labile ligands from the coordination sphere of the metal center.

First, we designed a library of triphenylphosphine-based self-activating gold(I)-catalysts bearing (thio)urea/squaramide motifs on the ligand, and we tested them in the cycloisomerization of *N*-propargylbenzamides. Experimental mechanistic studies, as well as DFT calculations, pointed out the role of the dual hydrogen bond donors in the activation of the gold(I)-chloride bond, allowing substrate coordination and catalytic turnover.

Second, we developed the Hydrogen Bonded Counterion-Directed Catalysis (HCDC), a novel approach for asymmetric gold(I) catalysis. HCDC relies on the use of (a)chiral gold(I)-catalysts embedded with hydrogen bond donors in combination with chiral counterions. The role of the hydrogen bond donor is to abstract the counterion from the coordination sphere of the metal center, while maintaining it close enough to allow for the transfer of the chiral information. This novel methodology allowed the transformation of 1,*n*-enynes with and without the addition of external nucleophiles in very high yields and enantioselectivities.

Finally, we completed the total synthesis of two members of the daucane family natural products, aspterric acid and shisanwilsonene A. Additionally, we synthesized the structure proposed for penigrisacid A by its isolation team and confirmed that it had been misassigned. A new structure has been proposed based on the experimental spectroscopic data as well as DFT-predicted NMR calculations.

General Objectives

The aims of this Doctoral Thesis were:

- The design and study of a novel family of self-activating gold(I) complexes embedded with hydrogen bond donors.
- The development of a novel approach for enantioselective gold(I)-catalysis, that relies on the hydrogen bonding interactions between a (a)chiral gold(I) complex bearing a hydrogen bond donor and a chiral counterion
- The divergent synthesis of sesquiterpene-derived natural products based on a previously developed gold(I)-catalyzed cascade reaction by our group, namely aspterric acid, penigrisacid A and schisanwilsonene A.

Each chapter of this manuscript provides a more detailed description of the corresponding objectives.

General Introduction

Homogeneous Gold(I) Catalysis

Origin of Gold Chemistry

With chemical symbol Au (from Latin *aurum*) and atomic number 79, gold has been present from very early in human history. Owing to its natural inertness and striking appearance, gold became a symbol of power and immortality across many ancient civilizations. Its importance was recognized in ancient Egypt era where it was known as "the flesh of gods" and closely associated with the sun god Ra. Egyptians believed gold had the power to purify the soul and facilitate the journey of the deceased to the afterlife. Since then, gold became a symbol of power and wealth and has been broadly applied to the production of coinage, jewelry, and more recently electronics (Figure 1).

Figure 1. Examples highlighting the importance of gold. From left to right: Tutankhamun's mask, jewels and computer processors.

Despite its unique properties, gold was long considered catalytically inactive.[1] The first example in homogeneous gold(I) catalysis was reported in 1986 by Ito and Hayashi, in the asymmetric aldol reaction of aldehydes with iso-cyanides to afford oxazolines **1**.[2] However, the field remained poorly developed until 1998, when Teles reported a gold(I)-catalyzed synthesis of acetals **2** via the addition of alcohols to alkynes.[3] A few years later, Tanaka extended this methodology, applying similar conditions to convert alkynes into ketones and aldehydes **3** (Scheme 1).[4]

1. Hashmi, A. S. K. *Gold Bull.* **2004**, *37*, 51–65.
2. Ito, Yoshihiko.; Sawamura, Masaya.; Hayashi, Tamio. *J. Am. Chem. Soc.* **1986**, *108*, 6405–6406.
3. Teles, J. H.; Brode, S.; Chabanas, M. *Angew. Chem. Int. Ed.***1998**, *37*, 1415–1418.
4. a) Mizushima, E.; Sato, K.; Hayashi, T.; Tanaka, M. *Angew. Chem. Int. Ed.***2002**, *41*, 4563–4565. b) Mizushima, E.; Hayashi, T.; Tanaka, M. *Org. Lett.* **2003**, *5*, 3349–3352.

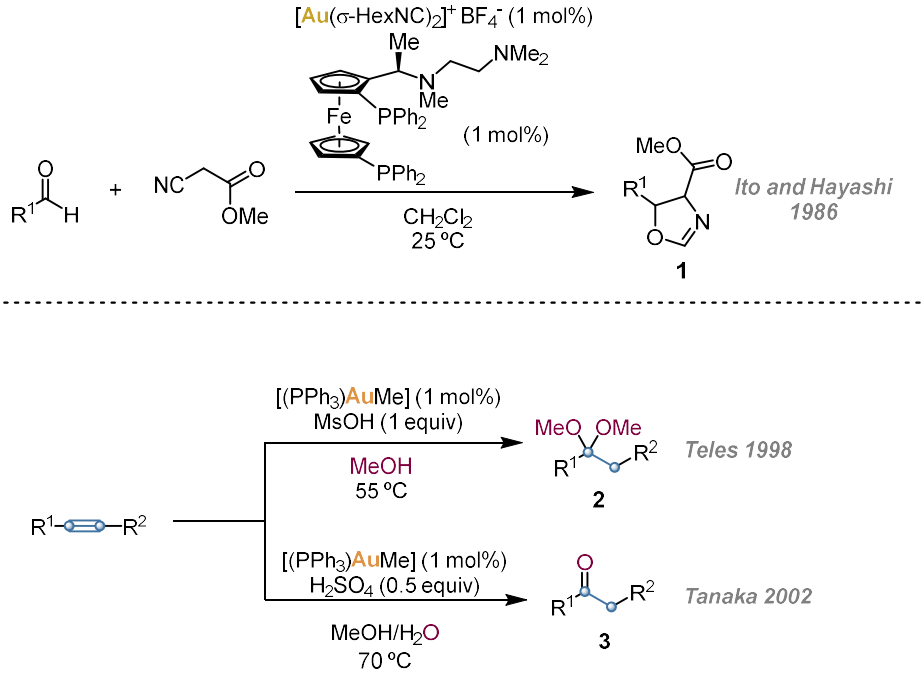

Scheme 1. First examples of the use of gold(I) in homogeneous catalysis.

Since then, during these last decades, homogeneous gold(I) catalysis has been extensively explored and developed into a versatile tool for constructing complex molecular architectures. Its ability to operate under mild conditions and orthogonally to other transition metals has made it a valuable tool in organic synthesis, enabling the efficient formation of carbon-carbon and carbon-heteroatom bonds. This unique catalytic activity has expanded the utility of gold in areas such as cyclizations, asymmetric synthesis, and cross-coupling reactions, further broadening its application in modern chemistry. [5]

Relativistic Effects and their Consequences in Gold(I) Catalysis

The high ability of gold(I) complexes to selectively activate π-bonds, along with some of its unique properties can be attributed in part to relativistic effects.[6] The relativistic effects arise from the high speed of electrons spinning around a heavy nucleus.[7] This results in an increase of the mass of the electrons leading to the contraction and stabilization of the core orbitals (orbitals *s* and to a lower extent orbitals *p*). This contraction of the more internal orbitals leads to a higher shielding of the nucleus. Hence, electrons present in the *d* and *f* orbitals are less attracted by the nucleus, resulting in a destabilization and expansion of these orbitals. This contraction/expansion of the orbitals is much more significant for those elements having their 4f and 5d orbitals filled, reaching a maximum for gold (Au electronic configuration: [Xe] 4f14 5d10 6s1) (Figure 2).

5. a) Fürstner, A. *Chem. Soc. Rev.* **2009**, *38*, 3208–3221. b) Hashmi, A. S. K.; Hutchings, G. J. *Angew. Chem. Int. Ed.***2006**, *45*, 7896–7936. c)Fensterbank, L.; Malacria, M. *Acc. Chem. Res.* **2014**, *47*, 953–965. d) Dorel, R.; Echavarren, A. M. *Chem. Rev.* **2015**, *115*, 9028–9072. e) Zheng, Z.; Ma, X.; Cheng, X.; Zhao, K.; Gutman, K.; Li, T.; Zhang, L. *Chem. Rev.* **2021**, *121*, 8979–9038.
6. a) Pyykkö, P. *Angew. Chem. Int. Ed.***2002**, *41*, 3573–3578. b) Schwarz, H. *Angew. Chem. Int. Ed.***2003**, *42*, 4442–4454. c) Pyykkö, P. *Angew. Chem. Int. Ed.***2004**, *43*, 4412–4456. d) Gorin, D. J.; Toste, F. D. *Nature* **2007**, *446*, 395–403.
7. Pyykko, P.; Desclaux. J. P. *Acc. Chem. Res.* **1979**, *12*, 276–281.

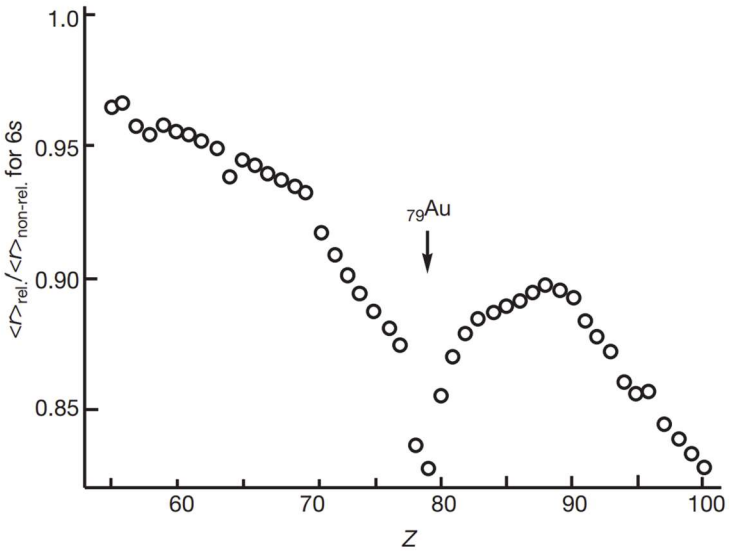

Figure 2. Calculated relativistic contraction of the 6s orbitals.[8]

The relativistic effects are also responsible of the characteristic color of gold(I), its higher electronegativity compared to other transition metals or its soft Lewis acidic character. The preference of gold(I) complexes to present a linear dicoordination[9] can also be explained by the relativistic effects. The hybridization of *s*/*d* or *s*/*p* orbitals is very efficient due to the small differences in energy among *s*, *p* and *d* states. These complexes do not undergo spontaneous oxidative addition[10] or promote β-hydride elimination.

Furthermore, the contraction of the orbital 6s on gold atom causes a strong Au–L interaction between the gold atom and the ligand. Therefore, the reactivity of gold(I)-catalyzed reactions can be easily tuned by modulation of the electronic and/or steric properties of the ligand.[11] Generally, complexes containing more donating *N*-heterocyclic carbenes are less electrophilic than those with phosphine-based ligands. Those with bulky phosphines or biarylphosphines display an intermediate electrophilicity that has proven to be highly convenient in catalysis. Moreover, gold(I) complexes bearing phosphite ligands are amongst the most electrophilic complexes and exhibit a carbocation-like character (Figure 3). [12,13]

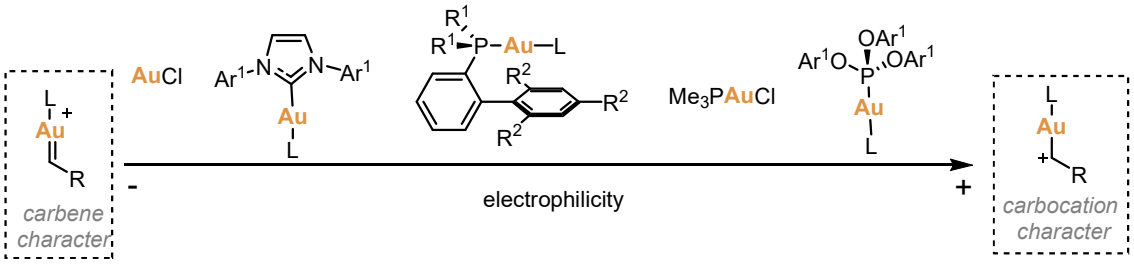

Figure 3. Effect of the ligand on the nature of gold(I) catalysts.

8. Graphic taken form ref. 6d.
9. Gimeno, M. C.; Laguna, A. *Chem. Rev.* **1997**, *97*, 511–522.
10. Livendahl, M.; Goehry, C.; Maseras, F.; Echavarren, A. M. *Chem. Commun.* **2014**, *50*, 1533–1536.
11. Gorin, D. J.; Sherry, B. D.; Toste, F. D. *Chem. Rev.* **2008**, *108*, 3351–3378.
12. Wang, Y.; Muratore, M. E.; Echavarren, A. M. *Chem. Eur. J.* **2015**, *21*, 7332–7339.
13. Zuccarello, G.; Zanini, M.; Echavarren, A. M. *Isr. J. Chem.* **2020**, *60*, 360–372.

As consequence of the relativistic effects, gold(I) is a soft Lewis acid, which preferentially binds to soft electrophiles, such as unsaturated C–C bonds. Calculations as well as experimental evidence on Au-alkyne and Au-alkene complexes have concluded that backdonation from the gold(I) center to the π system of a ligand accounts for a very small fraction of the bonding situation.[14] Thus, gold(I) coordination to alkynes can be partially rationalized by the Dewar-Chatt-Duncanson model:[15] a σ-interaction arises from the donation of electron density from the π-bond of the alkyne to the empty 6s orbital of the metal. However, in contrast to the classic model, the backdonation cannot happen towards the antibonding π* orbital of the alkyne, since these orbitals are too high in energy compared to the 5p orbitals of Au (due to the abovementioned relativistic effects) for significant overlap. The backbonding π-interaction consists instead, in the donation to lower-energy, non-bonding *p* orbitals (gold(I)-carbenes, Figure 4). This could explain the Lewis acidity of Au(I); the lack of backbonding from Au(I) into to the antibonding orbitals of the π-ligands could render them more electron deficient, facilitating nucleophilic addition.

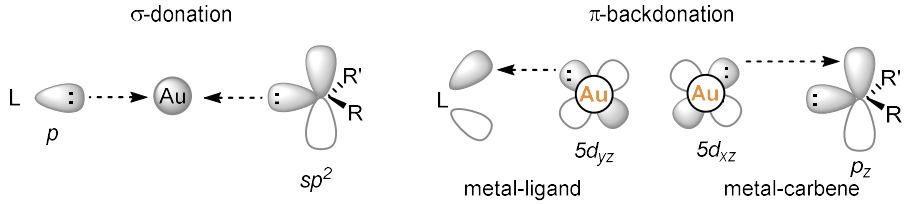

Figure 4. Bonding situation in gold(I)-coordination chemistry.

Gold(I) is known to have a high alkynophilicity. Thus in a system where both alkyne and alkenes are present, the gold(I) catalyst will coordinate with both but will preferentially activate the alkyne. This behavior is specially intriguing considering that gold(I) forms stronger bonds with alkenes[16] and can be explained by the kinetics of the coordination event. The activated alkyne LUMO has lower energy levels compared to those of alkenes. As a result, the lower energy levels of alkynes promote a favored nucleophilic attack, explaining the observed alkynophilicity. Typically, this attack occurs in an *anti*-fashion relative to the activated species **4** via an outer-sphere mechanism, following Markovnikov selectivity, giving rise to *trans*-alkenyl gold(I) species **5** (Scheme 2).[17]

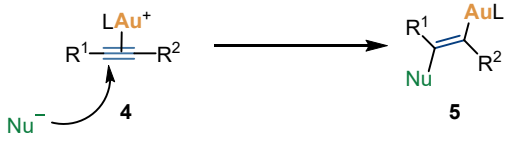

Scheme 2. Markovnikov nucleophilic attack to (η^2-alkyne)gold(I) complexes **4**.

Cycloisomerization of 1,*n*-Enynes

Among the gold(I)-catalyzed reactions studied, the cycloisomerizations of 1,*n*-enynes has had a significant impact on the field. The increase in molecular complexity as well as the atom economy

14. a) Hertwig, R. H.; Koch, W.; Schröder, D.; Schwarz, H.; Hrušák, J.; Schwerdtfeger, P. *J. Phys. Chem.* **1996**, *100*, 12253–12260. b) Xu, Q.; Imamura, Y.; Fujiwara, M.; Souma, Y. *J. Org. Chem.* **1997**, *62*, 1594–1598. c) Nechaev, M. S.; Rayón, V. M.; Frenking, G. *J. Phys. Chem. A* **2004**, *108*, 3134–3142.
15. a) Dewar, J. S. *Bull. Soc. Chim. Fr*. **1951**, *18*, C71–C79. b) Chatt, J., Duncanson, L. A. *J. Chem. Soc.* **1953**, 2939–2947. c) Salvi, N.; Belpassi, L.; Tarantelli, F. *Chem. Eur. J.* **2010**, *16*, 7231–7240.
16. a) Nechaev, M. S.; Rayón, V. M.; Frenking, G. *J. Phys. Chem. A* 2004, *108*, 3134–3142. b) Brown, T. J.; Dickens, M. G.; Widenhoefer, R. A. *Chem. Commun.* **2009**, 6451–6453. c) Brooner, R. E. M.; Widenhoefer, R. A. Angew. Chem. Int. Ed. **2013**, *52*, 11714–11724, *Angew. Chem.* **2013**, *125*, 11930–11941.
17. García-Mota, M.; Cabello, N.; Maseras, F.; Echavarren, A. M.; Pérez-Ramírez, J.; Lopez, N. *ChemPhysChem* **2008**, *9*, 1624–1629.

that can be achieved in a single chemical transformation from relatively simple molecules, made these reactions particularly interesting.[5] Depending on the substitution pattern at the alkene and alkyne, as well as on catalyst employed, the 1,6-enynes cycloisomerizations can follow different reaction pathways, leading to different products (Scheme 3).[18] The activation of the alkyne by gold(I) leads to the formation of a (η^2-alkyne)–metal complex **I** which, after nucleophilic attack from the alkene, produces cyclopropyl gold(I) carbene-like intermediates **II** or **VIII** through either *anti*-5-*exo*-dig or 6-*endo*-dig cyclizations respectively.[19]

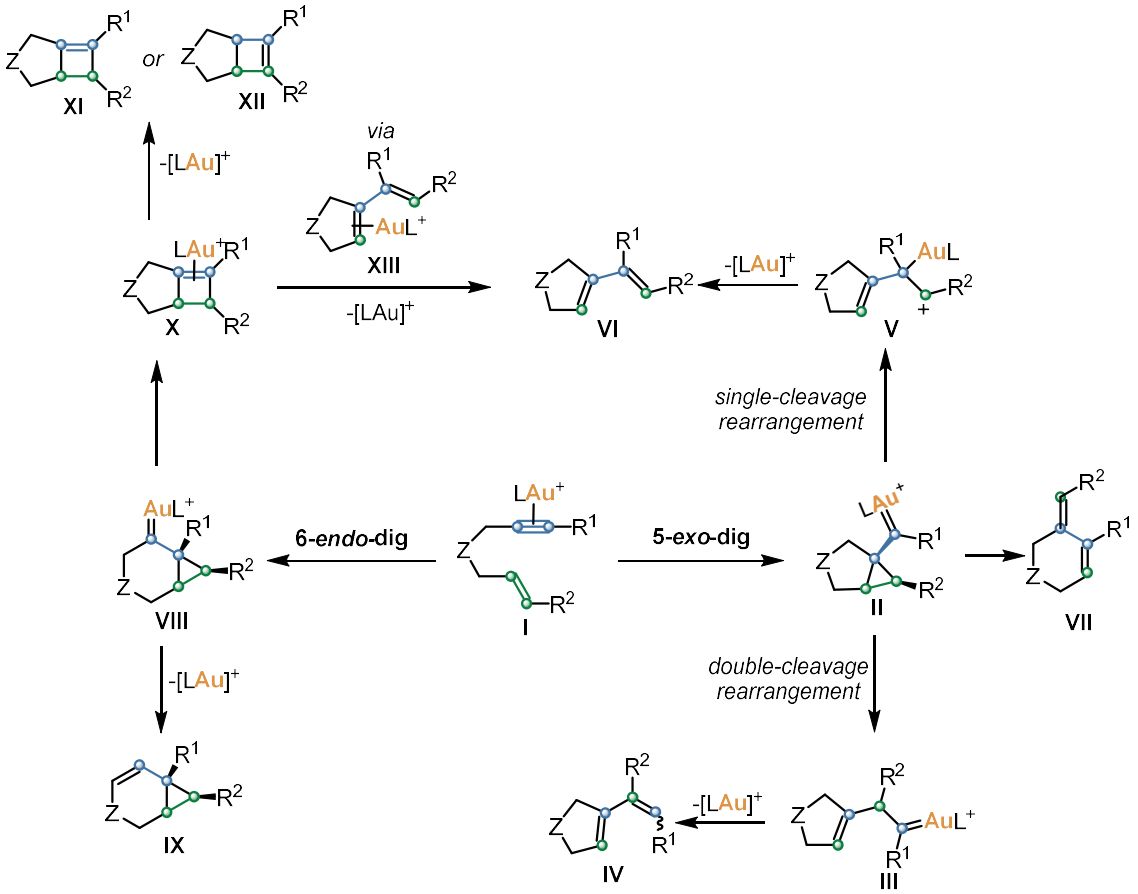

Scheme 3. General pathways for the gold(I)-catalyzed cycloisomerization of 1,6-enynes.

Intermediates **II** can further evolve to generate rearranged carbenes **III** through the formal insertion of the terminal alkene carbon into the alkyne carbons to eventually yield double-cleavage rearrangement products **IV** after α-proton elimination. While products with either configuration have been observed for this rearrangement, those with a *Z* configuration (R^2 = H) are often favored. Alternatively, if intermediate **II** undergoes a single-cleavage rearrangement, a formal 1,3-migration of the terminal carbon of the alkene takes place and gives rise to intermediate **V**, which after decoordination leads to product **VI**. Whether intermediate **II** undergoes single or double cleavage lies on the nature of the substituents attached to the alkyne. Electron-withdrawing substituents tend to promote the double-cleavage rearrangement, whereas electron-donating groups typically favor the formation of the single-cleavage diene. Additionally,

18. a) Nieto-Oberhuber, C.; López, S.; Muñoz, M. P.; Cárdenas, D. J.; Buñuel, E.; Nevado, C.; Echavarren, A. M. *Angew. Chem. Int. Ed.* **2005**, *44*, 6146–6148. b) Ferrer, C.; Raducan, M.; Nevado, C.; Claverie, C. K.; Echavarren, A. M. *Tetrahedron* **2007**, *63,* 6306–6316. c) Escribano-Cuesta, A.; Pérez–Galán, P.; Herrero-Gómez, E.; Sekine, M.; Braga, A. A. C.; Maseras, F.; Echavarren, A. M. *Org. Biomol. Chem.* **2012**, *10*, 6105–6111.
19. Nieto-Oberhuber, C.; Muñoz, M. P.; Buñuel, E.; Nevado, C.; Cárdenas, D. J.; Echavarren, A. M. *Angew. Chem. Int. Ed*. **2004**, *43*, 2402-2406, *Angew. Chem.* **2004**, *116*, 2456–2460.

six-membered ring compounds **VII** can also be generated from **II** through an alternative *endo*-type single-cleavage rearrangement, wherein the internal carbon of the double bond migrates toward C1 of the alkyne. [20]

On the other hand, intermediate **VIII,** product of 6-*endo*-dig cyclization of **I**, can undergo 1,2-migration affording product **IX**.[21] Furthermore, carbene **VIII** can undergo rearrangement to produce (η^2-cyclobutene)-gold(I) intermediate **X**. The opening of these complexes can form the same products of the single-cleavage rearrangement of **V** *via* 1,3-dienes **XIII**. Except some few cases reported where the highly strained cyclobutenes **XI**, product of a formal [2+2] cycloaddition, have been isolated starting from 1,6-enynes,[22] the more stable isomers **XII** are usually encountered.[21a,23]

In the case of 1,5-enynes[24] and 1,7-enynes[25] similar mechanisms are observed, being the formation of bicyclic derivatives more common when higher enynes are employed ($7 \leq n \leq 16$). [26] For example, in 2016 our group reported the enantioselective total synthesis rumphellaone A (**8**) and hushione (**9**) by a gold(I)-catalyzed [2+2] cycloaddition of a 1,10-enyne as the key step to build the cyclobutene motif (Scheme 4). [27]

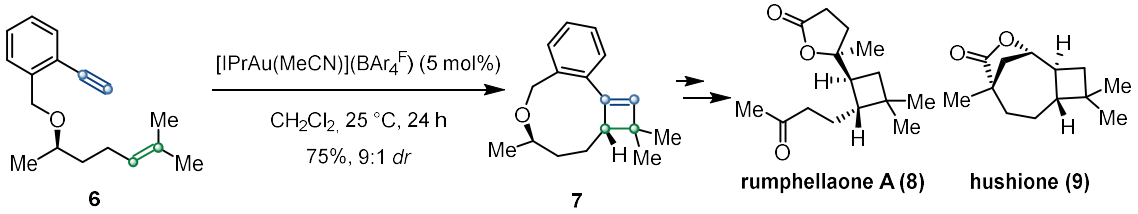

Scheme 4. Application of a Au(I)-catalyzed cyclization of 1,10-enyne **6** in the total synthesis of rumphellaone A (**8**) and hushione (**9**).

When an external nucleophile is present in the reaction mixture, cyclopropyl gold(I) carbene intermediates **II/VIII** can be trapped to generate the corresponding products (Scheme 5). For instance, when employing alcohols as nucleophiles, the alkoxycyclization products **9**/**11** from 1,6-enynes **8**/**10** form in a stereospecific fashion (Scheme 5a). Moreover, the Markovnikov product is usually obtained, as it can be seen in Scheme 5b where MeOH always attacks the most substituted carbon in intermediates **13** and **16**.[21a] Interestingly this process requires milder conditions when employing gold(I)-catalysts over other transition metals.[28]

20. Cabello, N.; Jiménez-Núñez, E.; Buñuel, E.; Cárdenas, D. J.; Echavarren, A. M. *Eur. J. Org. Chem*. **2007**, *25*, 4217–4223.
21. a) Nieto-Oberhuber, C.; Muñoz, M. P.; López, S.; Jiménez-Núñez, E.; Nevado, C.; Herrero-Gómez, E.; Raducan, M.; Echavarren, A. M. *Chem. Eur. J.* **2006**, *12*, 1677–1693. b) Lee, Y. T.; Kang, Y. K.; Chung, Y. K. *J. Org. Chem*. **2009**, *74*, 7922–7934.
22. a) Lee, S. I.; Kim, S. M.; Choi, M. R.; Kim, S. Y.; Chung, Y. K.; Han, W.-S.; Kang, S. O. *J. Org. Chem.* **2006,** *71*, 9366–9372. b) Brooner, R. E. M.; Brown, T. J.; Widenhoefer, R. A. *Angew. Chem. Int. Ed.* **2013**, *52*, 6259–6261, *Angew. Chem.* **2013**, *125*, 6379–6381.
23. Kim, N.; Brooner, R. E. M.; Widenhoefer, R. A. *Organometallics* **2017**, *36*, 673–678.
24. a) Sun, J.; Conley, M. P.; Zhang, L.; Kozmin, S. A. *J. Am. Chem. Soc.* **2006**, *128*, 9705–9710. b) López-Carrillo, V.; Huguet, N.; Mosquera, Á.; Echavarren, A. M. *Chem. Eur. J*. **2011**, *17*, 10972–10978
25. Cabello, N.; Rodríguez, C.; Echavarren, A. M. *Synlett* **2007**, 1753–1758. b) Huang, C.; Kothandaraman, P.; Koh, B. Q.; Chan, P. W. H. *Org. Biomol. Chem.* **2012**, *10*, 9067–9078.
26. a) Obradors, C.; Leboeuf, D.; Aydin, J.; Echavarren, A. M. *Org. Lett.* **2013**, *15*, 1576–1579.
27. Ranieri, B.; Obradors, C.; Mato, M.; Echavarren, A. M. *Org. Lett.* **2016**, *18*, 1614–1617.
28. Muñoz, M. P.; Adrio, J.; Carretero, J. C.; Echavarren, A. M. *Organometallics* **2005**, *24*, 1293–1300.

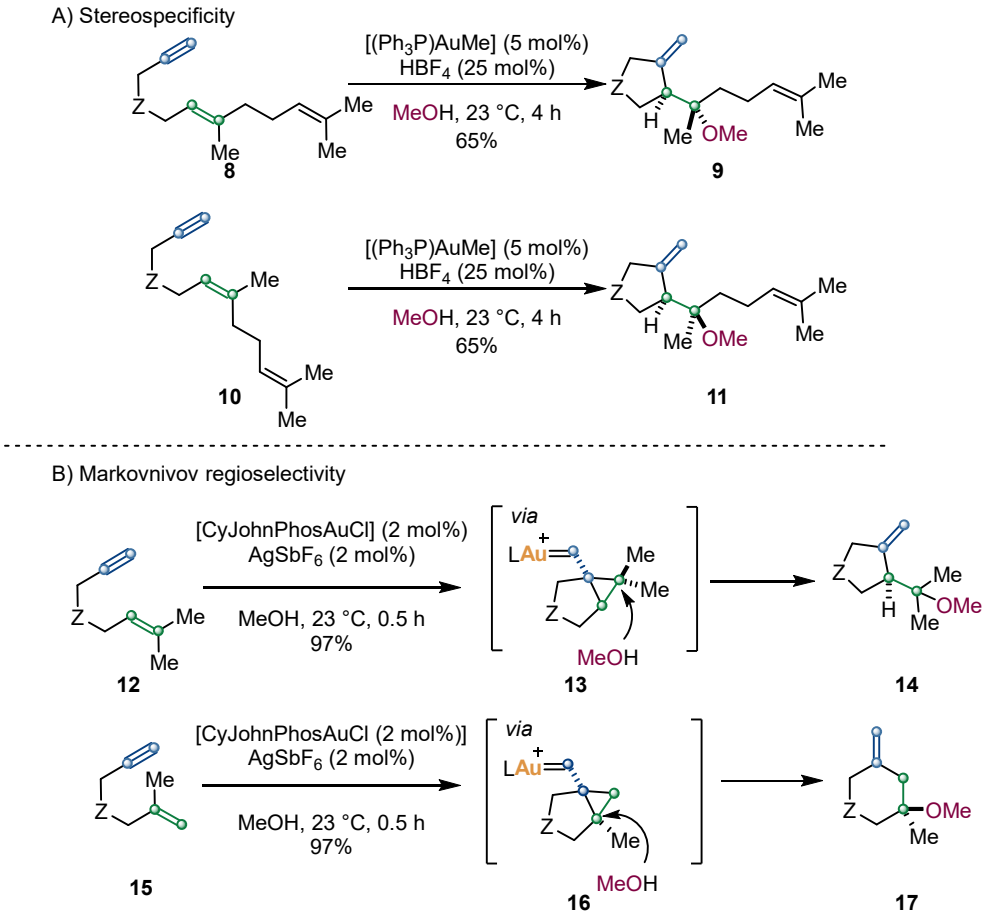

Scheme 5. Stereospecificity and regioselectivity of gold(I)-catalyzed alkoxycyclizations.

If the alkyne of the 1,6-enyne is substituted with an aryl ring tricyclic scaffold of type **19**, products of a formal [4+2] cycloaddition of **18,** are formed preferentially (Scheme 6).[21,29] The mechanism of this reaction starts with the formation of cyclopropyl gold(I) carbene **XIV-a** via a 5-*exo*-dig cyclization pathway that can open to form the cation **XIV-b**. Then, Friedel-Crafts-type reaction takes place to give **XV**, which upon re-aromatization and protodeauration leads to the formation of **19**.

29. Nieto-Oberhuber, C.; López, S.; Echavarren, A. M. *J. Am. Chem. Soc*. **2005**, *127*, 6178–6179.

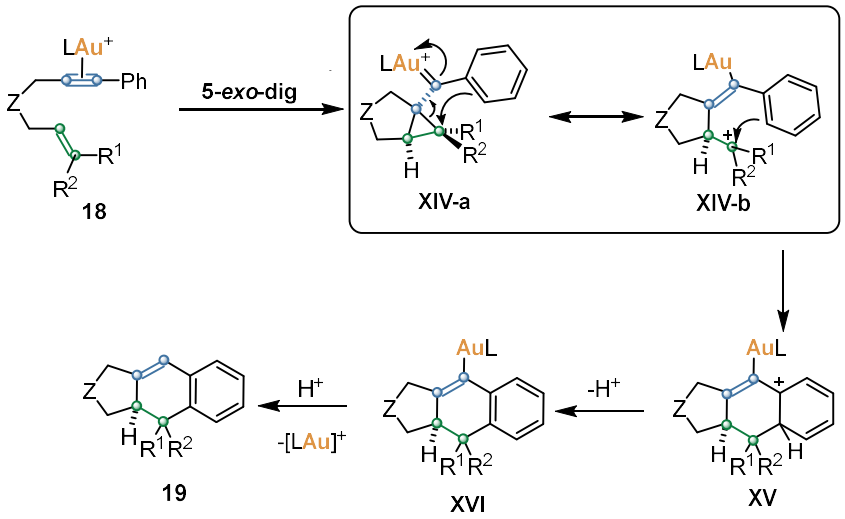

Scheme 6. Proposed mechanism for the formal [4+2] cycloadditions of enyne **18**.

Enantioselective Gold(I) Catalysis

The most popular strategy to build enantioenriched compounds relies on the use of chiral catalysts. Transition metal catalysis typically relies on the use of chiral ligands[30] or, less commonly, on chiral-at-metal complexes[31] Despite the progress made in the field of homogeneous gold(I) catalysis, the enantioselective version of these transformations remains underdeveloped.[32] This is in part due to the linear dicoordination of gold(I) catalysts, which places the chiral information far away from the reaction center. Furthermore, the free rotation of the L–Au and Au–substrate bonds and the outer-sphere mechanism of nucleophilic attack hamper the transfer of the stereochemical information from the ligand to the reaction center (Figure 5).

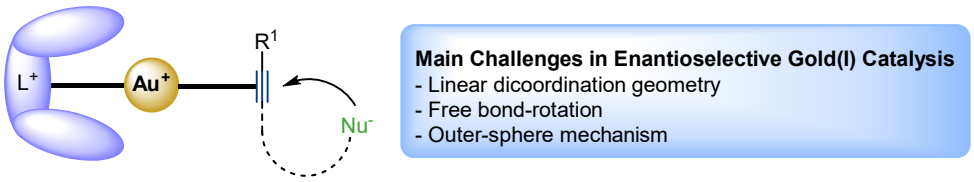

Figure 5. General coordination mode and main challenges associated with performing enantioselective gold(I) catalysis.

Three main strategies relying on different ligand designs have been successfully used to circumvent these challenges (Figure 6). The most widely employed is the use of binuclear axially chiral gold(I) complexes with phosphines or diaminocarbenes (Figure 6a). These complexes have

30. Fanourakis, A.; Docherty, P. J.; Chuentragool, P.; Phipps, R. J. *ACS Catal.* **2020**, *10*, 10672–10714.
31. Steinlandt, P. S.; Zhang, L.; Meggers, E. *Chem. Rev.* **2023**, *123*, 4764–4794
32. a) Widenhoefer, R. A. *Chem. Eur. J.* **2008**, *14*, 5382–5391. b) Michalak, M.; Kośnik, W. *Catalysts* **2019**, *9*, 890. c) Gade, A. B.; Urvashi; Patil, N. T. *Org. Chem. Front.* **2024**, *11*, 1858–1895.

been applied to cyclopropanations,[33] cycloisomerizations of 1,*n*-enynes,[34] hydrofunctionalizations of alkenes[35]and allenes,[36] as well as in other annulations.[37]

On the other hand, highly modular monodentate phosphoramidites[38] have proven to be very effective in allenene cyclizations[39] (Figure 6b). Finally, placing the chirality onto the counterion rather than in the gold catalyst itself is another strategy, entitled gold(I)-catalyzed Asymmetric Counterion-Directed Catalysis (ACDC), first introduced by Toste in 2007 (Figure 6c).[40,41]

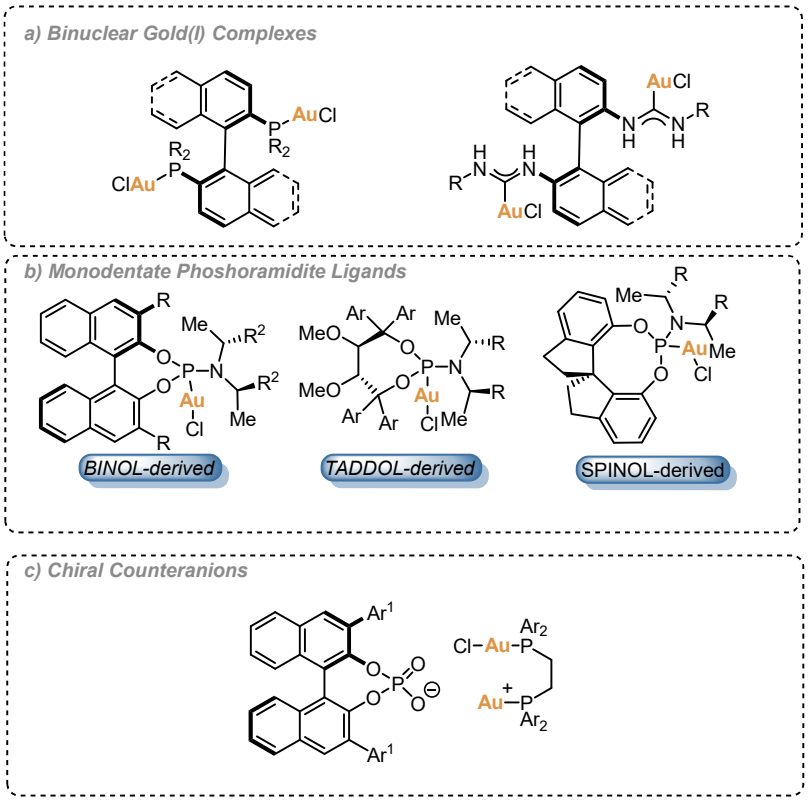

Figure 6. Different catalyst designs employed in enantioselective gold(I) catalysis.

33. a) Johansson, M. J.; Gorin, D. J.; Staben, S. T.; Toste, F. D. *J. Am. Chem. Soc.* **2005**, *127*, 18002–18003. b) Briones, J. F.; Davies, H. M. L. *J. Am. Chem. Soc.* **2012**, *134*, 11916–11919.
34. a) Chao, C.-M.; Beltrami, D.; Toullec, P. Y.; Michelet, V. *Chem. Commun.* **2009**, No. 45, 6988–6990. b) Chao, C.-M.; Vitale, M. R.; Toullec, P. Y.; Genêt, J.-P.; Michelet, V. *Chem. Eur. J.* **2009**, *15*, 1319–1323. c) Gawade, S. A.; Bhunia, S.; Liu, R.-S. *Angew. Chem. Int. Ed.***2012**, *51*, 7835–7838.
35. a) Bandini, M.; Bottoni, A.; Chiarucci, M.; Cera, G.; Miscione, G. P. *J. Am. Chem. Soc.* **2012**, *134*, 20690–20700. b) Mukherjee, P.; Widenhoefer, R. A. *Angew. Chem. Int. Ed.***2012**, *51*, 1405–1407. c) Lee, S. D.; Timmerman, J. C.; Widenhoefer, R. A. *Adv. Synth. Catal.* **2014**, *356*, 3187–3192. d)
36. Miles, D. H.; Veguillas, M.; Toste, F. D. *Chem. Sci.* **2013**, *4*, 3427–3431.
37. a) Zhou, G.; Liu, F.; Zhang, J. *Chem. Eur. J.* **2011**, *17*, 3101–3104. b) Huang, L.; Yang, H.; Zhang, D.; Zhang, Z.; Tang, X.; Xu, Q.; Shi, M. *Angew. Chem. Int. Ed.* **2013**, *52*, 6767–6771. c) Guo, R.; Li, K.-N.; Liu, B.; Zhu, H.-J.; Fan, Y.-M.; Gong, L.-Z. *Chem. Commun.* **2014**, *50*, 5451–5454. d) Sota, Y.; Yamamoto, M.; Murai, M.; Uenishi, J.; Uemura, M. *Chem. Eur. J.* **2015**, *21*, 4398–4404. e) Zi, W.; Wu, H.; Toste, F. D. *J. Am. Chem. Soc.* **2015**, *137*, 3225–3228.
38. a) Alonso, I.; Trillo, B.; López, F.; Montserrat, S.; Ujaque, G.; Castedo, L.; Lledós, A.; Mascareñas, J. L. *J. Am. Chem. Soc.* **2009**, *131*, 13020–13030. b) Teller, H.; Corbet, M.; Mantilli, L.; Gopakumar, G.; Goddard, R.; Thiel, W.; Fürstner, A. *J. Am. Chem. Soc.* **2012**, *134*, 15331–15342.
39. González, A. Z.; Benitez, D.; Tkatchouk, E.; Goddard, W. A.; Toste, F. D. *J. Am. Chem. Soc.* 2011, *133*, 5500– 5507.
40. Hamilton, G. L.; Kang, E. J.; Mba, M.; Toste, F. D. *Science* **2007**, *317*, 496–499.
41. Refer to the introduction of Chapter 2 for more information on the combination of gold(I)-catalysis and ACDC.

Our group has contributed to the design of novel gold(I) complexes for asymmetric catalysis.[42] For instance, in 2019 we reported the design of a new family of gold(I) catalysts based on a modified JohnPhos ligand, incorporating a C_2-symmetric 2,5-diarylpyrrolidine. These complexes demonstrated excellent enantioselectivity in various 1,6-enyne cyclizations, including [4+2] cycloadditions, the synthesis of azabicyclo[4.1.0]hept-4-enes, and alkoxycyclizations (Scheme 7). DFT calculations revealed that non-covalent π–π interactions between the enynes and the ligand are crucial for the selective encapsulation of substrates within the chiral pocket of the gold(I) complex.[43]

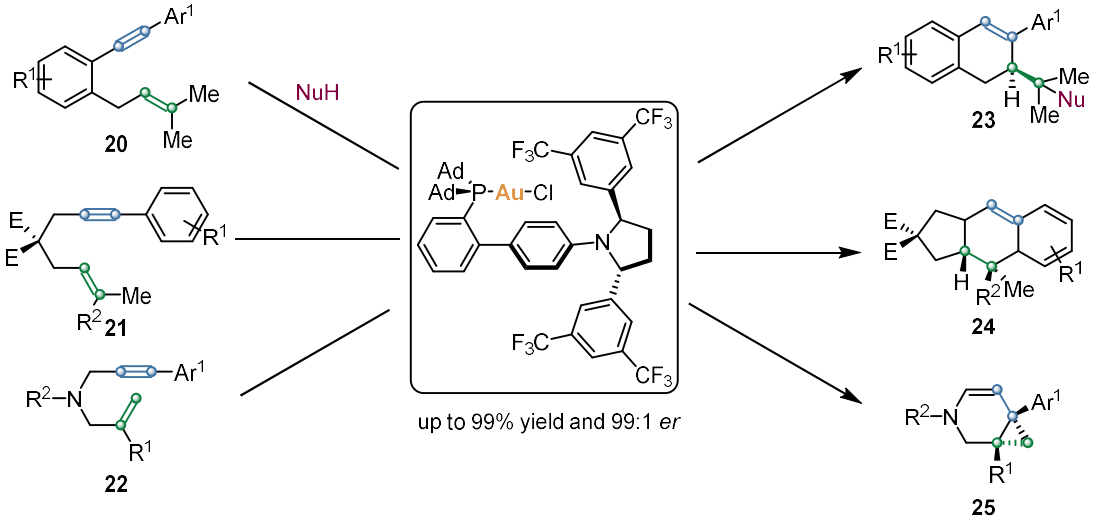

Scheme 7. Gold(I) catalysis with JohnPhos modified with a C_2-symmetric diarylpyrrolidine.

Building on this design, planar monodentate chiral 1,3-disubstituted ferrocene phosphine ligands were subsequently introduced.[44] These ligands were applied to highly enantioselective formal [4+2] cycloadditions of 1,6-enynes, leading to the formation of tricyclic scaffolds (Scheme 8A). More recently, shorter analogues of the original pyrrolidine ligands were developed and applied to the atroposelective cyclization of diarylacetylenes, yielding axially chiral indoles (Scheme 8B).[45] Additionally, in this last work, our group developed the NEST model, a tool specifically designed to account for steric effects in cylindrical-shaped complexes, which allows predicting experimental enantioselectivities.

42. Zuccarello, G.; Escofet, I.; Caniparoli, U.; Echavarren, A. M. *ChemPlusChem* **2021**, *86*, 1283–1296.
43. Zuccarello, G.; Mayans, J. G.; Escofet, I.; Scharnagel, D.; Kirillova, M. S.; Pérez-Jimeno, A. H.; Calleja, P.; Boothe, J. R.; Echavarren, A. M. *J. Am. Chem. Soc.* **2019**, *141*, 11858–11863.
44. Caniparoli, U.; Escofet, I.; Echavarren, A. M. *ACS Catal.* **2022**, *12*, 3317–3322.
45. Zuccarello, G.; Nannini, L. J.; Arroyo-Bondía, A.; Fincias, N.; Arranz, I.; Pérez-Jimeno, A. H.; Peeters, M.; Martín-Torres, I.; Sadurní, A.; García-Vázquez, V.; Wang, Y.; Kirillova, M. S.; Montesinos-Magraner, M.; Caniparoli, U.; Núñez, G. D.; Maseras, F.; Besora, M.; Escofet, I.; Echavarren, A. M. *JACS Au* **2023**, *3*, 1742–1754.

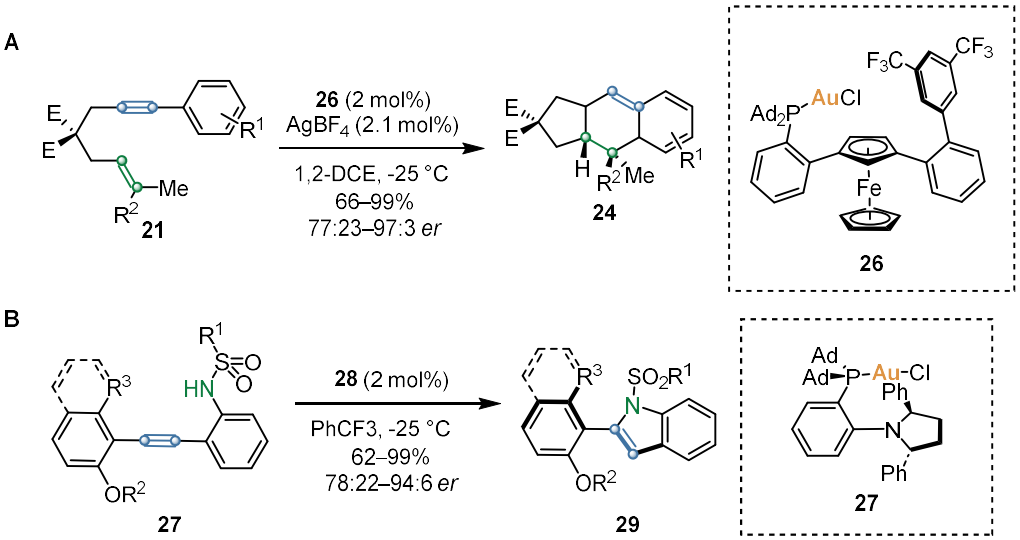

Scheme 8. New designs based on monodentate ligands developed by our group.

In the last years, the groups of Sollogoub, Fensterbank and Armspach, have developed different gold catalysts confined inside of cyclodextrins.[46] However, only moderate enantioselectivities were obtained in the cycloisomerization of 1,6-enynes. Inspired by those works and the seminal work by Iwasawa *et. al*,[47] our group reported in 2021 the use of achiral and chiral gold(I)-cavitand complexes which were applied to the alkoxycyclization of 1,6-enynes and the first total synthesis of carbazole alkaloid *(+)*-mafaicheenamine C. A combination of experimental and theoretical studies demonstrated that the cavity forces the enynes to adopt constrained conformations, leading to the high regio- and stereoselectivity observed.

46. a) Guitet, M.; Zhang, P.; Marcelo, F.; Tugny, C.; Jiménez-Barbero, J.; Buriez, O.; Amatore, C.; Mouriès-Mansuy, V.; Goddard, J.; Fensterbank, L.; Zhang, Y.; Roland, S.; Ménand, M.; Sollogoub, M. *Angew. Chem. Int. Ed.* **2013**, *52*, 7213–7218. b)Tugny, C.; del Rio, N.; Koohgard, M.; Vanthuyne, N.; Lesage, D.; Bijouard, K.; Zhang, P.; Meijide Suárez, J.; Roland, S.; Derat, E.; Bistri-Aslanoff, O.; Sollogoub, M.; Fensterbank, L.; Mouriès-Mansuy, V. *ACS Catal.* **2020**, *10*, 5964–5972. c) Zhu, X.; Xu, G.; Chamoreau, L.-M.; Zhang, Y.; Mouriès-Mansuy, V.; Fensterbank, L.; Bistri-Aslanoff, O.; Roland, S.; Sollogoub, M. *Chem. Eur. J.* **2020**, *26*, 15901–15909. d) Kaya, Z.; Andna, L.; Matt, D.; Bentouhami, E.; Djukic, J.-P.; Armspach, D. *Chem. Eur. J.* **2018**, *24*, 17921–17926. e) Kaya, Z.; Andna, L.; Matt, D.; Bentouhami, E.; Djukic, J.-P.; Armspach, D. *Eur. J. Org. Chem.* **2019**, *2019*, 4528–4537.
47. Schramm, M. P.; Kanaura, M.; Ito, K.; Ide, M.; Iwasawa, T. *Eur. J. Org. Chem.* **2016**, *2016*, 813–820.

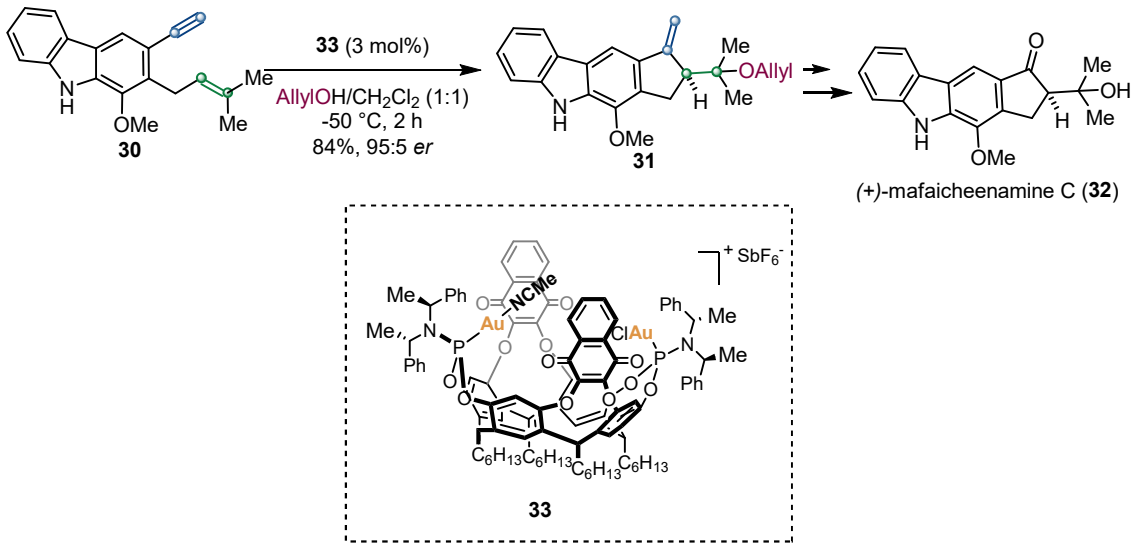

Scheme 9. First total synthesis of mafaicheenamine C by a chiral gold(I)-cavitand complex.

Gold(I) Catalysis in Total Synthesis

As mentioned in the previous sections, gold(I) catalysis constitutes a powerful tool for the electrophilic activation of C–C multiple bonds under mild reaction conditions. The strategic choice of the nucleophile can lead to the formation of a wide diversity of new C–C and C–heteroatom bonds.[48] When the nucleophilic attack takes place intramolecularly, complex polycyclic skeletons can be generated from relatively simple substrates, opening creative retrosynthetic disconnections. In the following section, selected examples will be presented to highlight the use of gold(I) catalysis in total synthesis.[49]

Initial steps

One of the first implementations of a gold(I)-catalyzed reaction in total synthesis was reported by Hashmi and coworkers in 2003 for the total synthesis of sesquiterpenoid jungianol (**37**) (Scheme 10).[50] The authors utilized a method previously reported by their group to transform furans into phenols.[51] According to independent mechanistic studies carried out in our group with Pt(II) for the same reaction,[52] the transformation starts with an intramolecular nucleophilic attack of the furan ring in **38** to the activated triple bond, resulting in the formation of cyclopropyl gold carbene **39**. This intermediate undergoes rearrangement into carbene **40**, which is then intramolecularly trapped by a nucleophilic attack on the carbonyl. Following deauration, oxepine **42** is generated,

48. a) Jiménez-Núñez, E.; Echavarren, A. M. *Chem. Rev.* **2008**, *108*, 3326–3350. b) Fürstner, A. *Chem. Soc. Rev.* **2009**, *38*, 3208–3221. c) Obradors, C.; Echavarren, A. M. *Acc. Chem. Res.* **2014**, *47*, 902–912. d) Fensterbank, L.; Malacria, M. *Acc. Chem. Res.* **2014,** *47*, 953–965. e) Dorel, R.; Echavarren, A. M. *Chem. Rev*. **2015**, *115*, 9028–9072. f) Pflästerer, D.; Hashmi, A. S. K. *Chem. Soc. Rev.* **2016***, 45*, 1331–1367
49. For detailed reviews on the application of gold catalysis in total synthesis, see: a) Rudolph, M.; Hashmi, A. S. K. *Chem. Soc. Rev.* **2008**, 37, 1766–1775. b) Rudolph, M.; Hashmi, A. S. K. *Chem. Soc. Rev.* **2012**, *41*, 2448– 2462. c) Zhang, Y.; Luo, T.; Yang, Z. *Nat. Prod. Rep.* **20**14, *31*, 489–503. d) Pflästerer, D.; Hashmi, A. S. K. *Chem. Soc. Rev.* **2016**, *45*, 1331–1367. e) Sugimoto, K.; Matsuya, Y. *Tetrahedron Lett.* **2017**, *58*, 4420–4426. f) Mayans, J. G.; Armengol-Relats, H.; Calleja, P.; Echavarren, A. M. *Isr. J. Chem.* **2018**, *58*, 639–658. g) Gu, Y.; Tan, C.; Gong, J.; Yang, Z. *Synlett* **2018***, 29*, 1552–1571. h) Lin, B.; Liu, T.; Luo, T. *Nat. Prod. Rep.* **2024**, *41*, 1091–1112.
50. Hashmi, A. S. K.; Ding, L.; Bats, J. W.; Fischer, P.; Frey, W. *Chem. Eur. J.* **2003**, *9*, 4339–4345.
51. Hashmi, A. S. K.; Frost, T. M.; Bats, J. W. *J. Am. Chem. Soc.* **2000**, *122*, 11553–11554.
52. a) Martín-Matute, B.; Cárdenas, D. J.; Echavarren, A. M. *Angew. Chem. Int. Ed.***2001**, *40*, 4754–4757. b) Martín-Matute, B.; Nevado, C.; Cárdenas, D. J.; Echavarren, A. M. *J. Am. Chem. Soc.* **2003**, *125*, 5757–5766.

which is in equilibrium with aryl oxide tautomer **43** and undergoes regioselective epoxide opening to yield phenol **35**. The natural product was synthesized in two steps from **35**, and its configuration was confirmed reassigning it to **37** instead of its previously proposed structure (**37'**).

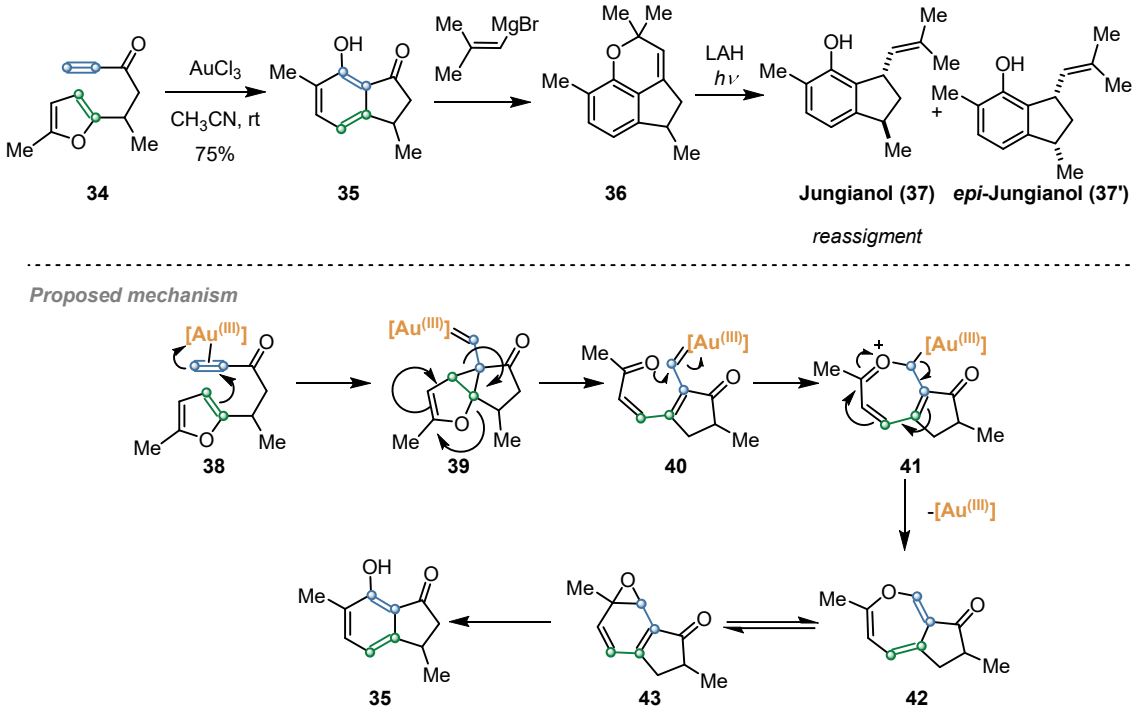

Scheme 10. Synthesis of jungianol **35** mediated by a gold(III)-catalyzed cyclization. LAH = $LiAlH_4$

Application of Gold(I) in Complex Systems

A good example of the functional group tolerance of gold(I) is the total synthesis of macrolactone bryostatin 16 (**47**) reported in 2008 by Trost and coworkers, featuring a late-stage gold(I)-catalyzed dihydropyran formation (Scheme 11).[53] Bryostatins are a group of natural products, showing promising anti-cancer activities, most of which present several features in common, including a 26-member macrolactone containing three embedded and highly functionalized pyran rings, as well as two *exo*-cyclic unsaturated esters and one congested C16–C17 *trans*-olefin. For the construction of ring C of bryostatin 16 (**47**), Trost and Dong performed a Pd-catalyzed alkyne-alkyne coupling macrocyclization on intermediate **44** to afford macrolide **45**. Exposure of **45** to a cationic gold(I) catalyst, in the presence of a mild base, led to the selective activation of the alkyne which upon nucleophilic attack of the vicinal alcohol via 6-*endo*-dig cyclization afforded dihydropyran product **46** in good yields. Compound **46** was acid-sensitive and was subsequently transformed into bryostatin 16 (**47**) in two steps. The use of a gold(I)-catalyzed nucleophilic cyclization was critical for the successful formation of the six-membered pyran ring over the five-membered furan product. The use of palladium for this step provided inseparable mixtures of the 5-*exo*-dig and 6-*endo*-dig cyclization products. More recently, the group of Trost and coworkers applied a very similar methodology for the synthesis of briostatin 3.

53. a) Trost, B. M.; Dong, G. *Nature* **2008**, *456*, 485–488. b) Trost, B. M.; Dong, G. *J. Am. Chem. Soc.* **2010**, *132*, 16403–16416.

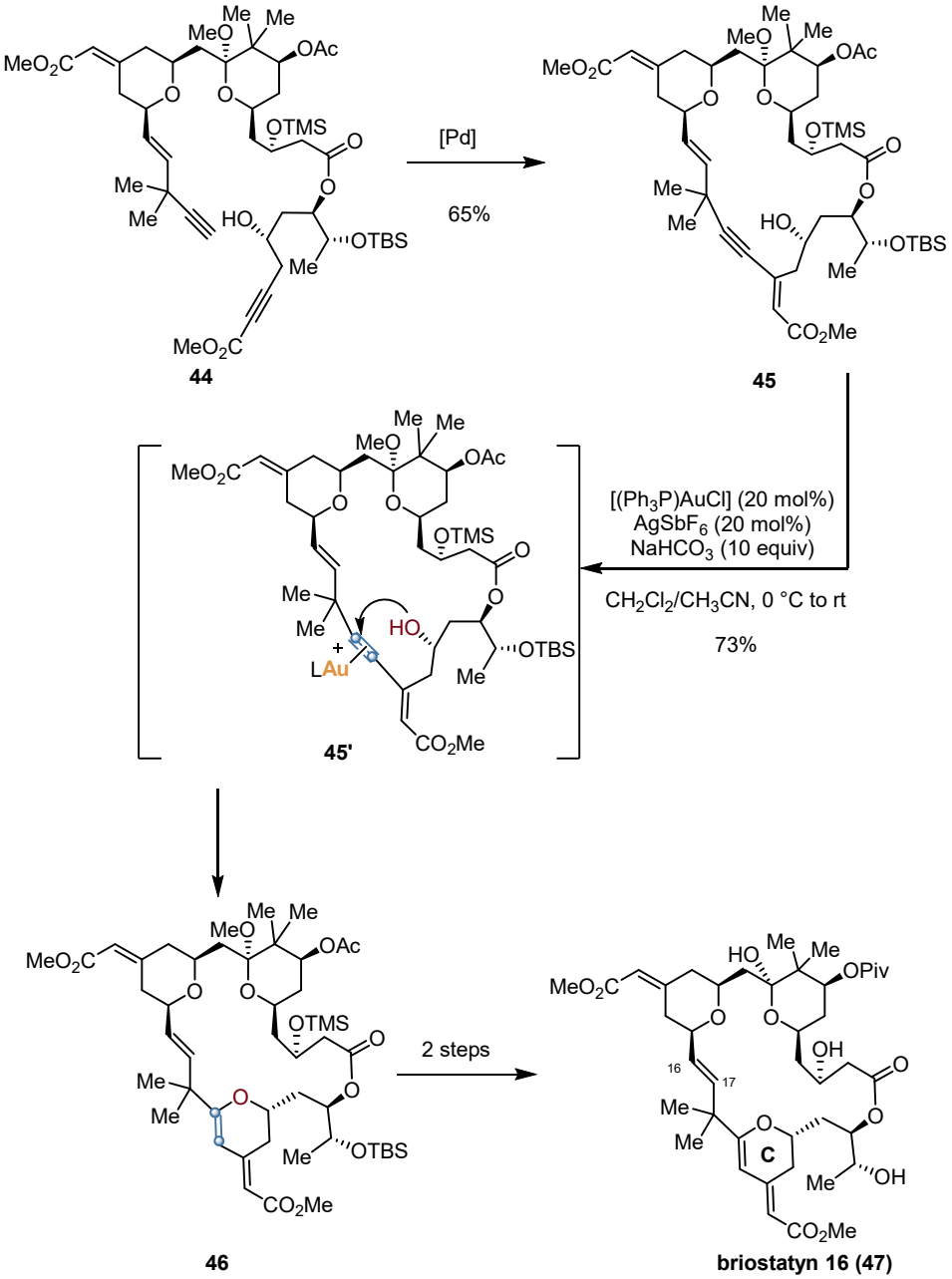

Scheme 11. Total synthesis of bryostatyn 16 (**47**) mediated by a gold(I)-tetrahydropyran synthesis.

Another excellent demonstration of the functional group tolerance of gold(I)-catalysis is Yu's glycosylation method, which employs glycosyl *ortho*-alkynylbenzoates as glycosyl donors, enabling glycosylation under very mild reaction conditions.[54] Upon activation of the alkyne by the gold catalyst, intramolecular nucleophilic attack of the carbonyl oxygen (Scheme 12) renders the cleavage of the glycosidic bond to give a molecule of isocumarine and the corresponding oxonium cation which can be trapped with the nucleophile of choice, usually alcohol or acids. This strategy has been successfully applied for the total synthesis of multiple saccharides.[54b] In comparison, more oxophilic Lewis acids lead to unwanted rearrangements and uncontrolled product distributions.[55]

54. a) Li, Y.; Yang, Y.; Yu, B. *Tetrahedron Letters* **2008**, *49*, 3604–3608. b) Li, W.; Yu, B. *Chem. Soc. Rev.* **2018**, *47*, 7954–7984.
55. Gauthier, C.; Legault, J.; Lavoie, S.; Rondeau, S.; Tremblay, S.; Pichette, A. *J. Nat. Prod.* **2009**, *72*, 72–81.

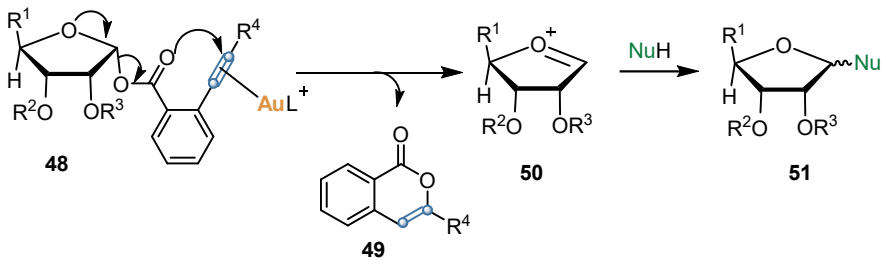

Scheme 12. Proposed mechanism for the gold(I)-catalyzed glycosylation developed by Yu and coworkers.

For instance, very recently the group of Zhang reported the Directed-Group-on-leaving-group (DGLG) strategy (Scheme 13), which was a modified version of Yu's glycosylation method, to regulate the configuration of the anomeric carbon.[56] In particular, they installed an oxazole ring on the *ortho*-alkynyl benzoate leaving group, which acted as a traceless directing group. After activation of the leaving group, the hydrogen bond acceptor facilitated the attack of the alcohol to the anomeric C–O bond, whose configuration was being controlled by the S_N2 nature of the transition state (**54**). This strategy was also applied to the synthesis of di and oligosaccharides with excellent yields and selectivity.

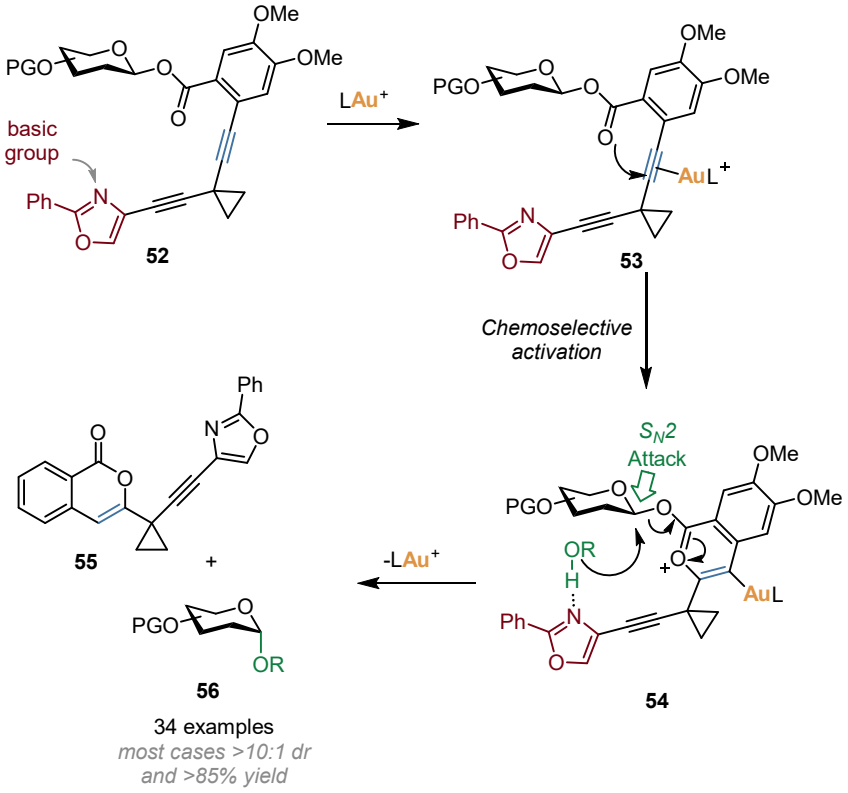

Scheme 13. Mechanism of the DGLG approach developed by Zhang and coworkers for glycosylations. PG = protecting group.

Enyne Cycloisomerizations

The cycloisomerization of enynes is probably the most used strategy for the construction of complex molecular systems from relatively simple starting material by means of gold(I)-catalysis.

56. Ma, X.; Zheng, Z.; Fu, Y.; Zhu, X.; Liu, P.; Zhang, L. *J. Am. Chem. Soc.* **2021**, *143*, 11908–11913.

Our group has exploited such reactions in the total synthesis of several natural products.[49f] The total synthesis of (-)-englerins A and B is a clear example where an oxatricyclic core was built in a formal [2+2+2] cycloaddition reaction from enyne **57** (Scheme 14, top). [57]

The reaction starts by the gold(I)-catalyzed 5-*exo*-dig cyclyzation of ketoenyne **57** (Scheme 14, bottom). Intramolecular trapping of the cyclopropyl gold(I) carbene **59** with the carbonyl group leads to oxocarbenium ion **60**. Finally, Prins-type cyclization of **60** and deauration delivers product **58** which was converted into englerin A (**59**) in 7 steps. This methodology allowed for a scale-up synthesis of **59** and several of its unnatural analogues, whose biological properties were tested.[58]

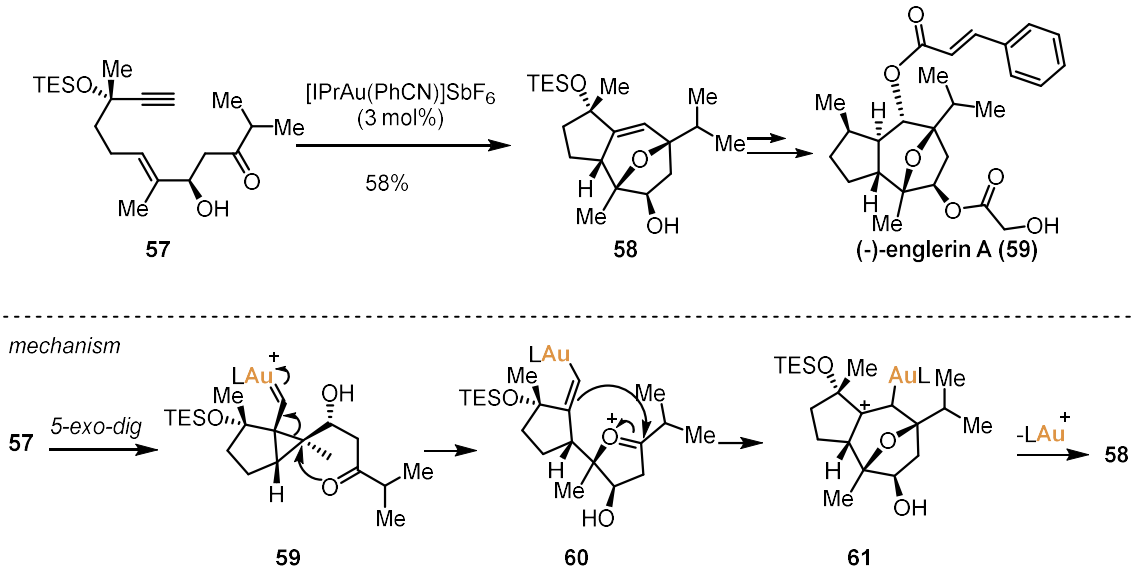

Scheme 14. Gold(I)-catalyzed cycloisomerization of enyne **57**, key step in the total synthesis of englerin A (**59**).

Finally, a more recent example on the use of gold(I)-catalyzed enyne cyclizations was recently reported by the Carreira group in the first enantioselective synthesis of (+)-aberrarone (**64**),[59] a diterpenoid featuring a 5-5-5-6 ring system that comprises four ketones and six continuous stereogenic centers (Scheme 15). The key reaction of the synthesis was a stereospecific gold(I)-catalyzed–tin-mediated tandem transformation of enantioenriched enyne **62** into the tetracyclic core of the natural product.[60] When enyne **62** was reacted with [JohnPhosAuNCMe]SbF_6, it underwent a Meyer–Schuster rearrangement generating a vinyl allene intermediate **66** which upon activation with gold(I) suffered a Nazarov cyclization, forming gold(I) carbene **67**. This intermediate readily reacted intramolecularly with the alkene to yield cyclopropene **69**. At this point, tin was introduced, promoting the intramolecular aldol condensation leading to pentacyclic product **63**.

57. a) Jiménez-Núñez, E.; Claverie, C. K.; Nieto-Oberhuber, C.; Echavarren, A. M. *Angew. Chem. Int. Ed.* **2006**, *45*, 5452–5455.b) Zhou, Q.; Chen, X.; Ma, D. *Angew. Chem. Int. Ed.* **2010**, *49*, 3513–3516. c) Molawi, K.; Delpont, N.; Echavarren, A. M. *Angew. Chem. Int. Ed.* **2010**, *49*, 3517–3519.
58. López-Suárez, L.; Riesgo, L.; Bravo, F.; Ransom, T. T.; Beutler, J. A.; Echavarren, A. M. *ChemMedChem* **2016**, *11*, 1003–1007. B) Wu, Z.; Suppo, J.-S.; Tumova, S.; Strope, J.; Bravo, F.; Moy, M.; Weinstein, E. S.; Peer, C. J.; Figg, W. D.; Chain, W. J.; Echavarren, A. M.; Beech, D. J.; Beutler, J. A. *ACS Med. Chem. Lett.* **2020**, *11*, 1711–1716.
59. Amberg, W. M.; Carreira, E. M. *J. Am. Chem. Soc.* **2022**, *144*, 15475–15479.
60. Lemière, G.; Gandon, V.; Cariou, K.; Hours, A.; Fukuyama, T.; Dhimane, A.-L.; Fensterbank, L.; Malacria, M. *J. Am. Chem. Soc.* **2009**, *131*, 2993–3006.

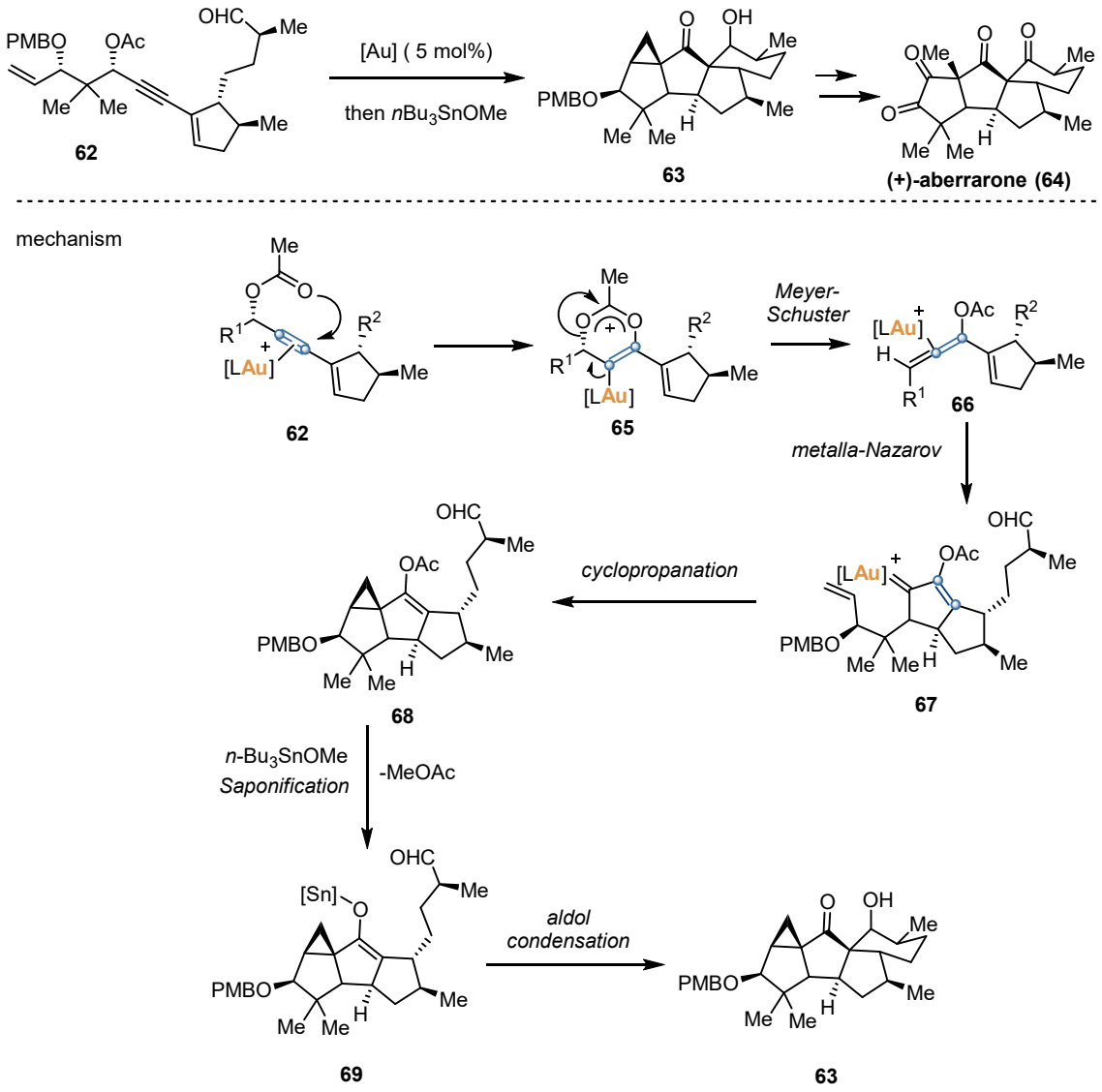

Scheme 15. Key step in the total synthesis of (+)-aberrarone (**64**) and its proposed mechanism. [Au] = [JohnPhosAu(MeCN)]SbF_6.

Chapter 1: Silver-Free Gold(I) Catalysis with Bifunctional Ligands

Introduction

Silver Salts as Chloride Scavengers in Gold(I) Catalysis

Gold(I) chloride complexes [LAuCl] are among the most used precatalysts in homogeneous gold(I) catalysis.[1] However, they usually present a linear dicoordinated geometry, thus requiring halide abstraction to allow substrate coordination and display meaningful levels of catalytic activity. The activation of the [LAuCl] is usually performed *in situ* by using external activators, the most employed being silver salts AgX (Scheme 1.1).[2] However, the use of silver salts to activate these precatalysts raises a series of issues, such as (1) practical problems; (2) interference of silver in catalysis ("silver effect"); and (3) incomplete chloride abstraction.

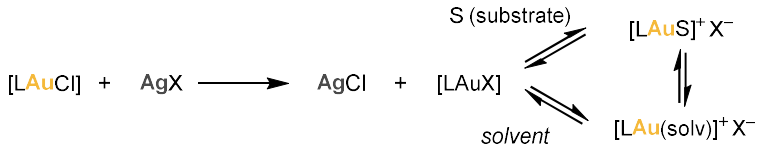

Scheme 1.1. Activation of Au(I) chloride precatalysts by chloride scavenging with silver salts.

The practical issues are associated with their high price, light and moisture sensitivity, the limited solubility in most used organic solvents and its tendency to be reduced to metallic silver. Furthermore, most silver(I) salts are hygroscopic which might cause the introduction of deleterious water in the system, leading to undesired reactions or to the formation of Au(I) oxonium species $[(LAu)_2OH]X$ which may also be catalytically active.[3] Additionally, work-up and recycling of the metals is also more difficult if there are two coinage metals in the system. Filtration of the reaction mixture through Celite® has become a common practice to remove the precipitated AgCl. However, it has been revealed that impurities on Celite® (bases or halides) can poison the catalyst[4] and filtration may not remove all traces of silver unless enough time has been allowed for all AgCl to precipitate.[5] The high metallophilic affinity of these two metals in their low oxidation state make it very difficult to completely remove all silver from the gold(I) catalysis solution and can also lead to a loss of gold to these same precipitates that are removed. In fact, in 2012 Straub[6] observed the formation of a heterobimetallic Ag/Au clusters **1.1** where a silver cation is coordinated to the Au–Cl bond of the catalyst (Scheme 1.2a). The same year Shi and coworkers classified a series of reactions in three types: (i) genuine gold(I), promoted only by [LAu]+; (ii) Au–Ag bi-metallic, catalyzed exclusively by Au/Ag mixture (Scheme 1.2b); (iii) silver assisted reactions presenting different reactivity with Au, Ag or Au/Ag mixtures.[7]

1. Schmidbaur, H.; Schier, *Z. Naturforschung,* **2011**, *66*, 329–350.
2. a) Fürstner, A. *Chem. Soc. Rev.* **2009**, *38*, 3208−3221. b) Shapiro, N. D.; Toste, F. D. *Synlett* **2010**, *5*, 675−691. c) Obradors, C.; Echavarren, A. M. *Acc. Chem. Res.* **2014**, *47*, 902−912. d) Fensterbank,L.; Malacria, M. *Acc. Chem. Res.* **2014**, *47*, 953−965. e) Dorel, R.; Echavarren, A. M. *Chem. Rev.* **2015**, *115*, 9028−9072. f) Pflästerer, D.; Hashmi, A. S. K. *Chem. Soc. Rev.* **2016**, *45*, 1331−1367.
3. a) Nesmeyanov, A. N.; Perevalova, E. G.; Struchkov, Yu. T.; Antipin, M. Yu.; Grandberg, K. I.; Dyadhenko, V. P. *Journal of Organometallic Chemistry* **1980**, *201*, 343–349. b)Yang, Y.; Ramamoorthy, V.; Sharp, P. R. *Inorg. Chem.* **1993**, *32*, 1946–1950. c) Sherry, B. D.; Toste, F. D. *J. Am. Chem. Soc.* **2004**, *126*, 15978–15979. d) Ramón, R. S.; Gaillard, S.; Poater, A.; Cavallo, L.; Slawin, A. M. Z.; Nolan, S. P. *Chem. Eur. J.* **2010**, *16*, 13729–13740. e) Gómez-Suárez, A.; Oonishi, Y.; Meiries, S.; Nolan, S. P. *Organometallics* **2013**, *32*, 1106–1111. f) Zhu, Y.; Zhou, W.; Petryna, E. M.; Rogers, B. R.; Day, C. S.; Jones, A. C. *ACS Catal.* **2016**, *6*, 7357–7362.
4. Kumar, M.; Hammond, G. B.; Xu, B. *Org. Lett.* **2014**, *16*, 3452–3455.
5. Zhu, Y.; Day, C. S.; Zhang, L.; Hauser, K. J.; Jones, A. C. *Chem. Eur. J.* **2013**, *19*, 12264–12271.
6. Weber, S. G.; Rominger, F.; Straub, B. F. *Eur. J. Inorg. Chem.* **2012**, *2012*, 2863–2867.
7. Wang, D.; Cai, R.; Sharma, S.; Jirak, J.; Thummanapelli, S. K.; Akhmedov, N. G.; Zhang, H.; Liu, X.; Petersen, J. L.; Shi, X. *J. Am. Chem. Soc.* **2012**, *134*, 9012–9019.

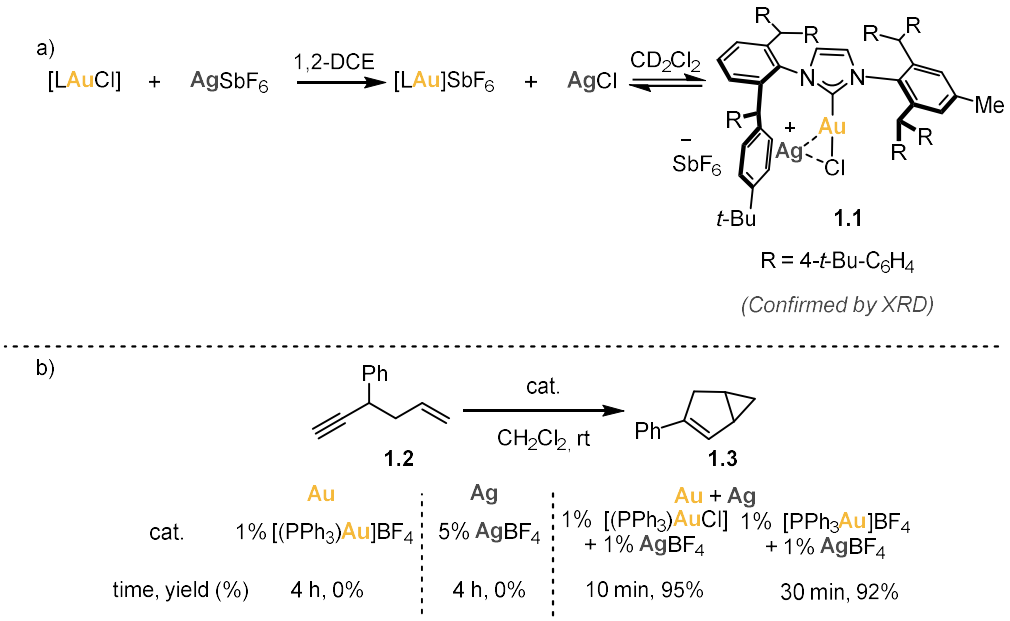

Scheme 1.2. a) Gold(I) complex with an arene stabilized silver cation coordinated to the Au-Cl bond. b) example of Shi's type ii) reaction, Au–Ag bimetallic reaction

Given that silver(I) is also catalytically active in some organic transformations of unsaturated organic substrates, its presence can lead to a different outcome of the reaction under study,[8] a term that has been coined as "silver effect". In 2009 Gagné and coworkers presented the first mechanistic study on the silver effect in Au(I)-catalyzed intramolecular hydroarylation of allenes.[9] It was found that Ag(I) was not interacting directly with reactants or products but caused the formation of a less reactive Ag/Au resting state, namely an argento-alkenyl Au(I) complex **1.6a** (Scheme 1.3a). The rate limiting step of that reaction was found to be the protodeauration, which happened fast from the resting state **1.6b**. However, when $AgNTf_2$ was added, a metathesis led to the formation of complex **1.6c**, whose protodemetallation was considerably slower than its digold(I) analog. Analogous conclusions were made later on in the hydroalkoxylation of alkynes.[10] Another example can be found in the regioselective switch observed from complete 5-*exo*-dig to 6-*endo*-dig in the intramolecular alkyne hydroamination of terminal alkynyl sulfamides **1.7** via the formation of σ-gold(I) π-silver(I) acetylides (**1.10**, Scheme 1.3b).[11] In conclusion, two main reasons can be found for the interference of silver in catalysis: a) Formation of off-cycle species with the catalytically active Au(I) intermediates of catalysis; thus, reducing the concentration of active Au(I);[10] b) Ag(I) catalysis promoting a different transformation than Au(I).[11]

8. Michelet, V.; Toullec, P. Y.; Genêt, J.-P. *Angew. Chem. Int. Ed.* **2008**, *47*, 4268–4315.
9. Weber, D.; Gagné, M. R. *Org. Lett.* **2009**, *11*, 4962–4965.
10. Zhdanko, A.; Maier, M. E. *ACS Catal.* **2015**, *5*, 5994–6004.
11. Veguillas, M.; Rosair, G. M.; Bebbington, M. W. P.; Lee, A.-L. *ACS Catal.* **2019**, *9*, 2552–2557.

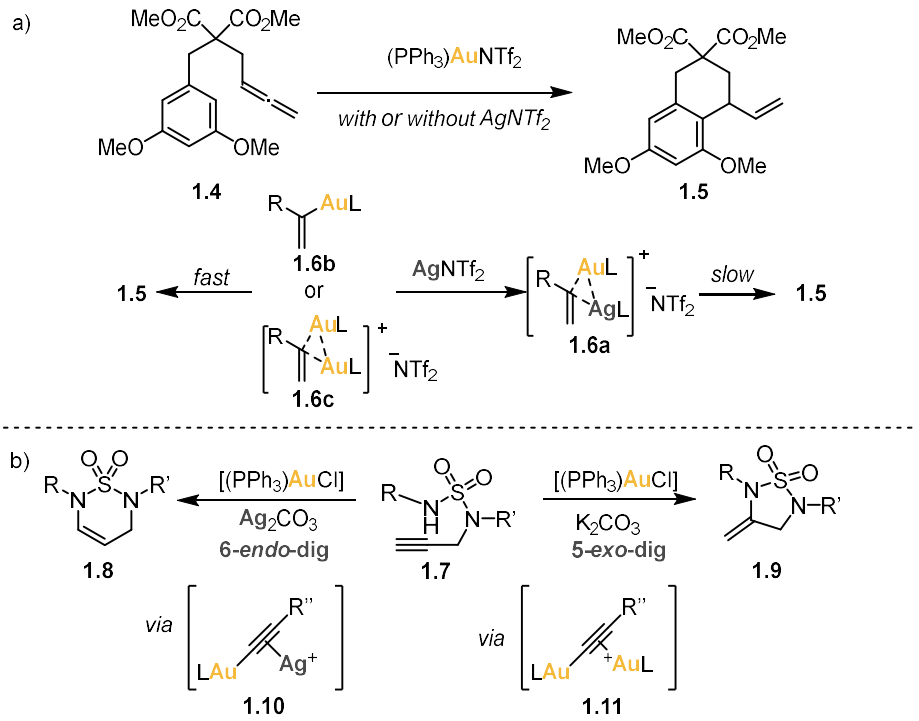

Scheme 1.3. Examples of the silver effect on gold(I) catalysis. a) formation of off-cycle species. b) different regioselectivity due to silver cation interference.

Chloride scavenging is not always quantitative, it is an associative ligand exchange equilibrium reaction that goes to completion only if performed in the presence of substrate, coordinating counterions or solvents (e.g. MeCN, THF, H_2O, toluene, etc.) to stabilize the LAu^+ cation (Scheme 1.1). In the absence of nucleophilic species, chloride abstraction can result in the formation of several species with different catalytic profiles.[12] Among these catalytically unactive species are chloride-bridged dinuclear Au(I) species that form upon the addition of an equimolar or excess amount of AgX to [LAuCl] in the absence of substrate and in a non-coordinating solvent (Scheme 1.4)[13c] but can also be prepared quantitatively by treating [LAuCl] precatalysts with 0.5 equiv of a silver salt. [13] These dinuclear complexes are less reactive compared to their mononuclear Au(I) counterparts in enyne cycloisomerizations. However, strongly coordinating substrates can cleave the Au–Cl bridge,[3,14,15] acting as a reservoir of active formal LAu^+, as Hashmi and coworkers

12. Franchino, A.; Montesinos-Magraner, M.; Echavarren, A. M. *Bull. Chem. Soc. J.* **2021**, *94*, 1099–1117.
13. a) Uson, R.; Laguna, A.; Castrillo, M. V. *Synth. React. Inorg. Met.-Org. Chem.* **1979**, *9*, 317–324. b) Bayler, A.; Bauer, A.; Schmidbaur, H. *Chem. Ber.* **1997**, *130*, 115–118. c) Homs, A.; Escofet, I.; Echavarren, A. M. *Org. Lett.* **2013**, *15*, 5782–5785. d) Pérez-Sánchez, J. C.; Herrera, R. P.; Concepción Gimeno, M. *Chem. Eur. J* **2024**, *30*, e202303585.
14. For an in deep analysis of ligand exchange in gold(I) catalysis: Zhdanko, A.; Ströbele, M.; Maier, M. E. *Chem. Eur. J.* **2012**, *18*, 14732–14744.
15. Bayrakdar, T. A. C. A.; Scattolin, T.; Ma, X.; Nolan, S. *Chem. Soc. Rev.* **2020**, *49*, 7044–7100.

demonstrated in the gold(I)-catalyzed transformation of ω-alkynyl furans (**1.15**) to phenols (**1.16**) (Scheme 1.4).[16]

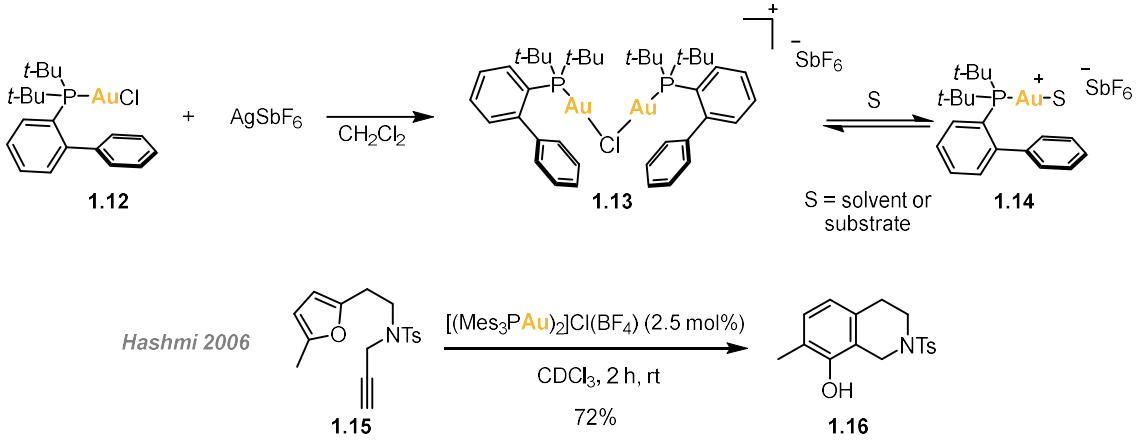

Scheme 1.4. Chloride-bridged digold(I) catalyst formation.

Silver-Free Activation for Au(I)-chloride Complexes

Alternative metal salts

As alternative to Ag(I) salts, the use of other transition metals as chloride scavengers has also been studied. Cu salts are particularly attractive when reactions have to be performed at elevated temperatures (the decomposition of cationic gold(I) complexes is more pronounced). Gandon and coworkers reported that both Cu(I) and Cu(II) salts were effective chloride scavengers for [(PPh_3)AuCl] in the Au-catalyzed intramolecular hydroxyalkylations of alkenes of type **1.17** (Scheme 1.5a).[17] Different Cu(I) and Cu(II) salts provided excellent yields compared to their analog Ag(I) salts. These results were rationalized by the lower scavenging ability of Cu salts (Cu(OTf) or $Cu(OTf)_2$) that generate the active complex [(PPh_3)Au(OTf)] in low concentration, maintaining a reservoir of more stable [(PPh_3)AuCl] during the course of the reaction. In contrast, AgOTf generates [(PPh_3)Au(OTf)] fast, which accelerates its decomposition into inactive [(PPh_3)$_2$Au(OTf)] and gold nanoparticles.[17] Later on, the group of Kamimura and coworkers presented a Au(I)-catalyzed 7-*exo*-dig cyclization of chiral *N*-tethered enynes **1.19** to form 1,4-oxazepan-7-ones **1.20** using [(PPh_3)AuCl]/$Cu(OTf)_2$ in refluxing 1,2-DCE with almost complete retention of the enantiomeric excess of the substrate.[18] Other Lewis acids, such as $Bi(OTf)_3$, $Zn(OTf)_2$, $Zn(ClO_4)_2$,[19] $In(OTf)_3$, $Yb(OTf)_3$, $Ga(OTf)_3$ or Me_3SiOTf have also proved to be

16. Hashmi, A. S. K.; Blanco, M. C.; Kurpejović, E.; Frey, W.; Bats, J. W. *Adv. Synt. Cat.* **2006**, *348*, 709–713. Corrigendum: Hashmi, A. S. K.; Blanco, M. C.; Kurpejović, E.; Frey, W.; Bats, J. W. *Adv. Synt. Cat.* **2006**, *348*, 792a–792a.
17. a) Guérinot, A.; Fang, W.; Sircoglou, M.; Bour, C.; Bezzenine-Lafollée, S.; Gandon, V. *Angew. Chem. Int. Ed.* **2013**, *52*, 5848–5852. b) w. Fang, F. Weizhen, M. Presset, A. Guérinot, C. Bour, S. Bezzenine-Lafollée, V. Gandon, *Org. Synth.* **2015**, *92*,117.c) Bour, C.; Gandon, V. *Synlett* **2015**, *26*, 1427–1436.
18. Kamimura, A.; Yamane, Y.; Yo, R.; Tanaka, T.; Uno, H. *J. Org. Chem.* **2014**, *79*, 7696–7702.
19. Demir, A. S.; Emrullahoğlu, M.; Buran, K. *Chem. Commun.* **2010**, *46*, 8032–8034.

efficient in the generation of $[LAuL']^+$ (L' = substrate, solvent or other weakly coordinating ligand).[20]

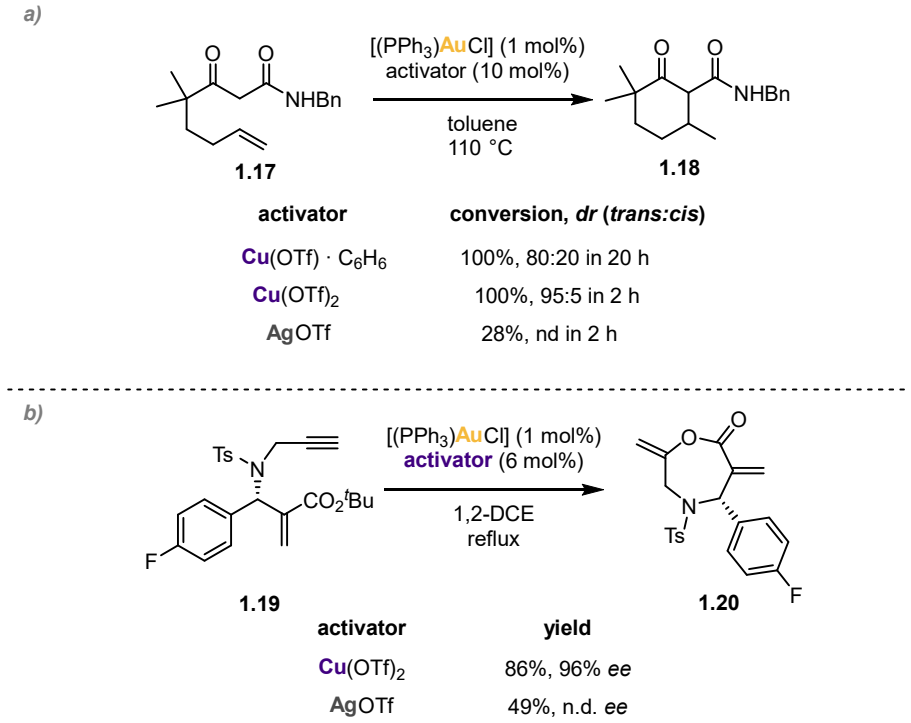

Scheme 1.5. Comparison of Cu salts with Ag(I) salts: a) in the intramolecular hydroalkylation of ene-*β*-ketoamide **1.18** and b) in the7-*exo*-dig cyclization of **1.19.**

Sodium and potassium salts of non-coordinating anions have also been employed as chloride scavengers.[12] In particular, $NaBAr_4^F$has been widely used as chloride scavenger due to the lower catalytic activity of Na^+.[21] Early examples of the use of $NaBAr_4^F$ as activator were reported by the group of Pérez for the activation of [(IPr)AuCl] in Au(I)-catalyzed cyclopropanation of alkenes and O–H, N–H and C–H insertions.[22] In 2017 our group reported the intermolecular [2+2] cycloaddition of alkynes **1.21** with alkenes **1.22** for the enantioselective synthesis of cyclobutenes **24** using JosiPhos-type digold(I) complexes **1.23** (Scheme 1.6).[23] A screening of metal salts revealed that the reaction outcome was highly dependent on the chloride scavenger employed. $NaBAr_4^F$ improved the yields compared to the Ag(I) salts that promoted the oligomerization of the electron-rich alkenes reducing the formation of the productive *σ,π*-(alkyne)-digold(I) complexes.[24] As for the use of potassium salts, some examples using $KB(C_6F_5)$ or KPF_6 have also

20. a)Wang, X.; Yao, Z.; Dong, S.; Wei, F.; Wang, H.; Xu, Z. *Org. Lett.* **2013**, *15*, 2234–2237. b)Fang, W.; Presset, M.; Guérinot, A.; Bour, C.; Bezzenine-Lafollée, S.; Gandon, V. *Chem. Eur. J.* **2014**, *20*, 5439–5446.
21. Nishida, H.; Takada, N.; Yoshimura, M.; Sonoda, T.; Kobayashi, H. *Bull. Chem. Soc. J.***1984**, *57*, 2600–2604.
22. Fructos, M. R.; Belderrain, T. R.; de Frémont, P.; Scott, N. M.; Nolan, S. P.; Díaz-Requejo, M. M.; Pérez, P. J. *Angew. Chem. Int. Ed.* **2005**, *44*, 5284–5288. B) Prieto, A.; Fructos, M. R.; Mar Díaz-Requejo, M.; Pérez, P. J.; Pérez-Galán, P.; Delpont, N.; Echavarren, A. M. *Tetrahedron* **2009**, *65*, 1790–1793. C) Delgado-Rebollo, M.; Beltrán, Á.; Prieto, A.; Díaz-Requejo, M. M.; Echavarren, A. M.; Pérez, P. J. *Eur. J. Inorg. Chem.* **2012**, *2012*, 1380–1386.
23. García-Morales, C.; Ranieri, B.; Escofet, I.; López-Suarez, L.; Obradors, C.; Konovalov, A. I.; Echavarren, A. M. *J. Am. Chem. Soc.* **2017**, *139*, 13628–13631.
24. Homs, A.; Obradors, C.; Lebœuf, D.; Echavarren, A. M. *Adv. Synt. Cat.* **2014**, *356*, 221–228.

been reported for gold(I)-catalyzed hydroaminations of alkynes[25] and the synthesis of oxazolines respectively.[26]

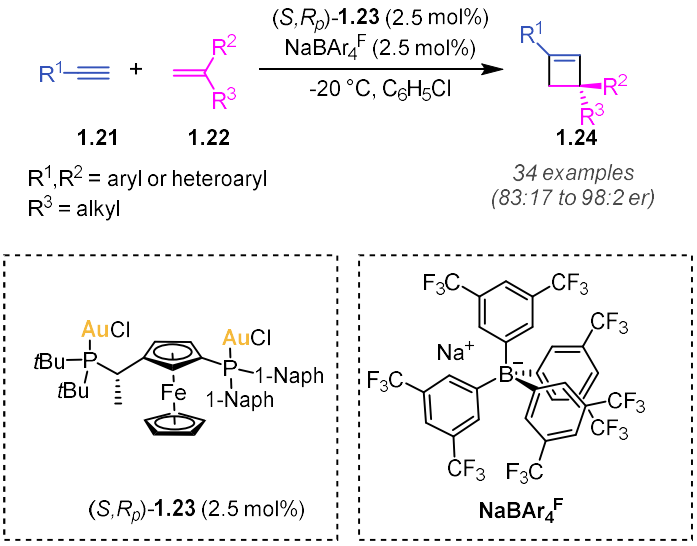

Scheme 1.6. Gold(I)-catalyzed enantioselective [2+2] cycloaddition of alkynes and alkynes promoted by $NaBAr^F$

As an alternative to the use of metal salts, the use of polar solvents is an attractive and simple approach, that relies in the dissociation of the Au–Cl bond facilitated by the polar solvent mixture. If working in aqueous media, special care must be taken on the ligand design, by introducing groups that improve their hydrophilicity, such as the introduction of sulfonate groups.[27] Nevertheless, there are some examples of silver-free gold(I) catalysis with conventional [(PPh_3)AuCl] and [IPrAuCl].[28] Very recently the group of Nolan and coworkers demonstrated that hexafluoroisopropanol (HFIP) could serve both as a solvent and activator in the additive-free cycloisomerization of benzamides **1.25a** and carboxylic acids **1.27** by forming intermolecular hydrogen bonds with the Cl ligand with surprisingly low catalyst loadings.[29] Additionally, they synthesized the corresponding Au–hexafluoroisopropoxide intermediate by independent methods, finding that it remained inactive unless the reaction occurred in HFIP or EtOH,[23c] emphasizing the crucial role of the solvent hydrogen-bonding network. Similarly, Lassaletta and Fernández very recently reported the intermolecular activation of [LAuCl] by using sulfonyl

25. a) Zeng, X.; Frey, G. D.; Kinjo, R.; Donnadieu, B.; Bertrand, G. *J. Am. Chem. Soc.* **2009**, *131*, 8690–8696. b) Zeng, X.; Soleilhavoup, M.; Bertrand, G. *Org. Lett.* **2009**, *11*, 3166–3169.
26. Pretorius, R.; Fructos, M. R.; Müller-Bunz, H.; Gossage, R. A.; Pérez, P. J.; Albrecht, M. *Dalton Trans.* **2016**, *45*, 14591–14602.
27. a) Almássy, A.; Nagy, C. E.; Bényei, A. C.; Joó, F. *Organometallics* **2010**, *29*, 2484–2490. b) Fernández, G. A.; Picco, A. S.; Ceolín, M. R.; Chopa, A. B.; Silbestri, G. F. *Organometallics* **2013**, *32*, 6315–6323. c)Tomás-Mendivil, E.; Toullec, P. Y.; Borge, J.; Conejero, S.; Michelet, V.; Cadierno, V. *ACS Catal.* **2013**, *3*, 3086–3098. d) Zhu, X.; Xu, G.; Chamoreau, L.-M.; Zhang, Y.; Mouriès-Mansuy, V.; Fensterbank, L.; Bistri-Aslanoff, O.; Roland, S.; Sollogoub, M. *Chem. Eur. J.* **2020**, *26*, 15901–15909.
28. a) Yao, X.; Li, C.-J. *Org. Lett.* **2006**, *8*, 1953–1955. b) Feng, E.; Zhou, Y.; Zhao, F.; Chen, X.; Zhang, L.; Jiang, H.; Liu, H. *Green Chem.* **2012**, *14*, 1888–1895. c) Li, F.; Wang, N.; Lu, L.; Zhu, G. *J. Org. Chem.* **2015**, *80*, 3538–3546.
29. a) Tzouras, N. V.; Gobbo, A.; Pozsoni, N. B.; Chalkidis, S. G.; Bhandary, S.; Hecke, K. V.; Vougioukalakis, G. C.; Nolan, S. P. *Chem. Commun.* **2022**, *58*, 8516–8519. b) Tzouras, N. V.; Zorba, L. P.; Kaplanai, E.; Tsoureas, N.; Nelson, D. J.; Nolan, S. P.; Vougioukalakis, G. C. *ACS Catal.* **2023**, *13*, 8845–8860. c) Arnaut, P.; Bracho Pozsoni, N.; Nahra, F.; Tzouras, N. V.; Nolan, S. P. *Dalton Trans.* **2024**, *53*, 11952–11958.

squaramides as external additives, instead of polar solvents, via hydrogen bonding to the chloride ligand.[30]

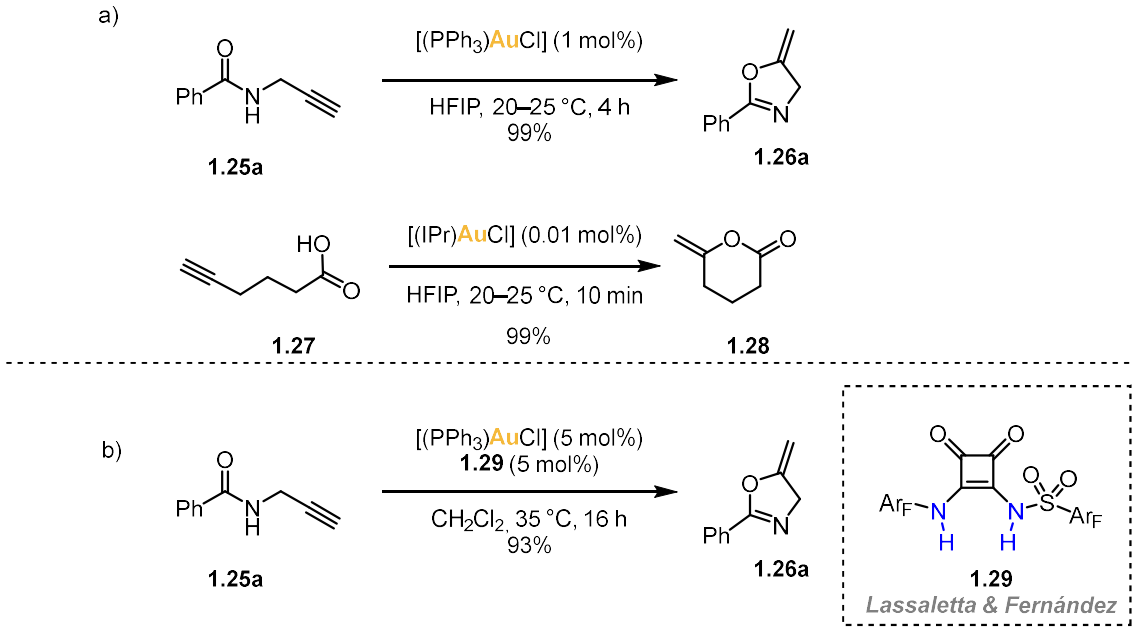

Scheme 1.7. a) HFIP promoted activation of gold(I)-chloride precatalysts. b) Sulfonyl squaramides as exogenous chloride scavengers.

Self-Activating Au(I) Chloride Complexes

The design of special ligands that allow for self-activation of the gold(I) chloride complexes has received special attention over the past decade.[31] Z-type ligands are σ-acceptor ligands acting as Lewis acids by accepting electron density from the metal center, which increases electrophilicity and modulates its catalytic activity. In 2019, Gabbaï reported complexes presenting a xanthylium **1.32** or acridinium unit **1.33** (Scheme 1.8). The carbenium center, with an empty p orbital, lower in energy than the analogous borane fragment, could serve as a more effective σ-acceptor ligand for gold(I), thus increasing the metal center's electrophilicity. The authors proposed a substrate push/carbenium pull mechanism to explain the observed activity in the cyclization of *N*-propargylbenzamide **1.30** (scheme 1.8).[32] More recently, the same group isolated complex **1.34** presenting a genuine Au–C^+ dative interaction. The activity of this complex could not be assessed with the cyclization of *N*-propargylbenzamide because it decomposed in the presence of the

30. a) Elías-Rodríguez, P.; Matador, E.; Benítez, M.; Tejero, T.; Díez, E.; Fernández, R.; Merino, P.; Monge, D.; Lassaletta, J. M. *J. Org. Chem.* **2023**, *88*, 2487–2492. b) Elías-Rodríguez, P.; Benítez, M.; Iglesias-Sigüenza, J.; Díez, E.; Fernández, R.; Lassaletta, J. M.; Monge, D. *Org. Lett.* **2024**, *26*, 5995–6000.
31. Pérez-Sánchez, J. C.; Herrera, R. P.; Gimeno, M. C. *Chem. Eur. J.* **2024**, *30*, e202401825.
32. a) Wilkins, L. C.; Kim, Y.; Litle, E. D.; Gabbaï, F. P. *Angew. Chem. Int. Ed.* **2019**, *58*, 18266–18270. b) Litle, E. D.; Wilkins, L. C.; Gabbaï, F. P. *Chem. Sci.* **2021**, *12*, 3929–3936.

amide. Nevertheless, 1,6-enyne **1.35** could be fully converted into the mixture of products **1.36** and **1.37** at room temperature in only 10 min without the addition of any additive.[33]

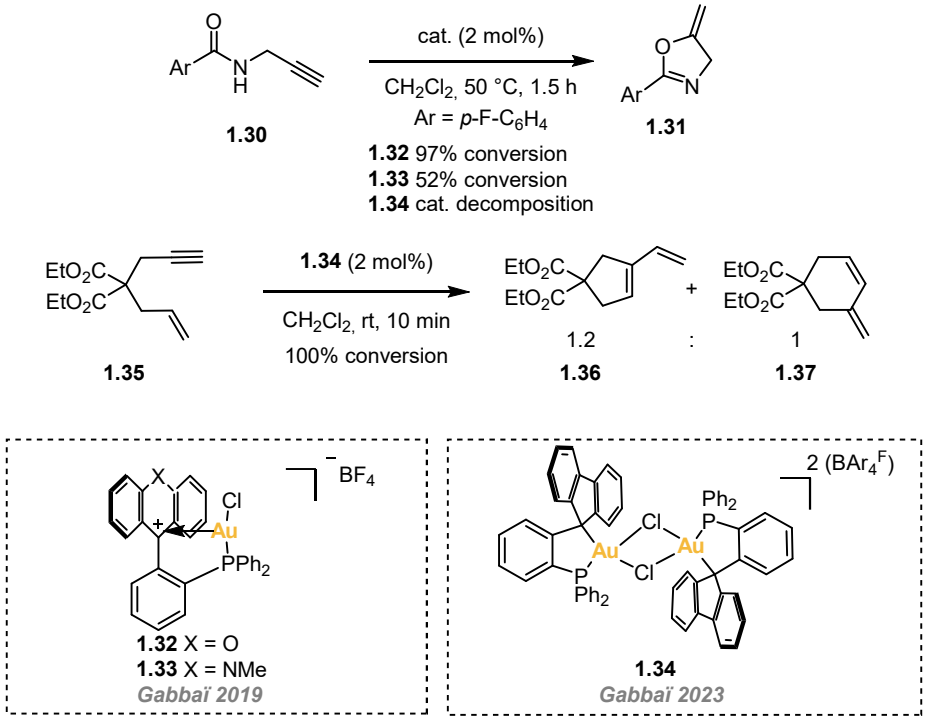

Scheme 1.8. Examples of silver-free gold(I)-catalysis with Z-type ligands.

Another type of design for self-activating complexes is the introduction of hydrogen bond donors in the second coordination sphere.[34] In 2017, Gabbaï and coworkers successfully prepared the first gold(I)-chloride catalyst capable of self-activation via H-bond interactions between a trifluoroacetamide scaffold in the ligand and the chloride.[35] In the solid state, the complex appeared as a dimer held by aurophilic interactions as well as H-bonds between the NH group of one molecule of catalyst and the chloride ligand of another molecule (Scheme 1.9). No activity was observed using [(PPh_3)AuCl] in combination with exogenous 2,2,2-trifluoro-*N*-phenylacetamide, pointing out the importance of tethering the H-bond donor to the ligand framework to mitigate the entropic cost of H-bonding. While this seminal work provided a compelling proof of concept, it only included one complex **1.38**, whose activity was modest and limited to the cyclization of *N*-propargyl benzamide. More recently, Helaja's group introduced NHC-based Au(I) complexes **1.39** (Scheme 1.9) incorporating an amide side arm, which was very active in the absence of additives (although traces of water had to be present in the solvent) but whose reactivity was once again restricted to the cyclization of *N*-propargylbenzamides **1.25**.[36]

33. Litle, E. D.; Gabbaï, F. P. *Chem. Commun.* **2023**, *59*, 603–606.
34. Reek, J. N. H.; de Bruin, B.; Pullen, S.; Mooibroek, T. J.; Kluwer, A. M.; Caumes, X. *Chem. Rev.* **2022**, *122*, 12308–12369.
35. Sen, S.; Gabbaï, F. P. *Chem. Commun.* **2017**, *53*, 13356–13358.
36. Seppänen, O.; Aikonen, S.; Muuronen, M.; Alamillo-Ferrer, C.; Burés, J.; Helaja, J. *Chem. Commun.* **2020**, *56*, 14697–14700.

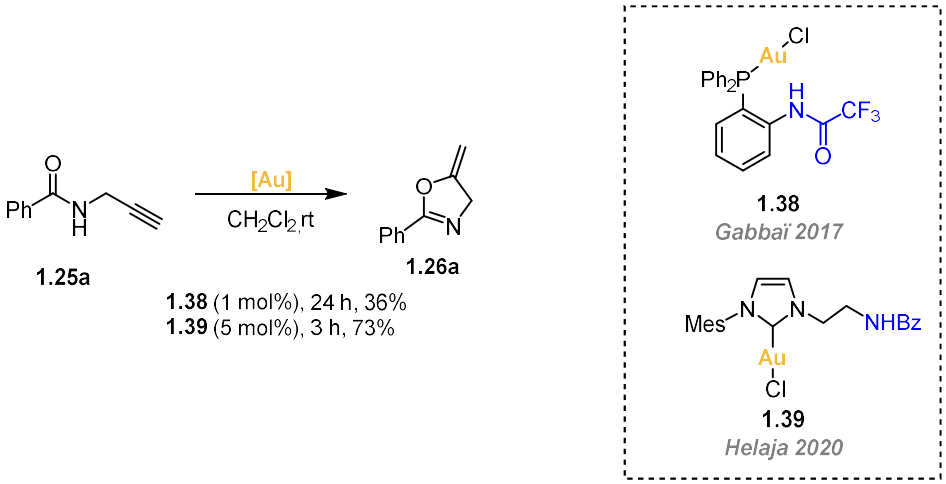

Scheme 1.9. H-Bond promoted silver-free gold(I) catalysis with **1.38** and **1.39**.

Marinetti, Guinchard and coworkers reported an example of a gold(I)-chloride complex with a chiral bifunctional phosphine ligand featuring a phosphoric acid moiety.[37] Complex **1.42** catalyzed the silver-free tandem cycloisomerization-indole addition reaction of 2-alkynyl enones, with high enantioselectivity and reactivity. The authors' hypothesis was that the Au-Cl bond is activated by weak basic nucleophiles via HCl abstraction, resulting in the reversible formation of a gold-phosphate catalyst **1.42'**. The chelation offered by the bidentate ligand might stabilize the catalytic active species (explaining the low catalyst loading employed) as well as allow substrate coordination because of the strain of the structure due to the bent geometry of the P–Au–O bond.

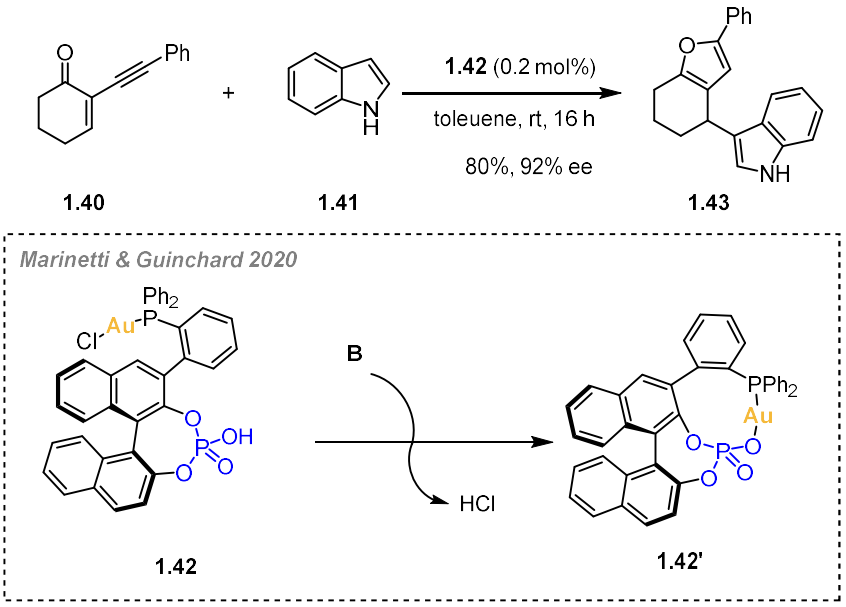

Scheme 1.10. Ligand-enabled silver-free gold(I) catalysis with **1.42**.

37. Zhang, Z.; Smal, V.; Retailleau, P.; Voituriez, A.; Frison, G.; Marinetti, A.; Guinchard, X. *J. Am. Chem. Soc.* **2020**, *142*, 3797–3805.

Objectives

In view of the importance of developing new silver-free methodologies, and inspired by the seminal work by Gabbaï and coworkers,[35] we envisioned the design of a new family of self-activating gold(I)-chloride complexes. We sought the preparation of a library of phosphino(thio)ureas and squaramides gold(I) chloride complexes as dual hydrogen bond donor groups.

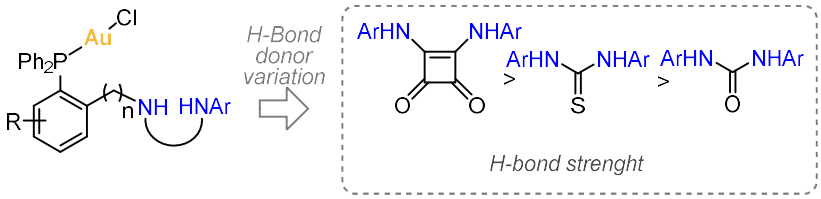

Scheme 1.11. Design of bidentate H-bond donor ligands.

To benchmark our system with the current literature we decided to test this reaction in the cycloisomerization of *N*-propargyl benzamides. We also decided to study the mechanism to gain some insight into the role of the H-bond donor unit present in the catalyst and to apply this system to other reactions.

Results and Discussion

To design new ligands capable of self-activation via intramolecular hydrogen bonding, we need to place the hydrogen bond donor relatively close to the Au-Cl bond. We envisioned that a good starting point could be ortho substituted triarylphosphines. Therefore, we prepared a library of twelve phosphine Au(I) chloride complexes featuring tethered squaramides (**A**–**C**), thioureas (**D** and **E**), and ureas (**F**, **G**–**I)** in the ortho position. The hydrogen bond donor group (HBD) was introduced onto the phosphine scaffold in a "late-stage" manner, as the final step in ligand synthesis. This approach facilitated the purification of intermediates and allowed for the diversification of the key HBD. We started by preparing phosphinosquaramide ligands **1.48a–c** by reaction of the corresponding primary amines **1.46a–c** with the mixed squarate **1.47** (Scheme 1.12). Reaction took place within a few minutes at room temperature, which could be judged by the rapid formation of a white precipitate, but they were left overnight. The phosphinosquaramide ligands **1.48a–c** were then purified by simple filtration in 79%, 38% and 57% yield respectively. The moderate yields are likely due to the partial solubility of the product in MeOH. However, purification of the substrate from the product by chromatography was not possible.

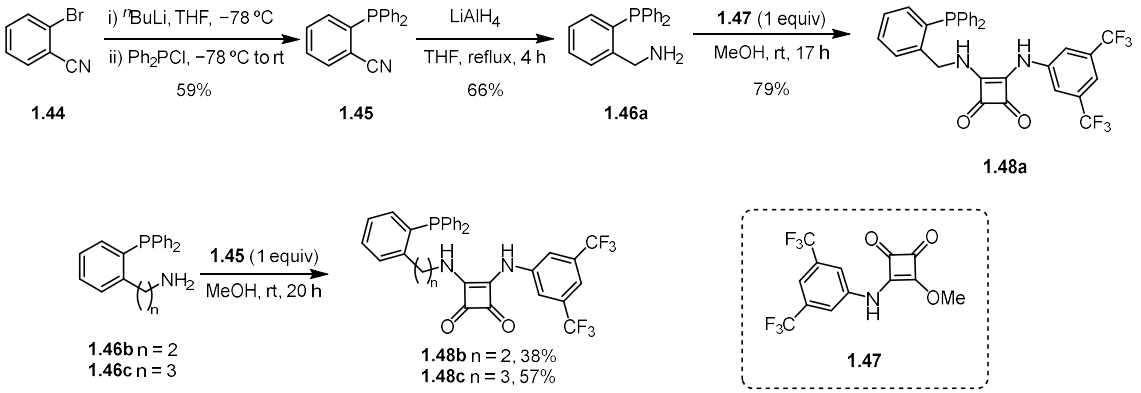

Scheme 1.12. Synthesis of phosphinosquaramide ligands **1.48a**–**c**.

Phosphino(thio)urea ligands **1.48d** and **1.48e** were prepared by reaction of the corresponding primary amines or anilines with the desired iso(thio)cyanates (Scheme 1.13). When primary amines were used, the reaction could be performed at room temperature in excellent yields (**1.46a,b**, 87 and 93% respectively). However, due to the lower nucleophilicity of anilines **1.49**, heating was required for urea formation, though this was not necessary for the thiourea analogues. Often, reaction did not reach complete conversion at room temperature (reaction was monitored by $^{31}P\{^{1}H\}$ NMR), while at higher temperatures afforded a mixture of products: the desired product and variable amounts of symmetrical ureas. The formation of these side products can be attributed to the reversibility of urea formation at high temperature, consistent with previous studies on the reversibility of thiourea formation at high[38] or moderate temperature in the presence of mild bases.[39] The formation of symmetrical ureas, which was more pronounced when less nucleophilic anilines **1.49b** and **1.49c** were used as starting materials, made purification more challenging consequently impacting the yields for ligands **1.48i–l** (42–60%).

38. Habib, N. S.; Rieker, A. *Synthesis* **1984**, 825–827.
39. Vlatković, M.; Feringa, B. L. *Tetrahedron* **2019**, *75*, 2188–2192.

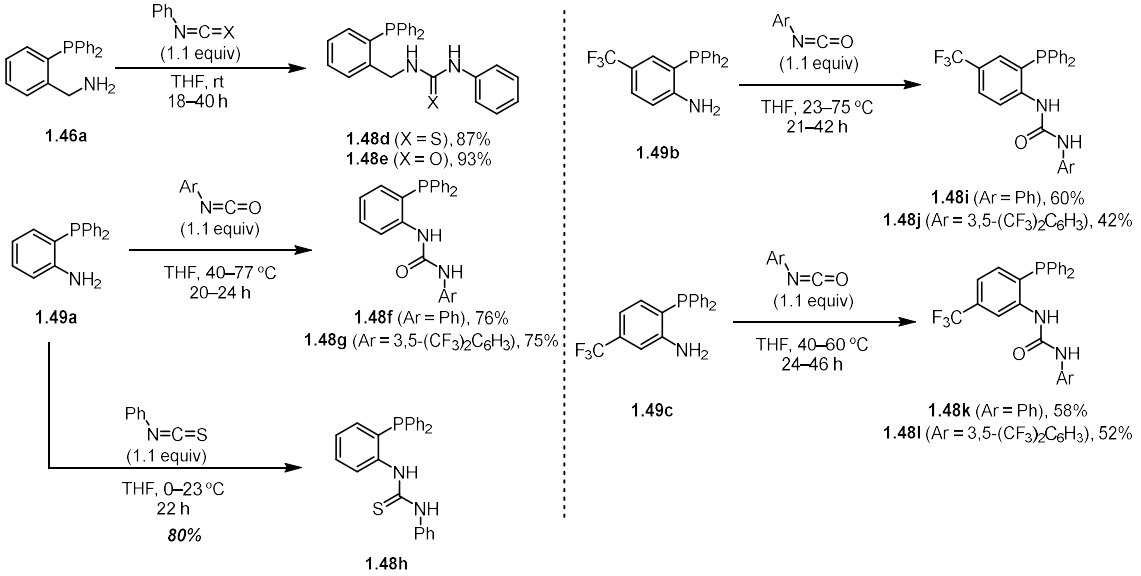

Scheme 1.13. Synthetic route towards the phosphino(thio)urea ligands.

Finally, ligand exchange with (dimethylsulfide)gold(I) chloride afforded complexes **A**–**L** as bench stable white solids after purification (Scheme 1.14). All complexes could be characterized by single-crystal X-ray diffraction, which provided valuable information on their connectivity and H-bonding ability in the solid state.[40] In principle, a longer distance of the Au–Cl bond compared to the PPh_3AuCl (approximately 2.28 Å)[41] indicates a weaker Au–Cl bond, thus a more active silver-free catalyst. However, in the solid state most of the complexes displayed either interactions with the solvent of crystallization or intermolecular interactions between two or more molecules of catalyst. Phosphinosquaramide complexes **A**–**C** were crystalized in DMSO[42] and show a bidentate H-bond interaction between the squaramide and the oxygen of dimethylsulfoxide as well as displaying Au–Cl distances of 2.282–2.287 Å. In phosphinourea complexes **E**, **I** and **K**, the Au–Cl bond lengths range from 2.275 to 2.283 Å, and the urea moiety engages in intermolecular H-bonds with another urea unit. Conversely, in the crystal structures of phosphinourea complexes **G**, **H**, **J** and **L**, the urea establishes H-bonds with the chloride atom of another [LAuCl] unit, leading to a weakening of the Au–Cl bond, as evidenced by its elongation to 2.297–2.326 Å. Complex **J** adopts a dimeric structure, closely resembling the one described by Gabbaï for complex **1.38**[35] stabilized by aurophilic interactions with a short Au–Au distance (3.077 Å) and with a less linear P–Au–Cl angle (169.67°). Finally, the X-ray structures of phosphinothiourea complexes **D** and **F** show a dimeric core with Au–Au distance of 3.416 Å for **F**. In these dimers, the thiourea of one molecule coordinates via S to the Au atom of another unit, while the displaced chloride ligands are stabilized by H-bonds with the thiourea NH groups and polar solvent molecules.

40. See Experimental Section for all X-ray structures.
41. Dunstan, S. P. C.; Healy, P. C.; Sobolev, A. N.; Tiekink, E. R. T.; White, A. H.; Williams, M. L. *J. Mol. Struct.* **2014**, *1072*, 253–259.
42. DMSO proved to be a very strong hydrogen bond acceptor, showing in all cases interactions of the hydrogen bond donor unit of the catalyst with it. Attempts to crystallize the complexes from CH_2Cl_2 or $CHCl_3$ mixtures in alkane solvents failed.

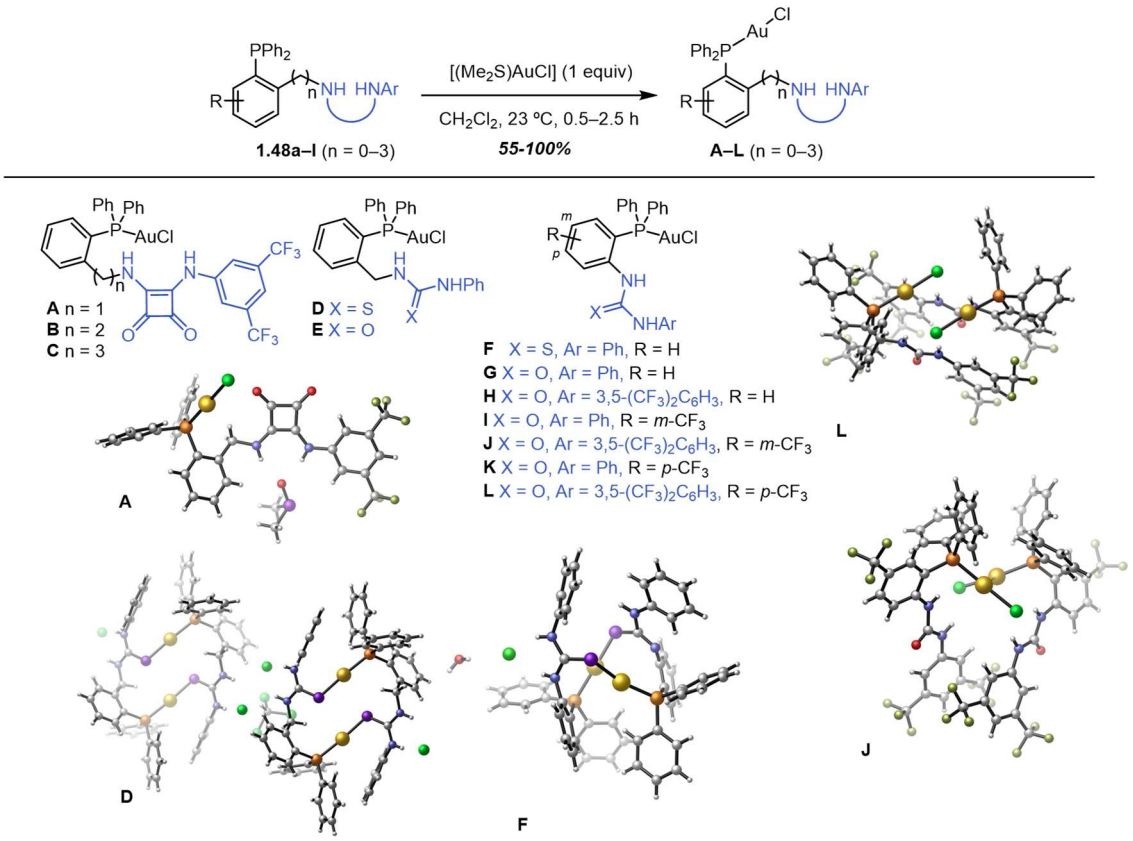

Scheme 1.14. Library of the new family of gold(I) complexes bearing squaramide and (thio)urea groups.

After preparing a library of complexes, we identified several that exhibited hydrogen bonding with either the chloride ligand (**G**, **H**, **J**, **L**) or the chloride anion (**D**, **F**) in the solid state, which although are not representative of the interactions present in solution served as a prove that intramolecular H-bonding of the HBD with the Cl was possible. To determine whether these H-bonding interactions would be sufficiently robust in solution to activate the metal center for catalysis, we conducted catalytic tests without silver additives. The cyclization of *N*-propargyl benzamide **1.25a** was selected as a benchmark reaction, as it is a model for silver-free Au(I) catalysis, employing the same conditions used by Gabbaï[35] for comparison. Another reason we chose this reaction is because under pure Au(I) catalysis it exclusively affords methylene oxazoline **1.26a**,[43] whereas isomerized oxazole **1.50a** is produced in the presence of Au(III) or Brønsted acid additives,[44,45] being thus ideally suited to discriminate a pure Au(I) catalysis from any catalytic activity arising from impurities or degradation/disproportionation products.

43. Hashmi, A. S. K.; Schuster, A. M.; Rominger, F. *Angew. Chem. Int. Ed.* **2009**, *48*, 8247–8249; *Angew. Chem.* **2009**, *121*, 8396–8398.
44. a) Milton, M. D.; Inada, Y.; Nishibayashi, Y.; Uemura, S. *Chem. Commun.* **2004**, 2712–2713; b) Hashmi, A. S. K.; Weyrauch, J. P.; Frey, W.; Bats, J. W. *Org. Lett.* **2004**, *6*, 4391–4394; c) Hashmi, A. S. K.; Rudolph, M.; Schymura, S.; Visus, J.; Frey, W. *Eur. J. Org. Chem.* **2006**, 4905–4909; d) Weyrauch, J. P.; Hashmi, A. S. K.; Schuster, A.; Hengst, T.; Schetter, S.; Littmann, A.; Rudolph, M.; Hamzic, M.; Visus, J.; Rominger, F.; Frey W.; Bats, J. W. *Chem. Eur. J.* **2010**, *16*, 956–963; e) Teci, M.; Hueber, D.; Pale, P.; Toupet, L.; Blanc, A.; Brenner, E.; Matt, D. *Chem. Eur. J.* **2017**, *23*, 7809–7818.
45. The following are a selection of mechanistic studies: a) Ref.43; b) Egorova, O. A.; Seo, H.; Kim, Y.; Moon, D.; Rhee, Y. M.; Ahn, K. H. *Angew. Chem. Int. Ed.* **2011**, *50*, 11446–11450. Corrigendum: Egorova, O. A.; Seo, H.; Kim, Y.; Moon, D.; Rhee, Y. M.; Ahn, K. H. *Angew. Chem. Int. Ed.* **2012**, *51*, 4511–4511.c) Lu, Z.; Han, J.; Okoromoba, O. E.; Shimizu, N.; Amii, H.; Tormena, C. F.; Hammond, G. B.; Xu, B. *Org. Lett.* **2017**, *19*, 5848–5851. d) Peng, H.; Akhmedov, N. G.; Liang, Y.-F.; Jiao, N.; Shi, X. *J. Am. Chem. Soc.* **2015**,

Table 1.1. Catalyst screening and control experiments for the cyclization of *N*-propargyl benzamide **1.25a**.

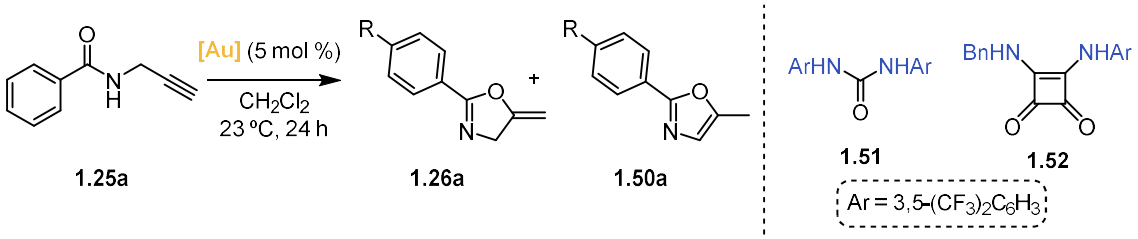

Entry	[Au]	**1.26a** [**1.50a**] yield[a] (%)	Entry	[Au]	**1.26a** [**1.50a**] yield[a] (%)
1	**A**	98	**15**	[(Ph_3P)AuCl]	<5
2	**B**	57	**16**	[(IPr)AuCl]	<5
3	**C**	<5 [5]	**17**	[(JohnPhos)AuCl]	5
4	**D**	6	**18**	[((2,4-$^tBu_2C_6H_3O)_3P$)AuCl]	<5
5	**E**	23	**19**[c]	[(Ph_3P)AuCl] + **1.51**	<5
6	**F**	<5	**20**[c]	[(Ph_3P)AuCl] + **1.52**	<5
7	**G**	23	**21**[c]	[(Ph_3P)AuCl] + $AgSbF_6$	95 [5]
8	**H**	76	**22**[c]	[(Ph_3P)AuCl] + $AgNTf_2$	95 [5]
9	**I**	65	**23**[c]	[(Ph_3P)AuCl] + AgOTf	81
10	**J**	96	**24**[c]	[(Ph_3P)AuCl] + $NaBAr^F{}_4$	99
11	**K**	64	**25**[c]	1,3-Diphenylurea	<5
12	**L**	99	**26**[c]	1,3-Diphenylthiourea	<5
13[b]	**1.38**	36	**27**[c]	Ligand **1.48i** or **1.48k**	<5
14	[(Me_2S)AuCl]	<5 [72]	**28**[c]	**A** + $^nBu_4NCl$	18

[a] Yields for **1.26a** and **1.50a** were determined by 1H NMR analysis using n-dodecane or tetraethoxysilane as internal standard. The remaining mass was unreacted starting material. [b] Data taken form ref. 35. [c] 5 mol% of the corresponding additive was added.

Complex **A**, featuring a pendant squaramide, along with complexes **J** and **L**, which incorporate electron-deficient aromatic ureas, delivered excellent yields of oxazoline **1.26a** in 24 h at 23 °C (95–98%, Table 1.1, entries 1, 10 and 12) outperforming the one shown by complex **1.38** (36% yield under the same conditions, Table 1.1, entry 13),[35] and highlighting the importance of ligand design to achieve catalytic efficiency. Comparing the performances of homologous phosphinosquaramide complexes **A**–**C**, a significant drop in activity is observed as the linker length increases (Table 1, entries 1–3). This suggests that the tether between the P and N atoms must have an optimal length (3 C atoms), likely minimizing the entropic cost of placing the H-bond donor near the Au–Cl bond. Phosphino(thio)urea complexes **D** and **E**, with the same optimal linker as phophinosquaramide **A**, provided much lower conversions (Table 1, entries 4–5), revealing that the nature of the H-bond donor group is also important. Stronger H-bond donor

137, 8912–8915. e) Dong, G.; Bao, M.; Xie, X.; Jia, S.; Hu, W.; Xu, X. *Angew. Chem. Int. Ed.* **2021**, *60*, 1992–1999; *Angew. Chem.* **2021**, *133*, 2020–2027.

groups on the ligand induce higher reactivity, which could be explained by a greater stabilization of the chloride ion via hydrogen bonding. This reactivity and H-bonding ability trend can be deduced also from the following two observations: 1) complexes **H**, **J** and **L** possessing electron-poor ureas systematically outperform their non-fluorinated counterparts **G**, **I**, and **K** (Table 1.1, entries 2 and 7–12) and 2) the activity of catalysts **I**–**L**, bearing an additional trifluoromethyl substituent on the internal aryl ring, surpass that of **H** and **G**. Finally, the difference in activity should not be attributed to the solubility of the catalysts, as all the complexes except **G** are soluble in CH_2Cl_2 (at the working concentrations, 5 mM). Phosphinothiourea complexes **D** and **F** were unreactive under these reaction conditions (Table 1.1, entries 4 and 6), likely because the thiourea moiety, as supported by the X-ray structures, binds too strongly to the metal center via the S atom, preventing ligand exchange with the substrate. This finding is also supported by the known thiophilicity of Au atoms.[46]

When using [(Me_2S)AuCl] (which could be found in traces in our complexes as it is used for the synthesis of most [LAuCl] precatalysts), oxazole **1.50a** formed exclusively (Table 1.1, entry 14).[47] As no formation of oxazole could be detected in the reactions using our designed catalysts, this result indirectly served as a prove of their purity as well as to corroborate that strongly coordinating ligands, such as phosphines[35] or carbenes, are required to impart sufficient stability to the Au(I) center during catalysis. On the other hand, common commercially available Au–Cl precatalysts bearing phosphine, carbene or phosphite ligands alone or in combination with urea **1.51** and squaramide **1.52** additives, did not promote reactivity, indicating that the H-bond donor employed must be linked to the ligand backbone[30] (Table 1.1, entries 15–20). Intermolecular chloride scavenging from [(Ph_3P)AuCl] using common additives such as $AgSbF_6$, $AgNTf_2$, AgOTf and $NaBAr^F{}_4$ affords high yields of product **1.26a** (Table 1.1, entries 21–24), while the reaction is not catalyzed by squaramides or (thio)ureas on their own (Table 1, entries 25–28). When an equimolar amount of chloride anions (TABCl was used as source of Cl^-) is added to the reaction of complex **A**, the yield for oxazoline product **1.26a** decreases from 98% to 18% (Table 1.1, entry 1 vs 28) indicating that the metal center is saturated with chloride anions.

Finally, starting materials presenting homopropargylic terminal alkynes or *N*-propargyl benzamide with an internal alkyne (**1.53** and **1.54**) did not react with our catalysts (Scheme 1.15).

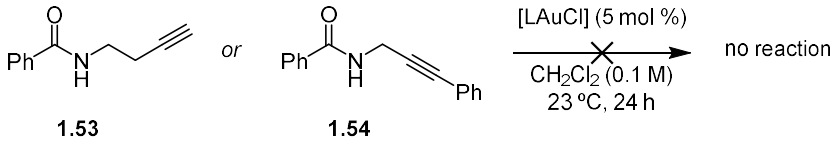

1.53 **1.54**

Scheme 1.15 Unsuccessful silver-free cyclization of **1.53** and **1.54**.

Mechanistic Studies on the Cycloisomerization of *N*-Propargylbenzamide

The gold(I) catalyzed cycloisomerization of *N*-propargylbenzamide **1.25a** has been previously studied and its mechanism has been elucidated[36,43,44d,48] and divided into 4 elementary steps: 1) gold(I) coordination to the alkyne, 2) attack of the carbonyl to the alkyne in a 5-*exo*-dig cyclization, 3) deprotonation of the oxazoline and 4) protodeauration.

46. a) Kepp, K. P. *Inorg. Chem.* **2016**, *55*, 9461–9470; b) Visbal, R.; Herrera, R. P.; Gimeno, M. C. *Chem. Eur. J.* **2019**, *25*, 15837–15845.
47. Decomposition of the catalyst was observed by the formation of a dark suspension.
48. Hashmi, A. S. K. *Pure Appl. Chem.* **2010**, *82*, 657–668.

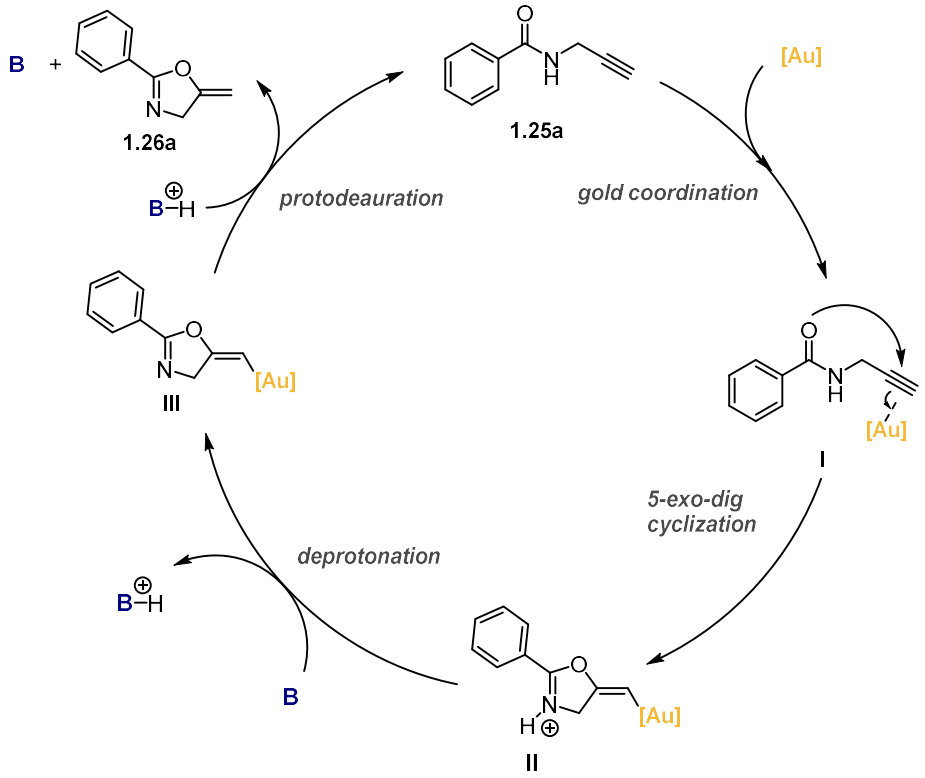

Scheme 1.16. Elementary steps in the gold(I)-catalyzed cyclization of **1.25a**.

To shed some light into the role of the H-bond donor motifs that we have introduced in our catalyst we performed some mechanistic studies on this reaction.

First, we monitored the reaction profile by ^{1}H NMR for 24 h (Figure 1.1) to get a correlation between catalytic activity and H-bonding ability for complexes **A**, **G**–**L**. The activity of our bifunctional complexes spans the range between a very fast catalytic activity of [(Ph_3P)AuCl]/$AgSbF_6$ (Figure 1.1, pink line) which gives almost full conversion after 1 h (99% yield), and the very slow [(Ph_3P)AuCl], which is barely active (Figure 1.1, light green line) with very little activity after 24 h (less than 5% **1.50a** could be observed). The fastest catalyst was phosphinosquaramide **A** although very similar to phosphinoureas **J** and **L**. The same conclusion can be taken for the comparison among analogous phosphinoureas as the ones commented in Table 1.1, where more electron-deficient phosphinoureas lead to more active catalysts.

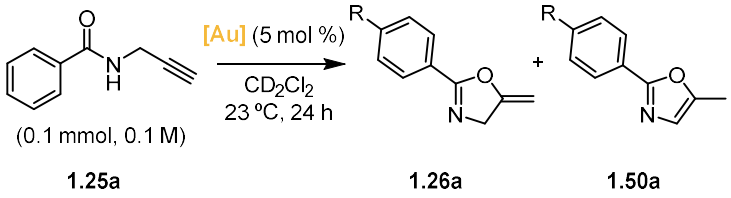

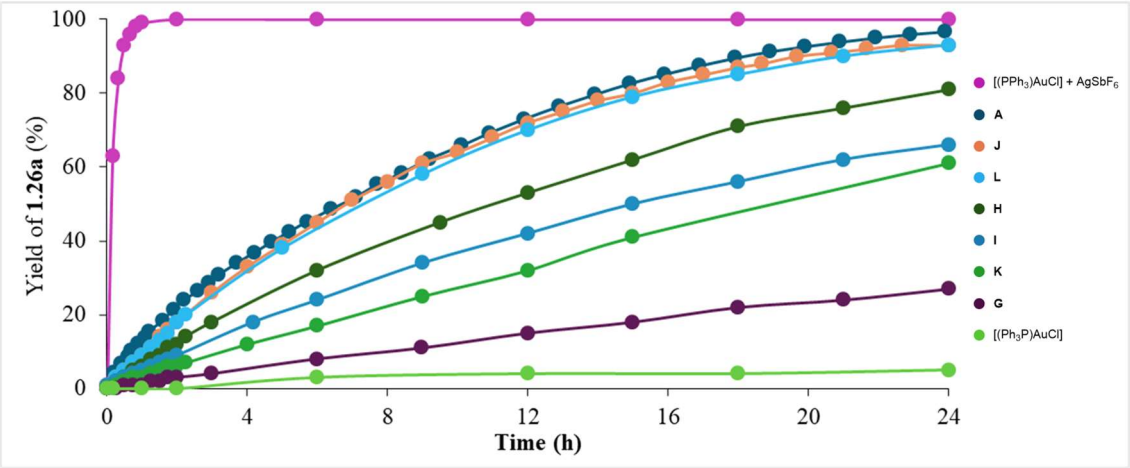

Figure 1.1 Comparison of the reaction monitoring by ^{1}H NMR with different gold(I) complexes.

Using complex **A**, the most active catalyst in this reaction, as well as one in which the ^{1}H NMR signals are easily assigned, the variation on the chemical shift on selected signals on both substrate and catalyst were monitored to determine possible resting states of the catalytic cycle (Figure 1.2).

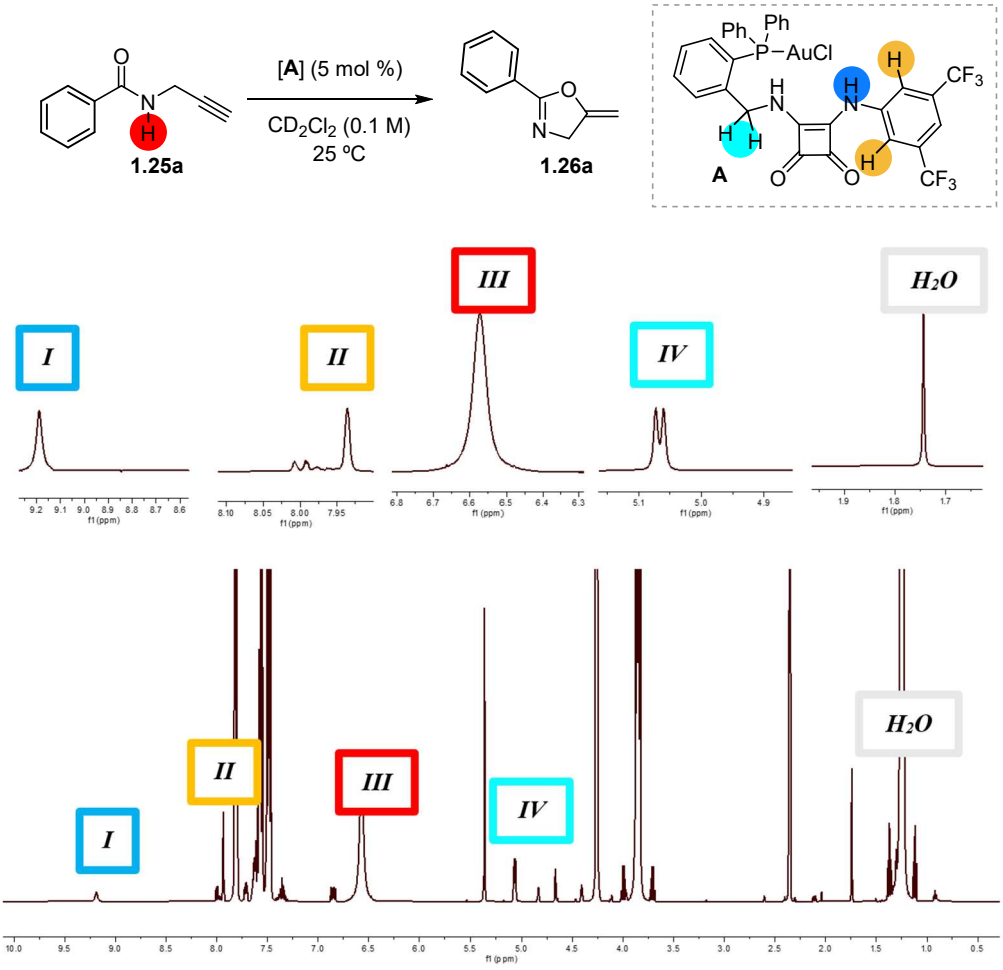

Figure 1.2. Characteristic signals by ^{1}H NMR in the reaction mixture of **1.25a** (100 mM) + A (5 mM). bottom: spectra from 0 to 10 ppm. Top: zoom in of the signals of interest.

The signals of 144 ^{1}H NMR spectra over the course of 24 h were then overlapped and analyzed. The more evident difference after 24 h is the shielding of the NH of the squaramide (highlighted in blue, Figure 1.2) by 0.45 ppm (Table 1.2). This can be explained by an involvement of that

proton in H-bond interactions that decrease over-time due to the consumption of the compound it is interacting with, for example the substrate.

Table 1.2. (De)shielding of ^{1}H NMR signals during the cyclization of **1.25a** to **1.26a** catalyzed by complex **A**

Signal	**δ_{in} (ppm, time 0)**	**δ_{fin} (ppm, 24 h)**	**$\delta\Delta$ ($\delta_{fin} - \delta_{in}$, ppm)**
I) NH_{squar} **(A)**	9.18	8.73	–0.45
II) $NH_{squar}C_{ipso}C_{ortho}H$ **(A)**	7.93	8.05	+0.12
III) C(O)NH **(1.25a)**	6.57	6.53	+0.04
IV) CH_2NH_{squar} **(A)**	5.07	4.94	–0.13
H_2O	1.74	1.81	+0.07

Kinetic studies on the cyclization of **1.25a** catalyzed by **A** in CD_2Cl_2 at 25 ºC were undertaken to get a better understanding on the turnover-limiting step. The data provided below was obtained from ^{1}H NMR studies using tetraethoxysilane as internal standard and further manipulated with Excel.

With the initial-rate method, the reaction was determined to be first order in catalyst (1.05 ± 0.02, Figures 1.3 and 1.4) which is common to most catalyzed transformations, as long as the catalyst does not form oligomers.

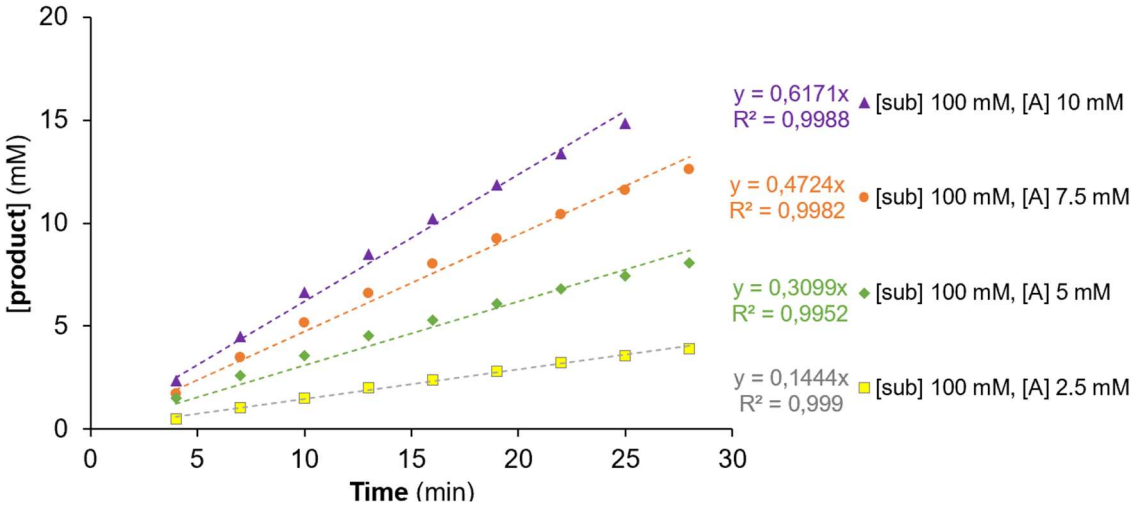

Figure 1.3. Reaction rate at different catalyst concentration. [sub] = concentration substrate **1.25a.**

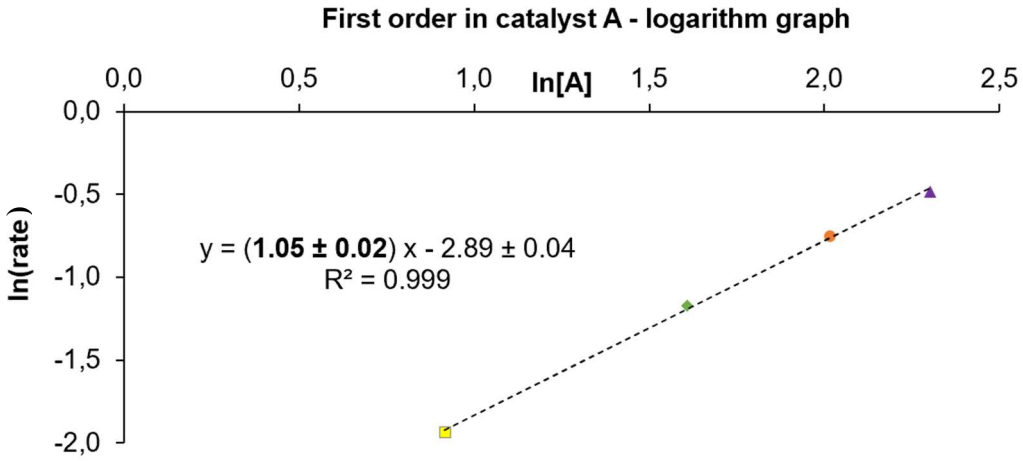

Figure 1.4. Logarithm graph of rate vs. [A], 1st order in catalyst indicated by the slope.

Some catalyst degradation was observed by ^{31}P NMR after 25 h when a new peak at *ca* 38 ppm appeared (Figure 1.5). This new peak was attributed to the formation $[L_2Au]^+$, which has been previously described in the literature indicating significant dissociation of the Au–Cl bond.[49] For instance, the group of Gandon and others observed the formation of $[(PPh_3)_2Au]$ at *ca* 45 ppm when treating PPh_3AuCl with AgOTf[17a] and other chloride scavengers.[14,49] Alternatively, a similar complex, was synthesized by Gabbaï's group through the combination of *o*-(diphenylphosphino)trifluoroacetanilide with [(tht)AuCl] in a 2:1 molar ratio and exhibited a broad ^{31}P NMR signal at 35.8 ppm. To confirm that the signals observed at 38.8 ppm corresponds to species of type $[(L)_2Au]Cl$ (where L is **1.48a**), we prepared this compound in a NMR tube (5 µM in CD_2Cl_2) following two independent methods:

- Exp. 1) $AgSbF_6$ (0.9 mg, 2.5 mmol, 1 equiv), complex **A** (2.1 mg, 2.5 mmol, 1 equiv) and ligand **1.48a** (1.5 mg, 2.5 mmol, 1 equiv) were dissolved in CD_2Cl_2 (500 mL). After 10 minutes, the $^{31}P\{^1H\}$ NMR spectrum of the mixture showed only a single peak, at 38.9 ppm: $[(L)_2Au]SbF_6$.

- Exp. 2) $[(Me_2S)AuCl]$ (0.7 mg, 2.5 mmol, 1 equiv) and ligand **1.48a** (2.3 mg, 3.8 mmol, 1.5 equiv) were dissolved in CD_2Cl_2 (500 mL). After 10 minutes, the $^{31}P\{^1H\}$ NMR spectrum of the mixture showed two peaks in a 1:1 ratio: a peak at 38.8 ppm corresponding to $[(L)_2Au]Cl$, and a peak at 29.4 ppm, corresponding to complex **A**, [(L)AuCl].

49. Wolf, J.; Huber, F.; Erochok, N.; Heinen, F.; Guérin, V.; Legault, C. Y.; Kirsch, S. F.; Huber, S. M. *Angew. Chem. Int. Ed.* **2020**, *59*, 16496–16500.

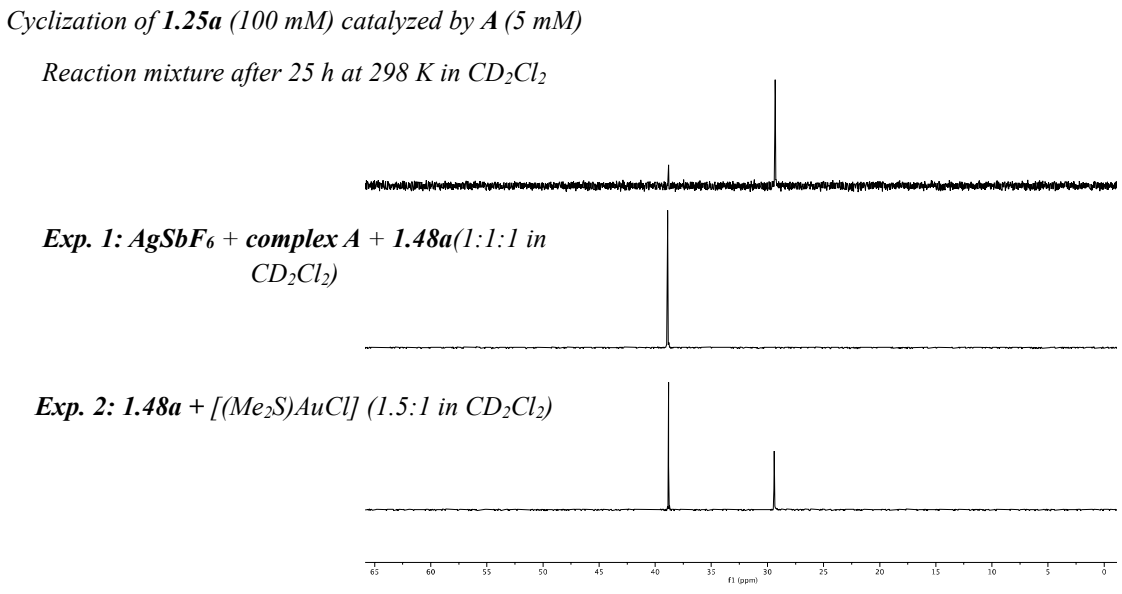

Figure 1.5. ^{31}P NMR studies on the cyclization of **1.25a** and the deactivation of catalyst **A**.

Thus, we can confirm that the species formed are solely derived from catalyst degradation and are not a result of reaction with substrate **1.25a** (also confirmed by the observation of the same species when reaction was run on substrates **1.25b–d**) and account for only a 1.3% of the catalyst added after 1.5 h and a 4.5% after 25 h.

On the other hand, an approximately zeroth order in substrate (0.20 ± 0.05, Figures 1.6 and 1.7) was determined by the initial-rate method.

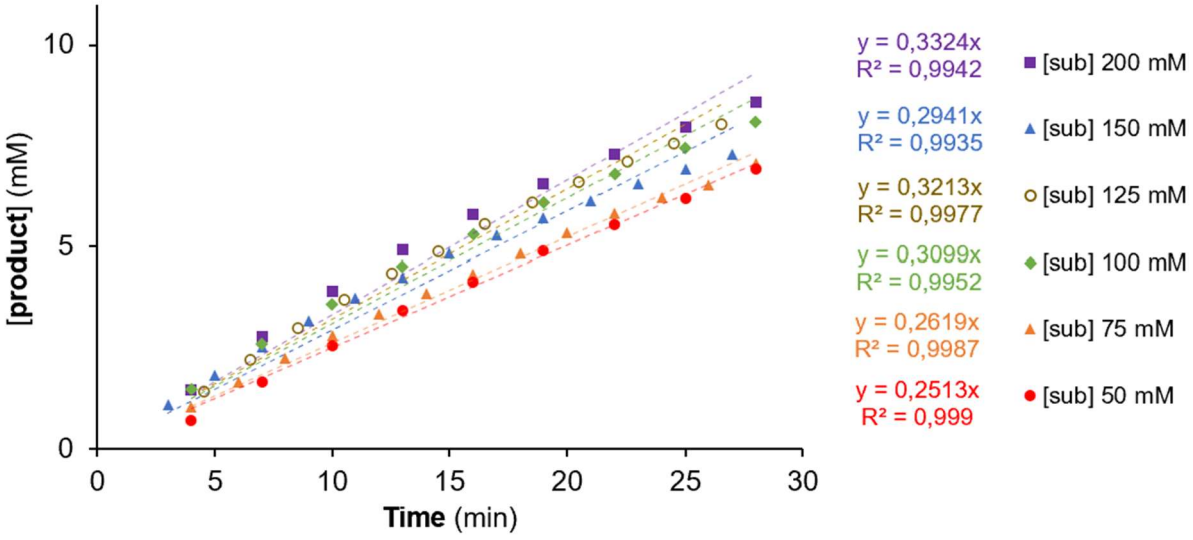

Figure 1.6. reaction rate at different substrate concentration. [sub] = concentration substrate **1.25a.**

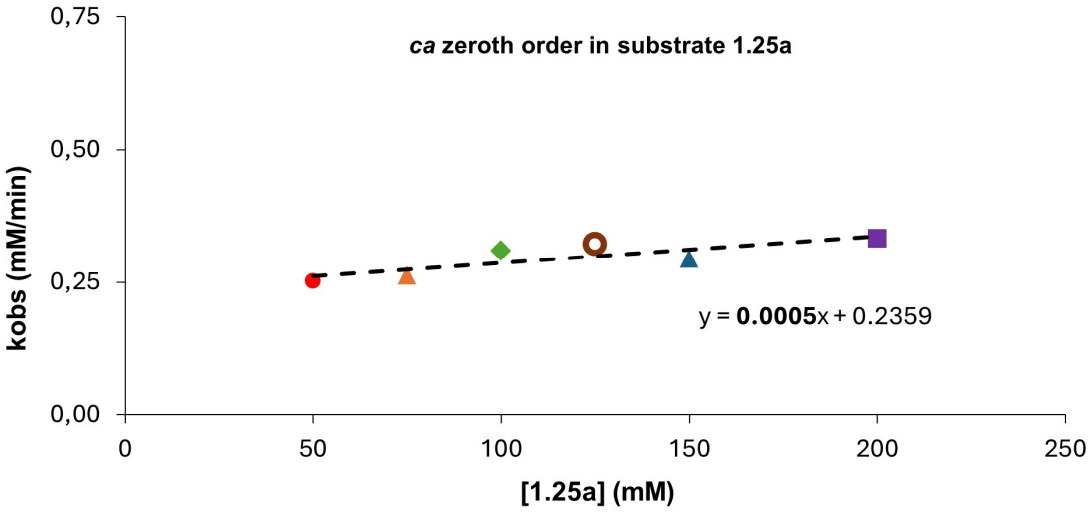

Figure 1.7. Determination order in substrate **1.25a.**

A zeroth order in substrate can be expected for unimolecular catalyzed transformations that follow the Briggs–Haldane kinetics[50] (the Michaelis–Menten regime[51] is regarded as a special case). This is the kinetic regime followed by most enzymatic transformations and unimolecular reactions with heterogenous and homogeneous catalysts,[52,53] provided that the Michaelis–Menten constant of the reaction (K_M) is much smaller than substrate concentration ([S]) (Scheme 1.17). If instead [S] was much smaller than K_M, a first order in substrate would be observed.

To apply the Briggs-Haldane kinetic model to our system some conditions must be fulfilled:

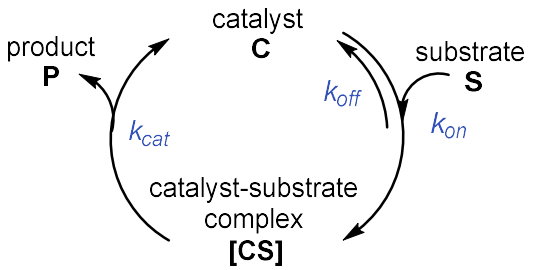

Scheme 1.17 Generic Briggs-Haldane scenario.

1) Diffusion is fast and not rate limiting, *i.e.* equilibration and reaction are slower than diffusion limit. This condition is assumed to be satisfied in homogeneous solutions with relatively slow reactions, like the one under study.

2) Formation of product [P] is irreversible, *i.e.* $\Delta G < 0$ and/or [S] >> [P]. In our case the reaction is spontaneous and in the initial rates the concentration of substrate is much larger than the concentration of products.

3) Catalyst C binds reversibly to substrate S. This condition is satisfied because the energy difference between C + S and CS as computed by DFT is low, and the barrier is also expected to be low (2.1 kcal/mol, see **DFT section**).

50. Briggs, G. E.; Haldane, J. B. *Biochem. J.* **1925**, *19*, 338–339.
51. a) Michaelis, L.; Menten, M. L. *Biochem. Z.* **1913**, *49*, 333–369; b) Johnson, K. A.; Goody, R. S. *Biochemistry* **2011**, *50*, 8264–8269; c) Michaelis, L.; Menten, M. L. *FEBS Lett.* **2013**, *587*, 2712–2720.
52. Blackmond, D. G. *Angew. Chem. Int. Ed.* **2005**, *44*, 4302–4320. Correction: *Angew. Chem. Int. Ed.* **2006**, *45*, 2162–2162.
53. Burés, J. *Top. Catal.* **2017**, *60*, 631–633

4) There is no significant catalyst degradation, meaning that the total concentration of catalyst **C** (both free and bound) during the reaction is constant. This condition is satisfied because only a minor degradation is observed (Figure 1.5)

5) The concentration of the activated substrate-catalyst complex [CS] rapidly reaches a steady state and remains constant (Quasi-steady-state approximation). Mathematically this means that the initial concentration of catalyst is much smaller than the sum of the initial concentration of substrate and K_M. In our case this condition is also satisfied because the catalyst loading is 5 mol% and K_M is ca 40 mM (see below for its determination), hence $[C]_0$ = 5 mM << 100mM + 40 mM. Additionally, we did not observe an induction period.

6) Rapid-equilibrium approximation (only for Michaelis-Menten kinetics). Substrate binding and dissociation are not rate limiting and occur much more rapidly than product formation, i.e. $k_{cat} << k_{off}$.

To calculate K_M the reaction progress kinetic analysis (RPKA) popularized by Blackmond[52] was applied to the entire reaction profile The data was obtained by ^{1}H NMR monitoring of the reaction under standard reaction conditions, [**1.25a**] of 0.1 M, catalyst **A** (5 mol%) in CD_2Cl_2. Data points for the concentration of reactant and product were measured every 10 min. A plot of the variation of [**1.26a**] against time was fitted to a polynomial equation that was derived into the rate equation. Finally, the Lineweaver–Burk plot was constructed (Figure 1.8).[54]

$$v = \frac{d[P]}{dt} = V_{MAX}\frac{[S]}{K_M+[S]} \quad \text{(Eq. 1.1)}$$

$$V_{MAX} = k_{cat}[C]_0 \quad \text{(Eq. 1.2)}$$

$$K_M = \frac{k_{off}+k_{cat}}{k_{on}} \quad \text{(Eq. 1.3)}$$

$$\frac{1}{v} = \frac{1}{V_{MAX}} + \frac{K_M}{V_{MAX}}\frac{1}{[S]} \quad \text{Lineweaver-Burk eq. (Eq. 1.4)}$$

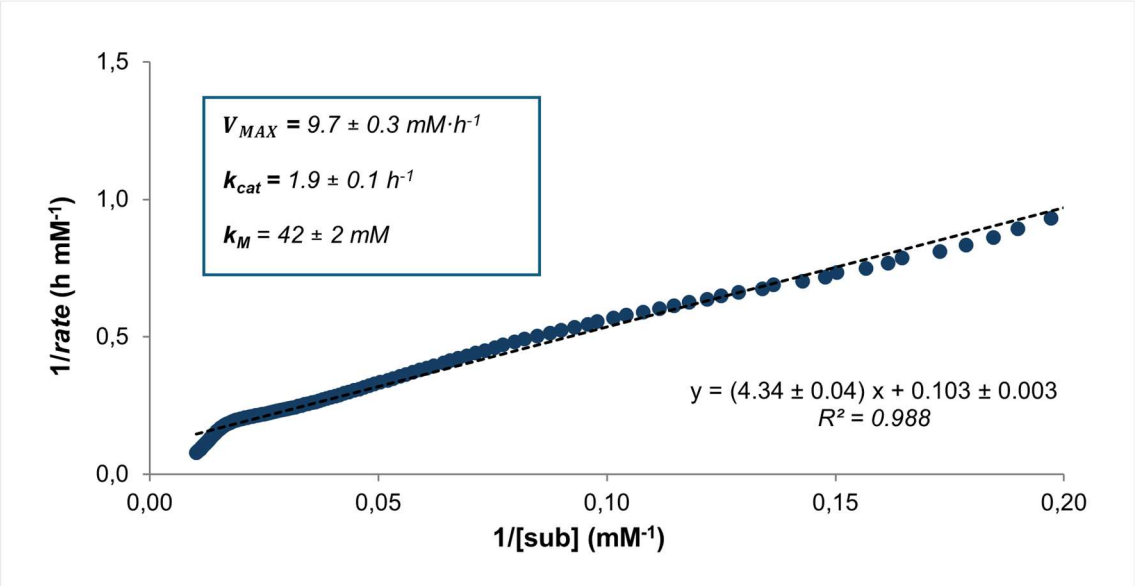

Figure 1.8 Lineweaver-Burk plot. [sub] = concentration substrate **1.25a**.

54. Lineweaver, H.; Burk, D. *J. Am. Chem. Soc.* **1934**, *56*, 658–666.

Given that the substrate concentration during the reaction fluctuates within the 0–100 mM range, and considering the K_M value, the transformation being studied seems to fall between the two limiting cases (zeroth and first order in substrate). This explains the fractional order in substrate, which lies between 0 and 1. Moreover, since the substrate concentration changes throughout the reaction, the reaction order with respect to the substrate is expected to vary as well. This variation in substrate order is a phenomenon that can be quantified by the elasticity coefficient (ε) introduced by Burés.[53] By applying the formula for deriving ε from K_M (Eq. 1.5) in Briggs–Haldane kinetic regimes the order in substrate can be determined at different stages of the reaction. The order was found to be closer to 0 at the beginning of the reaction (there is a large excess of substrate compared to catalyst) and to approach 1 as it progresses (Figure 1.9).

$$\varepsilon = \frac{K_M}{K_M + [S]} \qquad \text{(Eq. 1.5)}$$

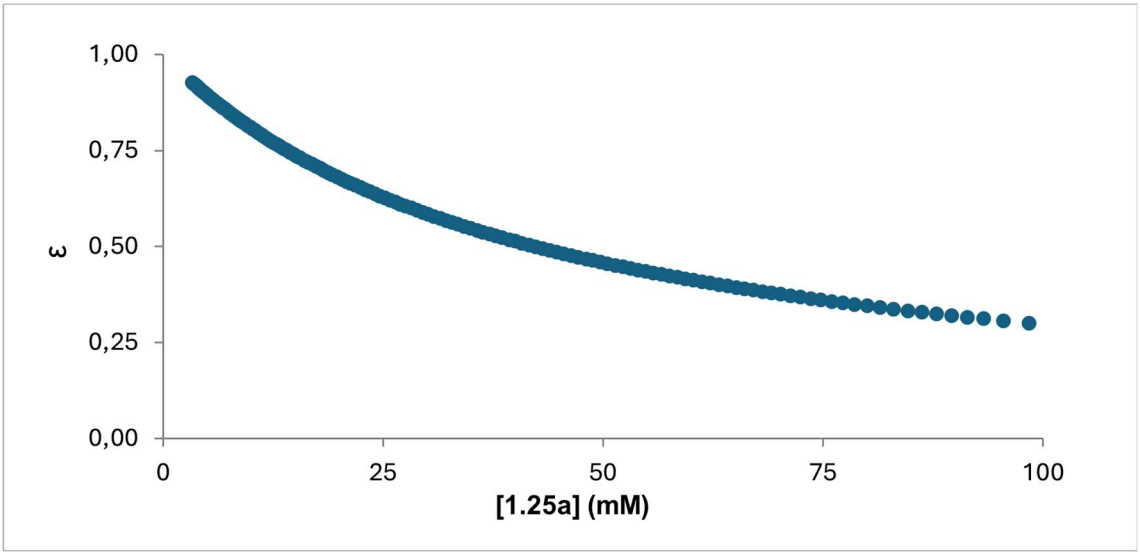

Figure 1.9 Elasticity coefficient graph.

Using the variable-time normalization analysis (VTNA) described by Burés,[55] an overall intermediate order in substrate of 0.4 was determined (Figure 1.10). This was calculated by the overlap of the curves of the reaction monitoring at different substrate concentration to the power of the order (X axis on Figure 1.10).[56] This result aligns well with the 0.2 order determined by initial-rate method (which only considers the beginning of the reaction).

55. a) Burés, J. *Angew. Chem. Int. Ed.* **2016**, *55*, 2028–2031; *Angew. Chem.* **2016**, *128*, 2068–2017; b) Burés, J. *Angew. Chem. Int. Ed.* **2016**, *55*, 16084–16087; *Angew. Chem.* **2016**, *128*, 16318–16321; c) Nielsen, C. D.-T.; Burés, J. *Chem. Sci.* **2019**, *10*, 348–353.
56. See Chapter 2 for more information on the application of the Burés method.

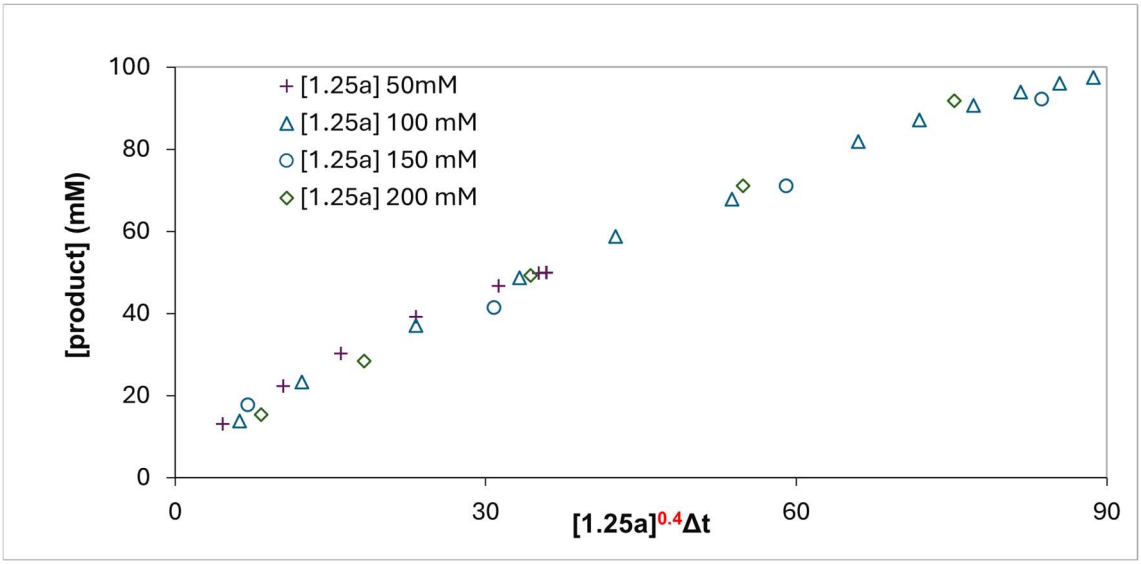

Figure 1.10 Order in substrate determined with the Burés method.

Next, the reaction progress with substrates with different electronics on the aromatic ring was compared. The reaction was found to be slower for electron-poor substrates bearing *p*-CF_3 (**1.25b**) and *p*-Cl (**1.25c**) substituents while it was considerably faster for electron rich substrates (**1.25d**) (Figure 1.11).

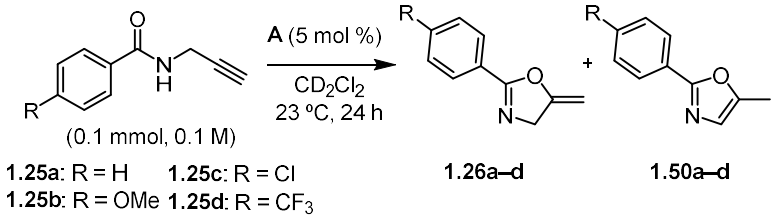

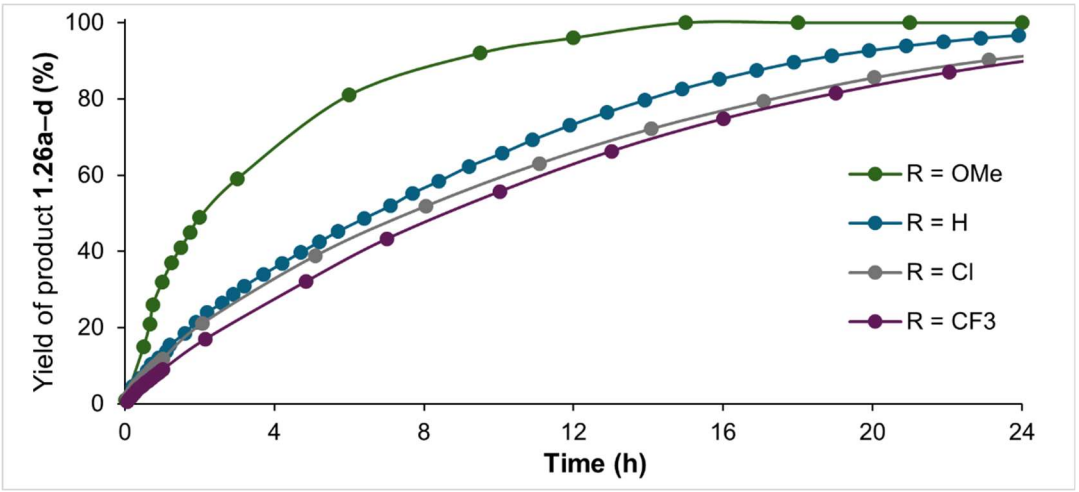

Figure 1.11 Reaction monitoring by ^{1}H-NMR for formation of product **1.26a-d**.

A Hammet analysis was performed comparing the initial rate of the reactions of substrates **1.25a–d**. A good correlation (R^2 = 0.987) was found using the standard σ values for para substituents (Figure 1.12).[57] A negative sensitivity constant ρ (–0.53 ± 0.04) indicates that in the transition state there is a build-up of positive charge, or a loss of negative charge. A significant positive charge build-up on the amide functionality occurs in the *5-exo-dig* cyclization. While the negative

57. Hansch, C.; Leo, A.; Taft, R. W. *Chem. Rev.* **1991**, *91*, 165–195.

sign of ρ could be consistent with amide addition as the turnover-limiting step, its low magnitude makes it very unlikely.

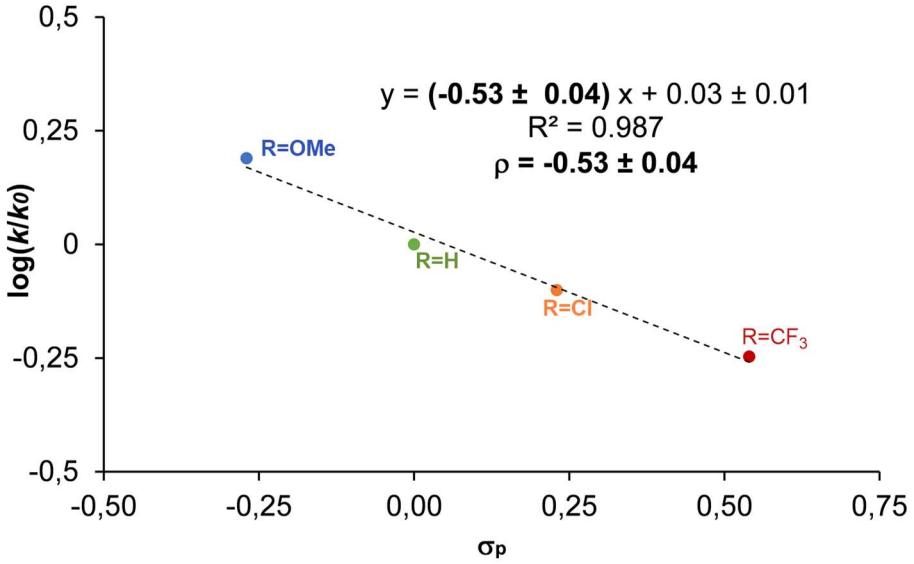

Figure 1.12 Hammet plot for the cycloisomerization of *N*-propargylbenzamides **1.25**.

Finally, the experimental activation thermodynamic parameters were determined via Eyring analysis.[58] An excellent correlation was observed in the 18–35 °C range, which suggests that only one mechanism is taking place for the formation of the desired product (Figure 1.13). The negative $\Delta S^{\neq}$ indicates that in the rate-determining step the system gets "ordered", which would rule out a dissociative chloride scavenging and supports and associative ligand exchange. However, the subsequent cyclization of the substrate could also imply a negative entropy. Finally, the calculated Gibbs free energy of activation at 298 K (21.5 ± 1.5 kcal mol^{-1}) is in good agreement with a slow reaction occurring at room temperature as well as the calculated energy for the cyclization step (see computational section).

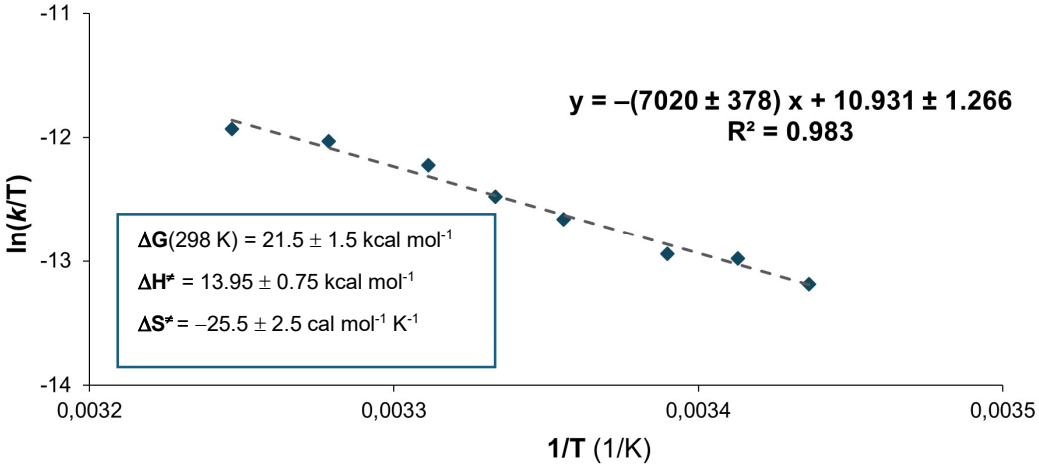

Figure 1.13 Eyring plot for the cyclization of **1.25a**, temperature range from 18 to 35 °C.

58. a) Eyring, H. *J. Chem. Phys.* **1935**, *3*, 107–115; b) M. G. Evans, M. Polanyi, *Trans. Faraday Soc.* **1935**, *31*, 875–894; c) Laidler, K. J.; King, M. C. *J. Phys. Chem.* **1983**, *87*, 2657–2664

Computational Studies

Generally, the chloride abstraction step has been mechanistically neglected in Au-catalyzed transformations, under the assumption that when using Ag salts, it is a fast, quantitative and irreversible process. However, recent studies have demonstrated that this is not the case in most reactions.[12] In order to get a better understanding on this often-overlooked step, we performed some computational studies for the Au–Cl bond activation using again complex **A** as we have performed most of the mechanistic studies with it. Both an associative and dissociative mechanism were considered at first.

A dissociative pathway would imply the formation of a LAu^+ intermediate before the substrate coordination. The stabilization of the Au atom was proposed to be provided by the coordination of an oxygen of a carbonyl unit of the squaramide (**Int_Ia**, Figure 1.14). However, no transition state could be detected for a dissociative pathway of the activation of the Au–Cl bond.

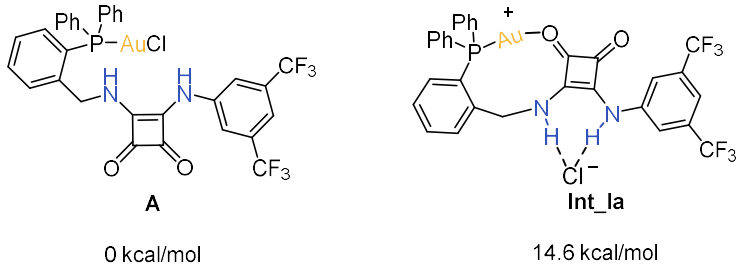

Figure 1.14 Energies calculated for the intermediates of a dissociative Cl abstraction.

On the other hand, an associative pathway in which the substrate participates in the chloride abstraction seemed more reasonable. An intermediate, more stable than substrate and catalyst, was found where the squaramide H-bonds with the carbonyl of the substrate (**Int_IIb,** Scheme 1.18). Then a remarkably low barrier of 6.7 Kcal/mol was detected for a transition state (**TS_II-IIIb**, Scheme 1.18), where the chloride displacement is stabilized by a triple H-bond established with the NH of the amide (**1.25a**) and the 2 NH of the squaramide of the catalyst. A very similar transition state was already calculated by Helaja and coworkers for a NHC-Au(I) chloride complex bearing a pendant tosylamide, with a 13.2 kcal/mol barrier with their system.[36] Thus, these calculations suggest that the bidentate HBD of our complex facilitates the chloride abstraction step. Furthermore, this low barrier indicates that the Au–Cl activation cannot be the turnover-limiting step on its own since the reaction requires several hours at room temperature to reach completion.

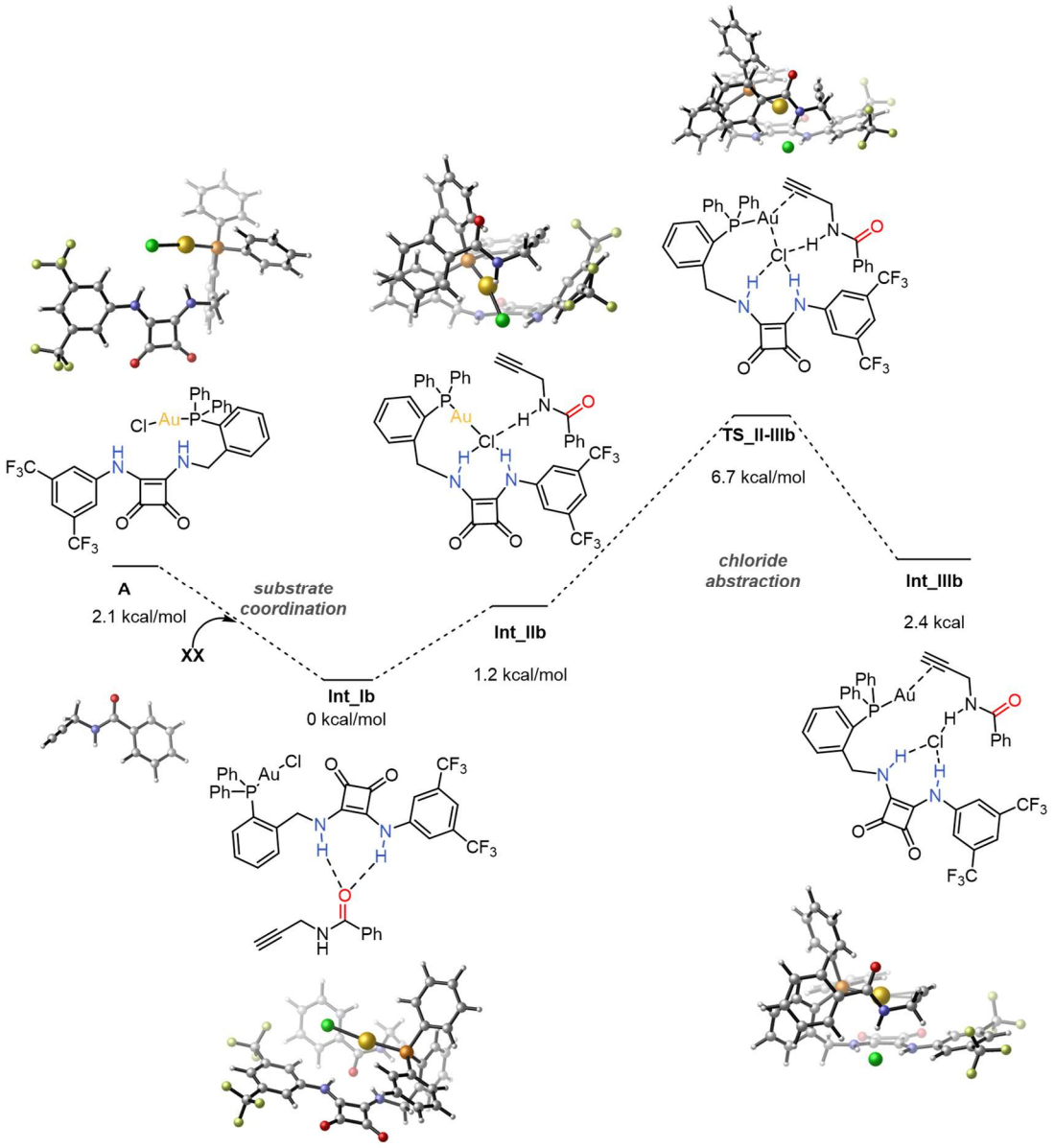

Scheme 1.18. Energy profile for the activation of the Au–Cl bond via an associative mechanism

Based on the collected computational and experimental data, the catalytic cycle depicted in Scheme 1.19 is proposed. Initially, complex **A** interacts with substrate **1.25a** forming intermediate **IV,** where the NH groups of the squaramide establish H-bonds with the carbonyl motif of the amide. Intermediate **IV** corresponds to the putative resting state of the catalytic cycle and computationally would correspond to the calculated **Int_Ib** (see Scheme 1.18), which was the lowest energy species located after considering several combinations of substrate and complex **A**. Experimentally, it was observed that complex **A** that was insoluble in CD_2Cl_2 readily dissolved when added to a solution of **1.25**. This could be explained by the complete formation of an intermediate between substrate and catalyst, upon mixing of the two, where the carbonyl group of the substrate H-bonds with the squaramide, breaking intermolecular H-bonds between squaramide units that make the catalyst insoluble otherwise. Further evidence is provided by monitoring the reaction mixture in CD_2Cl_2 by ^1H NMR. The signal for the most acidic squaramide NH (highlighted in blue in Scheme 1.18, see Table 1.2) shifts upfield by 0.45 ppm during the

reaction, suggesting increased shielding. This shift can be explained by the reduced involvement of that NH in hydrogen bonding as the reaction progresses, since the concentration of its H-bonding partner, **1.25a**, decreases with increasing conversion. From the resting state, the chloride abstraction step takes place with a 6.7 kcal/mol energy barrier followed by the 5-*exo*-dig cyclization the transition state of which could not be located. This hypothesis is based on the order in substrate being different to zero and the Hammett and Eyring plots.

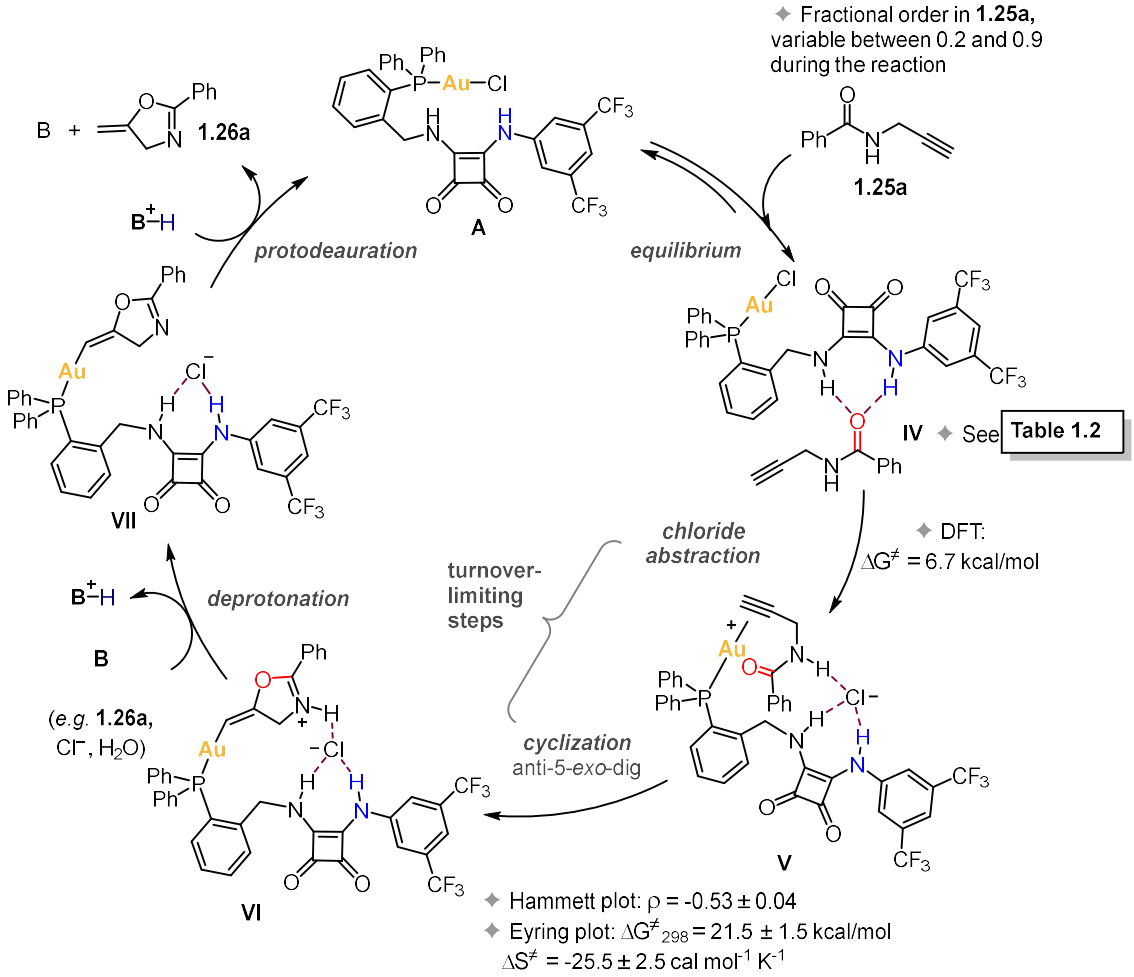

Scheme 1.19. Proposed catalytic cycle for the mechanism of the silver-free gold(I)-catalyzed cycloisomerization of **1.25a** with phosphinosquaramide **A**.

Deprotonation of intermediate **VI** by a basic species present in the reaction mixture (such as **1.26a**, adventitious water, or the chloride anion) is expected to occur readily, affording vinyl gold(I) species **VII**. Protodeauration of the latter would then liberate product **1.26a** and regenerate catalyst **A**. This mechanistic picture, while explaining all kinetic, computational and experimental results for the cyclization of **1.25a** catalyzed by **A**, contrasts previous studies on the same Au(I)-catalyzed reaction *in the presence of silver salts*.[45] Those studies rather point towards a turnover-limiting protodeauration step, based on the ^{1}H NMR observation[45a] and isolation[45b,c] of vinyl gold(I/III) complexes in the reaction of **1.25a**. This intriguing contrast highlights that the chloride abstraction step is far from obvious: the choice of a different chloride scavenging system (*e.g.* **A** as opposed to Ag salts) can implicate changes not only on the Au–Cl bond activation, but also on the following steps of the catalytic cycle.

Additional Reactions

Our new library of self-activating complexes was also tested in a range of other intra- and intermolecular reactions of alkynes. In the cycloisomerization of benzene-tethered 1,6-enyne bearing a terminal alkyne (**1.55,** Table 1.3), moderate to good activities were observed for complexes **A**, **K** and **L** (Table 1.3, entries 1, 10 and 11). The reaction did not reach full conversion but diene **1.56** was obtained as a single product. This reactivity sharply contrasts with previous studies, where dimers **1.57** and **1.58** emerged as the major products when external scavengers were employed.[59]

Table 1.3. Screening of complexes on the cycloisomerization of **1.55.**

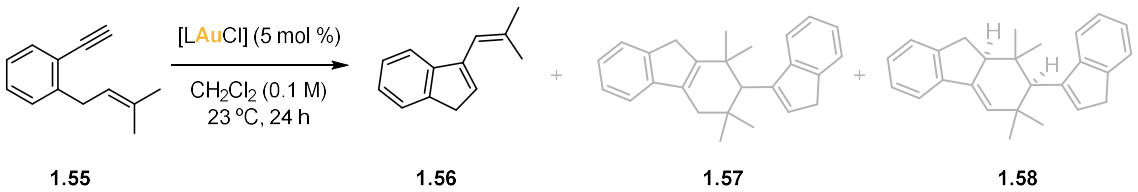

1.55 **1.56** **1.57** **1.58**

Entry	[LAuCl]	Yield (%)[a]
1	**A**	32
2	**B**	20
3	**C**	18
4	**D** or **F**	<5
5	**E**	<5
6	**H**	8
7	**I**	30
9	**J**	21
10	**K**	49
11	**L**	52
12	[(IPr)AuCl]	<5
13	[(JohnPhos)AuCl]	<5
14	[(Ph_3P)AuCl]	20

[a] Yields were determined by ^1H NMR analysis using mesitylene as internal standard.

Other intramolecular reactions were attempted, like the malonate tethered 1,6-enyne cyclization (Scheme 1.20). However, yields were low due to poor conversion which only got worse when modifying the tether or using an internal alkyne (no conversion was observed).

59. Álvarez-Pérez, M.; Frutos, M.; Viso, A.; Fernández de la Pradilla, R.; de la Torre, M. C.; Sierra, M. A.; Gornitzka, H.; Hemmert, C. *J. Org. Chem.* **2017**, *82*, 7546–7554.

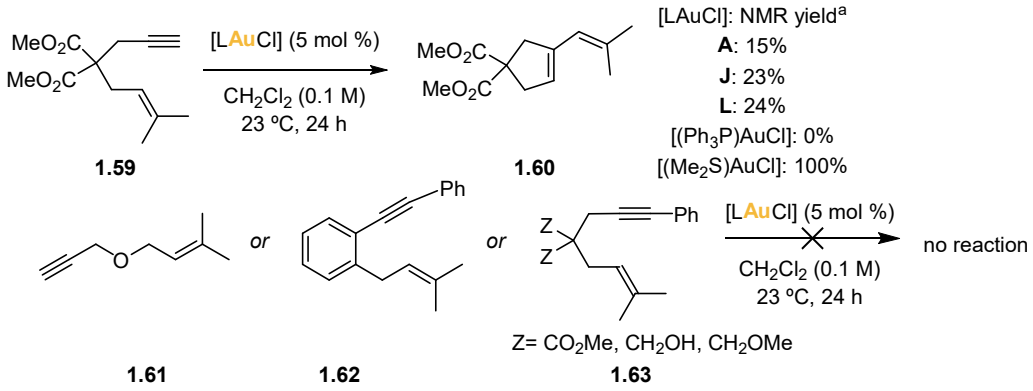

Scheme 1.20. Silver-free catalyzed intramolecular cycloisomerization of 1,6-enynes.[a] Yield was determined by NMR using mesitylene as internal standard.

In the case of intermolecular reactions, in addition to testing the most active catalysts in the previous transformations (**A**, **J** and **L**), we also evaluated **B** and **C** to determine whether the optimal linker length between P and squaramide is constant across different reactions. Indeed, in the case of the tandem cycloisomerization-indole addition of 2-alkynylenone **1.40** (Table 1.4), complex **B** (with an extra CH_2 compared to **A**) was the best catalyst providing furan **1.42** almost quantitatively.

Table 1.4. Intermolecular silver-free Au(I)-catalyzed tandem cycloisomerization-indole addition

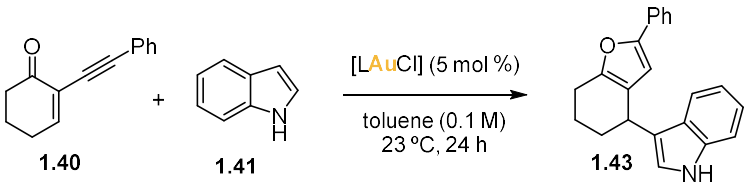

Entry	[LAuCl]	Yield (%)[a]
1	**A**	89
2	**B**	95
3	**C**	21
4	**J**	76
5	**L**	73
6	$(Ph_3P)AuCl$	29

[a] Yields were determined by ^1H NMR analysis using mesitylene as internal standard.

Very good activities were also observed for the hydrohydrazination of phenylacetylene (Table 1.5).[60] However, neither the hydroanilination of phenylacetylene,[61] nor the cyclopropanation using arylpropargyl acetate and styrene[62] or the hydration of alkynes[4,63] took place (Scheme 1.21).

60. a) Manzano, R.; Wurm, T.; Rominger, F.; Hashmi, A. S. K. *Chem. Eur. J* **2014**, *20*, 6844–6848. b) Hu, X.; Martin, D.; Bertrand, G. *New J. Chem.* **2016**, *40*, 5993–5996. c) Rotta-Loria, N. L.; Chisholm, A. J.; MacQueen, P. M.; McDonald, R.; Ferguson, M. J.; Stradiotto, M. *Organometallics* **2017**, *36*, 2470–2475.
61. a) Kong, L.; Ganguly, R.; Li, Y.; Kinjo, R. *Chem. Sci.* **2015**, *6*, 2893–2902. b) Tang, Y.; Benaissa, I.; Huynh, M.; Vendier, L.; Lugan, N.; Bastin, S.; Belmont, P.; César, V.; Michelet, V. *Angew. Chem. Int. Ed.* **2019**, *58*, 7977–7981.
62. Johansson, M. J.; Gorin, D. J.; Staben, S. T.; Toste, F. D. *J. Am.Chem. Soc.* **2005**, *127*, 18002−18003.
63. a) Ghosh, N.; Nayak, S.; Sahoo, A. K. *J. Org. Chem.* **2011**, *76*, 500–511.

Table 1.5. Screening of catalysts for the silver-free Au(I) catalyzed hydrohydrazination of phenylacetylene

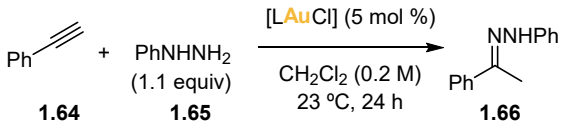

1.64 **1.65** **1.66**

Entry	[LAuCl]	Yield (%)[a]
1	**A**	89
2	**B**	95
3	**C**	21
4	**J**	76
5	**L**	73
6	$(Ph_3P)AuCl$	29

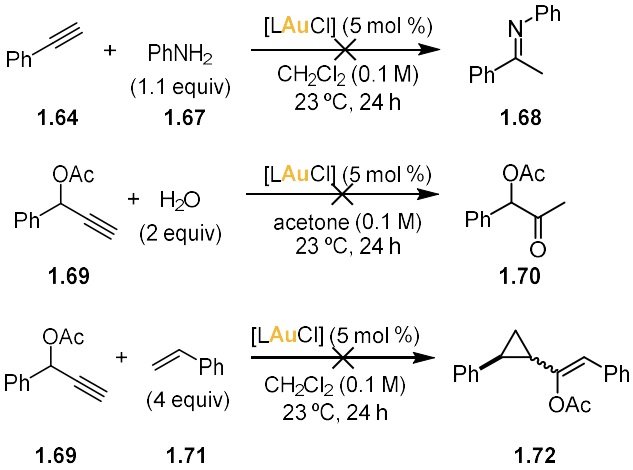

1.64 **1.67** **1.68**

1.69 **1.70**

1.69 **1.71** **1.72**

Scheme 1.21 Unsuccessful intermolecular silver-free Au(I) catalyzed reactions with our system.

Conclusions

A library of Au(I) chloride complexes featuring bifunctional phosphine ligands, which include common bidentate hydrogen-bond donors, has been prepared. The complexes varied in HB-donor strength (introduction of electro-withdrawing substituents or going form urea to thiourea or squaramide) and P-N linker distance. Most of the catalysts could be structurally characterized by X-ray diffraction, presenting in some cases HB interactions with the chloride ligand in the solid state. These complexes have been used as self-activating Au(I) catalysts in both intra- and intermolecular reactions of alkynes without the need of external activators or additives.

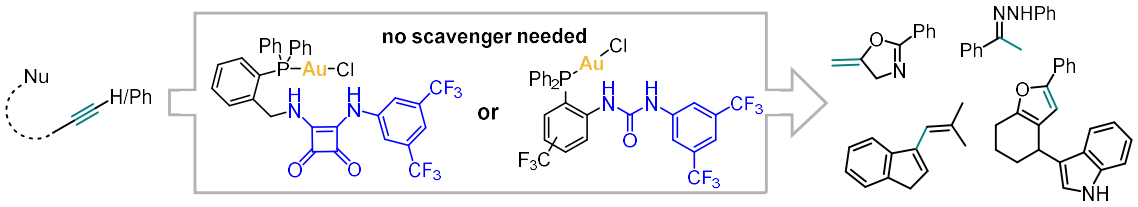

Scheme 1.22. Application of the self-activating phosphinosquaramide/phopshinourea gold(I) complexes.

Detailed kinetic studies on the cycloisomerization of *N*-propargylbenzamides revealed a correlation between the hydrogen-bonding ability and catalytic activity of the complexes. This indicates that hydrogen-bond interactions facilitate chloride abstraction from the Au(I) center. DFT calculations also showed a low energy barrier for the activation of the Au–Cl bond, promoted by a triple hydrogen bond with the squaramide ligand and the NH of the benzamide.

Experimental Part

General Remarks

Unless otherwise stated, reactions were performed with magnetic stirring under nitrogen or argon using standard Schlenk techniques. Room temperature (rt) indicates a temperature of approximately 23 ºC. Compound names were generated using ChemDraw. Chemicals were obtained from commercial suppliers and used as received. Anhydrous solvents were dried by passing through an activated alumina column on a PureSolv^{TM} Solvent Purification System (SPS, Innovative Technologies, Inc, MA) or taken from commercial bottles equipped with septa and molecular sieves. Solutions were evaporated using a Büchi rotary evaporator under reduced pressure at T ≤ 40 °C. Yields refer to chromatographically and spectroscopically pure homogenous material, unless otherwise stated. Analytical thin-layer chromatography (TLC) was carried out using aluminum sheets coated with 0.2 mm of silica gel (fluorescent-treated Merck Kieselgel 60 F254). Visualization was accomplished under UV light at 254 nm and by staining with an alkaline aqueous potassium permanganate solution, and ninhydrin or vanillin staining dips. Flash column chromatography (FCC) was carried out using PanReac Silica Gel 60 (40–63 μm) or employing the automated flash column chromatographer CombiFlash Companion. Preparative TLC was performed on 20 cm × 20 cm silica gel plates (2.0 mm or 1.0 mm silica thickness, Analtech). NMR spectra were recorded at 298 K (unless otherwise stated) on BrukerAvance Ultrashield NMR spectrometers operating at ^{1}H resonances of 300, 400 or 500 MHz. Proton and carbon chemical shifts (δ) are given in parts per million (ppm) relative to tetramethylsilane, referencing to the NMR solvent resonance.[64] ^{1}H NMR spectra are reported as follows: chemical shift (multiplicity, coupling constant, number of protons). The following abbreviations are used: s = singlet, d = doublet, t = triplet, q = quartet, quint = quintet, m = multiplet, br = broad signal, app = apparent. Coupling constants (*J*) are given in Hertz. ^{13}C, ^{31}P and ^{19}F NMR spectra were always acquired with proton decoupling. Two-dimensional NMR spectroscopy experiments (COSY, HSQC, HMBC and NOESY) were used to assist in the assignment of signals in ^{1}H and ^{13}C spectra. High-resolution mass spectra (HRMS) were recorded by ICIQ mass spectrometry staff on Bruker MicroTOF Focus or Maxis impact spectrometers equipped with an ESI or APCI source. Melting points were measured using a Mettler Toledo MP70 Melting Point apparatus. Elemental analysis was performed on a LECO CHNS 932 microanalyzer at the Universidad Computense de Madrid. Single-crystal X-ray diffraction (XRD) data were collected and refined by ICIQ XRD staff at 100 K on a Rigaku MicroMax-007HF, Mo Kα rotating anode, equipped with a Pilatus 200 K detector or on a Bruker APEX DUO, Mo Kα Microfocus source E025 IuS anode, equipped with an APEX DUO detector using omega scans.

64. Fulmer, G. R.; Miller, A. J. M.; Sherden, N. H.; Gottlieb, H. E.; Nudelman, A.; Stoltz, B. M.; Bercaw, J. E.; Goldberg, K. I. *Organometallics* **2010**, *29*, 2176–2179.

Synthetic Procedures and Analytical Data

The following compounds have already been reported and characterized: 3,4-dimethoxycyclobut-3-ene-1,2-dione;[65] 3-((3,5-bis(trifluoromethyl)phenyl)amino)-4-methoxycyclobut-3-ene-1,2-dione (**1.47**);[66] 2-(diphenylphosphino) benzonitrile (**1.45**);[67] (2-(diphenylphosphino)phenyl)methanamine (**1.46a**);[68] 3-(2-bromophenyl)propanenitrile.[69]

Ligand synthesis

3-((3,5-Bis(trifluoromethyl)phenyl)amino)-4-((2-(diphenylphosphino)benzyl)amino)cyclobut-3-ene-1,2-dione (1.48a)

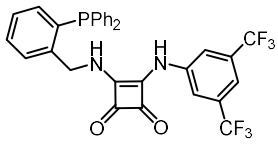

Under Ar, to a cloudy pale yellow solution of mixed squarate **1.47** (116.3 mg, 0.342 mmol, 1.0 equiv) in anhydrous MeOH (1.7 mL) was added a clear yellow solution of (2-(diphenylphosphino)phenyl)methanamine (100.0 mg, 0.343 mmol, 1.0 equiv) in MeOH (1 mL). Upon addition, the reaction mixture became a thick white suspension, which was stirred at 23 ºC for 17 h and then filtered on a sinter funnel. The collected solid was washed with MeOH (3 × 1 mL) and pentane (3 × 1 mL), and then dried under high vacuum, obtaining the title compound **1.48a** (162.4 mg, 0.271 mmol, 79% yield) as a white solid. **M.p.** 262°C. **^{1}H NMR** (400 MHz, DMSO-d_6, 16 mg in 0.5 mL) δ 9.78 (brs, 1H), 7.95 (s, 3H), 7.64 (s, 1H), 7.55 (dd, J = 7.7, 4.6 Hz, 1H), 7.47 (t, J = 7.5 Hz, 1H), 7.37–7.28 (m, 7H), 7.17 (t, J = 7.5 Hz, 4H), 6.86 (dd, J = 7.8, 4.3 Hz, 1H), 5.03 (s, 2H). **^{13}C NMR** (126 MHz, DMSO-d_6, 16 mg in 0.5 mL, insoluble at higher concentrations at 298 K, 1 aromatic C peak missing) δ 184.3, 180.5, 169.3, 162.3, 141.8 (d, J = 25.0 Hz), 141.2, 135.5 (d, J = 9.9 Hz), 133.6, 133.4 (d, J_{CP} = 19.6 Hz), 131.4 (q, J^2_{CF} = 32.2 Hz), 129.7, 129.2 (m), 128.9 (d, J_{CP} = 16.2 Hz), 128.8, 128.4, 123.2 (q, J^1_{CF} = 272.8 Hz), 117.9, 114.5, 46.3 (d, J^3_{CP} = 22.9 Hz). **^{31}P NMR** (162 MHz, DMSO-d_6) δ −14.0. **^{19}F NMR** (376 MHz, DMSO-d_6) δ −61.4. **HRMS** (ESI +) calculated for $[C_{31}H_{21}F_6N_2NaO_2P]^+$ [M + Na]$^+$ 621.1137 *m/z*; found 621.1131 *m/z*.

2-(2-(Diphenylphosphino)phenyl)acetonitrile (1.73)

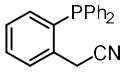

Under Ar, to a flame-dried microwave vial equipped with a stirring bar were added cesium carbonate (1.63 g, 5.00 mmol, 2.0 equiv), 1,1′-bis(diisopropylphosphino)ferrocene (75.3 mg, 0.18 mmol, 0.072 equiv), diacetoxypalladium (33.7 mg, 0.15 mmol, 0.06 equiv) and finally toluene (5.0 mL). Then 2-(2-bromophenyl)acetonitrile (325 µL, 490 mg, 2.50 mmol, 1 equiv) was added, followed by diphenylphosphine (0.52 mL, 3.0 mmol, 1.3 equiv). The mixture was heated to 130 °C and stirred for 72 h, after which volatiles were evaporated under reduced pressure. The crude oily residue was purified by FCC (99:1 CyH:EtOAc) to afford the title compound **1.73** (749 mg, 2.42 mmol, 97% yield estimating a 97%$_{w/w}$ purity) as an orange solid. **M.p.** 105–115 °C. **^{1}H NMR** (400 MHz, $CDCl_3$) δ 7.59 (dd, J = 7.7, 4.5 Hz, 1H), 7.49–7.39 (m, 7H), 7.32–7.19 (m, 5H), 6.90 (ddd, J = 7.7, 4.3, 1.4 Hz, 1H), 3.94 (d, J = 2.1 Hz, 2H). **^{13}C NMR** (101 MHz, $CDCl_3$) δ 136.1 (d, J_{CP} = 14.8 Hz), 134.8 (d, J_{CP} = 8.6 Hz), 134.4 (d, J_{CP} = 25.0 Hz), 134.0(d, J_{CP} = 19.8 Hz), 133.8, 129.8, 129.5, 129.0 (d, J_{CP} = 7.3 Hz), 128.7 (d, J_{CP} = 3.7 Hz), 128.5, 117.8 (d, J_{CP} = 3.4 Hz), 22.6 (d,

65. Liu, H.; Tomooka, C. S.; Xu, S. L.; Yerxa, B. R.; Sullivan, R. W.; Xiong, Y.; Moore, H. W. *Org. Synth.* **1999**, *76*, 189.
66. Yang, W.; Du, D. M. *Org. Lett.* **2010**, *12*, 5450–5453.
67. Zhang, L.; Yang, F.; Tao, G.; Qiu, L.; Duan, Z.; Mathey, F. *Eur. J. Inorg. Chem.* **2017**, 2355–2362.
68. Cahill, J. P.; Bohnen, F. M.; Goddard, R.; Krüger, C.; Guiry, P. J. *Tetrahedron Asymmetry* **1998**, *9*, 3831–3839.
69. Wolfe, J. R.; Rennels, R. A.; Buchwald, S. L. *Tetrahedron* **1996**, *52*, 7525–7546.

J^3_{CP} = 28.0 Hz). **^{31}P NMR** (162 MHz, $CDCl_3$) δ −12.1. **HRMS** (ESI +) calculated for $[C_{20}H_{16}NaNP]^+$ $[M+Na]^+$ 324.0913 *m/z*; found 324.0917 *m/z*.

2-(2-(Diphenylphosphino)phenyl)ethan-1-amine (1.46b)

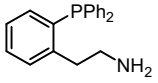

Following a modified literature procedure,[70] in the glovebox, to a flame-dried microwave vial equipped with a stirring bar was added lithium aluminium hydride (36.5 mg, 0.962 mmol, 1.0 equiv) followed by THF (1 mL). To the resulting grey suspension, a solution of aluminium trichloride (128.3 mg, 0.962 mmol, 1.0 equiv) in THF (1 mL) was added dropwise (vigorous bubbling observed), followed after 5 minutes by a solution of 2-(2-(diphenylphosphino)phenyl) acetonitrile **1.46b** (290.0 mg, 0.962 mmol, 1.0 equiv) in THF (2.8 mL). The microwave vial was capped and removed from the glovebox. The reaction mixture was stirred at 23 ºC under Ar atmosphere for 24 h, then carefully quenched under a flow of inert gas at 0 °C by adding dropwise a 5% solution of NaOH (until bubbling ceased). The aqueous phase was extracted with CH_2Cl_2 three times (3 × 30 mL). Combined organic phases were dried over $MgSO_4$, filtered and evaporated to afford the crude product **1.46b** (238.1 mg, 0.780 mmol, estimated 81% yield assuming an arbitrary 100% purity) as an orange oil, that was carried over as such to the next step (due to decomposition during purification attempts). **^{1}H NMR** (400 MHz, $CDCl_3$) δ 7.40–7.24 (m, 12H), 7.15 (td, *J* = 7.4, 1.7 Hz, 1H), 6.92 (ddd, *J* = 7.7, 4.3, 1.4 Hz, 1H), 3.04 (t, *J* = 7.0 Hz, 2H), 2.93 (t, *J* = 7.0 Hz, 2H), 1.50 (brs, 2H). **^{31}P NMR** (162 MHz, $CDCl_3$) δ −12.3.

3-((3,5-Bis(trifluoromethyl)phenyl)amino)-4-methoxycyclobut-3-ene-1,2-dione (1.48b)

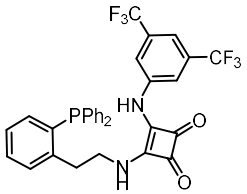

To a cloudy solution of mixed squarate **1.47** (264.5 mg, 0.780 mmol, 1.0 equiv) in MeOH (2 mL) was added a solution of 2-(2-(diphenylphosphino)phenyl)ethan-1-amine **1.46b** (238.1 mg, 0.780 mmol, 1.0 equiv) in MeOH (4 mL). The reaction mixture was stirred at 23 ºC for 20 h. The next day the precipitate that formed in the reaction mixture was collected on a sinter funnel, washed with MeOH (3 × 1 mL) and pentane (3 × 1 mL), and then dried under high vacuum, obtaining the title compound **1.48b** (180.0 mg, 0.294 mmol, 38% yield) as a white solid. **M.p.** 230–235 °C. **^{1}H NMR** (500 MHz, DMSO-d_6) δ 10.03 (brs, 1H), 8.00 (s, 2H), 7.76 (brs, 1H), 7.66 (s, 1H), 7.45–7.39 (m, 8H), 7.21–7.17 (m, 5H), 6.88–6.75 (m, 1H), 3.97–3.79 (m, 2H), 3.19–3.10 (m, 2H). **^{13}C NMR** (126 MHz, DMSO-d_6) δ 184.5, 180.4, 169.9, 162.2, 142.5(d, *J* = 25.9 Hz), 141.1, 136.0 (d, *J* = 11.0 Hz), 135.6 (d, *J* = 12.8 Hz), 133.2 (d, *J* = 19.3 Hz), 131.3 (q, J^2_{CF} = 32.2 Hz), 129.7, 129.4, 128.9, 128.8 (d, *J* = 6.9 Hz), 127.1, 123.1 (q, J^1_{CF} = 272.0 Hz), 117.9, 114.7, 44.7, 35.2 (d, J^3_{CP} = 20.1 Hz). **^{31}P NMR** (162 MHz, DMSO-d_6) δ −13.5. **^{19}F NMR** (376 MHz, DMSO-d_6) δ −61.8. **HRMS** (ESI +) calculated for $[C_{32}H_{23}F_6N_2NaO_2P]^+$ $[M + Na]^+$ 635.1294 *m/z*; found 635.1292 *m/z*.

3-(2-(Diphenylphosphino)phenyl)propanenitrile (1.74)

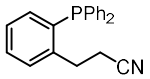

Under Ar, to a flame-dried microwave vial equipped with a stirring bar were added caesium carbonate (4.56 g, 14.0 mmol, 2.0 equiv), 1,1′-bis(diisopropylphosphino)ferrocene (211 mg, 0.504 mmol, 0.072 equiv) and diacetoxypalladium (94.0 mg, 0.42 mmol, 0.06 equiv) and finally toluene (14 mL). Then 3-(2-bromophenyl)propanenitrile[69] (1.47 g, 7.00 mmol, 1.0 equiv) was added, followed by diphenylphosphine (1.58 mL, 9.10 mmol, 1.3 equiv). The mixture was heated to 130 °C and stirred for 72 h, after which volatiles were evaporated under reduced pressure. The crude oily residue was purified by FCC (99:1 CyH:EtOAc) to afford the title compound **1.74** (1.37 g, 4.35

70. Nystrom, R. F. *J. Am. Chem. Soc.* **1955**, *77*, 2544–2545.

mmol, 62% yield) as a white solid. **M.p.** 100–110 °C. **^{1}H NMR** (400 MHz, $CDCl_3$) δ 7.40–7.31 (m, 7H), 7.30–7.24 (m, 5H), 7.20 (td, *J* = 7.4, 1.7 Hz, 1H), 6.93 (ddd, *J* = 7.8, 4.3, 1.3 Hz, 1H), 3.21 (td, *J* = 7.5, 1.3 Hz, 2H), 2.55 (td, *J* = 7.5, 1.1 Hz). **^{13}C NMR** (101 MHz, $CDCl_3$) δ 142.6 (d, J_{CP} = 25.3 Hz), 136.1 (d, J_{CP} = 9.6 Hz), 135.9, 134.2, 134.0 (d, J_{CP} = 19.7 Hz), 129.8 (d, J_{CP} = 4.9 Hz), 129.7, 129.2, 128.9 (d, J_{CP} = 7.1 Hz), 127.8, 119.3, 30.4 (d, J^3_{CP} = 21.7 Hz), 18.8 (d, J^4_{CP} = 4.8 Hz). **^{31}P NMR** (162 MHz, $CDCl_3$) δ −13.2. **HRMS** (ESI +) calculated for $[C_{21}H_{18}NNaP]^+$ [M + Na]$^+$ 338.1070 m/*z*; found 338.1077 *m/z.*

3-(2-(Diphenylphosphino)phenyl)propan-1-amine (1.46c)

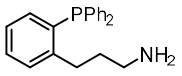

Following a modified literature procedure,[70] in the glovebox, to an oven-dried microwave vial equipped with a stirring bar was added lithium aluminium hydride (36.1 mg, 0.951 mmol, 1.0 equiv) followed by THF (1 mL). To the resulting grey suspension, a solution of aluminium trichloride (127 mg, 0.951 mmol, 1.0 equiv) in THF (1 mL) was added dropwise (vigorous bubbling observed), followed after 5 minutes by a solution of 3-(2-(diphenylphosphino)phenyl)propanenitrile **1.74** (300 mg, 0.951 mmol, 1.0 equiv) in THF (2.8 mL). The microwave vial was capped and removed from the glovebox. The reaction mixture was stirred at 23 ºC under Ar atmosphere for 48 h, then carefully quenched under a flow of inert gas at 0 °C by adding dropwise a 5% solution of NaOH (until bubbling ceased). The aqueous phase was extracted with CH_2Cl_2 three times (3 × 30 mL). Combined organic phases were dried over $MgSO_4$, filtered and evaporated to afford the crude product **1.46c** (293 mg, 0.918 mmol, 96% yield) as a yellow oil, that was carried over as such to the next step (due to decomposition during purification attempts). **^{1}H NMR** (400 MHz, $CDCl_3$) δ 7.37–7.22 (m, 12H), 7.10 (td, *J* = 7.3, 1.7 Hz, 1H), 6.86 (ddd, *J* = 7.7, 4.3, 1.4 Hz, 1H), 2.89 (t, *J* = 7.4 Hz, 2H), 2.66 (t, *J* = 6.9 Hz, 2H), 1.76–1.62 (m, 2H), 1.30 (brs, 2H). **^{31}P NMR** (162 MHz, $CDCl_3$) δ −12.3.

3-((3,5-Bis(trifluoromethyl)phenyl)amino)-4-((3-(2-(diphenylphosphino)phenyl)propyl)amino)cyclobut-3-ene-1,2-dione (1.48c)

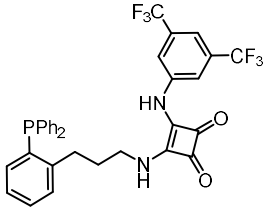

Under Ar, in an oven-dried microwave vial, to a cloudy solution of mixed squarate **1.47** (311 mg, 0.918 mmol, 1.0 equiv) in anhydrous MeOH (2 mL) was added a yellow solution of 3-(2-(diphenylphosphino)phenyl)propan-1-amine **1.46c** (293 mg, 0.918 mmol, 1.0 equiv) in anhydrous MeOH (5 mL). Upon addition, immediate formation of a precipitate was observed. The reaction mixture was sonicated for few minutes and the resulting slurry was stirred at 23 ºC for 20 h. The next day the precipitate that formed in the reaction mixture was collected on a sinter funnel, washed with MeOH (3 × 1 mL), and then dried under high vacuum, obtaining the title compound **1.47** (325.7 mg, 0.520 mmol, 57% yield) as a white solid. **M.p.** 180–184 °C. **^{1}H NMR** (500 MHz, DMSO-d_6) δ 10.16 (brs, 1H), 8.03 (brs, 2H), 7.75 (brs, 1H), 7.67 (s, 1H), 7.38–7.30 (m, 8H), 7.21–7.17 (m, 5H), 6.80–6.73 (m, 1H), 3.60 (m, 2H), 2.84 (m, 2H), 1.83 (m, 2H). **^{13}C NMR** (126 MHz, DMSO-d_6) δ 184.7, 180.5, 169.9, 162.3, 145.6 (d, J^2_{CP} = 25.4 Hz), 141.1, 136.2 (d, J^3_{CP} = 10.8 Hz), 134.9 (d, J^3_{CP} = 12.7 Hz), 133.3 (d, J^2_{CP} = 19.6 Hz), 133.0, 131.3 (q, J^2_{CF} = 32.2 Hz), 129.8, 129.2 (d, J^4_{CP} = 4.9 Hz), 128.9, 128.7 (d, J^3_P = 6.8 Hz), 126.5, 123.2 (q, J^1_{CF} = 272.0 Hz), 118.0, 114.7, 44.1, 32.2 (d, J^4_{CP} = 3.2 Hz), 30.7 (d, J^3_{CP} = 20.9 Hz). **^{31}P NMR** (202 MHz, DMSO-d_6) δ −13.6. **^{19}F NMR** (471 MHz, DMSO-d_6) δ −61.7. **HRMS** (ESI +) calculated for $[C_{33}H_{26}F_6N_2O_2P]^+$ [M + H]$^+$ 627.1631 m/*z*; found 627.1626 *m/z*.

1-(2-(Diphenylphosphino)benzyl)-3-phenylthiourea (1.48d)

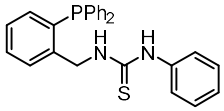

Under Ar, to a solution of (2-(diphenylphosphino)phenyl)methanamine[68] (146 mg, 0.501 mmol, 1 equiv) in anhydrous THF (5 mL), phenyl isothiocyanate (66 µL, 0.55 mmol, 1.1 equiv) was added. The reaction mixture was stirred at 23 ºC for 40 h, then volatiles were removed under reduced pressure. The crude product was purified by FCC (silica, CH_2Cl_2), obtaining 1-(2-(diphenylphosphino)benzyl)-3-phenylthiourea **1.48d** (185 mg, 0.434 mmol, 87% yield) as a white solid. **M.p.** 137–139 °C. **IR** (film, cm^{-1}) n 3373, 3200, 3054, 1529, 1496, 1434, 1315, 744, 696. **^{1}H NMR** (500 MHz, $CDCl_3$) δ 7.61 (brs, 1H), 7.58 (ddd, *J* = 7.7, 4.4, 1.3 Hz, 1H), 7.37–7.27 (m, 9H), 7.26–7.23 (m, 1H), 7.22–7.14 (m, 5H), 7.08 (dd, *J* = 7.3, 1.7 Hz, 2H), 6.89 (ddd, *J* =7.7, 4.6, 1.4 Hz, 1H), 6.62 (brs, 1H), 5.04 (d, *J* = 5.8 Hz, 2H). **^{13}C NMR** (126 MHz, $CDCl_3$) δ 180.6, 141.7 (d, J^2_{CP} = 24.2 Hz), 136.1, 135.9 (d, J_{CP} = 6.0 Hz), 135.8, 134.0, 133.9 (d, J_{CP} = 19.6 Hz), 130.3, 130.1 (d, J_{CP} = 5.4 Hz), 129.6, 129.1, 128.8 (d, J_{CP} = 7.0 Hz), 128.3, 127.3, 125.2, 48.2 (d, J^3_{CP} = 20.1). **^{31}P NMR** (202 MHz, $CDCl_3$) δ −12.7. **HRMS** (APCI +) calculated for $[C_{26}H_{24}N_2PS]^+$ $[M + H]^+$ 437.1392 m/*z*; found 437.1396 *m/z*.

1-(2-(Diphenylphosphino)benzyl)-3-phenylurea (1.48e)

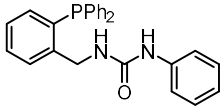

Under Ar, to a solution of (2-(diphenylphosphino)phenyl)methanamine[68] (146 mg, 0.501 mmol, 1 equiv) in anhydrous THF (5 mL), phenyl isocyanate (60 µL, 0.55 mmol, 1.1 equiv) was added. The reaction mixture was stirred at 23 ºC for 18 h, then volatiles were removed under reduced pressure. The crude product was purified by FCC (silica, CH_2Cl_2), obtaining the title compound **1.48e** (192 mg, 0.468 mmol, 93% yield) as a white solid. **M.p.** 179–181 °C. **^{1}H NMR** (500 MHz, $CDCl_3$) δ 7.48 (ddd, *J* = 7.7, 4.5, 1.3 Hz, 1H), 7.37–7.29 (m, 7H), 7.26–7.20 (m, 6H), 7.20–7.13 (m, 3H), 6.18 (s, 1H), 5.14 (t, *J* = 6.0 Hz, 1H), 4.60 (dd, *J* = 6.0, 1.3 Hz, 2H). **^{13}C NMR** (126 MHz, $CDCl_3$, signals listed for the phenyl urea major rotamer only) δ 155.4, 143.2 (d, J_{CP} = 24.1 Hz), 138.6, 136.2 (d, J_{CP} = 8.9 Hz), 135.5 (d, J_{CP} = 13.8 Hz), 134.0 (d, J_{CP} = 19.7 Hz), 133.9, 129.6, 129.5, 129.3, 129.1, 126.9 (d, J_{CP} = 7.0 Hz), 128.0, 123.7, 120.8, 43.4 (d, J^3_{CP} = 21.1 Hz). **^{31}P NMR** (202 MHz, $CDCl_3$) δ −12.6. **HRMS** (ESI +) calculated for $[C_{26}H_{23}N_2NaOP]^+$ $[M + Na]^+$ 433.1440 m/*z*; found 433.1442 *m/z*.

2-(Diphenylphosphino)aniline (1.49a)

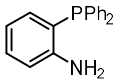

Following a modified literature procedure,[71] under Ar, CuI (19.1 mg, 0.100 mmol, 0.05 equiv), toluene (1.2 mL, previously degassed), diphenylphosphine (348 µL, 2.00 mmol, 1 equiv) and 1,2-dimethlethylenediamine (54 µL, 0.50 mmol, 0.25 equiv) were added in sequence to a flame-dried microwave vial. The mixture was stirred for 10 minutes, then 2-iodoaniline (438 mg, 2.00 mmol, 1 equiv), caesium carbonate (977 mg, 3.00 mmol, 1.5 equiv) and toluene (2.8 mL) were added in sequence. The reaction mixture was stirred in the sealed vial under Ar at 110 ºC for 22 h (reaction monitored by by GC-MS or ^{31}P NMR analysis). After cooling down to room temperature, the reaction mixture was partitioned between H_2O (15 mL) and EtOAc (15 mL). Phases were separated and the aqueous layer was extracted three times with EtOAc (3 × 15 mL). Combined organic phases were washed with brine, dried over Na_2SO_4, filtered and evaporated. The crude product was purified by FCC (silica, CyH:EtOAc 90:10 + 0.1% Et_3N), affording the title compound **1.49a** (337 mg, 1.22 mmol, 61% yield) as a white solid. Spectroscopic data match those previously reported.[72] **^{1}H NMR** (400 MHz, $CDCl_3$) δ 7.37–7.29 (m, 10H), 7.18 (ddd, *J* = 8.0, 7.2, 1.7 Hz, 1H), 6.79–6.74 (m, 1H), 6.72–6.66 (m, 2H), 4.14 (s,

71. Gelman, D.; Jiang, L.; Buchwald, S. L. *Org. Lett.* **2003**, *5*, 2315–2318.
72. Li, Y.; Das, S.; Zhou, S.; Junge, K.; Beller, M. *J. Am. Chem. Soc.* **2012**, *134*, 9727–9732.

2H). **^{31}P NMR** (161 MHz, $CDCl_3$) δ −17.3. **GC-MS** (ESI) *m/z* (%): 277 $[M]^+$ (100), 276 (59), 198 (70), 183 (29).

2-(Diphenylphosphino)-4-(trifluoromethyl)aniline (1.49b)

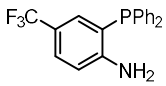

Under Ar, in a flame-dried microwave vial, diphenylphosphine (380 µL, 2.20 mmol, 1.1 equiv) was added to a stirred suspension of $Pd(OAc)_2$ (22.4 mg, 0.100 mmol, 0.05 equiv), dippf (50.2 mg, 0.120 mmol, 0.06 equiv), caesium carbonate (1.303 g, 4.00 mmol, 2 equiv), and 2-bromo-4-(trifluoromethyl)aniline (480 mg, 2.00 mmol, 1 equiv) in toluene (4 mL, previously degassed). The reaction mixture was stirred in the sealed vial under Ar at 120 ºC for 20 h (reaction monitored by GC-MS or ^{31}P NMR analysis). After cooling down to room temperature, volatiles were evaporated and the crude product was purified by FCC (silica, CyH:EtOAc 90:10 + 0.1% Et_3N), affording the title compound **1.49b** (540 mg, 1.56 mmol, 78% yield) as a yellow oil. **^{1}H NMR** (500 MHz, $CDCl_3$) δ 7.40–7.34 (m, 7H), 7.34–7.29 (m, 4H), 7.01 (dd, J = 5.6, 2.2 Hz, 1H), 6.70 (dd, J = 8.4, 5.0 Hz, 1H), 4.42 (brs, 2H). **^{13}C NMR** (126 MHz, $CDCl_3$) δ 152.4 (d, J_{CP} = 18.8 Hz), 134.4 (d, J_{CP} = 7.5 Hz), 133.8 (d, J^2_{CP} = 19.4 Hz), 131.5 (app quint, $J^3_{CF} = J^2_{CP}$ = 4.0 Hz), 129.4, 129.0 (d, J_{CP} = 7.0 Hz), 127.6 (q, J_{CF} = 3.6 Hz), 124.8 (q, J^1_{CF} = 271.0 Hz), 120.5 (qd, J^2_{CF} = 32.3 Hz, J^3_{CP} =2.3 Hz,), 119.5 (d, J_{CP} = 11.6 Hz), 114.8 (d, J_{CP} = 2.3 Hz). **^{31}P NMR** (202 MHz, $CDCl_3$) δ −17.1. **^{19}F NMR** (376 MHz, $CDCl_3$) δ −61.4. **HRMS** (APCI +) calculated for $[C_{19}H_{16}F_3NP]^+$ $[M + H]^+$ 346.0967 m/*z*; found 346.0966 *m/z*.

2-(diphenylphosphino)-5-(trifluoromethyl)aniline (1.49c)

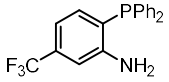

Under Ar, in a flame-dried microwave vial, diphenylphosphine (380 µL, 2.20 mmol, 1.1 equiv) was added to a stirred suspension of $Pd(OAc)_2$ (22.4 mg, 0.100 mmol, 0.05 equiv), dippf (50.2 mg, 0.120 mmol, 0.06 equiv), caesium carbonate (1.303 g, 4.00 mmol, 2 equiv), and 2-bromo-4-(trifluoromethyl)aniline (288 µL, 480 mg, 2.00 mmol, 1 equiv) in toluene (4 mL, previously degassed). The reaction mixture was stirred in the sealed vial under Ar at 120 ºC for 20 h (completion checked by GC-MS or ^{31}P NMR analysis). After cooling down to room temperature, volatiles were evaporated and the crude product was purified by FCC (silica, CyH:EtOAc 90:10 + 0.1% Et_3N), affording the title compound **1.49c** (439 mg, 1.27 mmol, 64% yield) as a white solid. **M.p.** 126–128 °C. **^{1}H NMR** (500 MHz, $CDCl_3$) δ 7.41–7.35 (m, 6H), 7.34–7.29 (m, 4H), 6.91-6.87 (m, 2H), 6.82 (dd, J = 7.7, 5.2 Hz, 1H), 4.28 (s, 2H). **^{13}C NMR** (126 MHz, $CDCl_3$) δ 149.7 (d, J^2_{CP} = 19.9 Hz), 134.7 (d, J_{CP} = 2.4 Hz), 134.4 (d, J_{CP} = 7.4 Hz), 133.9 (d, J^2_{CP} = 19.5 Hz), 132.4 (q, J^2_{CF} = 32.1 Hz), 129.4, 129.0 (d, J_{CP} = 7.3 Hz), 124.2 (q, J^1_{CF} = 272.3 Hz), 124.1 (d, J_{CP} = 11.8 Hz), 114.9 (m), 111.7 (app quint, $J^3_{CF} = J^3_{CP}$ = 3.8 Hz). **^{31}P NMR** (202 MHz, $CDCl_3$) δ −17.4. **^{19}F NMR** (376 MHz, $CDCl_3$) δ −63.2. **HRMS** (APCI +) calculated for $[C_{19}H_{16}F_3NP]^+$ $[M + H]^+$ 346.0967 m/*z*; found 346.0969 *m/z*.

1-(2-(Diphenylphosphino)phenyl)-3-phenylthiourea (1.48h)

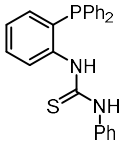

Under Ar, to a solution of 2-(diphenylphosphino)aniline **1.49a** (139 mg, 0.501 mmol, 1 equiv) in anhydrous THF (5 mL), phenyl isothiocyanate (66 µL, 0.55 mmol, 1.1 equiv) was added. The reaction mixture was stirred at 0 ºC for 4 h, then at 23 ºC for 18 h. Volatiles were removed under reduced pressure. The crude product was purified by FCC (silica, CyH:EtOAc 90:10 to 50:50), obtaining the title compound **1.48h** (165 mg, 0.400 mmol, 80% yield) as a white solid. **M.p.** 133–135 °C. **^{1}H NMR** (500 MHz, $CDCl_3$) δ 7.78 (dd, J = 8.0, 4.3 Hz, 1H), 7.74 (brs, 1H), 7.69 (s, 1H), 7.39 (td, J = 7.7, 1.6 Hz, 1H), 7.36–7.29 (m, 6H), 7.28–7.20 (m, 7H), 7.17 (t, J = 7.9 Hz, 1H), 7.12–7.09 (m, 2H), 6.83 (ddd, J = 7.7, 4.1, 1.5 Hz, 1H). **^{13}C NMR** (126 MHz, $CDCl_3$, one ^{31}P-coupled quaternary aromatic C not visible) δ 180.1, 140.8 (d, J_{CP} = 20.3 Hz), 136.4, 135.0 (d, J_{CP} = 9.3 Hz), 134.0 (d, J_{CP} = 19.9 Hz), 133.6, 129.8,

129.6, 129.4, 128.9 (d, J_{CP} = 7.3 Hz), 127.9 (d, J_{CP} = 2.1 Hz), 127.5, 127.4, 125.6. **^{31}P NMR** (202 MHz, $CDCl_3$) δ −13.8. **HRMS** (ESI –) calculated for $[C_{25}H_{20}N_2PS]^-$ [M – H]$^-$ 411.1090 m/*z*; found 411.1086 *m/z*.

1-(2-(Diphenylphosphino)phenyl)-3-phenylurea (1.48f)

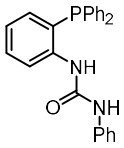

Under Ar, to a solution of 2-(diphenylphosphino)aniline **1.49a** (139 mg, 0.501 mmol, 1 equiv) in anhydrous THF (5 mL), phenyl isocyanate (60 µL, 0.55 mmol, 1.1 equiv) was added. The reaction mixture was stirred at 77 ºC for 24 h, then volatiles were removed under reduced pressure. The crude product was purified by FCC (silica, CH_2Cl_2 then CyH:EtOAc 90:10), obtaining the title compound **1.48f** (152 mg, 0.383 mmol, 76% yield) as a white solid. **M.p.** 164–166 °C. **^{1}H NMR** (500 MHz, $CDCl_3$) δ 7.96 (dd, J = 8.3, 3.0 Hz, 1H), 7.39–7.29 (m, 8H), 7.26–7.21 (m, 6H), 7.18–7.15 (m, 2H), 7.08 (t, *J* = 7.3 Hz, 1H), 7.04 (td, *J* = 7.5, 1.2 Hz, 1H), 6.88 (dd, J = 7.9, 3.0 Hz, 1H), 6.74 (s, 1H). **^{13}C NMR** (126 MHz, $CDCl_3$, signals listed for the phenyl urea major rotamer only) δ 153.4, 141.5 (d, J_{CP} = 18.3 Hz), 137.8, 134.9, 134.0, 133.9 (d, J_{CP} = 19.9 Hz), 130.4, 129.3 (d, J_{CP} = 2.8 Hz), 129.1, 128.9 (d, J_{CP} = 6.0 Hz), 128.2 (m), 124.8, 124.5, 123.3, 121.9. **^{31}P NMR** (202 MHz, $CDCl_3$) δ −16.9. **HRMS** (ESI –) calculated for $[C_{25}H_{20}N_2OP]^-$ [M – H]$^-$ 395.1319 m/*z*; found 395.1317 *m/z*.

1-(3,5-Bis(trifluoromethyl)phenyl)-3-(2-(diphenylphosphino)phenyl)urea (1.48g)

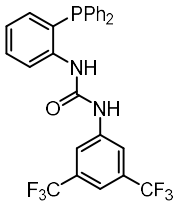

Under Ar, to a solution of 2-(diphenylphosphino)aniline **1.49a** (100 mg, 0.361 mmol, 1 equiv) in anhydrous THF (3 mL), 3,5-bis(trifluoromethyl)phenyl isocyanate (72 µL, 0.40 mmol, 1.1 equiv) was added. The reaction mixture was stirred at 40 ºC for 24 h, then volatiles were removed under reduced pressure. The crude product was purified by FCC (silica, CH_2Cl_2 then CyH:EtOAc 90:10), obtaining the title compound **1.48g** (145 mg, 0.271 mmol, 75% yield) as a white solid. **M.p.** 197–200 °C. **^{1}H NMR** (500 MHz, $(CD_3)_2CO$) δ 9.20 (brs, 1H), 8.10 (brs, 2H), 8.06–7.96 (m, 2H), 7.58 (brs, 1H) 7.49–7.35 (m, 7H), 7.34–7.22 (m, 4H), 7.10 (td, *J* = 7.3, 1.1 Hz, 1H), 6.90 (ddd, *J* = 7.7, 4.2, 1.5 Hz, 1H). **^{13}C NMR** (126 MHz, $(CD_3)_2CO$, signals listed for the major rotamer only) δ 153.3, 142.9, 142.7 (d, J_{CP} = 20.3 Hz), 136.3 (d, J_{CP} = 7.9 Hz), 134.6, 134.4 (d, J_{CP} = 19.6 Hz), 132.4 (q, J^2_{CF} = 32.9 Hz), 130.8, 130.0, 129.6 (d, J_{CP} = 7.0 Hz), 128.9 (d, J_{CP} = 10.9 Hz), 125.4, 124.4 (q, J^1_{CF} = 273.3 Hz), 124.3 (d, J_{CP} = 2.1 Hz), 119.0 (d, J_{CP} = 3.5 Hz), 124.3 (sept, J^3_{CF} = 4.1 Hz) **^{31}P NMR** (202 MHz, $(CD_3)_2CO$) δ −18.2. **^{19}F NMR** (376 MHz, $(CD_3)_2CO$) δ –63.3. **HRMS** (ESI +) calculated for $[C_{27}H_{20}F_6N_2OP]^+$ [M + H]$^+$ 533.1212 m/*z*; found 533.1223 *m/z*.

1-(2-(Diphenylphosphino)-4-(trifluoromethyl)phenyl)-3-phenylurea (1.48i)

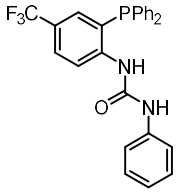

Under Ar, to a solution of phosphinoaniline **1.49b** (173 mg, 0.501 mmol, 1 equiv) in anhydrous THF (5 mL), phenyl isocyanate (60 µL, 0.55 mmol, 1.1 equiv) was added. The reaction mixture was stirred at 50 ºC for 5 h, then at 65 ºC for 16 h. After cooling to room temperature, volatiles were removed under reduced pressure and the crude product was purified by FCC (silica, CyH:EtOAc 90:10 + 0.1% Et_3N), obtaining the title compound **1.48i** (140 mg, 0.301 mmol, 60% yield) as a white solid. **M.p.** 203–205 °C. **^{1}H NMR** (500 MHz, $CDCl_3$) δ 8.33 (dd, *J* = 8.7, 4.3 Hz, 1H), 7.61 (d, *J* = 8.4 Hz, 1H), 7.57 (d, J = 8.1 Hz, 1H), 7.44–7.33 (m, 6H), 7.30 (t, *J* = 7.7 Hz, 2H), 7.23–7.14 (m, 7H), 7.13–7.09 (m, 1H), 6.37 (brs, 1H). **^{13}C NMR** (126 MHz, $CDCl_3$) δ 152.7, 144.9 (d, J^2_{CP} = 17.0 Hz), 137.0, 133.7 (d, J^2_{CP} = 19.9 Hz), 133.5 (d, J_{CP} = 6.2 Hz,), 130.9 (app quint, J^3_{CF} = J^2_{CP} = 3.2 Hz), 129.8, 129.7, 129.2 (d, J_{CP} = 7.3 Hz), 127.5 (q, J_{CF} = 3.2 Hz), 126.3 (d, J_{CP} = 13.2 Hz), 125.7, 125.4, 124.1 (q, J^1_{CF} = 272.1 Hz), 122.7, 121.0 (d, J_{CP} = 1.9 Hz). **^{31}P NMR** (202

MHz, $CDCl_3$) δ −17.8. **^{19}F NMR** (376 MHz, $CDCl_3$) δ −62.3. **HRMS** (ESI +) calculated for $[C_{26}H_{21}F_3N_2OP]^+$ $[M + H]^+$ 465.1338 m/*z*; found 465.1343 *m/z*.

1-(3,5-bis(trifluoromethyl)phenyl)-3-(2-(diphenylphosphino)-4-(trifluoromethyl)phenyl)urea (1.48j)

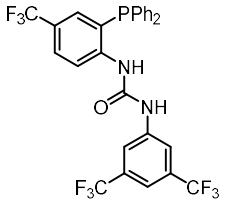

Under Ar, to a solution of phosphinoaniline **1.49a** (150 mg, 0.434 mmol, 1 equiv) in anhydrous THF (4.3 mL), 3,5-bis(trifluoromethyl)phenyl isocyanate (79 µL, 0.46 mmol, 1.05 equiv) was added. The reaction mixture was stirred at 23 ºC for 24 h, then at 75 ºC for 18 h. After cooling to room temperature, volatiles were removed under reduced pressure and the crude product was purified by FCC (silica, dry load, CyH:CH_2Cl_2 80:20 to 0:100), obtaining the title compound **1.48j** (110 mg, 0.183 mmol, 42% yield) as a white solid. **M.p.** 194–197 °C. **^{1}H NMR** (400 MHz, DMSO-d_6, 17 mg in 0.6 mL) δ 10.15 (brs, 1H), 8.67 (d, J = 5.7 Hz, 1H), 8.18 (dd, J = 8.5, 4.3 Hz, 1H), 8.02 (s, 2H), 7.77 (dd, J = 8.9, 2.2 Hz, 1H), 7.76 (s, 1H), 7.46–7.43 (m, 6H), 7.27–7.22 (m, 4H), 6.97 (m, 1H). **^{13}C NMR** (126 MHz, DMSO-d_6, 17 mg in 0.6 mL) δ 152.1, 145.2 (d, J^2_{CP} = 20.1 Hz), 141.3, 134.0 (d, J_{CP} = 8.6 Hz), 133.2 (d, J^2_{CP} = 19.5 Hz), 130.8 (q, J^2_{CF} = 32.7 Hz), 129.7 (m), 129.6, 129.1 (d, J_{CP} = 7.1 Hz), 128.3 (d, J_{CP} = 16.1 Hz), 126.9 (m), 124.0 (q, J^2_{CF} = 31.9 Hz), 124.0 (q, J^1_{CF} = 271.8 Hz), 123.3 (q, J^1_{CF} = 272.0 Hz), 122.7 (m), 117.9 (m), 114.8 (m). **^{31}P NMR** (202 MHz, DMSO-d_6) δ −18.0. **^{19}F NMR** (376 MHz, DMSO-d_6) δ −61.0 (3F), –61.8 (6F). **HRMS** (ESI +) calculated for $[C_{28}H_{19}F_9N_2OP]^+$ $[M + H]^+$ 601.1086 m/*z*; found 601.1088 *m/z*.

1-(2-(Diphenylphosphino)-5-(trifluoromethyl)phenyl)-3-phenylurea (1.48k)

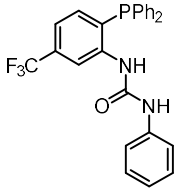

Under Ar, to a solution of phosphinoaniline **1.49c** (173 mg, 0.501 mmol, 1 equiv) in anhydrous THF (5 mL), phenyl isocyanate (60 µL, 0.55 mmol, 1.1 equiv) was added. The reaction mixture was stirred at 60 ºC for 24 h. After cooling to room temperature, volatiles were removed under reduced pressure and the crude product was purified by FCC (silica, CyH:CH_2Cl_2 70:30 to 0:100, then CH_2Cl_2:EtOAc 100:0 to 90:10), obtaining the title compound **1.48k** (136 mg, 0.293 mmol, 58% yield) as a white solid. **M.p.** 164–166 °C. **^{1}H NMR** (500 MHz, $CDCl_3$) δ 8.45 (dd, J = 4.3, 1.7 Hz, 1H), 7.42–7.34 (m, 7H), 7.31–7.27 (m, 2H), 7.24–7.13 (m, 8H), 6.94 (dd, J = 8.0, 4.4 Hz, 1H), 6.40 (brs, 1H). **^{13}C NMR** (126 MHz, $CDCl_3$) δ 152.9, 142.1 (d, J_{CP} = 13.8 Hz), 137.2, 134.3 (d, J_{CP} = 2.1 Hz), 133.8 (d, J_{CP} = 19.4 Hz), 133.7 (d, J_{CP} = 6.5 Hz), 132.3 (q, J^2_{CF} = 32.5 Hz), 130.9 (d, J_{CP} = 12.7 Hz), 129.8, 129.6, 129.1 (d, J_{CP} = 7.4 Hz, CH), 125.2, 124.0 (q, J^1_{CF} = 272.8 Hz, Cq), 122.6, 120.3 (m), 118.7 (CH). **^{31}P NMR** (202 MHz, $CDCl_3$) δ −17.4. **^{19}F NMR** (376 MHz, $CDCl_3$) δ −63.0. **HRMS** (ESI +) calculated for $[C_{26}H_{21}F_3N_2OP]^+$ $[M + H]^+$ 465.1338 m/*z*; found 465.1338 *m/z*.

1-(3,5-Bis(trifluoromethyl)phenyl)-3-(2-(diphenylphosphaneyl)-5-(trifluoromethyl)phenyl)urea (1.48l)

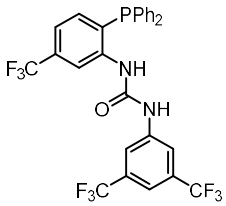

Under Ar, to a solution of phosphinoaniline **1.49c** (200 mg, 0.579 mmol, 1 equiv) in anhydrous THF (3 mL), 3,5-bis(trifluoromethyl)phenyl isocyanate (116 µL, 0.636 mmol, 1.1 equiv) was added. The reaction mixture was stirred at 40 ºC for 46 h, then volatiles were removed under reduced pressure. The crude product was purified by FCC (silica, CyH:EtOAc 95:5 to 80:20), obtaining the title compound **1.48l** (182 mg, 0.304 mmol, 52% yield) as a white solid. **M.p.** 178–183 °C. **^{1}H NMR** (500 MHz, $(CD_3)_2CO$) δ 9.36 (brs, 1H), 8.42 (d, J = 2.5 Hz, 1H), 8.21 (d, J = 6.4 Hz, 1H), 8.09 (s, 2H), 7.61 (brs, 1H), 7.49–7.38 (m, 7H), 7.37–7.25 (m,

4H), 7.08 (dd, J = 8.0, 3.7 Hz, 1H). **^{13}C NMR** (126 MHz, $(CD_3)_2CO$, signals listed for the major rotamer only) δ 153.1, 143.3 (d, J_{CP} = 20.0 Hz), 142.5, 135.4, 135.1 (d, J_{CP} = 7.4 Hz), 134.5 (d, J^2_{CP}= 19.8 Hz), 133.7 (d, J_{CP} = 13.9 Hz), 132.5 (q, J^2_{CF} = 33.0 Hz), 132.0 (q, J^2_{CF} = 32.3 Hz), 130.4, 129.9 (d, J_{CP} = 7.3 Hz), 125.0 (q, J^1_{CF} = 270.7 Hz), 124.4 (q, J^1_{CF} = 273.4 Hz), 121.2 (app q, J^3_{CF} = 3.9 Hz), 120.0 (m), 119.2 (m), 115.9 (app quint, J^3_{CF} = 4.2 Hz). **^{31}P NMR** (202 MHz, $(CD_3)_2CO$) δ −18.0. **^{19}F NMR** (376 MHz, $(CD_3)_2CO$) δ –63.1 (3F), –63.4 (6F). **HRMS** (ESI +) calculated for $[C_{28}H_{19}F_9N_2OP]^+$ $[M + H]^+$ 601.1086 m/*z*; found 601.1103 *m/z*.

Gold(I) complexes synthesis

Complex A

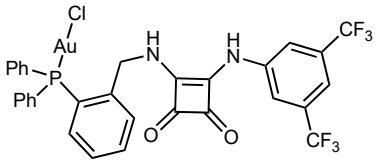

To a stirred suspension of **1.48a** (90.0 mg, 0.150 mmol, 1 equiv) in CH_2Cl_2 (1.5 mL), $[(Me_2S)AuCl]$ (44.3 mg, 0.150 mmol, 1 equiv) was added. After stirring at 23 ºC in the dark for 1 minute, the white suspension gradually became a pale-yellow solution. Upon further stirring (ca 5 minutes), the solution became cloudy and turned into a thick white suspension. The reaction mixture was stirred for 10 additional minutes, then diluted with CH_2Cl_2 until a solution was obtained.. This solution was filtered through a PTFE 0.2 mm syringe filter, and the filtrate was evaporated under reduced pressure providing the crude product as an off-white powder. The latter was purified by FCC (silica, dry load, CH_2Cl_2:EtOAc 50:50), affording complex **A** (120 mg, 0.144 mmol, 96% yield) as a white solid. **M.p.** 179 °C (decomposition). **^{1}H NMR** (500 MHz, DMSO-d_6, 15 mg in 0.5 mL) δ 10.03 (brs, 1H), 7.98 (s, 2H), 7.89 (brs, 1H), 7.75–7.72 (m, 2H), 7.66 (s, 1H), 7.65–7.48 (m, 11H), 6.85 (dd, J = 13.1, 7.7, 1H), 5.06 (d, J = 5.3 Hz, 2H). **^{13}C NMR** (126 MHz, DMSO-d_6, 15 mg in 0.5 mL) 184.6, 181.0, 169.4, 162.6, 141.0, 140.6 (d, J_{CP} = 10.8 Hz), 134.3 (d, J_{CP} = 14.1 Hz), 133.3 (d, J_{CP} = 7.6 Hz), 132.7, 132.6 (d, J^4_{CP} = 2.0 Hz), 131.3 (q, J^2_{CF} = 32.2 Hz), 130.6 (d, J_{CP} = 8.3 Hz), 129.8 (d, J_{CP} = 11.9 Hz), 128.8 (d, J_{CP} = 9.7 Hz), 127.1 (d, J^1_{CP} = 63.3 Hz), 126.2 (d, J^1_{CP} = 57.7 Hz), 122.1 (q, J^1_{CF} = 272.2 Hz), 118.0, 114.8, 46.0 (d, J^3_{CP} = 12.2 Hz). **^{31}P NMR** (202 MHz, DMSO-d_6, 15 mg in 0.5 mL) δ 28.1. **^{19}F NMR** (471 MHz, DMSO-d_6, 15 mg in 0.5 mL) δ −61.8. **HRMS** (ESI +) calculated for $[C_{31}H_{21}AuClF_6N_2NaO_2P]^+$ $[M + Na]^+$ 853.0491 *m/z*; found 853.0487 *m/z*. **Elemental analysis** calculated for $C_{31}H_{21}AuClF_6N_2O_2P$: C 44.81; H 2.55; N 3.37; found: C 44.65 ± 0.35; H 2.71 (below the 2.75 limit of quantitation); N 3.35 ± 0.30. **XRD**: crystals for single-crystal X-ray diffraction analysis were grown from DMSO at room temperature.

Complex B

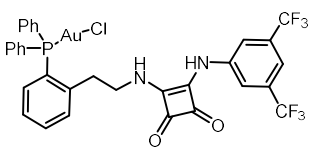

To a stirred suspension of **1.48b** (140 mg, 0.229 mmol, 1 equiv) in CH_2Cl_2 (2.3 mL), $[(Me_2S)AuCl]$ (67.3 mg, 0.229 mmol, 1 equiv) was added. After stirring for 15 minutes in the dark, the reaction mixture appeared as a clear pale-yellow solution. The solution was evaporated. The white-off solid crude was purified by FCC (CH_2Cl_2:EtOAc 100:0 to 90:10), affording complex **B** (151 mg, 0.179 mmol, 78% yield) as a white solid. **M.p.** 253–258 °C (decomposition). **^{1}H NMR** (400 MHz, $CDCl_3$) δ 8.84 (s, 1H), 8.07 (s, 2H), 7.71 (dd, J = 7.4, 5.3 Hz, 1H), 7.64–7.50 (m, 11H), 7.48 (s, 1H), 7.21 (tt, J = 7.5, 1.6 Hz, 1H), 6.70 (ddd, J = 13.0, 7.8, 1.3 Hz, 1H), 6.65–6.59 (m, 1H), 4.29 (q, J = 6.2 Hz, 2H), 3.19 (brt, J = 6.2 Hz, 2H). **^{13}C NMR** (126 MHz, $CDCl_3$) 183.9, 180.5, 169.0, 163.0, 141.2 (d, J = 12.0 Hz), 140.5, 134.6 (d, J = 13.8 Hz), 133.3 (d, J = 8.9 Hz), 132.9 (d, J_{CP} = 2.5 Hz), 132.7 (d, J_{CP} = 2.7 Hz), 132.7 (q, J^2_{CF} = 33.4 Hz), 131.2 (d, J = 8.7 Hz), 129.9 (d, J = 12.3 Hz), 127.9 (d, J = 10.2 Hz), 127.2 (d, J^1_{CP} = 64.9 Hz), 126.7 (d, J^1_{CP} = 62.9 Hz), 123.2 (q, J^1_{CF} = 272.0 Hz), 118.4 (d, J

= 4.1 Hz), 116.2 (m), 45.3, 35.1 (d, J^3_{CP} = 11.3 Hz). **^{31}P NMR** (202 MHz, $CDCl_3$) δ 30.2. **^{19}F NMR** (376 MHz, $CDCl_3$) δ −63.2. **HRMS** (ESI +) calculated for $[C_{32}H_{23}AuF_6N_2O_2P]^+$ $[M - Cl]^+$ 809.1062 *m/z*; found 809.1079 *m/z*; calculated for $[C_{32}H_{23}AuClF_6N_2NaO_2P]^+$ $[M + Na]^+$ 867.0648 *m/z*; found 867.0659 *m/z*; **Elemental analysis** calculated for $C_{32}H_{23}AuClF_6N_2O_2P$: C 45.49; H 2.74; N 3.32; found: C 45.62 ± 0.35; H 2.72 (below the 2.75 limit of quantitation); N 3.30 ± 0.30. **XRD**: crystals for single-crystal X-ray diffraction analysis were grown from DMSO at room temperature.

Complex C

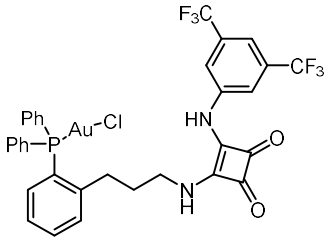

To a stirred suspension of **1.48c** (153 mg, 0.244 mmol, 1 equiv) in CH_2Cl_2 (2.4 mL), [(Me_2S)AuCl] (71.9 mg, 0.244 mmol, 1 equiv) was added. After stirring for 30 minutes in the dark, the reaction mixture was evaporated under reduced pressure. The solid residue was purified by FCC (CH_2Cl_2:EtOAc 100:0 to 90:10), affording complex **C** (151 mg, 0.176 mmol, 72% yield) as an off-white solid. **M.p.** 265–272 °C (decomposition). **^{1}H NMR** (500 MHz, DMSO-d_6) δ 10.11 (brs, 1H), 8.03 (s, 2H), 7.79–7.47 (m, 14H), 7.34 (t, *J* = 7.6 Hz, 1H), 6.75 (dd, *J* = 12.9, 7.8 Hz, 1H), 3.54 (q, *J* = 7.2 Hz, 2H), 2.94 (t, *J* = 8.1 Hz, 2H), 1.90–1.80 (m, 2H). **^{13}C NMR** (126 MHz, DMSO-d_6) δ 184.5, 180.6, 169.7, 162.4, 144.8 (d, J_{CP} = 11.9 Hz), 141.1, 134.2 (d, J_{CP} = 13.9 Hz), 132.9 (d, J_{CP} = 8.5 Hz), 132.4 (d, J^4_{CP} = 2.6 Hz), 132.3, 131.3 (q, J^2_{CF} = 32.4 Hz), 130.8 (d, J_{CP} = 8.9 Hz), 129.8 (d, J_{CP} = 11.8 Hz), 127.7 (d, J^1_{CP} = 63.2 Hz), 127.0 (d, J_{CP} = 9.9 Hz), 125.8 (d, J^1_{CP} = 60.7 Hz), 123.2 (q, J^1_{CF} = 272.8 Hz), 118.0, 114.7, 43.5, 31.9, 30.9 (d, J^3_{CP} = 11.8 Hz). **^{31}P NMR** (162 MHz, DMSO-d_6) δ 28.9. **^{19}F NMR** (471 MHz, DMSO-d_6) δ −61.7. **HRMS** (ESI +) calculated for $[C_{33}H_{25}AuClF_6N_2NaO_2P]^+$ $[M + Na]^+$ 881.0804 *m/z*; found 881.0811 *m/z*. **Elemental analysis** calculated for $C_{33}H_{25}AuClF_6N_2O_2P$: C 46.14; H 2.93; N 3.26; found: C 46.11 ± 0.35; H 2.98 ± 0.30; N 3.22 ± 0.30. **XRD**: crystals for single-crystal X-ray diffraction analysis were grown from DMSO at room temperature.

Complex D

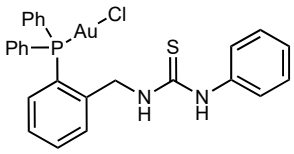

To a clear colorless solution of **1.48d** (100 mg, 0.234 mmol, 1 equiv) in CH_2Cl_2 (3 mL), [(Me_2S)AuCl] (69.7 mg, 0.237 mmol, 1.01 equiv) was added, obtaining a clear colorless solution. After stirring at 23 ºC for 2 h in the dark, the reaction mixture was evaporated under reduced pressure, obtaining a white solid that was no longer soluble in CH_2Cl_2. The solid was washed twice with CH_2Cl_2 (2 × 2 mL) decanting off the solvent, and dried under high vacuum, obtaining complex **D** (85.1 mg, 0.129 mmol, 55% yield) as a white solid. **M.p.** 196–199 °C. **^{1}H NMR** (500 MHz, DMSO-d_6, 303 K, 20 mg in 0.5 mL) δ 9.79 (brs, 1H), 8.26 (brs, 1H), 7.69–7.54 (m, 11H), 7.52–7.48 (m, 1H), 7.54–7.35 (m, 3H), 7.33 (t, *J* = 7.9 Hz, 2H), 7.13 (t, *J* = 7.3 Hz, 1H), 6.78 (dd, *J* = 13.0, 7.6 Hz, 1H), 4.91 (d, *J* = 5.0 Hz, 2H). **^{13}C NMR** (126 MHz, DMSO-d_6, 303 K, 20 mg in 0.5 mL) δ 180.6, 142.3 (d, J^2_{CP} = 10.4 Hz), 138.7, 134.2 (d, J_{CP} = 14.1 Hz), 132.7 (d, J_{CP} = 7.5 Hz), 132.5, 132.0, 129.8 (d, J_{CP} = 11.9 Hz), 128.7, 128.0 (d, J_{CP} = 7.0 Hz), 127.37 (d, J_{CP} = 9.7 Hz), 127.36 (d, J^1_{CP} = 62.9 Hz), 125.7 (d, J^1_{CP} = 57.4 Hz), 124.6, 123.6, 46.1 (d, J^3_{CP} = 14.0 Hz). **^{31}P NMR** (162 MHz, DMSO-d_6, 11 mg in 0.5 mL) δ 28.1. **HRMS** (ESI +) calculated for $[C_{26}H_{23}AuN_2PS]^+$ $[M - Cl]^+$ 623.0980 *m/z*; found 623.0979 *m/z*. **Elemental analysis** calculated for $C_{26}H_{23}AuClN_2PS$: C 47.39; H 3.52; N 4.25, S 4.87; found: C 45.31 ± 0.35; H 3.36 ± 0.30; N 4.02 ± 0.30; S 4.59 ± 0.35. **XRD**: crystals for single-crystal X-ray diffraction analysis were grown from $CHCl_3$ at 23 ºC.

Complex E

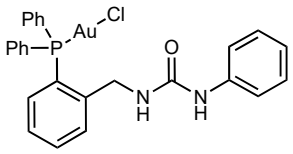

To a suspension of **1.48e** (96.0 mg, 0.234 mmol, 1 equiv) in CH_2Cl_2 (2.4 mL), [(Me_2S)AuCl] (68.9 mg, 0.234 mmol, 1 equiv) was added. After stirring at 23 ºC for 1 h in the dark, the reaction mixture was evaporated under reduced pressure, obtaining an off-white solid, that was dissolved in the minimum amount of CH_3CN. After stirring for a few minutes, a whitish solid precipitated, which was collected on a Buchner funnel, washed with CH_3CN (2 mL) and pentane (2 mL), and dried under high vacuum, obtaining complex **E** (85.2 mg, 0.133 mmol, 57% yield) as a white solid. **M.p.** 208 °C (decomposition). **^{1}H NMR** (500 MHz, $CDCl_3$, 6 mg in 0.5 mL) δ 7.66 (ddd, J = 7.8, 5.0, 1.3 Hz, 1H), 7.55–7.44 (m, 11H), 7.29–7.26 (m, 2H), 7.24–7.19 (m, 3H), 6.98 (tt, J = 7.3, 1.3 Hz, 1H), 6.75 (ddd, J = 13.2, 7.9, 1.3 Hz, 1H), 6.74 (brs, 1H), 5.47 (t, J = 6.0 Hz, 1H), 4.59 (d, J = 6.0 Hz, 2H). **^{13}C NMR** (126 MHz, $CDCl_3$, 6 mg in 0.5 mL) δ 155.3, 143.1 (d, J^2_{CP} = 10.8 Hz), 138.7, 134.6 (d, J_{CP} = 14.0 Hz), 133.4 (d, J_{CP} = 7.7 Hz), 132.5 (d, J^4_{CP} = 2.5 Hz), 132.5, 131.0 (d, J_{CP} = 9.0 Hz), 129.7 (d, J_{CP} = 12.1 Hz), 129.1, 127.9 (d, J_{CP} = 10.1 Hz), 127.9 (d, J^1_{CP} = 63.9 Hz), 125.9 (d, J^1_{CP} = 58.6 Hz), 123.3, 120.1, 42.9 (d, J^3_{CP} = 12.0 Hz). **^{31}P NMR** (202 MHz, CD_3Cl, 6 mg in 0.5 mL) δ 28.7. **HRMS** (ESI +) calculated for $[C_{26}H_{23}AuClN_2NaOP]^+$ $[M + Na]^+$ 665.0794 *m/z*; found 665.0789 *m/z*. **Elemental analysis** calculated for $C_{26}H_{23}AuClN_2OP$: C 48.58, H 3.61, N 4.36; found: C 48.22 ± 0.35; H 3.58 ± 0.30; N 4.36 ± 0.30. **XRD**: crystals for single-crystal X-ray diffraction analysis were grown from $ClCH_2CH_2Cl$/pentane at 23 ºC.

Complex F

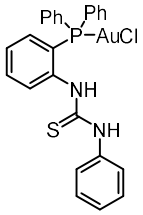

To a yellow solution of **1.48f** (85.0 mg, 0.206 mmol, 1 equiv) in CH_2Cl_2 (2.1 mL), [(Me_2S)AuCl] (60.7 mg, 0.206 mmol, 1 equiv) was added. After stirring at 23 ºC for 2 h in the dark, the reaction mixture was evaporated under reduced pressure, obtaining complex **F** as a pale yellow solid (133.0 mg, 0.205 mmol, 100% yield).

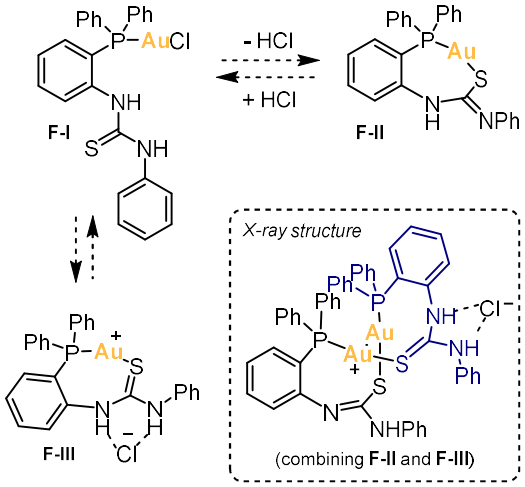

Scheme 1.23 Putative species for complex **F** present in solution based on NMR, XRD, HRMS and EA data.

^{1}H NMR and ^{31}P{^{1}H} NMR spectra at 298 K of complex **F** show very broad signals with unresolved multiplicity in $CDCl_3$, CD_2Cl_2 and DMSO-d_6, and to a lesser extent in CD_3CN. This was tentatively attributed to the dynamic nature of the complex (Scheme 1.23), with the thiourea S atom and the chloride competing for coordination at the Au(I) centre (**F-I** versus **F-III**), and to

the fact that the thiourea might be partially deprotonated (**F-I** versus **F-II**). Evidence for the deprotonation is provided in the solid state by the X-ray structure of **F**, and in solution by the under-integration of the signals in the ^{1}H NMR spectrum (19 aromatic H atoms and 2 NH protons are expected for **F**, but only 18–20 protons are seen). Since ^{1}H NMR signals were sharper in CD_3CN, this solvent was chosen to attempt a full NMR characterization, even if the complex is soluble in CD_3CN only at low concentrations. **M.p.** 160–165 °C (decomposition). **^{1}H NMR** (400 MHz, CD_3CN, 10 mg in 0.5 mL) δ 11.00–8.20 (brm, *ca* 1H), 7.90–7.05 (m, *ca* 16–18H), 7.04–6.90 (m, 1H). **^{13}C NMR** (126 MHz, CD_3CN, 10 mg in 0.5 mL; due to their broad nature, signals are listed without multiplicity) δ 179.8 (brs), 141.9 (brs), 137.9 (brs), 135.4, 135.3, 134.9 (m), 134.5, 134.0 (brs), 133.7, 133.3, 132.7 (brs), 130.6, 130.5, 130.0 (brs), 129.3 (brs), 128.8 (brs), 128.1 (brs), 126.7 (brs). **^{31}P NMR** (162 MHz, CD_3CN, 10 mg in 0.5 mL) δ 29.2 (brs). **HRMS** (ESI +) calculated for $[C_{25}H_{21}AuN_2PS]^+$ $[M - Cl]^+$ 609.0823 *m/z*; found 609.0847 *m/z*. **Elemental analysis** calculated for $C_{25}H_{21}AuClN_2PS$: C 46.56, H 3.28, N 4.34, S 4.97; found: C 44.95 ± 0.35; H 3.34 ± 0.30; N 4.12 ± 0.30; S 4.68 ± 0.35 (structure of complex **F** as **F-I** could not be confirmed). **XRD**: crystals for single-crystal X-ray diffraction analysis were grown from CH_2Cl_2/*n*-hexane at 5 ºC.

Complex G

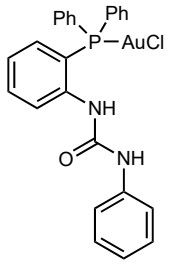

To a clear colorless solution of **1.48g** (90.0 mg, 0.227 mmol, 1 equiv) in CH_2Cl_2 (2.3 mL), [(Me_2S)AuCl] (66.9 mg, 0.227 mmol, 1 equiv) was added. After stirring at 23 ºC for 1 h in the dark, the reaction mixture appeared as a thick white suspension. The precipitated solid was collected on a synter funnel, washed with cyclohexane (2 mL) and dried under high vacuum, obtaining a ca 9:1 mixture (125 mg in total, white solid) of complex **G** and diphenylurea. This mixture was triturated in acetone three times, each time decanting off the solvent, thus isolating complex **G** (103.2 mg, 0.164 mmol, 72% yield) as an off-white solid. **M.p.** 225–234 °C (decomposition). **^{1}H NMR** (400 MHz, DMSO-d_6, 4 mg in 0.5 mL) δ 8.92 (s, 1H), 7.75 (s, 1H), 7.69–7.51 (m, 12H), 7.30–7.26 (m, 3H), 7.23 (t, J = 7.3 Hz, 2H), 6.95 (tt, J = 7.2, 1.3 Hz, 1H), 6.80 (ddd, J = 12.5, 7.9, 1.2 Hz, 1H). **^{13}C NMR** (126 MHz, DMSO-d_6, 4 mg in 0.5 mL) δ 152.4, 141.0 (d, J^2_{CP} = 7.9 Hz), 139.2, 134.0 (d, J_{CP} = 13.9 Hz), 133.2 (d, J_{CP} = 6.5 Hz), 132.4 (d, J_{CP} = 1.5 Hz), 132.2 (d, J^4_{CP} = 2.8 Hz), 129.6 (d, J_{CP} = 12.1 Hz), 128.63, 128.57, 128.0 (d, J^1_{CP} = 63.8 Hz), 125.4 (d, J_{CP} = 9.4 Hz), 122.0, 121.4 (d, J^1_{CP} = 62.1 Hz), 118.8. **^{31}P NMR** (162 MHz, DMSO-d_6, 4 mg in 0.5 mL) δ 25.3. **HRMS** (ESI +) calculated for $[C_{25}H_{21}AuClN_2NaOP]^+$ $[M + Na]^+$ 651.0638 *m/z*; found 651.0635 *m/z*. **Elemental analysis** calculated for $C_{25}H_{21}AuClN_2OP$: C 47.75, H 3.37, N 4.45; found: C 46.88 ± 0.35; H 3.36 ± 0.30; N 4.40 ± 0.30. **XRD**: crystals for single-crystal X-ray diffraction analysis were grown from $ClCH_2CH_2Cl$/*n*-hexane at 23 ºC.

Complex H

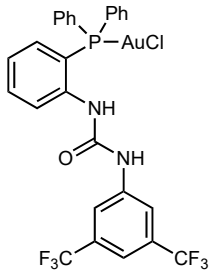

A solution of **1.48h** (120.0 mg, 0.225 mmol, 1 equiv) and [(Me_2S)AuCl] (66.4 mg, 0.225 mmol, 1 equiv) in CH_2Cl_2 (5 mL) was stirred in the dark at 23 ºC for 2.5 h, then filtered through a PTFE 0.2 mm syringe filter. The filtrate was evaporated under reduced pressure and the crude product was purified by FCC (silica, dry load, CyH:EtOAc 80:20), affording complex **H** (149.9 mg, 0.196 mmol, 87% yield) as an off-white solid. **M.p.** 135–138 °C. **^{1}H NMR** (500 MHz, $(CD_3)_2CO$, 22.5 mg in 0.5 mL) δ 8.87 (brs, 1H), 7.95 (s, 2H), 7.78–7.63 (m, 7H), 7.60–7.55 (m, 7H), 7.38 (tt, J = 7.7, 1.7 Hz, 1H), 6.95 (ddd, J = 12.5, 7.7, 1.2 Hz, 1H). **^{13}C NMR** (126 MHz, $(CD_3)CO$, 22.5 mg in 0.5 mL, signals listed

for the major rotamer only) δ 153.3, 142.4, 141.2 (d, J^3_{CP} = 7.6 Hz), 135.4 (d, J^2_{CP} = 14.2 Hz), 134.3 (d, J^3_{CP} = 6.9 Hz), 133.5 (d, J^4_{CP} = 1.9 Hz), 133.2 (d, J^4_{CP} = 2.5 Hz), 132.2 (q, J^2_{CF} = 33.0 Hz), 130.9 (d, J^3_{CP} = 6.0 Hz), 130.5 (d, J^2_{CP} = 12.1 Hz), 129.0 (d, J^1_{CP} = 63.8 Hz), 127.6 (d, J^2_{CP} = 9.8 Hz), 125.3 (d, J^1_{CP} = 61.2 Hz), 124.4 (q, J^1_{CF} = 273.2 Hz), 119.7, 115.8 (app quint, J^3_{CF} = 3.9 Hz). **^{31}P NMR** (162 MHz, $(CD_3)_2CO$) δ 26.4. **^{19}F NMR** (376 MHz, $(CD_3)_2CO$) δ –63.3. **HRMS** (ESI +) calculated for $[C_{27}H_{19}AuClF_6N_2NaOP]^+$ $[M + Na]^+$ 787.0386 *m/z*; found 787.0409 *m/z*. **Elemental analysis** calculated for $C_{27}H_{19}AuClF_6N_2OP$: C 42.40, H 2.50, N 3.66; found: C 42.46 ± 0.35; H 2.61 (below the 2.75 limit of quantitation); N 3.61 ± 0.30. **XRD**: crystals for single-crystal X-ray diffraction analysis were grown from CH_2Cl_2/*n*-hexane at –18 ºC.

Complex I

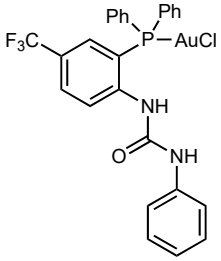

To a white suspension of **1.48i** (200.0 mg, 0.431 mmol, 1 equiv) in CH_2Cl_2 (4.3 mL), [(Me_2S)AuCl] (127.0 mg, 0.431 mmol, 1 equiv) was added. Upon addition, a clear colorless solution formed, that was stirred in the dark at 23 ºC for 30 minutes. Then cyclohexane was added until a white solid precipitated, and volatiles were removed under reduced pressure. The solid residue was collected on a synter funnel, washed with pentane (3 × 2 mL), 1:1 pentane: CH_2Cl_2 (2 mL) and pentane again (2 mL), then dried under high vacuum, obtaining complex **I** (278.4 mg, 0.399 mmol, 93% yield) as an off-white solid. **M.p.** 191–200 °C (decomposition). **^{1}H NMR** (300 MHz, $CDCl_3$, 10 mg in 0.5 mL) δ 8.17 (dd, *J* = 8.5, 4.9 Hz, 1H), 7.71 (d, *J* = 8.0 Hz, 1H), 7.60–7.43 (m, 10H), 7.40 (brs, 1H), 7.28 (brs, 1H), 7.23 (d, *J* = 4.2 Hz, 4H), 7.07 (app septet, *J* = 4.3 Hz, 1H), 6.88 (d, *J* = 12.6 Hz, 1H). **^{13}C NMR** (126 MHz, $CDCl_3$, 10 mg in 0.5 mL) δ 151.8, 144.1 (d, J_{CP} = 6.8 Hz), 137.2, 134.5 (d, J_{CP} = 14.2 Hz), 133.1 (d, J^4_{CP} = 2.6 Hz), 129.9 (d, J_{CP} = 12.4 Hz), 129.8 (m, 2C), 129.4, 126.3 (qd, J^2_{CF} = 33.4 Hz, J^3_{CP} = 9.9 Hz), 125.8 (d, J^1_{CP} = 65.2 Hz), 125.5 (d, J_{CP} = 5.2 Hz), 124.7 (brs), 123.5 (q, J^1_{CF} = 272.2 Hz), 121.5 (brs), 119.3 (d, J^1_{CP} = 60.5 Hz). **^{31}P NMR** (162 MHz, $CDCl_3$, 5 mg in 0.5 mL) δ 23.6. **^{19}F NMR** (376 MHz, $CDCl_3$, 5 mg in 0.5 mL) δ –62.3. **HRMS** (ESI +) calculated for $[C_{26}H_{20}AuClF_3N_2NaOP]^+$ $[M + Na]^+$ 719.0512 *m/z*; found 719.0501 *m/z*. **Elemental analysis** calculated for $C_{26}H_{20}AuClF_3N_2OP$: C 44.81, H 2.89, N 4.02; found: C 44.67 ± 0.35; H 3.03 ± 0.30; N 3.99 ± 0.30. **XRD**: crystals for single-crystal X-ray diffraction analysis were grown from $CHCl_3$/cyclohexane at 23 ºC.

Complex J

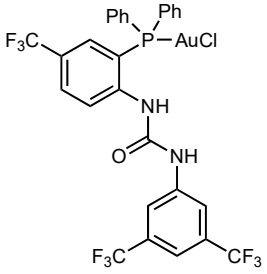

A solution of **1.48j** (206.3 mg, 0.344 mmol, 1 equiv) and [(Me_2S)AuCl] (101.2 mg, 0.344 mmol, 1 equiv) in CH_2Cl_2 (7 mL) was stirred in the dark at 23 ºC for 1 h. The reaction mixture was then filtered through a PTFE 0.2 mm syringe filter, and the filtrate was evaporated under reduced pressure. The crude product was purified by FCC (silica, dry load, CyH:EtOAc 90:10), affording complex **J** (272.8 mg, 0.327 mmol, 95% yield) as a white solid. **M.p.** 143–162 °C (decomposition). **^{1}H NMR** (400 MHz, CD_2Cl_2, 15 mg in 0.5 mL) δ 8.20 (brs, 1H), 8.04 (dd, *J* = 8.6, 4.9 Hz, 1H), 7.89 (s, 2H), 7.71 (d, *J* = 7.9 Hz, 1H), 7.58–7.46 (m, 12H), 6.97 (d, *J* = 12.6 Hz, 1H). **^{13}C NMR** (126 MHz, CD_2Cl_2, 15 mg in 0.5 mL) δ 151.3, 143.7 (d, J^2_{CP} = 6.6 Hz), 140.4, 134.9 (d, J_{CP} = 14.3 Hz), 133.5 (d, J^4_{CP} = 2.6 Hz), 132.1 (q, J^2_{CF} = 33.2 Hz), 130.3 (m), 130.2 (d, J_{CP} = 12.5 Hz), 130.0 (m), 127.0 (qd, J^2_{CF} = 33.2 Hz, J^3_{CP} = 9.9 Hz), 126.4 (d, J_{CP} = 5.5 Hz), 126.0 (d, J^1_{CP} = 65.6 Hz), 123.8 (q, J^1_{CF} = 272.5 Hz), 123.7 (q, J^1_{CF} = 272.6 Hz), 120.7 (d, J^1_{CP} = 60.6 Hz), 119.3 (q, J^3_{CF} = 3.8 Hz), 116.6 (app quint, J^3_{CF} = 3.8 Hz). **^{31}P NMR** (202 MHz, CD_2Cl_2, 5 mg in 0.5 mL) δ 23.3. **^{19}F NMR** (471 MHz, CD_2Cl_2, 5 mg in 0.5 mL) δ –63.1 (3F), –63.4 (6F). **HRMS**

(ESI +) calculated for $[C_{28}H_{18}AuClF_9N_2NaOP]^+$ [M + Na]$^+$ 855.0259 *m/z*; found 855.0276 *m/z*. **Elemental analysis** calculated for $C_{28}H_{18}AuClF_9N_2OP$: C 40.38, H 2.18, N 3.36; found: C 40.35 ± 0.35; H 2.38 (below the 2.75 limit of quantitation); N 3.33 ± 0.30. **XRD**: crystals for single-crystal X-ray diffraction analysis were grown from CH_2Cl_2 at 0 ºC.

Complex K

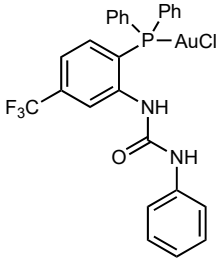

To a pale yellow solution of **1.48k** (100.0 mg, 0.215 mmol, 1 equiv) in CH_2Cl_2 (2.2 mL), [(Me_2S)AuCl] (63.4 mg, 0.215 mmol, 1 equiv) was added. The reaction mixture was stirred in the dark at 23 ºC for 1.5 h, then volatiles were evaporated under reduced pressure. The solid residue was purified by two sequential FCC (silica, dry load, CyH:EtOAc 80:20 to 50:50; silica, dry load, CyH:EtOAc 50:50), affording complex **K** (109.8 mg, 0.157 mmol, 73% yield) as an off-white solid. **M.p.** 220–224 °C (decomposition). **^{1}H NMR** (500 MHz, CD_2Cl_2, 10 mg in 0.5 mL) δ 8.28 (brd, *J* = 3.6 Hz, 1H), 7.59–7.56 (m, 2H), 7.54–7.46 (m, 8H), 7.33 (d, *J* = 8.2 Hz, 1H), 7.26–7.21 (m, 5H), 7.11 (brs, 1H), 7.08 (tt, *J* = 6.8, 1.7 Hz, 1H), 6.88 (dd, *J* = 12.5, 8.2 Hz, 1H). **^{13}C NMR** (126 MHz, CD_2Cl_2, 10 mg in 0.5 mL) δ 152.1, 141.9 (d, J^2_{CP} = 7.2 Hz), 137.7, 134.9 (d, J_{CP} = 14.3 Hz), 134.6 (qd, J^2_{CF} = 32.8 Hz, J_{CP} = 2.3 Hz), 134.2 (d, J_{CP} = 7.3 Hz), 132.2 (d, J^4_{CP} = 2.7 Hz), 130.1 (d, J_{CP} = 12.3 Hz), 129.6, 126.4 (d, J^1_{CP} = 65.1 Hz), 124.9, 124.0 (d, J^1_{CP} = 59.9 Hz), 123.8 (q, J^1_{CF} = 273.3 Hz), 123.0 (m), 121.8, 121.1 (dt, *J* = 10.5, 3.9 Hz). **^{31}P NMR** (202 MHz, CD_2Cl_2, 10 mg in 0.5 mL) δ 23.8. **^{19}F NMR** (471 MHz, CD_2Cl_2, 10 mg in 0.5 mL) δ –63.7. **HRMS** (ESI +) calculated for $[C_{26}H_{20}AuClF_3N_2NaOP]^+$ [M + Na]$^+$ 719.0512 *m/z*; found 719.0524 *m/z*. **Elemental analysis** calculated for $C_{26}H_{20}AuClF_3N_2OP$: C 44.81, H 2.89, N 4.02; found: C 45.09 ± 0.35; H 3.21 ± 0.30; N 3.85 ± 0.30. **XRD**: crystals for single-crystal X-ray diffraction analysis were grown from CH_2Cl_2/*n*-hexane at 0 ºC.

Complex L

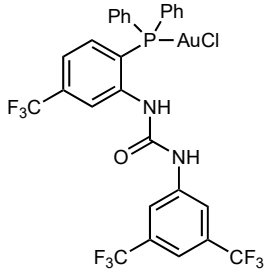

A solution of **1.48l** (130.0 mg, 0.217 mmol, 1 equiv) and [(Me_2S)AuCl] (63.4 mg, 0.217 mmol, 1 equiv) in CH_2Cl_2 (4 mL) was stirred in the dark at 23 ºC for 1.5 h, then filtered through a PTFE 0.2 mm syringe filter. The filtrate was evaporated under reduced pressure and the crude product was purified by FCC (silica, dry load, CyH:EtOAc 90:10), affording complex **L** (151.7 mg, 0.182 mmol, 84% yield) as a white solid. **M.p.** 172–177 °C (decomposition). **^{1}H NMR** (400 MHz, $(CD_3)_2CO$, 25 mg in 0.5 mL) δ 8.99 (brs, 1H), 8.11 (brs, 1H), 7.94 (s, 2H), 7.80 (brs, 1H), 7.76–7.67 (m, 5H), 7.66–7.56 (m, 7H), 7.18 (dd, *J* = 11.6, 8.3 Hz, 1H). **^{13}C NMR** (126 MHz, $(CD_3)_2CO$, 25 mg in 0.5 mL) δ 153.1, 142.1, 135.5 (d, J_{CP} = 14.4 Hz), 135.4, 134.4 (q, J^2_{CF} = 32.4 Hz), 133.6 (m), 132.3 (q, J^2_{CF} = 33.1 Hz), 130.7 (d, J_{CP} = 12.2 Hz), 129.7 (d, J^1_{CP} = 59.7 Hz), 128.1 (d, J^1_{CP} = 64.4 Hz), 126.9 (brs), 124.5 (q, J^1_{CF} = 273.2 Hz), 124.4 (q, J^1_{CF} = 273.2 Hz), 123.6 (brs), 118.9 (brs), 115.2 (m). **^{31}P NMR** (202 MHz, $(CD_3)_2CO$) δ 26.4. **^{19}F NMR** (471 MHz, $(CD_3)_2CO$) δ –63.3 (3F), –63.4 (6F). **HRMS** (ESI +) calculated for $[C_{28}H_{18}AuClF_9N_2NaOP]^+$ [M + Na]$^+$ 855.0259 *m/z*; found 855.0274 *m/z*. **Elemental analysis** calculated for $C_{28}H_{18}AuClF_9N_2OP$: C 40.38, H 2.18, N 3.36; found: C 40.09 ± 0.35; H 2.16 (below the 2.75 limit of quantitation); N 3.35 ± 0.30. **XRD**: crystals for single-crystal X-ray diffraction analysis were grown from CH_2Cl_2/*n*-pentane at 5 ºC.

3-(Benzylamino)-4-((3,5-bis(trifluoromethyl)phenyl)amino)cyclobut-3-ene-1,2-dione (1.52)

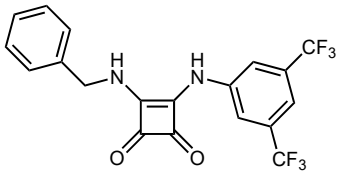

Following a modified literature procedure,[66] to a cloudy pale yellow solution of mixed squarate **1.47** (500 mg, 1.47 mmol, 1.0 equiv) in CH_2Cl_2 (7.0 mL) was added a clear yellow solution of benzylamine (160 µL, 1.47 mmol, 1.0 equiv). Upon addition, the reaction mixture became a very thick white suspension, to which additional CH_2Cl_2 (7.0 mL) was added. The reaction mixture was stirred at 23 ºC for 23 h and then filtered on a sinter funnel. The collected solid was washed with CH_2Cl_2 and then dried under high vacuum, obtaining the title compound **1.52** (579 mg, 1.40 mmol, 95% yield) as a white solid. Spectroscopic data match those previously reported.[73] **^{1}H NMR** (400 MHz, DMSO-d_6) δ 10.14 (brs, 1H), 8.09 (brs, 1H), 8.01 (s, 2H), 7.61 (s, 1H), 7.41–7.38 (m, 4H), 7.32 (app sextet, J = 4.1 Hz, 1H), 4.83 (d, J = 5.3 Hz, 2H). **^{13}C NMR** (101 MHz, DMSO-d_6) δ 184.8, 180.6, 169.4, 162.6, 141.1, 138.2, 131.3 (q, J^1_{CF} = 32.3 Hz), 128.7, 127.70, 126.68, 123.2 (q, J^2_{CF} = 272.9 Hz), 118.0 (brs), 114.7 (brs), 47.4. **^{19}F NMR** (376 MHz, DMSO-d_6) δ –62.0.

Substrate synthesis

***N*-(Prop-2-yn-1-yl)benzamide (1.25a)**

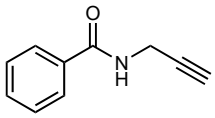

Under Ar, to a colorless solution of benzoyl chloride (3.55 mL, 30.6 mmol, 1.02 equiv) in anhydrous CH_2Cl_2 (67 mL) kept at 0 ºC, *N*-propargyl amine (0.86 mL, 30 mmol, 1.0 equiv) and then triethylamine (5.0 mL, 36 mmol, 1.2 equiv) were added dropwise at 0 ºC. The resulting suspension was allowed to warm up to room temperature and stirred at 23 ºC for 20 h, then a saturated NH_4Cl aqueous solution was added. Layers were separated, the aqueous phase was diluted with water and extracted twice with CH_2Cl_2. The combined organic phases were dried over Na_2SO_4, filtered and evaporated affording a beige solid. The latter was crystallized from CH_2Cl_2/pentane at 40–5 ºC, providing the first crop of the title compound (**1.25a**, 3.16 g, 19.8 mmol, 66% yield) as a white solid.

[Precisely, the crystallization was conducted as follows: the solid residue was dissolved in the minimum amount of CH_2Cl_2 at 40 ºC, then allowed to cool down to room temperature, at which point enough pentane was added to obtain a slightly cloudy solution. This solution was warmed up to 35 ºC until obtaining again a clear colorless solution, which was allowed to slowly cool down to 23 ºC and then was left standing at 5 ºC for 18 h, causing crystallization of an abundant off-white solid. The solid was collected by filtration on a sinter funnel, washed with pentane and dried under high vacuum. The mother liquor was evaporated and the residue purified by FCC (silica, CH_2Cl_2:EtOAc 100:0 to 90:10). Fractions containing the product were evaporated and the residue crystallized from CH_2Cl_2/pentane at 5 ºC, obtaining the second crop of the title compound (**1.25a**, 1.10 g, 6.91 mmol, 23% yield; overall yield 89%, 4.26 g, 26.8 mmol) as a white solid. Spectroscopic data match those previously reported.[74] **^{1}H NMR** (300 MHz, $CDCl_3$) δ 7.85–7.64 (m, 2H), 7.59–7.49 (m, 1H), 7.45–7.39 (m, 2H), 6.28 (brs, 1H), 4.27 (dd, J = 5.2, 2.6 Hz, 2H), 2.29 (t, J = 2.6 Hz, 1H). **^{13}C NMR** (75 MHz, $CDCl_3$) δ 167.2, 133.9, 132.0, 128.8, 127.1, 79.6, 72.1, 29.9.

73. Schaufelberger, D. F.; Seigel, K.; Ramström, O. *Chem. Eur. J.* **2020**, *26*, 15581–15588.
74. (a) Arcadi, A.; Cacchi, S.; Cascia, L.; Fabrizi, G.; Marinelli, F. *Org. Lett.* **2001**, *3*, 2501–2504. (b) Bacchi, A.; Costa, M.; Gabriele, B.; Pelizzi, G.; Salerno, G. *J. Org. Chem.* **2002**, *67*, 4450–4457. (c) Botta, M.; Corelli, G.; Petricci, E.; Seri, C. *Heterocycles* **2002**, *56*, 369–377.

4-Methoxy-*N*-(prop-2-yn-1-yl)benzamide (1.25b)

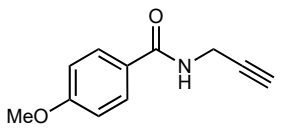

Under Ar, to a solution of *N*-propargyl amine (190 mL, 2.95 mmol, 1 equiv) and triethylamine (0.82 mL, 5.9 mmol, 2 equiv) in anhydrous CH_2Cl_2 (6 mL) kept at 0 ºC, 4-methoxybenzoyl chloride (400 µL, 2.95 mmol, 1 equiv) was added. The reaction mixture was stirred at 23 ºC for 24 h. Water (10 mL) and CH_2Cl_2 (10 mL) were added, and layers were separated. The organic phase was washed with brine (10 mL) and a saturated $NaHCO_3$ aqueous solution (10 mL), dried over Na_2SO_4, filtered and evaporated. The crude product was purified by FCC (silica, CyH:EtOAc 80:20 to 60:40), affording the title compound **1.25b** (353 mg, 1.87 mmol, 63% yield) as an off-white solid. Spectroscopic data match those previously reported.[75] **^{1}H NMR** (400 MHz, $CDCl_3$) δ 7.75 (d, *J* = 8.8 Hz, 2H), 6.92 (d, *J* = 8.9 Hz, 2H), 6.29 (brs, 1H), 4.24 (dd, *J* = 5.2, 2.6 Hz, 2H), 3.84 (s, 3H), 2.27 (t, *J* = 2.6 Hz, 1H). **^{13}C NMR** (101 MHz, $CDCl_3$) δ 166.8, 162.6, 129.0, 126.1, 114.0, 79.9, 71.9, 55.6, 29.9.

4-Chloro-*N*-(prop-2-yn-1-yl)benzamide (1.25c)

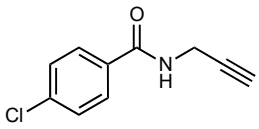

Following a modified literature procedure,[76] under Ar, to a solution of *N*-propargyl amine (320 µL, 5.00 mmol, 1 equiv), triethylamine (0.77 mL, 5.5 mmol, 1.1 equiv) and DMAP (12.2 mg, 0.100 mmol, 0.02 equiv) in anhydrous CH_2Cl_2 (25 mL) kept at 0 ºC, 4-chlorobenzoyl chloride (0.64 mL, 5.0 mmol, 1 equiv) was added. After stirring at 0 ºC for 15 minutes, the reaction mixture was stirred at 23 ºC for 17 h. A saturated NH_4Cl aqueous solution (20 mL) was added, layers were separated, and the aqueous phase was extracted twice with CH_2Cl_2 (2 × 20 mL). The combined organic phases were dried over Na_2SO_4, filtered and evaporated. The crude product was purified by FCC (silica, CyH:EtOAc 90:10 to 60:40), affording the title compound **1.25c** (950 mg, 4.92 mmol, 98% yield) as a white solid. Spectroscopic data match those previously reported.[75] **^{1}H NMR** (400 MHz, $CDCl_3$) δ 7.73 (d, *J* = 8.7 Hz, 2H), 7.40 (d, *J* = 8.6 Hz, 2H), 6.45 (brs, 1H), 4.23 (dd, *J* = 5.2, 2.6 Hz, 2H), 2.28 (t, *J* = 2.6 Hz, 1H). **^{13}C NMR** (75 MHz, $CDCl_3$) δ 166.3, 138.2, 132.2, 129.0, 128.6, 79.4, 72.2, 30.0.

***N*-(Prop-2-yn-1-yl)-4-(trifluoromethyl)benzamide (1.25d)**

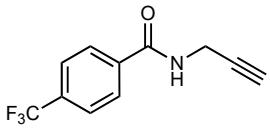

Following a modified literature procedure,[76] under Ar, to a solution of *N*-propargyl amine (320 µL, 5.00 mmol, 1 equiv), triethylamine (0.77 mL, 5.5 mmol, 1.1 equiv) and DMAP (12.2 mg, 0.100 mmol, 0.02 equiv) in anhydrous CH_2Cl_2 (25 mL) kept at 0 ºC, 4-(trifluoromethyl)benzoyl chloride (0.74 mL, 5.0 mmol, 1 equiv) was added. After stirring at 0 ºC for 15 minutes, the reaction mixture was stirred at 23 ºC for 17 h. A saturated NH_4Cl aqueous solution (20 mL) was added, layers were separated, and the aqueous phase was extracted twice with CH_2Cl_2 (2 × 20 mL). The combined organic phases were dried over Na_2SO_4, filtered and evaporated. The crude product was purified by FCC (silica, CyH:EtOAc 90:10 to 60:40), affording the title compound **1.25d** (887 mg, 3.90 mmol, 78% yield) as a white solid. Spectroscopic data match those previously reported.[75] **^{1}H NMR** (400 MHz, $CDCl_3$) δ 7.89 (d, *J* = 8.1 Hz, 2H), 7.69 (d, *J* = 8.2 Hz, 2H), 6.54 (brs, 1H), 4.26 (dd, *J* = 5.2, 2.6 Hz, 2H), 2.30 (t, *J* = 2.6 Hz, 1H). **^{13}C NMR** (75 MHz, $CDCl_3$) δ 166.1, 137.1, 133.7 (q, J^2_{CF} = 32.8 Hz), 127.7, 125.8 (q, J^3_{CF} = 3.7 Hz), 123.7 (q, J^1_{CF} = 272.7 Hz), 79.2, 72.3, 30.1. **^{19}F NMR** (376 MHz, $CDCl_3$) δ –63.1.

75. Senadi, G. C.; Guo, B.-C.; Hu, W.-P.; Wang, J.-J. *Chem. Commun.* **2016**, *52*, 11410–11413.
76. Hashmi, A. S. K.; Blanco Jaimes, M. C.; Schuster, A. M.; Rominger, F. *J. Org. Chem.* **2012**, *77*, 6394–6408.

((2-Bromophenyl)ethynyl)trimethylsilane (1.75)

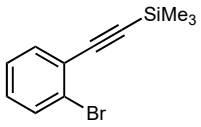

Following a modified literature procedure,[77] under Ar, bis(triphenylphosphine)palladium(II) dichloride (351 mg, 0.500 mmol, 0.025 equiv) and copper(I) iodide (95.2 mg, 0.500 mmol, 0.025 equiv) were suspended in anhydrous THF (40 mL), obtaining a yellow suspension that turned orange over 5 minutes. Next, triethylamine (14 mL, 100 mmol, 5 equiv) and 2-bromoiodobenzene (2.6 mL, 20 mmol, 1 equiv) were added in sequence, obtaining a slightly cloudy deep orange solution. Trimethylsilylacetylene (3.3 mL, 24 mmol, 1.2 equiv) was then added dropwise over 6 minutes, causing the reaction mixture to become a yellow suspension. After stirring 23 ºC for 1 h, during which an abundant white precipitate formed, the reaction mixture was diluted with Et_2O and filtered through Celite®. The filtrate was concentrated under reduced pressure and purified by FCC (silica, pentane), affording the title compound **1.75** (3.81 g, 15.0 mmol, 75% yield) as a yellow oil. Spectroscopic data match those reported in the literature.[78] **^{1}H NMR** (300 MHz, $CDCl_3$) δ 7.59 (dd, *J* = 8.0, 1.3 Hz, 1H), δ 7.51 (dd, *J* = 7.6, 1.8 Hz, 1H), δ 7.26 (td, *J* = 7.6, 1.3 Hz, 1H), δ 7.17 (td, *J* = 7.7, 1.8 Hz, 1H), 0.31 (s, 9H). **^{13}C NMR** (75 MHz, $CDCl_3$) δ 133.7, 132.5, 129.7, 127.0, 125.9, 125.4, 103.2, 99.8, 0.0.

Trimethyl((2-(3-methylbut-2-en-1-yl)phenyl)ethynyl)silane (1.76)

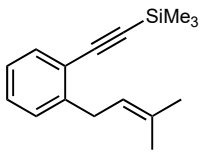

Following a literature procedure,[79] under Ar, to a pale yellow solution of ((2-bromophenyl)ethynyl)trimethylsilane **1.75** (3.66 g, 14.5 mmol, 1.0 equiv) in anhydrous THF (36 mL) kept at −78 °C, *n*-butyllithium (2.5 M solution in hexanes, 8.7 mL, 22 mmol, 1.5 equiv) was added dropwise, obtaining a brown solution. After stirring for 20 minutes at −78 °C, TMEDA (2.2 mL, 14.5 mmol, 1.0 equiv) was added dropwise. After stirring for 20 minutes at −78 °C, 1-bromo-3-methylbut-2-ene (2.5 mL, 22 mmol, 1.5 equiv) was added dropwise. The resulting yellow solution was left stirring for 1 h at −78 °C, then allowed to warm up to room temperature over 15 minutes. The reaction was carefully quenched by adding water (30 mL) and Et_2O (30 mL). Phases were separated and the aqueous layer was extracted with Et_2O (3 × 50 mL). The combined organic layers were washed with brine, dried over Na_2SO_4, filtered and evaporated to afford a yellow oil. The crude product was purified by FCC (silica, pentane) affording the title compound **1.76** (3.48 g, 14.4 mmol, 99% yield) as a pale-yellow oil. **^{1}H NMR** (300 MHz, $CDCl_3$) δ 7.51 (dd, *J* = 7.5, 1.0 Hz, 1H), δ 7.32–7.23 (m, 2H), δ 7.17 (td, *J* = 7.5, 1.7 Hz, 1H), 5.42 (hept, *J* = 7.3, 1.4 Hz, 1H), 3.60 (d, *J* = 7.3 Hz, 2H), 1.82–1.80 (m, 6H), 0.34 (s, 9H). **^{13}C NMR** (75 MHz, $CDCl_3$) δ 144.3, 132.8, 132.6, 128.8, 128.5, 125.7, 122.6, 122.5, 104.2, 98.2, 33.1, 25.9, 18.1, 0.16.

1-Ethynyl-2-(3-methylbut-2-en-1-yl)benzene (1.55)

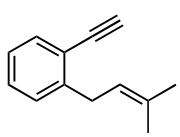

Following a modified literature procedure,[80] to a pale yellow solution of trimethyl((2-(3-methylbut-2-en-1-yl)phenyl)ethynyl)silane **1.76** (2.02 g, 8.33 mmol, 1 equiv) in MeOH (17 mL), potassium carbonate (1.27 g, 9.17 mmol, 1.1 equiv) was added. The resulting white suspension was stirred at 23 ºC for 2 h. A 1:1 brine:H_2O mixture (70 mL) was then added, and the aqueous phase was extracted with 1:1 CyH:EtOAc (3 × 60 mL). The combined organic phases were washed with brine, dried over Na_2SO_4, filtered and evaporated. The crude product was purified by FCC (silica, pentane),

77. Suzuki, Y.; Naoe, G.; Oishi, S.; Fujii, N.; Ohno, H. *Org. Lett.* **2012**, *14*, 326–329.
78. Rondeau-Gagné, S.; Curutchet, C.; Grenier, F.; Scholes, G. D.; Morin, J. -F. *Tetrahedron* **2010**, *66*, 4230-4242.
79. Gawade, S. A.; Bhunia, S.; Liu, R. -S. *Angew. Chem. Int. Ed.* **2012**, *51*, 7835–7838.
80. Ferrer, S.; Echavarren, A. M. *Org. Lett.* **2018**, *20*, 5784–5788.

affording the title compound **1.55** (1.11 g, 6.52 mmol, 78% yield) as a pale-yellow oil. Spectroscopic data match those reported in the literature.[79] **^{1}H NMR** (300 MHz, $CDCl_3$) δ 7.54 (d, *J* = 7.6 Hz, 1H), δ 7.36–7.25 (m, 2H), δ 7.20 (td, *J* = 7.5, 1.5 Hz, 1H), 5.40 (thept, *J* = 7.3, 1.4 Hz, 1H), 3.61 (d, *J* = 7.3 Hz, 2H), 3.32 (s, 1H), 1.82–1.80 (m, 6H). **^{13}C NMR** (75 MHz, $CDCl_3$) δ 144.5, 133.00, 132.96, 129.1, 128.5, 125.8, 122.4, 121.6, 82.6, 81.1, 33.0, 25.9, 18.1.

2-Iodocyclohex-2-en-1-one (1.77)

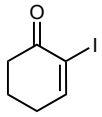

Following a modified literature procedure,[81] to a stirred solution of cyclohex-2-en-1-one (2.0 mL, 21 mmol, 1.0 equiv) in 1:1 THF:H_2O (100 mL), K_2CO_3 (3.7 g, 27 mmol, 1.3 equiv), I_2 (9.5 g, 37 mmol, 1.8 equiv) and DMAP (0.76 g, 6.2 mmol, 0.3 equiv) were added in sequence. The reaction mixture was protected from light (Aluminium foil) and stirred at 23 ºC for 4 h, after which EtOAc (120 mL) was added. Phases were separated and the organic phase was washed sequentially with a saturated aqueous solution of $Na_2S_2O_3$ (2 × 100 mL), a 0.1 M aqueous solution of HCl (2 × 80 mL) and brine (100 mL), then dried over Na_2SO_4 and filtered. Evaporation afforded the title compound **1.77** (3.9 g, 17 mmol, 81%) as a yellow oil, that solidified to a yellow solid after one night under high vacuum and was deemed pure enough to carry over to the next step. Spectroscopic data matched those reported in the literature.[81b] **^{1}H NMR** (300 MHz, $CDCl_3$) δ 7.76 (t, *J* = 4.4, 1H), 2.70–2.57 (m, 2H), 2.43 (td, *J* = 6.0, 4.5 Hz, 2H), 2.08 (dt, *J* = 12.2, 6.1 Hz, 2H).

2-(Phenylethynyl)cyclohex-2-en-1-one (1.40)

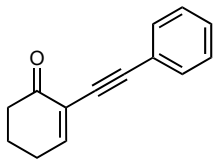

Following a modified literature procedure,[82] under Ar, to an oven-dried round-bottom flask equipped with a stirring bar were added 2-iodocyclohex-2-en-1-one **1.77** (3.51 g, 15.8 mmol, 1.0 equiv), copper(I) iodide (301 mg, 1.58 mmol, 0.10 equiv) and bis(triphenylphoshine)palladium(II) dichloride (555 mg, 0.79 mmol, 0.05 equiv), ethynylbenzene (3.5 mL, 31.6 mmol, 2.0 equiv) and finally THF (100 mL). The reaction mixture was cooled to 0 ºC, then diisopropylamine (6.2 mL, 47 mmol, 3.0 equiv) was added and the mixture was stirred for 1 h at 0 ºC. The reaction was quenched by adding a saturated aqueous solution of NH_4Cl (80 mL) followed by CH_2Cl_2 (80 mL). Layers were separated, the aqueous phase extracted with CH_2Cl_2 (2 × 80 mL), then the combined organic layers were washed with brine, dried over Na_2SO_4, filtered and evaporated. The crude product was purified without any delay by two sequential FCC (silica, CyH:EtOAc 100:0 to 90:10; silica, CyH:EtOAc 95:5), obtaining the product as an impure orange solid (2.29 g). The latter was further purified by washing it with CyH, obtaining the title compound **1.40** (1.09 g, 5.55 mmol, 35%) as a pale yellow solid. Spectroscopic data matched those reported in the literature.[82] **^{1}H NMR** (400 MHz, $CDCl_3$) δ 7.51–7.46 (m, 2H), 7.36 (t, *J* = 4.5 Hz, 1H), 7.33–7.28 (m, 3H), 2.59–2.41 (m, 4H), 2.07 (quint, *J* = 6.1 Hz, 2H). **^{13}C NMR** (101 MHz, $CDCl_3$) δ 195.6, 154.3, 131.9, 128.5, 128.3, 125.4, 123.0, 92.2, 83.9, 38.3, 26.6, 22.5.

81. a) Kraff, M. E.; Cran, J. W. *Synlett* **2005**, 1263–1266. b) Sundén, H.; Olsson, R. *Org. Biomol. Chem.* **2010**, *8*, 4831–4833.
82. Yao, T.; Zhang, X.; Larock, R. C. *J. Am. Chem. Soc.* **2004**, *126*, 11164–11165.

Procedure for reaction monitoring of catalytic reactions

5-Methylene-2-phenyl-4,5-dihydrooxazole (1.26a)

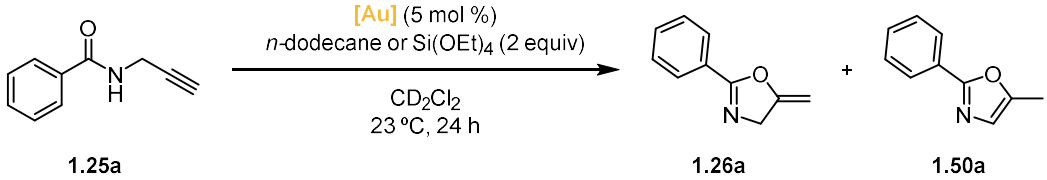

1.25a 1.26a 1.50a

In the glovebox, under Ar, a stock solution of amide **1.25a** (159.2 mg, 1.000 mmol, 10 equiv) in anhydrous CH_2Cl_2 (10 mL, 0.10 M solution) was prepared. This colorless stock solution (1.0 mL, 0.10 mmol, 1 equiv.) was added to a GC-MS vial equipped with a stirring bar and containing the desired [LAuCl] complex (0.05 equiv) and/or additive (0.05 equiv). The vial was capped, removed from the glovebox, and its content stirred in the dark (Al foil) at 23 ºC for 24 h. Then, the internal standard (*n*-dodecane, 45 µL, 0.2 mmol, 2 equiv; or tetraethoxysilane, 44 µL, 0.2 mmol, 2 equiv) was quickly added. Spectroscopic data for products **1.26a** and **1.50a** matched those reported in the literature.[44e] The following diagnostic signals were integrated to quantify the amount of starting material and products against internal standard: for substrate **1.25a**, peak at 4.27 ppm (dd, J = 5.2, 2.6 Hz, 2H); for product **1.26a**, peak at 4.80 ppm (q, J = 2.9 Hz, 1H); for product **1.50a**, peak at 2.40 ppm (d, J = 1.2 Hz, 3H); for *n*-dodecane, peak at 0.89 ppm (t, J = 7.2 Hz, 6H); for tetraethoxysilane, peak at 3.85 ppm (q, J = 7.0 Hz, 8H). **1.26a: ^{1}H NMR** (400 MHz, $CDCl_3$) δ 7.96 (d, J = 7.4 Hz, 2H), 7.55–7.47 (m, 1H), 7.43 (t, J = 7.5 Hz, 2H), 4.80 (q, J = 2.9 Hz, 1H), 4.64 (t, J = 2.7 Hz, 2H), 4.36 (q, J = 2.6 Hz, 1H). **1.50a: ^{1}H NMR** (400 MHz, $CDCl_3$) δ 8.09–7.83 (m, 2H) 7.50–7.38 (m, 3H), 6.87 (q, J = 1.2 Hz, 1H), 2.40 (d, J = 1.2 Hz, 3H).

1-Ethynyl-2-(3-methylbut-2-en-1-yl)benzene-3-(2-methylprop-1-en-1-yl)-1*H*-indene (1.56)

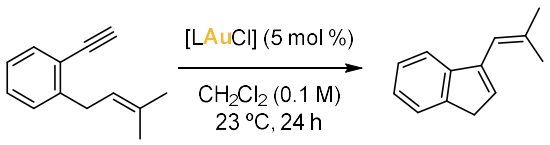

1.55 1.56

In the glovebox, under Ar, a stock solution of 1-ethynyl-2-(3-methylbut-2-en-1-yl)benzene **1.55** (42.6 mg, 0.250 mmol, 5 equiv) in anhydrous CH_2Cl_2 (2.5 mL, 0.10 M solution) was prepared. This colorless stock solution (0.5 mL, 0.05 mmol, 1 equiv.) was added to a GC-MS vial equipped with a stirring bar and containing the desired [LAuCl] complex (2.5 µmol, 0.05 equiv). The vial was capped, removed from the glovebox, and its content stirred in the dark (Al foil) at 23 ºC. After 24 h, the reaction was quenched by the addition of triethylamine (0.1 mL), then volatiles were removed under reduced pressure. The residue was dissolved in $CDCl_3$, then the internal standard (*n*-dodecane, 22.7 µL, 0.100 mmol, 2 equiv; or mesitylene, 13.9 µL, 0.100 mmol, 2 equiv) was added and the ^{1}H NMR spectrum was recorded. Spectroscopic data for isolated product **1.56** matched those reported in the literature.[83]

The following diagnostic signals were integrated to quantify the amount of starting material and product against internal standard: for substrate **1.55**, peak at 3.57 ppm (d, J = 7.3 Hz, 2H); for product **1.56**, peaks at 6.34 ppm (brs, 1H) and 6.19 (brs, 1H); for *n*-dodecane, peak at 0.89 ppm (t, J = 7.2 Hz, 6H); for mesitylene, peak at δ 6.76 ppm (s, 3H). **^{1}H NMR** (400 MHz, $CDCl_3$) δ

83. Madhushaw, R. J.; Lo, C. -Y.; Hwang, C. -W.; Su, M. -D.; Shen, H. -C.; Pal, S.; Shaikh, I. R.; Liu, R. -S. *J. Am. Chem. Soc.* **2004**, *126*, 15560−15565.

7.48 (*J* = 6.8 Hz, 1H), 7.40–7.20 (m, 3H), 6.34 (brs, 1H), 6.19 (brs, 1H), 3.45 (s, 2H), 1.97 (s, 3H), 1.93 (s, 3H).

Dimethyl 3-(2-methylprop-1-en-1-yl)cyclopent-3-ene-1,1-dicarboxylate (1.60)

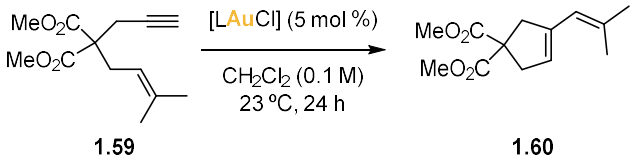

1.59 **1.60**

In the glovebox, under Ar, a stock solution of dimethyl 2-(3-methylbut-2-en-1-yl)-2-(prop-2-yn-1-yl)malonate **1.59** (59.6 mg, 50.0 µmol, 5 equiv) in anhydrous CH_2Cl_2 (2.50 mL, 0.10 M solution) was prepared. This colorless stock solution (0.5 mL, 0.05 mmol, 1 equiv) was added to a GC-MS vial equipped with a stirring bar and containing the desired [LAuCl] complex (2.5 µmol, 0.05 equiv). The vial was capped, removed from the glovebox, and its content stirred in the dark at 23 ºC. After 24 h, the reaction was quenched by the addition of triethylamine (0.1 mL), then volatiles were removed under reduced pressure. The residue was dissolved in $CDCl_3$, the internal standard (mesitylene, 13.9 µL, 0.100 mmol, 2 equiv) added and the ^{1}H NMR spectrum recorded.

Spectroscopic data for product dimethyl 3-(2-methylprop-1-en-1-yl)cyclopent-3-ene-1,1-dicarboxylate (**1.60**) matched those reported in the literature.[84] The following diagnostic signals were integrated to quantify the amount of starting material and product against internal standard: for substrate **1.59** peaks at 1.69 ppm (s, 3H) and 1.65 ppm (s, 3H); for product **1.60**, peak at 5.74 ppm (brs, 1H) ; for mesitylene, peak at δ 6.76 ppm (s, 3H). **^{1}H NMR** (400 MHz, $CDCl_3$) δ 5.74 (brs, 1H), 5.40 (brs, 1H, under residual CH_2Cl_2), 3.71 (s, 6H), 3.17–3.15 (m, 2H), 3.00 (brs, 1H), 1.82 (s, 3H), 1.79 (s, 3H).

1-Phenyl-2-(1-phenylethylidene)hydrazine (1.66)

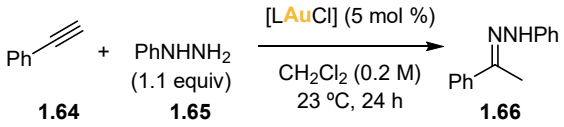

1.64 **1.65** **1.66**

In the glovebox, under Ar, a stock solution of phenylacetylene **1.64** (43.9 µL, 0.400 mmol, 4 equiv) in anhydrous CH_2Cl_2 (1.2 mL, 0.33 M solution) and a stock solution of phenylhydrazine **1.65** (43.3 µL, 0.440 mmol, 4.4 equiv) in anhydrous CH_2Cl_2 (0.8 mL, 0.55 M solution) were prepared. The stock solution of **1.64** (0.3 mL, 0.10 mmol, 1 equiv) and then the stock solution of **1.65** (0.2 mL, 0.11 mmol, 1.1 equiv) were added in sequence to a GC-MS vial equipped with a stirring bar containing the desired [LAuCl] complex (5.0 mmol, 0.05 equiv). The vial was capped, removed from the glovebox, and its content stirred in the dark (Al foil) at 23 ºC. After 24 h, the reaction was quenched by the addition of triethylamine (0.1 mL), then volatiles were removed under reduced pressure. The residue was dissolved in $CDCl_3$, then the internal standard (*n*-dodecane, 22.7 µL, 0.100 mmol, 1 equiv) was added and the ^{1}H NMR spectrum was recorded.

Spectroscopic data for product **1.66** matched those reported in the literature.[85] The following diagnostic signals were integrated to quantify the amount of starting material and product against internal standard: for substrate **1.64**, peak at 3.09 ppm (s, 1H); for product **1.66**, peak at 2.26 ppm (s, 3H); for *n*-dodecane, peak at 0.89 ppm (t, *J* = 7.2 Hz, 6H). **^{1}H NMR** (400 MHz, $CDCl_3$) δ 7.81–7.75 (m, 2H), 7.42–7.13 (m, 8H), 6.91 (t, *J* = 7.20 Hz, 1H), 2.26 (s, 3H).

84. Ferrer, S.; Echavarren, A. M. *Organometallics* **2018**, *37*, 781–786.
85. Yang, H.; Gabbaï, F. P. *J. Am. Chem. Soc.* **2015**, *137*, 13425–13432.

Tandem cycloisomerization-nucleophile addition

2-(Phenylethynyl)cyclohex-2-en-1-one (1.40)

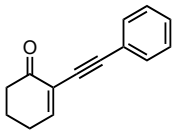

To an oven dried flask were added 2-iodocyclohex-2-en-1-one[86] (1.500 g, 6.756 mmol, 1 equiv), copper iodide (77.2 mg, 0.405 mmol, 6 mol%), bis(triphenylphosphine)palladium(II) dichloride (142.2 mg, 0.203 mmol, 3 mol%). After purging the system with argon THF (45 mL) was added followed by phenylacetylene (1.48 mL, 13.51 mmol, 2.0 equiv). The system was then degassed for 15 min by N_2 sparging with a N_2 balloon while sonicating in an ultrasound bath prior to the addition of diisopropylamine (2.66 mL, 20.27 mmol, 3 equiv) at 0 °C. The mixture was left stirring at the same temperature for 1 h. The reaction was quenched by addition of a saturated NH_4Cl aqueous solution (50 mL) followed by extraction with CH_2Cl_2 (50 mL x 3). The combined organic layers were washed with brine (50 mL), dried over Na_2SO_4, filtered and concentrated. The crude product was purified by FCC (silica, CyH:EtOAc, 98:2). Compound **1.40** was obtained as a pale orange solid (1.049 g, 5.345 mmol, 79% yield). Spectroscopic data for product 1a matched those reported in the literature.[86] **^{1}H NMR** (300 MHz, $CDCl_3$): δ 7.57 – 7.45 (m, 2H), 7.40 – 7.27 (m, 4H), 2.57 – 2.45 (m, 4H), 2.12 – 2.01 (m, 2H).

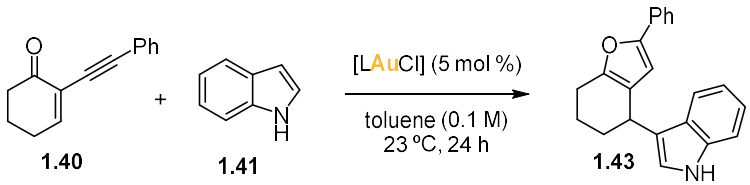

In the glovebox, under Ar, a stock solution of **1.40** (58.9 mg, 0.300 mmol, 6 equiv) in anhydrous toluene (1.8 mL, 0.17 M solution) and a stock solution of indole (38.7 mg, 0.330 mmol, 6.6 equiv) in anhydrous toluene (1.2 mL, 0.27 M solution) were prepared. The stock solution of **1.40** (0.3 mL, 0.05 mmol, 1 equiv) and then the indole stock solution (0.2 mL, 0.055 mmol, 1.1 equiv) were added in sequence to a GC-MS vial equipped with a stirring bar containing the desired [LAuCl] complex (2.5 μmol, 0.05 equiv). The vial was capped, removed from the glovebox, and its content stirred in the dark (Al foil) at 23 ºC. After 24 h, the reaction mixture was quenched by the addition of triethylamine (0.1 mL) and filtered through silica in a glass pipette, and volatiles were removed under reduced pressure. The residue was dissolved in $CDCl_3$, then the internal standard (1,1,2,2-tetrachloroethane, 10.6 μL, 0.100 mmol, 2 equiv) was added and the ^{1}H NMR spectrum was recorded. Spectroscopic data for product **1.43** matched those reported in the literature.[86] The following diagnostic signals were integrated to quantify the amount of starting material and product against internal standard: for substrate **1.40**, peak at 3.09 ppm (s, 1H); for product **1.43**, peak at 2.26 ppm (s, 3H); for *n*-dodecane, peak at 0.89 ppm (t, J = 7.2 Hz, 6H). **^{1}H NMR** (400 MHz, $CDCl_3$) δ 7.94 (brs, 1H), 7.63 (d, J = 8.0 Hz, 1H), 7.60 (dd, J = 8.4, 1.2 Hz, 2H), 7.38 (dt, J = 8.1, 0.8 Hz, 1H), 7.36–7.30 (m, 2H), 7.25–7.17 (m, 2H), 7.12 (ddd, J = 8.0, 7.0, 1.0 Hz, 1H), 6.88 (d, J = 2.0 Hz, 1H), 6.45 (s, 1H), 4.27 (t, J = 5.7 Hz, 1H), 2.85–2.69 (m, 2H), 2.23–2.10 (m, 2H), 2.03–1.91 (m, 2H), 1.91–1.79 (m, 1H).

86. Rauniyar, V.; Wang, Z. J.; Burks, H. E.; Toste, F. D. *J. Am. Chem. Soc*. **2011**, *133*, 8486–8489

Crystallographic Data[87]

Complex **A (CCDC2072784)**

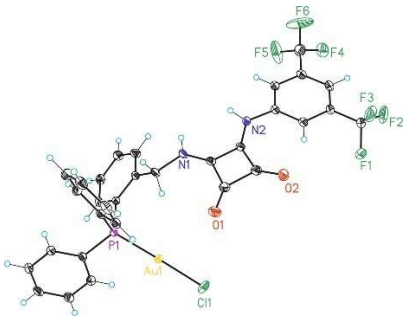

Table 1.6. Crystal data and structure refinement for AF-2-117 (complex **A**)

Identification code	af-2-117	
Empirical formula	$C_{33}H_{27}AuClF_6N_2O_3PS$	
Formula weight	909.01	
Temperature	100(2)K	
Wavelength	0.71073 Å	
Crystal system	monoclinic	
Space group	P 21/n	
Unit cell dimensions	a = 8.29650(10) Å	α = 90°.
	b = 10.97280(10) Å	β = 90.5230(10)°.
	c = 35.4708(4) Å	γ = 90°.
Volume	3228.98(6) $Å^3$	
Z	4	
Density (calculated)	1.870 Mg/m^3	
Absorption coefficient	4.827 mm^{-1}	
F(000)	1776	
Crystal size	0.120 x 0.050 x 0.050 mm^3	
Theta range for data collection	2.183 to 31.905°.	
Index ranges	-12<=h<=12,-16<=k<=16,-52<=l<=52	
Reflections collected	116023	
Independent reflections	10813[R(int) = 0.0421]	
Completeness to theta =31.905°	97.1%	
Absorption correction	Multi-scan	
Max. and min. transmission	1.00 and 0.79	
Refinement method	Full-matrix least-squares on F^2	
Data / restraints / parameters	10813/ 0/ 435	
Goodness-of-fit on F^2	1.052	
Final R indices [I>2sigma(I)]	R1 = 0.0271, wR2 = 0.0613	
R indices (all data)	R1 = 0.0362, wR2 = 0.0637	
Largest diff. peak and hole	2.404 and -0.845 $e.Å^{-3}$	

87. These data are provided free of charge by the joint Cambridge Crystallographic Data Centre (CCDC) and Fachinformationszentrum Karlsruhe Access Structures service. For more information access www.ccdc.cam.ac.uk/structures with the corresponding CCDC codes provided in this section.

Complex **B (CCDC2072785)**

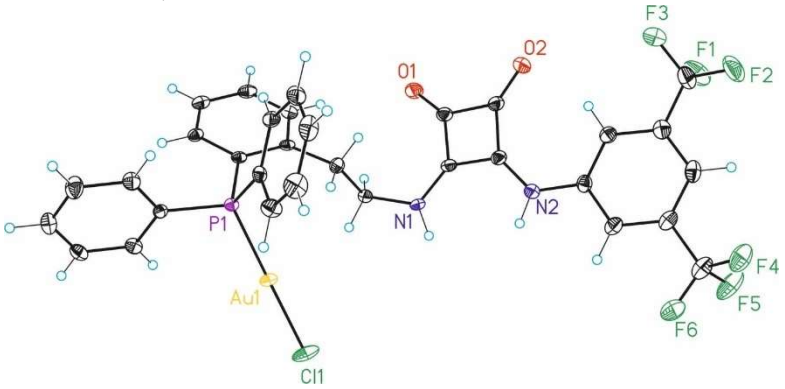

Table 1.7. Crystal data and structure refinement for MO_amz82cdm-05 (complex **B**)

Identification code	mo_AMZ82CDM-05	
Empirical formula	$C_{34}H_{29}AuClF_6N_2O_3PS$	
Formula weight	923.04	
Temperature	100(2)K	
Wavelength	0.71073 Å	
Crystal system	triclinic	
Space group	P -1	
Unit cell dimensions	a = 8.6507(18) Å	α = 100.657(5)°.
	b = 10.983(2) Å	β = 100.260(5)°.
	c = 18.744(4) Å	γ = 92.762(5)°.
Volume	1716.1(6) $Å^3$	
Z	2	
Density (calculated)	1.786 Mg/m^3	
Absorption coefficient	4.542 mm^{-1}	
F(000)	904	
Crystal size	0.200 x 0.040 x 0.030 mm^3	
Theta range for data collection	1.893 to 32.802°.	
Index ranges	-13<=h<=11,-16<=k<=16,0<=l<=28	
Reflections collected	20242	
Independent reflections	20242[R(int) = ?]	
Completeness to theta =32.802°	85.0%	
Absorption correction	Multi-scan	
Max. and min. transmission	0.74 and 0.58	
Refinement method	Full-matrix least-squares on F^2	
Data / restraints / parameters	20242/ 0/ 445	
Goodness-of-fit on F^2	1.036	
Final R indices [I>2sigma(I)]	R1 = 0.0392, wR2 = 0.1043	
R indices (all data)	R1 = 0.0468, wR2 = 0.1080	
Largest diff. peak and hole	2.219 and -2.066 e.$Å^{-3}$	

Complex **C (CCDC2072886)**

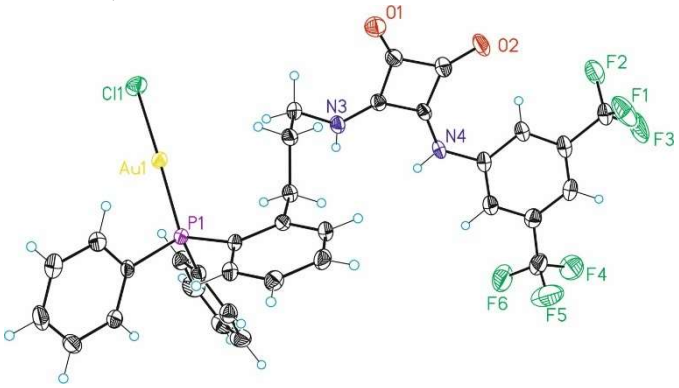

Table 1.8. Crystal data and structure refinement for AMZ-01-50_hklf5 (complex **C**)

Identification code	AMZ-01-50_hklf5	
Empirical formula	$C_{35}H_{31}AuClF_6N_2O_3PS$	
Formula weight	937.06	
Temperature	100(2)K	
Wavelength	0.71073 Å	
Crystal system	triclinic	
Space group	P -1	
Unit cell dimensions	a = 9.07231(19) Å	α = 92.7240(17)°.
	b = 10.5508(2) Å	β = 98.6197(18)°.
	c = 18.9633(5) Å	γ = 97.4765(16)°.
Volume	1775.25(7) $Å^3$	
Z	2	
Density (calculated)	1.753 Mg/m^3	
Absorption coefficient	4.392 mm^{-1}	
F(000)	920	
Crystal size	0.150 x 0.040 x 0.020 mm^3	
Theta range for data collection	2.293 to 29.778°.	
Index ranges	-12<=h<=12,-14<=k<=14,-26<=l<=26	
Reflections collected	24116	
Independent reflections	24116[R(int) = ?]	
Completeness to theta =29.778°	92.7%	
Absorption correction	Multi-scan	
Max. and min. transmission	1.00 and 0.90	
Refinement method	Full-matrix least-squares on F^2	
Data / restraints / parameters	24116/ 0/ 454	
Goodness-of-fit on F^2	1.098	
Final R indices [I>2sigma(I)]	R1 = 0.0350, wR2 = 0.0916	
R indices (all data)	R1 = 0.0395, wR2 = 0.0930	
Largest diff. peak and hole	1.221 and -0.919 e.$Å^{-3}$	

Complex **D (CCDC2072787)**

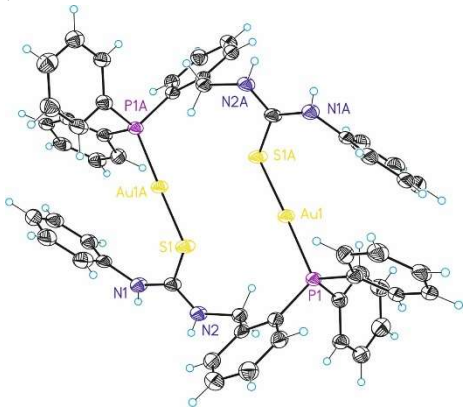

Table 1.9 Crystal data and structure refinement for SN038 (complex **D**)

Identification code	SN038	
Empirical formula	$C_{29}H_{26}AuClN_2PS$	
Formula weight	1017.01	
Temperature	100(2)K	
Wavelength	0.71073 Å	
Crystal system	triclinic	
Space group	P -1	
Unit cell dimensions	a = 12.8894(3) Å	α = 112.813(2)°.
	b = 13.2732(3) Å	β = 115.492(3)°.
	c = 14.2400(4) Å	γ = 96.3314(19)°.
Volume	1911.27(9) $Å^3$	
Z	2	
Density (calculated)	1.767 Mg/m^3	
Absorption coefficient	4.668 mm^{-1}	
F(000)	988	
Crystal size	0.250 x 0.150 x 0.100 mm^3	
Theta range for data collection	2.335 to 27.530°.	
Index ranges	-16<=h<=16,-17<=k<=17,-18<=l<=17	
Reflections collected	136984	
Independent reflections	8275[R(int) = 0.0745]	
Completeness to theta =27.530°	93.9%	
Absorption correction	Multi-scan	
Max. and min. transmission	1.00 and 0.62	
Refinement method	Full-matrix least-squares on F^2	
Data / restraints / parameters	8275/ 18/ 409	
Goodness-of-fit on F^2	1.094	
Final R indices [I>2sigma(I)]	R1 = 0.0481, wR2 = 0.1271	
R indices (all data)	R1 = 0.0603, wR2 = 0.1400	
Largest diff. peak and hole	4.363 and -1.474 e.$Å^{-3}$	

Complex **E (CCDC2072788)**

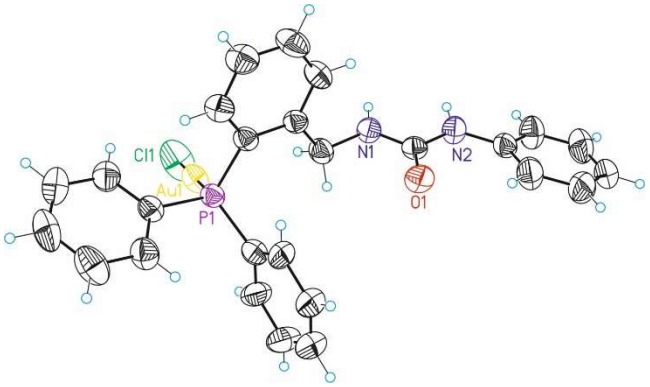

Table 1.10 Crystal data and structure refinement for SN037 (complex **E**)

Identification code	SN037	
Empirical formula	$C_{26}H_{23}AuClN_2OP$	
Formula weight	642.85	
Temperature	296(2)K	
Wavelength	0.71073 Å	
Crystal system	monoclinic	
Space group	P 21/c	
Unit cell dimensions	a = 10.5719(5) Å	α = 90°.
	b = 26.210(3) Å	β = 108.081(7)°.
	c = 9.4120(7) Å	γ = 90°.
Volume	2479.1(3) $Å^3$	
Z	4	
Density (calculated)	1.722 Mg/m^3	
Absorption coefficient	6.127 mm^{-1}	
F(000)	1248	
Crystal size	0.180 x 0.080 x 0.080 mm^3	
Theta range for data collection	2.170 to 29.644°.	
Index ranges	-14<=h<=14,-35<=k<=36,-13<=l<=13	
Reflections collected	70339	
Independent reflections	6637[R(int) = 0.0312]	
Completeness to theta =29.644°	94.9%	
Absorption correction	Multi-scan	
Max. and min. transmission	1.00 and 0.68	
Refinement method	Full-matrix least-squares on F^2	
Data / restraints / parameters	6637/ 108/ 325	
Goodness-of-fit on F^2	1.063	
Final R indices [I>2sigma(I)]	R1 = 0.0367, wR2 = 0.0868	
R indices (all data)	R1 = 0.0513, wR2 = 0.0924	
Largest diff. peak and hole	3.317 and -2.525 $e.Å^{-3}$	

Complex **F (CCDC2072789)**

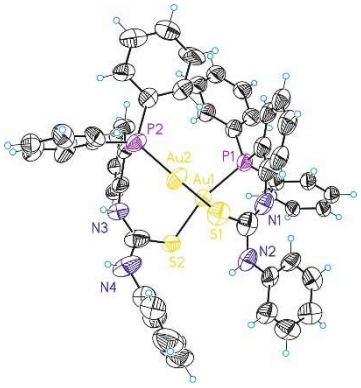

Table 1.11. Crystal data and structure refinement for sn033 (complex F)

Identification code	sn033	
Empirical formula	$C_{25.50}H_{22.50}Au\,Cl_{1.50}N_2\,O_{0.50}P\,S$	
Formula weight	678.13	
Temperature	100(2)K	
Wavelength	0.71073 Å	
Crystal system	triclinic	
Space group	P -1	
Unit cell dimensions	a = 13.2478(6)Å	α = 70.615(4)°.
	b = 14.4203(7)Å	β = 67.464(5)°.
	c = 14.6294(7)Å	γ = 79.009(4)°.
Volume	2428.5(2) $Å^3$	
Z	4	
Density (calculated)	1.855 Mg/m^3	
Absorption coefficient	6.394 mm^{-1}	
F(000)	1316	
Crystal size	0.100 x 0.100 x 0.050 mm^3	
Theta range for data collection	1.996 to 27.427°.	
Index ranges	-17<=h<=14,-18<=k<=17,-18<=l<=18	
Reflections collected	29191	
Independent reflections	9602[R(int) = 0.0789]	
Completeness to theta =27.427°	86.7%	
Absorption correction	Multi-scan	
Max. and min. transmission	1.00 and 0.66	
Refinement method	Full-matrix least-squares on F^2	
Data / restraints / parameters	9602/ 725/ 796	
Goodness-of-fit on F^2	1.924	
Final R indices [I>2sigma(I)]	R1 = 0.1271, wR2 = 0.2985	
R indices (all data)	R1 = 0.1990, wR2 = 0.3298	
Largest diff. peak and hole	6.392 and -3.031 e.$Å^{-3}$	

Complex **G (CCDC2072790)**

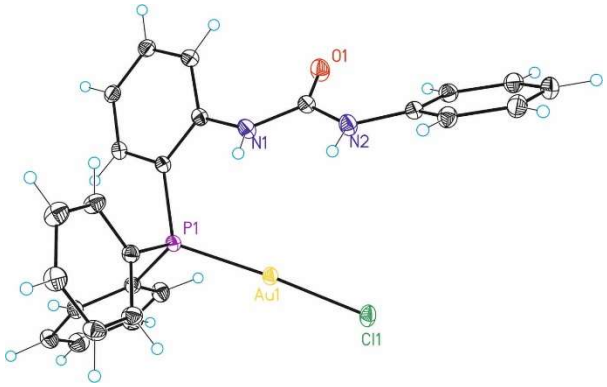

Table 1.12. Crystal data and structure refinement for AF-2-148 (complex **G**)

Identification code	AF-2-148	
Empirical formula	$C_{25}H_{21}AuClN_2OP$	
Formula weight	628.82	
Temperature	100(2)K	
Wavelength	0.71073 Å	
Crystal system	monoclinic	
Space group	P 21/n	
Unit cell dimensions	a = 9.73960(10) Å	α = 90°.
	b = 18.1322(2) Å	β = 102.7750(10)°.
	c = 12.73410(10) Å	γ = 90°.
Volume	2193.18(4) $Å^3$	
Z	4	
Density (calculated)	1.904 Mg/m^3	
Absorption coefficient	6.923 mm^{-1}	
F(000)	1216	
Crystal size	0.100 x 0.050 x 0.050 mm^3	
Theta range for data collection	2.421 to 45.554°.	
Index ranges	-19<=h<=19,-36<=k<=36,-25<=l<=25	
Reflections collected	215866	
Independent reflections	18492[R(int) = 0.0682]	
Completeness to theta =45.554°	99.2%	
Absorption correction	Multi-scan	
Max. and min. transmission	1.00 and 0.65	
Refinement method	Full-matrix least-squares on F^2	
Data / restraints / parameters	18492/ 0/ 280	
Goodness-of-fit on F^2	1.046	
Final R indices [I>2sigma(I)]	R1 = 0.0246, wR2 = 0.0588	
R indices (all data)	R1 = 0.0371, wR2 = 0.0627	
Largest diff. peak and hole	2.504 and -2.547 $e.Å^{-3}$	

Complex **H (CCDC2072791)**

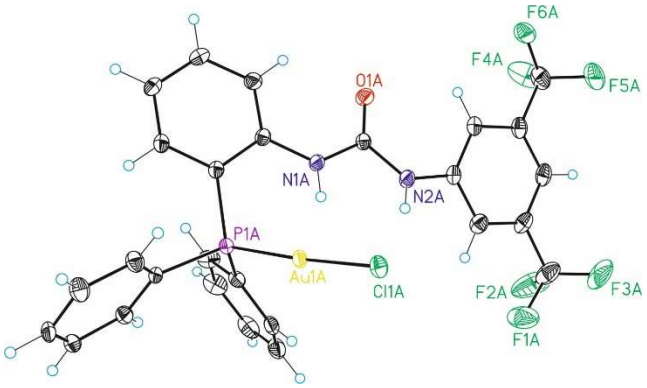

Table 1.13. Crystal data and structure refinement for AMZ-K2 (complex **H**)

Identification code	AMZ-K2	
Empirical formula	$C_{54}H_{38}Au_2Cl_2F_{12}N_4O_2P_2$	
Formula weight	1529.65	
Temperature	100(2)K	
Wavelength	0.71073 Å	
Crystal system	triclinic	
Space group	P -1	
Unit cell dimensions	a = 13.5048(2) Å	α = 97.5529(14)°.
	b = 13.8218(3) Å	β = 100.4450(14)°.
	c = 14.9022(2) Å	γ = 100.8732(15)°.
Volume	2646.62(8) $Å^3$	
Z	2	
Density (calculated)	1.919 Mg/m^3	
Absorption coefficient	5.787 mm^{-1}	
F(000)	1472	
Crystal size	0.150 x 0.100 x 0.080 mm^3	
Theta range for data collection	2.246 to 32.126°.	
Index ranges	-19<=h<=19,-20<=k<=17,-21<=l<=21	
Reflections collected	45241	
Independent reflections	16767[R(int) = 0.0255]	
Completeness to theta =32.126°	90.1%	
Absorption correction	Multi-scan	
Max. and min. transmission	1.00 and 0.87	
Refinement method	Full-matrix least-squares on F^2	
Data / restraints / parameters	16767/ 147/ 805	
Goodness-of-fit on F^2	1.025	
Final R indices [I>2sigma(I)]	R1 = 0.0263, wR2 = 0.0515	
R indices (all data)	R1 = 0.0412, wR2 = 0.0548	
Largest diff. peak and hole	1.357 and -0.893 $e.Å^{-3}$	

Complex **I (CCDC2072792)**

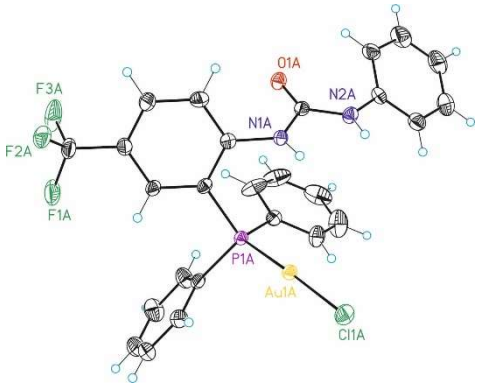

Table 1.14. Crystal data and structure refinement for mo_AF12151-05 (complex **I**)

Identification code	mo_AF12151-05	
Empirical formula	$C_{53}H_{41}Au_2Cl_5F_6N_4O_2P_2$	
Formula weight	1513.02	
Temperature	100(2)K	
Wavelength	0.71073 Å	
Crystal system	monoclinic	
Space group	P 21/n	
Unit cell dimensions	a = 22.8738(16) Å	α = 90°.
	b = 9.3434(6) Å	β = 110.7762(15)°.
	c = 27.0634(18) Å	γ = 90°.
Volume	5407.8(6) $Å^3$	
Z	4	
Density (calculated)	1.858 Mg/m^3	
Absorption coefficient	5.791 mm^{-1}	
F(000)	2920	
Crystal size	0.300 x 0.020 x 0.020 mm^3	
Theta range for data collection	1.610 to 33.875°.	
Index ranges	-35<=h<=33,0<=k<=14,0<=l<=41	
Reflections collected	21932	
Independent reflections	21932[R(int) = ?]	
Completeness to theta =33.875°	96.9%	
Absorption correction	Multi-scan	
Max. and min. transmission	0.74 and 0.52	
Refinement method	Full-matrix least-squares on F^2	
Data / restraints / parameters	21932/ 62/ 713	
Goodness-of-fit on F^2	1.030	
Final R indices [I>2sigma(I)]	R1 = 0.0476, wR2 = 0.1017	
R indices (all data)	R1 = 0.0676, wR2 = 0.1097	
Largest diff. peak and hole	2.964 and -2.245 $e.Å^{-3}$	

Complex **J (CCDC2072793)**

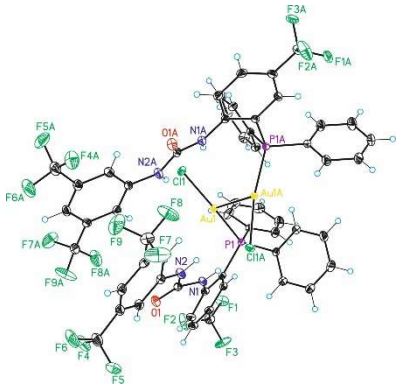

Table 1.15. Crystal data and structure refinement for mo_AF2220B_0m (complex **J**)

Identification code	mo_AF2220B_0m	
Empirical formula	$C_{29}H_{20}AuCl_3F_9N_2OP$	
Formula weight	917.76	
Temperature	100(2)K	
Wavelength	0.71073 Å	
Crystal system	monoclinic	
Space group	C 2/c	
Unit cell dimensions	a = 28.692(2) Å	α = 90°.
	b = 15.5102(13) Å	β = 133.0889(18)°.
	c = 19.7109(17) Å	γ = 90°.
Volume	6405.9(9) $Å^3$	
Z	8	
Density (calculated)	1.903 Mg/m^3	
Absorption coefficient	4.974 mm^{-1}	
F(000)	3536	
Crystal size	0.300 x 0.100 x 0.050 mm^3	
Theta range for data collection	1.633 to 33.154°.	
Index ranges	-44<=h<=25,-23<=k<=21,-29<=l<=30	
Reflections collected	43040	
Independent reflections	12107[R(int) = 0.0297]	
Completeness to theta =33.154°	99.1%	
Absorption correction	Multi-scan	
Max. and min. transmission	0.74 and 0.57	
Refinement method	Full-matrix least-squares on F^2	
Data / restraints / parameters	12107/ 64/ 460	
Goodness-of-fit on F^2	1.027	
Final R indices [I>2sigma(I)]	R1 = 0.0215, wR2 = 0.0412	
R indices (all data)	R1 = 0.0321, wR2 = 0.0438	
Largest diff. peak and hole	0.971 and -0.642 $e.Å^{-3}$	

Complex **K (CCDC2072794)**

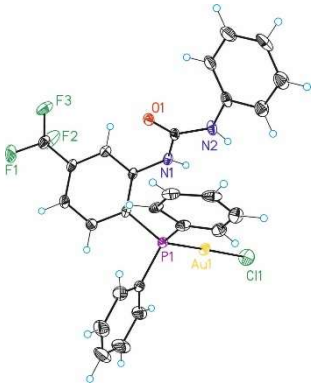

Table 1.16. Crystal data and structure refinement for mo_AF2135 (complex **K**)

Identification code	mo_AF2135	
Empirical formula	$C_{27}H_{22}AuCl_3F_3N_2OP$	
Formula weight	781.75	
Temperature	100(2)K	
Wavelength	0.71073 Å	
Crystal system	orthorhombic	
Space group	P b c a	
Unit cell dimensions	a = 17.8967(18) Å	α = 90°.
	b = 9.2995(9) Å	β = 90°.
	c = 33.374(3) Å	γ = 90°.
Volume	5554.5(9) $Å^3$	
Z	8	
Density (calculated)	1.870 Mg/m^3	
Absorption coefficient	5.688 mm^{-1}	
F(000)	3024	
Crystal size	0.200 x 0.100 x 0.020 mm^3	
Theta range for data collection	1.220 to 33.261°.	
Index ranges	-27<=h<=21,-14<=k<=14,-48<=l<=39	
Reflections collected	65974	
Independent reflections	10400[R(int) = 0.0529]	
Completeness to theta =33.261°	97.3%	
Absorption correction	Multi-scan	
Max. and min. transmission	0.74 and 0.55	
Refinement method	Full-matrix least-squares on F^2	
Data / restraints / parameters	10400/ 104/ 430	
Goodness-of-fit on F^2	1.069	
Final R indices [I>2sigma(I)]	R1 = 0.0390, wR2 = 0.0694	
R indices (all data)	R1 = 0.0611, wR2 = 0.0761	
Largest diff. peak and hole	2.221 and -2.009 $e.Å^{-3}$	

Complex **L (CCDC2072795)**

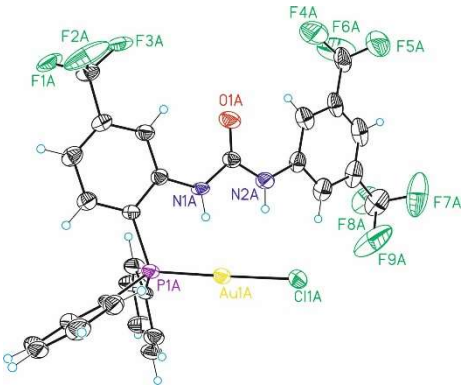

Table 1.17. Crystal data and structure refinement for AMZ-2-40_hklf5 (complex **L**)

Identification code	AMZ-2-40_hklf5	
Empirical formula	$C_{28.50}H_{19}AuCl_2F_9N_2OP$	
Formula weight	875.29	
Temperature	100(2)K	
Wavelength	0.71073 Å	
Crystal system	triclinic	
Space group	P -1	
Unit cell dimensions	a = 16.8101(4) Å	α = 88.2055(19)°.
	b = 17.7662(4) Å	β = 86.921(2)°.
	c = 22.7614(6) Å	γ = 63.318(2)°.
Volume	6064.9(3) $Å^3$	
Z	8	
Density (calculated)	1.917 Mg/m^3	
Absorption coefficient	5.163 mm^{-1}	
F(000)	3368	
Crystal size	0.250 x 0.200 x 0.100 mm^3	
Theta range for data collection	2.210 to 32.209°.	
Index ranges	-24<=h<=24,-25<=k<=25,-33<=l<=33	
Reflections collected	42797	
Independent reflections	42797[R(int) = ?]	
Completeness to theta =32.209°	94.2%	
Absorption correction	Multi-scan	
Max. and min. transmission	1.00 and 0.78	
Refinement method	Full-matrix least-squares on F^2	
Data / restraints / parameters	42797/ 6/ 1640	
Goodness-of-fit on F^2	1.047	
Final R indices [I>2sigma(I)]	R1 = 0.0486, wR2 = 0.1280	
R indices (all data)	R1 = 0.1076, wR2 = 0.1447	
Largest diff. peak and hole	1.913 and -2.114 $e.Å^{-3}$	

DFT Calculations

Computational methods

Calculations were carried out using the Gaussian09 package[88] at the density functional theory (DFT) level by means of the B3LYP[89] functional. Reported geometries and energies were calculated including the corrected dispersion GD3.[90] The 6-31G(d,p)[91] basis set was implemented on all atoms (C, H, N, O, F, P, Cl), except for Au for which the SDD[92] basis set and its corresponding ECP were used. All systems were calculated in CH_2Cl_2 whose solvation effects were accounted for using the implicit polarizable continuum model (PCM)[93]. Each stationary point was characterized by vibrational analysis. Transition states (TS) were identified by the presence of a single imaginary frequency while all minima presented only real frequencies. To further confirm the identity of the TS, relaxation experiments of the imaginary frequency were performed connecting reactants and products. Reported energies have been corrected with the thermal and entropic corrections by means of single point calculations at the 6-311G(d,p)[91] level on all atoms (C, H, N, O, F, P, Cl), except for Au for which the SDD basis set and ECP were used. Optimized geometries were visualized using CYLView.[94] A dataset collection of computational results of this chapter is available in the ioChem-BD[95] repository and can be accessed through: doi:10.19061/iochem-bd-1-350.

88. Gaussian 09, Revision D.01, M. J. Frisch, G. W. Trucks, H. B. Schlegel, G. E. Scuseria, M. A. Robb, J. R. Cheeseman, G. Scalmani, V. Barone, B. Mennucci, G. A. Petersson, H. Nakatsuji, M. Caricato, X. Li, H. P. Hratchian, A. F. Izmaylov, J. Bloino, G. Zheng, J. L. Sonnenberg, M. Hada, M. Ehara, K. Toyota, R. Fukuda, J. Hasegawa, M. Ishida, T. Nakajima, Y. Honda, O. Kitao, H. Nakai, T. Vreven, J. A. Montgomery, Jr., J. E. Peralta, F. Ogliaro, M. Bearpark, J. J. Heyd, E. Brothers, K. N. Kudin, V. N. Staroverov, T. Keith, R. Kobayashi, J. Normand, K. Raghavachari, A. Rendell, J. C. Burant, S. S. Iyengar, J. Tomasi, M. Cossi, N. Rega, J. M. Millam, M. Klene, J. E. Knox, J. B. Cross, V. Bakken, C. Adamo, J. Jaramillo, R. Gomperts, R. E. Stratmann, O. Yazyev, A. J. Austin, R. Cammi, C. Pomelli, J. W. Ochterski, R. L. Martin, K. Morokuma, V. G. Zakrzewski, G. A. Voth, P. Salvador, J. J. Dannenberg, S. Dapprich, A. D. Daniels, O. Farkas, J. B. Foresman, J. V. Ortiz, J. Cioslowski, D. J. Fox, Gaussian, Inc., Wallingford CT, **2013**.
89. a) A. D. Becke, *J. Chem. Phys.* **1993**, *98*, 5648–5652. b) C. Lee, W. Yang, R. G. Parr, *Phys. Rev. B.* **1988**, *37*, 785–789. c) S. H. Vosko, L. Wilk, M. Nusair, *Can. J. Phys.* **1980**, *58*, 1200–1211. d) P. J. Stephens, F. J. Devlin, C. F. Chabalowsky, M. J. Frisch, *J. Phys. Chem.* **1994**, *98*, 11623–11627.
90. S. Grimme, J. Antony, S. Ehrlich, H. Krieg, *J. Chem. Phys.* **2010**, *132*, 154104-1–19.
91. W. J. Hehre, R. Ditchfield, J. A. Pople, *J. Chem. Phys.* **1972**, 56, 2257–2261.
92. D. Andrae, U. Häussermann, M. Dolg, H. Stoll, H. Preuss, *Theor. Chim. Acta* **1990**, 77, 123–141.
93. E. Cancès, B. Mennucci, J. Tomasi, *J. Chem. Phys.* **1997**, 107, 3032−3041.
94. C. Y. Legault, CYLview 1.0b; Université de Sherbrooke, 2009; http://www.cylview.org.
95. Álvarez-Moreno, M.; De Graaf, C.; López, N.; Maseras, F.; Poblet, J. M.; Bo, C. *J. Chem. Inf. Model.* **2015**, *55*, 95–103.

Computed structures and energies

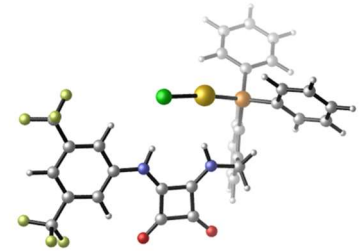

A

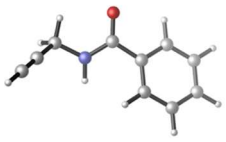

1.25

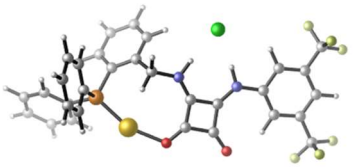

Int_Ia

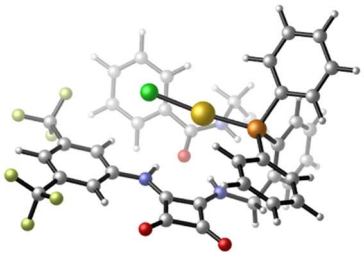

Int_Ib

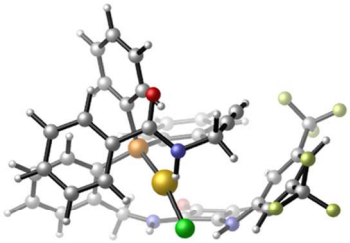

Int_IIb

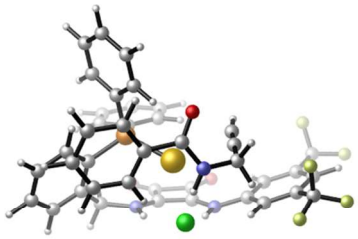

TS II-IIIb

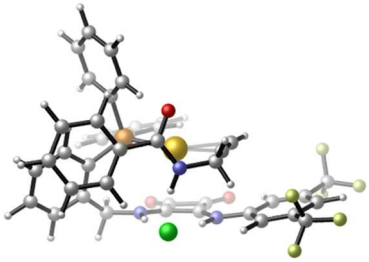

Int_IIIb

Table 1.18. Potential energies E and free energies in solution (G_{sol}), of relevant calculated structures for the activation of the Au-Cl bond using phosphinosquaramide **A** in the cyclization of *N*-propargylbenzamide **1.25a**.

	E (Hartree)	**G_{sol}[b] (Hartree)**
A	−2991.0742	−2990.6950

1.25	−516.5602	−516.4336
Int_Ia	−2991.0510	−2990.6726
Int_Ib	−3507.6681	−3507.1320
Int_IIb	−3507.6675	−3507.1301
TS_II-IIIb	−3507.6586	−3507.1213
Int_IIIb	−3507.6632	−3507.1282

Chapter 2: Gold(I)-Catalyzed Hydrogen Bonded Counterion-Directed Catalysis

Introduction

Counterion Effect in Gold(I) Catalysis

The counteranion plays a crucial role in determining the reactivity and selectivity of gold(I)-catalyzed reactions. Its properties, such as basicity, coordination ability, and steric bulk, significantly influence the energy barriers associated with various steps in the catalytic cycle.[1] The group of Hammond and coworkers established a relatively comprehensive scale indicating the affinity to the metal center of the most employed counterions in gold(I) catalysis, using the calculated dissociation energy of a triphenylphosphine gold chloride complex in CH_2Cl_2 (Table 2.1). The gold(I) affinity index (GAI), ranges from 0 to 10, where the bigger number indicates a higher affinity to gold(I), assigned to I^-. As expected, the affinity of the counterion toward the cationic gold(I) complex depended on the size and the charge distribution of the anion. Large, negatively charged, highly delocalized counterions presented a lower GAI (e.g., BF_4^-, CTf_3^-, SbF_6^-). On the other hand, counterions like TFA^- which are relatively small and have a more localized charge, form stronger interactions with the metal center (Table 2.1, entry 4).

Table 2.1. Gold affinity index of counterions.

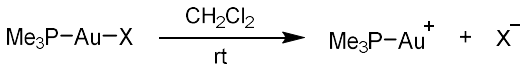

Entry	Counterion	ΔE (kJ/mol)[a]	GAI
1	I^-	143.8	10
2	Br^-	67.7	6.0
3	Cl^-	53.9	5.2
4	TFA^-	74	6.3
5	OAc^-	70.6	6.1
6	OTs^-	28	3.8
7	NTf_2^-	10.4	2.9
8	OTf^-	0	2.4
9	BF_4^-	-35.1	0.5
10	CTf_3^-	-40.5	0.2
11	SbF_6^-	-44.3	0
12	$Al[OC(CF_3)_3]_4^-$	<-45	<0
13	$BArF_4^-$	<-45	<0

[a] The energy difference refers to the dissociation energy, the difference between the neutral catalyst and the dissociated ion pairs.

For instance, Davies and coworkers demonstrated the crucial influence of anions in gold(I)-catalyzed synthesis of substituted pyrroles *via* the ring-opening of alkynyl aziridines **2.1** (Scheme

1. a) Jia, M.; Bandini, M. *ACS Catal.* **2015**, *5*, 1638–1652. b) Zuccaccia, D.; Del Zotto, A.; Baratta, W. *Coord. Chem. Rev,***2019**, *396*, 103–116. c) Lu, Z.; Li, T.; Mudshinge, S. R.; Xu, B.; Hammond, G. B. *Chem. Rev.* **2021**, *121*, 8452–8477.

2.1).[2] Specifically, they achieved the selective formation of regioisomeric disubstituted NTs pyrroles (**2.2** and **2.3**) using either [(PPh_3)AuOTf] or [(PPh_3)AuOTs] (Scheme 2.4). This divergent chemical outcome was explained by the differing basicities (*pKa* of the corresponding conjugate acids in DCE: HNO_3, −1.7; HBF_4, −10.3; TfOH, −11.4; Tf_2NH, −11.9; $HClO_4$, −13.0)[3] of the metal counterion and the reaction medium. The more basic OTs^- favored a rearomatization/protodeauration sequence (path a), leading to 2,5-disubstituted pyrroles (**2.2**). In contrast, the more electrophilic gold(I) complex (X = OTf) promoted a 1,2-aryl shift (path b), resulting in the major formation of 2,4-disubstituted pyrroles (**2.3**). These reports demonstrated that anions can significantly affect not only the chemical profile of gold(I) catalysis but also the overall kinetics. In solution, poorly dissociated counterions generally deliver a lower amount of catalytically active cationic gold species which result in reduced activities. In fact, in this example, they accounted for this matter by heating up the reaction in DCE, in the example with the more coordinating OTs anion.

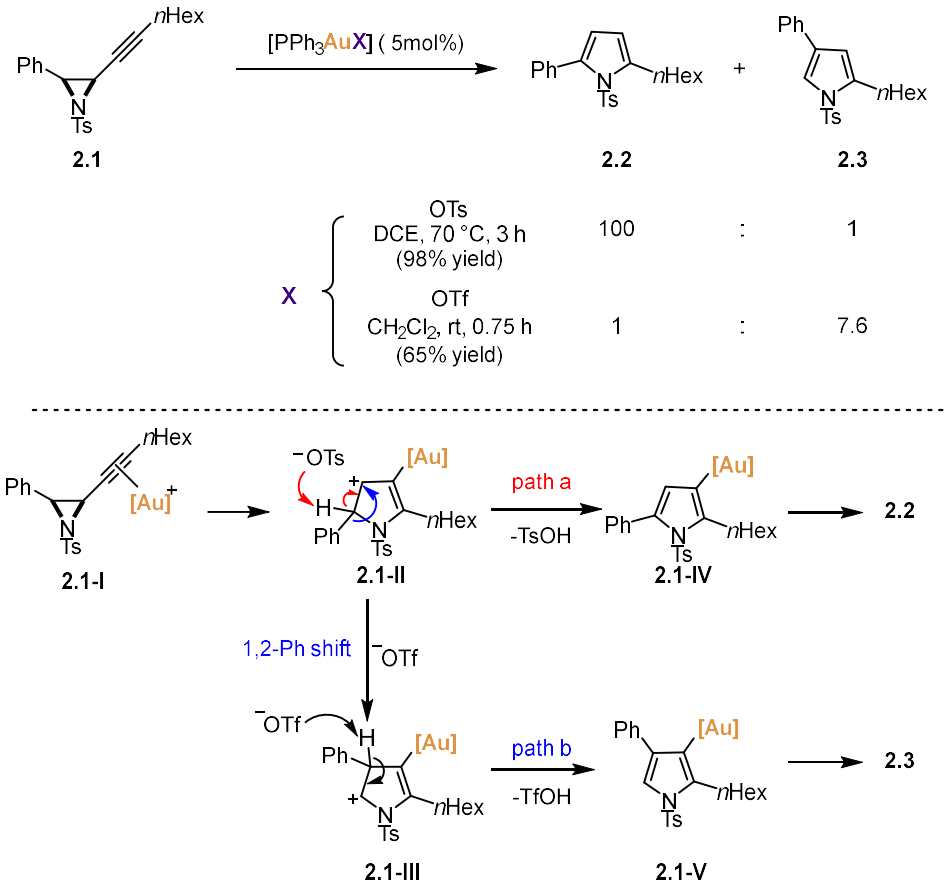

Scheme 2.1. Pivotal role of counterion in the outcome of gold(I)-catalyzed reactions.

Asymmetric Counterion Directed Catalysis (ACDC) in Gold(I) Catalysis

Performing enantioselective gold(I) catalysis has proven not trivial due to the special characteristics of this metal described in the **General Introduction**. Gold(I) complexes usually present a linear dicoordinated geometry,[4] which places the ligand on the opposite site of the

2. a) Davies, P. W.; Martin, N. *Org. Lett.* **2009**, *11*, 2293–2296. b) Davies, P. W.; Martin, N. *J. Organomet.* **2011**, *696*, 159–164.
3. a) Kütt, A.; Rodima, T.; Saame, J.; Raamat, E.; Mäemets, V.; Kaljurand, I.; Koppel, I. A.; Garlyauskayte, R. Yu.; Yagupolskii, Y. L.; Yagupolskii, L. M.; Bernhardt, E.; Willner, H.; Leito, I. *J. Org. Chem.* **2011**, *76*, 391–395.
4. Herrera, R. P.; Gimeno, M. C. *Chem. Rev.* **2021**, *121*, 8311–8363.

substrate, thus hampering transmission of the stereochemical information embedded in a chiral ligand to the reaction center. An alternative appealing strategy to chiral ligands consists in placing the stereochemical information not on the ligand, but on its counterion instead, in an approach termed "Asymmetric Counterion-Directed Catalysis" (ACDC).[5] In 2006, Mayer and List reported on their seminal work the asymmetric conjugate reduction of aldehydes **2.4** via iminium base-organocatalysis, using Hantzsch ester **2.5** as reducing agent. A chiral salt was generated by mixing an achiral secondary amine with a chiral BINOL-based phosphoric acid (***(R)*-TRIP-H**). The generation of chiral intermediate **2.7**, held by electrostatic interactions, rendered the whole process enantioselective and allowed the formation of product **2.6** in high yield and excellent enantioselectivities (Scheme 2.2). This work represented the first highly enantioselective transformation relying solely on the chirality of an anionic counterion to induce asymmetry.[5a]

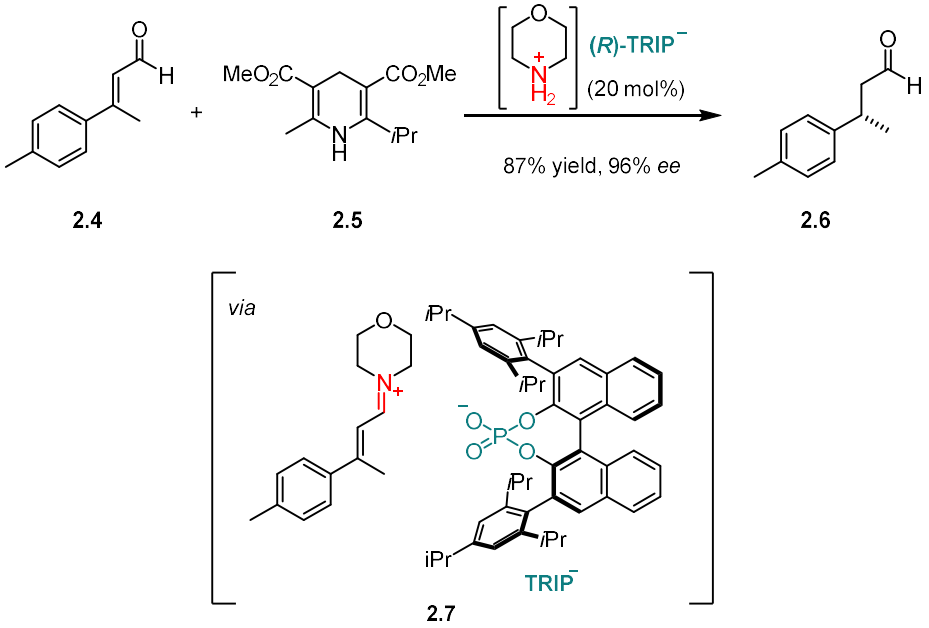

Scheme 2.2. First highly enantioselective application of ACDC.

When combining transition metal catalysis and chiral anions, an additional layer of complexity arises. The chiral anion's positioning relative to the reaction center, critical for achieving successful ACDC, is often influenced by difficult-to-predict electrostatic interactions with the cationic complex or intermediate, or by the presence of a protic group on the substrate. As a result, the non-covalent interactions essential for enantioinduction[6] are typically not built into the catalytic system from the start. Instead, they are identified during the optimization process through extensive trial and error and are usually understood only afterwards.[7]

In 2007, groundbreaking work by Toste and coworkers proved that it was possible to perform gold(I) catalysis enantioselectively by using achiral ligands together with chiral anions. They reported the combination of a dinuclear gold(I) complex with a chiral silver phosphate to realize

5. a) Mayer, S.; List, B. *Angew. Chem. Int. Ed.* **2006**, *45*, 4193–4195. b) Mukherjee, S.; List, B. *J. Am. Chem. Soc.* **2007**, *129*, 11336–11337. c) Phipps, R. J.; Hamilton, G. L.; Toste, F. D. *Nat. Chem.* **2012**, *4*, 603–614. d) Mahlau, M.; List, B. *Angew. Chem. Int.* Ed. **2013**, *52*, 518–533.
6. a) Neel, A. J.; Hilton, M. J.; Sigman, M. S.; Toste, F. D. *Nature* **2017**, *543*, 637–646. b) Fanourakis, A.; Docherty, P. J.; Chuentragool, P.; Phipps, R. J. *ACS Catal.* **2020**, *10*, 10672–10714.
7. a) Duarte, F.; Paton, R. S. *J. Am. Chem. Soc.* **2017**, *139*, 8886–8896. b) Orlandi, M.; Coelho, J. A. S.; Hilton, M. J.; Toste, F. D.; Sigman, M. S. *J. Am. Chem. Soc.* **2017**, *139*, 6803–6806. c) Shoja, A.; Reid, J. P. *J. Am. Chem. Soc.* **2021**, *143*, 7209–7215

the first metal-catalyzed ACDC for the cyclization of allenes (Scheme 2.3).[8] This encouraged the application of ACDC to other Au(I)-catalyzed transformations, in combination with both achiral[9] and chiral[10] gold(I) complexes.

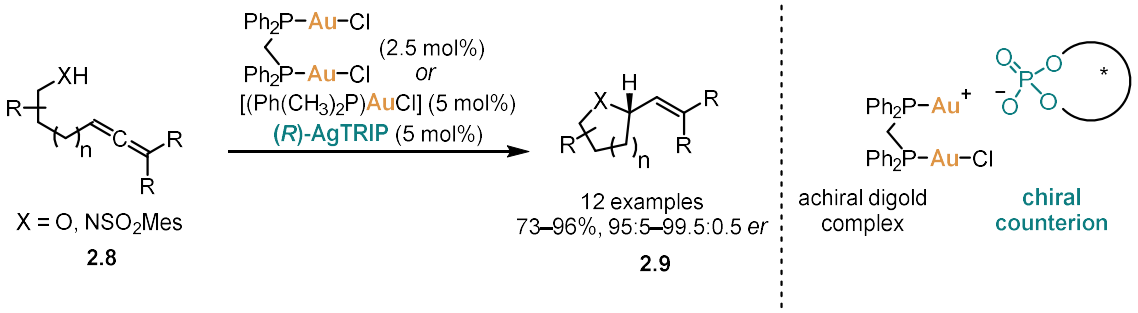

Scheme 2.3. Cyclization of allenols via gold(I)-catalyzed ACDC.

Nevertheless, nearly all examples of Au(I)-ACDC reported to date refer to reactions of prochiral allene substrates.[9,10] The only exceptions are the desymmetrization of diynes of type **2.7** described by the group of Czekelius (Scheme 2.4),[11] and cases of tandem Au/chiral acid catalysis wherein gold is generally not involved in the enantiodetermining step but rather participates on the formation of a prochiral intermediate.[12] To the best of our knowledge, all other attempts to apply the ACDC approach in more challenging asymmetric Au(I)-catalyzed reactions of alkynes,[9,10,13] which, unlike allenes, cannot be prochiral in themselves, were unsuccessful.

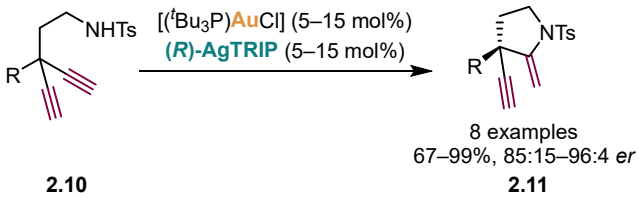

Scheme 2.4. Gold(I) catalyzed desymmetrization of diynes via ACDC.

Alternatively, the chiral anion can be precisely positioned by a rigid covalent linkage to the ligand, as in the "tethered counterion-directed catalysis" (TCDC) strategy recently disclosed by

8. Hamilton, G. L.; Kang, E. J.; Mba, M.; Toste, F. D. *Science* **2007**, *317*, 496–499.
9. a) LaLonde, R. L.; Wang, Z. J.; Mba, M.; Lackner, A. D.; Toste, F. D. *Angew. Chem. Int. Ed.* **2010**, *49*, 598–601. b) Miles, D. H.; Veguillas, M.; Toste, F. D. *Chem. Sci.* **2013**, *4*, 3427–3431. c) Zi, W.; Toste, F. D. *Angew. Chem. Int. Ed.* **2015**, *54*, 14447–14451. e) Pedrazzani, R.; An, J.; Monari, M.; Bandini, M. *Eur. J. Org. Chem.* **2021**, *2021*, 1732–1736. e) Liu, X.-S.; Tang, Z.; Si, Z.-Y.; Zhang, Z.; Zhao, L.; Liu, L. *Angew. Chem. Int. Ed.* **2022**, *61*, e202208874.
10. a) Aikawa, K.; Kojima, M.; Mikami, K. *Angew. Chem. Int. Ed.* **2009**, *48*, 6073–6077. b) Aikawa, K.; Kojima, M.; Mikami, K. *Adv. Synth. Cat.***2010**, *352*, 3131–3135. Corrigendum: Aikawa, K.; Kojima, M.; Mikami, K. *Adv. Synth. Cat.***2011**, *353*, 2882–2883. c) Barreiro, E. M.; Broggini, D. F. D.; Adrio, L. A.; White, A. J. P.; Schwenk, R.; Togni, A.; Hii, K. K. (Mimi). *Organometallics* **2012**, *31*, 3745–3754. d) Miles, D. H.; Veguillas, M.; Toste, F. D. *Chem. Sci.* **2013**, *4*, 3427. e) Handa, S.; Lippincott, D. J.; Aue, D. H.; Lipshutz, B. H. *Angew. Chem. Int. Ed.* **2014**, *53*, 10658–10662.
11. a) Mourad, A. K.; Leutzow, J.; Czekelius, C. *Angew. Chem. Int. Ed.* **2012**, *51*, 11149–11152. b) Spittler, M.; Lutsenko, K.; Czekelius, C. *J. Org. Chem.* **2016**, *81*, 6100–6105.
12. a) Han, Z.-Y.; Xiao, H.; Chen, X.-H.; Gong, L.-Z. *J. Am. Chem. Soc.* **2009**, *131*, 9182–9183. b) Muratore, M. E.; Holloway, C. A.; Pilling, A. W.; Storer, R. I.; Trevitt, G.; Dixon, D. J. *J. Am. Chem. Soc.* **2009**, *131*, 10796–10797. c) Liu, X.-Y.; Che, C.-M. *Org. Lett.* **2009**, *11*, 4204–4207. d) Tu, X.-F.; Gong, L.-Z. *Angew. Chem. Int. Ed.* **2012**, *51*, 11346–11349. e) Cala, L.; Mendoza, A.; Fañanás, F. J.; Rodríguez, F. *Chem. Commun.* **2013**, *49*, 2715. f) Zhou, S.; Li, Y.; Liu, X.; Hu, W.; Ke, Z.; Xu, X. *J. Am. Chem. Soc.* **2021**, *143*, 14703–14711.
13. a) Dorel, R.; Echavarren, A. M. *Chem. Rev.* **2015**, *115*, 9028–9072. b) Zuccarello, G.; Escofet, I.; Caniparoli, U.; Echavarren, A. M. *ChemPlusChem* **2021**, *86*, 1283–1296.

Marinetti, Guinchard and coworkers for the enantioselective Au(I)-catalyzed tandem cycloisomerization-nucleophile addition to 2-alkynyl enones (**1.40**), with and without the addition of Ag(I) additives (Scheme 2.5).[14] However, despite its elegance, this approach is the same as using a chiral ligand, so it is devoid of the flexibility and combinatorial potential offered by the original 2-component ACDC.

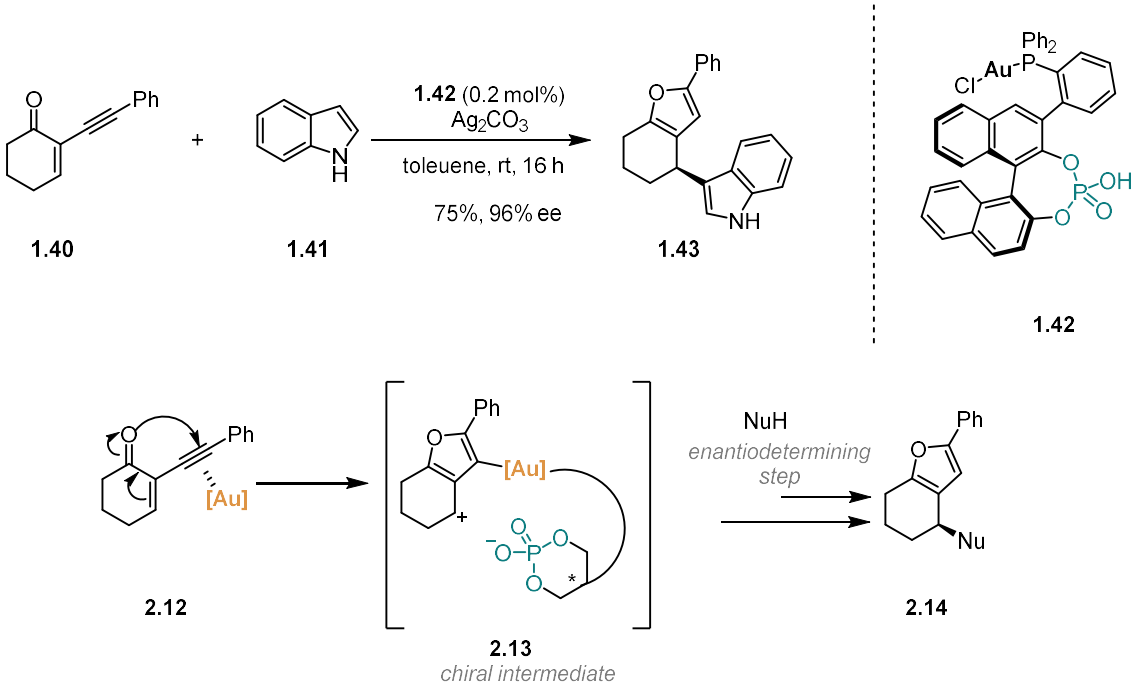

Scheme 2.5. Application of the Tethered Counterion-Directed Catalysis to the tandem cycloisomerization-nucleophile addition to 2-alkynyl-enones.

Anion Binding Catalysis

Anion binding catalysis operates on the principle that the catalyst forms hydrogen bonds with the anionic species, effectively modulating the electronic environment and spatial orientation of the cationic intermediate. This interaction stabilizes specific transition states over others, thereby influencing the outcome of the reaction in terms of both reactivity and enantioselectivity. This strategy is particularly valuable in reactions where traditional methods of asymmetric catalysis may be challenging, as it offers a way to exert control over the reaction's stereochemistry through non-covalent interactions with the anion. Consequently, anion binding catalysis has become a powerful tool in the development of highly enantioselective transformations.[5c,15] For example, Jacobsen and coworkers reported the asymmetric thiourea-catalyzed addition of silyl ketene acetals **2.16** to 1-chloroisochromanes **2.15** with excellent yields and enantioselectivities (Scheme 2.6).[16] The reaction proceeds through a dynamic kinetic resolution mechanism, as evidenced by the fact that the products are isolated in yields exceeding 50%, and the enantioselectivity remains consistent throughout the process. This suggests that racemization of the chloroether starting

14. a) Zhang, Z.; Smal, V.; Retailleau, P.; Voituriez, A.; Frison, G.; Marinetti, A.; Guinchard, X. *J. Am. Chem. Soc.* **2020**, *142*, 3797–3805. b) Yu, Y.; Zhang, Z.; Voituriez, A.; Rabasso, N.; Frison, G.; Marinetti, A.; Guinchard, X. *Chem. Commun.* **2021**, *57*, 10779–10782. c) Zhang, Z.; Sabat, N.; Frison, G.; Marinetti, A.; Guinchard, X. *ACS Catal.* **2022**, *12*, 4046–4053. d) Yu, Y.; Daghmoum, M.; Sabat, N.; Zhang, Z.; Frison, G.; Marinetti, A.; Guinchard, X. *Adv. Synth. Cat.***2024**, *366*, 2613–2622.
15. a) Doyle, A. G.; Jacobsen, E. N. *Chem. Rev.* **2007**, *107*, 5713–5743.b) Nishikawa, Y. *Tetrahedron Lett.* **2018**, *59*, 216–223. c) Ovian, J. M.; Vojáčková, P.; Jacobsen, E. N. *Nature* **2023**, *616*, 84–89.
16. Reisman, S. E.; Doyle, A. G.; Jacobsen, E. N. *J. Am. Chem. Soc.* **2008**, *130*, 7198–7199.

materials likely occurs via the in-situ formation of oxocarbenium ions **2.18**, facilitated by thiourea-assisted chloride dissociation. Support for chloride-binding catalysis was provided by the fact that addition of 10 mol% nBu$_4$NCl resulted in complete inhibition of the reaction. The presence and configuration of an aryl group in the amide component of the catalyst had a large impact on the reaction rate and enantioselectivity, which could be indicative of this group's involvement in stabilizing interactions in the rate-determining transition state (Scheme 2.6).

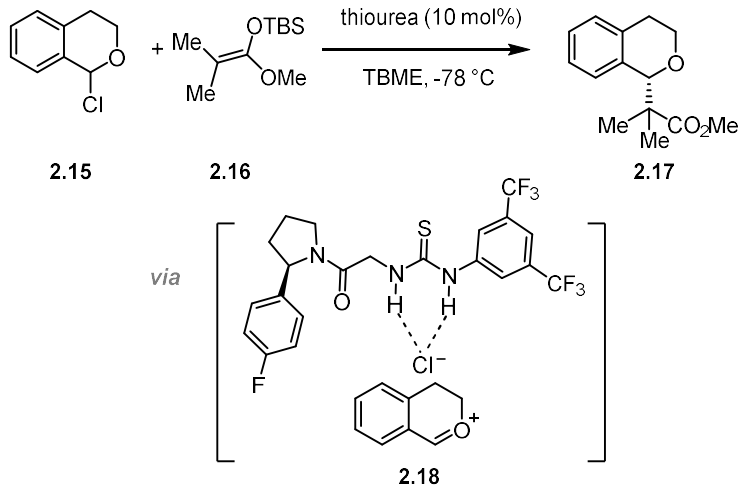

Scheme 2.6. Enantioselective thiourea-catalyzed additions to oxocarbenium ions.

The beneficial effects of hydrogen-bond donors (HBD) in transition-metal catalysis have also been well-documented.[12,17] Achiral HBD have been used as additives to boost the reactivity of organometallic complexes, likely by reducing the coordination strength of anionic ligands (Scheme 2.7).[17] Additionally, chiral organic compounds containing hydrogen-bond donor (HBD) components have been employed as cocatalysts in asymmetric transition-metal-catalyzed transformations.[12,18] In the proposed mechanisms for stereo-induction in these cases, the organocatalyst typically either functions as a ligand on the metal or associates with other organic components in the reaction.

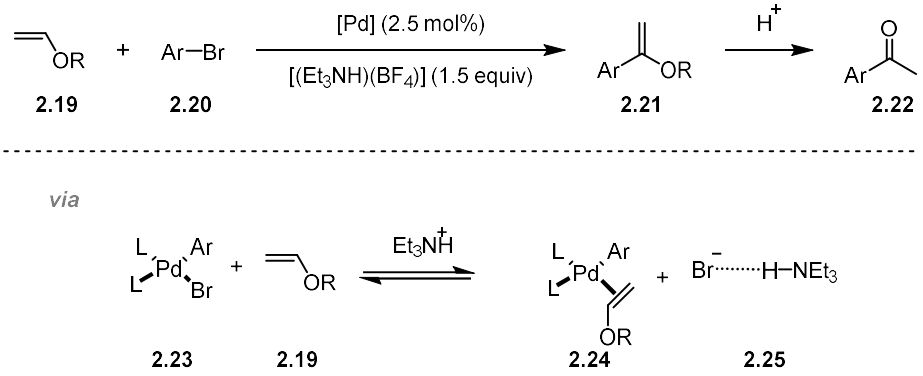

Scheme 2.7. Reaction acceleration by ligand dissociation mediated by a HBD.

17. a) Mo, J.; Xiao, J. *Angew. Chem. Int. Ed.* **2006**, *45*, 4152–4157. b) Ruan, J.; Iggo, J. A.; Berry, N. G.; Xiao, J. *J. Am. Chem. Soc.* **2010**, *132*, 16689–16699. c)Farney, E. P.; Chapman, S. J.; Swords, W. B.; Torelli, M. D.; Hamers, R. J.; Yoon, T. P. *J. Am. Chem. Soc.* **2019**, *141*, 6385–6391.
18. a) Simlandy, A. K.; Ghosh, B.; Mukherjee, S. *Org. Lett.* **2019**, *21*, 3361–3366. Zhang, X.; Li, S.; Yu, W.; Xie, Y.; Tung, C.-H.; Xu, Z. *J. Am. Chem. Soc.* **2022**, *144*, 6200–6207. b) Li, M.-L.; Yu, J.-H.; Li, Y.-H.; Zhu, S.-F.; Zhou, Q.-L. *Science* **2019**, *366*, 990–994. c) Furniel, L. G.; Echemendía, R.; Burtoloso, A. C. B. *Chem. Sci.* **2021**, *12*, 7453–7459. d) Zhang, X.; Li, S.; Yu, W.; Xie, Y.; Tung, C.-H.; Xu, Z. *J. Am. Chem. Soc.* **2022**, *144*, 6200–6207.

Objectives

Given the difficulties encountered in enantioselective gold(I) catalysis posed by the linear dicoordination of gold(I) catalysts, our objective was to develop a novel methodology for asymmetric gold(I)-catalysis. In our previous work, we demonstrated that ligands bearing bidentate hydrogen bond donors could remove the chloride anionic ligand from the coordination sphere, allowing reactivity on the gold center. We envisioned that, if we used chiral counterions, instead of achiral ones,[8] we should be able to anchor it with the hydrogen bond donors, close enough to the reaction center to allow transfer of the stereochemical information.

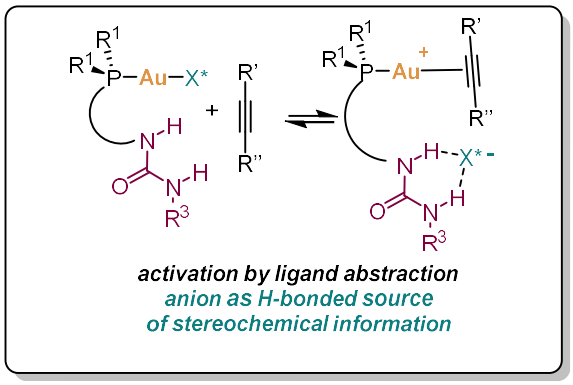

Scheme 2.8. H-Bonded Counterion-Directed Catalysis (HCDC). X* = chiral counterion.

Thus in order to expand the application of chiral asymmetric counterion directed catalysis, we decided to explore the use of this novel approach in the activation of alkyne-containing susbtrates.

Results and Discussion

Phosphinourea Au(I)-Chloride Complex Synthesis

As mentioned in Chapter 1, choosing the order in which the functional groups were to be introduced, (thio)urea and phosphine scaffolds, was very important. To introduce the phosphine group (PR_2) we realized that standard conditions for Pd-catalyzed cross-coupling of bromoaniline **2.26a,** with di-*tert*-butylphosphine under standard literature conditions for Pd–P couplings ($Pd(OAc)_2$, 1,1′-bis(diisopropylphosphino)ferrocene and NaO^{t}Bu in toluene),[19] afforded the desired product **2.27a** alongside significant amounts of Buchwald–Hartwig side product **2.27H**. To optimize the reaction, a screening of bases was undertaken. It was found that milder bases, such as K_3PO_4, promote P–C, but not C–N bond formation (Table 2.2, entry 7, 98% conversion to the desired phosphine **2.27a**).

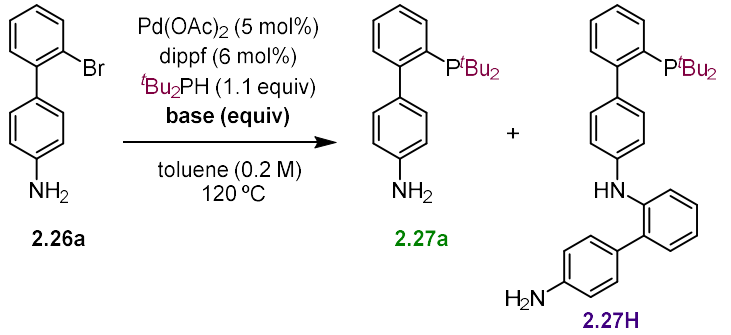

Table 2.2. Base screening for the optimization of the P–C coupling reaction.

Entry	Base (equiv)	pK_{BH+} in H_2O taken from Bordwell pKa Table	Time (h)	$^{31}P\{^1H\}$ crude NMR 2.26a:2.27a:2.27H:others
1	NaO^{t}Bu (1.4)	17	15	35:**46**:**19**:0
2	NaO^{t}Bu (3.6)	17	15	25:**44**:**31**:0
3	NaO^{t}Bu (1.1)	17	65	26:**57**:**17**:0
4	KO^{t}Bu (1.1)	17	65	29:**18**:**35**:18
5	K_2CO_3 (1.1)	10.3, 3.6	65	12:**86**:**0**:2
6	Cs_2CO_3 (1.1)	10.3, 3.6	65	8:**86**:**6**:0
7	K_3PO_4 (1.1)	12.3, 7.2, 2.1	65	2:**98**:**0**:0
8	K_2HPO_4 (1.1)	7.2, 2.1	65	10:**85**:**5**:0
9	KH_2PO_4 (1.1)	2.1	65	100:**0**:**0**:0

The optimized cross-coupling could be performed on multigram scale and allowed the introduction of different phosphine substituents on the biphenyl scaffold without the need to protect the free amine group in high yields (Scheme 2.10, **2.27a–e**).

19. Murata, M.; Buchwald, S. L. *Tetrahedron* **2004**, *60*, 7397–7403.

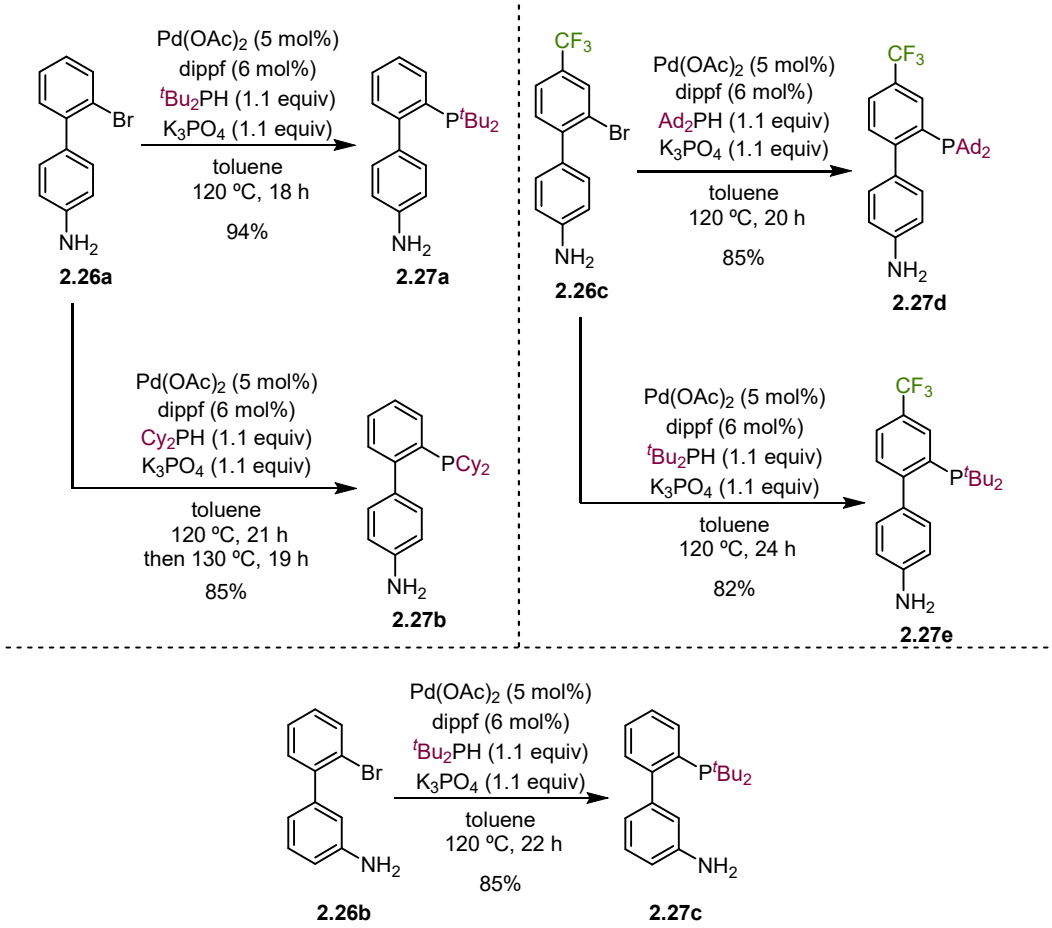

Scheme 2.9. Synthesis of phosphinoanilines **2.27**.

Phosphinoanilines **2.27a–e** were then allowed to react with the iso(thio)cyanate of choice for the late-stage introduction of the key HBD on the ligands (Scheme 2.10, **2.28–2.40**). Urea formation proceeded with excellent yields in THF at reflux, whereas it was observed that hindered diarylthioureas decompose into aniline and isothiocyanate upon heating[20] or in the presence of bases.[21] Therefore, the yield for the thiourea formation was improved by lowering the reaction temperature to 23 ºC while increasing the concentration, and never warming up the product above 30 ºC during work-up and purification. When using cyclohexyl isocyanate, the addition of silica gel to the reaction mixture improved conversion.

20. Habib, N.; Rieker, A. *Synthesis* **1984**, *10*, 825–827.
21. Vlatkovíc, M.; Feringa, B. L. *Tetrahedron* **2019**, *75*, 2188–2192.

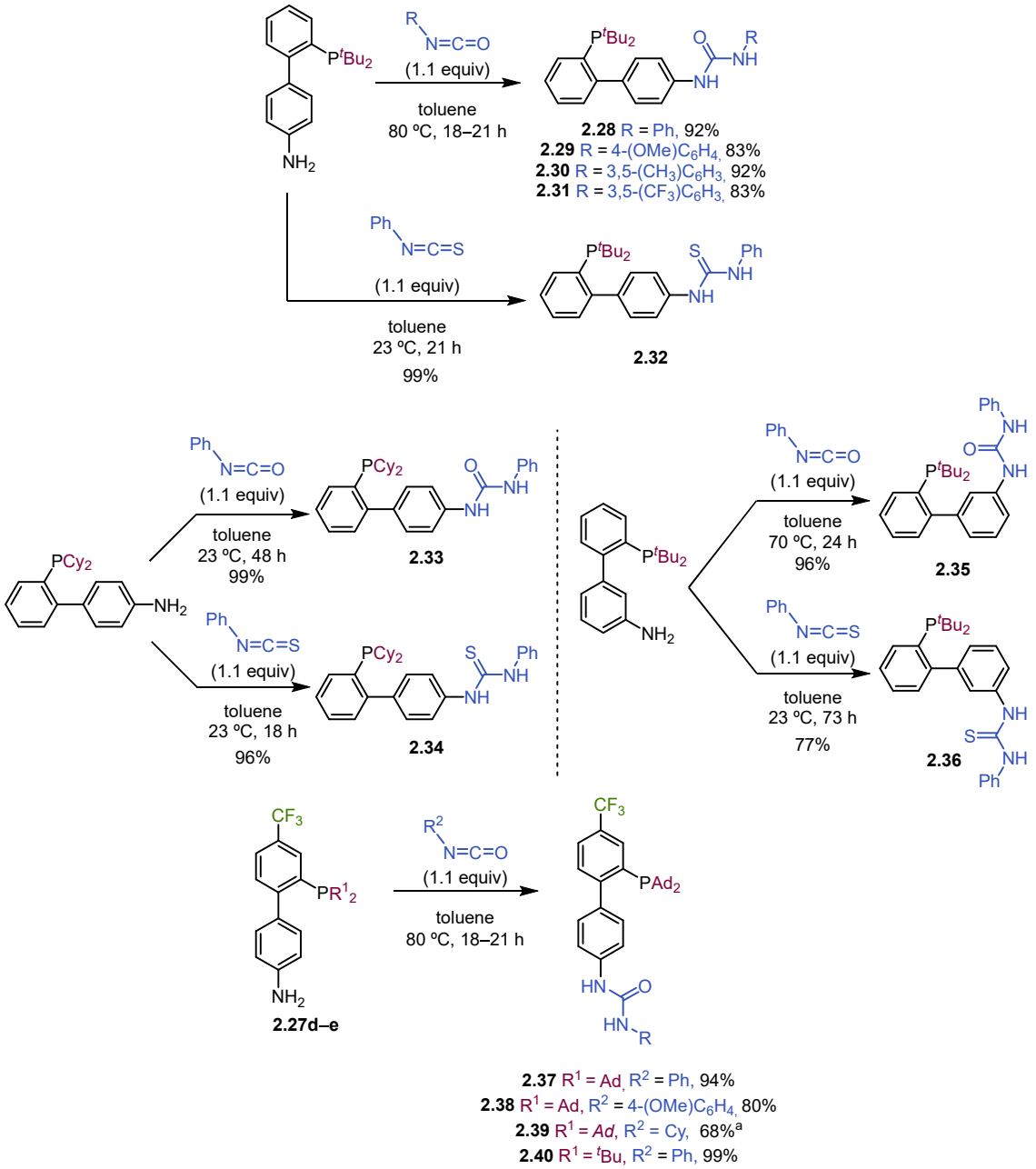

Scheme 2.10. Synthesis of the JohnPhos (thio)urea-type ligands. [a] silica (pore size 60 Å, 40–63 µm particle size) added. Reaction carried out at 80 ºC for 24 h and then at 90 °C for 4 h.

Finally, ligand exchange with [(Me_2S)AuCl] in CH_2Cl_2 afforded the preparation of 13 novel bifuncional complexes **Au1**–**Au13** in excellent yields (Scheme 2.11).

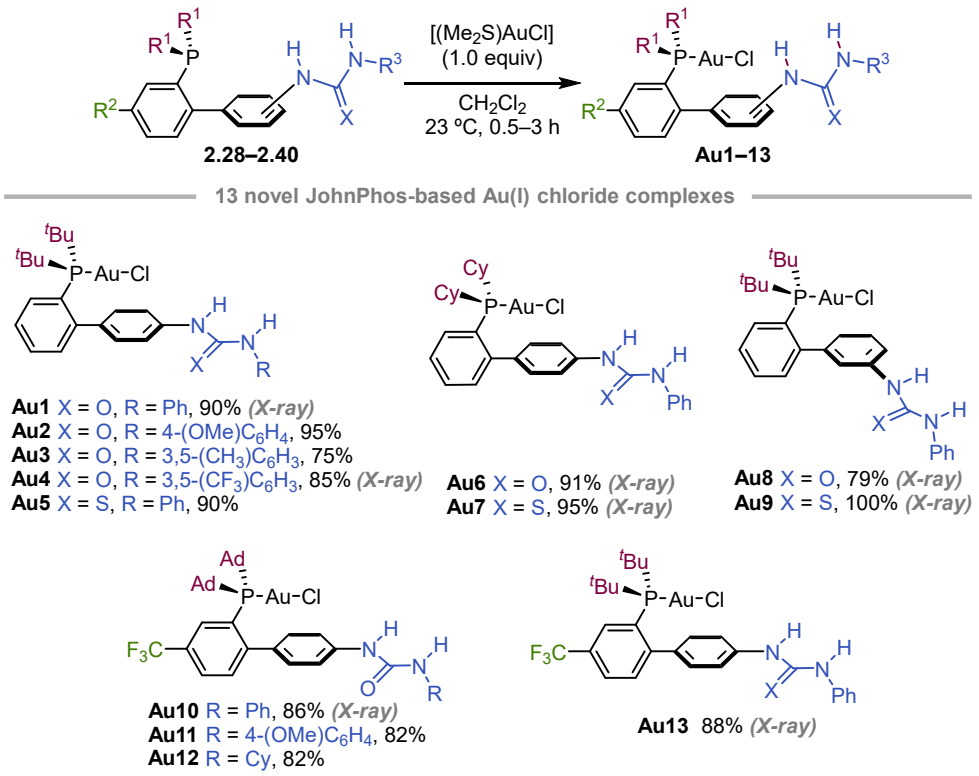

Scheme 2.11. Synthesis and library of JohnPhos-type urea gold(I) complexes.

Some of the complexes could be characterized by single crystal X-ray diffraction (see experimental part for all the structures). In the solid state, all phosphinourea Au(I) complexes[22] displayed an intact Au–Cl bond with the P–Au–Cl axis almost parallel to the biphenyl axis. The urea moiety generally adopts an *anti,anti*-conformation (for example in **Au1**, **Au6**, **Au10** and **Au13**) but in some cases also displayed the rare[23] *anti,syn*-conformation (**Au4** and **Au8**) (Figures 2.1 and 2.2).

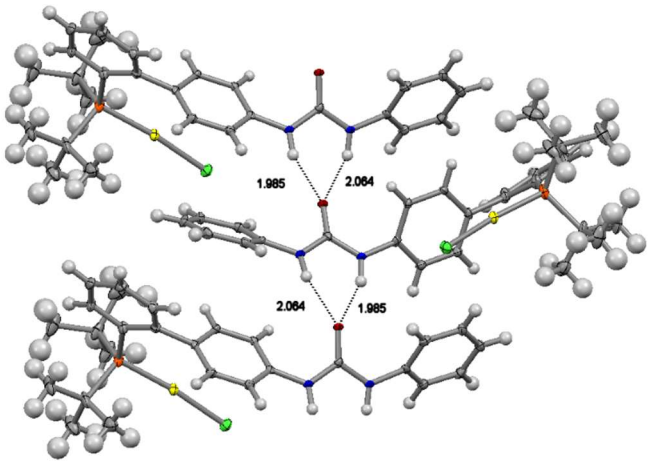

Figure 2.1. Single X-ray diffraction of **Au1**, displaying an *anti,anti*-conformation in the intermolecular HB with another molecule of catalyst. Visualized using Mercury program.

22. Campbell, M. J.; Toste, F. D. *Chem. Sci.* **2011**, *2*, 1369–1378.
23. Luchini, G.; Ascough, D. M. H.; Alegre-Requena, J. V.; Gouverneur, V.; Paton, R. S. *Tetrahedron* **2019**, *75*, 697–702.

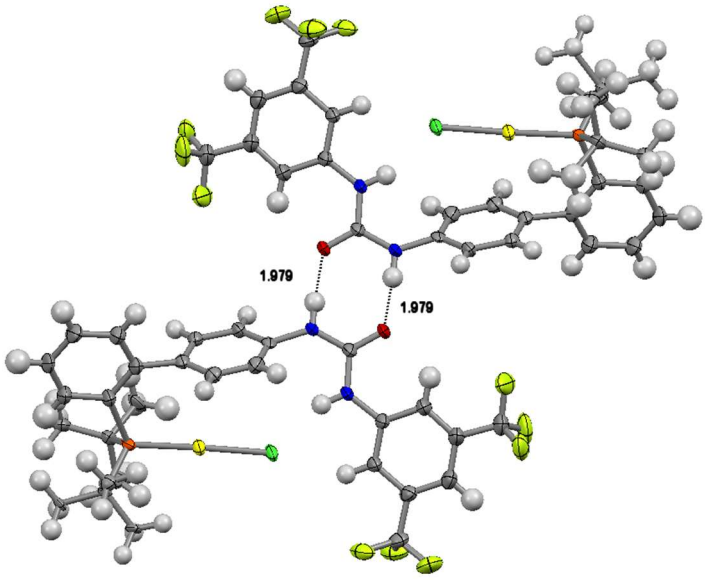

Figure 2.2. Single X-ray diffraction of **Au6**, displaying a *syn,anti*-conformation in the intermolecular HB with another molecule of catalyst. Visualized using Mercury program.

Different degrees of out-of-plane twisting of the aryl substituents could also be observed (Figure 2.3, **Au1** vs. **Au10**). The urea group establishes H-bonds either with another urea unit or chloride ligands, depending on the ligand scaffold (Figures 2.1 and 2.2).

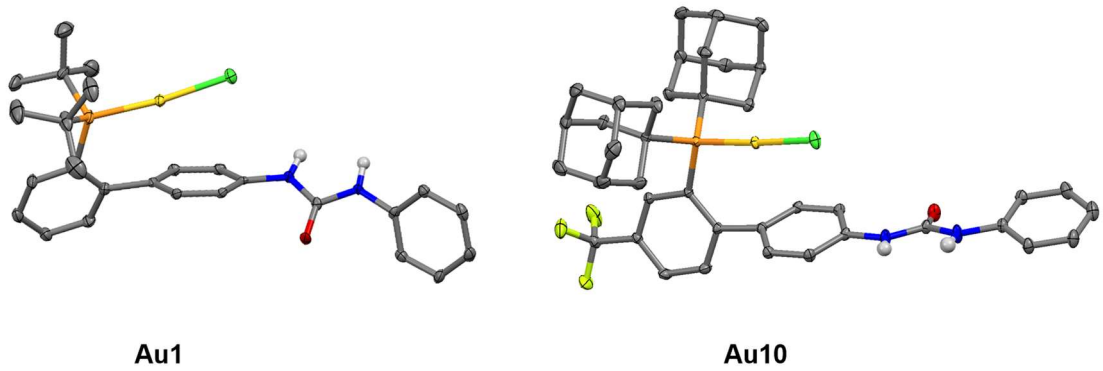

Figure 2.3. Comparison of the out of plane twist of the aryl substituent in complexes **Au1** and **Au10**. Visualized using Mercury program, H atoms, except N–H, were omitted for clarity.

In the case of phosphinothiourea Au(I) complex **Au7**, in *para* position in the biphenyl scaffold, presented a classical P–Au–Cl structure with intramolecular NH–Cl interactions (Figure 2.4 left). However, as already observed in Chapter 1 for triphenyl-based phosphino(thio)urea complexes (**D** and **F**), in the case of **Au9**, with the thiourea in the *meta* position of the biphenyl scaffold, the S atom coordinated to gold with an almost linear P–Au–S axis. Meanwhile the Cl^- anion is stabilized by a dual H-bond interaction with the NH groups (Figure 2.4 right).

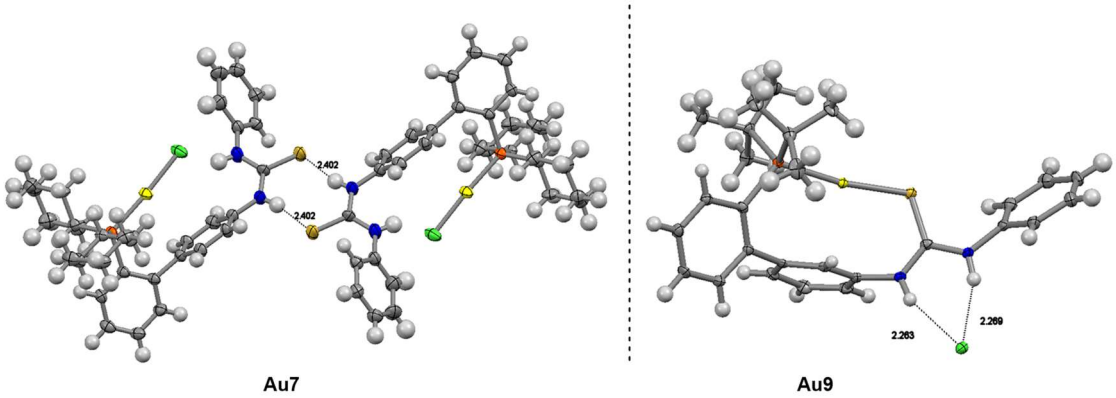

Figure 2.4. Single X-ray diffraction of phosphitothiourea gold(I)-complexes. On the left: **Au7**, displaying a classical P–Au–Cl linear coordination. On the right: **Au9**, displaying a Au–S bond and a displaced chloride ligand stabilized by the HB of the thiourea. Visualized using Mercury program.

Chiral Counterion Synthesis

The chiral anion was introduced as a metal salt with a countercation capable of abstracting the chloride from the Au(I) center, such as Ag(I), Cu(II) and Na(I).[24] Based on previous work by our group, in which phosphate anion containing silver salts **Ag0** and **TRIPAg** proved to be too coordinating,[25,26] we envisioned that less basic phosphoramidate salts bearing an *N*-sulfonyl group (Scheme 2.12) could be a better option for counterion abstraction via H-bond interaction. A library of 14 metal salts (**Ag0**-**Ag10**, **Na6** and **Cu6**) was prepared in 2–3 steps from commercially available 3,3'-(*R*)-BINOL, (*R*)-VAPOL and (*R*)-VANOL: first generation of a phosphorylchloride intermediate which was then trapped with the desired nucleophile. Ag(I) and Na(I) salts were prepared by reaction of the corresponding phosphoric acid or phosphoramide with Ag_2CO_3 (**TRIPAg**, **Ag0**-**Ag10**) and Na_2CO_3 ((*R*)-**Na6**) respectively. On the other hand, salt metathesis of (*R*)-**Ag6** with $CuCl_2 \cdot H_2O$ resulted in the best approach for the preparation of (*R*)-**Cu6**.

24. Fang, W.; Presset, M.; Guérinot, A.; Bour, C.; Bezzenine-Lafollée, S.; Gandon, V. *Chem. Eur. J.* **2014**, *20*, 5439–5446.
25. Raducan, M.; Moreno, M.; Bour, C.; Echavarren, A. M. *Chem. Commun.* **2011**, *48*, 52–54.
26. Commercially available **(*R*)-Ag0** and **(*R*)-TRIPAg** were employed.

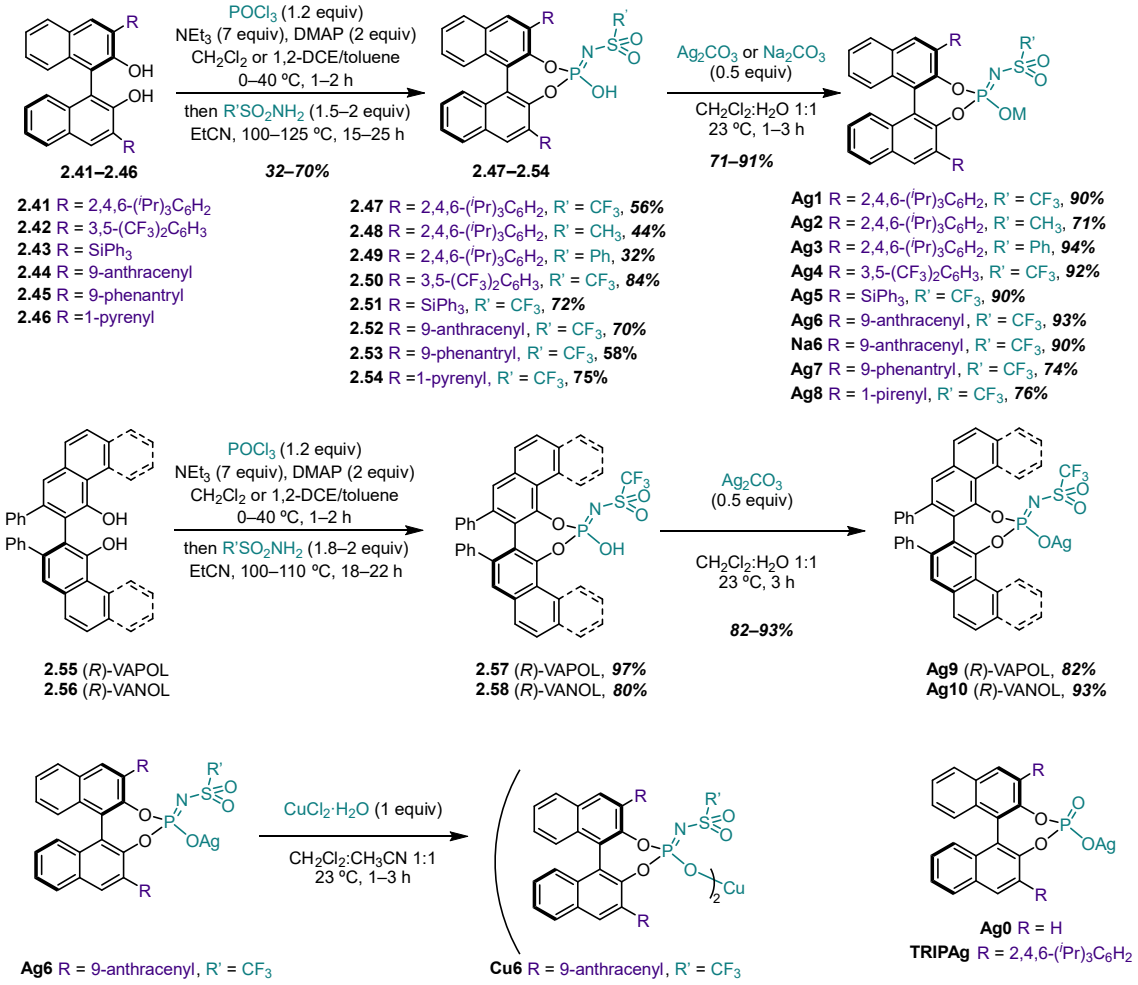

Scheme 2.12. Synthetic route towards the synthesis of BINOL based chiral metal salts.

Crystals of (*R*)-**Ag6** could be grown from a toluene/pentane mixture, revealing a dimeric structure where the anion behaves as a bidentate *O,O*-ligand through the phosphoryl and sulfonyl O atoms (Figure 2.5). The Ag(I) centers are further stabilized by η^2-interactions with the anthracenyl substituents, with one of the centers also binding to a molecule of toluene in a η^1/η^2 fashion.

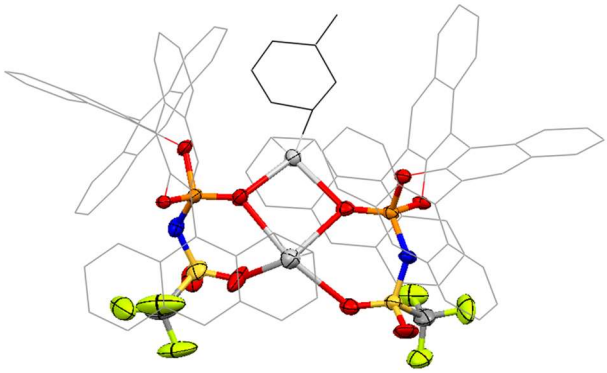

[(Ag6)$_2$·toluene]

Figure 2.5. Single crystal XRD of (*R*)-**Ag6**, displayed with ORTEP ellipsoid at 50% probability level; BINOL scaffold and toluene in wireframe; solvent and all H atoms omitted for clarity.

Application of HCDC in Catalysis

Formal [4+2] cycloaddition and other 1,6-enyne cyclization reactions

Having built the library of JohnPhos-based [LAuCl] complexes and chiral anions, to validate the HCDC design, we investigated the formal gold(I)-catalyzed [4+2] cycloaddition of 1,6-enynes of type **2.59** (Table 2.3).[27,28] As previously studied by our group, this reaction did not proceed using [(PPh_3)AuCl] and phosphate salt **AgTRIP,** in the absence of an H-bond donor.[25] Some representative examples from the library of triphenylphosphine based phosphinourea and phosphinosquaramide gold(I) complexes from Chapter 1, Scheme 1.14, were also tested. We commenced by screening different silver salts in combination with phosphinourea gold(I) chloride **Au1** at room temperature. This complex combined with **AgTRIP** was catalytically inactive, whereas together with less basic *N*-triflyl phosphoramidate[29] salt **Ag1** afforded the desired product **2.60a** in good yield and encouraging 79:21 *er* (Table 2.3, entries 1–2). The more basic *N*-mesyl and *N*-phenylsulfonyl analogues **Ag2** and **Ag3** induced comparable enantioselectivity, but much lower reactivity (Table 2.3, entries 3–4). There was a clear relationship between reactivity and basicity: less basic counterions originating from stronger parent Brønsted acids (*N*-Triflyl phosphoric amide **2.41** has a pK_a[30] value 0.9 units lower than the corresponding phosphoric acid **TRIPH**)[31] are essential for reactivity, presumably because they coordinate less strongly to the cationic Au(I) center (which is isolobal to a H^+),[32] and therefore can be abstracted more easily via H-bonds. Among *N*-triflyl phosphoramidate salts, **Ag1** provided better enantiocontrol than **Ag4** and **Ag5** (Table 2.3, entries 5–6), which bear different groups at the 3,3'-positions of the binaphthol backbone. Overall, the results summarized in Table 2.3 indicate that, for a given anion, substitution at phosphorous influences basicity and coordinating ability, hence reactivity, while 3,3'-substituents are responsible for enantioselectivity.[33]

27. a) Nieto-Oberhuber, C.; López, S.; Echavarren, A. M. *J. Am. Chem. Soc.* **2005**, *127*, 6178–6179. b)Nieto-Oberhuber, C.; Pérez-Galán, P.; Herrero-Gómez, E.; Lauterbach, T.; Rodríguez, C.; López, S.; Bour, C.; Rosellón, A.; Cárdenas, D. J.; Echavarren, A. M. *J. Am. Chem. Soc.* **2008**, *130*, 269–279.
28. Previous asymmetric versions of the formal [4+2] cycloaddition of enyne **2.59**: a) Chao, C.-M.; Vitale, M. R.; Toullec, P. Y.; Genêt, J.-P.; Michelet, V. *Chem. Eur. J.* **2009**, *15*, 1319–1323. b) Pradal, A.; Chao, C.-M. Vitale, M. R.; Toullec, P. Y; Michelet, V. *Tetrahedron* **2011**, *67*, 4371–4377. c) Delpont, N.; Escofet, I.; Pérez-Galán, P.; Spiegl, D.; Raducan, M.; Bour, C.; Sinisi, R.; Echavarren, A. M. *Catal. Sci. Technol.* **2013**, *3*, 3007–3012. d) Aillard, P.; Dova, D.; Magné, V.; Retailleau, P.; Cauteruccio, S.; Licandro, E.; Voituriez, A.; Marinetti, A. *Chem. Commun.* **2016**, *52*, 10984–10987. e) Zuccarello, G.; Mayans, J. G.; Escofet, I.; Scharnagel, D.; Kirillova, M. S.; Pérez-Jimeno, A. H.; Calleja, P.; Boothe, J. R.; Echavarren, A. M. *J. Am. Chem. Soc.* **2019***, 141*, 11858–11863. f) Magné, V.; Sanogo, Y.; Demmer, C. S.; Retailleau, P.; Marinetti, A.; Guinchard, X.; Voituriez, A. *ACS Catal.* **2020**, *10*, 8141–8148. g) Caniparoli, U.; Escofet, I.; Echavarren, A. M. *ACS Catal.* **2022**, *12*, 3317–3322. h) Zuccarello, G.; Nannini, L. J.; Arroyo-Bondía, A.; Fincias, N.; Arranz, I.; Pérez-Jimeno, A. H.; Peeters, M.; Martín-Torres, I.; Sadurní, A.; García-Vázquez, V.; Wang, Y.; Kirillova, M. S.; Montesinos-Magraner, M.; Caniparoli, U.; Núñez, G. D.; Maseras, F.; Besora, M.; Escofet, I.; Echavarren, A. M. *JACS Au* **2023**, *3*, 1742–1754.
29. Nakashima, D.; Yamamoto, H. *J. Am. Chem. Soc.* **2006**, *128*, 9626–9627
30. Christ, P.; Lindsay, A. G.; Vormittag, S. S.; Nuedörfl, J.-M.; Berkessel, A.; O'Donoghue, A. C. *Chem. Eur. J.* **2011**, *17*, 8524–8528.
31. a) Akiyama, T. *Chem. Rev.* **2007**, *107*, 5744–5758. b) Terada, M. *Chem. Commun.* **2008**, 4097–4112. c) Akiyama, T.; Mori, K. *Chem. Rev.* **2015**, *115*, 9277–9306. d) Parmar, D.; Sugiono, E.; Raja, S.; Rueping, M. *Chem. Rev.* **2014**, *114*, 9047–9153. Correction: Parmar, D.; Sugiono, E.; Raja, S.; Rueping, M. *Chem. Rev.* **2017**, *117*, 10608–10620.
32. Raubenheimer, H. G.; Schmidbaur, H. *Organometallics* **2012**, *31*, 2507–2522.
33. Reid, J. P.; Goodman, J. M. *J. Am. Chem. Soc.* **2016**, *138*, 7910–7917.

Table 2.3. Screening of silver salts in combination with Au1.

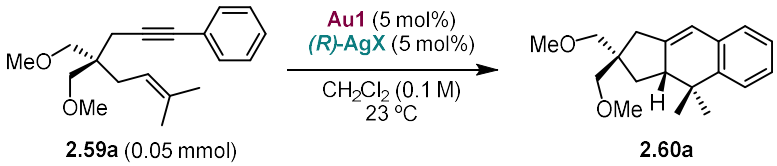

2.59a (0.05 mmol) **2.60a**

Entry	*(R)*-Ag salt	Solvent	Time	2.60a (%)[a]	2.59a (%)[a]	2.60a *er*[b]
1	**AgTRIP**	CH_2Cl_2	4 d	0	89	-
2	**Ag1**	CH_2Cl_2	4.5 h	70	0	79:21
3	**Ag2**	CH_2Cl_2	4.5 h	7	>95	81.5:18.5
4	**Ag3**	CH_2Cl_2	4.5 h	9	90	83.5:16.5
5	**Ag4**	CH_2Cl_2	4.5 h	42	47	57:43
6	**Ag5**	CH_2Cl_2	4.5 h	22	74	51:49

[a] Determined by ^{1}H NMR using dodecane as internal standard. [b] Determined by HPLC on chiral stationary phase.

The library of gold(I) complexes was also evaluated with the optimal silver salt *(R)*-**Ag1**. The presence of the urea group on the ligand is important for reactivity and essential for enantioselectivity, as [(JohnPhos)AuCl] with **Ag1** delivered product **2.60a** in lower yield and racemic form (Table 2.4, entries 1–2). These findings proved the role of the hydrogen bond donor to remove the counterion but keeping it close enough to transfer its stereochemical information to gold. Complexes **A**, **C**, **E** and **G**, equipped with urea or squaramide groups on triarylphosphine scaffolds (catalysts prepared in Chapter 1, see Scheme 1.14), were poorly active and afforded (close to) racemic product (Table 2.4, entries 3–6). These poor results with triarylphopshine scaffolds proved that this design of gold(I) complexes was not a good fit for this specific reaction. Increasing the acidity of the urea in **Au1** by introducing a 3,5-bistrifluoromethylaryl motif, **Au4**, only resulted in erosion on the yield and enantioselectivity (Table 2.4, entry 7). Complex **Au5**, the thiourea analogue of **Au1**, was completely inactive (Table 2.4, entry 8), most likely due to the S atom of the thiourea coordinating too strongly to the metal center, preventing substrate activation (consistent with the results obtained in Chapter 1 with the thiourea gold(I) catalysts). When cyclohexyl groups were present on the phosphine (**Au6**), instead of *t*Bu, **2.60a** was obtained in moderate yield and lower stereoselectivity (Table 2.4, entry 1 vs. 9), probably due to an increase of the steric hindrance around the Au(I) center. Moving the urea group from the *para* to the *meta* position of the biphenyl scaffold (**Au8**) led to an inversion of the enantioselectivity (Table 2.4, entry 1 vs.10). Remarkably, both enantiomers of the product can thus be obtained preferentially using the same enantiomer of the chiral anion, in combination with a different achiral cocatalyst.

Table 2.4. Screening of Au(I) complexes in combination with (*R*)-**Ag1**.

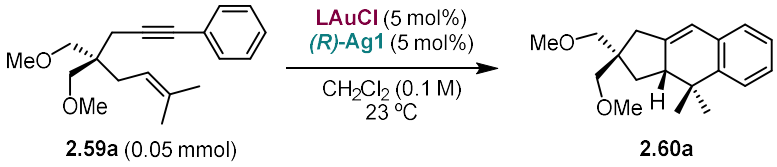

2.59a (0.05 mmol) **2.60a**

Entry	LAuCl	Time (h)	2.60a (%)[a]	2.59a (%)[a]	2.60a *er*[b]
1	**Au1**	4.5	70	0	79:21

2	[(JohnPhos)AuCl]	6	40	59	50:50
3	**A**	4.5	15	35	47.5:52.5
4	**C**	24	46	50	56:44
5	**E**	44	10	86	45:55
6	**G**	44	32	46	50:50
7	**Au4**	4.5	45	0	68.5:31.5
8	**Au5**	44	0	89	-
9	**Au6**	4.5	34	12	62.5:37.5
10	**Au8**	4.5	70	0	27.5:72.5

[a] Determined by ^{1}H NMR using dodecane as internal standard, after filtration of the reaction mixture through silica. [b] Determined by HPLC analysis on chiral stationary phase.

Overall, the dataset emphasizes that the presence of a H-bond donor on the ligand is essential for both reactivity and enantiocontrol. Simply including a chiral anion in the reaction mixture is insufficient to effectively transfer stereochemical information, as its proximity to the reaction center cannot be ensured without a strategically placed H-bond donor. These findings support the original design concept, where the pendant urea was intended to facilitate both anion abstraction and precise positioning of the chiral source (see objectives). Parallel screening showed that enantiocontrol generally increased at –20 °C, thus the subsequent set of experiments was performed at this temperature. The importance of H-bonding within the catalytic system is also reflected in solvent effects. For example, the performance of the optimal **Au1**/**Ag1** combination improved when CH_2Cl_2 was replaced with benzene (Table 2.5, entry 1 vs. 2). A qualitative correlation was observed between solvent polarity (defined by E^N_T values, Table 2.5)[34] and enantioselectivity levels, aligning with the notion that H-bonding interactions between the urea and the anion are favored in apolar solvents. The least polar solvent in either the chlorinated or aromatic series (chloroform for entries 7–9 and toluene for entries 10–14 in Table 2.5) produced the product with the highest enantiomeric ratio, reaching up to 94.5:5.5 *er*.

Table 2.5. Solvent and complex screening with (*R*)-**Ag1** at –20 °C.

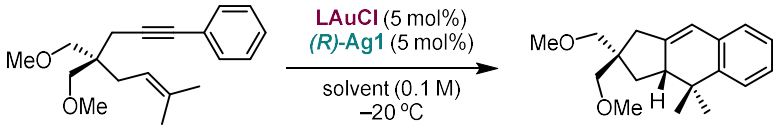

2.59a (0.05 mmol) **2.60a**

Entry	LAuCl	solvent	E^N_T[34]	time (h)	2.60a (%)[a]	2.59a (%)[a]	2.60a *er*[b]
1	**Au1**[c]	CH_2Cl_2	0.309	4.5	70	0	79:21
2	**Au1**[c]	C_6H_6	0.111	0.7	90	0	87:13
3	**Au1**	CH_2Cl_2	0.309	18	>95	6	92:8
4	**Au2**	CH_2Cl_2	0.309	18	95	0	94:6
5	**Au3**	CH_2Cl_2	0.309	18	67	28	90:10
6	**Au4**	CH_2Cl_2	0.309	18	84	18	84:16

34. Reichardt, C. *Chem. Rev.* **1994**, *94*, 2319–2358.

7	**Au1**	$CHCl_3$	0.259	24	39	54	93:7
8	**Au1**	CH_2Cl_2	0.309	24	85	10	92:8
9	**Au1**	1,2-DCE	0.327	24	60	40	88:12
10	**Au1**	toluene	0.099	24	>95	0	94.5:5.5
11	**Au1**	$C_6H_5CF_3$	-	24	89	0	90.5:9.5
12	**Au1**	*o*-xylene	-	24	86	14	93:7
13	**Au1**	C_6H_5F	0.194	24	75	36	90:10
14	**Au1**	C_6H_5Cl	0.188	24	>95	0	91:9

[a] Determined by ^{1}H NMR using dodecane as internal standard, after filtration of the reaction mixture through silica. [b] Determined by HPLC analysis on chiral stationary phase. [c] Reaction performed at rt, 23 °C. Best results highlighted in red.

Once having identified toluene as the best solvent, a final fine-tuning of the catalytic system was performed (Table 2.6). Further lowering the temperature or increasing the concentration did not improve the yield or the enantioselectivity of the reaction. In fact, the reaction was not complete after 24 h at −40 ºC.

Table 2.6. Effect of temperature and concentration with Au1 and (R)-Ag1.

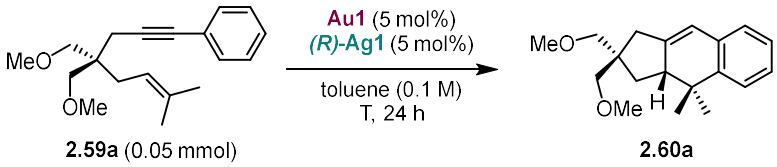

2.59a (0.05 mmol) **2.60a**

Entry	T (ºC)	conc (M)	2.60a (%)[a]	2.59a (%)[a]	2.60a *er*[b]
1	–20	0.1	>95	0	94.5:5.5
2	–30	0.1	>95	0	95.5:4.5
3	–30	0.2	94	5	95.5:4.5
4	–40	0.1	32	70	95.3:4.7
5	–40	0.2	38	70	96:4

[a] Determined by ^{1}H NMR against internal standard, after filtration of the reaction mixture through silica. [b] Determined by HPLC analysis on chiral stationary phase.

A new screening of the combination of gold(I) complexes and chiral counterions was attempted, this time in toluene at −20 °C. The initial setup used **Ag1**, a silver complex featuring 2,4,6-triisopropylbenzene groups at the 3,3' positions of the BINOL ligand. However, when replaced with **Ag6,** which bears a 9-anthracenyl substituent instead, a significant improvement in enantioselectivity at the cost of lower reactivity was observed (as shown in Table 2.7, entry 1 vs 4). Switching to more electrophilic complex **Au10** with a trifluoromethyl group *meta* to the phosphine increased the yield to 78% (Table 2.7, entries 4–6) with still some unreacted **2.59a**. Nevertheless, with this new **Au10/Ag6** combination, the temperature could be increased to −10 °C, reaching full conversion in excellent yields and enantioselectivities. Additionally, **Na6** and **Cu6** were evaluated as potential alternatives, but neither demonstrated sufficient ability to scavenge the halide from the Au(I) complexes under these reaction conditions (Table 2.7, entries 10–11).

Table 2.7. Final fine-tuning of the reaction conditions.

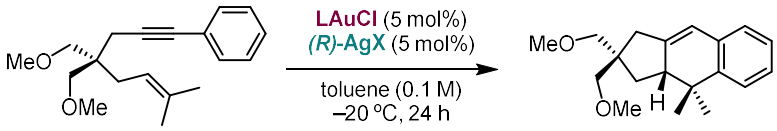

2.59a (0.05 mmol) **2.60a**

Entry	LAuCl	*(R)*-AgX	2.60a (%)[a]	2.59a (%)[a]	2.60a *er*[b]
1	**Au1**	**Ag1**	>95	0	94.5:5.5
2	**Au2**	**Ag1**	>95	0	94:6
3	**Au3**	**Ag1**	88	8	91:9
4	**Au1**	**Ag6**	50	50	98:2
5	**Au2**	**Ag6**	54	36	98:2
6	**Au10**	**Ag6**	78	19	98:2
7	**Au11**	**Ag6**	66	36	98:2
8	**Au12**	**Ag6**	28	63	98:2
9[c]	**Au10**	**Ag6**	>95	0	98:2
10[c]	**Au10**	**Na6**	0	>95	-
11[c]	**Au10**	**Cu6**	0	93	-

[a] Determined by ^{1}H NMR against internal standard, after filtration of the reaction mixture through silica. [b] Determined by HPLC analysis on chiral stationary phase. [c] At –10 °C. Best results highlighted in red.

In conclusion, **Au10** presenting a CF_3 *meta* to the phosphine and a simple phenyl urea, offered the right balance between electronic activation and steric hindrance (Table 2.8, entries 7 and 8). Finally, a catalyst loading screening revealed that it could be reduced to 2 mol% with minimal impact on the yield and enantioselectivity. However, further reductions resulted in sluggish reactions and incomplete conversions. Surprisingly, when reaction was scaled up to 1.0 and 2.0 mmol scale, it could be performed under air, allowing us to increase reaction concentration and reducing the catalyst loading to 2 and 1 mol% respectively, obtaining the desired product in excellent yields and enantioselectivities (Table 2.8, entries 8–10). This catalyst loading is the lowest reported so far in asymmetric cycloadditions of enynes **2.59a**, which is remarkable considering that all previous methods relied on stereochemical information covalently embedded in a chiral ligand.[27] We also tested the ratio of Au:Ag but no significant differences could be detected (Table 2.8, entries 11–12).

Table 2.8. Catalyst loading screening and scale-up tests with Au10 and (R)-Ag6.

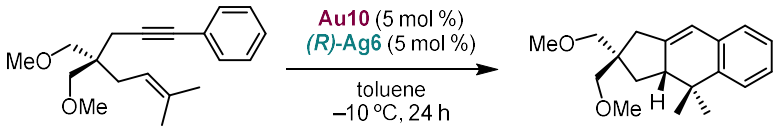

2.59a (x mmol) **2.60a**

Entry	scale (mmol)	catalyst loading (x mol %)	conc (M)	2.60a (%)[a]	2.59a (%)[a]	2.60a *er* (%)[b]
1	0.05	5	0.1	>95	0	98:2

2	0.05	4	0.1	>95	0	98:2
3	0.05	3	0.1	>95	0	97.5:2.5
4	0.05	2	0.1	94	3	97.5:2.5
5	0.05	1	0.1	71	20	97.5:2.5
6	0.05	0.5	0.1	7	81	96:4
7	0.05	0.5	0.2	18	70	98:2
8[c]	0.15	5	0.1	93 (is.)	-	98:2
9[d]	1.0	2	0.3	97 (is.)	-	98:2
10[d,e]	2.0	1	0.6	99 (is.)	-	98:2
11	0.05	[Au] 10, [Ag] 5	0.1	92	9	96:4
12	0.05	[Au] 5, [Ag] 10	0.1	>95	0	96:4

[a] Determined by ^{1}H NMR against internal standard, after filtration of the reaction mixture through silica. [b] Determined by HPLC analysis on chiral stationary phase. [c] Isolated yield. [d] Under air. [e] Toluene technical grade.

Scope of the formal [4+2] 1,6-enyne cycloisomerization

With the optimal conditions for substrate **2.59a** (**Au10**/**Ag6**), the substrate scope of the formal [4+2] cycloaddition of 1,6-enynes **2.59** was assessed using 5 mol% of the catalyst for practical purposes. The effect of the linker in the substrate was first studied (Scheme 2.13). Enynes **2.59a–h** bearing various linkers underwent cyclization to deliver the corresponding products **2.60a–h** in high yield (84–95%) and with excellent enantioselectivity (96.5:3.5 to 98:2 *er*). The reaction demonstrated remarkable functional group tolerance, accommodating not only ethers (**2.60a**, **2.60b**) but also allyl (**2.60c**), ester (**2.60d**, **2.60h**), carbamate (**2.60e**), tosylate (**2.60f**), and acetal groups (**2.60g**). This versatility highlights the robustness of the catalytic system across a wide range of substrates. As for variations on the alkyne moiety, products with electron-poor as well as electron-rich groups at the *para* (**2.60i–l**), *ortho* (**2.60m–n**) and *meta* position (**2.60o–p**) of the aromatic ring were obtained with good to excellent yield and enantiocontrol (85–98%, 89.5:10.5 to 98.5:1.5 *er*). Moreover, substrates with more complex alkyne terminus, such as **2.59q** and **2.59r**, which bear 1-naphthyl and 2-benzothiophenyl groups, respectively, also reacted smoothly. These substrates not only underwent the transformation efficiently but also retained high levels of enantioselectivity, demonstrating that the system can handle larger and more structurally diverse substituents.

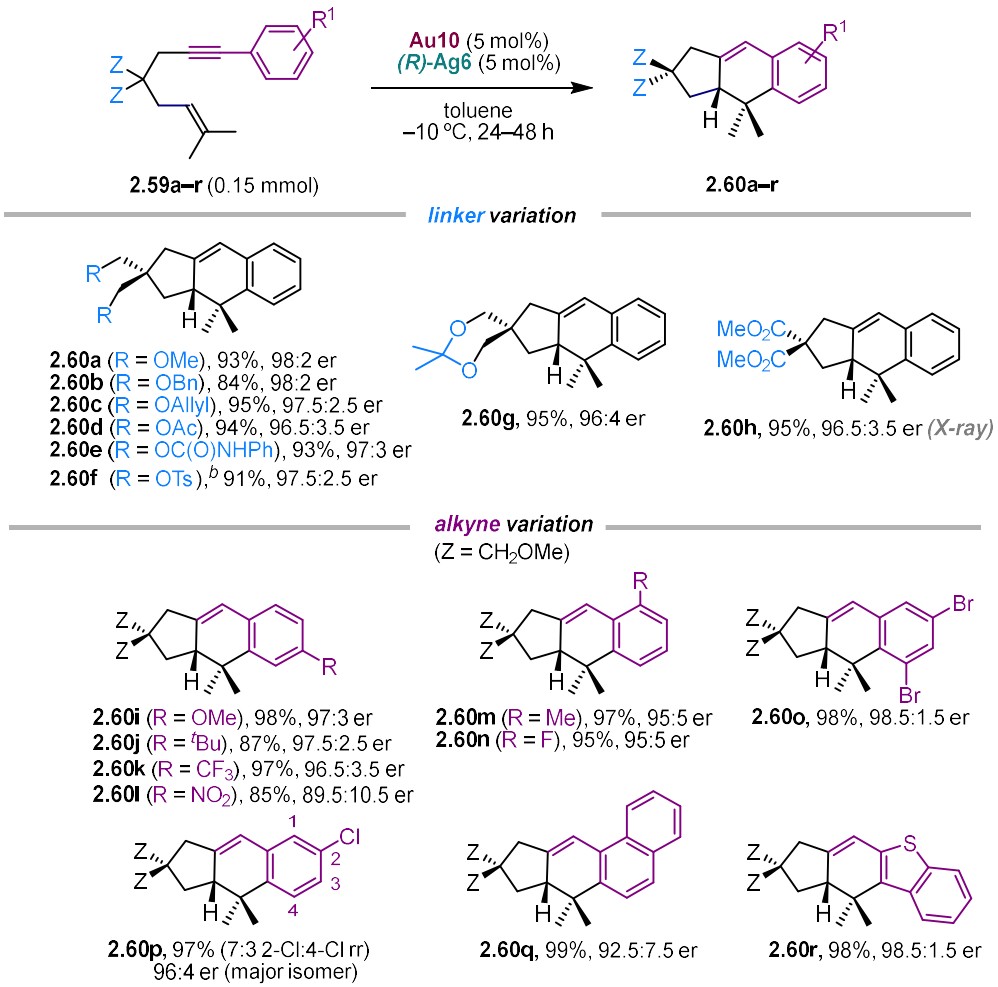

Scheme 2.13. Scope formal [4+2] cycloaddition of enyne **2.59**, effect of the linker and alkyne substituent on the substrate. [a] Reaction performed under Ar or N_2 in anhydrous toluene (0.1 or 0.2 M), unless otherwise stated. Yields of material isolated after purification, *er* determined by HPLC or SFC on chiral stationary phase. [b] Reaction carried out at 23 °C.

Compared to linker and alkyne variations, the catalytic system showed higher sensitivity to structural changes in the alkene (compare **2.60a** with **2.60s–w** in Scheme 2.13 and Scheme 2.14), in line with the fact that the chiral catalytic system needs to discriminate the two enantiotopic faces of the double bond. Thus, enynes **2.59s** and **2.59t** possessing geranyl or *trans*-cinnamyl groups cyclized to products **2.60s** and **2.60t** in less than 48 h (90–99% yield, 89:11–95.5:4.5 *er*), even though higher temperatures and/or catalyst loadings were required. Nevertheless, this represents a significant improvement over previous chiral gold catalysts that require 7–14 days at room temperature.[27e] Enyne **2.59u** possessing a *cis*-cinnamyl substituent afforded product **2.60u** in lower yield (48%, due to a competing cycloisomerization to an achiral diene product) and enantioselectivity (82:18 *er*). Formation of epimeric products **2.60t** and **2.60u** highlights the stereospecificity of the reaction with respect to the alkene configuration. More hindered substrates such as **2.59v** and **2.59w**, bearing respectively a cyclohexene or a tetrasubstituted alkene, delivered products **2.60v** and **2.60w** in good yield (61–95%) and moderate enantioselectivity (80:20–85:15 *er*), which is also remarkable considering that such bulky enynes were never engaged in this cycloisomerization, let alone asymmetrically.

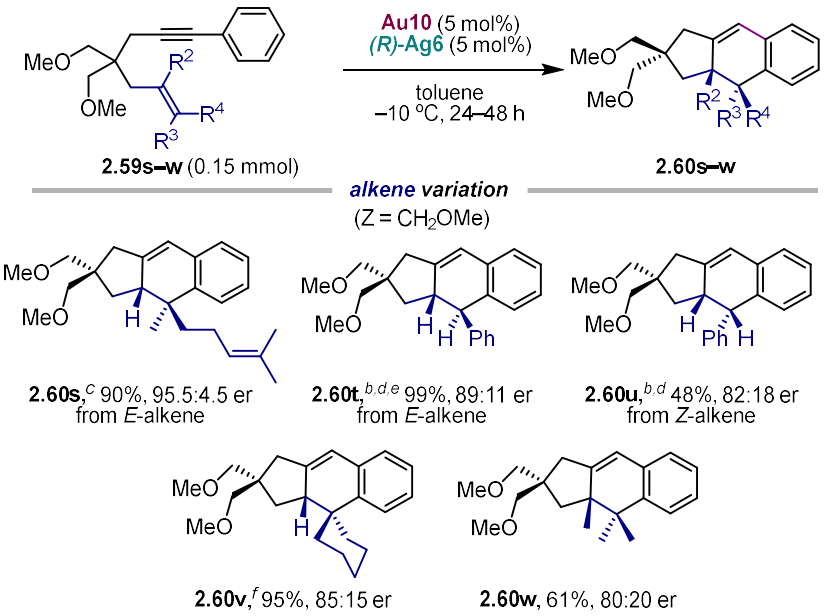

Scheme 2.14. Scope formal [4+2] cycloaddition of enyne **2.59**, effect of alkene substitution. [a] Reaction performed under Ar or N_2 in anhydrous toluene (0.1 or 0.2 M), unless otherwise stated. Yields of material isolated after purification, *er* determined by HPLC or SFC on chiral stationary phase. [b] At 23 °C. [c] At 0 °C. [d] Carried out with 10 mol% **Au10** and (*R*)-**Ag6**. [e] Including 5% of inseparable 6-*endo*-isomer. [f] Reaction time: 96h.

Finally, some of the substrates that did not give satisfactory results, either because the reactivity was too slow or because they yielded complex mixture of products, are depicted in Scheme 2.15. Reaction with **2.59x** was very slow, with only a 37% yield after 48 h, though with a promising 89:11 *er*. On the other hand, substrates **2.59y–z** led to complex mixtures.

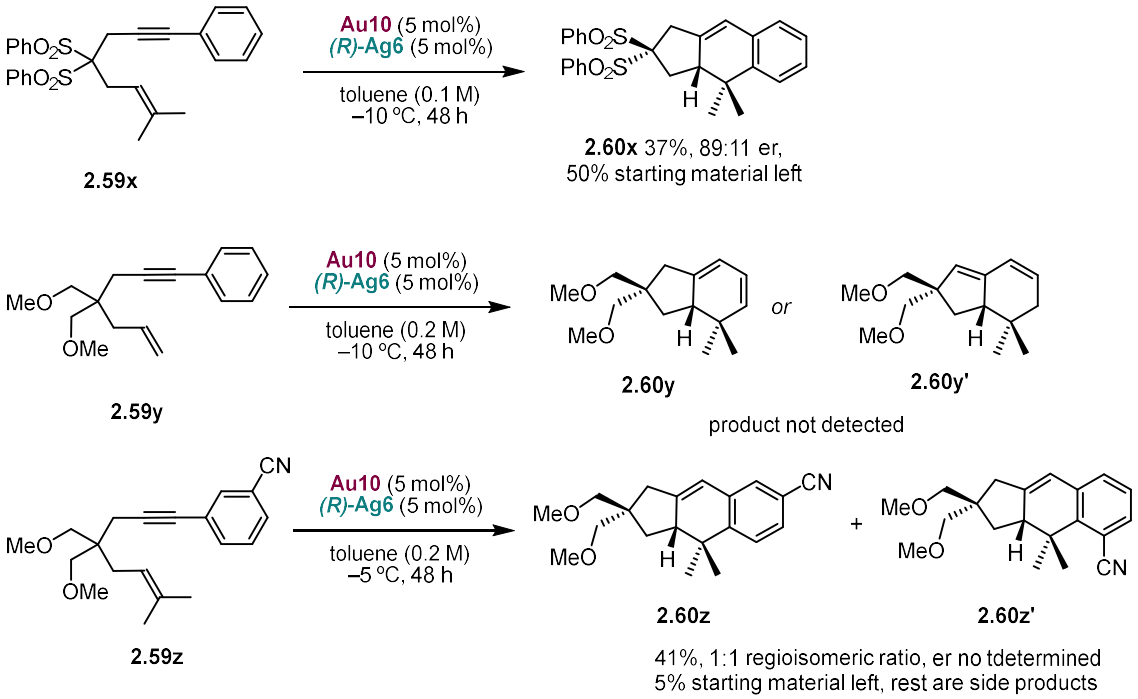

Scheme 2.15. Unsuccessful substrates on the application of the HCDC approach with the current library of catalyst.

Additional reactions with the JohnPhos-type gold(I)-urea catalysts

Judging by the enantioselectivity of the 5-*exo*-dig cyclizations presented in Scheme 2.13, the key interaction between the urea and the anion is not disrupted by H-bond acceptors on the substrates (such as ester, carbamate, tosylate and nitro groups in **2.59d–f**, **2.59h, 2.59l**), even though they are present in large excess with respect to the chiral anion. Protic additives with H-bond donor ability were also tolerated, as spiking the reaction of model enyne **2.59a** with 5 equiv-of methanol still delivered product **2.60a** in 80% NMR yield and 97:3 *er*. These observations suggest that H-bonding between the urea and the anion is strong enough to make for an effective and robust catalytic system, even if it is based on non-covalent interactions. To further prove this point, the **Au10/Ag6** catalytic system was also applied to the 6-*endo*-dig cyclization of enynes, with and without the addition of protic exogenous nucleophiles (Scheme 2.16).

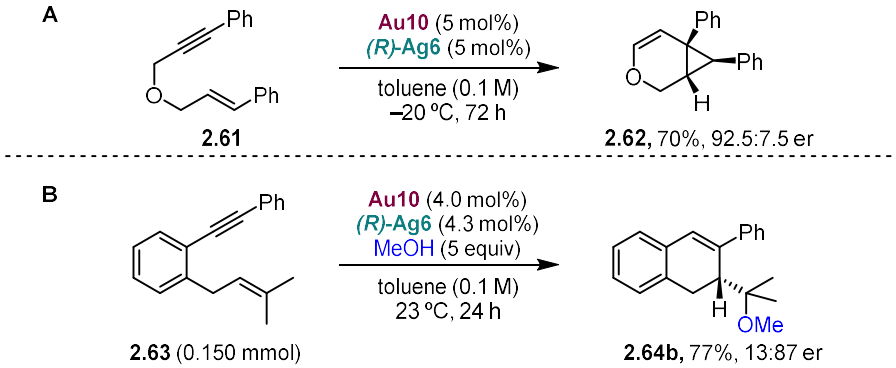

Scheme 2.16. cyclization of enynes **2.61** and **2.63** with and without the addition of nucleophiles.

O-Tethered enyne **2.61** was converted to oxabicyclo[4.1.0]hept-4-ene **2.62** in 70% yield and 92.5:7.5 *er* (Scheme 2.16A).[35] Initial tests for the methoxycyclization of benzene tethered enyne **2.63** were promising (Scheme 2.16B), so we performed a quick screening of the reaction conditions to fine-tune the catalytic system (Table 2.9). Reducing the temperature led to incomplete conversion of the substrate, which could be solved by increasing the catalyst loading to 4 mol%, but the difference in enantioselectivities when compared to standard conditions was not significative (Table 2.9, entries 1–3). Variations on equiv of nucleophile or reaction concentration did not lead to significant changes (Table 2.9, entries 4–7). Changing to more polar trifluorotoluene or 1,2-DCE led to a drop on enantioselectivity (Table 2.9, entries 4–7). Finally, using more active (*R*)-**Ag1** and lowering the temperature to –20 °C still was not enough to get useful levels of activity.

Table 2.9. Screening for the enantioselective gold(I)-catalyzed 6-*endo*-dig cyclization of **2.63** with nucleophile addition.

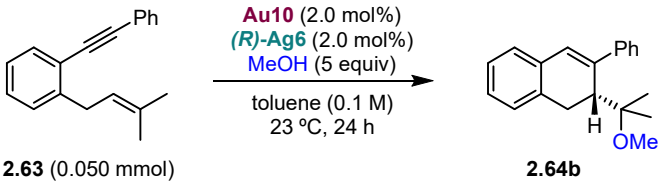

Entry	Variation from std conditions	T (° C)	Time (h)	2.63(%)[a]	2.63b (%)[a]	2.63b *er*[b]

35. a) M. Chao, D. Beltrami, Y. Toullec, V. Michelet, *Chem.Comm.*, **2009**, 6988–6990. b) Teller, H.; Corbet, M.; Mantilli, L.; Gopakumar, G.; Goddard, R.; Thiel, W.; Fürstner, A. *J. Am. Chem. Soc.* **2012**, *134*, 15331–15342.

1	none	23	15.5	0	77	13:87
2	0 ºC	0	15.5	39	33	11.5:88.5
3	0 ºC, 4 mol % cat	0	15.5	0	72	10.5:89.5
4	MeOH 2.5 equiv	27	19.5	0	70	12:88
5	MeOH 10 equiv	27	19.5	0	83	13.5:86.5
6	0.05 M	27	19.5	0	75	12:88
7	0.20 M	27	19.5	0	76	13.5:86.5
8	trifluorotoluene instead of toluene	23	19.5	0	64	20:80
9	1,2-DCE instead of toluene	23	19.5	0	81	20.5:79.5
10	–20 ºC, 4 mol % cat, 3 equiv MeOH	–20	22	62	20	*nd*
11	–20 ºC, 4 mol % cat, 3 equiv MeOH, **Au13** instead of **Au10**	–20	22	87	25	*nd*
12	–20 ºC, 4 mol % cat, 3 equiv MeOH, *(R)*-**Ag1** instead of *(R)*-**Ag6**	–20	22	74	8	*nd*

[a] Determined by ^{1}H NMR analysis of the crude reaction mixture against internal standard (1,1,2,2-tetrachloroethane). [b] Determined by HPLC analysis on chiral stationary phase. *nd* = Not determined.

A small scope of the reaction was then done to test the extent and versatility of the nucleophiles that could be tolerated (Scheme 2.17). Cyclization of benzene-tethered enyne **2.63** followed by the addition of *O*-based nucleophiles[28e,35b,36] delivered compounds **2.64a−e** in moderate to good yield and *er* (55−77%, 88.5:11.5 to 92.5:7.5 *er*). The first successful addition of a *N*-centered nucleophile to enynes of type **2.63** was demonstrated, obtaining azide **2.64f** in 62% yield and 90:10 *er*. Instead, fluoride addition afforded product **2.64g** in 69% yield and 61:39 *er*. The low enantiocontrol in the formation of **2.64g** can be explained by the strong tendency of the fluoride ion to H-bond with the urea,[37] thus preventing the key interaction that keeps the chiral anion close to the reaction center.

36. Sanjuán, A. M.; Martínez, A.; García-García, P.; Fernández-Rodríguez, M. A.; Sanz, R. *Beilstein J. Org. Chem.* **2013**, *9*, 2242–2249
37. a) Pfeifer, L.; Engle, K. M.; Pidgeon, G. W.; Sparkes, H. A.; Thompson, A. L.; Brown, J. M.; Gouverneur, V. *J. Am. Chem. Soc.* **2016**, *138*, 13314–13325. b) Ibba, F.; Pupo, G.; Thompson, A. L.; Brown, J. M.; Claridge, T. D. W.; Gouverneur, V. *J. Am. Chem. Soc.* **2020**, *142*, 19731–19744.

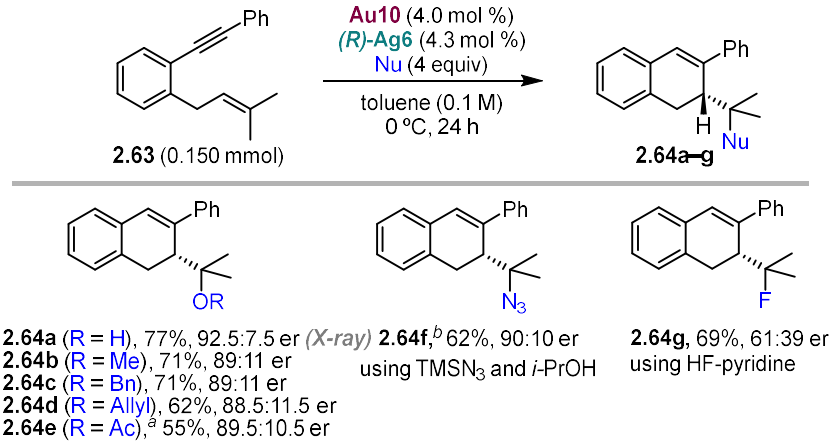

Scheme 2.17. Scope of the gold(I)-catalyzed 6-*endo*-dig cyclization with exogenous nucleophile addition employing the HCDC strategy for asymmetric gold(I) catalysis. [a] Reaction run for 48 h. [b] Reaction carried out at 23 °C.

Importantly, derivatization of the water- and azide-addition products (Scheme 2.18) gave access to *O*- and *N*-derivatives equivalent to the formal addition of noncompetent nucleophiles, thus expanding the scope and underlying the usefulness of this enantioselective protocol. For example, alcohol **2.64a** was transformed into benzoate **2.64h**, as well as into diene **2.65**, which displays the core of the carexane natural products.[28e,38] Triazole **2.64i**, primary amine **2.64j**, and amide **2.64k** were easily obtained from azide **2.64f** without erosion of the enantiopurity, as expected.

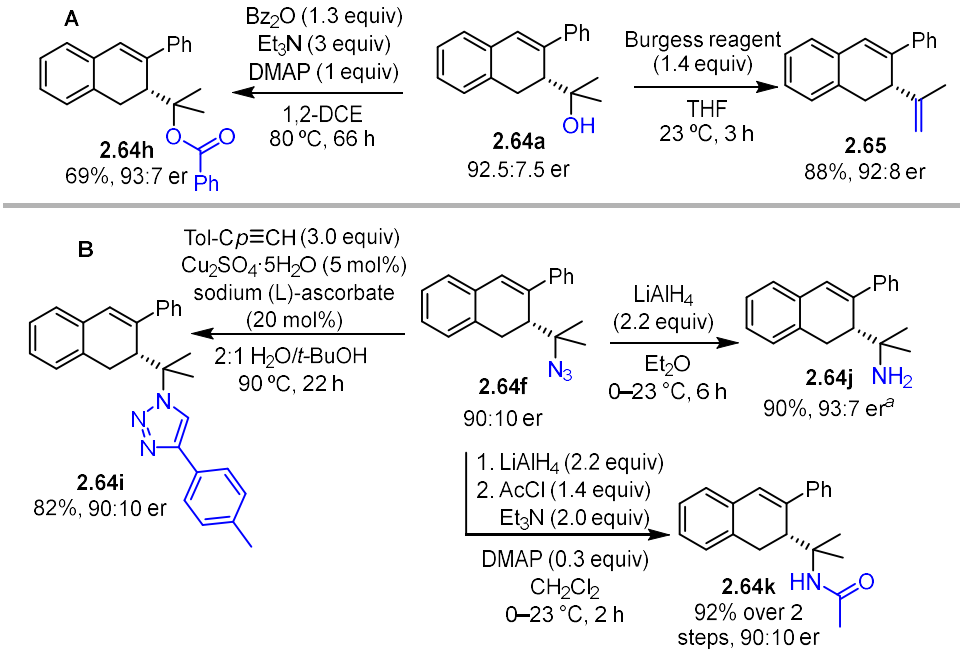

Scheme 2.18. Derivatization of product **2.64** from the 6-endo-dig cyclization/nucleophile addition of enyne **2.63**. A) prepared from water addition product **2.64a**. B) prepared from NaN_3 addition product **2.64f**. [a] Prepared from a batch of **2.64f** with 93:7 *er*.

On the other hand, when the internal aryl alkynes on the 1,6-enyne substrates were changed for terminal alkynes **2.66** and **2.68**, a drop on the enantioselectivities was observed (Scheme 2.19). For instance, the methoxy- and ethoxycyclization of the terminal alkyne analogue to benzene-

38. D'Abrosca, B.; Fiorentino, A.; Golino, A.; Monaco, P.; Oriano, P.; Pacifico, S. *Tetrahedron Lett.* **2005**, *46*, 5269–5272.

tethered enyne **2.63** (**2.66**) afforded product **2.67** in a 94% yield with a 78.5:21.5 *er*, which could be improved to 87:13 *er* at the cost of reduced conversion by lowering the temperature to −78 °C. On the 5-*exo*-dig cycloisomerization of *O*-linked enyne **2.68** the stereocenters generated on the gold(I) carbene are lost upon protodeauration step. To keep those newly generated chiral centers, the gold(I) carbene was trapped *in situ* with diphenyl sulfoxide, affording bicyclic ether **2.69**.[39] Under non-optimized conditions, cyclopropyl aldehyde **2.69** was produced in 42% yield with a 83:17 *er*, representing a significant improvement over the previously reported enantioselective synthesis, which achieved a poor 48.5:51.5 enantiomeric ratio.[40]

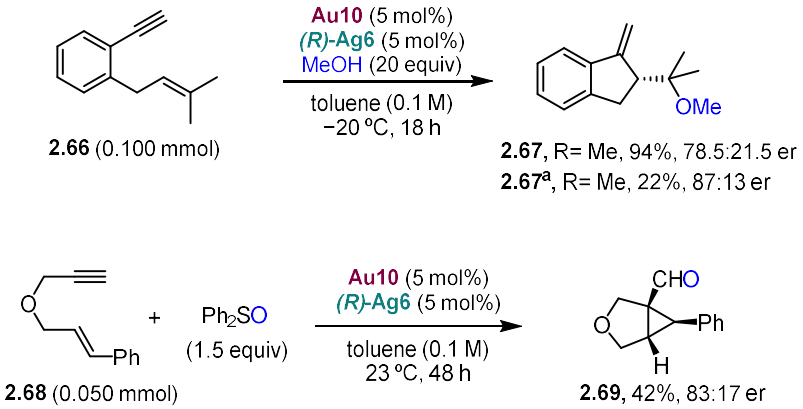

Scheme 2.19. Gold(I)-catalyzed nucleophile addition to 1,6-enyne bearing terminal alkynes. [a] Reaction carried out at −78 °C with 5 equiv of the corresponding nucleophile.

Single-crystal X-ray diffraction of products **2.60h** and **2.64a** and comparison of optical rotations with available literature values[28e] indicated that the newly created stereocenters are (*R*)-configured in both the 5-*exo*-dig and 6-*endo*-dig cyclizations. This means that in the enantio-determining step of both cyclizations, the *Si* face of the alkene attacks the Au(I)-activated alkyne, delivering the corresponding cyclopropyl Au(I) carbene intermediates (Scheme 2.20).

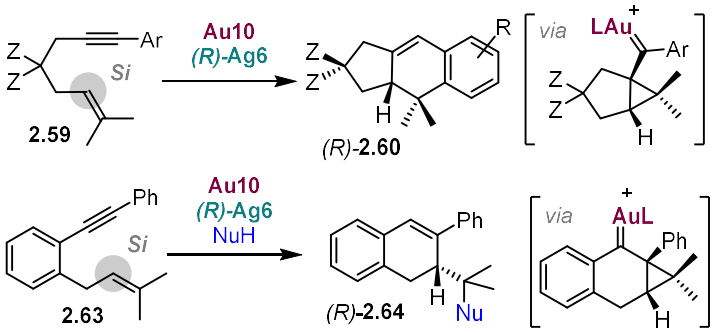

Scheme 2. 20. Enantiofacial selectivity in the enantiodetermining step of the gold(I)-catalyzed formal (4+2) cycloaddition and 6-*endo*-dig cyclization with nucleophile addition using **Au10** and (*R*)-**Ag6**.

Mechanistic study on the HCDC gold(I)-catalyzed formal [4+2] cycloaddition

To shed some light onto the mechanistic aspects of our newly developed approach for enantioselective gold(I)-catalysis we decided to perform some mechanistic studies on its application in the formal [4+2] cycloaddition of enyne **2.59a**. As part of these investigations, cationic complex **Au14** was synthesized by reacting **Au10** with an equimolar amount of **$AgSbF_6$** in the presence of acetonitrile (Scheme 2.21), which acts as a labile ligand and stabilizes the

39. Witham, C. A.; Mauleón, P.; Shapiro, N. D.; Sherry, B. D.; Toste, F. D. *J. Am. Chem. Soc.* **2007**, *129*, 5838−5839.
40. Wang, W.; Yang, J.; Wang, F.; Shi, M. *Organometallics* **2011**, *30*, 3859–3869.

generated gold cation. The structure of **Au14** was confirmed through X-ray diffraction, revealing that in the solid state, the urea forms hydrogen bonds with the fluoride of the SbF_6 counteranion. In contrast, when **$AgSbF_6$** was replaced by (*R*)-**Ag6**, the neutral complex **Au15** was obtained. Although we could not get a good enough crystal for X-ray analysis, NMR analysis confirmed the absence of acetonitrile incorporation (by comparison of the signals of residual acetonitrile[41] with those of the coordinated one in **Au14**) and we could detect the peak of the expected product by HRMS using ESI as ionization method.

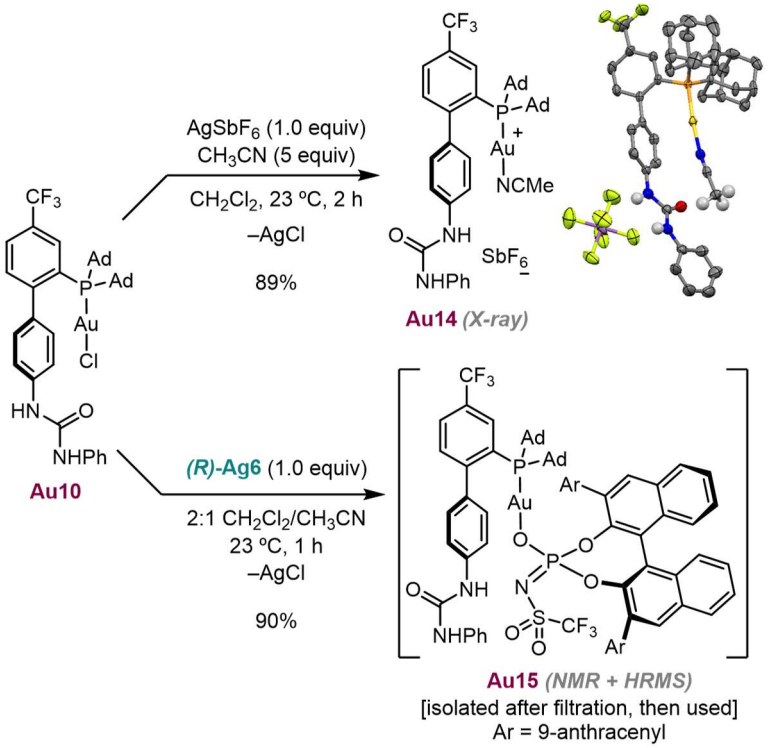

Scheme 2.21. Synthesis of cationic gold(I) complex **Au14** and neutral one **Au15**.

Some control experiments were then carried out this time with the optimal chiral counterion (*R*)-**Ag6**. Preactivated complex **Au15** delivered product **2.60a** with yield and enantioselectivity comparable to the *in situ* combination of **Au10** and (*R*)-**Ag6** (Table 2.10, entry 1 vs 2). As already demonstrated with the combination of **Ag1** with JohnPhosAuCl (Table 2.4, entry 2) that resulted in the formation of 40% of product as a racemic mixture. When **Ag6** was used in combination with the same precatalyst, no reactivity could be observed (Table 2.10, entry 3), which again showed that the urea is essential for displacing the chiral anion from Au and keeping it close to the reaction center allowing it to transfer its stereochemical information. This finding was further supported by ligand exchange experiments where cationic [JohnPhosAu(NCMe)]SbF_6 was treated with either **Ag6** or **Na6**, delivering some of the desired product but as a racemate (Table 2.10, entries 5 and 6). Interestingly, when cationic phosphinourea complex **Au14** was combined with **Ag6** the product was also obtained as a racemate within 1 h. In contrast, when **Na6** was used, product **2.60a** was obtained with 79:21 *er*. Adding 15-crown-5 ether to chelate the Na+ resulted in an increase of the enantiomeric ratio of the product to 90:10. These, results could indicate that the counteranion has a preference for Ag^+ over Au^+. Thus, to attain high enantioselectivity using this H-bonded system, it is crucial to associate the generation of catalytically competent Au(I) center to the removal of other cations, which could "kidnap" the chiral anion, leading to racemic

41. Residual non coordinated acetonitrile (compared to **Au14**) in the sample could not be removed even after washing the compound with alkanes and keeping it in the vacuum line for several days.

background reactivity (since Ag^+ nor Na^+ are active in this reaction, and the reaction was relatively fast). When using silver salts, precipitation of AgCl ensures that most of the Ag^+ is removed from deleterious solution equilibria with the anion rendering "naked" counterion that can interact with Au^+.

Table 2.10. Control experiments in the gold(I)-catalyzed formal cycloisomerization of **2.59a**.

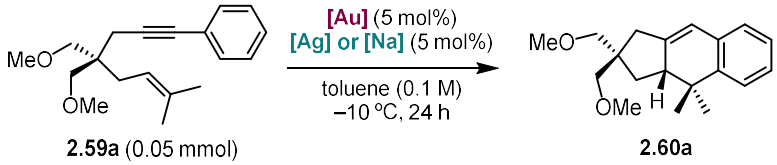

2.59a (0.05 mmol) **2.60a**

Entry	[Au]	[Na or Ag]	Yield (%)[a]	er[b]
1	**Au10**	*(R)*-Ag6	>95	98:2
2	**Au15**	-	>95	93:7
3	[(JohnPhos)AuCl]	*(R)*-Ag6	0	-
4	**Au10**	*(R)*-Na6	0	-
5	[(JohnPhos)Au(NCMe)]SbF_6	*(R)*-Ag6	24	50:50
6	[(JohnPhos)Au(NCMe)]SbF_6	*(R)*-Na6	3	50:50
7[c]	**Au14**	*(R)*-Ag6	>95	50:50
8	**Au14**	*(R)*-Na6	>95	79:21
9[d]	**Au14**	*(R)*-Na6	>95	90:10
10	**Au4**	(R)-Ag6	76	92:8

[a] Yields determined by ^{1}H NMR against dodecane as internal standard. [b] Determined by HPLC on chiral stationary phase. [c] Reaction was complete within 1 h. [d] 15-Crown-5 ether (1 equiv) was added

The non-linear effects were investigated by examining the *er* of the product as a function of the *er* of the **Ag6** salt. This was accomplished by mixing (*R*)-**Ag6** with varying amounts of (*S*)-**Ag6** to create a series of **Ag6** mixtures with known enantiomeric ratios. The resulting product *er* was then plotted against the *er* of the **Ag6** mixture (Figure 2.6). If a linear correlation is observed, it indicates that only one molecule of the chiral catalyst is involved in the enantio-determining step.[42] In this study, small deviations from the expected values, particularly the 4% enantiomeric excess (ee) observed for the product obtained from a supposedly racemic mixture of (*S*)-**Ag6** and (*R*)-**Ag6**, can be attributed to experimental errors. These errors likely stem from challenges in handling the silver salt stock solutions, such as dealing with small volumes and low weights, as well as potential slight differences in the enantiopurity of (*S*)-**Ag6** and (*R*)-**Ag6**. Although the ee for each enantiomer was assumed to be >99%, it may vary slightly depending on the optical purity of the commercial binaphthol starting materials. Overall, these results support the conclusion that only one chiral anion is involved in the enantio-determining step, consistent with the formation of the expected 1:1 urea complex.[43]

42. Geiger, Y.; Achard, T.; Maisse-François, A.; Bellemin-Laponnaz, S. *Chem. Sci.* **2020**, *11*, 12453–12463.
43. a) Amendola, V.; Fabbrizzi, L.; Mosca, L. *Chem. Soc. Rev.* **2010**, *39*, 3889–3915. b) Blažek Bregović, V.; Basarić, N.; Mlinarić-Majerski, K. *Coord. Chem. Rev,***2015**, *295*, 80–124.

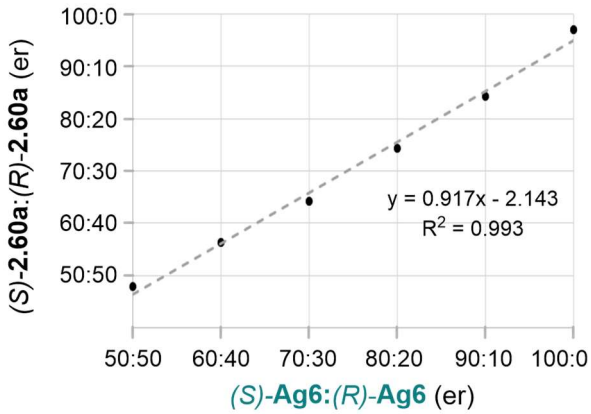

Figure 2.6. Non-linear effects study on the **Au10**/**Ag6**-catalyzed cyclization of **2.59a** with linear regression.

To our surprise, crystals suitable for X-ray analysis of a triethylammonium salt of **Ag6** grew by slow evaporation of a reaction mixture (experiment with 50:50 ratio of **Ag6** enantiomers) after quenching with Et_3N and diluting with CH_2Cl_2. Comparing the crystal structures of (*R*)-**Ag6** and the analogous triethylammonium salt (*R*)-**Et_3NH6**, we can observe that the P–O and S–O bonds are nearly parallel, forming a ~3 Å-wide "pincer" with the two oxygen atoms (Figures 2.7).

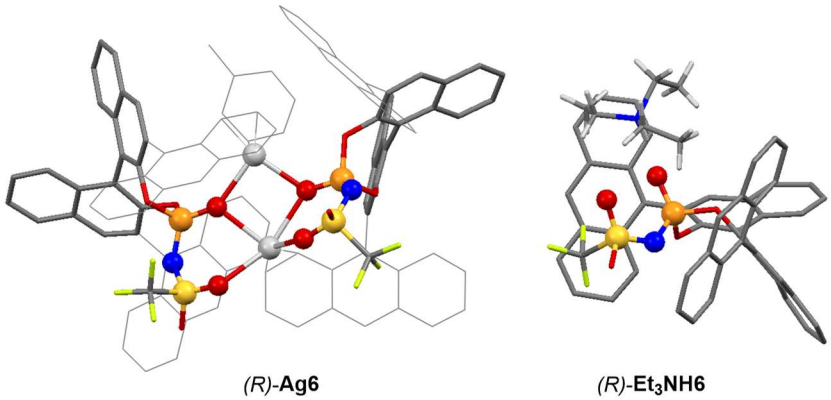

Figure 2.7 X-ray structures of (*R*)-**Ag6** and (*R*)-**Et_3NH6**, solvent molecules and H atoms (except those of triethyl ammonium) omitted for clarity.

We envisioned that the H-bonding interactions should be detectable between the urea of the gold(I) complex and the phosphoramidate group of the chiral anion. To do so we needed to avoid chloride scavenging, since using (*R*)-**Ag6** resulted in poorly resolved spectra (due to the formation of **Au15** and chloride bridged species), so (*R*)-**Na6** was used instead. **Au10** was also switched for **Au4** since the latter, despite similar reactivity to the former (Table 2.10, entry 1 vs 10), was more easily monitored by ^1H NMR. At first, no variation on the NMR was observed, presumably pointing to the chiral anion remaining associated with Na^+, without interacting at all with the neutral urea. However, when adding 15-crown-5 ether, to force dissociation of the sodium cation without undesired scavenging the chloride (Table 2.10, entry 9), we could observe a shift on the signals NH_a and NH_b of the urea (Figure 2.8). Titration of complex **Au4** (10 mM in CD_2Cl_2 at 25 °C), in the presence of an excess of crown ether, with increasing amounts of (*R*)-**Na6** resulted in clear deshielding of both NH signals of the urea, indicating their engagement in H-bonding interactions with the anion (Figure 2.8). The establishment of such H-bonds during the reaction is expected to be entropically more favorable in reaction with (*R*)-**Ag6** because after AgCl precipitation, the Au(I)-bound chiral anion should already be close to the H-bond donor.

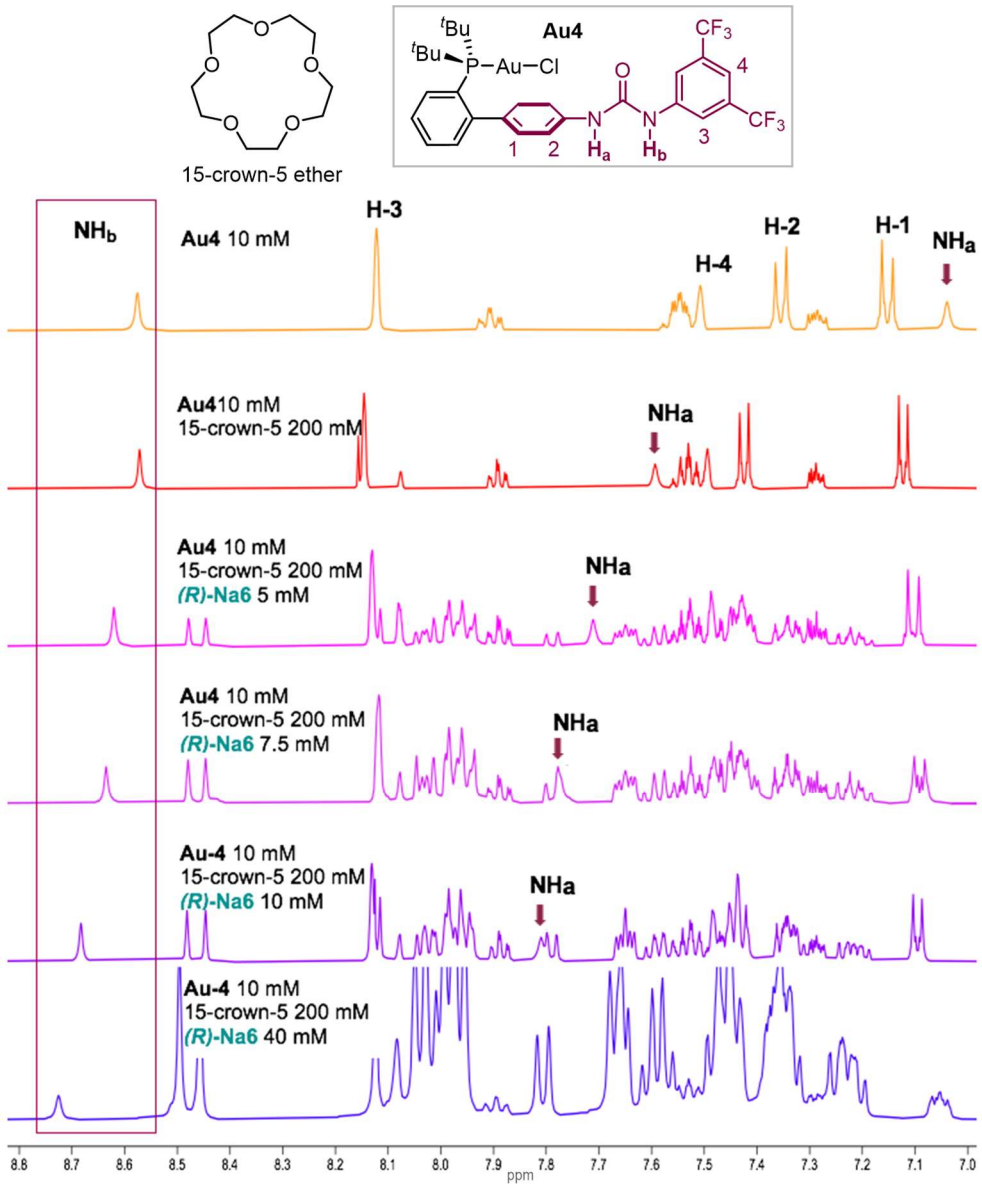

Figure 2.8 ^{1}H NMR monitoring of **Au4** with (*R*)-**Na6** in the presence of 15-crown-5 ether.

Kinetic studies

Reaction progress kinetic studies were conducted on the cycloisomerization of **2.59a** to **2.60a** catalyzed by **Au10**/(*R*)-**Ag6** system in toluene-d_8 at −10 °C. We chose the variable time normalization analysis (VTNA), introduced by Burés.[44] In contrast to the initial rates that only explains the reaction behavior at the beginning of the reaction (until ca. 20% or less usually), VTNA allows the analysis of the whole reaction profile, which can lead to the analysis of catalyst degradation or changes in the reaction order of some components. Another advantage of the Burés method is that fewer sets of conditions are needed to determine the reaction order in one component of the reaction and the data interpretation is done simply by direct visual comparison of reaction profiles.[44] The profiles of experiments differing in concentration of one reactant, R, will only overlay when the time axis is replaced by the time integral of [R] raised to the correct

44. a) Burés, J. *Angew. Chem. Int. Ed.* **2016**, *55*, 2028–2031. b) Burés, J. *Angew. Chem. Int. Ed.* **2016**, *55*, 16084–16087. c) Nielsen, C. D.-T.; Burés, J. *Chem. Sci.* **2019**, *10*, 348–353.

power of α (order in R) [Eq. (1)]. The data provided below was obtained from ^{1}H NMR studies using tetrachloroethane or *n*-dodecane as internal standard and further manipulated with Excel.

$$\int_{t=0}^{t=n}[R]^{\alpha}dt = \sum_{i=1}^{n}\left(\frac{[[R]_i+[R]_{i-1}}{2}\right)^{\alpha}(t_i - t_{i-1}) \quad \text{(Eq. 1)}$$

Following this method, the reaction was determined to be approximately first order in catalyst (0.9) and 0.5 order in substrate (Figures 2.9 and 2.10). A first-order dependence on catalyst is typical for most catalyzed reactions, provided the catalyst does not decompose or form inactive species. The partial, non-integer order in substrate is consistent with unimolecular catalyzed reactions that follow Briggs-Haldane kinetics and have a Michaelis-Menten constant (K_M)[45] close to the substrate concentration.

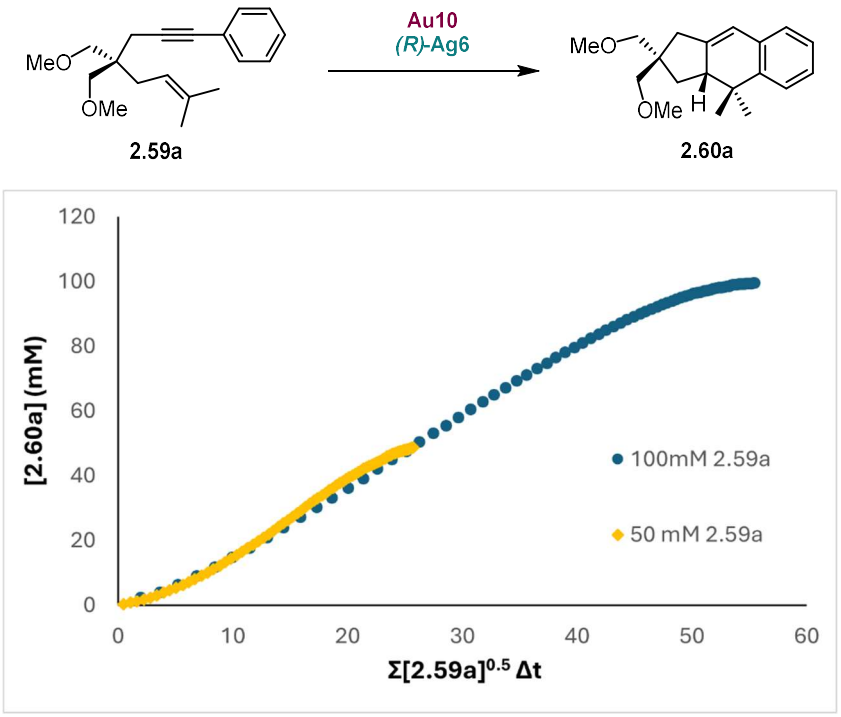

Figure 2.9. 0.5 Order in substrate determined by VTNA analysis.

45. a) Michaelis, L.; Menten, M. L. *Biochem. Z.* **1913**, *49*, 333–369. b) Johnson, K. A.; Goody, R. S. *Biochemistry* **2011**, *50*, 8264–8269.

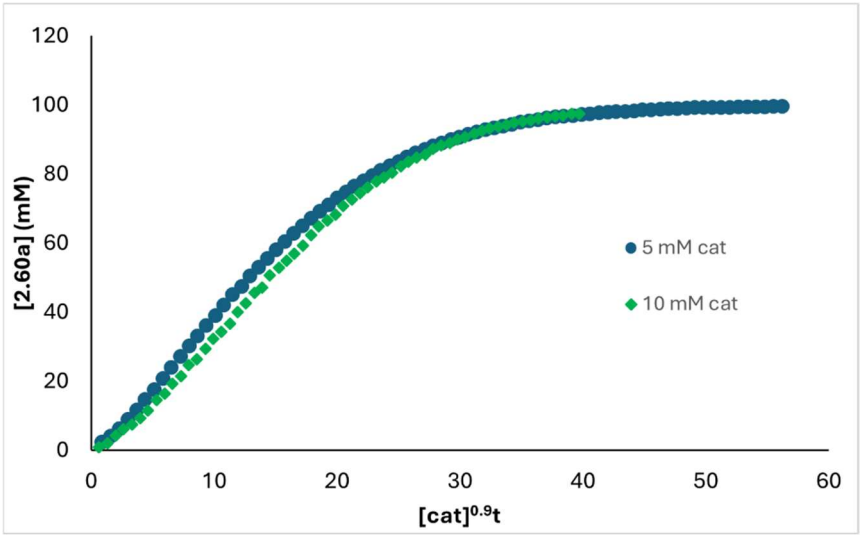

Figure 2.10 0.9 order in catalyst **Au10** determined by VTNA.

^{1}H NMR monitoring showed clean conversion of enyne **2.59a** to product **2.60a** (Figure 2.11). An initial induction period was observed, likely due to a non-instantaneous chloride abstraction. The plot shows a relatively quick conversion at the beginning and a plateau at around 10 h. The data in Figure 2.11 was fitted to a polynomial equation that was further derived to the rate equation (Figure 2.12).

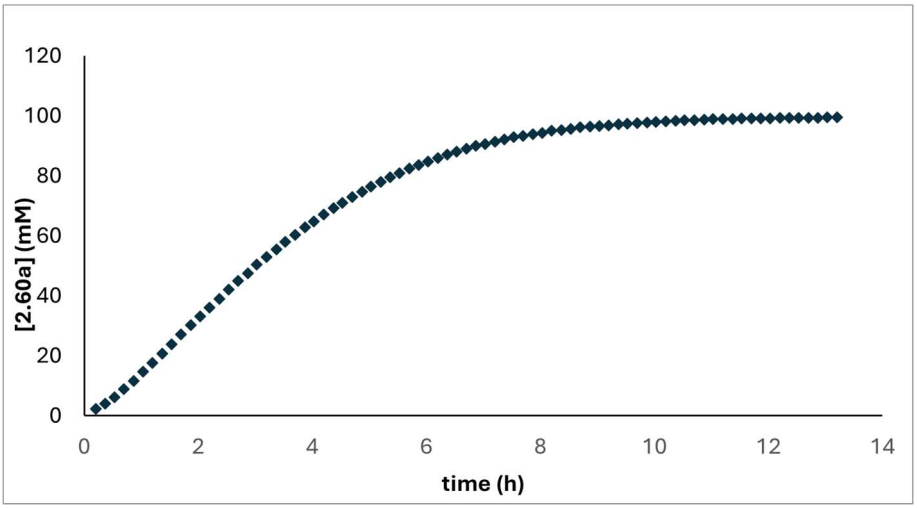

Figure 2.11. ^{1}H NMR monitoring of the standard reaction of substrate **2.59a** (100 mM initial concentration) to product **2.60a**, catalyzed by **Au10** and (*R*)-**Ag6** (5 mM).

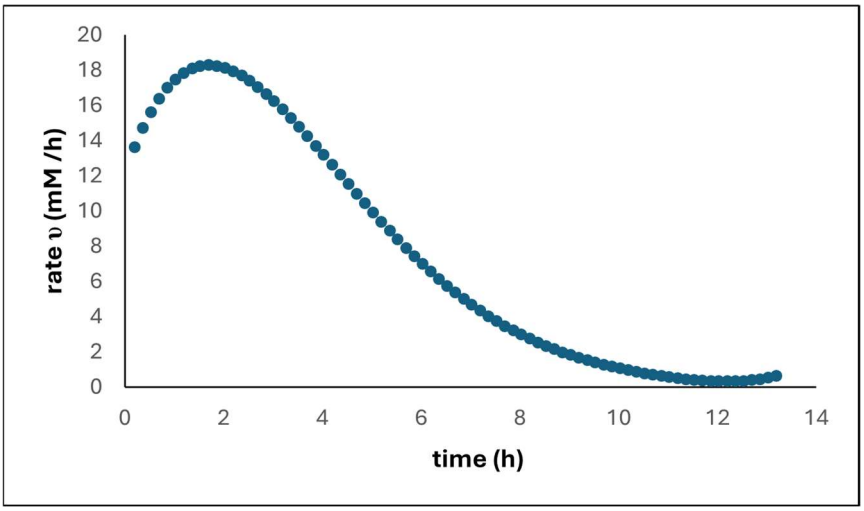

Figure 2.12. Derived differential of the ^{1}H NMR monitoring of the standard reaction in **Figure 2.10**.

A double reciprocal Lineweaver-Burk plot was constructed,[46] using data in the 1.5−10 h time range (Figure 2.13), by plotting the reciprocal of the reaction rate against the reciprocal of substrate concentration. The Michaelis-Menten constant (K_M) and V_{MAX} were calculated to be 74 ± 4 mM and 7.1 ± 0.4 h^{-1} respectively.[47,48] Given that substrate concentrations ranged from 0−100 mM during the reaction, this intermediate K_M value justifies the partial order in substrate determined by VTNA.

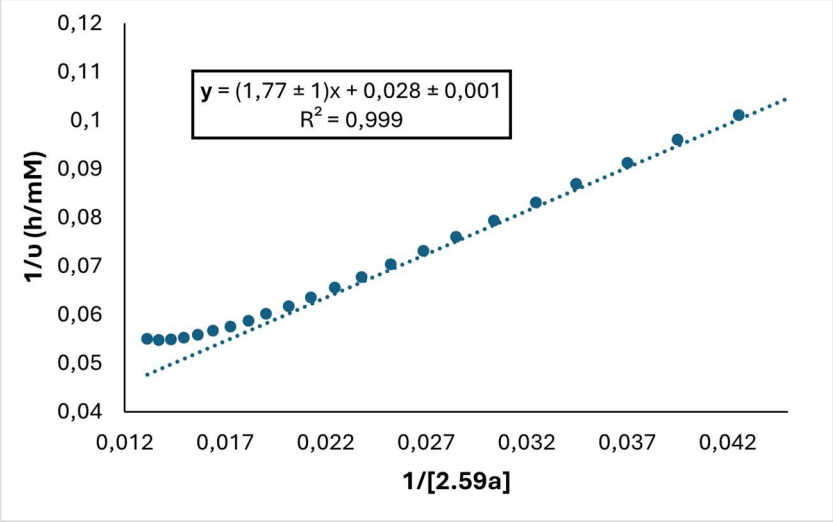

Figure 2.13. Lineweaver-Burk plot, using data from points 1.5–10 h.

The experimentally observed 0.5 order in substrate aligns with the elasticity coefficient (ε),[49] which, as mentioned in Chapter 1, predicts the variations in order in substrate for Briggs-Haldane kinetic regimes based on K_M and substrate concentration (Figure 2.14). [48]

46. Lineweaver, H.; Burk, D. *J. Am. Chem. Soc.* **1934**, *56*, 658–666.
47. The uncertainty refers not to experimental variation but to mathematical error of the linear regression, determined using Excel LINEST routine.
48. See Chapter 1 for more information on Briggs-Haldane kinetics and the determination of K_M and V_{max}.
49. Burés, J. *Top. Catal.* **2017**, *60*, 631–633.

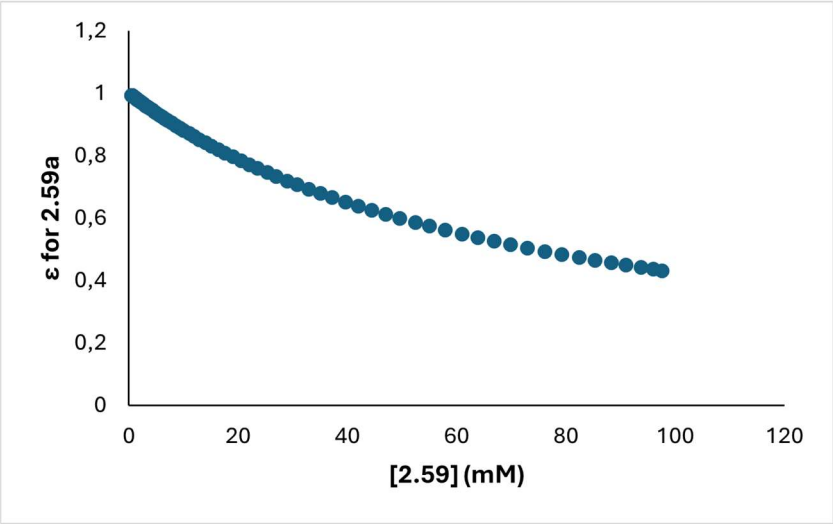

Figure 2.14 Variation of the elasticity coefficient for the order in substrate **2.59a** against **[2.59a]**.

DFT Studies

Some DFT studies were performed on a model diphenylurea in combination with our phosphoramidate **Ag6** counterion were performed to gain some insights into the possible conformers and the interaction between the hydrogen bond donor and the anion.[50] After screening several conformers, the most stable was found to be **U-I** presenting a bidentate hydrogen bond interaction to the phosphoryl oxygen atom. However, **U-II**, a conformer where the NH groups bond to both the phosphoryl and sulfonyl oxygen atoms is only 0.8 kcal/mol higher in energy. Interestingly, most inputs with the urea NH groups placed to H-bond with both the PO and the SO groups were optimized to output geometries with the urea H-bonding exclusively to the phosphoryl moiety.

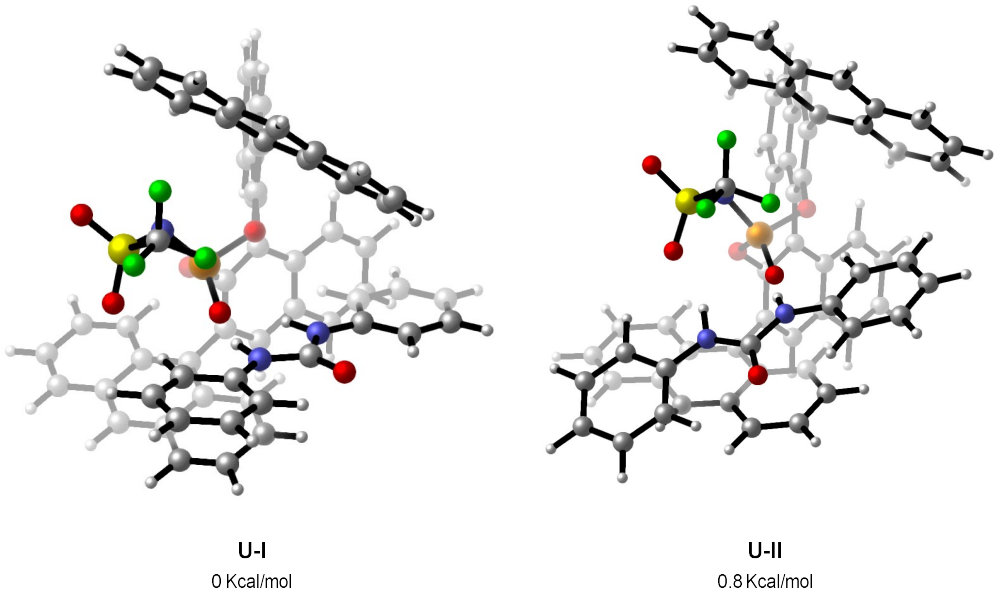

Figure 2.15 CYLview representation of the most stable conformers of the interaction between the anion from (*R*)-**Ag6** and a model diphenylurea, calculated by DFT. Visualized with CYLView program. Color code: P, orange; F, green; O, red; N, blue; S, yellow; C, gray; and H, white.

50. Calculations were carried out using B3LYP/6-31G(d) (C, H, P, O, F, N, S)//B3LYP-D3/6-311G(d,p) and SDD (Au) and with toluene as solvent (PCM).

The optimized *anti,anti*-diphenylurea presented a 2.1 Å H–H distance between the NH groups (similar to the distance observed in **Au10** in the solid state), not matching with the larger anionic O,O pincers (structures where the urea H-bonds to two sulfonyl O atoms are significantly higher in energy (ΔGsol ≥ 10 kcal/mol). The same was observed for structures where the urea NH groups H-bond to the N atom of the anion and to an O atom (either from the phosphoryl or the sulfonyl groups, ΔGsol ≥ 5 kcal/mol).

Proposed Mechanism for the Gold(I)-Catalyzed Formal [4+2] Cycloaddition

A proposed mechanism is depicted in Scheme 2.22 for the enantioselective formal [4+2] cycloaddition of enyne **2.59** catalyzed by **Au10**/(*R*)-**Ag6**, considering all experimental, spectroscopic and kinetic evidence discussed above as well as previous studies on this cycloisomerization.

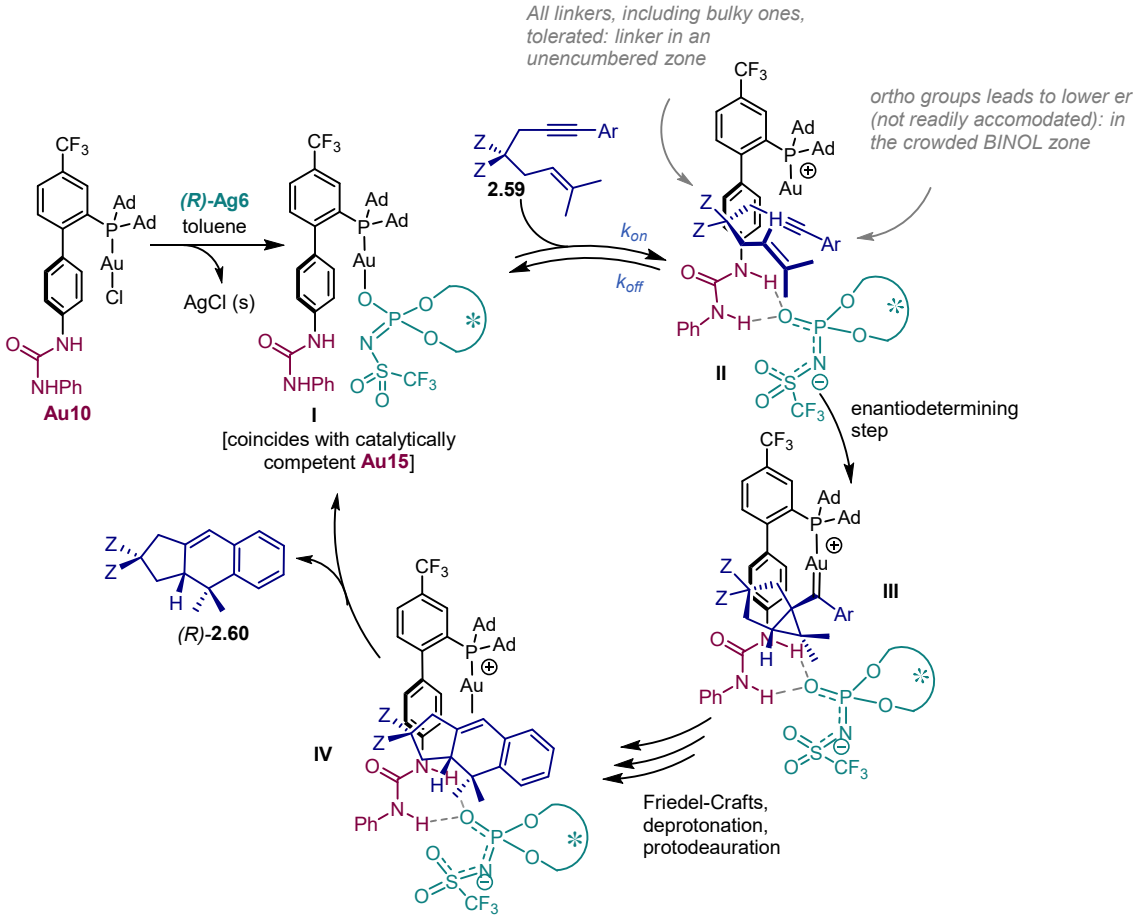

Scheme 2.22 Proposed mechanism for the gold(I)-catalyzed enantioselective formal [4+2] cyclization of enyne **2.59** using the HCDC approach, with **Au10** and (*R*)-**Ag6.**

Upon mixing the Au(I) chloride complex **Au10** with (*R*)-**Ag6**, a neutral complex **I** is formed, featuring a phosphoramidate anionic ligand, coinciding the previously prepared and catalytically competent **Au15**. The expected chloride scavenging, which leads to the precipitation of AgCl, matches the observed transformation of a thick whitish suspension of **Au10** and enyne in toluene into a solution with only some precipitate when (*R*)-**Ag6** is added. We propose that neutral complex **I** reversibly coordinates with enyne **2.59** leading to cationic complex **II**, where the anion is hydrogen-bonded to the pendant urea, and the alkyne coordinates to Au. This equilibrium could be explained by the partial order in substrate observed in the Briggs–Haldane kinetics. Additionally, in a model system, spectroscopic evidence of hydrogen bonding between the anion

and both NH groups of the urea was observed (see NMR titration in Figure 2.8). Regarding the precise geometrical arrangement, we propose that the NH groups establish two hydrogen bonds with the phosphoryl oxygen atom. This hypothesis is supported by solid-state observations and density functional theory (DFT) calculations with implicit solvent models described above. **Au10**, presenting a 2.0 Å H–H distance between the urea NH groups in the solid state (Figure 2.3) is not wide enough to chelate to both P–O and S–O of **Ag6** (Figure 2.7) as also observed in the DFT calculations with the model diphenyl urea (Figure 2.15).

The enyne orientation is expected to happen as shown in complex **II** (Scheme 2.22), with the arene pointing toward the more crowded BINOL region and the linker occupying a less hindered area. This would be consistent with the lower *er* observed in the cyclization of aryl *ortho*-substituted substrates **2.59m–n** and **2.59q** (95:5 and 92.5:7.5 respectively), which would not be as accommodated as others, and with the catalyst ability to tolerate instead bulky linkers **2.59a–q**. At this point, the C–C bond formation takes place, this being the enantiodetermining step, [27,28e] via the attack of the *Si* face of the alkene to the activated alkyne, forming cyclopropyl gold(I) carbene **III**. The alkene attack being the enantiodetermining step is also in line with the fact that variations in the alkene moiety led to large changes on the enantiomeric ratios. From this point, and based on previous reports on this reaction, intermediate **III** undergoes Friedel-Crafts-type ring expansion, deprotonation of the Wheland intermediate and protodeauration yielding intermediate **IV**.[27,28e] Finally, product to substrate ligand exchange is most likely mediated by the anion via the intermediacy of species **I**, thus closing the cycle and releasing product **2.60**.

Enantioselective Gold(I)-Catalyzed Addition to 2-Alkynyl Enones

As exemplified in the cases above, when using hydrogen-bonded counterion-directed catalysis, the factors that most influence the stereochemical outcome are: 1) the strength and geometry of the H-bond donor, 2) its relative position in the metal complex, and 3) the nature of the chiral counteranion (basicity and steric bulk). In light of the previous extensive screening of reaction conditions, we decided to screen these parameters systematically for the enantioselective gold(I)-catalyzed addition to 2-alkynyl enones to expand the scope of the HCDC as well as benchmark it with previously reported ACDC-based reports.[14a,51,52] A library of our previously prepared phosphine Au(I) chloride complexes equipped with a urea or squaramide groups on triphenylphosphine-[53] or JohnPhos-type scaffolds was evaluated (Scheme 2.23). These complexes vary in terms of phosphine, H-bond donor and linker between the two families.

51. First reported in: a) T. Yao, X. Zhang, R. C. Larock, *J. Am. Chem. Soc.* **2004**, *126,* 11164–11165; other selected gold-catalyzed versions: b) T. Yao, X. Zhang, R. C. Larock, *J. Org. Chem*. **2005**, *70*, 7679–7685; c) X. Liu, Z. Pan, X. Shu, X. Duan, Y. Liang, *Synlett* **2006**, 1962–1964; seminal reports employing other transition-metal catalysts: d) N. T. Patil, H. Wu, Y. Yamamoto, *J. Org. Chem*. **2005**, *70*, 4531–4534; e) C. H. Oh, V. R. Reddy, A. Kim, C. Y. Rhim, *Tetrahedron Lett.* **2006**, *47*, 5307–5310; f) Y. Xiao, J. Zhang, *Angew. Chem. Int. Ed.* **2008**, *47*, 1903–1906; g) W.-L. Chen, J. Li, Y.-H. Zhu, L.-T. Ye, W. Hu, W.-M. Mo, *ARKIVOC* **2011**, 381–392; h) H. Gao, J. Zhang, *Chem. Eur. J.* **2012**, *18*, 2777–2782
52. For reports on the enantioselective reaction of 2-alkynyl enones **1.40** and **2.70**: a) V. Rauniyar, Z. J. Wang, H. E. Burks, F. D. Toste, *J. Am. Chem. Soc*. **2011**, *133*, 8486–8489; b) G. Force, Y. L. T. Ki, K. Isaac, P. Retailleau, A. Marinetti, J.-F. Betzer, *Adv. Synth. Catal*. **2018**, *360*, 3356–3366; c) Y. Yu, Z. Zhang, A. Voituriez, N. Rabasso, G. Frison, A. Marinetti, X. Guinchard, *Chem. Commun.* **2021**, *57*, 10779–10782
53. These were a selected group of catalysts from **Chapter 1**, varying in linker length between P and hydrogen bond donor and in acidity.

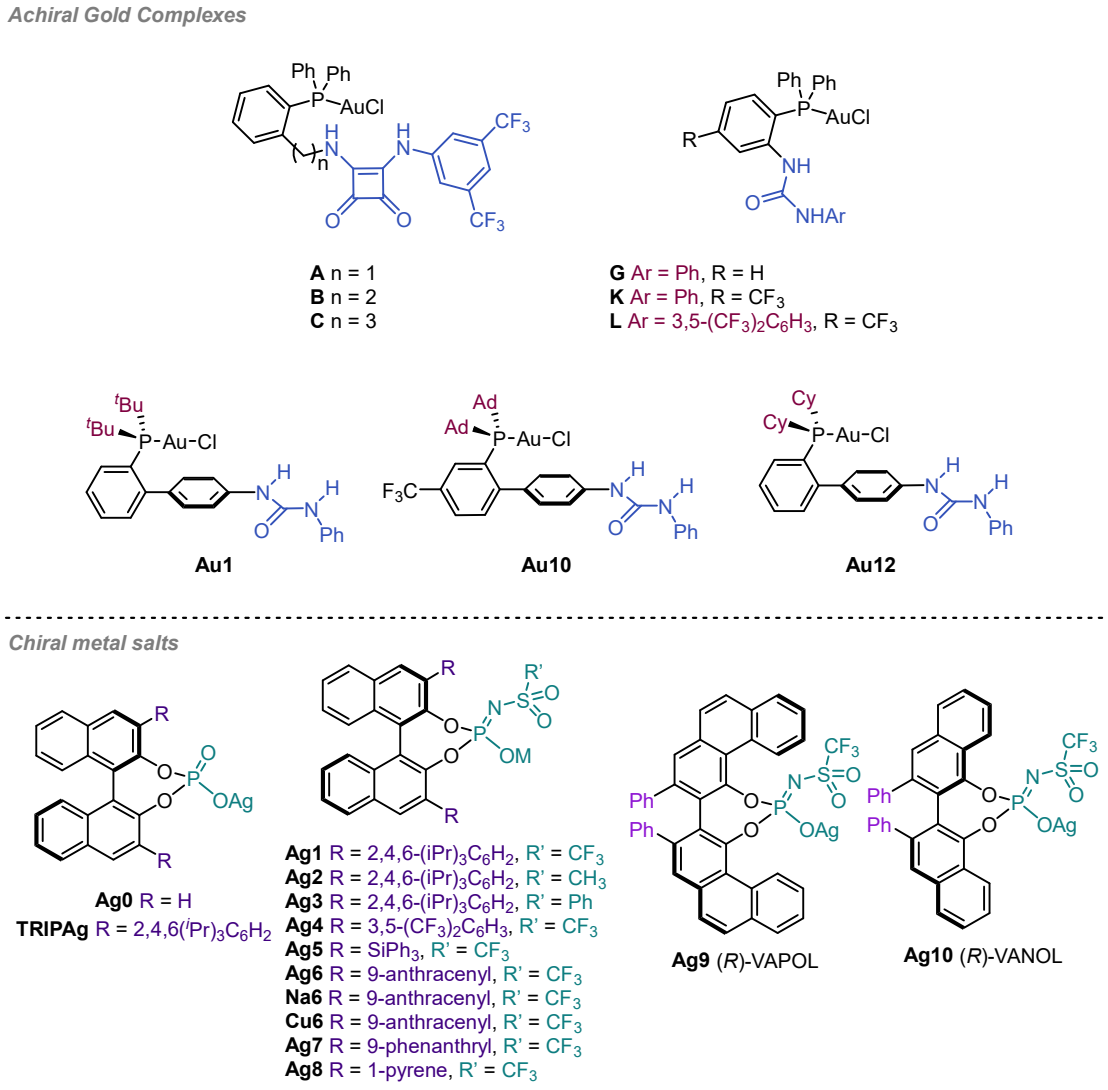

Scheme 2.23. Library employed in the study of the tandem gold(I)-catalyzed cycloisomerization/nucleophile addition reaction.

In Chapter 1, complex **A**–**L** already showed promising reactivities in the silver-free Au(I)-catalyzed tandem cyclization-indole addition to enone **1.40**, albeit as a racemic mixture.[48] Upon addition of chiral salt (*R*)-**Ag1** to reaction with complex **C**, the catalytic efficiency improved notably, delivering the desired product in high yield and with promising enantioselectivities in favor of the (*S*) enantiomer (Table 2.11, entry 1).[54] As already observed in the previous case, concentration had little impact on the enantioselectivity (Table 2.11, entries 1–3). Interestingly, when catalyzed by Ag(I) salt (*R*)-**Ag1** alone, the reaction afforded the *R*-enantiomer of the product preferentially, opposite to the one observed when combined with achiral phosphinosquaramide Au(I) complex **C**. This switch in enantioinduction points to the fact that a very different chiral pocket forms upon interaction between the H-bond donor and the chiral anion. Commercially available precatalysts [JohnPhosAuCl] and [(PPh_3)AuCl] in combination with (*R*)-**Ag1** delivered the product in quantitative yields but with lower *er* and with a preference for the same enantiomer

[54]. For the discussion on the determination of the absolute configuration of the products of catalysis with either Au(I) + Ag(I), see below.

as the silver salt alone.[55] Finally, no considerable changes were observed when switching (*R*)-**Ag1** for its phosphate analogue (*R*)-**TRIPAg**.

Table 2.11. Preliminar studies on the model cycloisomerization-indole addition to 2-alkynyl enone **1.40**.

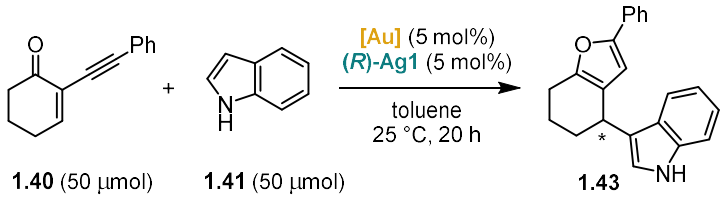

1.40 (50 μmol) **1.41** (50 μmol) **1.43**

Entry	[Au]	Conditions	Yield (%)[a]	er[b]
1	**C**	0.1 M	>95	62:38
2	**C**	0.2 M	>95	61:39
3	**C**	0.05 M	>95	62:38
4	-	0.1 M	55	27.5:72.5
5	[JohnPhosAuCl]	0.1 M	>95	42:58
6	[(PPh_3)AuCl]	0.1 M	>95	40:60
7	**C**	**AgTRIP** instead of **Ag1**	>95	64:36

[a] Yield determined by ^{1}H-NMR analysis against 1,1,2,2-tetrachoroethane as internal standard. [b] *er* determined by HPLC on chiral stationary phase.

With these promising results, we proceeded to screen various combinations of gold chloride complexes and chiral metal salts using High Throughput Experimentation (HTE) (Table 2.12). This method, which allows for the setup of multiple reactions with minimal consumption of substrates, catalysts and time, is ideal for a multicomponent reaction, like the H-bonded counterion-directed catalysis under study. With the HCDC approach we can do permutations of several parameters, for example, the combination of two catalysts. In this screening, six chiral salts five Ag(I) and a Cu(II) were tested, either individually or in combination with seven Au(I) complexes, resulting in a total of 56 reactions on a 10-μmol scale. To simplify the results, HTE data is provided as a heat map, where the color scale goes from blue to red indicating enantio-enrichment of product **1.43**. In general, results varied significantly when comparing the same Au(I) complex with different chiral salts, or different Au(I) complexes with the same chloride scavenger. Reactions without the Au(I) catalyst usually had moderate to good conversion, while full conversion was observed when Au(I) was added. Complexes **A**–**C**, which vary in linker length between the phosphine aromatic ring and the squaramide, exhibited significant differences in enantiocontrol (Table 2.12, columns 1–3). **C**, bearing the longest and most flexible linker, delivered the best result, achieving up to 86:14 *er* when paired with (*R*)-**Ag6**. In fact, catalyst flexibility can sometimes enhance enantiocontrol by potentially maximizing attractive non-covalent interactions throughout the catalytic cycle.[56] When comparing the acidity of the H-bond donor in complexes **G**–**L** (Table 2.12, columns 4–6), in 5 out of 6 cases the use of **L**, which possesses the most acidic urea, resulted in higher enantioselectivity in favor of product (*R*)-**1.43**. This trend suggests that a stronger H-bonding interaction with the anion is beneficial for enantiocontrol in this reaction. Phosphinosquaramide complexes **A**–**C** and JohnPhos-type

55. See below for more examples of commercially available catalyst in combination with our chiral metal salts.
56. For a review about flexibility in ligand design, including examples of H-bond donors, see: Crawford, J.; Sigman, M. *Synthesis* **2019**, *51*, 1021–1036.

phosphinourea complex **Au12** favored the formation of (*R*)-**1.43**, in up to 81:5:18.5 *er* when mixed with (*R*)-**Ag6**. All in all, these data highlight the effect on enantiocontrol played by the relative position of the H-bond donor with respect to the Au(I) center and the nature of the H-bond donor.

Table 2.12. Results on the HTE screening of combination of AuX complexes with halide scavengers bearing a chiral counterion.

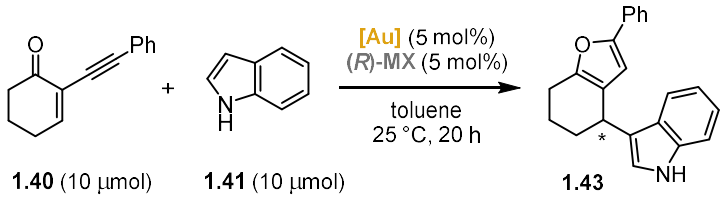

1.40 (10 μmol) **1.41** (10 μmol) **1.43**

	A	B	C	G	K	L	Au12	No gold
(*R*)-Ag1	56.5:43.5	61.5:38.5	63.5:46.5	39.5:60.5	38:62	35.5:64.5	76.5:23.5	23:77
(*R*)-Ag2	63:36	48.5:51	59:41	42:58	45.5:54.5	37.5:62.5	79.5:20.5	14.5:85.5
(*R*)-Ag3	66.5:33.5	54:46	58:42	42:58	46.5:53.5	30.5:69.5	72:28	13.5:86.5
(*R*)-Ag4	61.5:38.5	66.5:33.5	76.5:23.5	35.5:64.5	39.5:60.5	47:53	66.5:33.5	34.5:65.5
(*R*)-Ag5	63:37	46:54	60.5:39.5	46:54	42:58	35.5:64.5	73.5:26.5	28.5:71.5
(*R*)-Ag6	55:45	73.5:26.5	86:14	36.5:63.5	42:58	23.5:76.5	81.5:18.5	29.5:70.5
(*R*)-Cu6	56:44	70.5:29.5	83.5:16.5	36:64	38:62	25.5:74.5	76:24	35:65

90:10–80:20
80:20–70:30
70:30–60:40
60:40–50:50
50:50–40:60
40:60–30:70
30:70–20:80
20:80–10:90

[a]*er* is given in a heat map, where color indicates enantiocontrol according to the legend on the right part.
[b]*er* was determined by UPC[2] on chiral stationary phase.

As for the other component of the reaction, the chiral Ag(I)[52b] and Cu(II)[52a] phosphoramidate salts, in line with previous reports, were capable of catalyzing this reaction alone, without the addition of the Au(I) catalysts, although with lower yields and favoring the formation of the (*R*)-enantiomer (Table 2.12, column 8). Comparing (*R*)-**Ag1–3**, differing only on the *N*-sulfonyl substituents on the phosphoramidate (thus differing in their basicity), in the absence of Au(I) (Table 2.11, column 8, lines 1–3), the more acidic (*R*)-**Ag1** (with a N-triflyl group) gave the product with the lowest *er* (23:77). These results are consistent with the high enantioselectivities observed in previous work by Toste and others when more basic phosphate anions were employed.[52a,b] Additionally, variations in enantiocontrol were noted when *N*-triflyl phosphoramidate salts with different substituents at the 3,3'-positions of the BINOL backbone ((*R*)-**Ag4–6**) were evaluated. Among these, (*R*)-**Ag6** and (*R*)-**Cu6** emerged as the most effective salts, both featuring a BINOL-derived phosphoramidate scaffold with 9-anthracenyl groups at the 3,3'-positions which, in combination with **Au3**, gave the desired product in 86:14 *er* and 83.5:16.5 *er* respectively. In conclusion, the HTE results showed several factors influence enantiocontrol: 1) the basicity of the counteranion ((*R*)-**Ag1–3**); 2) the substituents in the 3,3' position of the

BINOL scaffold of the anion; and 3) the strength (**Au4–6**) and the relative position of the hydrogen-bond donor (**Au1–3**). Given the interplay of these multiple factors, a combinatorial approach resulted in the most effective method of identifying the optical catalytic system.

The next step on the optimization was performing the reaction in a bigger scale in the lab, to validate the results obtained and further screen some conditions that cannot be optimized efficiently in an HTE lab, like solvent and temperature. Thus, the best results, combination of **C** with (*R*)-**Ag6** and (*R*)-**Cu6,** were reproduced agreeing with the HTE results (Table 2.13 entries 1–2). Since the countercation also seemed to affect the enantioselectivity of the reaction we also tested chiral salt (*R*)-**Na6**, with **C** and without the addition of Au(I) (Table 2.13, entries 3 and 6). Although on its own (*R*)-**Na6** was not catalytically active, in combination with **C** gave the desired product in high yield but lower *er* compared to its Ag(I) and Cu(II) analogue (Table 2.13, entries 1 and 2 vs 3). This difference could arise from the chloride scavenging ability of the three cations, Ag(I), Cu(II) and Na(I). As already reported in the work by Gandon and coworkers, [24] the scavenging ability of Cu(II) and Na(I) is not as good as Ag(I) leading to incomplete and reversible scavenging.[57] This implies that there is potentially **C,** with its Au–Cl bond intact, which has demonstrated to be active on its own in this reaction (Table 2.13, entry 7), leading to background racemic formation of the product lowering the *er* of the final mixture. JohnPhos-type urea **Au12** also performed considerably well in the HTE experiments, so we also tested it in a bigger scale together with other JohnPhos-type complexes **Au1** and **Au10**, but catalyst **C** was superior in terms of enantioselectivity in this reaction. Seeing how highly conjugated systems in 3,3'-positions of the BINOL scaffold were beneficial we decided to also test chiral salts (*R*)-**Ag7–10** which also featured polycyclic aromatic moieties (Table 2.13, entries 11–18). (*R*)-**Ag7** and (*R*)-**Ag8**, bearing 9-phenathryl and 2-pyrenyl groups respectively, gave comparable results to (*R*)-**Ag6**, which still was the best one among them (Table 2.13, entries 1 vs 11 and 12). On the other hand, the (*R*)-**VANOL** and (*R*)-**VAPOL** derived chiral metal salts provided poor enantiocontrol (Table 2.13, entries 13–14). These results further highlighted that highly conjugated substituents in 3,3'-position increase the enantioselectivity of the reaction under study. Finally, we observed that the Au:Ag ratio on the system had no effect on the enantioselectivity (Table 2.13, entries 19–20). This can be explained by the fact that reaction is very fast when using the Au/Ag system, but relatively slow when using Ag(I) alone. Therefore, as soon as the cationic gold(I) complex forms, it outperforms the remaining chiral silver salt in the media.

Table 2.13. Validation of HTE experiments in the lab and additional tests.

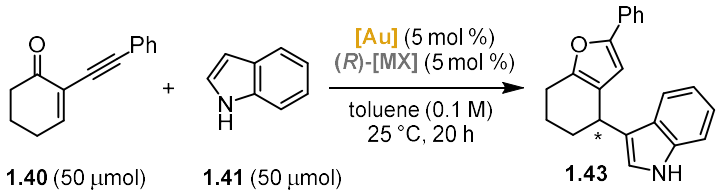

1.40 (50 μmol) **1.41** (50 μmol) **1.43**

Entry	[Au]	[MX]	Yield (%)[a]	er[b]
1	**C**	**(*R*)-Ag6**	87	89:11
2	**C**	**(*R*)-Cu6**	79	83:17
3	**C**	**(*R*)-Na6**	86	81:19
4	**-**	**(*R*)-Ag6**	87	30.5:69.5

57. We also observed in Figure 2.8 that we need to force the dissociation of the Na cation from **Na6** to observe interactions of the urea with the counterion.

5	**-**	**(*R*)-Cu6**	68	28:72
6	**-**	**(*R*)-Na6**	0	-
7	**C**	**-**	21	50:50
8	**Au12**	**(*R*)-Ag6**	>95	80:20
9	**Au1**	**(*R*)-Ag6**	>95	78:22
10	**Au10**	**(*R*)-Ag6**	>95	80:20
11	**C**	**(*R*)-Ag7**	>95	87:13
12	**C**	**(*R*)-Ag8**	>95	80:20
13	**C**	**(*R*)-Ag9**	>95	62:38
14	**C**	**(*R*)-Ag10**	>95	55:45
15	-	**(*R*)-Ag7**	92	30:70
16	-	**(*R*)-Ag8**	>95	49:51
17	-	**(*R*)-Ag9**	61	44:56
18	-	**(*R*)-Ag10**	90	43:57
19[c]	**C**	**(*R*)-Ag6**	>95	86.5:13.5
20[d]	**C**	**(*R*)-Ag6**	>95	87:13

[a] Yield determined by ^{1}H-NMR analysis against 1,1,2,2-tetrachloroethane as internal standard. [b] *er* determined by HPLC on chiral stationary phase. [c] 2:1 Au:Ag ratio was used. [d] 1:0.5 Au:Ag ratio was used.

Next, we performed a solvent and temperature screen with the best combination of catalyst, **C/(*R*)-Ag6** (Table 2.14). Once again, polar solvents led to lower enantioselectivities (Table 2.14, entries 1–3), pointing to possible interference with both the ion-pairing and the hydrogen-bonding (refer to Table 2.3 and 2.5 for more examples and for a comparison on polarity). Among the more apolar solvents (Table 2.14, entries 4–7), toluene worked best in terms of enantioselectivity. Lowering the temperature allowed increasing the *er* to 92:8 when reaction was performed at −10 °C in toluene (Table 2.14, entry 8). Further lowering the temperature did not give better results (Table 2.14, entry 9). At that point we realized that the reaction was much faster than we expected (usually it was left overnight), in fact after 1 h the reaction was already complete, which allowed us to lower the catalyst loading to 1 mol% with a 4 h reaction time for the standard starting material **1.40** (Table 2.14, entry 10).

Table 2.14. Solvent and temperature screening.

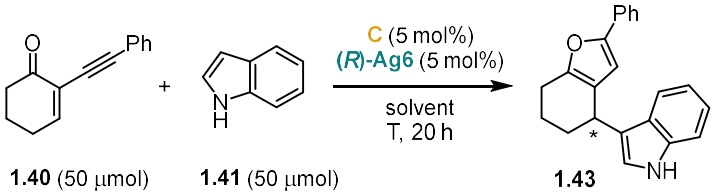

1.40 (50 μmol) **1.41** (50 μmol) **1.43**

Entry	solvent	T (°C)	Yield (%)[a]	er[b]
1	1,2-DCE	25	79	69:31
2	$CHCl_3$	25	81	75:25
3	THF	25	79	66:34

4	trifluorotoluene	25	58	78:22
5	benzene	25	>95	87:13
6	*p*-xylene	25	77	86:14
7	toluene	25	87	89:11
8[c]	toluene	-10	>95	92:8
9[d]	toluene	-20	66	92:8
10[e]	toluene	-10	72	92:8
11[f]	toluene	-10	83	92:8

[a] Yield determined by ^{1}H-NMR analysis against 1,1,2,2-tetrachloroethane as internal standard. [b] *er* determined by HPLC on chiral stationary phase. [c] Reaction was stopped after 5 h. [d] Reaction stopped after 2 h. [e] Reaction stopped after 1 h, yield given for the isolated compound. [f] Reaction performed at 1 mol% loading and stopped after 4 h, yield given for the isolated compound.

Once having optimized the reaction for the model substrate, we tested a scope of the tandem cycloisomerization-nucleophile addition to enones **1.40** and **2.70a–k** on 0.15 mmol scale with 1 mol% loading of **C** and (*R*)-**Ag6** using indoles as nucleophiles (Scheme 2.24). Indoles substituted at the 5-position with either electron-donating or electron-withdrawing groups on the aromatic ring proved to be effective nucleophiles, leading to the formation of products **2.72a** and **2.72b**. However, indoles bearing substituents at the 2- or 1-position resulted in lower *er* for products **2.72c** and **2.72d**. When the 3-position on the indole was blocked, the product of C-2 attack **2.72e** was obtained instead. Modifications on the enone were then studied (Scheme 2.24 bottom). Variations on the electronics of the aromatic ring on the alkyne terminus affected the enantioselectivity (**2.72f–l**) although to a lower extent than steric effects, as a methyl substituent in *ortho* position of the aryl ring, resulted in the formation of product **2.72h** in lower yield and enantioselectivity. The aromatic ring could be replaced by 3-thienyl or cyclohexyl alkyne groups yielding furans with heteroaromatic and alkyl substituents, though with moderate yields and enantioselectivities (**2.72m–n**). Furthermore, the ring size of the cyclohexenone was modified to cyclopentenone and cycloheptenone substrates **2.70j** and **2.70k** generating the corresponding bicyclic furans **2.72o** and **2.72p** in good yields, with 86:14 and 85:15 *er*, respectively.

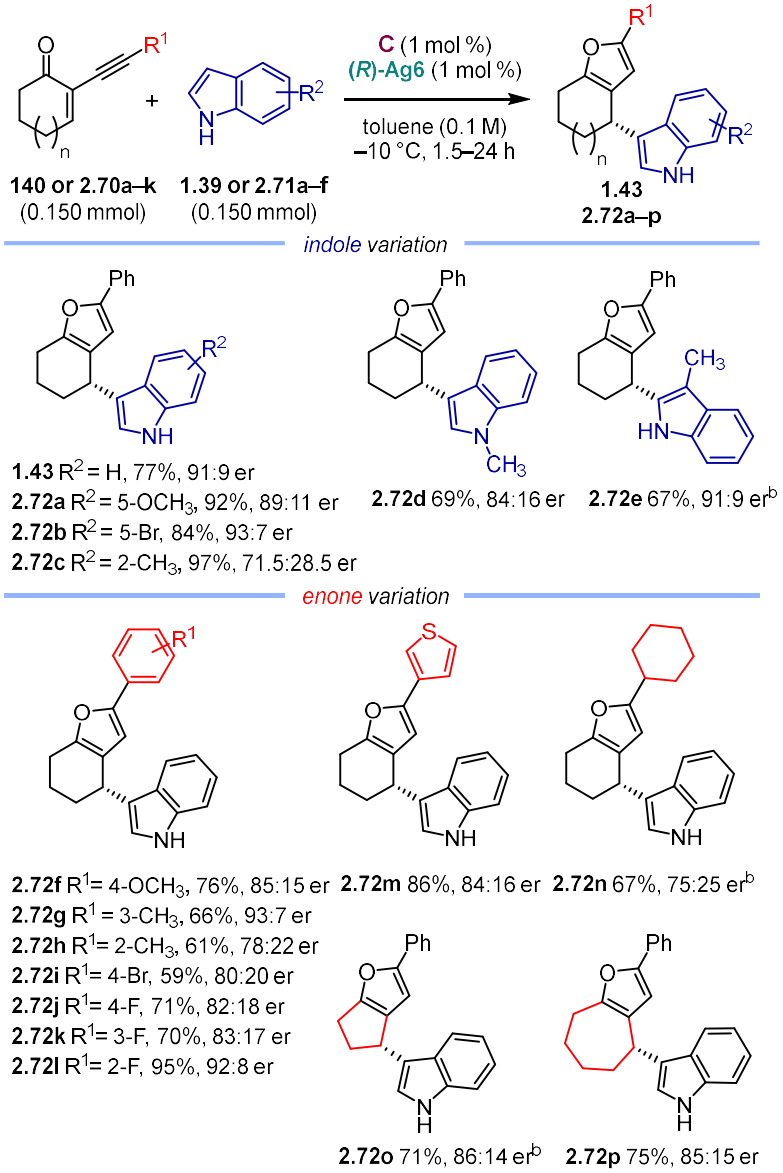

Scheme 2.24. Scope of the gold(I)-catalyzed indole nucleophile addition to 2-alkynyl enones **1.40** and **2.70**.[a] Reactions were performed under Ar or N_2 atmosphere in anhydrous toluene. Yields given for isolated material after purification. *er* determined by HPLC or SFC on a chiral stationary phase. [b] Reaction carried out with 3 mol% catalyst loading.

To test the robustness of our methodology we decided to perform a small screening of *N*- and *O*-centered nucleophiles (Scheme 2.25). Addition of aniline to the standard substrate required 24 h to reach completion and provided the corresponding product **2.73a** with low enantioselectivities (62:38 *er*). These results could point to the aniline interfering with the key hydrogen-bond interaction of the squaramide with the chiral counterion, which at the same time would also affect its nucleophilicity. Carbamates on the other hand were excellent nucleophiles, providing after just 1 h furans **2.73b** and **2.73c** in 95:5 *er*. When using primary alcohols, moderate enantioselectivities could be observed (**2.73d–f**). However, propargylic and allyl alcohols delivered the desired ethers **2.73e** and **2.73f**, with no side-products of further reactivity of the alkyne, nor the vinyl group. When more sterically hindered secondary alcohols (**2.73g–h**), phenols (**2.73i**) or 1-naphtols (**2.73j**), were used instead an increase on the enantioselectivity was observed, suggesting that to a certain degree, bulking up the steric hindrance on the nucleophile might be beneficial for the enantiofacial discrimination of the carbocation intermediate. The use of water led to the formation

of ether **2.73k**, which results from the nucleophilic attack by the secondary alcohol formed upon the addition of water, in 85% yield and 95:5 *er*. In contrast to previous reports, where the meso compound isomer to **2.73k** was obtained, with our system **2.73k** could be obtained as a single diastereomer.

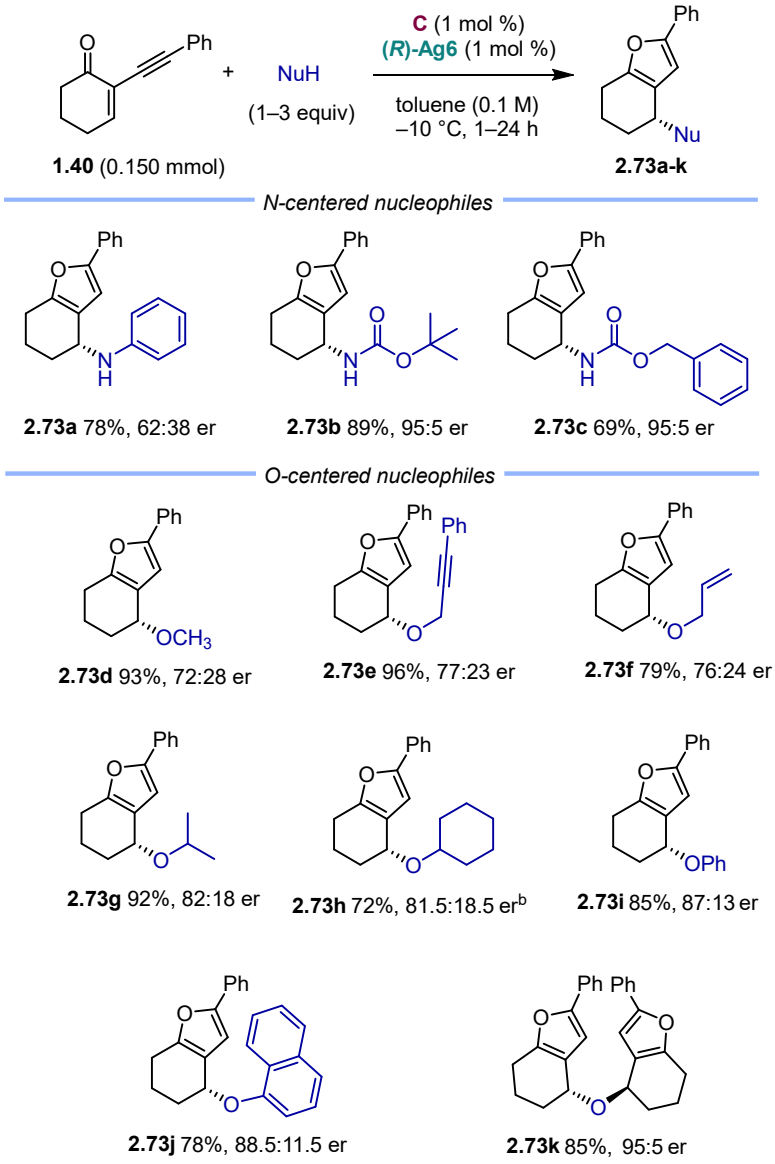

Scheme 2.25 Scope on the enantioselective addition of N- and O- nucleophiles to enone **1.40**. [a] Reactions were performed under Ar or N_2 atmosphere in anhydrous toluene. Yields given for isolated material after purification. *er* determined by HPLC or SFC on a chiral stationary phase. [b] Reaction carried out with 3 mol% catalyst loading.

The reaction was found sensitive to steric effects on the alkyne aromatic ring and to the H-bonding ability of the nucleophile (**2.73** and **2.73d**). The absolute configuration of products **1.43**,[14a, 52a,b] **2.72a-e**,[14a] **2.73a**,[14a] **2.73c**,[14a] **2.73i**[14a] and **2.73k**[14a] could be assigned by comparison with the sign of the optical rotation reported in the literature.[58] The configuration of the rest of the products was assigned by analogy assuming a uniform stereochemical mechanism, where the H-bonded anion shields the *Si* face of carbocation **2.74** generated upon cyclization of enone **1.40** (Scheme 2.26).

[58]. The comparison of the order of elution of the enantiomers by HPLC reproducing the same conditions as in the literature was also used as means to determine the absolute configuration of the product.

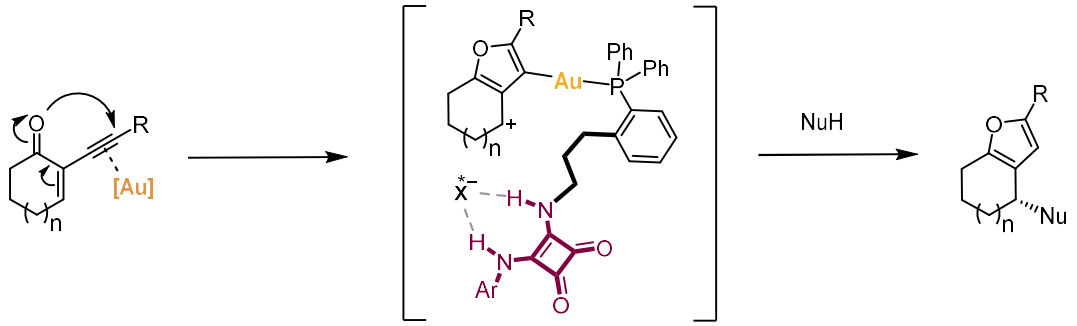

Scheme 2.26 Proposed simplified mechanism of tandem cyclization-nucleophile addition of enone **1.40** via the formation of chiral intermediate **2.74** where Si face is blocked by the chiral anion towards nucleophile addition. X* = Chiral anion.

Hydrogen-Bonded Matched Ion Pair Gold(I) Catalysis

Having demonstrated that hydrogen bond donors embedded in the catalyst can abstract the chiral counterions from the gold coordination sphere in the previous section, our next goal was the combination of chiral hydrogen bond donors with chiral counterions. We believed that this approach might lead to the formation of match/mismatch scenarios among catalysts and the generation of a chiral pocket that would allow the transformation of small molecules with high enantioselectivies. In previous work by our group, we reported the preparation of modular chiral BINOL-based phosphite ligands by trapping of the P–Cl intermediate by a phenol.[28c] These gold(I)-phosphite complexes presented promising levels of enantioselectivity in the formal [4+2] cycloisomerization of enyne **2.59a** (up to 88% ee). Given that our lab already had a collection of chiral (*R*)-BINOLs, we developed a one-pot, two-step method to synthesize eight chiral gold(I)-phosphitoureas. This was achieved by reacting the corresponding (*R*)-binaphtol **2.41–2.44** with PCl_3 and subsequently trapping the resulting P–Cl intermediate with phenyl-hydroxy urea **U** (Scheme 2.27). Urea groups were positioned at the *para*-, *meta*-, or *ortho*- positions relative to the phosphite to evaluate the directing influence of the hydrogen-bond donor. Finally, ligand exchange with [$(Me_2S)AuCl$] in CH_2Cl_2, afforded the desired phosphitourea gold(I) complexes **Au16–Au23**.

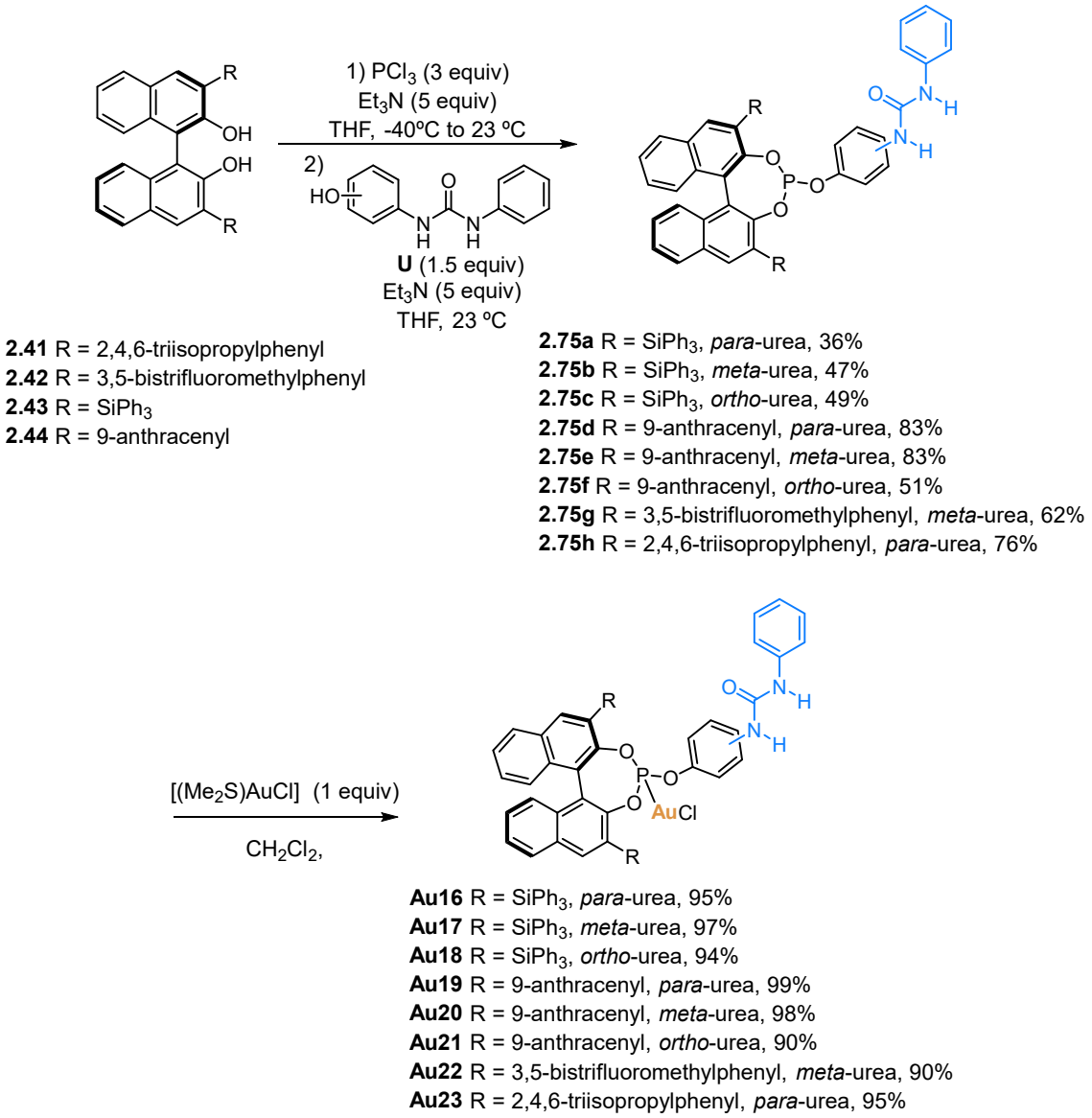

2.41 R = 2,4,6-triisopropylphenyl
2.42 R = 3,5-bistrifluoromethylphenyl
2.43 R = $SiPh_3$
2.44 R = 9-anthracenyl

2.75a R = $SiPh_3$, *para*-urea, 36%
2.75b R = $SiPh_3$, *meta*-urea, 47%
2.75c R = $SiPh_3$, *ortho*-urea, 49%
2.75d R = 9-anthracenyl, *para*-urea, 83%
2.75e R = 9-anthracenyl, *meta*-urea, 83%
2.75f R = 9-anthracenyl, *ortho*-urea, 51%
2.75g R = 3,5-bistrifluoromethylphenyl, *meta*-urea, 62%
2.75h R = 2,4,6-triisopropylphenyl, *para*-urea, 76%

Au16 R = $SiPh_3$, *para*-urea, 95%
Au17 R = $SiPh_3$, *meta*-urea, 97%
Au18 R = $SiPh_3$, *ortho*-urea, 94%
Au19 R = 9-anthracenyl, *para*-urea, 99%
Au20 R = 9-anthracenyl, *meta*-urea, 98%
Au21 R = 9-anthracenyl, *ortho*-urea, 90%
Au22 R = 3,5-bistrifluoromethylphenyl, *meta*-urea, 90%
Au23 R = 2,4,6-triisopropylphenyl, *para*-urea, 95%

Scheme 2.27 Synthesis of chiral phosphitourea gold(I)-complexes.

We then proceeded to test the complexes in the formal [4+2] cycloaddition to compare these newly prepared phosphite gold(I) complexes **Au16–23** with the JohnPhos-type-urea gold(I) complexes **Au1–13** (Table 2.15). The complexes **Au16–18** and **Au20** were not catalytically active without the addition of a chloride scavenger (Table 2.15, entries 1–4). When (*R*)-**Ag6** was added to the reaction mixture, no conversion could be detected for complexes **Au16** and **Au17** while it was very moderate with **Au18** and **Au20** after 3 days and with moderate enantioselectivities (Table 2.15, entries 5–8). Seeing how 9-anthracenyl substituents in 3,3'-positions (i.e. complexes **Au20**) seemed to work better we also tested complexes **Au19** and **Au21**, bearing ureas in *para*- and *ortho*-position relative to the phosphite, respectively. Again, conversion was moderate for **Au19** and **Au20** (although it could be improved in some cases by allowing it to react for 5 days) but the *er* were promising (Table 2.15, entries 9–11). Using (*S*)-**Ag6** instead, the reactivities were even lower and no significant improvement on the *er* could be detected (Table 2.15, entry 12–14). We then tested the combination of **Au19** with $AgSbF_6$ and $NaBAr_4^F$, which lead to very good yield and enantioselectivities with the former but no reactivity with the latter (Table 2.15, entries 15 and 16). However, since it was not the aim of this project to use achiral scavengers, we did not study this any further.

Table 2.15 Screening of chiral gold(I)-catalyst in the formal [4+2] cycloisomerization of **2.59a**.

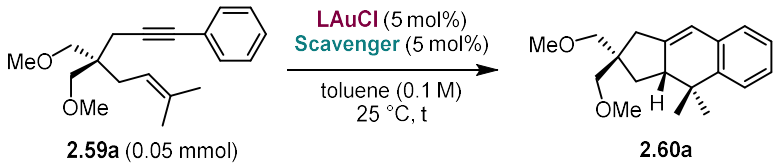

2.59a (0.05 mmol) **2.60a**

Entry	(*R*)-[Au]	scavenger	time (h)	yield (%)[a]	er[b]
1	**Au16**	None	48	0	-
2	**Au17**	None	48	0	-
3	**Au18**	None	48	0	-
4	**Au20**	None	48	0	-
5	**Au16**	**(R)-Ag6**	72	0	-
6	**Au17**	**(R)-Ag6**	72	0	-
7	**Au18**	**(R)-Ag6**	72	31	37.5:62.5
8	**Au20**	**(R)-Ag6**	72	42	81.5:18.5
9	**Au19**	**(R)-Ag6**	48	50	77.5:22.5
10	**Au20**	**(R)-Ag6**	120	84	80:20
11	**Au21**	**(R)-Ag6**	120	6	65:35
12	**Au19**	**(S)-Ag6**	48	28	82:18
13	**Au20**	**(S)-Ag6**	120	17	82:18
14	**Au21**	**(S)-Ag6**	120	4	61:39
15	**Au19**	**$AgSbF_6$**	22	88	95:5
16	**Au19**	**$NaBAr_4^F$**	72	0	-

[a] Yield determined by ^{1}H-NMR analysis against 1,1,2,2-tetrahloroethane as internal standard. [b] *er* determined by HPLC on chiral stationary phase.

The results in Table 2.15 suggested that the problem was the substrate, an internal alkyne might be too hindered for our catalytic system. Thus, we decided to switch to the nucleophile addition reaction to 1,6-enyne **2.76a** bearing a terminal alkyne.[39,40,59] Preliminary results showed that

59. For previous reports on the racemic gold(I)-catalyzed addition of nucleophiles to 1,6-enyne **2.76a** see: a) Nieto-Oberhuber, C.; Muñoz, M. P.; Buñuel, E.; Nevado, C.; Cárdenas, D. J.; Echavarren, A. M. *Angew. Chem. Int. Ed.* **2004**, *43*, 2402–2406. b) Nieto-Oberhuber, C.; Muñoz, M. P.; López, S.; Jiménez-Núñez, E.; Nevado, C.; Herrero-Gómez, E.; Raducan, M.; Echavarren, A. M. *Chem. Eur. J.* **2006**, *12*, 1677–1693. Corrigendum: Nieto-Oberhuber, C.; Muñoz, M. P.; López, S.; Jeménez-Núñez, E.; Nevado, C.; Herrero-Gómez, E.; Raducan, M.; Echavarren, A. M. *Chem. Eur. J.* **2008**, *14*, 5096–5096. c)Toullec, P. Y.; Genin, E.; Leseurre, L.; Genêt, J.-P.; Michelet, V. *Angew. Chem. Int. Ed.* **2006**, *45*, 7427–7430. d) ref 35a. e) Amijs, C. H. M.; López-Carrillo, V.; Raducan, M.; Pérez-Galán, P.; Ferrer, C.; Echavarren, A. M. *J. Org. Chem.* **2008**, *73*, 7721–7730. f) Leseurre, L.; Chao, C.-M.; Seki, T.; Genin, E.; Toullec, P. Y.; Genêt, J.-P.; Michelet, V. *Tetrahedron* **2009**, *65*, 1911–1918. g) Miller, R.; Carreras, J.; Muratore, M. E.; Gaydou, M.; Camponovo, F.; Echavarren, A. M. *J. Org. Chem.* **2016**, *81*, 1839–1849. For enantioselective versions see: h) Chao, C.-M.; Genin, E.; Toullec, P. Y.; Genêt, J.-P.; Michelet, V.*J. Organomet.* **2009**, *694*, 538–545. i) Matsumoto, Y.; Selim, K. B.; Nakanishi, H.; Yamada, K.; Yamamoto, Y.; Tomioka, K. *Tetrahedron Lett.* **2010**, *51*, 404–406. j) ref. 28b. k) Yamada, K.; Matsumoto, Y.; Selim, K. B.; Yamamoto, Y.; Tomioka, K. *Tetrahedron* **2012**, *68*, 4159–4165. l) Gung, B. W.; Holmes, M. R.; Jones, C. A.; Ma, R.; Barnes, C. L. *Tetrahedron Lett.* **2016**, *57*, 3912–3915. m) Tugny, C.; del Rio, N.; Koohgard, M.; Vanthuyne, N.; Lesage, D.; Bijouard, K.; Zhang, P.; Meijide Suárez, J.; Roland, S.; Derat, E.; Bistri-Aslanoff, O.; Sollogoub, M.; Fensterbank, L.;

gold(I) complexes bearing 3,3'-9-anthracenyl substituents on the BINOL (**Au19–21**) provided better yields and enantioselectivities (Table 2.16). To avoid the formation of the products of non-productive cyclization of enyne **2.76a** without the addition of nucleophile **2.76'** and **2.76"**, 3 equiv of NuH were employed and catalyst was added last to the reaction mixture. Complexes bearing *para*-urea showed much higher reactivity and enantioselectivities (Table 2.16, entries 1–6). Highly conjugated 9-anthracenyl systems worked better than their bulky $SiPh_3$ analogues. The combination of (*R*)-BINOL based gold(I)-urea complexes with (*R*)-**Ag6** resulted in the indole and EtOH addition products in up to 95:5 and 98:2 *er* respectively (Table 2.16, entries 4 and 8). On the other hand, the use of the (*S*)-enantiomer of **Ag6** delivered the products in only 61.5:38.5 *er* for indole addition and 57:43 *er* for EtOH. This was a clear case of a match/mismatch scenario, in which in contrast to previous combinations of two BINOL-based cation/anion ion pairs,[9b,10b,10e] the resulting matched catalyst was the (*R*)/(*R*) ion combination.

Table 2.16. Preliminary studies on the enantioselective gold(I)-catalyzed nucleophile addition to 1,6-enyne **2.76a**.

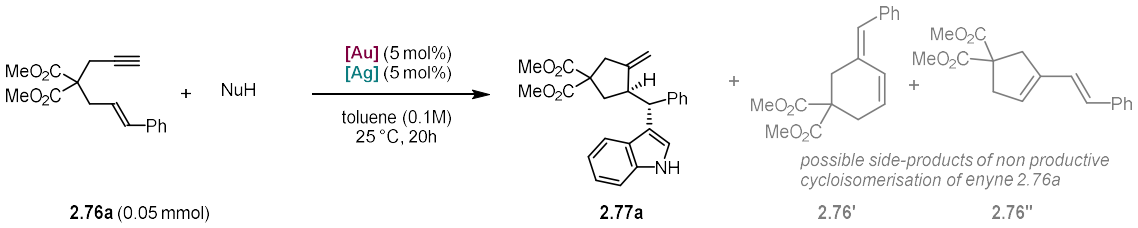

Entry	[Au]	[Ag]	NuH	Time (h)	Yield (%)[a]	*er*[b]
1	Au16	(*R*)-Ag6	Ind	44	61	78:22
2	Au17	(*R*)-Ag6	Ind	44	69	54:46
3	Au18	(*R*)-Ag6	Ind	44	6	50:50
4	Au19	(*R*)-Ag6	Ind	44	82	95:5
5	Au20	(*R*)-Ag6	Ind	44	74	60:40
6	Au21	(*R*)-Ag6	Ind	44	39	54:46
7	Au19	(*S*)-Ag6	Ind	44	61	61.5:38.5
8	Au16	(*R*)-Ag6	EtOH	14	87	98:2
9	Au16	(*S*)-Ag6	EtOH	14	85	57:43
10	Au19	(*R*)-Ag6	EtOH	14	67	91:9
11	Au19	(*S*)-Ag6	EtOH	14	53	47:53

[a]Yield determined by ^{1}H-NMR analysis against 1,1,2,2-tetrahloroethane as internal standard. [b]*er* determined by HPLC on chiral stationary phase. Ind = 1*H*-Indole

We then conducted a high-throughput experimentation (HTE) screening to optimize the solvent (Tables 2.17) and catalyst combinations (Tables 2.18 and 2.19) for the indole addition reaction.[60]

Mouriès-Mansuy, V. *ACS Catal.* **2020**, *10*, 5964–5972. n) Martín-Torres, I.; Ogalla, G.; Yang, J.-M.; Rinaldi, A.; Echavarren, A. M. *Angew. Chem. Int. Ed.* **2021**, *60*, 9339–9344. o) Martinez, T.; Vanitcha, A.; Troufflard, C.; Vanthuyne, N.; Forté, J.; Gontard, G.; Lemière, G.; Mouriès-Mansuy, V.; Fensterbank, L. *Angew. Chem. Int. Ed.* **2021**, *60*, 19879–19888.

60. Achiral resorcinol [4]arenes gold(I) cavitands bearing urea motifs were also tested. These were prepared by Gala Ogalla and will not be included in this Thesis. Please refer to the Doctoral Thesis of Gala Ogalla or the original manuscript (reference: Martí, À.; Ogalla, G.; Echavarren, A. M. *ACS Catal.* **2023**, *13*, 10217–10223.) for more information.

The **Au19–21** complexes were selected for solvent screening, as they demonstrated superior performance compared to their $SiPh_3$ analogs. These complexes were evaluated in six different solvents: two aromatic (trifluorotoluene and toluene), two chlorinated (1,2-DCE and $CHCl_3$), and two ethers (cyclopentyl methyl ether and 1,4-dioxane). Among these solvents, very similar results were obtained for toluene, $CHCl_3$, CPME and 1,4-dioxane, while more polar DCE and trifluorotoluene provided the desired product in lower yields and enatioselectivities. 1,4-dioxane was chosen for further optimization since it provided the best results.

Table 2.17. High-throughput screening of solvents for the gold(I)-catalyzed nucleophile addition to enyne **2.76a**, yield shown.[a]

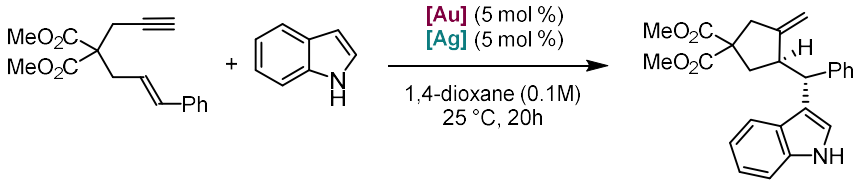

2.76a (5 μmol) **1.41** (15 μmol) **2.77a**

	$CF_3C_6H_5$	$CH_3C_6H_5$	1,2-DCE	$CHCl_3$	CPME	1,4-Dioxane
Au19	88 (92.5:7.5)	87 (95.5:4.5)	99 (87:13)	90 (96:4)	92 (96.5:3.5)	93 (97:3)
Au20	77 (46.5:53.5)	71 (57:43)	75 (58.5:41.5)	40 (55:45)	79 (69:31)	81 (71:29)
Au21	75 (44:56)	50 (55:45)	73 (43:57)	34 (53:47)	63 (34.5:65.5)	5 (35.5:64.5)

[a] Yield for the solvent screening calculated using naphtalene as internal standard in the UPC^2. *er* determined by UPC^2 on chiral stationary phase, in brackets. CPME = cyclopentyl methyl ether.

For the catalyst combination HTE (Tables 2.18 and 2.19), we introduced chiral phosphates **(*R*)-Ag0** and **(*R*)-TRIPAg** into the screening. As anticipated, these were unreactive when paired with the gold(I) phosphites (Table 2.18, rows 1–2). We also screened the *meta*- and *ortho*-urea analogs of **(*R*)-Au19** to explore the directing effects of the hydrogen-bond donor in this reaction when combined with various chiral counterions. Overall, the reactivity of this catalytic system followed a clear trend: the *para*-urea **(*R*)-Au19** delivered the highest enantioselectivities, followed by the *meta*-urea **(*R*)-Au20**, and the *ortho*-urea **(*R*)-Au21** which exhibited the lowest reactivity and, in most cases, a complete switch in the preferred enantiomer (Table 2.18 and 2.19, rows 2–4). Comparing the 3,3'-substituents on the binaphtol scaffold of the gold(I) complexes with *para*-urea, 9-anthracenyl substituents (**(*R*)-Au19**) outperformed both $SiPh_3$ (**(*R*)-Au16**) and 2,4,6-triisopropylphenyl (**(*R*)-Au23**). The optimal combination was **(*R*)-Au19** with **(*R*)-Ag1**, **(*R*)-Ag6**, or **(*R*)-Ag8** (Table 2.19, row 2), which produced product **2.77a** with 99:1, 98:2, and 95.5:4.5 *er* respectively.

Table 2.18. High-throughput screening of gold (I) complexes and chiral silver salts in 1,4-dioxane, yield shown.[a]

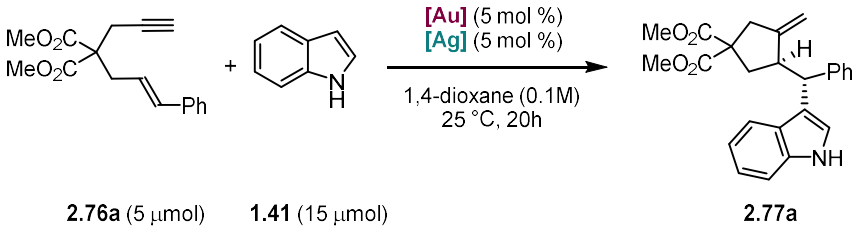

2.76a (5 μmol) **1.41** (15 μmol) **2.77a**

	Ag0	TRIPAg	Ag1	Ag3	Ag4	Ag5	Ag6	Ag8	Ag9	Ag10
Au16	6	0	76	3	66	64	72	68	53	55
Au19	6	0	78	40	71	71	79	79	76	75
Au20	9	0	61	4	40	57	66	56	43	49
Au21	0	0	4	0	9	0	6	7	34	33
Au23	0	0	33	0	17	13	47	42	61	55

[a] Yield for the solvent screening calculated using naphtalene as internal standard in the UPC^2. In all cases (*R*)-Ag was used.

Table 2.19. High-throughput screening of gold (I) complexes and chiral silver salts in 1,4-dioxane, *er* shown.[a]

	Ag0	Ag1	Ag3	Ag4	Ag5	Ag6	Ag8	Ag9	Ag10
Au16	58:42	92.5:7.5	-	68:32	72.5:27.5	90:10	84:16	55:45	65:35
Au19	71.5:28.5	99:1	95.5:4.5	93.5:6.5	88:12	98:2	95.5:4.5	87.5:12.5	87.5:12.5
Au20	24.5:75.5	71:29	48.5:51.5	62.5:27.5	55.5:44.5	73:27	53:47	48:52	34:66
Au21	-	68:32	-	31.5:68.5	-	42.5:57.5	45:55	46:54	38.5:61.5
Au22	-	62:38	-	67.5:32.5	55:45	61.5:38.5	55:45	64:36	48:52

99:1–90:10
90:10–80:20
80:20–70:30
70:30–60:40
60:40–50:50
50:50–40:60
40:60–30:70
30:70–20:80

[a] *er* determined by UPC^2 on chiral stationary phase. In all cases (*R*)-Ag was used. Results represented as a heatmap.

The most promising results from the HTE were then verified by reproducing them on a larger scale in the lab (Table 2.20). Control experiments showed that neither the (*R*)-**Au19** nor (*R*)-**Ag1** were active on their own (Table 2.20, entries 5–6). The achiral JohnPhos-type urea Au(I) complex **Au10**, was also tested together with (*R*)-**Ag1** in the reaction of **2.76a** with indole **1.41**, although poor reactivity and low enantio-induction was observed (Table 2.20, entry 7). Finally, an achiral silver salt was tested, $AgSbF_6$, in combination with (*R*)-**Au19** (Table 2.20, entry 9) resulting in lower yield and enantioselectivities than those observed with the matched dual chiral system.

Table 2.20. Additional control experiments on the gold(I)-catalyzed addition of indole to 1,6-enyne **2.76a**.

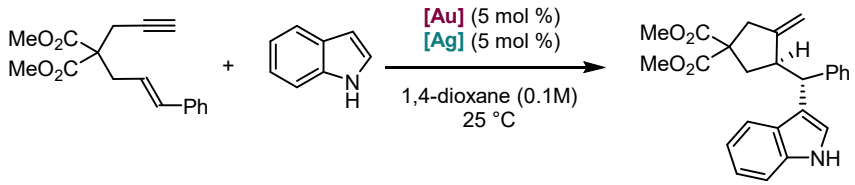

2.76a (0.05 mmol) **1.41** (0.15 mmol) **2.77a**

entry	[Au]	[Ag]	Time (h)	Yield (%)[b]	*er* [c]
1	Au16	(*R*)-Ag1	14	82	91:9
2	Au19	(*R*)-Ag1	14	93	>99:1
3	Au19	(*R*)-Ag6	14	98	97.5:2.5
4	Au19	(*R*)-Ag8	14	90	95:5
5	Au19	-	24	0	-
6	-	(*R*)-Ag6	24	0	-
7	Au10	(R)-Ag6	44	61	61.5:38.5
8	Au12	(*R*)-Ag1	24	18	52:48
9	Au19	$AgSbF_6$	24	76	92.5:7.5

[a]Yield determined by ^{1}H-NMR analysis against 1,1,2,2-tetrahloroethane as internal standard. [b]*er* determined by HPLC on chiral stationary phase

We then examined the scope of the reaction using the optimal combination of (*R*)-**Au19** and (*R*)-**Ag1** for the nucleophile addition to enyne **2.76** (Scheme 2.28). The reactions of 1,6-enyne **2.76** were performed on a 0.10 mmol scale, at 2 mol% catalyst loading. The cycloisomerization of the starting material was favored when the alkene of the substrate was more reactive or when the nucleophile used was less nucleophilic. It was observed that the competitive cycloisomerization without nucleophile addition could be avoided by lowering the temperature of the reaction and changing the solvent to toluene. Therefore, two conditions were used depending on the nature of the nucleophile and the reactivity of the substrate: conditions A using 1,4-dioxane at room temperature, or conditions B using toluene at temperatures ranging from room temperature to −10 °C. Substituents in the 1,2 and 5-position of indole were well tolerated (**2.77a–e**). Electron-rich aromatic arenes, such as 1,3,5-trimethoxybenzene (**2.77f**), 1,3-dimethoxybenzene (**2.77g**) and *N,N*-dimethylaniline (**2.77h**) also performed well, obtaining the desired product with excellent yields and enantioselectivities. The system was also compatible with heteroatom-centered nucleophiles, such as anilines (**2.77i–k**); a carbamate (**2.77l**); water (**2.77m**) and alcohols (**2.77n–r**). Furthermore, the presence of terminal alkenes on the nucleophile did not affect the reaction outcome (**2.77r**). 1,6-Enynes with varying alkene substitutions yielded the corresponding compounds **2.77t–ad** in good to excellent yields and high enantioselectivities, except for those with *para*- or *ortho*-anisole groups, which produced **2.77w** and **2.77z** with 87:13 and 93:7 *er*, respectively (Scheme 2.28).

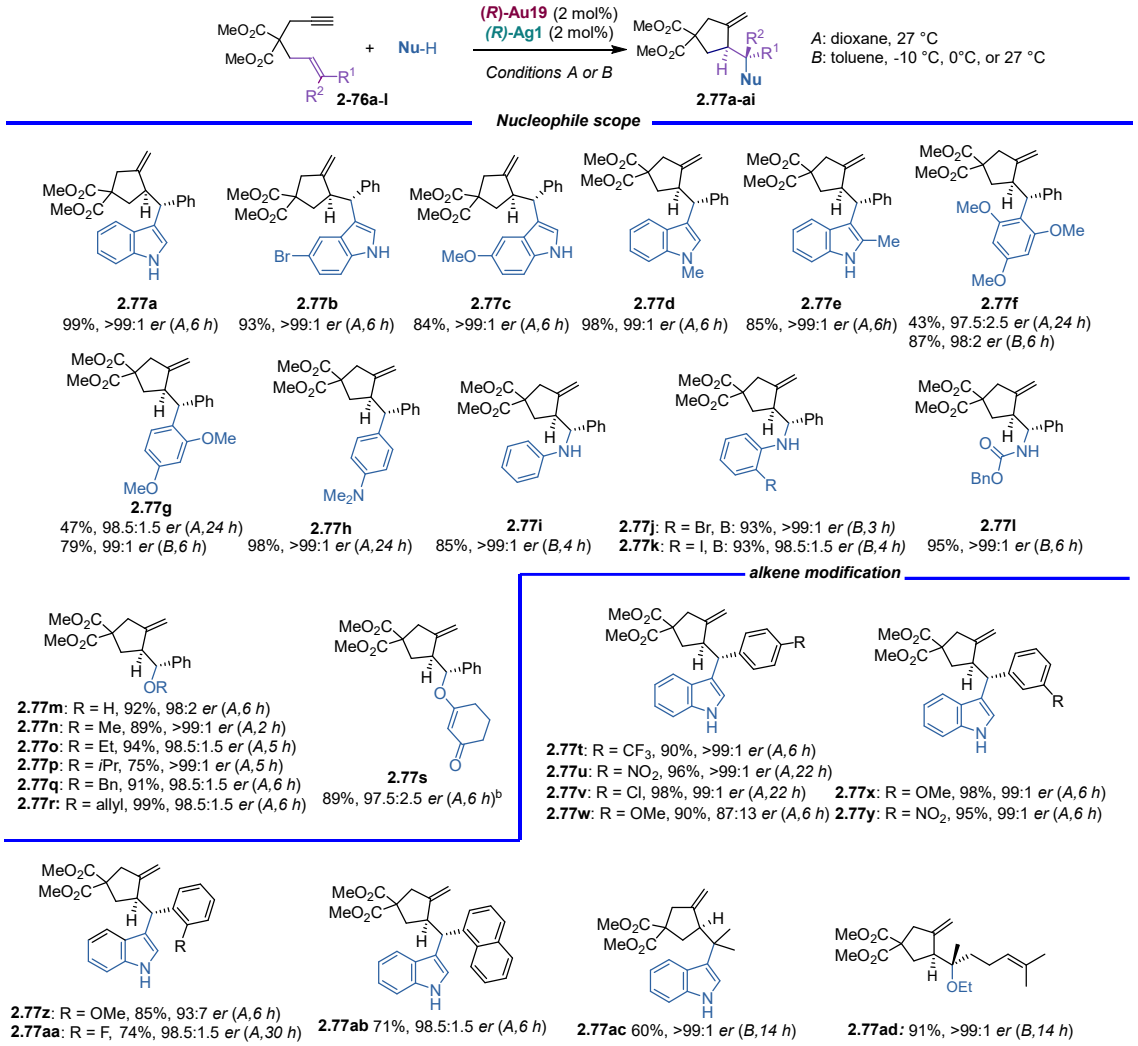

Scheme 2.28. Variations in the nucleophile and the alkene moiety of the enyne in the scope of the gold(I)-catalyzed tandem 5-*exo*-dig cycloisomerization/nucleophile addition to enyne **2.76**. [a]Yields given for isolated material after purification, *er* were determined using a HPLC or SFC on chiral stationary phase. Products obtained as single diastereomers. [b]1,3-cyclohexandione (2.0 equiv) was used as nucleophile.

Next, the effect of the tether on the reaction outcome was studied (Scheme 2.29). Substituting the malonate with a dimethylether tether favored unproductive cycloisomerization without nucleophile addition, leading to **2.77ae** in moderate yield. However, increasing the ester size from methyl to isopropyl reduced enantioselectivity to 93:7 *er* in **2.77af**, indicating that the tether plays a crucial role in the folding of the 1,6-enyne within the catalyst's chiral pocket. Changing from a malonate tether to an *N*-tosyl group resulted in reduced enantioselectivity, yielding **2.77ag** with a 78:22 *er*. However, using (*R*)-**Au23** in combination with (*R*)-**Ag5** significantly improved the outcome, producing adducts **2.77ag** and **2.77ah**, as well as aldehyde **2.77ai**, formed through oxidation of the gold(I) carbene intermediate with diphenylsulfoxide,[39] with enantioselectivities ranging from 98:2 to >99:1 *er*.

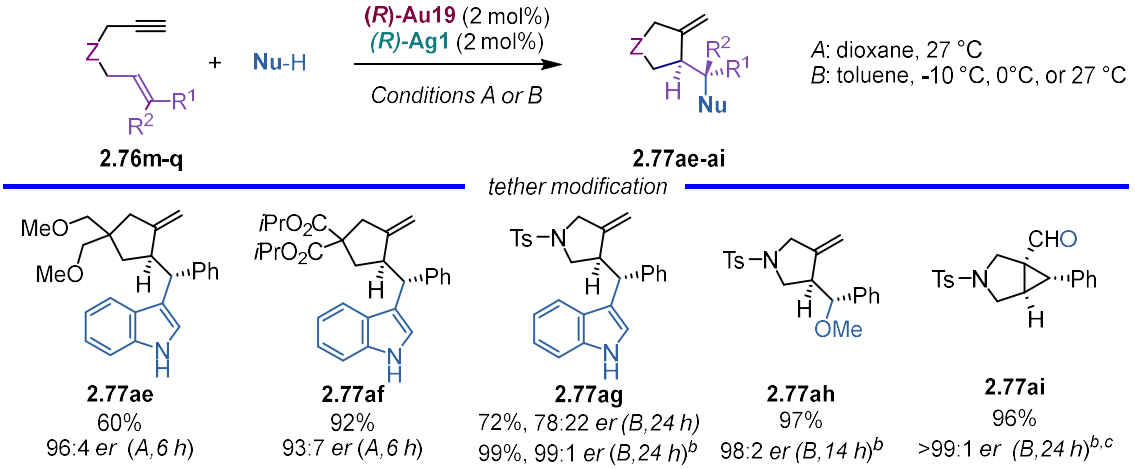

Scheme 2.29. Modifications in the tether of enyne **2.76**. [a]Yields given for isolated material after purification, *er* were determined using a HPLC or SFC on chiral stationary phase. [b]Reaction carried out using (*R*)-**Au23** and (*R*)-**Ag5** at a 3 mol% catalyst loading. [c]Diphenylsulfoxide (1.5 equiv) was used as nucleophile.

The absolute configurations of **2.77v** and **2.77ai** were confirmed to be (*S,S*) and (*R,S*) by X-ray diffraction. The configuration of the rest of the products was assigned by comparison and assuming a uniform stereochemical mechanism. Before our work, the absolute configuration of these products had only been assigned once by the group of Michelet[61] by the preparation of diastereomers with enantioenriched **2.77m** and (*S*)-α-methoxyphenyl acetic acid followed by purification by flash chromatography (Scheme 2.30). It was determined that the major diastereomer was (*S,R,S*)-**2.78** by comparing the chemical shift variation in the ^{1}H NMR spectra of the benzylic proton (marked in red in Scheme 2.30) due to the shielding of the methoxy group.[62] However, as we observed discrepancies between the values of the optical rotation of our products, whose absolute configuration was assigned by X-ray diffraction, and the ones reported in the literature, we conclude that the previous assignment could be mistaken. Therefore, previous publications[28b,59h,59i,59m,63] that relied on those values for the assignment of the configuration of their products should be revised.

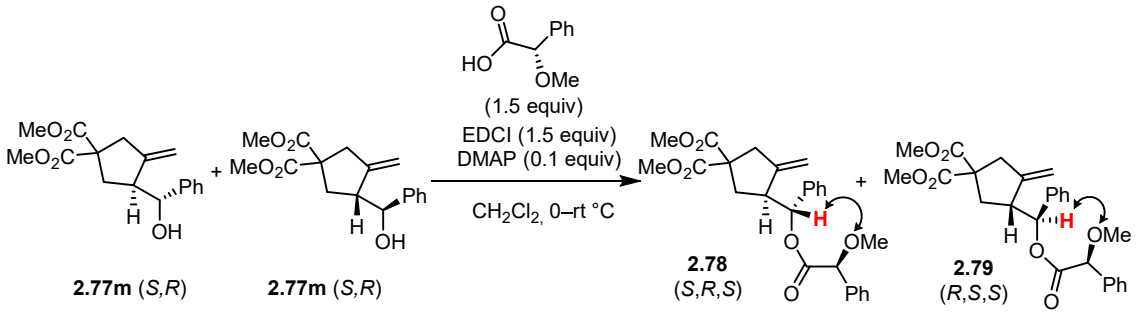

Scheme 2.30 Michelet's attempt on the determination of the absolute configuration of **2.77m.**

To further prove the utility of this reaction, the derivatization of selected products from the scope into more complex ones was performed (Scheme 2.31). For instance, the *ortho*-iodoaniline addition product (**2.77k**) was used in an intramolecular Heck[59g] reaction with the concomitant

61. Charruault, L.; Michelet, V.; Taras, R.; Gladiali, S.; Genêt, J. P. *Chem. Commun.* **2004**, *4*, 850–851.
62. a) Wu, B.; Mosher, H. S. *J. Org. Chem.*, **1986**, *51*, 1904–1906. b) Trost, B. M.; Belletire, J. L.; Godelski, S.; McDougal, P. G.; Balkovec, J. M. *J. Org. Chem.*, **1986**, *51*, 2370–2374. c) Ohtani, I.; Kusumi, T.; Kashman, Y.; Kakisawa, H. *J. Am. Chem. Soc.*, **1991**, *113*, 4092–4096.
63. Michelet, V.; Charruault, L.; Gladiali, S.; Genêt, J. P. *Pure Appl. Chem.* **2006**, *78*, 397–407.

formation of a new stereocenter to form 3,4-dihydroquinoline **2.77k'**. Ring-closing metathesis of the allyl alcohol addition product (**2.77r**) with the second-generation Grubbs catalyst[64] rendered bicyclic ether **2.77r'** with no erosion on the enantioselectivity. Finally, the allylic position in pyrrolidine **2.77ah** was oxidized to lactam **2.77ah'** with moderate yield and no erosion on the enantioselectivity using $NaClO_2$ and *N*-hydroxyphtalamide.

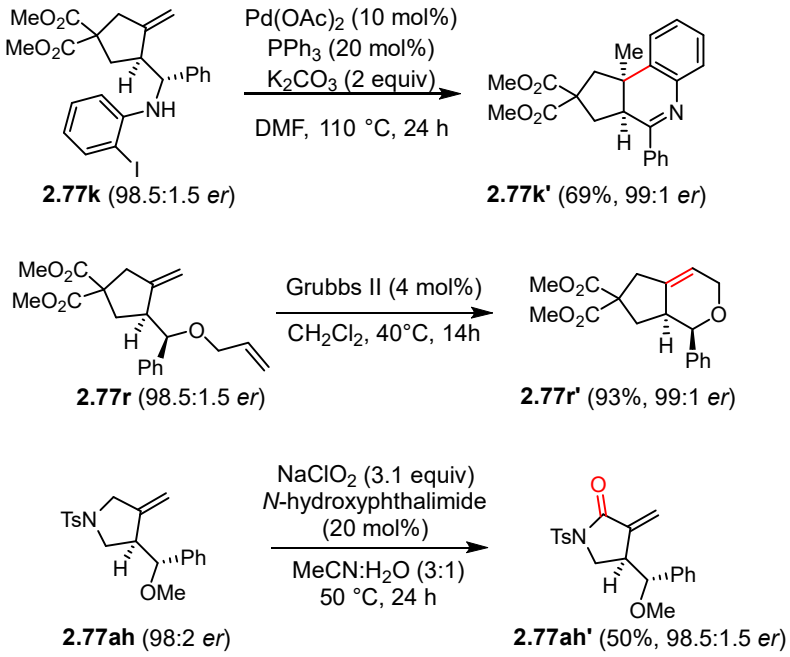

Scheme 2.31. Product derivatization into more complex products.

Computational Studies on the Tandem Cyclization/Nucleophile Addition

In order to gain some insights into the role of the urea and the possible secondary interactions involved in the enantioselective cyclization step, DFT studies[65] were performed using chiral (*R*)-**Au19** and the phosphoramidate chiral counterion from (*R*)-**Ag6,** which experimentally led to **2.77a** in a 95:5 *er* (**Ag6** was chosen because we envisioned that the rigidity of the polyaromatic unit would facilitate the calculations leading to less conformers). The mechanism of this specific reaction has not, to our knowledge, been studied computationally before. However, the mechanism is expected to be closely related to previously described cyclizations of 1,6-enynes, bearing a terminal alkyne, followed by nucleophile addition to the gold carbene intermediate generated upon attack of the alkene to the alkyne.[59] Upon activation of the alkyne in enyne **2.76a** through gold coordination, a 5-*exo*-dig cyclization occurs (Scheme 2.32). During this step, the system must differentiate between the two enantiotopic faces of the alkene, making it the enantiodetermining step. Following this, a stereospecific nucleophile attack takes place on the cyclopropyl gold carbene intermediate.[66] This attack is directed by the already stereodefined intermediate **I,** ultimately yielding a product where the nucleophile adds trans to H^1.

64. Chao, C. M.; Toullec, P. Y.; Michelet, V. *Tetrahedron Lett.* **2009**, *50*, 3719–3722.
65. Calculations were carried our using B3LYP/6-31G(d) (C, H, P, O, F, N, S)//B3LYP-D3/6-311G(d,p) and SDD (Au) and with toluene as solvent (PCM).
66. Escofet, I.; Armengol-Relats, H.; Bruss, H.; Besora, M.; Echavarren, A. M *Chem. Eur. J.* **2020**, *26*, 15738–15745.

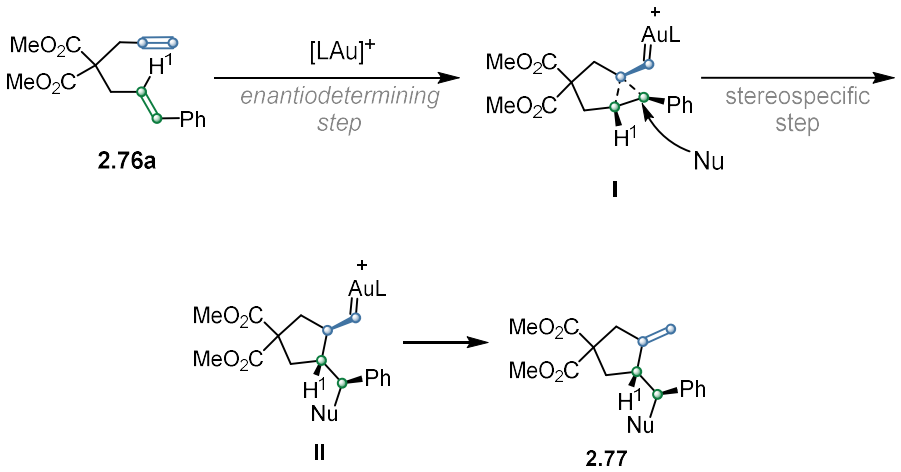

Scheme 2.32. Simplified mechanism for the gold(I)-catalyzed cascade cycloisomerization-nucleophile addition to enyne **2.76a**.

In our computational studies, we focused on the enantio-determining step. Two possible pathways for the 5-*exo*-dig cyclization were considered (Figure 2.16), one for each enantiotopic face (*Re* or *Si*) of the alkene. Among the tested conformers leading to either enantiomer of the product,[67] two pathways stood out with the lowest transition state (TS) connecting intermediates **Int1a**–**Int2a** and **Int3a**–**Int4a** with 6.9 and 7.9 Kcal/mol respectively. A Curtin-Hammet scenario[68] was observed, where the two orientations of the alkene (**Int1a** and **Int3a**) are in equilibrium, with the less stable intermediate (**Int1a**) exhibiting the lowest energy barrier of 2.0 Kcal/mol. Thus, the major product arises from $\mathbf{TS_{int1a\text{-}2a}}$, giving rise to **Int2a** with an absolute *R*-configuration by reaction through the *Re* face of the alkene, which after indole nucleophile trapping renders product **2.77a** with an *S* absolute configuration which agrees with the experimental results. Hydrogen bond interactions between both chiral units could be observed in all the intermediates calculated, suggesting they might serve as anchor for additional stabilizing interactions.

67. The difference among them was on the (*R*)-**Au19**/substrate/(*R*)-**Ag6** folding and the HB-interaction between urea and phosphoramidate.
68. a) Chakraborty, S.; Saha, C. *Reson* **2016**, *21*, 151–171. b) Takahashi, S.; Sato, H.; Hiraoka, S. American Chemical Society (ACS) April 4, 2023.

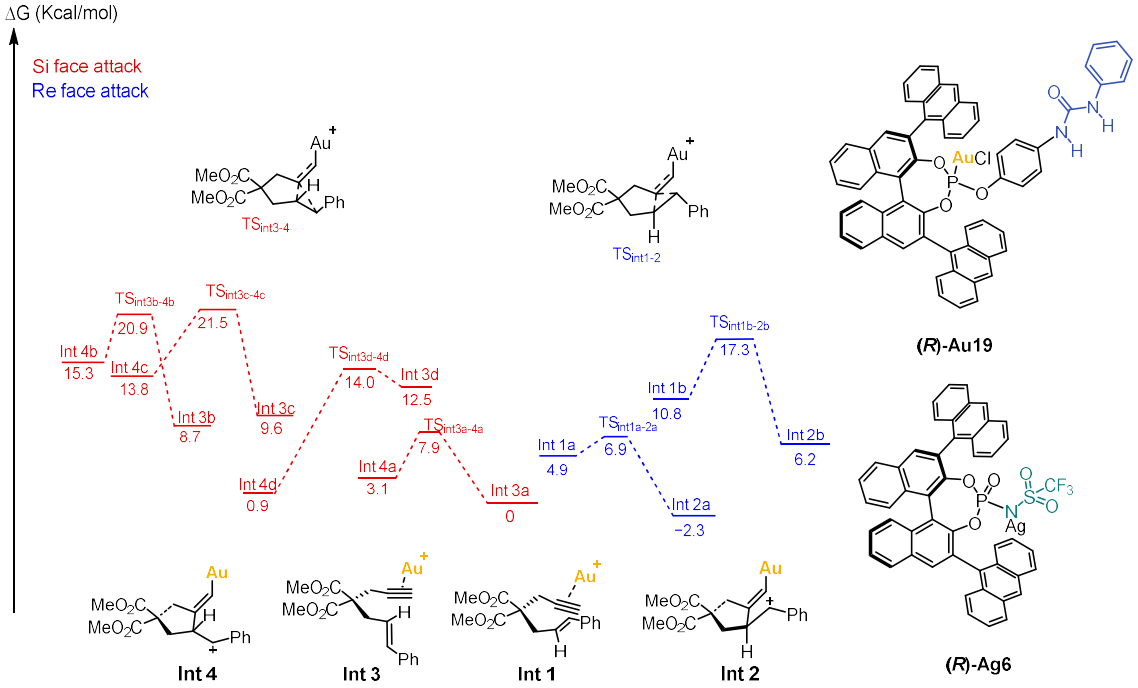

Figure 2.16. Free energy profiles for the 5-*exo*-dig cyclization for the matched case of the cyclization of **2.76a** using (*R*)-**Au19** and the counterion from (*R*)-**Ag6**. Pathways for the *Si* and *Re* face attack of the alkene are depicted in red and blue respectively. A, b, c and d refer to different conformers. Energy values are given in Kcal/mol and represent the relative free energies to **Int3a** which was chosen as the zero point.

NCI plots were used to visualize the non-covalent interactions in the transition states. Weak attractive interactions are represented by green surfaces, while strong, attractive interactions are blue (corresponding to the hydrogen bond interactions) and strong repulsive interactions are red. All intermediates were found to share extended and strong attractive non-covalent interactions based on π-π stackings or C–H-π agnostic interactions. **TS$_{int1a-2a}$** presented a strong dual hydrogen bond interaction (Figure 2.17) to the oxygen of the phosphoramidate P=O (2.15 and 1.90 Å), which, together with the T-shaped-π attractive interaction between the C–H of the urea and the pi-system of the binaphtol counterion, brings the two components closer together. Additionally, more stabilizing interactions were observed, including a strong sandwich-type π-π system (3.49 Å) and a T-shaped interaction between the urea's carbonyl π system and the *para*-C–H of the cinnamyl group (2.88 Å).

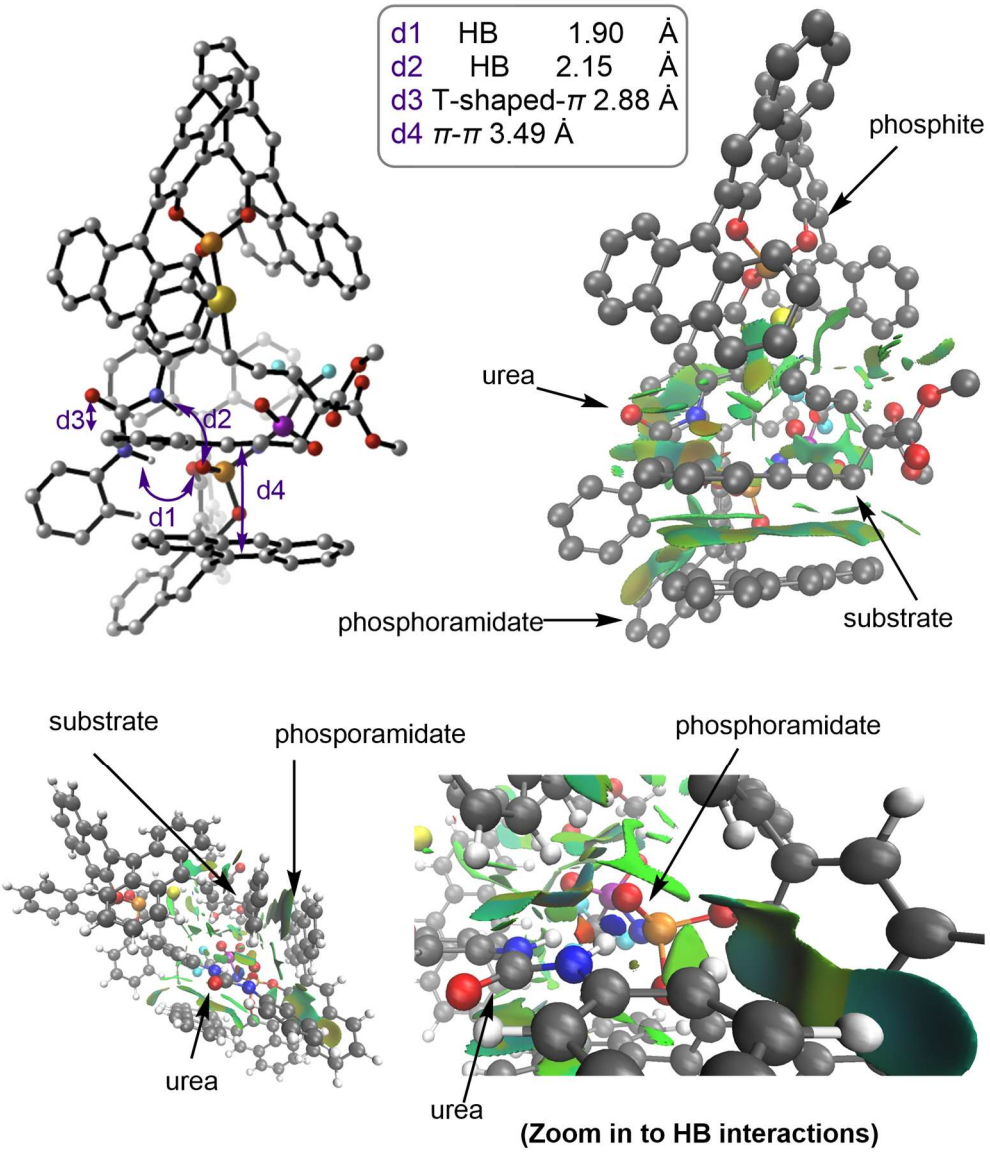

Figure 2.17 NCI plots and CYLview representations of $\mathbf{TS_{int1a\text{-}2a}}$ from different perspectives. In some cases H atoms are omitted for clarity. Color code: P, orange; Au, yellow; F, cyan; O, red; N, blue; S, purple; C, grey; and H, white.

In contrast, $\mathbf{TS_{int3a\text{-}4a}}$ (Figure 2.18) displayed hydrogen bond interactions with both the P=O (2.00 Å) and S=O (2.00 Å) bonds which approximates the counterion and the gold (I) complex favoring two strong attractive T-shaped-π interactions of the substrate with the anthracenyl motifs of gold (3.32 Å) and with the counterion (2.52 Å) which play the major role in stabilizing the transition state.

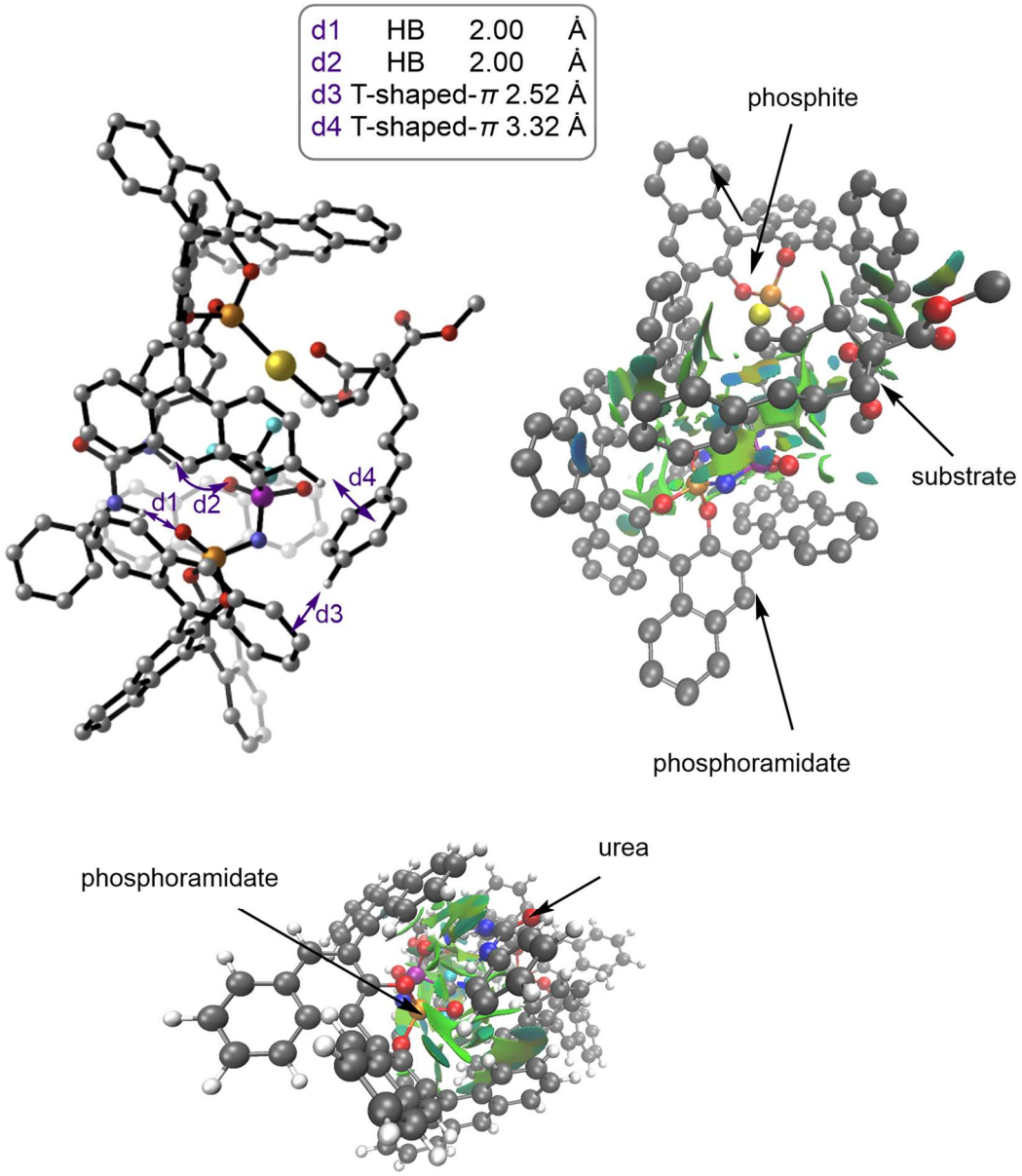

Figure 2.18 NCI plots and CYLview representations for $\mathbf{TS_{int3a\text{-}4a}}$ from different perspectives. In some cases H atoms are omitted for clarity. Color code: P, orange; Au, yellow; F, cyan; O, red; N, blue; S, purple; C, grey; and H, white.

Conclusions

The concept of asymmetric gold(I)-catalyzed H-bonded Counterion-Directed Catalysis has been introduced. This new methodology is based on H-bonding interactions between a chiral anion and a suitably positioned H-bond donor group on the ligands of gold(I) complexes. The presence of such interactions was demonstrated experimentally by NMR and structure–activity studies with modified ligands and chiral salts, as well as by the observed solvent and fluoride effects. Mechanistic studies allowed to elucidate the role of the hydrogen bond donor and the metal scavenger. First we demonstrated that excellent yields and enantioselectivities could be obtained simply by mixing an achiral phosphinourea/phosphinosquaramide gold(I) complex with a chiral counterion in four different enantioselective cyclization of 1,*n*-enynes.

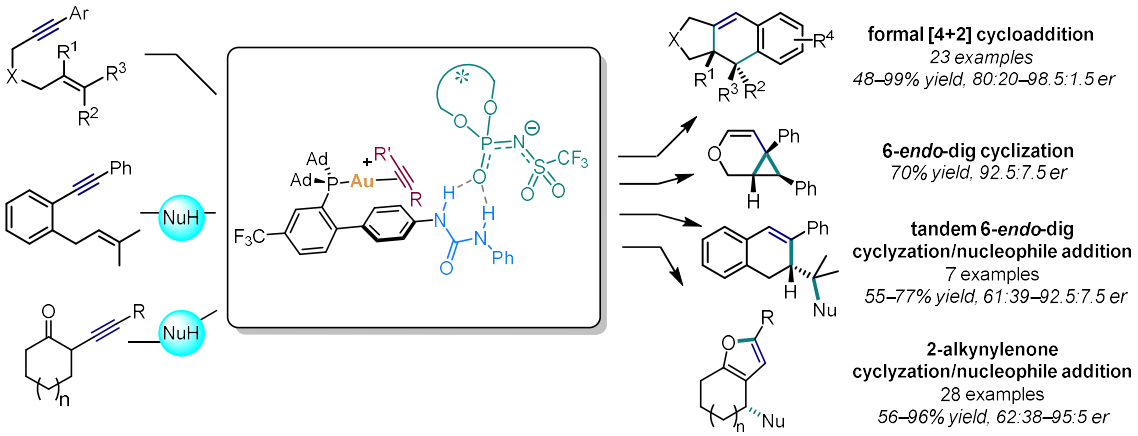

Scheme 2.33. Application of the gold(I) catalyzed HCDC for the activation of alkyne-containing substrates, using an achiral gold(I) complex and a chiral counterion. In green bonds generated during the reaction.

Finally, the enantioselective reaction of 1,6-enynes with *O*-, *N*-, and *C*-nucleophiles was developed by matched ion pair gold(I) catalysis combining a chiral phosphitourea gold(I) complex and a chiral phosphoramidate. Very high levels of enantiocontrol were achieved (up to >99:1 *er*) for a broad scope of substrates.

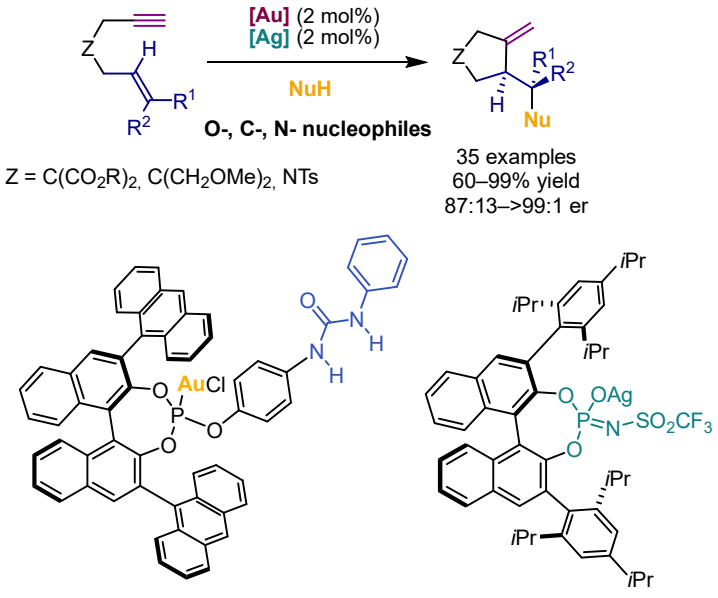

Scheme 2.34 Matched ion pair gold(I) catalysis enabled by H-bonded interactions.

Experimental Part

General Remarks

The general information has been provided in the experimental section of Chapter 1.

Synthetic Procedures and Analytical Data

Synthesis and characterization of ligands and Au(I) complexes

General Procedure GP1: P–C coupling

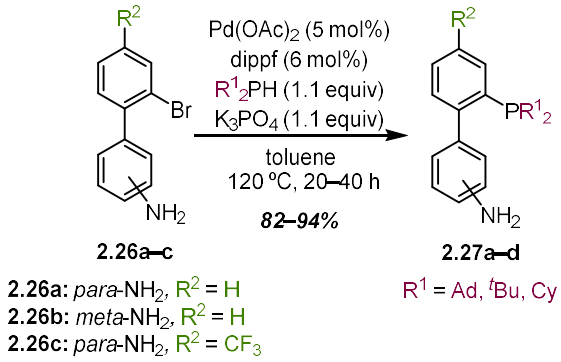

Following a modified literature procedure,[19] under Ar, to an oven-dried microwave vial equipped with a stirring bar the following compounds were added sequentially: 1,1′-bis(diisopropylphosphino)ferrocene (0.06 equiv), diacetoxypalladium (0.05 equiv), anhydrous potassium phosphate tribasic (1.1 equiv), aryl bromide **2.26** (1.0 equiv) and finally anhydrous toluene (0.2 M concentration). At this point, the desired secondary phosphine (1.1 equiv) was added. The mixture was stirred at 120 ºC in the sealed MW-vial for the time indicated in the single procedures, then volatiles were evaporated under reduced pressure. The crude residue was purified by FCC to afford aminophosphine **2.27**.

Note: Before stopping the reaction, conversion was checked by $^{31}P\{^{1}H\}$ NMR analysis of an aliquot of the reaction mixture (ca 0.1 mL) diluted in a deuterated solvent (ca 0.4 mL) and prepared under Ar, to avoid oxidation of unreacted secondary phosphine. Consumption of aryl bromide **2.26** was monitored by GC-MS.

General Procedure GP2: (thio)urea formation in JohnPhos base systems

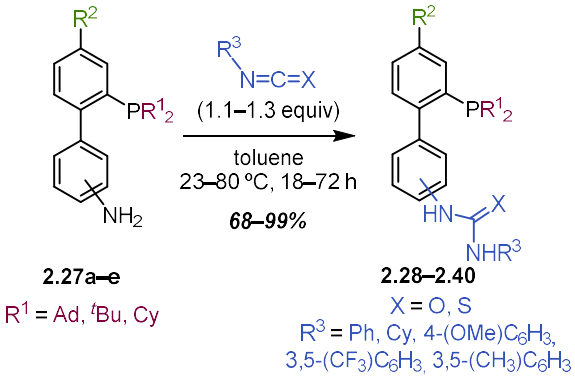

Under Ar, to a solution of aminophosphine **2.27** in anhydrous THF (0.1–0.3 M), the desired iso(thio)cyanate (1.1 equiv) was added. The reaction mixture was stirred at the temperature and for the time indicated in the single procedures (until substrate consumption as assessed by $^{31}P\{^{1}H\}$

NMR), then volatiles were evaporated under reduced pressure. The crude residue was purified by FCC to afford (thio)ureaphosphine ligand **2.28–2.40**.

General Procedure GP3: gold(I) ligand exchange

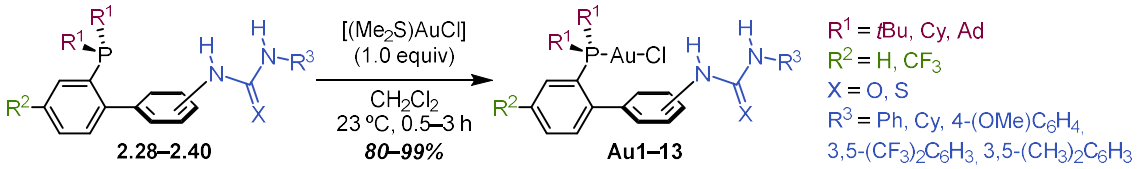

Under air, to a stirred solution or suspension of (thio)ureaphosphine ligand **2.28–2.40** (1.0 equiv) in CH_2Cl_2, [$(Me_2S)AuCl$] (1.0 equiv) was added, followed by additional CH_2Cl_2 (final concentration 0.06 M). The resulting solution was stirred in the dark at 23 ºC for 0.5–3 h, then filtered through a 0.2 mm PTFE syringe filter. The filtrate was evaporated under reduced pressure (T ≤ 37 °C) and the crude product was purified as described in the single procedures, yielding complexes **Au1–13**.

2-Bromo-4'-nitro-4-(trifluoromethyl)-1,1'-biphenyl (2.80)

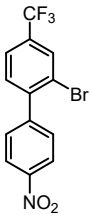

In a Schlenk flask, under Ar, 2-bromo-1-iodo-4-(trifluoromethyl)benzene (2.00 g, 5.70 mmol, 1.0 equiv), (4-nitrophenyl)boronic acid (1.05 g, 6.27 mmol, 1.1 equiv), [$(PPh_3)_2PdCl_2$] (0.060 g, 0.085 mmol, 0.015 equiv) and potassium carbonate (1.97 g, 14.3 mmol, 2.5 equiv) were suspended in H_2O (3.0 mL) and dimethoxyethane (17.5 mL). The resulting yellow suspension was degassed by bubbling Ar for 5 minutes while stirring. The resulting orange mixture was stirred at 80 ºC for 16 h (after which GC-MS analysis indicated incomplete conversion) and then 110 °C for 5 h. The reaction mixture was diluted with water (20 mL) and EtOAc (20 mL). Layers were separated and the aqueous phase was extracted with EtOAc (3 × 30 mL). The combined organic phases were washed with brine (50 mL), dried over Na_2SO_4, filtered and evaporated. The crude product was purified by automated FCC (silica, dry load, CyH:EtOAc 100:0 slowly to 96:4, then to 90:10). Compound **2.80** was obtained as a pale yellow solid (1.44 g, 4.16 mmol, 73% yield). **M.p.** 88–90 °C. **IR** (film from $CDCl_3$, cm^{-1}) υ 1521, 1345, 1319, 1173, 1132, 1083. **^{1}H NMR** (300 MHz, $CDCl_3$) δ 8.37–8.26 (m, 2H), 8.01–7.87 (m, 1H), 7.73–7.64 (m, 1H), 7.65–7.54 (m, 2H), 7.46 (d, J = 7.9 Hz, 1H). **^{13}C NMR** (101 MHz, $CDCl_3$) δ 147.9, 146.2, 144.1, 132.3 (q, J = 33.4 Hz), 131.3, 130.6 (q, J = 3.8 Hz), 130.4, 124.7 (q, J = 3.7 Hz), 123.7, 123.1 (q, J = 272.8 Hz), 122.6. **^{19}F NMR** (376 MHz, $CDCl_3$) δ −62.5. **HRMS** (APCI +) calculated for $[C_{13}H_7BrF_3NO_2]^{\cdot+}$ $[M]^{\cdot+}$ 344.9607 *m/z*; found 344.9610 *m/z*.

2'-Bromo-4'-(trifluoromethyl)-[1,1'-biphenyl]-4-amine (2.26c)

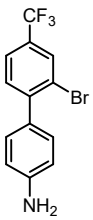

To a pale-yellow suspension of 2-bromo-4'-nitro-4-(trifluoromethyl)-1,1'-biphenyl **2.80** (1.62 g, 4.67 mmol, 1.0 equiv) in AcOH (9 mL) and H_2O (3 mL), iron powder (2.09 g, 37.4 mmol, 8.0 equiv) was added. The resulting mixture was stirred at 23 °C for 3 min (turned red-brown) and then at 80 ºC for 1 h. The reaction was cooled to 23 °C and filtered through a sintered glass funnel washing with the minimal amount of H_2O, CH_2Cl_2 and AcOH. The filtrate was evaporated till a brown residue was obtained, which was then dissolved in 5%$_{w/w}$ aqueous NaOH (60 mL) and CH_2Cl_2 (50 mL). Upon basification, the color changed from brown to blue-grey (ensure the pH of the organic phase is >12). Layers were separated and the aqueous phase was extracted with CH_2Cl_2 (3 × 50 mL). The combined organic phases were washed with brine (80 mL), dried over Na_2SO_4, filtered and evaporated. The crude product was purified by automated FCC (silica, dry load, CyH:CH_2Cl_2 80:20 to 0:100, product eluting in CyH:CH_2Cl_2 50:50). Compound **2.26c** was obtained as a pale yellow solid (1.30 g, 4.11

mmol, 88% yield). **M.p.** 68–70 °C. **IR** (film from $CDCl_3$, cm^{-1}) υ 3490, 3395, 1621, 1604, 1317, 1293, 1167, 116, 1081, 1057, 813. **^{1}H NMR** (400 MHz, $CDCl_3$) δ 8.02–7.95 (m, 1H), 7.66–7.58 (m, 1H), 7.51–7.41 (m, 1H), 7.33–7.23 (m, 2H), 6.82–6.69 (m, 2H), 3.86 (br s, 1H). **^{13}C NMR** (101 MHz, $CDCl_3$) 146.7, 146.4–146.2 (m), 131.6, 130.4, 130.20 (q, J = 3.9 Hz), 130.17 (q, J = 32.6 Hz), 129.9, 124.2 (q, J = 3.6 Hz), 123.4 (q, J = 270.6 Hz), 123.1, 114.5. **^{19}F NMR** (376 MHz, $CDCl_3$) δ −62.5. **HRMS** (ESI+) calculated for $[C_{13}H_{10}BrF_3N]^+$ $[M+H]^+$ 315.9943 *m/z*; found 315.9938 *m/z*.

2'-(Di-*tert*-butylphosphanyl)-[1,1'-biphenyl]-4-amine (2.27a)

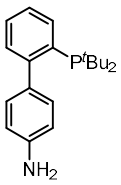

Prepared following general procedure **GP1**, using 2'-bromo-[1,1'-biphenyl]-4-amine **2.26a** (500 mg, 2.01 mmol, 1.0 equiv) and di-*tert*-butyl phosphine (410 µL, 2.22 mmol, 1.1 equiv) in toluene (10 mL) at 120 °C for 18 h. The crude product was purified by FCC (silica, liquid load in CH_2Cl_2, CH_2Cl_2:EtOAc 90:10 to 70:30). Compound **2.27a** was obtained as a beige solid (596 mg, 1.89 mmol, 94% yield). **M.p.** 106–107 °C. **IR** (film from $CDCl_3$, cm^{-1}) υ 3344, 2957, 2937, 2892, 2860, 1621, 1517, 1459. **^{1}H NMR** (400 MHz, $CDCl_3$): d 7.90–7.83 (m, 1H), 7.34 (tdd, J = 7.4, 1.5, 0.8 Hz, 1H), 7.29 (dd, J = 7.5, 1.8 Hz, 1H), 7.27–7.22 (m, 1H), 7.10–7.00 (m, 2H), 6.67 (d, J = 8.3 Hz, 2H), 3.65 (br s, 2H), 1.14 (d, J = 11.5 Hz, 18H). **^{13}C NMR** (101 MHz, $CDCl_3$): δ 151.4 (d, J = 32.1 Hz), 144.8, 136.1, 135.0, 135.5 (d, J = 3.3 Hz), 134.5 (d, J = 7.2 Hz), 131.7 (d, J = 4.1 Hz), 131.0 (d, J = 5.8 Hz), 128.5 (d, J = 1.3 Hz), 125.4, 32.9 (d, J = 25.3 Hz), 30.9 (d, J = 15.5 Hz). **^{31}P NMR** (162 MHz, $CDCl_3$): δ 21.6. **HRMS** (ESI +) calculated for $[C_{20}H_{29}NP]^+$ $[M+H]^+$ 314.2032 *m/z*; found 314.2033 *m/z*.

2'-(Dicyclohexylphosphanyl)-[1,1'-biphenyl]-4-amine (2.27b)

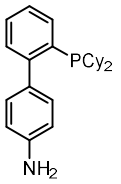

Prepared following general procedure **GP1**, using 2'-bromo-[1,1'-biphenyl]-4-amine **2.26a** (300 mg, 1.21 mmol, 1.0 equiv) and dicyclohexylphosphine (269 µL, 2.22 mmol, 1.1 equiv) in toluene (6 mL) at 120 °C for 21 h and then at 130 °C for 19 h. The crude product was purified by FCC (silica, liquid load in CH_2Cl_2, CH_2Cl_2:EtOAc 100:0 to 90:10, product eluting in pure CH_2Cl_2). Compound **2.27b** was obtained as a yellow solid (376.8 mg, 1.03 mmol, 85% yield). **IR** (film from $CDCl_3$, cm^{-1}) υ 3460 (broad), 3351 (broad), 3212, 2920, 2847, 1620, 1517, 1461, 1446, 728. **^{1}H NMR** (400 MHz, $CDCl_3$) δ 7.57 (dt, J = 7.6, 2.1 Hz, 1H), 7.38–7.24 (m, 3H), 7.14–7.08 (m, 2H), 6.73–6.67 (m, 2H), 3.65 (s, 2H), 1.90–1.78 (m, 2H), 1.76–1.53 (m, 10H), 1.32–0.95 (m, 10H). **^{13}C NMR** (101 MHz, $CDCl_3$) δ 150.7 (d, J = 27.9 Hz), 145.1, 134.1, 133.4 (d, J = 6.2 Hz), 132.9 (d, J = 3.0 Hz), 131.6 (d, J = 4.4 Hz), 130.5 (d, J = 5.1 Hz), 128.2, 126.0, 114.3, 34.8 (d, J = 14.6 Hz), 30.5 (d, J = 17.0 Hz), 29.4 (d, J = 9.0 Hz), 27.4 (d, J = 7.5 Hz), 27.3 (d, J = 3.3 Hz), 26.5. **^{31}P NMR** (162 MHz, $CDCl_3$) δ –9.9. **HRMS** (APCI +) calculated for $[C_{24}H_{33}NP]^+$ $[M+H]^+$ 366.2345 *m/z*; found 366.2347 *m/z*.

2'-(Di-*tert*-butylphosphaneyl)-[1,1'-biphenyl]-3-amine (2.27c)

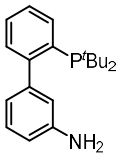

Prepared following general procedure **GP1**, using 2'-bromo-[1,1'-biphenyl]-3-amine **2.26b (**500 mg, 2.02 mmol, 1 equiv) and di-*tert*-butyl phosphine (410 µL, 2.22 mmol, 1.1 equiv) in toluene (10 mL) at 120 ºC for 22 h. The crude product was purified by FCC (silica, CH_2Cl_2:EtOAc 95:5 to 50:50). Compound **2.27c** was obtained as a pale orange solid (537 mg, 1.71 mmol, 85% yield). It could be recrystallized from warm EtOAc to an off-white solid. **M.p.** 121–122 °C. **IR** (film from $CDCl_3$, cm^{-1}) υ 3341, 2958, 2938, 2892, 2860, 1618, 1605, 1585, 1460. **^{1}H NMR** (500 MHz, $CDCl_3$): δ 7.88 (dt, J = 7.5, 1.5 Hz, 1H), 7.34 (tdd, J = 7.5, 1.6, 0.8 Hz, 1H), 7.31 (td, J = 7.5, 1.8 Hz, 1H), 7.25 (ddd, J = 7.2, 4.0, 1.8 Hz, 1H), 7.12 (t, J = 7.7 Hz, 1H), 6.66–6.63 (m, 2H), 6.57–6.55 (m, 1H), 3.63 (br s, 2H), 1.14 (d, J^3_{HP} = 11.5 Hz, 18H). **^{13}C NMR** (126 MHz, $CDCl_3$): δ 151.6 (d, J_{CP} = 33.3 Hz), 145.23, 145.17

(d, J_{CP} = 7.3 Hz), 135.7 (d, J_{CP} = 28.1 Hz), 135.4 (d, J_{CP} = 3.2 Hz), 130.5 (d, J_{CP} = 6.2 Hz), 128.4, 128.1, 125.7, 121.5 (d, J_{CP} = 3.9 Hz), 117.7 (d, J_{CP} = 3.2 Hz), 113.5, 32.9 (d, J^{1}_{CP} = 25.5 Hz), 30.9 (d, J^{2}_{CP} = 15.6 Hz). **^{31}P NMR** (202 MHz, $CDCl_3$): δ 21.6. **HRMS** (ESI +) calculated for $[C_{20}H_{29}NP]^+$ $[M+H]^+$ 314.2032 *m/z*; found 314.2028 *m/z*.

2'-(Di(adamantan-1-yl)phosphaneyl)-4'-(trifluoromethyl)-[1,1'-biphenyl]-4-amine (2.27d)

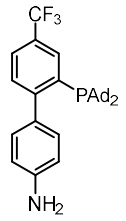

Prepared following general procedure **GP1**, using 2'-bromo-4'-(trifluoromethyl)-[1,1'-biphenyl]-4-amine **2.26c (**500.0 mg, 1.58 mmol, 1 equiv) and di-1-adamantyl phosphine (526 mg, 1.74 mmol, 1.1 equiv) in toluene (8 mL) at 120 ºC for 20 h. The crude product was purified by automated FCC (silica, dry load, CyH:EtOAc 100:0 to 80:20). Compound **2.27d** was obtained as an off-white solid with very pale pink/orange hues (799 mg, 1.49 mmol, 85% yield). **M.p.** 247–249 °C (decomposition). **IR** (film from $CDCl_3$, cm^{-1}) υ 2902, 2847, 1619, 1602, 1323, 1299, 1137, 1117, 1084, 1068, 821. **^{1}H NMR** (500 MHz, $CDCl_3$) d 8.13 (br s, 1H), 7.58 (d, *J* = 8.0 Hz, 1H), 7.37 (dd, *J* = 8.0, 3.8 Hz, 1H), 7.04 (d, *J* = 8.4 Hz, 2H), 6.69 (d, *J* = 8.4 Hz, 2H), 3.70 (br s, 2H), 1.98–1.82 (m, 18 H), 1.68–1.63 (m, 12 H). **^{13}C NMR** (126 MHz, $CDCl_3$) δ 155.4 (d, J_{CP} = 31.0 Hz), 145.4, 134.8 (d, J_{CP} = 31.0 Hz), 133.3 (quint, J_{CF} = J_{CP} = 3.7 Hz), 133.1 (d, J_{CP} = 6.7 Hz),131.6 (d, J_{CP} = 4.1 Hz), 131.3 (d, J_{CP} = 5.6 Hz), 127.0 (q, J^{2}_{CF} = 31.9 Hz), 124.9 (q, J_{CF} = 3.3 Hz), 124.6 (q, J^{1}_{CF} = 273.0 Hz), 114.3, 42.0 (d, J^{2}_{CP} = 13.0 Hz), 37.7 (d, J^{1}_{CP} = 26.4 Hz), 37.0, 29.0 (d, J^{3}_{CP} = 8.6 Hz). **^{31}P NMR** (202 MHz, $CDCl_3$) δ 24.1. **^{19}F NMR** (471 MHz, $CDCl_3$) δ –62.4. **HRMS** (ESI +) calculated for $[C_{33}H_{40}F_3NP]^+$ $[M+H]^+$ 538.2845 *m/z*; found 538.2848 *m/z*.

2'-(Di-*tert*-butylphosphaneyl)-4'-(trifluoromethyl)-[1,1'-biphenyl]-4-amine (2.27e)

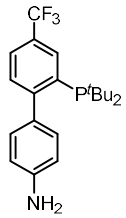

Prepared following general procedure **GP1**, using 2'-bromo-4'-(trifluoromethyl)-[1,1'-biphenyl]-4-amine **2.26c (**200 mg, 0.633 mmol, 1 equiv) and di-*tert*-butyl phosphine (129 µL, 0.696 mmol, 1.1 equiv) in toluene (3.1 mL) at 120 ºC for 24 h. The crude product was purified by automated FCC (silica 40 g, dry load, CyH:EtOAc 100:0 to 80:20, product eluted in CyH:EtOAc 85:15). Compound **2.27e** was obtained as an off-white solid (198 mg, 0.519 mmol, 82% yield). **M.p**. 158 °C. **IR** (film from $CDCl_3$, cm^{-1}) υ 3355, 2953, 2896, 1618, 1322, 1120, 1083, 1069, 821. **^{1}H NMR** (400 MHz, $CDCl_3$) δ 8.16 (br s, 1H), 7.58 (d, *J* = 8.1 Hz, 1H), 7.37 (dd, *J* = 8.0, 3.9 Hz, 1H), 7.06 (d, *J* = 8.5 Hz, 2H), 6.69 (d, *J* = 8.5 Hz, 2H), 3.70 (br s, 2H), 1.14 (d, J^{3}_{HP} = 11.7 Hz, 18H). **^{13}C NMR** (126 MHz, $CDCl_3$) δ 154.9 (d, J_{CP} = 30.0 Hz), 145.5, 137.3 (d, J_{CP} = 31.2 Hz), 132.9 (d, J_{CP} = 6.6 Hz), 132.2 (quint, J_{CF} = J_{CP} = 3.9 Hz), 131.5 (d, J_{CP} = 4.3 Hz), 131.3 (d, J_{CP} = 5.4 Hz), 127.5 (q, J^{2}_{CF} = 32.0 Hz), 125.1 (q, J_{CF} = 3.7 Hz), 124.6 (q, J^{1}_{CF} = 272.0 Hz), 114.3, 33.0 (d, J^{1}_{CP} = 25.7 Hz), 30.8 (d, J^{2}_{CP} = 15.5 Hz). **^{31}P NMR** (162 MHz, $CDCl_3$) δ 21.6. **^{19}F NMR** (471 MHz, $CDCl_3$) δ –62.5. **HRMS** (ESI +) calculated for $[C_{21}H_{28}F_3NP]^+$ $[M+H]^+$ 382.1906 *m/z*; found 382.1914 *m/z*.

***N*^{2}-(2'-(Di-*tert*-butylphosphaneyl)-[1,1'-biphenyl]-4-yl)-[1,1'-biphenyl]-2,4'-diamine (2.27H)**

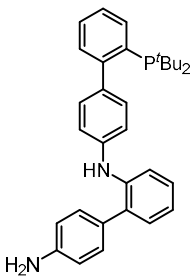

Isolated as a side product from a coupling reaction between 2'-bromo-[1,1'-biphenyl]-4-amine **2.26a** (50.0 mg, 0.200 mmol, 1 equiv) and di-*tert*-butyl phosphine (41 µL, 0.22 mmol, 1.1 equiv) in toluene (1 mL) at 120 ºC for 24 h, according to **GP1** except for using NaO^{t}Bu (26.9 mg, 0.280 mmol, 1.4 equiv) as a base. The crude material was purified by FCC with two sequential columns (silica, dry load, CH_2Cl_2:EtOAc 100:0 to 70:30). Compound **2.27H** was obtained as an orange oil that solidified to a pale brown solid (13.5 mg, 0.028 mmol, 14% yield). **M.p.** 62–64 °C. **IR** (film from $CHCl_3$, cm^{-1}) υ 3388,

2957, 2936, 2892, 2859, 1620, 1517, 1458, 1309, 1179, 830, 755, 745. **^{1}H NMR** (300 MHz, $CDCl_3$) δ 7.91 (d, *J* = 7.6 Hz, 1H), 7.48–7.22 (m, 8H), 7.17 (d, *J* = 8.2 Hz, 2H), 7.05 (d, *J* = 8.4 Hz, 2H), 6.96 (t, *J* = 7.4 Hz, 1H), 6.80 (d, *J* = 8.4 Hz, 2H), 5.78 (br s, 1H, NH), 3.77 (br s, 2H, NH), 1.17 (d, J^3_{HP} = 11.6 Hz, 18H). **^{13}C NMR** (101 MHz, $CDCl_3$) δ 1541.2 (d, J_{CP} = 32.1 Hz), 145.9, 141.6, 140.8, 136.8 (d, J_{CP} = 7.0 Hz), 135.8 (d, J_{CP} = 27.2 Hz), 135.6 (d, J_{CP} = 3.3 Hz), 131.6 (d, J_{CP} = 4.2 Hz), 131.6 (d, J_{CP} = 7.1 Hz), 131.0, 130.9, 130.6, 129.1, 128.5, 127.7, 125.6, 120.4, 117.5, 116.4, 115.6, 32.9 (d, J^1_{CP} = 25.2 Hz), 30.9 (d, J^2_{CP} = 15.4 Hz). **^{31}P NMR** (162 MHz, $CDCl_3$) δ 21.5. **HRMS** (ESI +) calculated for $[C_{32}H_{28}N_2P]^+$ $[M+H]^+$ 481.2767 *m/z*; found 481.2753.

1-(2'-(Di-*tert*-butylphosphanyl)-[1,1'-biphenyl]-4-yl)-3-phenylurea (2.28)

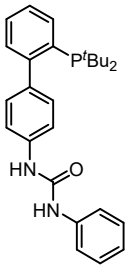

Prepared following general procedure **GP2**, using aminophosphine **2.27a** (200 mg, 0.638 mmol, 1.0 equiv) and phenylisocyanate (76 µL, 0.702 mmol, 1.1 equiv) in THF (6.4 mL) at 77 °C for 18 h. The crude product was purified by FCC (silica, dry load, CH_2Cl_2: EtOAc 98:2 to 80:20). Ligand **2.28** was obtained as a white solid (255 mg, 0.587 mmol, 92% yield). **M.p.** 214–216 °C. **IR** (film from $CDCl_3$, cm^{-1}) υ 3331, 29577, 2936, 2893, 2859, 1654, 1598, 1545, 1499, 1313, 1231. **^{1}H NMR** (400 MHz, $CDCl_3$) δ 7.88 (d, *J* = 7.5 Hz, 1H), 7.43–7.29 (m, 8H), 7.26–7.20 (m, 3H), 7.10 (tt, *J* = 7.2, 1.3 Hz, 1H), 6.91 (br s, 1H), 6.86 (br s, 2H), 1.13 (d, *J* = 11.6 Hz, 18H). **^{13}C NMR** (126 MHz, $CDCl_3$) δ 153.6, 150.7 (d, J^1_{CP} = 32.2 Hz), 140.1 (d, J_{CP} = 7.3 Hz), 138.3, 136.4, 135.9, 135.5 (d, J_{CP} = 3.3 Hz), 131.6 (d, J_{CP} = 4.0 Hz), 130.7 (d, J_{CP} = 6.1 Hz), 129.4, 128.6, 126.0, 124.3, 121.3, 120.4, 32.9 (d, J^1_{CP} = 24.8 Hz), 30.9 (d, J^2_{CP} = 15.3 Hz). **^{31}P NMR** (162 MHz, $CDCl_3$) δ 21.3. **HRMS** (ESI +) calculated for $[C_{27}H_{34}N_2OP]^+$ $[M+H]^+$ 433.2403 *m/z*; found 433.2407 *m/z*.

1-(2'-(Di-*tert*-butylphosphanyl)-[1,1'-biphenyl]-4-yl)-3-(4-methoxyphenyl)urea (2.29)

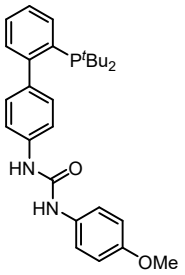

Prepared following general procedure **GP2**, using aminophosphine **2.27a** (100 mg, 0.319 mmol, 1.0 equiv) and 1-isocyanato-4-methoxybenzene (45 µL, 0.35 mmol, 1.1 equiv) in THF (6.4 mL) at 80 °C for 19 h. The crude product was purified by FCC (silica, dry load, CH_2Cl_2: EtOAc 100:0 to 70:30). Ligand **2.29** was obtained as a white solid (123 mg, 0.265 mmol, 83% yield). **M.p.** 220 °C (decomposition). **IR** (film from acetone-d_6, cm^{-1}) υ 3326, 2956, 2938, 2893, 2860, 1650, 1598, 1542, 1243, 1229. **^{1}H NMR** (400 MHz, acetone-d_6) δ 8.05 (br s, 1H), 7.98 (br s, 1H), 7.96–7.92 (m, 1H), 7.52 (d, *J* = 8.5 Hz, 2H), 7.45 (d, *J* = 9.1 Hz, 2H), 7.42–7.35 (m, 2H), 7.28–7.24 (m, 1H), 7.17 (d, *J* = 8.5 Hz, 2H), 6.86 (d, *J* = 9.0 Hz, 2H), 3.76 (s, 3H), 1.13 (d, *J* = 11.4 Hz, 18H). **^{13}C NMR** (126 MHz, acetone-d_6) δ 156.2, 153.7, 152.0 (d, J^1_{CP} = 32.8 Hz), 139.4, 138.4 (d, J_{CP} = 7.2 Hz), 136.6, 136.4, 136.3 (d, J_{CP} = 3.1 Hz), 133.9, 131.9 (d, J_{CP} = 4.4 Hz), 131.5 (d, J_{CP} = 6.0 Hz), 129.5, 126.6, 121.4, 118.0, 114.8, 55.7, 33.2 (d, J^1_{CP} = 26.3 Hz), 31.1 (d, J^2_{CP} = 15.8 Hz). **^{31}P NMR** (162 MHz, acetone-d_6) δ 20.9. **^{31}P NMR** (162 MHz, $CDCl_3$) δ 21.3. **HRMS** (ESI +) calculated for $[C_{28}H_{36}N_2O_2P]^+$ $[M+H]^+$ 463.2509 *m/z*; found 463.2505 *m/z*.

1-(2'-(Di-*tert*-butylphosphaneyl)-[1,1'-biphenyl]-4-yl)-3-(3,5-dimethylphenyl)urea (2.30)

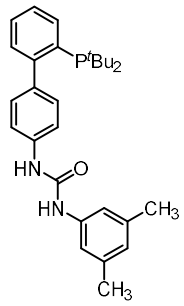

Prepared following general procedure **GP2**, using aminophosphine **2.27a** (80.5 mg, 0.257 mmol, 1.0 equiv) and 1-isocyanato-3,5-dimethylbenzene (40 µL, 0.28 mmol, 1.1 equiv) in THF (2.5 mL) at 80 °C for 20 h. The crude product was purified by FCC (silica, dry load, CH_2Cl_2: EtOAc 100:0 to 85:15). Ligand **2.30** was obtained as a white solid (111.5 mg, 0.240 mmol, 92% yield). **M.p.** 135 °C (decomposition). **IR** (film from acetone-d_6, cm^{-1}) υ 3331, 2956, 2938, 2893, 1653, 1613, 1596, 1558, 1535, 1519, 1459, 1310, 1219. **^{1}H NMR** (400 MHz, acetone-d_6) δ 8.11 (s, 1H), 8.03 (s, 1H), 7.98–7.91 (m, 1H), 7.53 (d, J = 8.5 Hz, 2H), 7.46–7.34 (m, 2H), 7.30–7.22 (m, 1H), 7.22–7.14 (m, 4H), 6.64 (s, 1H), 2.24 (s, 6H), 1.13 (d, J = 11.4 Hz, 18H). **^{13}C NMR** (126 MHz, acetone-d_6) δ 153.5, 152.0 (d, J^1_{CP} = 32.8 Hz), 140.8, 139.3, 138.9, 138.5 (d, J_{CP} = 7.2 Hz), 136.5 (d, J_{CP} = 28.3 Hz), 136.3 (d, J_{CP} = 3.1 Hz), 131.9 (d, J_{CP} = 4.4 Hz), 131.5 (d, J_{CP} = 6.0 Hz), 129.5, 126.6, 124.6, 118.1, 117.3, 33.1 (d, J^1_{CP} = 26.3 Hz), 31.1 (d, J^2_{CP} = 15.8 Hz), 21.5. **^{31}P NMR** (162 MHz, acetone-d_6) δ 20.9. **HRMS** (ESI +) calculated for $[C_{29}H_{38}N_2OP]^+$ $[M+H]^+$ 461.2716 *m/z*; found 461.2720 *m/z*.

1-(3,5-Bis(trifluoromethyl)phenyl)-3-(2'-(di-*tert*-butylphosphanyl)-[1,1'-biphenyl]-4-yl)urea (2.31)

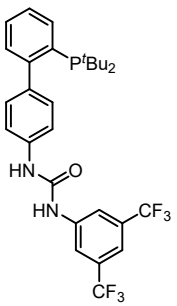

Prepared following general procedure **GP2**, using aminophosphine **2.26a** (200 mg, 0.638 mmol, 1.0 equiv) and 1-isocyanato-3,5-bis(trifluoromethyl)benzene (121 µL, 0.702 mmol, 1.1 equiv) in THF (6.4 mL) at 77 °C for 21 h. The crude product was purified by FCC (silica, dry load, CH_2Cl_2: EtOAc 95:5 to 80:20). Ligand **2.31** was obtained as a white solid (300 mg, 0.529 mmol, 83% yield). **IR** (film from acetone-d_6, cm^{-1}) υ 3336, 2940, 1666, 1571, 1473, 1387, 1277, 1177, 1134. **^{1}H NMR** (400 MHz, acetone-d_6) δ 8.82 (s, 1H), 8.38 (s, 1H), 8.23 (s, 2H), 7.99–7.87 (m, 1H), 7.61 (s, 1H), 7.55 (d, J = 8.5 Hz, 2H), 7.46–7.36 (m, 2H), 7.31–7.25 (m, 1H), 7.22 (d, J = 8.1 Hz, 2H), 1.13 (d, J = 11.4 Hz, 18H). **^{13}C NMR** (126 MHz, acetone-d_6): δ 153.2, 151.8 (d, J^1_{CP} = 32.9 Hz), 143.1, 139.4 (d, J_{CP} = 7.2 Hz), 138.4, 136.6, 136.3 (d, J_{CP} = 3.1 Hz), 132.5 (q, J^2_{CF} = 32.9 Hz), 132.0 (d, J_{CP} = 4.3 Hz), 131.4 (d, J_{CP} = 6.0 Hz), 129.5, 126.72, 124.5 (q, J^1_{CF} = 271.9 Hz), 119.2–118.9 (m), 118.7, 115.7–115.2 (m), 33.2 (d, J^1_{CP} = 26.2 Hz), 31.1 (d, J^2_{CP} = 15.8 Hz).**^{31}P NMR** (162 MHz, acetone-d_6): δ 21.3. **^{19}F NMR** (376 MHz, acetone-d_6) δ −62.5. HRMS (ESI +) calculated for $[C_{29}H_{32}F_6N_2OP]^+$ $[M+H]^+$ 569.2151 *m/z*; found 569.2143 *m/z*.

1-(2'-(Di-*tert*-butylphosphanyl)-[1,1'-biphenyl]-4-yl)-3-phenylthiourea (2.32)

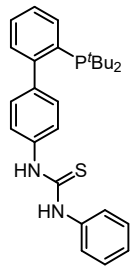

Prepared following general procedure **GP2**, using aminophosphine **2.26a** (203 mg, 0.648 mmol, 1.0 equiv) and isothiocyanatobenzene (85 µL, 0.712 mmol, 1.1 equiv) in THF (2.2 mL) at 23 °C for 21 h. The crude product was purified by FCC (silica, dry load, CH_2Cl_2: EtOAc 97:3 to 70:30). Ligand **2.32** was obtained as a pale yellow solid (287 mg, 0.640 mmol, 99% yield). **M.p.** 163 °C. **IR** (film from $CDCl_3$, cm^{-1}) υ 2957, 2929, 2857, 2160, 1239, 1034, 832, 756. **^{1}H NMR** (400 MHz, $CDCl_3$) δ 7.93–7.86 (m, 1H), 7.81 (br s, 1H), 7.73 (br s, 1H), 7.50–7.34 (m, 8H), 7.34–7.23 (m, 4H), 1.13 (d, J = 11.7 Hz, 18H). **^{13}C NMR** (126 MHz, $CDCl_3$) δ 180.0, 150.2 (d, J^1_{CP} = 32.1 Hz), 142.8 (d, J_{CP} = 6.1 Hz), 137.4, 135.6 (d, J_{CP} = 12.9 Hz), 135.5 (d, J_{CP} = 10.9 Hz), 131.9 (d, J_{CP} = 4.1 Hz), 130.6 (d, J_{CP} = 6.1 Hz), 129.7, 128.7 (d, J_{CP} = 0.8 Hz), 127.2, 126.3, 125.5, 124.0, 33.0 (d, J^1_{CP} = 24.0 Hz), 30.8 (d, J^2_{CP} = 15.2 Hz). **^{31}P NMR** (162 MHz, $CDCl_3$) δ 21.2. **HRMS** (ESI +) calculated for $[C_{27}H_{34}N_2SP]^+$ $[M+H]^+$ 449.2175 *m/z*; found 449.2172 *m/z*.

1-(2'-(Dicyclohexylphosphanyl)-[1,1'-biphenyl]-4-yl)-3-phenylurea (2.33)

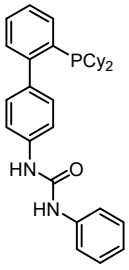

Prepared following general procedure **GP2**, using aminophosphine **2.26b** (127 mg, 0.347 mmol, 1.0 equiv), phenylisocyanate (41 µL, 0.382 mmol, 1.1 equiv) in THF (5 mL) at 23 °C for 48 h. The crude product was purified by FCC (silica, dry load, CH_2Cl_2: EtOAc 95:5). Ligand **2.33** was obtained as a white solid (166 mg, 0.343 mmol, 99% yield). **M.p.** 172 °C. **IR** (film from $CDCl_3$, cm^{-1}) υ 3332, 2923, 2849, 1654, 1597, 1499, 1444, 1231. **^{1}H NMR** (400 MHz, $CDCl_3$) δ 7.60–7.56 (m, 1H), 7.38–7.32 (m, 8H), 7.26–7.22 (m, 2H), 7.15–7.10 (m, 1H), 6.70 (d, J = 17.5 Hz, 2H), 1.87–1.77 (m, 2H), 1.74–1.60 (m, 8H), 1.57 (s, 2H), 1.31–0.97 (m, 10H). **^{13}C NMR** (101 MHz, $CDCl_3$) δ 153.5, 150.0 (d, J^I_{CP} = 28.2 Hz), 139.3, 138.1, 136.6, 134.2 (d, J_{CP} = 20.8 Hz), 133.1 (d, J_{CP} = 3.3 Hz), 131.8 (d, J_{CP} = 4.3 Hz), 130.4 (d, J_{CP} = 5.2 Hz), 129.5 (d, J_{CP} = 2.0 Hz), 126.7, 124.5, 121.5, 121.4, 120.5, 34.9 (d, J_{CP} = 14.1 Hz), 30.6 (d, J_{CP} = 17.1 Hz), 29.4 (d, J_{CP} = 8.7 Hz), 27.4 (d, J_{CP} = 7.2 Hz), 27.3 (d, J_{CP} = 2.9 Hz), 26.5. **^{31}P NMR** (162 MHz, $CDCl_3$) δ –10.1. **HRMS** (APCI +) calculated for $[C_{31}H_{38}N_2OP]^+$ $[M+H]^+$ 485.2716 *m/z*; found 485.2716 *m/z*.

1-(2'-(Dicyclohexylphosphanyl)-[1,1'-biphenyl]-4-yl)-3-phenylurea (2.34)

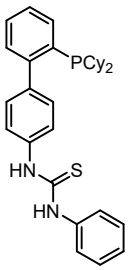

Prepared following general procedure **GP2**, using aminophosphine **2.26b** (120 mg, 0.328 mmol, 1.0 equiv), isothiocyanatobenzene (43 µL, 0.361 mmol, 1.1 equiv) in THF (11 mL) at 23 °C for 18 h. The crude product was purified by FCC (silica, dry load, CH_2Cl_2: EtOAc 100:0 to 95:5). Ligand **2.34** was obtained as a pale yellow solid (157 mg, 0.313 mmol, 96% yield). **M.p.** 161–163 °C. **IR** (film from $CDCl_3$, cm^{-1}) υ 3179, 3052, 2922, 2848, 2222, 1523, 1496, 1447, 1314, 731. **^{1}H NMR** (400 MHz, $CDCl_3$) δ 7.97 (br s, 1H), 7.87 (br s, 1H), 7.59 (dt, J = 6.8, 2.3 Hz, 1H), 7.48–7.27 (m, 12H), 1.91–1.75 (m, 2H), 1.73–1.59 (m, 8H), 1.54 (d, J = 13.1 Hz, 2H), 1.29–0.97 (m, 10H). **^{13}C NMR** (101 MHz, $CDCl_3$) δ 179.9, 149.6 (d, J^I_{CP} = 28.4 Hz), 141.8 (d, J_{CP} = 6.3 Hz), 137.4, 135.7, 134.1 (d, J_{CP} = 20.7 Hz), 133.1 (d, J_{CP} = 3.3 Hz), 132.0 (d, J_{CP} = 4.4 Hz), 130.2 (d, J_{CP} = 5.2 Hz), 129.7, 128.5, 127.2, 127.0, 125.5, 124.1, 34.9 (d, J_{CP} = 13.8 Hz), 30.6 (d, J_{CP} = 17.1 Hz), 29.4 (d, J_{CP} = 8.6 Hz), 27.3 (d, J_{CP} = 6.2 Hz), 27.2 (d, J_{CP} = 1.8 Hz), 26.5. **^{31}P NMR** (162 MHz, $CDCl_3$) δ –10.2. **HRMS** (ESI +) calculated for $[C_{31}H_{38}N_2PS]^+$ $[M+H]^+$ 501.2488 *m/z*; found 501.2505 *m/z*.

1-(2'-(Di-*tert*-butylphosphaneyl)-[1,1'-biphenyl]-3-yl)-3-phenylurea (2.35)

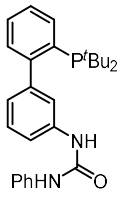

Prepared following general procedure **GP2**, using aminophosphine **B3** (200 mg, 0.638 mmol, 1 equiv) and phenyl isocyanate (76 µL, 0.70 mmol, 1.1 equiv) in THF (6.4 mL) at 70 ºC for 24 h. The crude product was purified by FCC (silica, dry load, CH_2Cl_2:EtOAc 98:2 to 50:50, product eluted in CH_2Cl_2:EtOAc 90:10 to 50:50). Ligand **2.35** was obtained as a pale orange solid (265 mg, 0.613 mmol, 96% yield). It tended to precipitate from EtOAc as an off-white solid. **M.p.** 173–174 °C (EtOAc). **IR** (film from $CHCl_3$, cm^{-1}) υ 3321, 2958, 2938, 2893, 2861, 1648, 1599, 1552, 1500, 1462, 1445, 1310, 909, 733. **^{1}H NMR** (500 MHz, $CDCl_3$, 298 K) □ 7.89 (m, 1H), 7.39–7.31 (m, 6H), 7.28–7.24 (m, 4H), 7.08–7.04 (m, 2H), 6.93 (br s, 1H, NH), 6.68 (br s, 1H, NH), 1.09 (d, J^3_{HP} = 11.7 Hz, 18H). **^{1}H NMR** (500 MHz, $CDCl_3$, 323 K) δ 7.89 (dt, J = 7.4, 1.4 Hz, 1H), 7.39–7.27 (m, 10H), 7.08–7.04 (m, 2H), 6.84 (br s, 1H [underintegrates], NH), 6.59 (br s, 1H [underintegrates], NH), 1.11 (d, J^3_{HP} = 11.6 Hz, 18H). **^{13}C NMR** (126 MHz, $CDCl_3$, 298 K, rotamers observed in 7:3 ratio) δ 154.01 (major rotamer, CO), 153.94 (minor rotamer, CO), 150.3 (d, J_{CP} = 31.5 Hz), 145.2 (d, J_{CP} = 7.1 Hz), 138.31 (major rotamer), 138.24 (minor rotamer), 136.24 (major rotamer), 136.20 (minor rotamer), 135.56, 135.54, 130.7 (d, J_{CP} = 6.1 Hz), 129.1, 128.7 (d, J_{CP} = 5.2 Hz),

127.7, 126.2, 124.04 (major rotamer), 123.98 (minor rotamer), 121.3 (major rotamer), 121.1 (major rotamer), 33.0 (d, J^{1}_{CP} = 24.2 Hz), 30.8 (d, J^{2}_{CP} = 15.2 Hz). **^{13}C NMR** (126 MHz, $CDCl_3$, 323 K, rotamers observed in 6:4 ratio): δ 153.9 (major rotamer, CO), 153.8 (minor rotamer, CO), 150.5 (d, J_{CP} = 32.2 Hz), 145.4 (d, J_{CP} = 7.1 Hz), 138.5 (major rotamer), 138.4 (minor rotamer), 136.44 (major rotamer), 136.39 (minor rotamer), 135.8, 135.61, 135.59, 130.7 (d, J_{CP} = 6.1 Hz), 129.2, 128.7 (d, J_{CP} = 11.9 Hz), 127.81 (d, J_{CP} = 3.1 Hz, major rotamer), 127.75 (d, J_{CP} = 3.1 Hz, minor rotamer), 126.3, 126.1, 126.0, 124.10 (major rotamer), 124.05 (minor rotamer), 121.4, 121.3, 121.2, 33.1 (d, J^{1}_{CP} = 24.9 Hz), 30.9 (d, J^{2}_{CP} = 15.3 Hz). **^{31}P NMR** (202 MHz, $CDCl_3$) δ 20.9. **HRMS** (ESI +) calculated for $[C_{27}H_{34}N_2OP]^+$ $[M+H]^+$ 433.2403 *m/z*; found 433.2396 *m/z*.

1-(2'-(Di-*tert*-butylphosphaneyl)-[1,1'-biphenyl]-3-yl)-3-phenylthiourea (2.36)

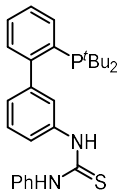

Prepared following general procedure **GP2**, using aminophosphine **2.27c** (200 mg, 0.638 mmol, 1 equiv) and phenyl isothiocyanate (84 µL, 0.71 mmol, 1.1 equiv) in THF (3.2 mL) at 23 ºC for 73 h. The crude product was purified by FCC (silica, dry load, CH_2Cl_2:EtOAc 100:0 to 80:20, product eluted in CH_2Cl_2:EtOAc 95:5). Ligand **2.36** was obtained as a pale yellow solid (221 mg, 0.493 mmol, 77% yield). **M.p.** 157 °C. **IR** (film from $CHCl_3$, cm^{-1}) υ 3169, 2959, 2938, 2893, 2861, 1598, 1536, 1471, 1362, 909, 733. **^{1}H NMR** (400 MHz, $CDCl_3$) δ 8.07 (br s, 1H, NH), 8.02 (br s, 1H, NH), 7.88 (dt, *J* = 7.6, 1.6 Hz, 1H), 7.46–7.38 (m, 5H), 7.37–7.33 (m, 3H), 7.30–7.26 (m, 1H), 7.25–7.17 (m, 3H), 1.00 (d, J^{3}_{HP} = 11.8 Hz, 18H). **^{13}C NMR** (126 MHz, $CDCl_3$, 298 K, rotamers observed in 7:3 ratio) δ 180.5 (CS), 149.5 (d, J_{CP} = 30.4 Hz), 145.4 (d, J_{CP} = 7.2 Hz), 138.3, 135.6 (d, J_{CP} = 3.5 Hz), 135.2 (d, J_{CP} = 26.8 Hz), 134.6, 130.6 (d, J_{CP} = 6.0 Hz), 129.9, 129.5, 129.0, 126.8, 126.6, 126.1, 123.6, 33.0 (d, J^{1}_{CP} = 23.2 Hz), 30.6 (d, J^{2}_{CP} = 14.8 Hz). **^{31}P NMR** (162 MHz, $CDCl_3$) δ 20.7. **HRMS** (ESI +) calculated for $[C_{27}H_{34}N_2PS]^+$ $[M+H]^+$ 449.2157 *m/z*; found 449.2162 *m/z*.

1-(2'-(Diadamantan-1-yl)phosphaneyl)-4'-(trifluoromethyl)-[1,1'-biphenyl]-4-yl)-3-phenylurea (2.37)

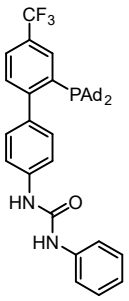

Prepared following general procedure **GP2**, using aminophosphine **2.27d** (800 mg, 1.49 mmol, 1 equiv) and phenyl isocyanate (180 µL, 1.66 mmol, 1.1 equiv) in THF (15 mL) at 80 ºC for 21 h. The crude product was purified by FCC (silica, dry load, CyH:EtOAc 85:15). Ligand **2.37** was obtained as an off-white solid (929 mg, 1.40 mmol, 94% yield). **M.p.** 213 °C. **IR** (film from $CHCl_3$, cm^{-1}) υ 3329 (broad), 2901, 2848, 2410, 1644, 1599, 1499, 1445, 1322, 1126, 754. **^{1}H NMR** (400 MHz, $CDCl_3$) δ 8.13 (s, 1H), 7.61 (d, *J* = 10.9 Hz, 2H), 7.55 (d, *J* = 8.0 Hz, 1H), 7.33 (d, *J* = 8.5 Hz, 2H), 7.32–7.25 (m, 2H), 7.23 (dd, *J* = 11.0, 4.8 Hz, 3H), 7.12 (d, *J* = 8.3 Hz, 2H), 7.07–6.98 (m, 1H), 1.92–1.72 (m, 18H), 1.72–1.56 (m, 12H). **^{13}C NMR** (101 MHz, $CDCl_3$) δ 154.6 (d, J^{1}_{CP} = 31.4 Hz), 154.2, 138.3, 137.1, 134.8, 134.5, 133.2 (app quint, J_{CP} = J_{CF} =3.4 Hz), 131.2 (d, J_{CP} = 3.3 Hz), 131.1, 129.3, 127.5 (q, J^{2}_{CF} = 31.9 Hz), 124.9 (d, J_{CP} = 3.3 Hz), 124.5 (q, J^{1}_{CF} = 272.9 Hz), 124.0, 121.0, 119.6, 42.0 (d, J_{CP} = 12.8 Hz), 37.7 (d, J^{1}_{CP} = 25.7 Hz), 36.9, 28.9 (d, J_{CP} = 8.6 Hz). **^{31}P NMR** (162 MHz, $CDCl_3$) δ 23.7. **^{9}F NMR** (471 MHz, $CDCl_3$) δ −62.5. **HRMS** (ESI +) calculated for $[C_{40}H_{45}F_3N_2OP]^+$ $[M+H]^+$ 657.3216 *m/z*; found 657.3209 *m/z*.

1-(2'-(Diadamantan-1-yl)phosphaneyl)-4'-(trifluoromethyl)-[1,1'-biphenyl]-4-yl)-3-(4-methoxyphenyl)urea (2.38)

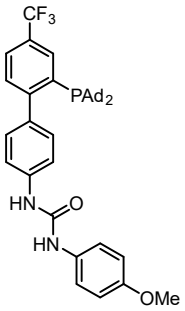

Prepared following general procedure **GP2**, using aminophosphine **2.27d** (200 mg, 0.372 mmol, 1 equiv) and phenyl isocyanate (53 µL, 0.409 mmol, 1.1 equiv) in THF (3.7 mL) at 80 ºC for 19 h. The crude product was purified by FCC (silica, dry load, CyH:EtOAc 80:20). Ligand **2.38** was obtained as an off-white solid (205.5 mg, 0.299 mmol, 80% yield). **M.p.** 208–210 °C. **IR** (film from $CHCl_3$, cm^{-1}) υ 3318 (broad), 2901, 2847, 2412, 1511, 1450, 1323, 1244, 1126. **^{1}H NMR** (400 MHz, $CDCl_3$) δ 8.15 (s, 1H), 7.58 (d, J = 7.9 Hz, 1H), 7.41–7.32 (m, 3H), 7.31–7.26 (m, 1H), 7.26–7.19 (m, 3H), 7.15 (d, J = 8.3 Hz, 2H), 6.86–6.79 (m, 2H), 3.76 (s, 3H), 1.93–1.78 (m, 18H), 1.76–1.53 (m, 12H). **^{13}C NMR** (101 MHz, $CDCl_3$) δ 157.0, 154.7 (d, J_{CP} = 29.8 Hz), 154.5, 137.9 (d, J_{CP} = 6.7 Hz), 137.3, 134.8, 134.5, 133.2 (app quint, J_{CP} = J_{CF} = 3.4 Hz), 131.1 (d, J_{CP} = 3.7 Hz), 130.7, 127.5 (q, J^2_{CF} = 31.9 Hz), 124.9 (d, J_{CP} = 3.3 Hz), 124.5 (q, J^1_{CF} = 272.9 Hz), 124.1, 119.2, 114.6, 55.6, 42.0 (d, J_{CP} = 12.8 Hz), 37.7 (d, J_{CP} = 25.7 Hz), 36.9, 28.9 (d, J_{CP} = 8.6 Hz). **^{31}P NMR** (162 MHz, $CDCl_3$) δ 23.7. **^{9}F NMR** (471 MHz, $CDCl_3$) δ −62.5. **HRMS** (ESI +) calculated for $[C_{41}H_{47}F_3N_2O_2P]^+$ $[M+H]^+$ 687.3322 *m/z*; found 687.3314 *m/z*.

1-Cyclohexyl-3-(2'-(diadamantan-1-yl)phosphaneyl)-4'-(trifluoromethyl)-[1,1'-biphenyl]-4-yl)urea (2.39)

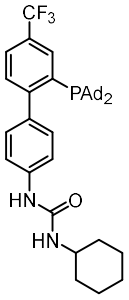

Prepared following general procedure **GP2**, using aminophosphine **2.27d** (80 mg, 0.372 mmol, 1 equiv), cyclohexyl isocyanate (38 µL, 0.409 mmol, 1.1 equiv) and silica gel (pore size 60 Å, 40–63 µm particle size, 100 mg) in THF (1.4 mL) at 80 ºC for 24 h and then at 90 °C for 4 h. The crude product was purified by FCC (silica, dry load, CH_2Cl_2:EtOAc 96:4 to 90:10). Ligand **2.39** was obtained as an off-white solid (67.0 mg, 0.101 mmol, 68% yield). **M.p.** 219–227 °C. **IR** (film from $CHCl_3$, cm^{-1}) υ 3332 (broad), 2926, 2901, 2848, 2472, 2406, 1632, 1541, 1519, 1450, 1322, 1126. **^{1}H NMR** (500 MHz, $CDCl_3$, 32.0 mg in 0.5 mL) δ 8.13 (s, 1H), 7.58 (d, J = 8.0 Hz, 1H), 7.36–7.31 (m, 3H), 7.15 (d, J = 8.2 Hz, 2H), 6.97 (s, 1H), 5.15 (d, J = 8.0 Hz, 1H), 3.73–3.63 (m, 1H), 2.00–1.93 (m, 2H), 1.91–1.75 (m, 19H), 1.75–1.53 (m, 16H), 1.45–1.29 (m, 2H), 1.21–1.05 (m, 3H).**^{13}C NMR** (126 MHz, $CDCl_3$, 32.0 mg in 0.5 mL) δ 155.5, 154.7 (d, J_{CP} = 31.3 Hz), 138.0, 137.6 (d, J_{CP} = 6.7 Hz), 134.8 (d, J_{CP} = 31.4 Hz), 133.3 (app quint, J_{CP} = J_{CF} =3.4 Hz), 131.3 (d, J_{CP} = 4.0 Hz), 131.1 (d, J_{CP} = 5.5 Hz), 127.4 (q, $J2_{CF}$ = 32.0 Hz), 124.9 (d, J_{CP} = 3.3 Hz), 124.5 (q, $J1_{CF}$ = 272.5 Hz), 119.4, 49.1, 42.0 (d, J_{CP} = 12.9 Hz), 37.7 (d, $J1_{CP}$ = 26.1 Hz), 37.0, 33.8, 28.9 (d, J_{CP} = 8.6 Hz), 25.7, 25.0. **^{31}P NMR** (202 MHz, $CDCl_3$, 32.0 mg in 0.5 mL) δ 20.6. **^{9}F NMR** (471 MHz, $CDCl_3$) δ −62.5. **HRMS** (ESI +) calculated for $[C_{40}H_{51}F_3N_2OP]^+$ $[M+H]^+$ 663.3686 *m/z*; found 663.3678 *m/z*.

1-(2'-(Di-*tert*-butylphosphaneyl)-4'-(trifluoromethyl)-[1,1'-biphenyl]-4-yl)-3-phenylurea (2.40)

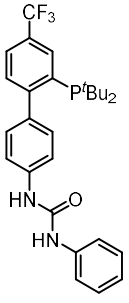

Prepared following general procedure **GP2**, using aminophosphine **2.27e** (750 mg, 1.97 mmol, 1 equiv) and phenyl isocyanate (220 µL, 2.02 mmol, 1.05 equiv) in THF (12 mL) at 80 ºC for 16 h. The crude product was purified by FCC (silica, dry load, CyH:EtOAc 100:0 slowly to 80:20, product eluted in CyH:EtOAc 85:15). Ligand **2.40** was obtained as an off-white solid (973 mg, 1.94 mmol, 99% yield). **M.p.** 226–229 °C. **IR** (film from $CHCl_3$, cm^{-1}) υ 3327 (broad), 2938, 2862, 1649, 1602, 1553, 1322, 1125. **^{1}H NMR** (400 MHz, $(CD_3)_2SO$, 30 mg in 0.5 mL) δ 8.73 (d, J = 7.2 Hz,

2H), 8.09 (s, 1H), 7.79 (d, J = 8.1 Hz, 1H), 7.52–7.44 (m, 5H), 7.29 (t, J = 7.7 Hz, 2H), 7.18 (d, J = 8.0 Hz, 2H), 6.98 (t, J = 7.1 Hz, 1H), 1.09 (d, J = 11.7 Hz, 18H). **^{13}C NMR** (126 MHz, $(CD_3)_2SO$, 30 mg in 0.5 mL) δ 154.4 (d, J = 31.2 Hz), 152.5, 139.7, 138.7, 136.7 (d, J_{CP} = 32.7 Hz), 135.1 (d, J_{CP} = 6.6 Hz), 131.4 (d, J_{CP} = 5.2 Hz), 131.2 (app quint, J_{CP} = J_{CF} =3.4 Hz), 130.6 (d, J_{CP} = 4.3 Hz), 128.8, 126.3 (q, J_{CF} = 31.5 Hz), 125.4, 124.2 (q, J_{CF} = 272.5 Hz), 121.8, 118.2, 117.1, 32.4 (d, J^1_{CP} = 26.3 Hz), 30.2 (d, J^2_{CP} = 15.5 Hz). **^{31}P NMR** (202 MHz, $(CD_3)_2SO$, 30 mg in 0.5 mL) δ 17.3. **^{9}F NMR** (471 MHz, $(CD_3)_2SO$, 30 mg in 0.5 mL) δ –60.9. **HRMS** (ESI +) calculated for $[C_{28}H_{33}F_3N_2OP]^+$ $[M+H]^+$ 501.2277 *m/z*; found 501.2278 *m/z*.

Complex Au1

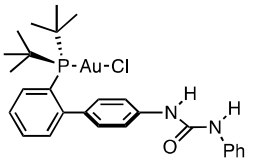

Prepared following general procedure **GP3**, using ligand **2.28** (100 mg, 0.222 mmol, 1.0 equiv) in CH_2Cl_2 (3.7 mL) at 23 °C for 1 h. After filtration, the crude product was purified by FCC (silica, dry load, CyH:EtOAc 70:30), obtaining **Au1** (131 mg, 0.197 mmol, 90% yield) as an off-white solid. **M.p.** 194–197 °C. **IR** (film from $CDCl_3$, cm^{-1}) υ 3344, 2938, 2234, 1596, 1536, 1499, 1442, 1311, 1231. **^{1}H NMR** (400 MHz, $CDCl_3$) δ 8.08 (br s, 1H), 7.86 (td, J = 7.5, 1.9 Hz, 1H), 7.59–7.54 (m, 2H), 7.53–7.46 (m, 2H), 7.41–7.35 (m, 2H), 7.32–7.27 (m, 3H), 7.13–7.07 (m, 2H), 7.06–6.99 (m, 1H), 6.94 (br s, 1H),1.42 (d, J = 15.7 Hz, 18H). **^{13}C NMR** (101 MHz, $CDCl_3$) δ 154.1, 149.7 (d, J_{CP} = 13.4 Hz), 139.1 (d, J_{CP} = 14.8 Hz), 138.2 (d, J_{CP} = 6.6 Hz), 133.6 (d, J_{CP} = 7.3 Hz), 133.5 (d, J_{CP} = 2.9 Hz), 130.9 (d, J_{CP} = 2.4 Hz), 130.3, 127.0 (d, J_{CP} = 6.9 Hz), 126.3, 125.8, 123.1, 122.7, 120.5, 37.9 (d, J^1_{CP} = 25.8 Hz), 31.0 (d, J^2_{CP} = 6.6 Hz). **^{31}P NMR** (162 MHz, $CDCl_3$) δ 63.3. **HRMS** (ESI +) calculated for $[C_{27}H_{33}AuN_2OP]^+$ $[M - Cl]^+$ 629.1991 *m/z*; found 629.1991 *m/z*. **Elemental analysis** calculated for $C_{27}H_{33}AuClN_2OP$: C 48.77, H 5.00, N 4.21, found: C 48.65 ± 0.35, H 4.95 ± 0.30, N 4.11 ± 0.30. **XRD**: crystals for single-crystal X-ray diffraction analysis were grown from a solution in CH_2Cl_2/*n*-hexane/cyclohexane at ca –25 ºC.

Complex Au2

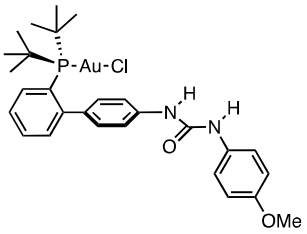

Prepared following general procedure **GP3**, using ligand **2.29** (100 mg, 0.216 mmol, 1.0 equiv) in CH_2Cl_2 (4 mL) at 23 °C for 1 h. After filtration, the crude product was purified by FCC (silica, dry load, CyH:EtOAc 65:35 to 50:50), obtaining **Au2** (143 mg, 0.205 mmol, 95% yield) as a pink solid. **M.p.** 140 °C (decomposition). **IR** (film from CD_2Cl_2, cm^{-1}) υ 3342, 2955, 2239, 1597, 1538, 1509, 1465, 1230. **^{1}H NMR** (400 MHz, $CDCl_3$, 20.0 mg in 0.6 mL) δ 7.89–7.79 (m, 2H), 7.54–7.46 (m, 2H), 7.43 (d, J = 8.8 Hz, 2H), 7.38 (d, J = 8.3 Hz, 2H), 7.28 7.31–7.26 (m, 1H), 7.08 (d, J = 8.2 Hz, 2H), 7.03 (br s, 1H), 6.84 (d, J = 8.9 Hz, 2H), 3.77 (s, 3H), 1.41 (d, J = 15.6 Hz, 18H). **^{13}C NMR** (101 MHz, $CDCl_3$, 20 mg in 0.6 mL) δ 156.1, 154.5, 149.7 (d, J_{CP} = 13.4 Hz), 139.0, 138.2 (d, J_{CP} = 6.7 Hz), 133.6 (d, J_{CP} = 7.3 Hz), 133.5 (d, J_{CP} = 2.8 Hz), 131.9, 130.9 (d, J_{CP} = 2.2 Hz), 130.3, 127.0 (d, J_{CP} = 6.9 Hz), 126.2, 125.8, 122.9 (d, J_{CP} = 23.6 Hz), 114.3, 55.6, 37.9 (d, J^1_{CP} = 25.8 Hz), 31.0 (d, J_{CP} = 6.6 Hz). **^{31}P NMR** (162 MHz, $CDCl_3$, 20.0 mg in 0.6 mL) δ 63.2. **HRMS** (ESI +) calculated for $[C_{28}H_{35}AuClN_2O_2P]^+$ $[M + Na]^+$ 717.1683 *m/z*; found 717.1664 *m/z*.

Complex Au3

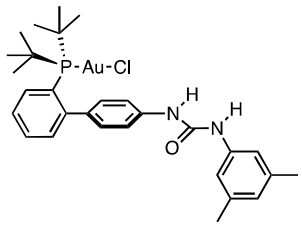

Prepared following general procedure **GP3**, using ligand **2.30** (50 mg, 0.109 mmol, 1.0 equiv) in CH_2Cl_2 (3 mL) at 23 °C for 1 h. After filtration, the crude product was purified by FCC (silica, dry load, CyH:EtOAc 80:20 to 70:30), obtaining **Au3** (56 mg, 0.081 mmol, 75% yield) as a pale yellow solid. **M.p.** 209 °C (decomposition). **IR** (film from $CDCl_3$, cm^{-1}) ʋ 3338, 2955, 2920, 2862, 2229, 1595, 1556, 1531, 1465, 1310, 1202. **^{1}H NMR** (400 MHz, $CDCl_3$, 20.0 mg in 0.6 mL) δ 7.90–7.76 (m, 2H), 7.49 (dq, J = 16.5, 7.3 Hz, 2H), 7.39 (d, J = 8.2 Hz, 2H), 7.33–7.27 (m, 2H), 7.16 (br s, 3H), 7.07 (d, J = 8.2 Hz, 2H), 6.68 (s, 1H), 2.27 (s, 6H), 1.41 (d, J = 15.7 Hz, 18H). **^{13}C NMR** (101 MHz, $CDCl_3$, 20 mg in 0.5 mL) δ 154.1, 149.7 (d, J_{CP} = 13.4 Hz), 138.9 (d, J^1_{CP} = 46.8 Hz), 138.6, 138.0 (d, J_{CP} = 6.7 Hz), 133.6 (d, J_{CP} = 7.3 Hz), 133.5 (d, J_{CP} = 2.7 Hz), 130.8 (d, J_{CP} = 2.1 Hz), 130.2, 127.0 (d, J_{CP} = 6.9 Hz), 126.2, 125.9, 125.2, 122.6, 118.6, 37.9 (d, J^1_{CP} = 25.7 Hz), 31.0 (d, J^2_{CP} = 6.7 Hz), 21.5. **^{31}P NMR** (162 MHz, $CDCl_3$, 20.0 mg in 0.6 mL) δ 63.2. **HRMS** (ESI +) calculated for $[C_{29}H_{37}AuClN_2NaOP]^+$ $[M + Na]^+$ 715.1890 *m/z*; found 715.1879 *m/z*. **Elemental analysis** calculated for $C_{29}H_{37}AuClN_2OP$: C 50.26, H 5.38, N 4.04, found: C 50.11 ± 0.35, H 5.40 ± 0.30, N 3.84 ± 0.30.

Complex Au4

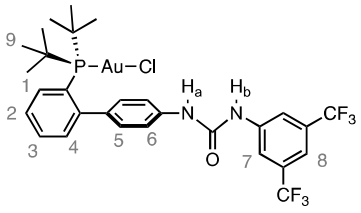

Under air, to a stirred suspension of ligand **2.31** (150.0 mg, 0.264 mmol, 1 equiv) in CH_2Cl_2 (3.5 mL), [(Me_2S)AuCl] (78.5 mg, 0.267 mmol, 1.01 equiv) was added, followed by additional CH_2Cl_2 (0.9 mL, final concentration 0.06 M). The resulting pale-yellow solution was stirred in the dark at 23 ºC for 30 minutes, then filtered through a 0.2 mm PTFE syringe filter. The filtrate was evaporated under reduced pressure. The crude product was purified by FCC (silica, dry load, pentane:EtOAc 90:10 to 65:35, product eluting in pentane:EtOAc 70:30), obtaining **Au4** (180.1 mg, 0.225 mmol, 85% yield) as a white solid. **M.p.** 268–271 °C (decomposition). **IR** (film from CD_2Cl_2, cm^{-1}) ʋ 3351, 2959, 1716, 1565, 1530, 1473, 1388, 1278, 1177, 1132. **^{1}H NMR** (400 MHz, CD_2Cl_2, 4.0 mg in 0.5 mL, 10 mM) δ 8.58 (br s, 1H, N$\underline{H}_b$), 8.12 (s, 2H, C$\underline{H}$-7), 7.93–7.89 (m, 1H, C$\underline{H}$-1/2/3/4), 7.58–7.52 (m, 2H, C$\underline{H}$-1/2/3/4), 7.51 (br s, 1H, C$\underline{H}$-8), 7.35 (d, J = 8.4 Hz, 2H, C$\underline{H}$-6), 7.30–7.27 (m, 1H, C$\underline{H}$-1/2/3/4), 7.15 (d, J = 8.4 Hz, 2H, C$\underline{H}$-5), 7.04 (br s, 1H, N$\underline{H}_a$), 1.43 (d, J^3_{HP} = 15.7 Hz, C$\underline{H}_3$-9). **^{13}C NMR** (126 MHz, CD_2Cl_2, 20 mg in 0.5 mL) δ 153.1 ($\underline{C}$O), 149.7 (d, J^2_{CP} = 13.1 Hz, PC$\underline{C}$C-4), 141.7 (N$\underline{C}$C-7), 138.84 (N$\underline{C}$C-6), 138.78 (PCC$\underline{C}$C-5), 134.0 (d, J_{CP} = 3.0 Hz, $\underline{C}$-1/2/3/4), 133.8 (d, J_{CP} = 7.3 Hz, $\underline{C}$-1/2/3/4), 131.9 (q, J^2_{CF} = 33.0 Hz, $\underline{C}$-CF_3), 131.2 (d, J_{CP} = 2.2 Hz, $\underline{C}$-1/2/3/4), 130.7 ($\underline{C}$-5), 127.5 (d, J_{CP} = 7.0 Hz, $\underline{C}$-1/2/3/4), 126.0 (d, J^1_{CP} = 46.8 Hz, P$\underline{C}$C-1), 123.9 (q, J^1_{CF} = 272.5 Hz, $\underline{C}F_3$), 121.8 ($\underline{C}$-6), 119.3 (br s, $\underline{C}$-7), 115.8 (app quint, J^3_{CF} = 4.0 Hz, $\underline{C}$-8), 38.2 (d, J^1_{CP} = 26.0 Hz, P$\underline{C}$C-9), 31.1 (d, J^2_{CP} = 6.6 Hz, $\underline{C}$-9). **^{31}P NMR** (162 MHz, CD_2Cl_2, 4.9 mg in 0.5 mL) δ 63.6. **^{19}F NMR** (376 MHz, CD_2Cl_2, 4.9 mg in 0.5 mL) δ −63.4. **HRMS** (ESI +) calculated for $[C_{29}H_{32}AuClF_6N_2OP]^+$ $[M + H]^+$ 801.1505 *m/z*; found 801.1495 *m/z*. **Elemental analysis** calculated for $C_{29}H_{31}AuClF_6N_2OP$: C 43.49, H 3.90, N 3.50, found: C 43.56 ± 0.35, H 3.91 ± 0.30, N 3.49 ± 0.30. **XRD**: crystals for single-crystal X-ray diffraction analysis were grown from a solution in CH_2Cl_2/*n*-hexane at ca –25 ºC.

Complex Au5

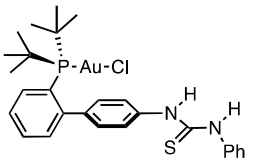

Prepared following general procedure **GP3**, using ligand **2.32** (92.6 mg, 0.206 mmol, 1.0 equiv) in CH_2Cl_2 (3.7 mL) at 23 °C for 1 h. The reaction mixture was filtered obtaining **Au5** (128.8 mg, 0.186 mmol, 90% yield) as a pale yellow solid. **M.p.** 173 °C (decomposition). **IR** (film from $CDCl_3$, cm^{-1}) υ 3184, 3176, 3057, 2955, 2923, 2901, 2864, 2238, 2214, 1548, 1515, 1497, 1466, 729. **^{1}H NMR** (500 MHz, $CDCl_3$, 298 K) δ 11.26 (br s, 1H), 9.62 (br s, 1H), 7.83 (td, J = 7.6, 1.6 Hz, 1H), 7.62–7.44 (m, 6H), 7.36 (t, J = 7.9 Hz, 2H), 7.31–7.28 (m, 1H), 7.22 (t, J = 7.4 Hz, 1H), 7.14 (d, J = 8.1 Hz, 2H), 1.37 (d, J = 15.6 Hz, 18H). **^{13}C NMR** (126 MHz, $CDCl_3$, 323 K) δ 176.8, 149.5 (d, J_{CP} = 13.3 Hz), 141.1, 138.3, 137.4, 133.9–133.4 (m) overlapping with 133.6 (d, J_{CP} = 13.3 Hz), 131.1 (d, J_{CP} = 2.3 Hz), 130.9, 129.0, 127.2 (d, J_{CP} = 6.8 Hz), 126.8, 126.3 (d, J_{CP} = 2.3 Hz), 126.0, 125.5, 38.1 (d, J^1_{CP} = 25.6 Hz), 31.0 (d, J^2_{CP} = 6.7 Hz). **^{31}P NMR** (162 MHz, $CDCl_3$) δ 63.8. **HRMS** (ESI +) calculated for $[C_{27}H_{33}AuN_2PS]^+$ [M – Cl]$^+$ 645.1762 *m/z*; found 645.1770 *m/z*.

Complex Au6

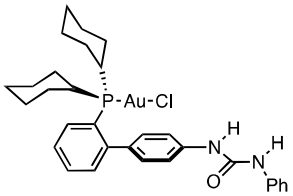

Prepared following general procedure **GP3**, using ligand **2.33** (120 mg, 0.248 mmol, 1.0 equiv) in CH_2Cl_2 (5 mL) at 23 °C for 3 h. After filtration, the crude product was purified by FCC (silica, dry load, CH_2Cl_2:EtOAc 98:2 to 95:5), obtaining **Au6** (161 mg, 0.225 mmol, 91% yield) as a white solid. **M.p.** 267–270 °C (decomposition). **IR** (film from $CDCl_3$, cm^{-1}) υ 3342, 2927, 2852, 2236, 1596, 1535, 1498. **^{1}H NMR** (400 MHz, $CDCl_3$) δ 7.89 (s, 1H), 7.63–7.57 (m, 1H), 7.54 (dd, J = 8.2, 1.2 Hz, 2H), 7.52–7.46 (m, 2H), 7.42–7.38 (m, 2H), 7.35–7.28 (m, 3H), 7.14–7.09 (m, 2H), 7.07–6.98 (m, 2H), 2.23–2.09 (m, 2H), 2.06–1.96 (m, 2H), 1.89–1.72 (m, 4H), 1.71–1.57 (m, 4H), 1.48–1.07 (m, 10H). **^{13}C NMR** (101 MHz, $CDCl_3$) 153.9, 149.2 (d, J_{CP} = 12.3 Hz), 139.0 (d, J_{CP} = 2.9 Hz), 137.4 (d, J_{CP} = 6.3 Hz), 132.9 (d, J_{CP} = 7.4 Hz), 132.8 (br s), 130.9 (d, J_{CP} = 2.4 Hz), 130.4. 129.0, 127.7 (d, J_{CP} = 7.9 Hz), 125.1, 124.6, 123.3, 122.2, 120.6, 36.7 (d, J^1_{CP} = 34.0 Hz), 31.0 (d, J^3_{CP} = 4.0 Hz), 29.3, 26.7 (d, J^2_{CP} = 12.0 Hz), 26.5 (d, J^2_{CP} = 14.6 Hz), 25.7. **^{31}P NMR** (162 MHz, $CDCl_3$) δ 42.7. **HRMS** (ESI +) calculated for $[C_{31}H_{38}AuClN_2OP]^+$ [M + H]$^+$ 717.2070 *m/z*; found 717.2052 *m/z*. **XRD**: crystals for single-crystal X-ray diffraction analysis were grown from a solution in $CHCl_3$/*n*-hexane/cyclohexane at ca 20 ºC.

Complex Au7

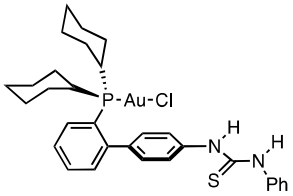

Prepared following general procedure **GP3**, using ligand **2.34** (100 mg, 0.200 mmol, 1.0 equiv) in CH_2Cl_2 (2 mL) at 23 °C for 2 h. The crude compound was filtrated obtaining **Au7** (143 mg, 0.195 mmol, 95% yield) as a pale yellow solid. **M.p.** 171–173 °C. **IR** (film from CD_2Cl_2, cm^{-1}) υ 3177 (broad), 3053, 2926, 2851, 1724, 1594, 1548, 1497, 1315. **^{1}H NMR** (500 MHz, $CDCl_3$, 323 K) δ 7.61 (d, J = 7.8 Hz, 2H), 7.57–7.47 (m, 5H), 7.40–7.31 (m, 3H), 7.23–7.18 (m, 2H), 7.17–7.13 (m, 2H), 2.22–2.08 (m, 2H), 1.97 (br s, 2H), 1.90–1.74 (m, 4H), 1.73–1.55 (m, 4H), 1.41–1.11 (m, 11H). **^{13}C NMR** (126 MHz, $CDCl_3$, 323 K) δ 178.6, 149.3 (d, J_{CP} = 12.8 Hz), 138.8, 138.1, 132.8 (d, J_{CP} = 7.4 Hz), 132.2 (d, J_{CP} = 3.6 Hz), 131.0 (d, J_{CP} = 2.3 Hz), 130.9, 128.9, 128.0 (d, J_{CP} = 7.5 Hz), 126.3, 125.6, 125.3, 125.1 (br s), 124.9, 37.0 (d, J^1_{CP} = 33.4 Hz), 31.1 (d, J^3_{CP} = 4.0 Hz), 29.4, 26.8 (d, J^2_{CP} = 12.5 Hz), 26.6 (d, J^2_{CP} = 14.4 Hz), 25.8. **^{31}P NMR** (203 MHz, $CDCl_3$, 323 K) δ 41.8. **HRMS** (ESI +) calculated for $[C_{31}H_{37}AuN_2PS]^+$ [M – Cl]$^+$ 697.2075 *m/z*; found 697.2079 *m/z*. **XRD**:

crystals for single-crystal X-ray diffraction analysis were grown from a solution in $ClCH_2CH_2Cl$/*n*-hexane/pentane at room temperature.

Complex Au8

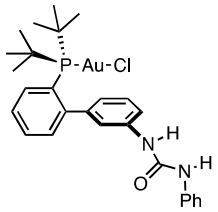

Prepared following general procedure **GP3**, using ligand **2.35** (150 mg, 0.347 mmol, 1 equiv) in CH_2Cl_2 (3.5 mL) at 23 ºC for 1 h. After evaporation of volatiles, the crude product was purified by FCC (silica, liquid load in CH_2Cl_2, CH_2Cl_2:EtOAc 100:0 to 90:10), obtaining **Au8** (183 mg, 0.275 mmol, 79% yield) as a pale pink solid. **M.p.** 145–170 °C (decomposition). **IR** (film from $CHCl_3$, cm^{-1}) υ 3347 (strong), 2957, 2235, 1705, 1657, 1597, 1590, 1542 (strong), 1499, 1469, 1442, 1309, 1215, 732. **^{1}H NMR** (400 MHz, $CDCl_3$) δ 7.86–7.82 (m, 1H), 7.81 (br s, 1H, N<u>H</u>), 7.53–7.45 (m, 4H), 7.40–7.30 (m, 4H), 7.24–7.20 (m, 2H), 7.15 (br s, 1H, N<u>H</u>), 6.98 (tt, J = 7.3, 1.0 Hz, 1H), 6.85 (dt, J = 7.0, 1.6 Hz, 1H), 1.40 (d, J^3_{HP} = 15.6 Hz, 9H), 1.38 (d, J^3_{HP} = 15.7 Hz, 9H). **^{13}C NMR** (101 MHz, $CDCl_3$) δ 153.9 (<u>C</u>O), 149.6 (d, J_{CP} = 13.3 Hz), 143.6 (d, J_{CP} = 6.6 Hz), 139.1, 138.5, 133.5 (d, J_{CP} = 2.8 Hz), 133.4 (d, J_{CP} = 7.4 Hz), 138.9 (d, J_{CP} = 2.3 Hz), 129.7, 128.8, 127.1 (d, J_{CP} = 7.0 Hz), 126.0 (d, J_{CP} = 46.0 Hz), 125.3, 123.5, 123.0, 122.1, 120.3, 38.1 (d, J^1_{CP} = 25.8 Hz), 37.9 (d, J^1_{CP} = 25.6 Hz), 31.0 (d, J^2_{CP} = 14.8 Hz), 30.9 (d, J^2_{CP} = 14.6 Hz). **^{31}P NMR** (162 MHz, $CDCl_3$) δ 63.6. **HRMS** (ESI +) calculated for $[C_{27}H_{33}AuN_2OP]^+$ [M – Cl]$^+$ 629.1991 *m/z*, found 629.1981 *m/z*; calculated for $[C_{27}H_{33}AuClN_2NaOP]^+$ [M + Na]$^+$ 687.1577 *m/z*; found 687.1567 *m/z*. **XRD**: crystals for single-crystal X-ray diffraction analysis were grown from a solution in EtOAc/*n*-hexane/$CDCl_3$ at ca 5 ºC.

Complex Au9

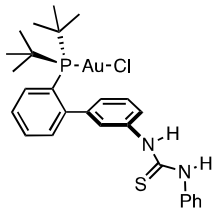

Prepared following general procedure **GP3**, using ligand **2.36** (150 mg, 0.334 mmol, 1 equiv) in CH_2Cl_2 (3.5 mL) at 23 ºC for 1 h. After filtration and evaporation of volatiles, **Au9** was obtained (228 mg, 0.334 mmol, 100% yield) as a pale yellow solid. For the sake of simplicity, the compound is depicted as a classical phosphine Au(I) chloride complex, but single crystal X-ray diffraction shows instead a P–Au–S linear motif, with the displaced chloride anion H-bonded to the two NH groups. ^{1}H NMR in $CDCl_3$ indeed suggests that the highly deshielded NH groups are engaged in H-bonding. Broad signals in ^{1}H and ^{31}P spectra at 298 K indicate a dynamic behavior on NMR time scale. By HRMS the chloride was not detected, in analogy with other phosphinothiourea Au(I) complexes.[69] **M.p.** 145–171 °C (decomposition). **IR** (film from $CHCl_3$, cm^{-1}) υ 2955 (broad, strong), 2215, 1551 (strong), 1497, 1470, 1367, 913, 730. **^{1}H NMR** (500 MHz, $CDCl_3$) δ 12.24 (br s, 1H, N<u>H</u>), 11.98 (br s, 1H, N<u>H</u>), 7.86 (t, J = 7.7 Hz, 1H), 7.64–7.59 (m, 1H), 7.56–7.44 (m, 6H), 7.38–7.34 (m, 3H), 7.27–7.25 (m, 1H), 7.13–7.08 (m, 1H), 1.49 (d, J^3_{HP} = 15.9 Hz, 9H), 1.15 (d, J^3_{HP} = 16.0 Hz, 9H). **^{13}C NMR** (126 MHz, $CDCl_3$) δ 179.3 (weak br s, <u>C</u>S), 148.1 (d, J_{CP} = 12.4 Hz), 142.3 (weak br s), 137.6 (br s), 137.5, 134.2 (br s), 132.6 (br s), 131.6, 130.5 (br s), 130.3, 128.9, 128.2 (br s), 127.8 (d, J_{CP} = 6.8 Hz), 126.6, 126.3, 38.3 (d, J^1_{CP} = 23.6 Hz), 37.4 (d, J^1_{CP} = 22.6 Hz), 32.1 (br s), 30.0 (br s). **^{31}P NMR** (202 MHz, $CDCl_3$) δ 67.1 (br s). **HRMS** (ESI +) calculated for $[C_{27}H_{33}AuN_2PS]^+$ [M – Cl]$^+$ 645.1762 *m/z*, found 645.1759 *m/z*. **XRD**: crystals for single-crystal X-ray diffraction analysis were grown from a solution in CH_2Cl_2/$CDCl_3$ at ca 5 ºC.

69. For more information check complexes **D** and **F** from Chapter 1.

Complex Au10

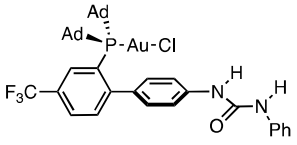

Prepared following general procedure **GP3**, using ligand **2.37** (100 mg, 0.152 mmol, 1 equiv) in CH_2Cl_2 (1.5 mL) at 23 ºC for 2 h. After evaporation of volatiles, the crude product was purified by FCC (silica, solid load, CyH:EtOAc 70:30), obtaining **Au10** (117 mg, 0.131 mmol, 86% yield) as an off-white solid. **M.p.** 290 °C (decomposition). **IR** (film from $CHCl_3$, cm^{-1}) υ 3339 (broad), 2904, 2850, 2232, 1594, 1529, 1323, 1130, 728. **^{1}H NMR** (500 MHz, $CDCl_3$, 40 mg in 0.5 mL) δ 8.11 (d, J = 6.6 Hz, 1H), 8.05 (s, 1H), 7.75 (d, J = 8.1 Hz, 1H), 7.52 (d, J = 7.7 Hz, 2H), 7.48–7.43 (m, 3H), 7.41 (dd, J = 8.0, 3.8 Hz, 1H), 7.31–7.23 (m, 2H), 7.07–7.02 (m, 2H), 7.00 (d, J = 7.4 Hz, 1H), 2.21–2.07 (m, 12H), 2.02 (s, 6H), 1.68 (s, 12H). **^{13}C NMR** (126 MHz, $CDCl_3$, 40 mg in 0.5 mL) δ 154.0, 153.9 (d, J_{CP} = 12.1 Hz), 139.6, 139.1, 136.5 (d, J_{CP} = 6.2 Hz), 134.4 (d, J_{CP} = 6.7 Hz), 131.0 (app quint, $J_{CP} = J_{CF}$ = 3.4 Hz), 129.8, 128.9, 127.1, 125.4, 125.0, 123.8 (q, J^1_{CF} = 272.2 Hz), 123.1, 122.5, 120.4, 43.0 (d, J^1_{CP} = 22.5 Hz), 42.3 (d, J_{CP} = 2.0 Hz), 36.3, 28.6 (d, J^2_{CP} = 9.9 Hz). **^{31}P NMR** (162 MHz, $CDCl_3$, 20 mg in 0.5 mL) δ 65.1. **^{19}F NMR** (376 MHz, $CDCl_3$, 20 mg in 0.5 mL) δ –62.4. **HRMS** (ESI +) calculated for $[C_{40}H_{44}AuClF_3N_2NaOP]^+$ $[M + Na]^+$ 911.2390 *m/z*; found 911.2414 *m/z*. **XRD**: crystals for single-crystal X-ray diffraction analysis were grown from a solution in CH_2Cl_2 at ca 5 ºC.

Complex Au11

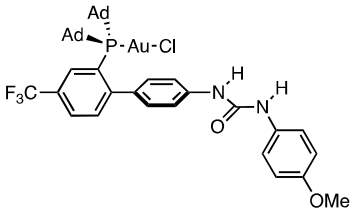

Prepared following general procedure **GP3**, using ligand **2.38** (100.0 mg, 0.146 mmol, 1 equiv) in CH_2Cl_2 (1.5 mL) at 23 ºC for 2 h. After evaporation of volatiles, the crude product was purified by FCC (silica, solid load, CyH:EtOAc 70:30), obtaining **Au11** (116.5 mg, 0.127 mmol, 82% yield) as a brown solid. **M.p.** 215 °C (decomposition). **IR** (film from $CHCl_3$, cm^{-1}) 3343 (broad), 2904, 2850, 2232, 1535, 1509, 1323, 1229, 1174, 1130, 729. **^{1}H NMR** (500 MHz, $CDCl_3$, 40 mg in 0.5 mL) δ 8.10 (d, J = 6.5 Hz, 1H), 7.81 (br s, 1H), 7.75 (d, J = 8.1 Hz, 1H), 7.50–7.37 (m, 5H), 7.29 (br s, 1H), 7.04 (d, J = 8.5 Hz, 2H), 6.83 (d, J = 9.0 Hz, 2H), 3.76 (s, 3H), 2.18–2.07 (m, 12H), 2.02 (s, 6H), 1.68 (s, 12H). **^{13}C NMR** (126 MHz, $CDCl_3$, 40 mg in 0.5 mL) δ 156.1, 154.4, 153.9 (d, J_{CP} = 12.4 Hz), 139.7, 136.4 (d, J_{CP} = 6.1 Hz), 134.4 (d, J_{CP} = 6.7 Hz), 131.9, 131.1, 129.8, 128.6 (qd, J = 32.9, 6.8 Hz), 127.1 (app quint, $J_{CP} = J_{CF}$ = 3.4 Hz), 125.1 (d, J_{CP} = 42.2 Hz), 123.8 (q, J^1_{CF} = 272.7 Hz), 122.9, 122.4, 114.3, 55.6, 43.0 (d, J_{CP} = 22.5 Hz), 42.3 (d, J_{CP} = 2.1 Hz), 36.3, 28.6 (d, J_{CP} = 9.9 Hz). **^{31}P NMR** (162 MHz, $CDCl_3$, 20 mg in 0.5 mL) δ 65.0. **^{19}F NMR** (376 MHz, $CDCl_3$, 20 mg in 0.5 mL) δ –62.4. **HRMS** (ESI +) calculated for $[C_{41}H_{46}AuClF_3N_2NaO_2P]^+$ $[M + Na]^+$ 941.2495 *m/z*; found 941.2531 *m/z*.

Complex Au12

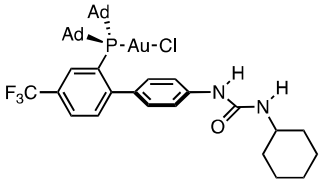

Prepared following general procedure **GP3**, using ligand **2.39** (67.0 mg, 99.4 µmol, 1 equiv) in CH_2Cl_2 (1.0 mL) at 23 ºC for 30 min. After evaporation of volatiles, the crude product was purified by FCC (silica, solid load, CyH:EtOAc 80:20 to 70:30), obtaining **Au12** (116.5 mg, estimated 99%$_{w/w}$ purity, 81.0 µmol, 82% yield) as a white solid. **M.p.** 257 °C (decomposition). **IR** (film from $CHCl_3$, cm^{-1}) 3339 (broad), 2905, 2851, 2233, 1532, 1323, 1130, 728. **^{1}H NMR** (500 MHz, $CDCl_3$, 40 mg in 0.5 mL, containing 1%$_{w/w}$ of pentane) δ 8.10 (d, J = 6.6 Hz, 1H), 7.75 (d, J = 8.1 Hz, 1H), 7.43 (d, J = 3.8 Hz, 1H), 7.36 (d, J = 8.4 Hz, 2H), 7.02 (d, J = 8.4 Hz, 2H), 6.89 (s, 1H), 5.84 (d, J = 8.0 Hz, 1H), 3.77–3.55 (m, 1H), 2.21–2.06 (m, 12H), 2.06–1.96 (m, 8H), 1.77–1.64 (m, 14H), 1.61–1.56 (m, 1H),

1.45–1.24 (m, 5H). **^{13}C NMR** (126 MHz, $CDCl_3$, 40 mg in 0.5 mL, containing 1%$_{w/w}$ of pentane) δ 155.5, 154.0 (d, J_{CP} = 12.7 Hz), 140.1, 136.0 (d, J_{CP} = 6.2 Hz), 134.4 (d, J_{CP} = 6.7 Hz), 131.0 (app quint, $J_{CP} = J_{CF}$ = 3.4 Hz), 129.8, 128.7 (qd, J = 33.0, 6.7 Hz), 127.0, 125.25 (d, J^1_{CP} = 42.1 Hz), 123.8 (d, J^1_{CF} = 272.6 Hz), 122.3, 49.5, 42.9 (d, J^1_{CP} = 22.5 Hz), 42.2 (d, J^3_{CP} = 2.1 Hz), 36.3, 33.6, 28.6 (d, J^2_{CP} = 9.9 Hz), 25.7, 25.3. **^{31}P NMR** (162 MHz, $CDCl_3$, 20 mg in 0.5 mL): δ 64.9. **^{19}F NMR** (376 MHz, $CDCl_3$, 20 mg in 0.5 mL): δ –62.4. **HRMS** (ESI +) calculated for $[C_{40}H_{50}AuClF_3N_2NaOP]^+$ $[M + Na]^+$ 917.2859 *m/z*; found 917.2881 *m/z*.

Complex Au13

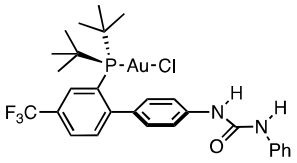

Prepared following modified general procedure **GP3**, using ligand **2.40** (80.0 mg, 0.153 mmol, 1 equiv) in CH_2Cl_2 (3.0 mL) at 23 ºC for 2 min. To the resulting pale-yellow solution was added pentane until a white precipitate formed. Solvent was decanted off and the resulting solid was washed with CH_2Cl_2:pentane (1:1, 2 × 1 mL) and pentane (3 × 1 mL). Complex **Au13** (98.7 mg, 0.135 mmol, 88% yield) was obtained as a beige solid. **M.p.** 258–262 °C (decomposition). **IR** (film from $CHCl_3$, cm^{-1}) υ 3354, 2973, 1710, 1587, 1521, 1499, 1321, 1166, 1131. **^{1}H NMR** (500 MHz, $(CD_3)_2SO$, 18 mg in 0.5 mL) δ 8.75–8.62 (m, 1H), 8.13–7.97 (m, 1H), 7.62–7.50 (m, 3H), 7.47 (d, J = 7.8 Hz, 2H), 7.29 (t, J = 7.7 Hz, 2H), 7.09 (d, J = 8.3 Hz, 2H), 7.01–6.92 (m, 1H), 1.35 (d, J = 15.9 Hz, 18H). **^{13}C NMR** (126 MHz, $(CD_3)_2SO$, 18 mg in 0.5 mL) δ 153.4 (d, J_{CP} = 12.4 Hz), 152.4, 140.0 (d, J^1_{CP} = 69.0 Hz), 134.4 (d, J_{CP} = 6.6 Hz), 133.8 (d, J_{CP} = 6.2 Hz), 129.7 (app quint, $J_{CP} = J_{CF}$ = 3.4 Hz), 129.0, 128.8, 127.52, 127.50 (qd, J = 33.0, 6.9 Hz), 126.7 (d, J_{CP} = 43.5 Hz), 123.7 (q, J^1_{CF} = 272.5 Hz), 121.8, 118.5, 118.1, 37.5 (d, J^1_{CP} = 24.5 Hz), 30.1 (d, J^2_{CP} = 6.6 Hz). **^{31}P NMR** (162 MHz, $(CD_3)_2SO$, 18 mg in 0.5 mL) δ 64.9. **^{19}F NMR** (376 MHz, $(CD_3)_2SO$, 18 mg in 0.5 mL) δ –62.4. **HRMS** (ESI +) calculated for $[C_{40}H_{50}AuClF_3N_2NaOP]^+$ $[M + Na]^+$ 917.2859*m/z*; found 917.2881 *m/z*. **Elemental analysis** calculated for $C_{28}H_{32}AuClF_3N_2OP$: C 45.88, H 4.40, N 3.82, found: C 44.91 ± 0.35, H 4.22 ± 0.30, N 3.74 ± 0.30. **XRD**: crystals for single-crystal X-ray diffraction analysis were grown from a solution in DMSO/CH_2Cl_2/*n*-pentane at room temperature.

Complex Au14

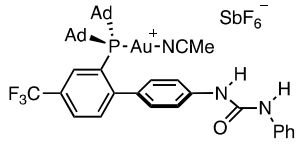

Following a modified literature procedure,[70] $AgSbF_6$ (19.4 mg, 56.2 µmol, 1 equiv, weighted in a vial in the glovebox) was added under air to a stirred cloudy whitish solution of **Au10**, 50.0 mg, 56.2 µmol, 1 equiv) in CH_3CN (15 µL, 281 µmol, 5 equiv) and CH_2Cl_2 (2.8 mL). Additional CH_2Cl_2 (1.0 mL) was added. Within 1 minute, precipitation of a white solid was observed. The suspension was stirred at 23 ºC for 2 h in the dark, then filtered through Celite® washing with CH_2Cl_2. Evaporation of the filtrate afforded an off-white powder, that was dissolved in CH_2Cl_2 and transferred into a tared vial. The solution was evaporated under reduced pressure and the resulting solid was dried overnight under high vacuum, affording **Au14** (56.8 mg, 50.2 µmol, 89% yield) as an off-white powder. **M.p.** 216 °C (decomposition). **IR** (film from $CHCl_3$, cm^{-1}) υ 3394 (broad), 2905, 2851, 1523, 1324, 1129, 1075, 656. **^{1}H NMR** (500 MHz, CD_2Cl_2, 21 mg in 0.5 mL) δ 8.11 (d, J = 7.2 Hz, 1H), 7.85 (d, J = 8.1 Hz, 1H), 7.75–7.68 (m, 2H), 7.57 (br s, 1H, NH), 7.54 (dd, J = 8.0, 3.9 Hz, 1H), 7.47 (d, J = 7.8 Hz, 2H), 7.44 (br s, 1H, NH), 7.35 (t, J = 7.9 Hz, 2H), 7.15 (d, J = 8.4 Hz, 2H), 7.10 (t, J = 7.3 Hz, 1H), 2.30 (s, 3H, CH_3CN), 2.17–2.11 (m, 6H), 2.08–2.02 (m, 12H), 1.76–1.68 (m, 12H). **^{13}C NMR** (126 MHz, CD_2Cl_2, 21 mg in 0.5 mL) δ 153.7 (weak br s, CO), 153.4 (d, J_{CP} = 11.0 Hz), 139.8 (weak br s), 138.5, 135.9 (weak br

70. de Orbe, E. M.; Echavarren, A. M. *Org. Synth.* **2016**, *93*, 115–126.

s), 134.7 (d, J_{CP} = 6.6 Hz), 130.9 (app quint, $J_{CP} = J_{CF}$ = 3.4 Hz), 130.3, 129.6, 129.5 (qd, J^2_{CF} = 32.8 Hz, J_{CP} = 7.6 Hz), 128.2 (m), 124.1 (q, J^1_{CF} = 272.6 Hz), 124.0 (br s), 123.6, 123.2, 121.5, 120.0 (br s), 119.8 (br s), 119.5 ($CH_3\underline{C}N$), 43.6 (d, J^1_{CP} = 23.6 Hz), 42.7, 36.3, 29.0 (d, J_{CP} = 10.0 Hz), 2.31 ($\underline{C}H_3CN$). **^{31}P NMR** (162 MHz, CD_2Cl_2, 21 mg in 0.5 mL) δ 62.5 (br s). **^{19}F NMR** (376 MHz, CD_2Cl_2, 21 mg in 0.5 mL) δ –62.8. **HRMS** (ESI +) calculated for $[C_{40}H_{44}AuF_3N_2OP]^+$ [M – CH_3CN – SbF_6]$^+$ [**Au14**]$^+$ 853.2804 *m/z*, found 853.2766 *m/z*. **XRD**: crystals for single-crystal X-ray diffraction were grown from a solution in CH_2Cl_2/cyclohexane at room temperature and confirmed the structure of complex **Au14** as drawn.

Complex Au15

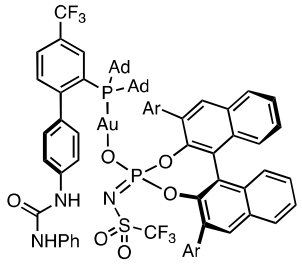

Ar = 9-anthracenyl
Tentative structure

(*R*)-**Ag6** (28.4 mg, 30.3 μmol, 1.01 equiv, derived from (*R*)-BINOL scaffold) was added under air to a stirred colorless solution of **Au10**, 26.7 mg, 30.0 μmol, 1.00 equiv) in CH_3CN (1 mL) and CH_2Cl_2 (2 mL). Immediate cloudiness was observed, and within 2 minutes precipitation of an off-white solid was observed. The suspension was stirred at 23 ºC for 1 h in the dark, then filtered through a small, sintered glass funnel. The clear filtrate was evaporated under reduced pressure at 30 ºC until 2 mL total volume, at which point precipitation of more off-white solid had happened. The suspension was filtered through a PTFE 0.2 μm syringe filter into a tared vial, washing with CH_2Cl_2 (ca 0.3 mL). The filtrate was evaporated under reduced pressure at 30 ºC and dried under high vacuum for 30 minutes, obtaining **Au15** (47.1 mg, 27.3 μmol, 90% yield) as a yellow solid. **Au15** was employed as such in catalytic tests. In **Au15**, the $^{31}P\{^1H\}$ NMR signal for the phosphine (62.8 ppm) moved upfield with respect to **Au10** (65.1 ppm), indicating chloride scavenging (compare with **Au14**, 62.5 ppm). The $^{31}P\{^1H\}$ NMR signal for the phosphoramidate anion (5.3 ppm) in **Au15** moved upfield with respect to the salt **Ag6** (ca 6 ppm) but remained well above the one of neutral phosphoramidate **2.52** (ca 0 ppm, depending on concentration), thus ruling out protonation of the anion. **M.p.** 305 °C (dec.). **^{1}H NMR** (400 MHz, CD_2Cl_2, 11 mg in 0.5 mL) δ 8.40–3.36 (m, 2H), 8.13 (br s, 1H), 8.07–7.97 (m, 6H), 7.95–7.89 (m, 1H), 7.85 (d, *J* = 8.1 Hz, 1H), 7.82–7.69 (m, 6H), 7.65–7.48 (m, 8H), 7.44–7.32 (m, 5H), 7.14–6.75 (m, 10H), 6.26 (br s, 1H), 6.01 (br s, 1H), 2.10–1.79 (m, 18 H), 1.75–1.39 (m, 12H, overlapping with H_2O peak, s at δ 1.55 ppm). **^{13}C NMR** (126 MHz, CD_2Cl_2, 15 mg in 0.5 mL; given the numerous peaks and couplings with ^{19}F and ^{31}P, aromatic signals are listed as observed without taking multiplicity into account, and with 2 decimal digits) δ 154.27, 154.19, 153.06, 147.90, 147.82, 147.22, 147.15, 140.91, 139.99, 134.75, 134.70, 134.61, 134.15, 133.55, 133.29, 133.21, 132.42, 132.24, 131.92, 131.91, 131.77, 131.75, 131.69, 131.35, 131.17, 131.14, 131.12, 131.05, 130.91, 130.84, 130.22, 129.30, 129.09, 128.78, 128.70, 128.54, 128.46, 128.04, 127.86, 127.84, 127.67, 127.62, 127.40, 127.28, 127.18, 127.06, 126.83, 126.81, 126.29, 126.18, 125.98, 125.81, 125.64, 125.37, 125.23, 125.16, 125.05, 123.54, 123.52, 123.09, 122.83, 122.82, 121.94, 121.10, 118.65, 118.53, 117.57, 43.6 (app t, *i.e.* two overlapping doublets, J^1_{CP} = 23.5 Hz), 42.6 (d, J_{CP} = 12.2 Hz), 36.3 (d, J_{CP} = 9.2 Hz), 29.0 (d, J_{CP} = 9.9 Hz). **^{31}P{^{1}H} NMR** (162 MHz, CD_2Cl_2, 30 mg in 0.5 mL, δ same as 11 mg in 0.5 mL) δ 62.8 (br s, $Ad_2\underline{P}Ar$), 5.3 (s, $O_3\underline{P}NTf$), integrations 1.00:0.93. **^{19}F{^{1}H} NMR** (376 MHz, CD_2Cl_2, 30 mg in 0.5 mL, δ same as 11 mg in 0.5 mL): δ –62.7 ($ArC\underline{F}_3$), –79.8 ($SO_2\ C\underline{F}_3$), integrations 1.00:0.93. **HRMS** (ESI–) on the filtered reaction mixture, calculated for $[C_{89}H_{72}AuClF_6N_3O_6P_2S]^-$ [M + Cl]$^-$ 1718.3881 *m/z*, found 1718.3882 *m/z*; calculated for $[C_{49}H_{28}F_3NO_5P_2S]^-$ [anion]$^-$ 830.1383 *m/z*, found 830.1381 *m/z*.

General Procedure GP4: phosphoramidate formation

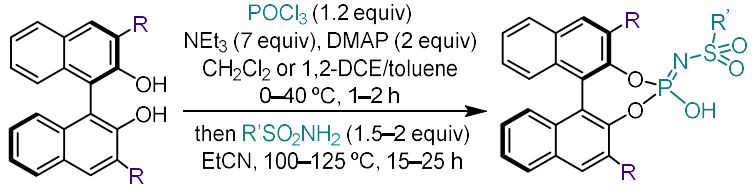

2.41 R = 2,4,6-(^{i}Pr)$_3$C$_6$H$_2$
2.42 R = 3,5-(CF$_3$)$_2$C$_6$H$_3$
2.43 R = SiPh$_3$
2.44 R = 9-anthracenyl
2.45 R = 9-phenantryl
2.46 R =1-pyrenyl

2.47 R = 2,4,6-(^{i}Pr)$_3$C$_6$H$_2$, R' = CF$_3$, ***56%***
2.48 R = 2,4,6-(^{i}Pr)$_3$C$_6$H$_2$, R' = CH$_3$, ***44%***
2.49 R = 2,4,6-(^{i}Pr)$_3$C$_6$H$_2$, R' = Ph, ***32%***
2.50 R = 3,5-(CF$_3$)$_2$C$_6$H$_3$, R' = CF$_3$, ***84%***
2.51 R = SiPh$_3$, R' = CF$_3$, ***72%***
2.52 R = 9-anthracenyl, R' = CF$_3$, ***70%***
2.53 R = 9-phenantryl, R' = CF$_3$, **58%**
2.54 R =1-pyrenyl, R' = CF$_3$, **75%**

Adapting a reported procedure,[29] under Ar, a flame-dried Schlenk tube equipped with a stir bar was charged with the desired binaphthol **2.41–2.46** (1 equiv). Anhydrous CH_2Cl_2, anhydrous Et_3N (7 equiv) and phosphoryl chloride (1.2 equiv) were added in sequence at 0 °C. After 5 minutes, 4-(dimethylamino)pyridine (2 equiv) was added at 0 °C. The mixture was then stirred at 23–40 °C for 1–2 h. Anhydrous solvent (propionitrile, 1,2-DCE and/or toluene) and then the desired sulfonamide (1.5–2 equiv) were added at room temperature. The resulting mixture was heated in the sealed Schlenk tube at 100–125 °C for 15–25 h. Then, the reaction mixture was cooled to room temperature, quenched by addition of water and extracted three times with CH_2Cl_2 (or Et_2O). The combined organic layers were washed once with a saturated $NaHCO_3$ aqueous solution and then twice with aqueous 4 M HCl, filtered and concentrated. The crude product was purified by FCC (silica, CyH:EtOAc solvent mixtures), dissolved in EtOAc (or Et2O, or CH_2Cl_2, 15 mL), washed twice with aqueous 4 M HCl (5 mL) and evaporated, affording phosphoramidate **2.47–2.54**.

Note: a common side product in this reaction is the phosphoric acid diester. Its presence can be easily checked by $^{31}P\{^1H\}$ NMR in $CDCl_3$: the phosphoramidate resonates ca 5 ppm upfield from the phosphoric acid diester. On TLC (CyH:EtOAc 8:2) the acid remains on the baseline, while the desired phosphoramidate moves to higher RF. Nevertheless, when purifying the crude by FCC, the acid side product often coelutes with the phosphoramidate, at least partially. We found that mixed fractions can be successfully purified by PTLC on silica plates (ca 100 mg per 2000 micron silica plate) in CyH:EtOAc eluent mixtures.

(*R*)-2.47

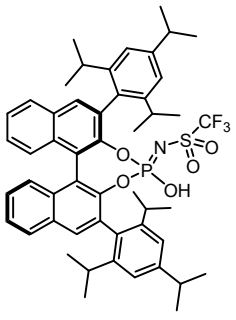

Prepared following general procedure **GP4**, using binaphthol (*R*)-**2.41** (400 mg, 0.579 mmol, 1.0 equiv), CH_2Cl_2 (2.9 mL), Et_3N (565 µL, 4.05 mmol, 7 equiv) and $POCl_3$ (65 µL, 0.70 mmol, 1.2 equiv), obtaining a yellow suspension at 0° C. After the addition of DMAP (141 mg, 1.16 mmol, 2 equiv) at 23 °C, the resulting pink suspension was stirred at 23 °C for 1 h, during which it turned orange. Then, propionitrile (2.9 mL) and trifluoromethanesulfonamide (130 mg, 0.869 mmol, 1.5 equiv) were added and the resulting brown suspension was heated at 100 °C for 18 h. After work-up, the crude was purified by FCC (dry load, silica, CyH:EtOAc 100:0 to 80:20). After acidification and evaporation, compound (*R*)-**2.47** was obtained as an off-white solid (286 mg, 0.324 mmol, 56% yield). Spectroscopic data of (*R*)-**2.47** matched the

previously reported ones.[71] **M.p.** 173–176 °C (lit:[72] 170–175 °C, sample containing 10 mol % of the corresponding phosphoric acid diester). **IR** (film from $CHCl_3$, cm^{-1}) ʋ 2960, 2870, 1194, 1148, 1116, 975. **^{1}H NMR** (400 MHz, $CDCl_3$) δ 8.00–7.95 (m, 4H), 7.58–7.54 (m, 2H), 7.40–7.33 (m, 3H), 7.30–7.27 (m, 1H), 7.18–7.16 (m, 1H), 7.15–7.12 (m, 2H), 7.06–7.04 (m, 1H), 4.20 (br s, 1H), 3.00–2.88 (m, 2H), 2.81–2.70 (m, 2H), 2.65–2.51 (m, 2H), 1.32–1.14 (m, 30H), 1.10 (d, *J* = 6.8 Hz, 3H), 1.01 (d, *J* = 6.8 Hz, 3H), 0.95 (d, *J* = 6.8 Hz, 3H). **^{13}C NMR** (101 MHz, $CDCl_3$, listed as observed except for the CF_3 quartet) δ 149.6, 149.2, 148.0, 147.9, 147.4, 147.2, 145.8, 145.7, 145.1, 145.0, 133.2, 133.1, 132.50, 132.46, 132.4, 132.3, 131.6, 131.2, 130.91, 130.87, 130.54, 130.49, 128.6, 128.5, 127.46, 127.43, 126.8, 126.7, 126.39, 126.35, 122.0, 121.9, 121.3, 121.2, 121.1, 120.5, 119.1 (q, *J* = 320.3 Hz), 34.6, 34.5, 31.5, 31.2, 31.1, 30.7, 27.03, 26.84, 25.4, 25.3, 24.3, 24.2, 24.1, 23.25, 23.20, 23.0, 22.8. **^{31}P NMR** (162 MHz, $CDCl_3$) δ −1.0 (for comparison, the corresponding phosphoric acid diester peak was observed in the crude and in mixed fractions at 4.0−4.5 ppm). **^{19}F NMR** (376 MHz, $CDCl_3$) δ −77.3. **$[\alpha]^{24.6}_D$** −36 (c 1.0, $CHCl_3$); lit.[72] **$[\alpha]^{20.0}_D$** −24 (c 1.0, $CHCl_3$, sample containing 10 mol % of the corresponding phosphoric acid diester); (*S*) enantiomer lit.[71] **$[\alpha]^{27.9}_D$** +30 (c 0.42, CH_2Cl_2).

(*R*)-2.48

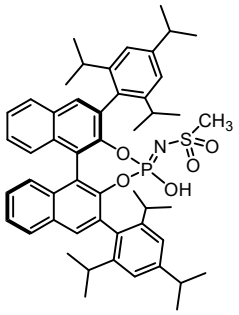

Prepared following general procedure **GP4**, using binaphthol (*R*)-**2.41** (100 mg, 0.145 mmol, 1.0 equiv), CH_2Cl_2 (0.9 mL), Et_3N (140 µL, 1.01 mmol, 7 equiv) and $POCl_3$ (16 µL, 0.17 mmol, 1.2 equiv), obtaining a yellow solution at 0° C. After the addition of DMAP (35.4 mg, 0.289 mmol, 2 equiv) at 0 °C, the resulting pink cloudy solution was stirred at 23 °C for 1 h. Then, propionitrile (0.7 mL) and methanesulfonamide (22.0 mg, 0.232 mmol, 1.6 equiv) were added and the resulting yellow solution was heated at 100 °C for 20 h. After work-up, the crude was purified by automated FCC (dry load, silica, CyH:EtOAc 90:10 to 0:100, desired product eluting in CyH:EtOAc 70:30 to 30:70, immediately after the corresponding phosphoric acid diester). After acidification and evaporation, compound (*R*)-**2.48** was obtained as an off-white solid (52.8 mg, 0.0639 mmol, 44% yield). Spectroscopic data of (*R*)-**2.48** matched the previously reported ones. **^{1}H NMR** (400 MHz, $CDCl_3$) δ 7.99–7.93 (m, 4H), 7.58–7.51 (m, 2H), 7.38–7.32 (m, 3H), 7.29 (br s, 1H), 7.16 (br s, 2H), 7.14 (br s, 1H), 7.03 (br s, 1H), 2.99–2.83 (m, 3H), 2.77–2.67 (m, 1H), 2.63–2.52 (m, 2H), 2.43 (s, 3H), 1.30 (d, *J* = 7.6 Hz, 6H), 1.28–1.21 (m, 22H), 1.10 (d, *J* = 6.8 Hz, 3H), 1.00 (d, *J* = 6.7 Hz, 3H), 0.96 (d, *J* = 6.8 Hz, 3H). **^{13}C NMR** (101 MHz, $CDCl_3$, listed as observed) δ 149.9, 149.2, 148.7, 148.3, 147.2, 146.2, 146.05, 145.93, 144.64, 144.56, 132.94, 132.85, 132.6, 132.4, 132.3, 131.8, 131.2, 130.84, 130.80, 130.7, 130.3, 128.6, 128.5, 127.5, 126.8, 126.5, 126.4, 122.1, 121.7, 121.63, 121.57, 121.3, 120.3, 42.1, 34.58, 34.54, 31.6, 31.4, 31.2, 30.8, 27.1, 27.0, 25.5, 25.2, 24.4, 24.24, 24.19, 23.32, 23.30, 23.2, 23.1. **^{31}P NMR** (162 MHz, $CDCl_3$) δ −1.3 (for comparison, the corresponding phosphoric acid diester peak was observed in the crude and in mixed fractions at 5.5−6.0 ppm).

71. Borovika, A.; Nagorny, P. *Tetrahedron* **2013**, *69*, 5719–5725.
72. Knipe, P. C.; Smith, M. D. *Org. Biomol. Chem.* **2014**, *12*, 5094–5097.

(*R*)-2.49

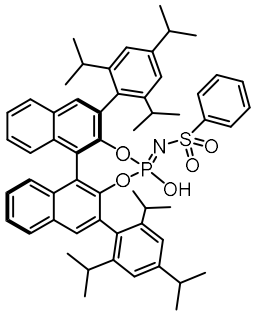

Prepared following general procedure **GP4**, using binaphthol (*R*)-**2.41** (150 mg, 0.217 mmol, 1.0 equiv), CH_2Cl_2 (1.1 mL), Et_3N (212 µL, 1.52 mmol, 7 equiv) and $POCl_3$ (24 µL, 0.26 mmol, 1.2 equiv), obtaining a yellow solution at 0 °C. After the addition of DMAP (53.0 mg, 0.434 mmol, 2 equiv) at 0 °C, the resulting pink suspension was stirred at 23 °C for 1 h. Then, propionitrile (1.1 mL) and benzenesulfonamide (45.6 mg, 0.347 mmol, 1.6 equiv) were added and the resulting mixture was heated at 100 °C for 19 h. After work-up, the crude was purified by automated FCC (dry load, silica, CyH:EtOAc 90:10 to 0:100, desired product eluting in CyH:EtOAc 90:10, initially coeluting with the corresponding phosphoric acid diester). After acidification and evaporation, compound (*R*)-**2.49** was obtained as an off-white solid (62.0 mg, 0.0639 mmol, 32% yield). **M.p.** 192 °C. **IR** (film from $CHCl_3$, cm^{-1}) υ 2959, 2929, 2868, 1383, 1315, 1174, 903, 751, 732. **^{1}H NMR** (500 MHz, $CDCl_3$) δ 7.97–7.91 (m, 4H), 7.57–7.51 (m, 2H), 7.42 (tt, *J* = 7.3, 1.1 Hz, 1H), 7.36–7.31 (m, 5H), 7.29–7.27 (m, 1H), 7.29–7.27 (m, 1H), 7.25–7.21 (m, 4H), 7.13 (d, *J* = 1.7 Hz, 1H), 7.10 (d, *J* = 1.7 Hz, 1H), 3.04–2.94 (m, 2H), 2.88–2.80 (m, 1H), 2.77–2.69 (m, 1H), 2.67–2.55 (m, 2H), 1.33 (app ddd, *J* = 6.9, 3.5, 1.6 Hz, 12H), 1.28–1.21 (m, 10H), 1.20 (d, *J* = 6.7 Hz, 3H), 1.13 (d, *J* = 6.8, Hz, 3H), 1.12 (d, *J* = 6.8, Hz, 3H), 0.98 (d, *J* = 6.8 Hz, 3H), 0.95 (d, *J* = 6.8 Hz, 3H). **^{13}C NMR** (101 MHz, $CDCl_3$, listed as observed) δ 149.8, 148.7, 148.6, 148.3, 147.2, 146.4, 146.14, 146.05, 145.23, 145.16, 140.0, 133.3, 133.13, 133.09, 132.7, 132.5, 132.4, 131.6, 131.1, 130.9, 130.5, 130.4, 130.3, 128.7, 128.5, 127.7, 127.6, 127.5, 126.8, 126.5, 126.3, 122.22, 122.19, 121.8, 121.3, 121.5, 121.3, 120.5, 34.57, 34.55, 31.6, 31.3, 31.2, 30.6, 27.3, 27.0, 25.6, 25.2, 24.32, 24.29, 24.26, 24.15, 23.3, 23.2, 23.13, 23.08. **^{31}P NMR** (162 MHz, $CDCl_3$) δ −1.8 (for comparison, the corresponding phosphoric acid diester peak was observed in the crude and in mixed fractions at 5.5−6.0 ppm). **HRMS** (ESI −) calculated for $[C_{56}H_{61}NO_5PS]^-$ $[M-H]^-$ 890.4014 *m/z*; found 890.4017 *m/z*. **[α]$^{24.6}_D$** −56 (c 1.0, $CHCl_3$).

(*R*)-2.50

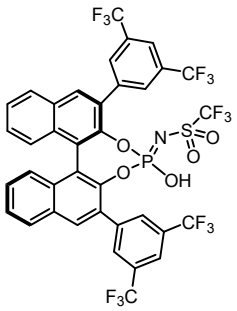

Prepared following general procedure **GP4**, using binaphthol (*R*)-**2.42** (100 mg, 0.141 mmol, 1.0 equiv), CH_2Cl_2 (0.7 mL), Et_3N (137 µL, 0.985 mmol, 7 equiv) and $POCl_3$ (16 µL, 0.17 mmol, 1.2 equiv), obtaining a yellow suspension at 0° C. After the addition of DMAP (34.4 mg, 0.281 mmol, 2 equiv) at 23 °C, the resulting pink cloudy solution was stirred at 23 °C for 1 h. Then, propionitrile (0.7 mL) and trifluoromethanesulfonamide (32.5 mg, 0.218 mmol, 1.55 equiv) were added and the resulting mixture was heated at 100 °C for 15 h. After work-up, the crude was purified by automated FCC (dry load, silica, CyH:EtOAc 90:10 to 0:100, desired product eluting in CyH:EtOAc 70:30). After acidification and evaporation, compound (*R*)-**2.50** was obtained as a beige solid (107.0 mg, 0.118 mmol, 84% yield). Spectroscopic data of (*R*)-**2.50** matched the previously reported ones.[73] **^{1}H NMR** (500 MHz, acetone-d_6) δ 8.53 (d, *J* = 6.9 Hz, 2H), 8.48 (s, 2H), 8.41 (s, 2H), 8.25 (d, *J* = 8.4 Hz, 2H), 8.12 (d, *J* = 10.4 Hz, 2H), 7.68–7.62 (m, 2H), 7.51–7.44 (m, 3H), 7.39 (d, *J* = 8.5 Hz, 1H). **^{31}P NMR** (202 MHz, acetone-d_6) δ 1.7. **^{19}F NMR** (471 MHz, acetone-d_6) δ −63.23 (6F), −63.25 (6F), −80.09 (3F).

73. Tay, J.-H.; Arguelles, A. J.; Nagorny, P. *Org. Lett.* **2015**, *17*, 3774–3777.

(*R*)-2.51

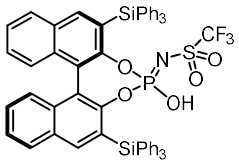

Prepared following general procedure **GP4**, using binaphthol (*R*)-**2.43** (95.0 mg, 0.118 mmol, 1.0 equiv), CH_2Cl_2 (0.6 mL), Et_3N (115 µL, 0.828 mmol, 7 equiv) and $POCl_3$ (13 µL, 0.14 mmol, 1.2 equiv), obtaining a yellow solution at 0° C. After the addition of DMAP (28.9 mg, 0.237 mmol, 2 equiv) at 23 °C, the resulting orange suspension was stirred at 23 °C for 1 h. Then, propionitrile (0.6 mL) and trifluoromethanesulfonamide (27.3 mg, 0.183 mmol, 1.55 equiv) were added and the resulting mixture was heated at 100 °C for 15 h. After work-up, the crude was purified by automated FCC (dry load, silica, CyH:EtOAc 100:0 to 0:100, desired product eluting in CyH:EtOAc 60:40). After acidification and evaporation, compound (*R*)-**2.51** was obtained as a beige solid (84.6 mg, 0.0850 mmol, 72% yield). Spectroscopic data of (*R*)-**2.51** matched the previously reported ones.[74] **^{1}H NMR** (500 MHz, $CDCl_3$) δ 8.28 (s, 1H), 8.05 (s, 1H), 7.90 (d, *J* = 8.2 Hz, 1H), 7.80 (d, *J* = 8.1 Hz, 1H), 7.76–7.72 (m, 6H), 7.67–7.64 (m, 6H), 7.55–7.34 (m, 22H), 7.26 (d, *J* = 8.5 Hz, 1H), 7.20 (d, *J* = 8.5 Hz, 1H), 3.81 (br s, 1H). **^{31}P NMR** (202 MHz, $CDCl_3$) δ −6.2 (for comparison, the corresponding phosphoric acid diester peak was observed in the crude and in mixed fractions at 1.5−2.0 ppm). **^{19}F NMR** (471 MHz, $CDCl_3$) δ −77.8.

(*R*)-2.52

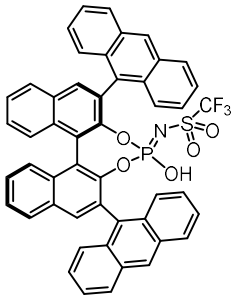

Prepared following general procedure **GP4**, using binaphthol (*R*)-**2.44** (450 mg, 0.704 mmol, 1.0 equiv), $ClCH_2CH_2Cl_2$ (1.0 mL) and toluene (9.0 mL). The pale yellow suspension was cooled to 0° C, and Et_3N (0.69 mL, 4.9 mmol, 7 equiv) was added at 0 °C, obtaining a bright yellow cloudy solution, that after stirring for 5 minutes formed a crystalline precipitate. $POCl_3$ (79 µL, 0.845 mmol, 1.2 equiv) was added at 0 °C, obtaining a darker yellow solution. DMAP (172 mg, 1.41 mmol, 2 equiv) was then added at 0 °C as a solution in $ClCH_2CH_2Cl_2$ (2.0 mL). The resulting pale yellow creamy suspension was stirred at 23 °C for 40 minutes and at 40 °C for 50 minutes. After cooling to room temperature, trifluoromethanesulfonamide (189 mg, 1.27 mmol, 1.8 equiv) was added as a solution in propionitrile (3.0 mL) and the resulting mixture was heated at 125 °C for 25 h in a sealed Schlenk flask. After work-up, *without* drying the combined organic phases with Na_2SO_4, the crude was purified by automated FCC (dry load, silica, CyH:EtOAc 80:20 to 50:50). After acidification and evaporation, compound (*R*)-**2.52** was obtained as a beige solid (408 mg, 0.491 mmol, 70% yield). Spectroscopic data of (*R*)-**2.52** matched the previously reported ones.[75] **M.p.** 264 °C (decomposition; lit:[75] 281–283 °C). **IR** (film from $CHCl_3$, cm^{-1}) υ 3054, 1445, 1402, 1295, 1198, 1099, 956, 891. **^{1}H NMR** (400 MHz, $CDCl_3$) δ 8.56 (s, 1H), 8.39 (s, 1H), 8.17 (d, *J* = 7.9 Hz, 2H), 8.08–8.04 (m, 3H), 8.03–7.97 (m, 2H), 7.79–7.52 (m, 11H), 7.51–7.29 (m, 6H), 7.01–6.94 (m, 1H), 6.91–6.82 (m, 1H), 5.29 (br s, 1H). **^{13}C NMR** (101 MHz, $CDCl_3$, listed as observed except for CF_3 quartet) δ 146.3, 146.2, 145.4, 145.3, 134.6, 132.8, 132.7, 132.1, 131.9, 131.6, 131.3, 131.0, 130.9, 130.8, 130.7, 130.5, 130.0, 129.9, 129.1, 128.9, 128.84, 128.81, 128.7, 128.4, 128.1, 128.0, 127.8, 127.6, 127.5, 127.1, 126.9, 126.6, 126.1, 125.8, 125.6, 125.4, 125.3, 125.1, 125.0, 122.5, 122.1, 118.2 (q, *J* = 321.1 Hz). **^{31}P NMR** (162 MHz, $CDCl_3$) δ −1.5 (for comparison, the corresponding phosphoric acid diester peak was observed in the crude and in mixed fractions

74. Villar, L.; Uria, U.; Martínez, J. I.; Prieto, L.; Reyes, E.; Carrillo, L.; Vicario, J. L. *Angew. Chem. Int. Ed.* **2017**, *56*, 10535–10538.
75. Zhao, P.; Cheng, A.; Wang, X.; Ma, J.; Zhao, G.; Li, Y.; Zhang, B. Zhao, *Chin. J. Chem.* **2020**, *38*, 565–569.

at 5.0−6.5 ppm). **^{19}F NMR** (376 MHz, $CDCl_3$) δ −78.3. **$[\alpha]^{24.3}_D$** −21 (c 1.0, $CHCl_3$, unstable readings, average of 8 datasets, each with 10 measurements).

(*R*)-2.53

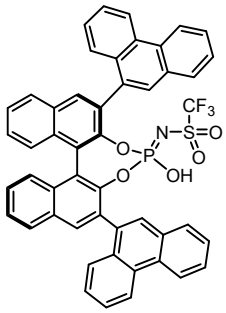

Prepared following general procedure **GP4**, using binaphthol (*R*)-**2.45** (100 mg, 0.157 mmol, 1.0 equiv), 1,2-DCE (0.7 mL), toluene (2.1 mL), Et_3N (153 µL, 1.10 mmol, 7 equiv) and $POCl_3$ (17.6 µL, 0.188 mmol, 1.2 equiv), obtaining a yellow suspension at 0 °C. After the addition of DMAP (38.3 mg, 0.383 mmol, 2 equiv) at 23 °C, the resulting brown suspension was stirred at 23 °C for 50 min then heated to 40 °C for 1 h, the reaction mixture stayed as a brown suspension. Then, propionitrile (0.7 mL) and trifluoromethanesulfonamide (42.0 mg, 0.282 mmol, 1.8 equiv) were added and the resulting brown solution was heated at 120 °C for 18 h. After work-up, the crude was purified by FCC (dry load, silica, CyH:EtOAc 100:0 to 80:20). After acidification and evaporation, compound (*R*)-**2.53** was obtained as a beige solid (76 mg, 0.091 mmol, 58% yield). Spectroscopic data for product (*R*)-**2.53** matched those reported in the literature.[75] According to ^{31}P NMR and ^{19}F NMR analysis, compound (*R*)-**2.53** mainly existed as three isomers in $CDCl_3$ solution due to the restricted rotation of the 3,3'-phenanthryl groups. **^{1}H NMR** (400 MHz, $CDCl_3$): δ 8.78 – 8.52 (m, 4H), 8.24 – 8.16 (m, 2H), 8.15 – 7.96 (m, 4H), 7.89 – 7.73 (m, 3H), 7.70 – 7.54 (m, 11H), 7.54 – 7.38 (m, 5H). **^{31}P NMR** (162 MHz, $CDCl_3$) δ −0.5, −1.1, −1.5. **^{19}F NMR** (376 MHz, $CDCl_3$) δ −78.1, −78.2, −78.4.

(*R*)-2.54

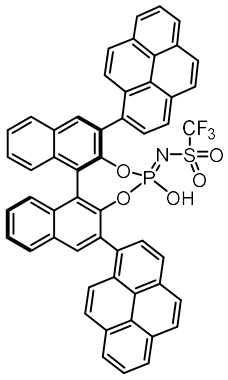

Prepared following general procedure **GP4**, using binaphthol (*R*)-**2.46** (100 mg, 0.146 mmol, 1.0 equiv), 1,2-DCE (0.6 mL), toluene (1.8 mL), Et_3N (141 µL, 1.02 mmol, 7 equiv) and $POCl_3$ (16.3 µL, 0.175 mmol, 1.2 equiv), obtaining a yellow suspension at 0 °C. After the addition of DMAP (35.6 mg, 0.291 mmol, 2 equiv) at 25 °C, the resulting brown suspension was stirred at 25 °C for 40 min then heated to 40 °C for 50 min during which it stayed as a yellow suspension. Then, propionitrile (0.6 mL) and trifluoromethanesulfonamide (39.1 mg, 0.262 mmol, 1.8 equiv) were added and the resulting orange solution was heated at 110 °C for 23 h. After work-up, the crude was purified by FCC (dry load, silica, CyH:EtOAc 100:0 to 80:20). After acidification and evaporation, compound (*R*)-**2.54** was obtained as a yellow solid (113 mg, 93% weight purity, 0.109 mmol, 75% yield). Traces of grease could not be removed, and the compound was used as such. According to ^{31}P NMR and ^{19}F NMR analysis, compound (*R*)-**2.54** mainly existed as four isomers in $CDCl_3$ solution due to the restricted rotation of the 3,3'-pyren-1-yl groups. Similar behavior has been reported previously in the literature for the corresponding phosphoric acid.[76] **M.p.** 237 °C (decomposition). **IR** (film from $CHCl_3$, cm^{-1}) ν 3043 (broad), 2926, 2853, 1288, 1199, 1151, 1102, 980, 846, 753. **^{1}H NMR** (400 MHz, 22 mg in 0.5 mL $CDCl_3$): δ 8.29 – 8.14 (m, 3H), 8.13 – 7.95 (m, 8H), 7.94 – 7.84 (m, 4H), 7.84 – 7.70 (m, 5H), 7.69 – 7.52 (m, 5H), 7.52 – 7.06 (m, 3H), 5.58 (brs, 1H). **^{13}C NMR** (101 MHz, $CDCl_3$, no couplings reported due to complexity, peaks listed as observed) δ 143.9, 134.3, 134.2, 134.1, 134.0, 133.5, 133.3, 133.2, 133.1, 132.9, 132.6, 132.53, 132.48, 132.4, 132.1, 132.1, 132.0, 131.8, 131.7, 131.6, 131.45, 131.41, 131.36, 131.32, 131.26, 131.2, 131.14, 131.11, 131.0, 130.94, 130.86, 130.81, 130.79, 130.7, 130.6, 130.0, 129.9, 129.8, 129.6, 129.4, 129.4, 129.36, 129.3,

76. Shin, N. Y.; Ryss, J. M.; Zhang, X.; Miller, S. J.; Knowles, R. R. *Science* **2019**, *366*, 364–369.

129.24, 129.19, 129.0, 128.94, 128.89, 128.82, 128.79, 128.7, 128.6, 128.4, 128.3, 128.0, 127.96, 127.9, 127.8, 127.72, 127.67, 127.63, 127.59, 127.50, 127.4 (d = 22.7 Hz), 127.36, 127.32, 127.28, 127.2, 127.17, 127.1, 127.0, 126.98, 126.9, 126.8, 126.76, 126.7, 126.61, 126.58, 126.0, 125.98, 125.9, 125.8, 125.4, 125.32, 125.29, 125.26, 125.22, 125.20, 125.16, 125.1, 125.07, 125.05, 125.03, 124.99, 124.9, 124.8, 124.75, 124.7, 124.65, 124.63, 124.5, 124.47, 124.4, 124.3, 124.2, 124.1, 124.08, 123.9, 121.8. **^{31}P NMR** (162 MHz, $CDCl_3$) δ −1.9, −2.3, −2.9, −3.4. **^{19}F NMR** (376 MHz, $CDCl_3$) δ −77.6, −78.2, −78.5, −78.8. **HRMS** (ESI +) calculated for $[C_{53}H_{28}F_3NO_5PS]^+$ [M - H]$^+$ 878.1383 *m/z*; found 878.1391 *m/z*. **[α]$^{24.0}_D$** −331 (c 0.385, $CHCl_3$).

***(R)*-2.57**

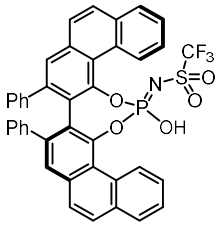

Prepared following general procedure **GP4**, using binaphthol (*R*)-**2.55** (98 mg, 0.182 mmol, 1.0 equiv), 1,2-DCE (0.6 mL), toluene (1.2 mL), Et_3N (178 μL, 1.27 mmol, 7 equiv) and $POCl_3$ (20.4 μL, 0.218 mmol, 1.2 equiv), obtaining a yellow suspension at 0 °C. After the addition of DMAP (44.5 mg, 0.291 mmol, 2 equiv) at 25 °C, the resulting yellow suspension was stirred at 25 °C for 1 h then heated to 40 °C for 1 h, the reaction mixture stayed as a yellow suspension. Then, propionitrile (0.6 mL) and trifluoromethanesulfonamide (39.1 mg, 0.262 mmol, 1.8 equiv) were added and the resulting yellow solution was heated at 110 °C for 28 h. After work-up, the crude was purified by FCC (dry load, silica, CyH:EtOAc 100:0 to 80:20). After acidification and evaporation, compound (*R*)-**2.57** was obtained as a beige solid (129 mg, 0.176 mmol, 97% yield). Spectroscopic data for product (*R*)-**2.57** matched those reported in the literature.[77] **^{1}H NMR** (400 MHz, $CDCl_3$): δ 9.63 – 9.42 (m, 2H), 7.94 (dd, *J* = 14.8, 7.7 Hz, 2H), 7.82 (t, *J* = 9.3 Hz, 2H), 7.78 – 7.63 (m, 6H), 7.58 (d, *J* = 2.2 Hz, 2H), 7.16 – 7.07 (m, 2H), 6.99 – 6.91 (m, 4H), 6.55 – 6.32 (m, 4H), 4.68 (brs, 1H). **^{31}P NMR** (162 MHz, $CDCl_3$) δ −1.7. **^{19}F NMR** (376 MHz, $CDCl_3$) δ −78.1.

(*R*)-2.58

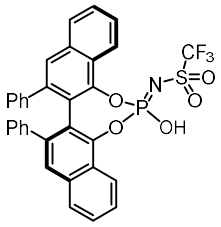

Prepared following general procedure **GP4**, using binaphthol (*R*)-**2.56** (100 mg, 0.228 mmol, 1.0 equiv), CH_2Cl_2 (1.1 mL), Et_3N (220 μL, 1.58 mmol, 6.9 equiv) and $POCl_3$ (26.0 μL, 0.280 mmol, 1.2 equiv), obtaining a yellow suspension at 0 °C. After the addition of DMAP (55.7 mg, 0.456 mmol, 2 equiv) at 25 °C, the resulting orange suspension was stirred at 25 °C for 1 h. Then, propionitrile (1.1 mL) and trifluoromethanesulfonamide (68.0 mg, 0.456 mmol, 2.0 equiv) were added and the resulting orange solution was heated at 100 °C for 18 h. After work-up, the crude was purified by FCC (dry load, silica, CyH:EtOAc 100:0 to 80:20). After acidification and evaporation, compound (*R*)-**2.58** was obtained as a beige solid (115 mg, 0.182 mmol, 80% yield). Spectroscopic data for product (*R*)-**2.58** matched those reported in the literature.[77] **^{1}H NMR** (500 MHz, $CDCl_3$): δ 8.43 (dd, *J* = 8.5, 1.1 Hz, 1H), 8.32 (dd, *J* = 8.2, 1.3 Hz, 1H), 7.88 – 7.76 (m, 2H), 7.68 – 7.63 (m, 1H), 7.63 – 7.53 (m, 4H), 7.49 (s, 1H), 7.15 – 7.08 (m, 2H), 7.00 – 6.87 (m, 4H), 6.51 – 6.37 (m, 4H), 5.90 (brs, 1H). **^{31}P NMR** (202 MHz, $CDCl_3$) δ 1.1. **^{19}F NMR** (471 MHz, $CDCl_3$) δ −77.3.

77. Desai, A. A.; Wulff, W. D. *Synthesis* **2010**, 3670–3680.

(*R*)-Ag1

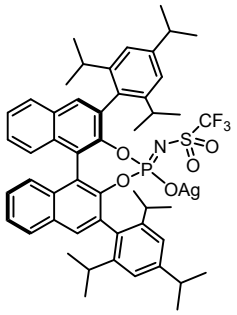

Whenever possible, all steps of this procedure were carried out in the dark. Following a reported procedure,[72] Ag_2CO_3 (15.9 mg, 0.058 mmol, 0.5 equiv) and distilled H_2O (1.0 mL) were added to a stirred solution of phosphoramidate *(R)*-**2.47** (102.0 mg, 0.115 mmol, 1 equiv) in CH_2Cl_2 (1.0 mL). The resulting biphasic mixture was vigorously stirred under air at 23 °C in the dark for 1 h, then diluted with CH_2Cl_2 (5 mL) and distilled H_2O (5 mL). The aqueous layer was extracted with CH_2Cl_2 (3 × 5 mL), then the combined organic phases were filtered over Celite® washing with additional CH_2Cl_2. The filtrate was concentrated and dried under high vacuum affording (*R*)-**Ag1** (102.2 mg, 0.103 mmol, 90% yield) as an off-white powder. Spectroscopic data of (*R*)-**Ag1** matched those reported in the literature.[72] **M.p.** 224–229 °C (dec.). **^{1}H NMR** (400 MHz, $CDCl_3$) δ 7.98–7.94 (m, 2H), 7.92–7.89 (m, 2H), 7.56–7.52 (m, 1H), 7.49 (dt, *J* = 8.1, 3.9 Hz, 1H), 7.36–7.27 (m, 5H), 7.13 (d, *J* = 1.6 Hz, 1H), 7.07 (d, *J* = 1.6 Hz, 1H), 7.01 (d, *J* = 1.6 Hz, 1H), 3.01 (septet, *J* = 6.8 Hz, 1H), 2.95–2.75 (m, 4H), 2.67 (septet, *J* = 6.8 Hz, 1H), 1.35 (d, *J* = 6.9 Hz, 6H), 1.32–1.19 (m, 21H), 1.15 (d, *J* = 6.8 Hz, 3H), 1.03 (d, *J* = 6.8 Hz, 3H), 0.90 (d, *J* = 6.8 Hz, 3H). **^{13}C NMR** (101 MHz, $CDCl_3$, listed as observed, CF_3 quartet not visible) δ 151.4, 151.1, 148.6, 147.8, 147.1, 147.0, 145.6, 145.5, 133.1, 132.9, 132.5, 132.2, 131.7, 131.6, 131.0, 130.8, 128.5, 128.3, 127.60, 127.57, 126.5, 126.1, 125.9, 125.6, 123.11, 123.09, 121.7, 121.42, 121.40, 120.5, 120.4, 34.5, 34.4, 31.7, 31.2, 31.10, 30.96, 27.0, 26.8, 25.4, 25.3, 25.2, 24.9, 24.45, 24.36, 24.0, 23.51, 23.47, 22.3. **^{31}P NMR** (162 MHz, $CDCl_3$) δ −9.0. **^{19}F NMR** (376 MHz, $CDCl_3$) δ −78.0. **$[\alpha]^{24.9}_D$** −27 (c 1.0, $CHCl_3$); lit.[72] **$[\alpha]^{20.0}_D$** −39 (c 0.61, $CHCl_3$, prepared from a 9:1 mixture of phosphoramidate and phosphoric acid diester).

(*R*)-Ag2

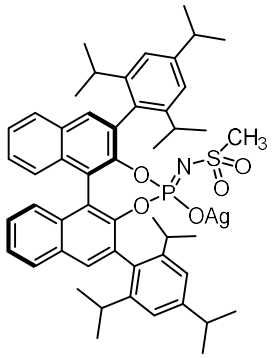

Whenever possible, all steps of this procedure were carried out in the dark. Ag_2CO_3 (8.3 mg, 0.030 mmol, 0.5 equiv) and distilled H_2O (1.2 mL) were added to a stirred pale-yellow solution of phosphoramidate *(R)*-**2.48** (50.0 mg, 0.060 mmol, 1 equiv) in CH_2Cl_2 (1.2 mL). The resulting biphasic mixture was vigorously stirred under air at 23 °C in the dark for 2 h, then diluted with CH_2Cl_2 (5 mL) and distilled H_2O (5 mL). The aqueous layer was extracted with CH_2Cl_2 (3 × 5 mL), then the combined organic phases were filtered over Celite® washing with additional CH_2Cl_2. The filtrate was concentrated and dried under high vacuum affording (*R*)-**Ag2** (40.0 mg, 0.042 mmol, 71% yield) as a pale beige powder. **M.p.** 215 °C (dec.). **^{1}H NMR** (500 MHz, CD_2Cl_2) δ 7.97 (d, *J* = 8.1 Hz, 1H), 7.93–7.91 (m, 2H), 7.85 (s, 1H), 7.51 (t, *J* = 7.6 Hz, 1H), 7.48 (t, *J* = 7.2 Hz, 1H), 7.32–7.32 (m, 3H), 7.18 (d, *J* = 8.5 Hz, 1H), 7.15–7.14 (m, 1H), 7.12–7.08 (m, 3H), 2.99–2.76 (m, 4H), 2.75–2.67 (m, 1H), 2.66–2.57 (m, 1H), 2.11 (s, 3H), 1.36 (br d, *J* = 6.6 Hz, 3H), 1.28–1.08 (m, 27H), 0.98 (d, *J* = 6.8 Hz, 3H), 0.94 (d, *J* = 6.8 Hz, 3H). **^{13}C NMR** (126 MHz, CD_2Cl_2, listed as observed) δ 150.3, 150.0, 149.3, 148.8, 148.6, 147.5, 147.3, 147.2, 146.6, 146.5, 133.0, 132.5, 132.4, 132.2, 131.4, 131.3, 131.0, 128.6, 128.5, 127.6, 127.4, 126.6, 126.0, 125.9, 122.8, 121.9, 121.4, 121.0, 116.8 (br s), 41.9, 34.8, 34.5, 31.8, 31.5, 31.40, 31.7, 26.9, 26.8, 25.0, 24.8, 24.7, 24.4, 24.3, 24.13, 24.05, 23.6, 22.9. **^{31}P NMR** (202 MHz, CD_2Cl_2) δ 9.3. **HRMS** (MALDI +, pyrene, CH_2Cl_2) calculated for $[C_{51}H_{59}AgNO_5PS]^+$ $[M]^{\cdot+}$ 935.2897 *m/z*; found 935.2897 *m/z*. **Elemental analysis** calculated for $C_{51}H_{59}AgNO_5PS$: C 65.38, H 6.35, N 1.49, S 3.42; found: C 66.12 ± 0.35, H 6.65 ± 0.30, N 1.42 ± 0.30, S 3.20 ± 0.35. **$[\alpha]^{25.2}_D$** −20 (c 0.68, $CHCl_3$).

(*R*)-Ag3

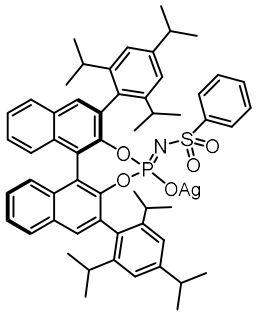

Whenever possible, all steps of this procedure were carried out in the dark. Ag_2CO_3 (8.8 mg, 0.032 mmol, 0.5 equiv) and distilled H_2O (1.2 mL) were added to a stirred pale yellow solution of phosphoramidate *(R)*-**2.49** (57.0 mg, 0.064 mmol, 1 equiv) in CH_2Cl_2 (1.2 mL). The resulting biphasic mixture was vigorously stirred under air at 23 °C in the dark for 2.5 h, then diluted with CH_2Cl_2 (5 mL) and distilled H_2O (5 mL). The aqueous layer was extracted with CH_2Cl_2 (3 × 5 mL), then the combined organic phases were filtered over Celite® washing with additional CH_2Cl_2. The filtrate was concentrated and dried under high vacuum affording (*R*)-**Ag3** (60.0 mg, 0.060 mmol, 94% yield) as a pale beige powder. **M.p.** 221 °C (dec.). **^{1}H NMR** (500 MHz, CD_2Cl_2) δ 7.92 (d, *J* = 8.2 Hz, 2H), 7.86 (s, 1H), 7.82 (s, 1H), 7.50–7.47 (m, 2H), 7.29–7.10 (m, 10H), 6.94 (t, *J* = 7.6 Hz, 2H), 6.89 (br s, 1H), 3.05 (septet, *J* = 6.9 Hz, 1H), 2.95–2.80 (m, 2H), 2.74–2.67 (m, 1H), 2.66–2.54 (m, 1H), 2.43–2.25 (m, 1H), 1.40–1.32 (m, 9H), 1.21 (d, *J* = 6.7 Hz, 6H), 1.15 (d, *J* = 6.8 Hz, 3H), 1.10–1.04 (m, 6H), 1.00–0.96 (m, 6H), 0.94 (d, *J* = 6.8 Hz, 3H), 0.92 (d, *J* = 6.8 Hz, 3H). **^{13}C NMR** (126 MHz, CD_2Cl_2, listed as observed) δ 149.6, 149.4 (br s), 148.5, 148.3, 147.8, 147.14, 147.07, 146.5, 146.4, 144.5, 133.0, 132.92, 132.87, 132.8, 132.7 (br s), 132.2, 132.1, 131.5 (br s),131.3, 131.04, 130.99, 129.1, 128.6, 128.4, 127.6, 127.5, 126.7, 126.6, 126.0, 125.94, 125.86, 123.0, 122.1, 121.9 (br s), 121.5, 118.4 (br s), 34.8, 34.1, 31.6, 31.50, 31.47, 31.4, 27.1, 26.5, 25.0, 24.91, 24.88, 24.7, 24.6 (br s), 24.4, 23.9, 23.1, 22.7. **^{31}P NMR** (202 MHz, CD_2Cl_2) δ 9.9. **HRMS** (MALDI +, pyrene, CH_2Cl_2) calculated for $[C_{56}H_{61}AgNO_5PS]^+$ $[M]^+$ 977.3054 *m/z*; found 977.3054 *m/z*. **Elemental analysis** calculated for $C_{56}H_{61}AgNO_5PS$: C 67.33, H 6.15, N 1.40, S 3.21; found: C 66.97 ± 0.35, H 6.29 ± 0.30, N 1.43 ± 0.30, S 3.15 ± 0.35. **$[\alpha]^{25.3}_D$** +16 (c 1.0, $CHCl_3$).

(*R*)-Ag4

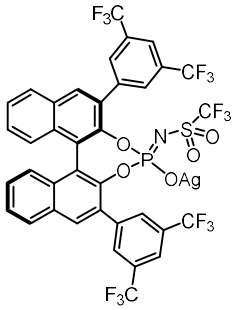

Whenever possible, all steps of this procedure were carried out in the dark. Ag_2CO_3 (16.5 mg, 0.060 mmol, 0.5 equiv) and distilled H_2O (1.5 mL) were added to a stirred pale-yellow solution of phosphoramidate *(R)*-**2.50** (108.0 mg, 0.120 mmol, 1 equiv) in CH_2Cl_2 (1.5 mL). The resulting biphasic mixture was vigorously stirred under air at 23 °C in the dark for 3 h, then diluted with CH_2Cl_2 (5 mL) and distilled H_2O (5 mL). The aqueous layer was extracted with CH_2Cl_2 (3 × 5 mL), then the combined organic phases were filtered over Celite® washing with additional CH_2Cl_2. The filtrate was concentrated and dried under high vacuum affording (*R*)-**Ag4** (111.0 mg, 0.110 mmol, 92% yield) as a pale beige powder. **M.p.** 195 °C (dec.). **^{1}H NMR** (500 MHz, CD_3CN) δ 8.51 (s, 2H), 8.34 (s, 2H), 8.26 (d, *J* = 6.8 Hz, 2H), 8.13–8.08 (m, 2H), 8.03 (app d, *J* = 4.7 Hz, 2H), 7.58 (app q, *J* = 4.7 Hz, 2H), 7.43–7.37 (m, 2H), 7.35 (d, *J* = 8.3 Hz, 1H), 7.29 (d, *J* = 8.5 Hz, 1H). **^{13}C NMR** (126 MHz, CD_3CN) δ 146.4 (d, *J* = 11.2 Hz), 145.7 (d, *J* = 9.2 Hz), 140.7 (d, *J* = 7.3 Hz), 133.4 (dd, *J* = 8.6, 1.1 Hz), 132.9, 132.64, 132.56, 132.54, 132.28, 132.26, 132.2, 132.1 (dd, *J* = 4.0, 1.1 Hz), 132.0 (d, *J* = 12.8 Hz), 131.7–131.6 (m), 131.5, 131.4, 130.8, 130.7, 129.8, 128.3 (d, *J* = 13.0 Hz), 127.4 (d, *J* = 12.7 Hz), 127.1 (d, *J* = 11.2 Hz), 124.7 (qd, *J* = 272.0, 8.9 Hz), 124.1 (dd, *J* = 47.3, 2.5 Hz), 122.4 (septet, *J* = 3.8 Hz), 122.2 (septet, *J* = 3.6 Hz), 121.0 (qd, *J* = 321.0, 5.2 Hz). **^{31}P NMR** (202 MHz, CD_3CN) δ 3.7. **^{31}P NMR** (162 MHz, CD_2Cl_2) δ 6.7. **^{19}F NMR** (471 MHz, CD_3CN) δ −63.10 (6F), −63.12 (6F), −80.9 (3F). **^{19}F NMR** (376 MHz, CD_2Cl_2) δ −63.1 (6F), −63.2 (6F), −80.5 (3F). **HRMS** (MALDI +, pyrene, CH_2Cl_2) calculated for

$[C_{37}H_{16}AgF_{15}NNaO_5PS]^+$ $[M+Na]^+$ 1031.9190 *m/z*; found 1031.9172 *m/z*. **$[\alpha]^{25.4}_D$** −183 (c 1.0, $CHCl_3$).

(*R*)-Ag5

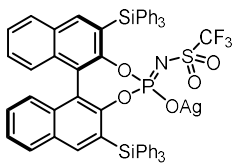

Whenever possible, all steps of this procedure were carried out in the dark. Ag_2CO_3 (12.3 mg, 0.045 mmol, 0.5 equiv) and distilled H_2O (1.0 mL) were added to a stirred pale-yellow solution of phosphoramidate *(R)*-**2.51** (89.0 mg, 0.089 mmol, 1 equiv) in CH_2Cl_2 (1.0 mL). The resulting biphasic mixture was vigorously stirred under air at 23 °C in the dark for 3 h, then diluted with CH_2Cl_2 (5 mL) and distilled H_2O (5 mL). The aqueous layer was extracted with CH_2Cl_2 (3 × 5 mL), then the combined organic phases were filtered over Celite® washing with additional CH_2Cl_2. The filtrate was concentrated and dried under high vacuum affording (*R*)-**Ag5** (88.5 mg, 0.080 mmol, 90% yield) as a pale beige powder. **M.p.** 246–250 °C (dec.). **^{1}H NMR** (500 MHz, CD_2Cl_2) δ 8.22 (s, 1H), 8.13 (s, 1H), 7.91 (d, *J* = 8.2 Hz, 1H), 7.77 (d, *J* = 8.1 Hz, 1H), 7.71–7.66 (m, 6H), 7.56–7.48 (m, 7H), 7.43–7.34 (m, 2H), 7.32–7.28 (m, 1H), 7.25–7.10 (m, 20H). **^{13}C NMR** (126 MHz, CD_2Cl_2, listed as observed except for CF_3 qd) δ 151.8, 151.7, 151.54, 151.46, 142.45, 142.42, 137.4, 136.7, 135.1, 134.9, 134.6, 134.2, 131.3, 131.1, 129.2, 129.1, 129.0, 128.6 (br s), 128.4, 128.3, 127.4, 126.81, 126.75, 126.23, 126.20, 125.85, 125.82, 125.77 (br s), 122.1, 121.8, 120.0 (qd, *J* = 321.7, 7.6 Hz). **^{31}P NMR** (162 MHz, CD_2Cl_2) δ 4.1. **^{19}F NMR** (376 MHz, CD_2Cl_2) δ −79.3. **HRMS** (MALDI +, pyrene, CH_2Cl_2) calculated for $[C_{57}H_{40}Ag_2F_3NO_5PSSi_2]^+$ $[M+Ag]^+$ 1207.9952 *m/z*; found 1207.9967 *m/z*. **Elemental analysis** calculated for $C_{57}H_{40}AgF_3NO_5PSSi_2$: C 62.07, H 3.66, N 1.27, S 2.91; found: C 62.44 ± 0.35, H 3.98 ± 0.30, N 1.29 ± 0.30, S 2.69 ± 0.35. **$[\alpha]^{24.9}_D$** −94 (c 1.0, $CHCl_3$).

(*R*)-Ag6

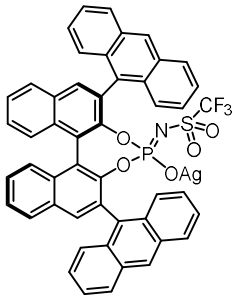

Whenever possible, all steps of this procedure were carried out in the dark. Ag_2CO_3 (49.9 mg, 181 μmol, 0.5 equiv) and distilled H_2O (3.5 mL) were added to a stirred pale brown solution of phosphoramidate *(R)*-**2.52** (300 mg, 361 μmol, 1 equiv) in CH_2Cl_2 (3.5 mL). The resulting biphasic mixture was vigorously stirred under air at 23 °C in the dark for 3 h, then diluted with CH_2Cl_2 (75 mL) and distilled H_2O (15 mL). Pale beige flocks formed in the organic phase, but all material solubilized when warmed up to 30 °C. Layers were separated and the aqueous one was extracted with CH_2Cl_2 (3 × 10 mL), then the combined organic phases were washed with distilled water (15 mL) and filtered over Celite® washing with additional CH_2Cl_2. The filtrate was concentrated and dried under high vacuum affording (*R*)-**Ag6** (315 mg, 336 μmol, 93% yield) as a dark beige/military green powder. Traces of EtOAc (3 mol % judging by ^{1}H NMR integrations, carried over from the phosphoramidate, corresponding to <0.5%$_{w/w}$), H grease and silicon grease could not be removed, therefore the salt was used as such. **M.p.** 330 °C (dec.). **^{1}H NMR** (100 MHz, 38 mg in 0.6 mL $CDCl_3$) δ 8.40 (s, 1H), 8.07–7.91 (m, 7H), 7.82 (d, *J* = 8.5 Hz, 1H), 7.79 (d, *J* = 8.4 Hz, 1H), 7.71 (d, *J* = 8.5 Hz, 1H), 7.66–7.48 (m, 8H), 7.43–7.37 (m, 2H), 7.35–7.21 (m, 3H), 7.13 (d, *J* = 8.4 Hz, 1H), 6.87 (br s, 1H), 5.78–5.60 (m, 2H). **^{13}C NMR** (126 MHz, 38 mg in 0.6 mL $CDCl_3$, listed as observed except for CF_3 q) δ 147.6, 147.5, 146.3, 146.2, 134.5, 133.2, 133.1, 132.8, 132.0, 131.9, 131.7, 131.6, 131.6, 131.48, 131.45, 131.3, 131.13, 131.07, 130.95, 130.92, , 130.4, 129.94, 129.92, 129.8, 129.4 (br s), 128.8, 128.7, 128.6, 128.1, 127.8, 127.6, 127.5, 127.3, 127.2, 127.1, 127.0, 126.5, 126.4, 126.3, 126.1, 125.90, 125.86, 124.7, 123.14, 123.12, 123.07 (br s), 122.01, 121.99, 118.8 (qd, *J* = 321.8, 2.5 Hz), 118.4 (br s), 116.1 (br s). **^{31}P NMR** (162 MHz, 38 mg in 0.6 mL $CDCl_3$) δ 6.5. **^{19}F NMR** (376 MHz, 38 mg in 0.6 mL $CDCl_3$) δ −80.1. **HRMS**

(MALDI +, pyrene, CH_2Cl_2) calculated for $[C_{49}H_{28}AgF_3NO_5PS]^+$ $[M]^+$ 937.0423 *m/z*; found 937.0448 *m/z*. **Elemental analysis** calculated for $C_{49}H_{28}AgF_3NO_5PS$: C 62.70, H 3.01, N 1.49, S 3.42; found: C 61.76 ± 0.35, H 3.26 ± 0.30, N 1.62 ± 0.30, S 3.36 ± 0.35. **$[\alpha]^{26.4}_D$** −225 (c 1.0, $CHCl_3$, *(R)*-**Ag6**).

An analogous procedure was followed for the synthesis of (*S*)-**Ag6** where commercially available (*S*)-**2.52** was employed. All data matched that of its (*R*)-enantiomer but the alphaD for which: **$[\alpha]^{26.4}_D$** +242 (c 1.0, $CHCl_3$, *(S)*-**Ag6**).

(*R*)-Na6

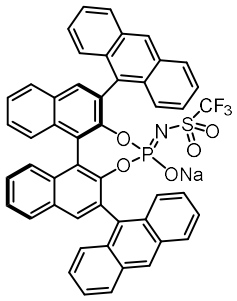

Whenever possible, all steps of this procedure were carried out in the dark. Finely ground Na_2CO_3 (6.5 mg, 61 µmol, 0.5 equiv) and distilled H_2O (1.2 mL) were added to a pale brown solution of phosphoramidate *(R)*-**2.52**100 mg, 120 µmol, 1 equiv) in CH_2Cl_2 (1.2 mL). The resulting biphasic mixture was vigorously stirred under air at 23 °C in the dark for 5 minutes, after which a white solid precipitated and additional H_2O (1.0 mL) and CH_2Cl_2 (1.0 mL) were added. After stirring for 1 h, the reaction mixture was diluted with CH_2Cl_2 (40 mL) and distilled H_2O (15 mL). Brine (10 mL) was added to remove the white interphase between the two layers, and phases were separated. The aqueous layer was extracted with CH_2Cl_2 (3 × 15 mL), then the combined organic phases were dried over Na_2SO_4, filtered, concentrated under reduced pressure and dried under high vacuum affording (*R*)-**Na6** (92.1 mg, 108 µmol, 90% yield) as a beige powder. Traces of EtOAc (5 mol % judging by ^{1}H NMR integrations, carried over from the phosphoramidate, corresponding to 0.5%$_{w/w}$) and traces of H grease could not be removed, therefore the salt was used as such. **M.p.** 342 °C (dec.). **^{1}H NMR** (500 MHz, 10 mg in 0.5 mL CD_2Cl_2) δ 8.38 (s, 1H), 8.16 (s, 1H), 8.10–8.06 (m, 3H), 8.03 (d, *J* = 8.2 Hz, 1H), 7.97–7.92 (m, 1H), 7.90 (d, *J* = 8.5 Hz, 1H), 7.84 (d, *J* = 8.5 Hz, 1H), 7.79 (d, *J* = 8.4 Hz, 1H), 7.78 (dd, *J* = 8.2, 0.7 Hz, 1H), 7.77–7.73 (m, 1H), 7.67–7.61 (m, 3H), 7.59 (dd, *J* = 8.8, 0.8 Hz, 1H), 7.56 (ddd, *J* = 8.2, 7.0, 1.2 Hz, 1H), 7.53–7.48 (m, 2H), 7.47–7.43 (m, 2H), 7.42–7.38 (m, 1H), 7.36–7.24 (m, 4H), 6.28–6.23 (m, 1H), 6.19–6.14 (m, 1H). **^{13}C NMR** (126 MHz, 10 mg in 0.5 mL CD_2Cl_2, listed as observed except for CF_3 q) δ 147.6, 147.5, 146.6, 146.5, 134.7, 134.0, 133.3, 133.1, 132.1, 132.0, 131.92, 131.87, 131.8, 131.6, 131.5, 131.1, 131.00, 130.98, 130.95, 130.8, 130.4, 129.7, 129.3, 129.0, 128.9, 128.5, 128.4, 128.2, 128.01, 127.96, 127.8, 127.63, 127.60, 127.4, 126.7, 126.52, 126.49, 126.42, 126.35, 126.2, 126.0, 125.8, 125.3, 125.2, 125.1, 123.32, 123.30, 122.53, 122.51, 119.0 (q, *J* = 321.6 Hz). **^{31}P NMR** (202 MHz, 10 mg in 0.5 mL CD_2Cl_2) δ 6.8. **^{19}F NMR** (376 MHz, 10 mg in 0.5 mL CD_2Cl_2) δ −81.5. **HRMS** (ESI +) calculated for $[C_{49}H_{28}F_3NNa_2O_5PS]^+$ $[M+Na]^+$ 876.1168 *m/z*; found 876.1146 *m/z*. **$[\alpha]^{26.4}_D$** +29 (c 1.0, $CHCl_3$).

(*R*)-Cu6

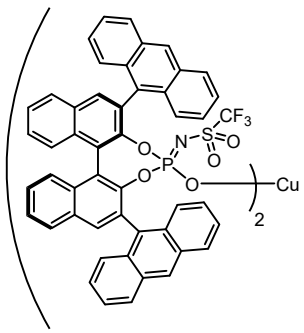

Whenever possible, all steps of this procedure were carried out in the dark. Adapting a reported procedure,[72] copper(II) chloride dihydrate (4.6 mg, 27 µmol, 1 equiv) was added to a stirred yellow solution of silver phosphoramidate salt *(R)*-**Ag6** (50.0 mg, 53.3 µmol, 2 equiv) in 1:1 CH_3CN:CH_2Cl_2 (2.0 mL). The resulting biphasic mixture was vigorously stirred under air at 23 °C in the dark for 21 h, then filtered over Celite® washing with minimal CH_2Cl_2. The filtrate was concentrated, the dark yellow residue dissolved in CH_2Cl_2 (1 mL) and filtered again over Celite® washing with minimal CH_2Cl_2. The filtrate was evaporated and dried under high vacuum affording (*R*)-**Cu6** (41.0 mg, 23.8 µmol, 88% yield)

as a pale brown powder. Due to the paramagnetic nature of Cu(II), NMR analysis was not informative. **M.p.** 322–340 °C. **HRMS** (MALDI +, pyrene, CH_2Cl_2) calculated for $[C_{98}H_{56}CuF_6N_2O_{10}P_2S_2]^+$ $[M]^+$ 1723.2046 *m/z*; found 1723.2057 *m/z*. **$[\alpha]^{25.2}_D$** −55 (c 0.44, $CHCl_3$, unstable readings, average of 5 datasets, each with 10 measurements). **$[\alpha]^{26.2}_D$** −88 (c 0.77, $CHCl_3$ unstable readings, average of 4 datasets, each with 10 measurements).

(*R*)-Ag7

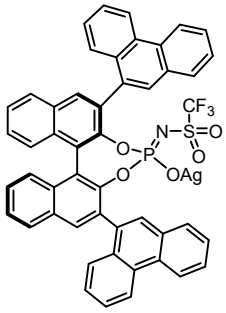

Whenever possible, all steps of this procedure were carried out in the dark. Following a reported procedure,[3] Ag_2CO_3 (9.8 mg, 35.6 μmol, 0.5 equiv) and distilled H_2O (0.7 mL) were added to a stirred solution of phosphoramidate *(R)*-**2.53** (59.3 mg, 71.3 μmol, 1 equiv) in CH_2Cl_2 (0.7 mL). The resulting biphasic mixture was vigorously stirred under air at 23 °C in the dark for 4 h, then diluted with CH_2Cl_2 (5 mL) and distilled H_2O (5 mL). The aqueous layer was extracted with CH_2Cl_2 (3 × 5 mL), then the combined organic phases were filtered over Celite® washing with additional CH_2Cl_2. The filtrate was concentrated and dried under high vacuum affording (*R*)-**Ag7** (66.5 mg, 75% weight purity, 53.1 μmol, 74% yield) as brown powder. Traces of grease could not be removed and the compound was used as such. (*R*)-**Ag7** was a mixture of rotamers in solution due to the restricted rotation of the 3,3'-phenanthyl groups. C_6D_6 was chosen as solvent because it was found that less rotamers are present in aromatic solvents. **M.p.** 189–192 °C. **IR** (film from $CHCl_3$, cm^{-1}) ν 2923, 2854, 1450, 1195, 1092, 995, 750. **^{1}H NMR** (300 MHz, 16 mg in 0.5 mL C_6D_6) δ 8.73 (d, *J* = 17.4 Hz, 1H), 8.66 – 8.41 (m, 2H), 8.41 – 8.02 (m, 3H), 8.01 – 7.90 (m, 1H), 7.90 – 7.76 (m, 2H), 7.76 – 7.59 (m, 6H), 7.52 (q, *J* = 7.7 Hz, 2H), 7.45 – 7.19 (m, 8H), 7.13 – 7.03 (m, 3H). **^{13}C NMR** (126 MHz, 16 mg in 0.5 mL C_6D_6, peaks listed as observed, no couplings reported due to complexity) δ 147.7, 147.6, 147.5, 147.4, 146.6, 146.55, 146.47, 141.5, 137.6, 135.9, 134.5, 134.0, 133.8, 133.6, 133.4, 133.3, 133.2, 133.1, 132.9, 132.7, 132.55, 132.49, 132.4, 132.3, 132.1, 131.9, 131.84, 131.81, 131.77, 131.5, 131.4, 131.1, 130.9, 130.8, 130.7, 130.4, 130.0, 129.3, 129.2, 129.1, 128.89, 128.86, 127.8, 127.6, 127.5, 127.41, 127.4¡35, 127.3, 127.2, 127.1, 127.02, 126.98, 126.8, 126.69, 126.66, 126.6, 126.4, 126.21, 126.16, 126.11, 126.06, 126.0, 125.9, 123.3, 123.24, 123.16, 122.8, 122.6, 122.4, 122.3. **^{31}P NMR** (122 MHz, 16 mg in 0.5 mg C_6D_6) δ 3.3, 3.0. **^{19}F NMR** (282 MHz, 16 mg in 0.5 mL C_6D_6) δ −79.3, −80.1. **HRMS** (ESI +) calculated for $[C_{49}H_{28}AgF_3NNaO_5PS]^+$ $[M + Na]^+$ 960.0321 *m/z*; found 960.0316 *m/z*. **Elemental analysis** calculated for $C_{49}H_{28}AgF_3NO_5PS$: C 62.70, H 3.01, N 1.49, S 3.42, found: C 62.74 ± 0.35, H 3.95 ± 0.30, N 1.54 ± 0.30, S 3.19 ± 0.35. **$[\alpha]^{27.3}_D$** −102 (c 0.80, $CHCl_3$).

(*R*)-Ag8

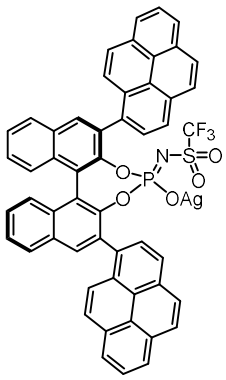

Whenever possible, all steps of this procedure were carried out in the dark. Following a reported procedure,[3] Ag_2CO_3 (9.7 mg, 35.2 μmol, 0.5 equiv) and distilled H_2O (0.7 mL) were added to a stirred solution of phosphoramidate *(R)*-**2.54** (62.0 mg, 70.5 μmol, 1 equiv) in CH_2Cl_2 (0.7 mL). The resulting biphasic mixture was vigorously stirred under air at 23 °C in the dark for 3 h, then diluted with CH_2Cl_2 (5 mL) and distilled H_2O (5 mL). The aqueous layer was extracted with CH_2Cl_2 (3 × 5 mL), then the combined organic phases were filtered over Celite® washing with additional CH_2Cl_2. The filtrate was concentrated and dried under high vacuum affording (*R*)-**Ag8** (60.6 mg, 87% weight purity, 53.4 μmol, 76% yield) as a yellow powder. Traces of grease could not be removed, and the compound was used as such.

(*R*)-**Ag8** was a mixture of rotamers in solution due to the restricted rotation of the 3,3'-pyren-1-yl groups. C_6D_6 was chosen as solvent because it was found that less rotamers are present in aromatic solvents. **M.p.** 216 °C (decomposition). **IR** (film from $CHCl_3$, cm^{-1}) ν 2924, 2853, 1197, 846. **^{1}H NMR** (400 MHz, 22 mg in 0.5 mL C_6D_6) δ 8.90 – 8.72 (m, 1H), 8.52 – 8.35 (m, 1H), 8.22 – 8.08 (m, 1H), 7.99 (t, *J* = 8.4 Hz, 1H), 7.96 – 7.80 (m, 4H), 7.80 – 7.55 (m, 11H), 7.55 – 7.34 (m, 4H), 7.25 (dq, *J* = 12.6, 6.9 Hz, 3H), 7.13 – 7.06 (m, 2H). **^{13}C NMR** (101 MHz, 22 mg in 0.5 mL C_6D_6, peaks listed as observed, no couplings reported due to complexity): δ 133.6, 133.5, 133.4, 133.2, 133.0, 132.6, 132.4, 132.1, 131.8, 131.6, 131.4, 131.2, 131.0, 130.8, 130.2, 130.1, 129.1, 129.0, 128.6, 127.4, 127.2, 127.0, 126.4, 126.2, 126.0, 125.8, 125.5, 125.4, 125.2, 125.2, 124.9. **^{31}P NMR** (162 MHz, 22 mg in 0.5 mL C_6D_6) δ 7.7, 7.2, 6.3. **^{19}F NMR** (376 MHz, 22 mg in 0.5 mL C_6D_6) δ −78.7, −80.3. **HRMS** (ESI +) calculated for $[C_{53}H_{28}AgF_3NNaO_5PS]^+$ $[M + Na]^+$ 1008.0321 *m/z*; found 1008.0354 *m/z*. **Elemental analysis** calculated for $C_{53}H_{28}AgF_3NO_5PS$: C 64.52, H 2.86, N 1.42, S 3.25, found: C 64.09 ± 0.35, H 3.58 ± 0.30, N 1.52 ± 0.30, S 3.16 ± 0.35. **$[\alpha]^{27.5}_D$** −218 (c 0.8, $CHCl_3$).

(*R*)-Ag9

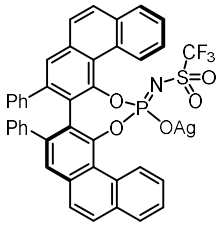

Whenever possible, all steps of this procedure were carried out in the dark. Following a reported procedure,[3] Ag_2CO_3 (18.6 mg, 67.6 μmol, 0.5 equiv) and distilled H_2O (1.4 mL) were added to a stirred solution of phosphoramidate *(R)*-**2.57** (98.9 mg, 0.135 mmol, 1 equiv) in CH_2Cl_2 (1.4 mL). The resulting biphasic mixture was vigorously stirred under air at 23 °C in the dark for 3 h, then diluted with CH_2Cl_2 (5 mL) and distilled H_2O (5 mL). The aqueous layer was extracted with CH_2Cl_2 (3 × 5 mL), then the combined organic phases were filtered over Celite® washing with additional CH_2Cl_2. The filtrate was concentrated and dried under high vacuum affording (*R*)-**Ag9** (92.8 mg, 0.111 mmol, 82% yield) as a beige powder. **M.p.** 273 °C (decomposition). **IR** (film from $CHCl_3$, cm^{-1}) ν 3057, 2924, 332, 1200, 1128, 1087, 1018. **^{1}H NMR** (500 MHz, CD_2Cl_2): δ 10.06 (d, *J* = 8.3 Hz, 1H), 9.80 (d, *J* = 8.2 Hz, 1H), 8.22 (dd, *J* = 12.5, 8.1 Hz, 2H), 8.06 – 7.92 (m, 4H), 7.78 – 7.64 (m, 2H), 7.40 (t, *J* = 7.4 Hz, 1H), 7.28 (t, *J* = 7.5 Hz, 1H), 7.18 – 7.02 (m, 4H), 7.02 – 6.93 (m, 4H), 6.67 – 6.61 (m, 2H), 6.61 – 6.53 (m, 2H). **^{13}C NMR** (126 MHz, CD_2Cl_2): δ 148.3 (d, *J* = 10.8 Hz), 147.5 (d, *J* = 10.1 Hz), 142.5 (d, *J* = 12.8 Hz), 139.8 (d, *J* = 38.1 Hz), 135.4, 135.2, 135.2, 130.9, 130.3 (d, *J* = 34.3 Hz), 129.8, 129.7, 129.2, 129.1, 129.00, 128.9, 128.8, 128.33, 128.31, 128.15, 128.12, 127.7 (d, *J* = 2.4 Hz), 127.5 (d, *J* = 2.3 Hz), 127.2 (d, *J* = 10.7 Hz), 122.13 (d, *J* = 3.2 Hz), 122.07 (d, *J* = 2.6 Hz), 120.1 (q, *J* = 322.8 Hz). **^{31}P NMR** (202 MHz, CD_2Cl_2) δ 4.6. **^{19}F NMR** (471 MHz, CD_2Cl_2) δ −80.1. **HRMS** (ESI +) calculated for $[C_{41}H_{24}AgF_3NNaO_5PS]^+$ $[M + Na]^+$ 860.0008 *m/z*; found 860.0046 *m/z*. **Elemental analysis** calculated for $C_{41}H_{24}AgF_3NO_5PS$: C 58.73, H 2.89, N 1.67, S 3.82, found: C 57.88 ± 0.35, H 3.26 ± 0.30, N 1.70 ± 0.30, S 3.61 ± 0.35. **$[\alpha]^{27.2}_D$** −113 (c 0.24, $CHCl_3$).

(*R*)-Ag10

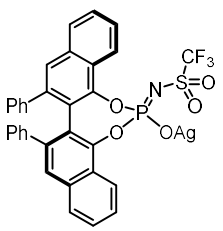

Whenever possible, all steps of this procedure were carried out in the dark. Following a reported procedure,[3] Ag_2CO_3 (18.6 mg, 67.6 μmol, 0.5 equiv) and distilled H_2O (1.4 mL) were added to a stirred solution of phosphoramidate *(R)*-**2.58** (85.0 mg, 0.135 mmol, 1 equiv) in CH_2Cl_2 (1.4 mL). The resulting biphasic mixture was vigorously stirred under air at 23 °C in the dark for 3 h, then diluted with CH_2Cl_2 (5 mL) and distilled H_2O (5 mL). The aqueous layer was extracted with CH_2Cl_2 (3 × 5 mL), then the combined organic phases were filtered over Celite® washing with additional CH_2Cl_2. The filtrate was concentrated and dried under high vacuum affording (*R*)-**Ag10** (92.0 mg, 0.120 mmol, 93%

yield) as a red powder. **M.p.** 266 °C (decomposition). **IR** (film from $CHCl_3$, cm^{-1}) ν 3055, 2925, 1487, 1363, 1275, 1211, 1081, 966, 759. **^{1}H NMR** (300 MHz, CD_2Cl_2): δ 8.55 (s, 1H), 8.40 (d, *J* = 8.0 Hz, 1H), 7.68 (d, *J* = 8.8 Hz, 2H), 7.49 (d, *J* = 12.7 Hz, 3H), 7.43 – 7.19 (m, 3H), 7.10 (q, *J* = 7.6 Hz, 2H), 6.89 (dt, *J* = 12.1, 7.3 Hz, 4H), 6.44 (dd, *J* = 13.0, 7.6 Hz, 4H). **^{13}C NMR** (75 MHz, CD_2Cl_2): δ 146.6, 145.6 (d, *J* = 9.6 Hz), 141.1 (d, *J* = 21.4 Hz), 140.0 (d, *J* = 12.3 Hz) 134.5, 129.3, 129.1, 128.2, 127.8, 127.4, 127.3, 127.2 (d, *J* = 4.3 Hz), 126.2, 125.7 (d, *J* = 2.8 Hz), 124.2, 123.2, CF_3 quartet overlapping/not emerging from baseline. **^{31}P NMR** (122 MHz, CD_2Cl_2) δ 3.9. **^{19}F NMR** (282 MHz, CD_2Cl_2) δ −78.5. **HRMS** (ESI +) calculated for $[C_{33}H_{20}AgF_3NNaO_5PS]^+$ [M + Na]$^+$ 759.9695 *m/z*; found 759.9709 *m/z*. **Elemental analysis** calculated for $C_{33}H_{20}AgF_3NO_5PS$: C 53.68, H 2.73, N 1.90, S 4.34, found: C 54.17 ± 0.35, H 3.20 ± 0.30, N 1.98 ± 0.30, S 4.28 ± 0.35. **$[\alpha]^{27.2}_D$** −622 (c 0.83, $CHCl_3$).

Synthesis of substrates [4+2]

Enynes **2.59a**, **2.59d**, **2.59h**, **2.59i**, **2.59j**, **2.59k**, **2.59l**, **2.59m**, **2.59n**, **2.59o, 2.59s** and **2.59t** were prepared following literature procedures[28e, 78] and their spectroscopic data matched the previously reported ones.

2-(3-Methylbut-2-en-1-yl)-2-(3-phenylprop-2-yn-1-yl)propane-1,3-diol (2.81)

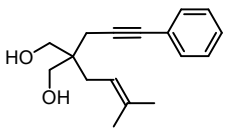

Following a literature procedure,[79] under Ar a 100-mL 2-neck flask was charged with lithium aluminium hydride (970 mg, 25.6 mmol, 4.27 equiv) and Et_2O (60 mL). The grey suspension was cooled to 0 °C before adding enyne **2.50h**[78] dropwise (1.88 g, 5.98 mmol, 1 equiv), rinsing with Et_2O (2 × 2 mL). The ice bath was removed, and the reaction mixture stirred at room temperature for 3 h. Then the reaction was carefully quenched under Ar flow by slowly adding H_2O (1 mL), 15%$_{w/w}$ aqueous NaOH (1 mL) and H_2O (3 mL). Since bubbling was still observed, additional water was added (5 mL), until gas evolution ceased. The mixture was stirred for 15 minutes, $MgSO_4$ was added and the mixture stirred for other 15 minutes. The precipitate was removed by filtration through Celite® washing with EtOAc and the solvent was evaporated. The crude residue was purified by automated FCC (dry load, CyH:EtOAc 90:10 to 0:100, product eluting in CyH:EtOAc 40:60). Diol **2.81** (1.53 g, 5.92 mmol, 99% yield) was obtained as a yellow oil that solidified to a pale beige solid upon standing. **M.p.** 54 °C. **IR** (film from $CDCl_3$, cm^{-1}) υ 3364 (broad, strong), 2966, 2914, 2882, 1490, 1442, 1030, 756, 691. **^{1}H NMR** (500 MHz, $CDCl_3$) δ 7.41–7.37 (m, 2H), 7.30–7.37 (m, 2H), 5.24–5.19 (m, 1H), 3.74 (d, *J* = 10.8 Hz, 2H), 3.69 (d, *J* = 11.0 Hz, 2H), 2.60–2.20 (m, 4H, 2O<u>H</u> + C<u>H</u>$_2$), 2.15 (d, *J* = 7.8 Hz, 2H), 1.74 (s, 3H), 1.68 (s, 3H). **^{13}C NMR** (75 MHz, $CDCl_3$) δ 135.3, 131.7, 128.4, 127.9, 123.8, 118.9, 87.0, 83.1, 68.1, 43.4, 30.5, 26.3, 22.6, 18.1. **HRMS** (ESI +) calculated for $[C_{17}H_{22}NaO_2]^+$ [M+Na]$^+$ 281.1512 *m/z*; found 281.1504 *m/z*.

(((2-(3-Methylbut-2-en-1-yl)-2-(3-phenylprop-2-yn-1-yl)propane-1,3-diyl)bis(oxy)) bis(methylene))dibenzene (2.59b)

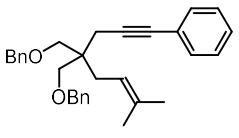

Following a modified literature procedure,[80] under Ar, sodium hydride (67.0 mg, 60% in mineral oil, 1.68 mmol, 2.16 equiv) was added to solution of diol **2.81** (200 mg, 1 equiv, 774 μmol) in anhydrous DMF (3 mL) kept at 0 ºC. The resulting off-white suspension was left stirring for 30 min at the same temperature before dropwise addition of benzyl bromide (202 μL, 1.70 mmol, 2.20 equiv) at 0 ºC, then it was warmed up to 23 ºC. After 1.5 h, tetrabutylammonium iodide (14.3 mg,

78. Nieto-Oberhuber, C.; López, S.; Echavarren, A. M. *J. Am. Chem. Soc*. **2005**, *127*, 6178–6179.
79. Surendra, K.; Corey, E. J. *J. Am. Chem. Soc.* **2014**, *136*, 10918–10920.
80. Trieselmann, T.; Hoffmann, R. W.; Menzel, K. *Eur. J. Org. Chem.* **2002**, 1292–1304.

38.7 μmol, 0.05 equiv) was added and the mixture stirred for 18 h at 23 ºC. The resulting pale beige suspension was quenched by addition of water (7 mL) and saturated aqueous NH_4Cl solution (7 mL). Et_2O (20 mL) was then added and layers were separated. The aqueous phase was extracted with Et_2O (3 × 20 mL) and the combined organic phases were dried over Na_2SO_4, filtered and evaporated. The crude product was purified by automated FCC (silica, CyH:EtOAc 100:0 to 90:10). Compound **2.59b** was obtained as a colorless oil (180 mg, 410 μmol, 53% yield). **IR** (film from $CDCl_3$, cm^{-1}) υ 3030, 2909, 2856, 1491, 1453, 1362, 1092,1072, 1028, 753, 733, 693. **^{1}H NMR** (300 MHz, $CDCl_3$) δ 7.45–7.25 (m, 15H), 5.25–5.10 (m, 1H), 4.53 (s, 4H), 3.47 (d, *J* = 8.9 Hz, 2H), 3.44 (d, *J* = 8.9 Hz, 2H), 2.49 (s, 2H), 2.24 (d, *J* = 7.8 Hz, 2H), 1.72 (s, 3H), 1.66 (s, 3H). **^{13}C NMR** (75 MHz, $CDCl_3$) δ 139.0, 134.6, 131.7, 128.4, 128.3, 127.6, 127.5, 127.4, 124.3, 119.5, 87.8, 82.4, 73.4, 72.2, 43.4, 30.4, 26.3, 23.2, 18.1. **HRMS** (ESI +) calculated for $[C_{31}H_{34}NaO_2]^+$ $[M+Na]^+$ 461.2451 *m/z*; found 461.2459 *m/z*.

(4,4-Bis((allyloxy)methyl)-7-methyloct-6-en-1-yn-1-yl)benzene (2.59c)

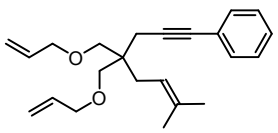

Under Ar, in a microwave vial, to solution of diol **2.81** (200 mg, 0.774 mmol, 1.0 equiv) in THF (2 mL) at room temperature were sequentially added sodium hydroxide (186 mg, 4.64 mmol, 6 equiv) and tetrabutylammonium iodide (5.7 mg, 16 μmol, 0.02 equiv). The vial was capped and allyl bromide (402 μL, 4.64 mmol, 6.0 equiv) was added dropwise. The reaction was stirred at 70 °C for 19 h. Since TLC (CyH:EtOAc 9:1) analysis indicated the presence of putative monoprotected diol, additional allyl bromide (402 μL, 4.64 mmol, 6.0 equiv) was added ad the reaction mixture stirred at 70 °C for 24 h. The reaction mixture was then cooled to room temperature and filtered through a sintered glass funnel washing with Et_2O (15 mL). To the filtrate, saturated NH_4Cl aqueous solution (15 mL) was added, layers were separated and the aqueous phase was extracted with Et_2O (2 × 20 mL). The combined organic phases were dried over Na_2SO4, filtered and evaporated. The crude product was purified by automated FCC (silica, CyH:EtOAc 100:0 to 94:6, product eluting in CyH:EtOAc 97:3). Compound **2.59c** was obtained as a yellow oil (163 mg, 0.482 mmol, 62% yield). **IR** (film from $CDCl_3$, cm^{-1}) υ 2970, 2910, 2856, 1490, 1442, 1137, 1086, 989, 922, 755, 691. **^{1}H NMR** (400 MHz, $CDCl_3$) δ 7.43–7.37 (m, 2H), 7.32–7.26 (m, 3H), 5.92 (ddt, *J* = 17.2, 10.6, 5.4 Hz, 2H), 5.29 (dq, *J* = 17.3, 1.7 Hz, 2H), 5.24–5.18 (m, 1H), 5.15 (dq, *J* = 10.4, 1.4 Hz, 2H), 4.00 (t, *J* = 1.5 Hz, 2H), 3.98 (t, *J* = 1.5 Hz, 2H), 3.42–3.34 (m, 4H), 2.44 (s, 2H), 2.20 (d, *J* = 7.9 Hz, 2H), 1.77–1.72 (m, 3H), 1.69–1.64 (m, 3H). **^{13}C NMR** (101 MHz, $CDCl_3$) δ 135.4, 134.5, 131.7, 128.3, 127.6, 124.4, 119.5, 116.3, 87.8, 82.4, 72.4, 72.0, 43.3, 30.4, 26.3, 23.2, 18.0. **HRMS** (ESI +) calculated for $[C_{23}H_{30}NaO_2]^+$ $[M+Na]^+$ 361.2138 *m/z*; found 361.2122 *m/z*.

2-(3-Methylbut-2-en-1-yl)-2-(3-phenylprop-2-yn-1-yl)propane-1,3-diyl bis(phenylcarbamate) (2.59e)

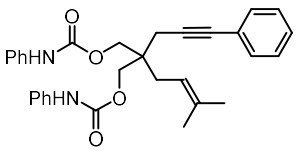

Under Ar, in a microwave vial, phenyl isocyanate (210 μL, 1.94 mmol, 2.5 equiv) was added to a stirred solution of diol **2.81** (200 mg, 774 μmol, 1.0 equiv) in anhydrous 1,2-DCE (7.0 mL). The reaction mixture was then stirred at 40 ºC for 23 h. The reaction mixture was evaporated and the crude residue was purified by FCC (silica, CyH:EtOAc 90:10 to 80:20) affording two fractions: the first one containing pure compound **2.59e** as a white solid (125 mg, 251 μmol, 33% yield) and the second one containing monoprotected diol and diphenylurea in 1:0.25 ratio (170 mg overall). This fraction was then resubjected to the reaction conditions using phenyl isocyanate (50 μL, 0.46 mmol, 1.3 equiv) in anhydrous 1,2-DCE (3.0 mL) at 70 °C for 24 h. The reaction mixture was then evaporated and the crude product was purified by FCC (silica, CyH:EtOAc 90:10 to 80:20, desired product eluting in 86:14), affording compound **2.59e** as a

white solid (129 mg, 260 μmol, 72% yield for the "resubmission" reaction). Combining both batches, compound **2.69e** was thus obtained as a white solid (254 mg, 511 μmol, 66% yield). **M.p.** 141 °C. **IR** (film from $CDCl_3$, cm^{-1}) υ 3317, 1706, 1600, 1535, 1501, 1444, 1314, 1217, 1062. **^{1}H NMR** (400 MHz, $CDCl_3$) δ 7.43–7.33 (m, 6H), 7.33–7.26 (m, 7H), 7.11–7.03 (m, 2H), 6.68 (br s, 2H), 5.27–5.15 (m, 1H), 4.23 (s, 4H), 2.53 (s, 2H), 2.28 (d, *J* = 7.8 Hz, 2H), 1.74 (s, 3H), 1.67 (s, 3H). **^{13}C NMR** (101 MHz, $CDCl_3$) δ 153.4, 137.8, 136.3, 131.8, 129.2, 128.4, 128.0, 123.7, 123.6, 118.9, 117.6, 85.5, 83.5, 66.9, 41.8, 30.5, 26.3, 23.4, 18.1. **HRMS** (ESI +) calculated for $[C_{31}H_{32}N_2NaO_4]^+$ $[M+Na]^+$ 519.2254 *m/z*; found 519.2240 *m/z*.

2-(3-Methylbut-2-en-1-yl)-2-(3-phenylprop-2-yn-1-yl)propane-1,3-diyl Bis(4-methylbenzene-sulfonate) (2.59f)

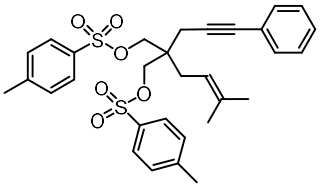

Under Ar, in a MW vial, a pale-yellow solution of *p*-toluenesulfonyl chloride (221 mg, 1.16 mmol, 3.0 equiv) in anhydrous pyridine (0.5 mL) was added to a solution of diol **2.81** (100 mg, 0.387 mmol, 1.0 equiv) in anhydrous pyridine (0.5 mL) at 23 °C. The resulting pale-yellow solution was stirred at 60 ºC for 20 h. Then, the yellow cloudy solution was cooled to room temperature, obtaining a yellow suspension. CH_2Cl_2 (10 mL) and 2.5 M aqueous HCl (10 mL) were added, layers were separated and the aqueous phase was extracted with CH_2Cl_2 (2 × 10 mL). The combined organic layers were dried over Na_2SO_4, filtered and evaporated. The crude product was purified by FCC (silica, CyH:CH_2Cl_2 50:50 to 10:90, product started eluting in CyH:CH_2Cl_2 25:75). The use of CH_2Cl_2 as a coeluent was found to be essential to avoid precipitation of the product during FCC, with negative impact on final yield. Compound **2.59f** was obtained as a white solid (172.6 mg, 0.305 mmol, 79% yield). **M.p.** 124 °C. **IR** (film from $CDCl_3$, cm^{-1}) υ 3556, 2916, 1598, 1491, 1358, 1189, 1175, 1097, 963, 839, 668. **^{1}H NMR** (400 MHz, $CDCl_3$) δ 7.79–7.72 (m, 4H), 7.32–7.27 (m, 6H), 7.26–7.23 (m, 1H), 7.20–7.15 (m, 2H), 4.92–4.83 (m, 1H), 3.88 (s, 4H), 2.37 (s, 6H), 2.33 (s, 2H), 2.11 (d, *J* = 7.8 Hz, 2H), 1.66–1.62 (m, 3H), 1.62–1.58 (m, 3H). **^{13}C NMR** (101 MHz, $CDCl_3$) δ 145.2, 137.4, 132.3, 131.7, 130.1, 128.3, 128.2, 128.1, 123.2, 116.2, 84.0, 83.9, 70.3, 42.2, 29.2, 26.2, 22.4, 21.8, 18.2. **HRMS** (ESI +) calculated for $[C_{31}H_{34}NaO_6S_2]^+$ $[M+Na]^+$ 589.1689 *m/z*; found 589.1668 *m/z*.

2,2-Dimethyl-5-(3-methylbut-2-en-1-yl)-5-(3-phenylprop-2-yn-1-yl)-1,3-dioxane (2.59g)

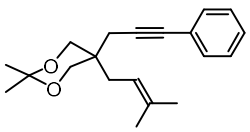

Following a modified literature procedure,[81] under Ar, 2,2-dimethoxypropane (0.67 mL, 5.42 mmol, 7.0 equiv) was added to a solution of diol **2.81** (200 mg, 0.774 mmol, 1.0 equiv) and pyridinium *p*-toluenesulfonate (19.5 mg, 77.4 μmol, 0.10 equiv) in anhydrous CH_2Cl_2 (7 mL). The resulting colorless solution was stirred at room temperature for 2 h. Then, saturated aqueous $NaHCO_3$ (20 mL) was added, and the aqueous phase was extracted with CH_2Cl_2 (3 × 20 mL). The combined organic layers were washed with brine (30 mL), dried over Na_2SO_4, filtered and evaporated. The crude product was purified by FCC (silica, CyH:EtOAc 100:0 to 94:6, product eluting in CyH:EtOAc 96:4). Compound **2.59g** was obtained as a white solid (166 mg, 0.557 mmol, 72% yield). **IR** (film from $CDCl_3$, cm^{-1}) υ 2990, 2966, 2934, 2912, 2860, 1490, 1451, 1442, 1371, 1195, 1067, 830, 756, 691. **^{1}H NMR** (500 MHz, $CDCl_3$) δ 7.41–7.34 (m, 2H), 7.29–7.24 (m, 3H), 5.14 (ddt, *J* = 9.3, 6.5, 1.4 Hz, 1H), 3.74 (d, *J* = 11.7 Hz, 2H), 3.69 (d, *J* = 11.7 Hz, 2H), 2.55 (s, 2H), 2.17 (d, *J* = 7.9 Hz, 2H), 1.75–1.72 (m, 3H), 1.69–1.66 (m, 3H), 1.42 (s, 6H). **^{13}C NMR** (126 MHz, $CDCl_3$) δ 135.6, 131.7, 128.3, 127.8, 124.0, 118.1, 98.2, 87.0, 83.1,

81. Katagiri, K.; Kodera, H.; Tayu, M.; Saito, N. *Chem. Lett.* **2019**, *48*, 768–770.

67.1, 36.9, 31.3, 26.2, 25.6, 23.5, 22.4, 18.1. **HRMS** (ESI +) calculated for $[C_{20}H_{26}NaO_2]^+$ $[M+Na]^+$ 321.1825 *m/z*; found 321.1823 *m/z*.

1-(4,4-Bis(methoxymethyl)-7-methyloct-6-en-1-yn-1-yl)-3-chlorobenzene (2.59p)

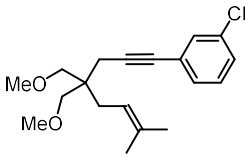

Following a modified literature procedure, under Ar, $[(Ph_3P)_2PdCl_2]$ (5.0 mg, 7.1 μmol, 0.01 equiv) and copper(I) iodide (2.7 mg, 14.3 μmol, 0.02 equiv) were sequentially added to a stirred yellow solution of 4,4-bis(methoxymethyl)-7-methyloct-6-en-1-yne[28e] (150 mg, 0.713 mmol, 1.0 equiv) in triethylamine (3.8 mL). To the resulting orange suspension was added 1-chloro-3-iodobenzene (106 μL, 0.856 mmol, 1.2 equiv) and the mixture was stirred at 23 °C for 22 h. The reaction was quenched with saturated NH_4Cl aqueous solution (20 mL). Layers were separated and the aqueous phase was extracted with EtOAc (3 × 30 mL). The combined organic layers were dried over Na_2SO_4, filtered and evaporated. The crude product was purified by FCC (silica, CyH:EtOAc 100:0 to 95:5). Compound **2.59p** was obtained as a pale yellow oil (227 mg, 0.707 mmol, 99% yield). **IR** (film from $CDCl_3$, cm^{-1}) υ 2976, 2886, 2809, 592, 1475, 1106, 782. **^{1}H NMR** (400 MHz, $CDCl_3$) δ 7.40 (t, *J* = 1.6 Hz, 1H), 7.32–7.20 (m, 3H), 5.23–5.15 (m, 1H), 3.37 (s, 6H), 3.32 (d, *J* = 9.0 Hz, 2H), 3.29 (d, *J* = 9.0 Hz, 2H), 2.42 (s, 2H), 2.17 (d, *J* = 7.9 Hz, 2H), 1.80–1.73 (m, 3H), 1.71–1.66 (m, 3H). **^{13}C NMR** (101 MHz, $CDCl_3$) δ 134.7, 134.1, 131.6, 129.8, 129.5, 127.9, 126.0, 119.3, 89.2, 81.1, 74.6, 59.4, 43.2, 30.4, 26.3, 23.1, 17.9. **HRMS** (ESI +) calculated for $[C_{19}H_{25}ClNaO_2]^+$ $[M+Na]^+$ 343.1435 *m/z*; found 343.1438 *m/z*.

1-(4,4-Bis(methoxymethyl)-7-methyloct-6-en-1-yn-1-yl)naphthalene (2.59q)

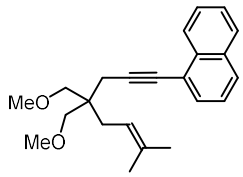

Following a modified literature procedure, [28e] under Ar, to a stirred yellow solution of 4,4-bis(methoxymethyl)-7-methyloct-6-en-1-yne[28e] (170 mg, 0.808 mmol, 1.0 equiv) in triethylamine (3.8 mL) at 20 °C were sequentially added $[(Ph_3P)_2PdCl_2]$ (5.7 mg, 8.08 μmol, 0.01 equiv) and copper(I) iodide (3.1 mg, 16.2 μmol, 0.02 equiv). To the resulting orange suspension was added 1-iodonaphtalene (142 μL, 0.970 mmol, 1.2 equiv) and the mixture was stirred at 20 °C for 22 h. The reaction was quenched with saturated NH_4Cl aqueous solution (20 mL). Layers were separated and the aqueous phase was extracted with EtOAc (3 × 30 mL). The combined organic layers were dried over Na_2SO_4, filtered and evaporated. The crude product was purified by FCC (silica, CyH:EtOAc 100:0 to 96:4). Compound **2.59q** was obtained as a pale-yellow oil (243 mg, 0.722 mmol, 89% yield). **IR** (film from $CDCl_3$, cm^{-1}) υ 2974, 2875, 2808, 1449, 1136, 1196, 1105, 798, 772. **^{1}H NMR** (400 MHz, $CDCl_3$) δ 8.43 (d, *J* = 8.3 Hz, 1H), 7.89–7.85 (m, 1H), 7.81 (d, *J* = 8.3 Hz, 1H), 7.69 (dd, *J* = 7.1, 1.0 Hz, 1H), 7.59 (ddd, *J* = 8.3, 6.8, 1.4 Hz, 1H), 7.53 (ddd, *J* = 8.1, 6.9, 1.4 Hz, 1H), 7.44 (dd, *J* = 8.2, 7.2 Hz, 1H), 5.39–5.25 (m, 1H), 3.47–3.39 (m, 10H), 2.64 (s, 2H), 2.31 (d, *J* = 7.9 Hz, 2H), 1.84–1.78 (m, 3H), 1.74 (s, 3H). **^{13}C NMR** (101 MHz, $CDCl_3$): δ 134.7, 133.7, 133.3, 130.2, 128.3, 128.0, 126.6, 126.4, 126.3, 125.3, 122.0, 119.4, 92.7, 80.4, 74.7, 59.4, 43.2, 30.5, 26.3, 23.5, 17.9. **HRMS** (ESI +) calculated for $[C_{23}H_{28}NaO_2]^+$ $[M+Na]^+$ 359.1982 *m/z*; found 359.1977 *m/z*.

2-(4,4-Bis(methoxymethyl)-7-methyloct-6-en-1-yn-1-yl)benzo[*b*]tiophene (2.59r)

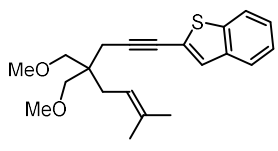

Prepared by Dr Ulysse Caniparoli. Under Ar, copper(I) iodide (2.7 mg, 14 μmol, 0.02 equiv), $[(Ph_3P)_2PdCl_2]$ (5.0 mg, 7.1 μmol, 0.01 equiv), anhydrous triethylamine (2.0 mL) and 2-bromobenzo[*b*]thiophene (152 mg, 0.713 mmol, 1.0 equiv) were added sequentially to a MW vial. The mixture was stirred for 15 min, then 4,4-bis(methoxymethyl)-7-methyloct-6-en-1-yne[28e] (150 mg, 0.713 mmol, 1.0 equiv) was added and the resulting mixture stirred at 60 °C for 20 h. The reaction

mixture was diluted with *i*-PrOH (2 mL), then cysteine (ca 5 mg) and active charcoal (ca 5 mg) were added. The mixture was stirred for 1 h, filtered over Celite® and the filter cake was washed with Et_2O (20 mL). Saturated NH_4Cl aqueous solution (20 mL) was added to the filtrate and layers were separated. The aqueous phase was extracted with Et_2O (3 × 30 mL). The combined organic layers were washed with 5% aqueous citric acid solution (20 mL), brine (20 mL), dried over $MgSO_4$, filtered and concentrated under reduced pressure. The crude product was purified by FCC (silica, pentane:Et_2O 98:2). Compound **2.59r** was obtained as a pale-yellow oil (237 mg, 0.692 mmol, 97% yield). **^{1}H NMR** (300 MHz, $CDCl_3$) δ 7.76–7.69 (m, 2H), 7.37–7.31 (m, 3H), 5.21–5.15 (m, 1H), 3.37 (s, 6H), 3.30 (s, 4H), 2.47 (s, 2H), 2.17 (d, *J* = 7.8 Hz, 2H), 1.76 (s, 3H), 1.68 (s, 3H). **^{13}C NMR** (101 MHz, $CDCl_3$) δ 139.9, 139.3, 134.9, 127.7, 125.2, 124.7, 123.6, 122.0, 119.2, 94.3, 75.9, 59.5, 43.3, 30.5, 26.3, 23.6, 18.0. **HRMS** (ESI +) calculated for $[C_{21}H_{26}NaO_2S]$+ [M+Na]+ 365.1546 *m/z*; found 365.1543 *m/z*.

(*E*)-2-(3,7-Dimethylocta-2,6-dien-1-yl)-2-(3-phenylprop-2-yn-1-yl)propane-1,3-diol (2.82)

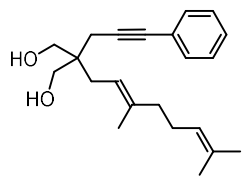

Under Ar, to a suspension of lithium aluminium hydride (625 mg, 16.5 mmol, 4.0 equiv) in anhydrous Et_2O (20 mL) kept at 0 ºC, was added dimethyl (*E*)-2-(3,7-dimethylocta-2,6-dien-1-yl)-2-(3-phenylprop-2-yn-1-yl)[78] (1.58 g, 4.13 mmol, 1 equiv) as a solution in anhydrous Et_2O (8 mL) and the mixture was left stirring at 23 ºC. After 3 h the reaction was carefully quenched under Ar flow by slowly adding water (0.6 mL), followed by a 15%$_{w/w}$ aqueous solution of NaOH (0.6 mL) and then water again (1.2 mL). The mixture was stirred for 15 min, then $MgSO_4$ was added and the mixture stirred for other 15 min (a biphasic mixture with insoluble solids formed). The precipitate was removed by filtration through Celite® and the filtrate was evaporated. The crude product was purified by FCC (silica, CyH:EtOAc 9:1 to 7:3). Compound **2.82** was obtained as a colorless oil (1.25 g, 3.84 mmol, 93% yield). **^{1}H NMR** (300 MHz, $CDCl_3$) δ 7.45–7.35 (m, 2H), 7.33–7.24 (m, 3H), 5.22 (t, *J* = 7.9 Hz, 1H), 5.06 (t, *J* = 6.7 Hz, 1H), 3.81–3.64 (m, 4H), 2.47 (s, 2H), 2.22–2.00 (m, 8H) 1.69 (s, 3H), 1.67 (s, 3H), 1.61 (s, 3H). **^{13}C NMR** (75 MHz, $CDCl_3$) δ 138.8, 131.8, 131.7, 128.4, 127.9, 124.3, 123.8, 119.0, 87.0, 83.1, 68.2, 43.6, 40.2, 30.4, 26.7, 26.0, 22.6, 17.9, 16.3. **HRMS** (ESI +) calculated for $[C_{22}H_{30}NaO_2]^+$ $[M+Na]^+$ 349.2138 *m/z*; found 349.2144 *m/z*.

(*E*)-(4,4-Bis(methoxymethyl)-7,11-dimethyldodeca-6,10-dien-1-yn-1-yl)benzene (2.59s)

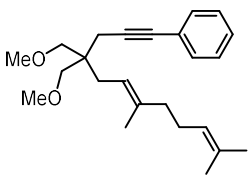

Under Ar, to a suspension of sodium hydride (447 mg, 60% in mineral oil, 11.2 mmol, 2.4 equiv) in anhydrous THF (20 mL) kept at 0 ºC, was added diol **2.82** (1.22 g, 3.72 mmol, 1.0 equiv) dropwise as a solution in anhydrous THF (15 mL). The mixture was left stirring for 30 min before adding iodomethane (0.81 mL, 13 mmol, 3.5 equiv) and then it was warmed up to 23 ºC for 2 h. The reaction was cooled to 0 ºC and diluted with Et_2O (50 mL) and a saturated aqueous solution of NH_4Cl (50 mL) was added. Layers were separated and the aqueous phase was extracted with Et_2O (2 × 80 mL). The combined organic layers were washed with brine (80 mL), dried over $MgSO_4$, filtered and evaporated. The crude product was purified by FCC (silica, CyH:EtOAc 98:2 slowly to 95:5). Compound **2.59s** was obtained as a colorless oil (1.179 g, 3.33 mmol, 89% yield). Spectroscopic data match those previously reported.[28e] **^{1}H NMR** (300 MHz, $CDCl_3$) δ 7.46–7.34 (m, 2H), 7.33–7.26 (m, 3H), 5.23–5.12 (m, 1H), 5.13–5.03 (m, 1H), 3.36 (s, 6H) 3.32 (d, *J* = 9.0 Hz, 2H), 3.28 (d, *J* = 9.0 Hz, 2H), 2.39 (s, 2H), 2.16 (d, *J* = 7.9 Hz, 2H), 2.13–1.98 (m, 4H), 1.69 (s, 3H), 1.65 (s, 3H), 1.61 (s, 3H). **^{13}C NMR** (75 MHz, $CDCl_3$) δ 138.2, 131.7, 131.4, 128.3, 127.6, 124.6, 124.3, 119.5, 87.6, 82.4, 74.6, 59.4, 43.2, 40.3, 30.1, 26.7, 25.9, 23.0, 17.8, 16.1.

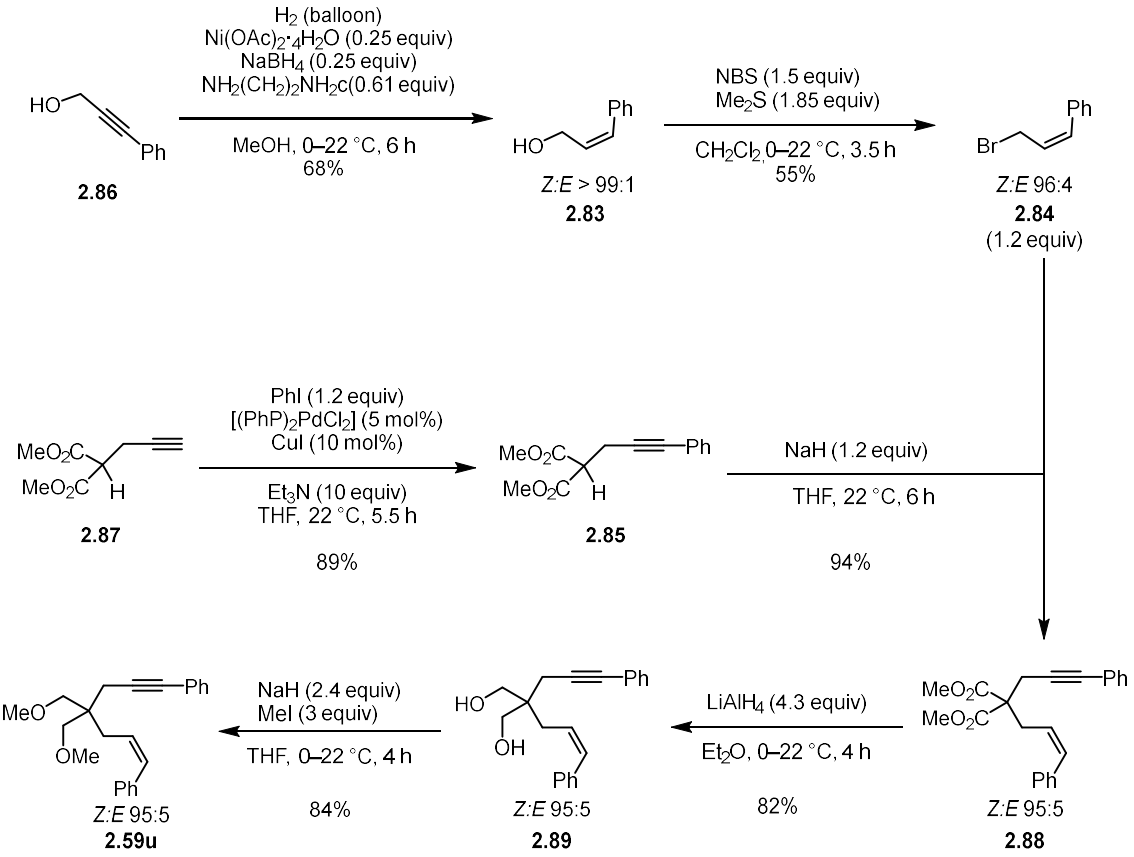

Enyne **2.59u** was prepared according to the route shown below. Compounds **2.83**,[82] **2.84**[83] and **2.85**[84] were prepared following literature procedures and their spectroscopic data matched the previously reported ones.

Dimethyl (*Z*)-2-(3-phenylallyl)-2-(3-phenylprop-2-yn-1-yl)malonate (2.88)

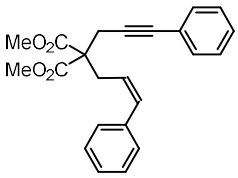

Following a modified literature procedure,[85] under Ar, to a whitish suspension of sodium hydride (58.5 mg, 60%$_{w/w}$, 1.46 mmol, 1.2 equiv) in anhydrous THF (8.0 mL) kept at 0 °C, a solution of dimethyl 2-(3-phenylprop-2-yn-1-yl)malonate[84] **2.85** (300 mg, 1.22 mmol, 1.0 equiv) in anhydrous THF (1.0 mL) was added dropwise. During the addition, foaming was observed, and the mixture turned into a pale-yellow solution. After stirring at 0 °C for 15 min, a solution of (*Z*)-(3-bromoprop-1-en-1-yl)benzene[83] **2.84** (288 mg, 1.46 mmol, 1.2 equiv) in anhydrous THF (3 mL) was added and the resulting pale yellow suspension was stirred at 23 °C for 6 h. The reaction was quenched with brine (15 mL) and the aqueous phase was extracted with Et_2O (3 × 20 mL). The combined organic phases were dried over Na_2SO_4, filtered and evaporated. The crude product was purified by automated FCC (silica, liquid load, CyH:EtOAc 100:0 to 80:20, product eluting in CyH:EtOAc 90:10). Compound **2.88** was obtained as a yellow oil (417 mg, 1.15 mmol, 94% yield, 95:5 *Z*:*E* ratio as judged by ^{1}H NMR). **IR** (film from $CDCl_3$, cm^{-1}) υ 3022, 2953, 1736, 1437, 1292, 1209. **^{1}H NMR** (400 MHz, $CDCl_3$) δ 7.37–7.29 (m, 4H), 7.26–7.14 (m, 6H), 6.63 (d, *J* = 11.7 Hz, 1H), 5.54 (dt, *J* = 11.7, 7.5 Hz, 1H), 3.71 (s, 6H), 3.22 (dd, *J* = 7.5, 1.8 Hz, 2H), 3.06 (s, 2H). **^{13}C NMR** (101 MHz, $CDCl_3$) δ 170.5, 136.9,

82. Davies, S. G.; Fletcher, A. M.; Roberts, P. M.; Thomson, J. E.; Zammit, C. M. *Chem. Commun.* **2013**, *49*, 7037–7039.
83. Vyas, D. J.; Oestreich, M. *Chem. Commun.* **2010**, *46*, 568–570.
84. Gasperini, D.; Maggi, L.; Dupuy, S.; Veenboren, R. M. P.; Cordes, D. B.; Slawin, S. M. Z.; Nolan, S. P. *Adv. Synth. Catal.* **2016**, *358*, 3857–3862.
85. Schiller, R.; Pour, M.; Fáková, H.; Kuneš, J.; Císařová, I. *J. Org. Chem.* **2004**, *69*, 6761–6765.

133.2, 131.8, 128.9, 128.4, 128.1, 128.0, 127.0, 125.0, 123.1, 84.1, 83.8, 57.5, 52.9, 31.0, 23.9. **HRMS** (ESI +) calculated for $[C_{23}H_{22}NaO_4]^+$ $[M+Na]^+$ 385.1410 *m/z*; found 385.1402 *m/z*.

(*Z*)-2-(3-Phenylallyl)-2-(3-phenylprop-2-yn-1-yl)propane-1,3-diol (2.89)

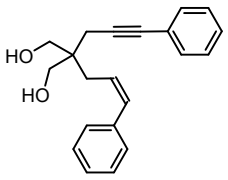

Under Ar, to a suspension of lithium aluminum hydride (160 mg, 4.22 mmol, 4.3 equiv) in anhydrous Et_2O (8 mL) kept at 0 ºC, was added (*Z*)-2-(3-phenylallyl)-2-(3-phenylprop-2-yn-1-yl)malonate **2.88** (356 mg, 0.982 mmol, 1.0 equiv, 95:5 *Z*:*E*) dropwise over 2 min as a solution in anhydrous Et_2O (2 mL). The mixture was stirred at 23 ºC for 4 h, then the reaction was carefully quenched under Ar flow at 0 ºC by slowly adding water (0.2 mL), followed by a 15%$_{w/w}$ aqueous solution of NaOH (0.2 mL) and then water again (0.6 mL). The resulting white suspension was diluted with Et_2O (5 mL) and stirred for 15 min, then $MgSO_4$ was added and the mixture stirred for another 15 min (a biphasic mixture with insoluble solids formed). The precipitate was removed by filtration through Celite®, washed with Et_2O and EtOAc and the solvent was evaporated. Compound **2.89** (247 mg, 0.806 mmol, 82% yield, 95:5 *Z*:*E* ratio as judged by ^{1}H NMR) was obtained as a pale yellow dense oil that solidified to a beige solid upon standing, and was pure enough to be used directly in the next step. **^{1}H NMR** (400 MHz, $CDCl_3$) δ 7.44–7.17 (m, 10H), 6.65 (d, *J* = 11.7 Hz, 1H), 5.82 (dt, *J* = 11.7, 7.7 Hz, 1H), 3.78–3.64 (m, 4H), 2.55 (dd, *J* = 7.7, 1.7 Hz, 2H), 2.51 (s, 2H), 2.39 (s, 2H). **^{13}C NMR** (101 MHz, $CDCl_3$) δ 137.3, 132.1, 131.7, 128.9, 128.4, 128.3, 127.9, 126.9, 126.8, 123.5, 86.33, 83.28, 67.6, 43.3, 30.0, 22.6. **HRMS** (ESI +) calculated for $[C_{21}H_{22}NaO_2]^+$ $[M+Na]^+$ 329.1512 *m/z*; found 359.1511 *m/z*.

(*Z*)-(4,4-Bis(methoxymethyl)hept-1-en-6-yne-1,7-diyl)dibenzene (2.59u)

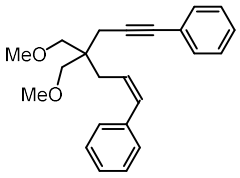

Under Ar, to a suspension of sodium hydride (68.9 mg, 60% in mineral oil, 1.72 mmol, 2.4 equiv) in anhydrous THF (2.5 mL) kept at 0 ºC, was added (*Z*)-2-(3-phenylallyl)-2-(3-phenylprop-2-yn-1-yl)propane-1,3-diol **2.89** (220 mg, 0.718 mmol, 1.0 equiv, 95:5 *Z*:*E*) dropwise as a solution in anhydrous THF (3.5 mL). The mixture was stirred for 10 min before adding iodomethane (204 µL, 2.15 mmol, 3.0 equiv) and then it was warmed up to 23 ºC for 4 h. The reaction was cooled to 0 ºC, diluted with Et_2O (10 mL) and NH_4Cl (10 mL). Layers were separated and the aqueous phase was extracted with Et_2O (4 × 10 mL). The combined organic layers were dried over Na_2SO_4, filtered and evaporated. The crude product was purified by FCC (silica, liquid load, pentane:EtOAc 98:2 slowly to 95:5). Compound **2.59u** was obtained as a pale-yellow oil (201 mg, 0.601 mmol, 84% yield, 95:5 *Z*:*E* ratio as judged by ^{1}H NMR). **IR** (film from $CDCl_3$, cm^{-1}) υ 2888, 2809, 1490, 1444, 1196, 1100, 756, 691. **^{1}H NMR** (400 MHz, $CDCl_3$) δ 7.42 (d, *J* = 7.2 Hz, 2H), 7.40–7.21 (m, 8H), 6.63 (d, *J* = 11.8 Hz, 1H), 5.86 (dt, *J* = 11.8, 7.6 Hz, 1H), 3.47–3.37 (m, 4H), 3.37 (s, 6H), 2.65 (dd, *J* = 7.6, 1.8 Hz, 2H), 2.55 (s, 2H). **^{13}C NMR** (101 MHz, $CDCl_3$) δ 137.7, 131.7, 131.4, 128.9, 128.20, 128.19, 127.6, 127.5, 126.6, 124.0, 87.0, 82.6, 74.6, 59.3, 42.8, 30.7, 23.3. **HRMS** (ESI +) calculated for $[C_{23}H_{26}NaO_2]^+$ $[M+Na]^+$ 357.1825 *m/z*; found 357.1811 *m/z*.

(2-Bromoethylidene)cyclohexane (2.90)

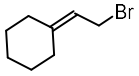

Following a modified literature procedure,[86] under Ar, dimethylsulfide (209 µL, 2.85 mmol, 1.2 equiv) was added dropwise to a white suspension of *N*-bromosuccinimide (465 mg, 2.61 mmol, 1.1 equiv) in anhydrous CH_2Cl_2 (6.0 mL) kept at 0 ºC, forming a yellow solution. After 30 min, the reaction mixture was cooled to −20 ºC

86. Cho, H.; Shi, J. E.; Lee, S.; Jeon, H.; Park, S.; Kim, S. *Org. Lett.* **2018**, *20*, 6121–6125.

and 2-cyclohexylideneethan-1-ol[87] (300 mg, 2.38 mmol, 1.0 equiv) was added as a solution in anhydrous CH_2Cl_2 (6.0 mL) (reaction mixture turned into a white suspension and 5 min later into a colorless solution). The resultant colorless solution was then warmed up to 0 ºC and stirred for 2 h at 0 ºC, followed by 1 h at 23 ºC. The mixture was diluted with water (10 mL) and Et_2O (10 mL). Layers were separated and the aqueous phase (that presented pH ca 1) was extracted with Et_2O (3 × 15 mL). The combined organic layers were washed with brine (20 mL), dried over Na_2SO_4, filtered and evaporated. Compound **2.90** was obtained as a pale-yellow oil (405 mg, 2.14 mmol, 90% yield) and was used without further purification in the next step. **^{1}H NMR** (400 MHz, $CDCl_3$) δ 5.43 (tquint, *J* = 8.5, 1.1 Hz, 1H), 3.98 (d, *J* = 7.1 Hz, 2H), 2.24–2.14 (m, 2H), 2.14–2.04 (m, 2H), 1.62–1.42 (m, 6H).

Dimethyl 2-(2-cyclohexylideneethyl)-2-(3-phenylprop-2-yn-1-yl)malonate (2.91)

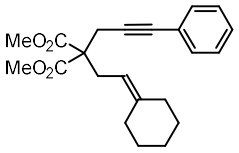

Under Ar, to a grey suspension of sodium hydride (195 mg, 60% in mineral oil, 4.87 mmol, 1.2 equiv) in anhydrous THF (30 mL) kept at 0 ºC, was added dropwise a solution of dimethyl 2-(3-phenylprop-2-yn-1-yl)malonate[84] (1.00 g, 4.06 mmol, 1.0 equiv) in anhydrous THF (5 mL). The mixture was stirred at 0 ºC for 20 min before dropwise addition of a solution of alkyl bromide **2.90** (921 mg, 4.87 mmol, 1.2 equiv) in anhydrous THF (5 mL). The reaction mixture was stirred at 23 ºC for 3 h. A saturated aqueous NH_4Cl solution (30 mL) and Et_2O (30 mL) were added, and layers separated. The aqueous phase was extracted with Et_2O (2 × 30 mL) and the combined organic layers were dried over Na_2SO_4, filtered and evaporated. The crude product was purified by FCC (silica, CyH:EtOAc 95:5 to 90:10). Compound **2.91** was obtained as a pale-yellow oil (997 mg, 4.06 mmol, 69% yield). **IR** (film from $CDCl_3$, cm^{-1}) υ 29226, 2853, 1735, 1436, 1289, 1218, 1176. **^{1}H NMR** (500 MHz, $CDCl_3$) δ 7.38–7.33 (m, 2H), 7.31–7.25 (m, 3H), 4.89 (t, *J* = 7.9 Hz, 1H), 3.76 (s, 6H), 3.00 (s, 2H), 2.85 (d, *J* = 7.9 Hz, 2H), 2.23–2.17 (m, 2H) 2.08 (d, *J* = 5.8 Hz, 2H), 1.56–1.46 (m, 6H). **^{13}C NMR** (126 MHz, $CDCl_3$) δ 170.8, 145.2, 131.8, 128.3, 128.0, 123.4 113.9, 84.8, 83.4, 57.7, 52.9, 37.7, 30.1, 29.1, 28.8, 28.1, 26.9, 23.5. **HRMS** (ESI +) calculated for $[C_{22}H_{26}NaO_4]^+$ $[M+Na]^+$ 377.1723 *m/z*; found 377.1721 *m/z*.

2-(2-Cyclohexylideneethyl)-2-(3-phenylprop-2-yn-1-yl)propane-1,3-diol (2.92)

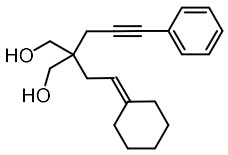

Under Ar, to a suspension of lithium aluminium hydride (171 mg, 4.51 mmol, 4.0 equiv) in anhydrous Et_2O (18 mL) kept at 0 ºC, was added dimethyl 2-(2-cyclohexylideneethyl)-2-(3-phenylprop-2-yn-1-yl)malonate **2.91** (400 mg, 1.13 mmol, 1 equiv) as a solution in anhydrous Et_2O (6 mL) and the mixture was stirred at 23 ºC. After 2 h the reaction was carefully quenched under Ar flow by slowly adding water (0.2 mL), followed by a 15%$_{w/w}$ aqueous solution of NaOH (0.2 mL) and then water again (0.6 mL). The mixture was stirred for 15 min, then $MgSO_4$ was added and the mixture stirred for another 15 min (a biphasic mixture with insoluble solids formed). Finally, the precipitate was removed by filtration through Celite® and the solvent was evaporated. The crude product was purified by FCC (silica, CyH:EtOAc 9:1 to 7:3). Compound **2.92** was obtained as a white solid (260 mg, 0.87 mmol, 77% yield). **M.p** 117 °C. **IR** (film from $CDCl_3$, cm^{-1}) υ 3387 (broad), 2926, 2852, 1444, 1027, 755. **^{1}H NMR** (300 MHz, $CDCl_3$) δ 7.44–7.35 (m, 2H), 7.33–7.27 (m, 3H), 5.16 (t, *J* = 7.9 Hz, 1H), 3.76 (d, *J* = 10.9 Hz, 2H), 3.70 (d, *J* = 10.9 Hz, 2H), 2.48 (s, 2H), 2.30–2.05 (m, 8H) 1.59–1.49 (m, 6H). **^{13}C NMR** (75 MHz, $CDCl_3$) δ 143.6, 131.7, 128.4, 127.9, 123.8, 115.4, 86.9, 83.1, 68.3, 43.4, 37.8, 29.5, 28.92, 28.90, 28.0, 27.0, 22.6. **HRMS** (ESI +) calculated for $[C_{20}H_{26}NaO_2]^+$ $[M+Na]^+$ 321.1825 *m/z*; found 321.1818 *m/z*.

87. Comito, R. J.; Finelli, F. G.; Macmillan, D. W. C. *J. Am. Chem. Soc.* **2013**, *135*, 9358–9361.

(6-Cyclohexylidene-4,4-bis(methoxymethyl)hex-1-yn-1-yl)benzene (2.59v)

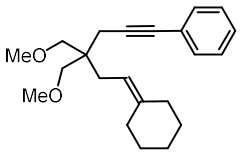

Under Ar, to a suspension of sodium hydride (77.2 mg, 60% in mineral oil, 1.93 mmol, 2.4 equiv) in anhydrous THF (1.5 mL) kept at 0 ºC, was added 2-(2-cyclohexylideneethyl)-2-(3-phenylprop-2-yn-1-yl)propane-1,3-diol **2.92** (240 mg, 0.804 mmol, 1.0 equiv) dropwise as a solution in anhydrous THF (2.5 mL). The mixture was left stirring for 10 min before adding iodomethane (150 µL, 2.41 mmol, 3.0 equiv) and then it was warmed up to 23 ºC for 2 h. Then, the reaction was cooled to 0 ºC and diluted with Et_2O (10 mL) and an aqueous saturated solution of NH_4Cl (10 mL). Layers were separated and the aqueous phase was extracted with Et_2O (2 × 30 mL). The combined organic layers were washed with brine (20 mL), dried over $MgSO_4$, filtered and evaporated. The crude product was purified by FCC (silica, CyH:EtOAc 100:0 slowly to 95:5). Compound **2.59v** was obtained as a colorless oil (230 mg, 0.705 mmol, 88% yield).**IR** (film from $CDCl_3$, cm^{-1}) υ 2922, 2852, 1490, 1445, 1102, 755, 691. **^{1}H NMR** (300 MHz, $CDCl_3$) δ 7.44–7.35 (m, 2H), 7.32–7.23 (m, 3H), 5.11 (t, *J* = 7.9 Hz, 1H), 3.35 (s, 6H), 3.31 (d, *J* = 9.0 Hz, 2H), 3.30 (d, *J* = 9.0 Hz, 2H), 2.39 (s, 2H), 2.24–2.07 (m, 6H), 1.64–1.43 (m, 6H). **^{13}C NMR** (75 MHz, $CDCl_3$) δ 142.9, 131.7, 128.3, 127.6, 124.3, 115.9, 87.6, 82.4, 74.6, 59.5, 43.0, 37.8, 29.2, 29.0, 28.8, 28.1, 27.1, 23.0. **HRMS** (ESI +) calculated for $[C_{22}H_{30}NaO_2]^+$ $[M+Na]^+$ 349.2138 *m/z*; found 349.2133 *m/z*.

1-Chloro-2,3-dimethylbut-2-ene (2.93)

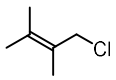

Following a literature procedure,[88] under Ar, dimethylsulfide (1.10 mL, 14.9 mmol, 1.6 equiv) was added dropwise to solution of *N*-chlorosuccinimide (1.99 g, 14.9 mmol, 1.6 equiv) in anhydrous CH_2Cl_2 (84 mL) kept at 0 ºC. After 30 min, the resulting white suspension was cooled to −20 ºC and 2,3-dimethylbut-2-en-1-ol[89] (932 mg, 9.31 mmol, 1.0 equiv) was added dropwise as a solution in anhydrous CH_2Cl_2 (6.0 mL). The reaction mixture was then warmed up to 0 ºC, stirred for 1 h at 0 ºC and then for 1 h at 23 ºC. The mixture was poured into an ice-cold brine (40 mL) and Et_2O (40 mL). Layers were separated and the aqueous phase (that presented pH ca 1) was extracted with Et_2O (3 × 50 mL). The combined organic layers were washed with ice-cold brine (40 mL), dried over $MgSO_4$, filtered and evaporated. Compound **2.93** was obtained as a pale yellow liquid (984 mg, ca 70% purity a judged by ^{1}H NMR, 5.81 mmol, 62% yield) and immediately used without further purification in the next reaction. **^{1}H NMR** (400 MHz, $CDCl_3$) δ 4.13 (s, 2H), 1.83 (s, 6H), 1.71 (s, 3H).

Dimethyl 2-(2,3-Dimethylbut-2-en-1-yl)-2-(3-phenylprop-2-yn-1-yl)malonate (2.94)

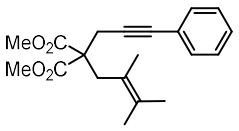

Under Ar, to a grey suspension of sodium hydride (84 mg, 60% in mineral oil, 2.1 mmol, 0.8 equiv) in anhydrous THF (15 mL) kept at 0 ºC, was added dropwise a solution of dimethyl 2-(3-phenylprop-2-yn-1-yl)malonate[84] (659 mg, 2.68 mmol, 1.0 equiv) in anhydrous THF (5 mL) and the mixture was left stirring at the same temperature for 15 min before dropwise addition of 1-chloro-2,3-dimethylbut-2-ene **2.93** (984 mg, ca 70% purity, 5.81 mmol, 2.2 equiv) as a solution in anhydrous THF (5 mL). The reaction mixture was left stirring at 23 ºC for 18 h. A saturated aqueous NH_4Cl solution (20 mL) was added, and the aqueous phase was extracted with EtOAc (3 × 15 mL). The combined organic layers were washed with brine, dried over $MgSO_4$, filtered and evaporated. The crude product was purified by FCC (silica, CyH:EtOAc 1:0 to 9:1). Compound **2.94** was obtained as a pale-yellow oil (307 mg, 0.934 mmol, 35% yield). **IR** (film from $CDCl_3$, cm^{-1}) υ 2952, 1736, 1435, 1295, 1215, 1140, 757, 692. **^{1}H NMR** (300 MHz, $CDCl_3$) δ 7.42–7.32 (m, 2H), 7.31–7.23 (m, 3H), 3.75 (s, 6H), 3.00 (s, 2H), 2.99 (s, 2H), 1.79–1.76 (m, 3H), 1.67 (s, 3H), 1.59 (s, 3H).

88. Trend, R. M.; Ramtohul, Y. K.; Stoltz, B. M. *J. Am. Chem. Soc.* **2005**, *127*, 17778–17788.
89. Lauterbach, L.; Hou, A.; Dickschat, J. S. *Chem. Eur. J.* **2021**, *27*, 7923–7929.

^{13}C NMR (126 MHz, $CDCl_3$) δ 171.3, 131.7, 131.3, 128.3, 128.0, 123.4, 121.9, 85.6, 83.6, 57.7, 52.7, 37.1, 23.7, 21.23, 21.21, 19.2. **HRMS** (ESI +) calculated for $[C_{20}H_{24}NaO_4]^+$ $[M+Na]^+$ 351.1567 *m/z*; found 351.1563 *m/z*.

2-(2,3-Dimethylbut-2-en-1-yl)-2-(3-phenylprop-2-yn-1-yl)propane-1,3-diol (2.95)

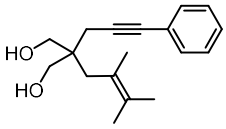

Under Ar, to a suspension of lithium aluminum hydride (160 mg, 4.21 mmol, 4.0 equiv) in anhydrous Et_2O (20 mL) kept at 0 ºC, was added dimethyl 2-(2,3-dimethylbut-2-en-1-yl)-2-(3-phenylprop-2-yn-1-yl)malonate **2.94** (346 mg, 1.05 mmol, 1 equiv) as a solution in anhydrous Et_2O (8 mL) and the mixture was left stirring at 23 ºC. After 5 h the reaction was carefully quenched under Ar flow by slowly adding water (0.3 mL), followed by a 15%$_{w/w}$ aqueous solution of NaOH (0.3 mL) and then water again (0.9 mL). The mixture was stirred for 15 min, then MgSO4 was added and the mixture stirred for other 15 min (a biphasic mixture with insoluble solids formed). Finally, the precipitate was removed by filtration through Celite® and the solvent was evaporated. The crude product was purified by FCC (silica, CyH:EtOAc 9:1 to 7:3). Compound **2.95** was obtained as a colorless oil (277 mg, 1.02 mmol, 97% yield). **IR** (film from $CDCl_3$, cm^{-1}) υ 3373 (broad), 2957, 2926, 1490, 1442, 1028, 756. **^{1}H NMR** (300 MHz, $CDCl_3$) δ 7.45–7.36 (m, 2H), 7.33–7.27 (m, 3H), 3.76 (s, 4H), 2.57 (s, 2H), 2.31 (s, 2H), 2.26 (s, 2H), 1.81–1.71 (m, 6H) 1.67 (s, 3H). **^{13}C NMR** (75 MHz, $CDCl_3$) δ 131.7, 129.5, 128.4, 127.9, 124.3, 123.8, 87.4, 83.5, 68.7, 44.7, 37.3, 23.6, 21.6, 21.4, 21.1. **HRMS** (ESI +) calculated for $[C_{18}H_{24}NaO_2]^+$ $[M+Na]^+$ 295.1669 *m/z*; found 295.1667 *m/z*.

(4,4-Bis(methoxymethyl)-6,7-dimethyloct-6-en-1-yn-1-yl)benzene (2.59w)

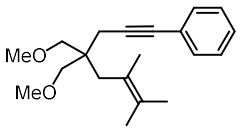

Under Ar, to a suspension of sodium hydride (85.6 mg, 60% in mineral oil, 2.14 mmol, 2.4 equiv) in anhydrous THF (1.5 mL) kept at 0 ºC, was added 2-(2,3-dimethylbut-2-en-1-yl)-2-(3-phenylprop-2-yn-1-yl)propane-1,3-diol **2.95** (243 mg, 0.892 mmol, 1.0 equiv) dropwise as a solution in anhydrous THF (2.5 mL). The mixture was left stirring for 10 min before adding iodomethane (167 µL, 2.68 mmol, 3.0 equiv) and then it was warmed up to 23 ºC for 3 h. The reaction was cooled to 0 ºC and diluted with Et_2O (10 mL) and NH_4Cl (10 mL). Layers were separated and the aqueous phase was extracted with Et_2O (2 × 30 mL). The combined organic layers were washed with brine (20 mL), dried over $MgSO_4$, filtered and evaporated. The crude product was purified by FCC (silica, CyH:EtOAc 100:0 to 95:5). Compound **2.59w** was obtained as a colorless oil (160 mg, 95% purity judged by ^{1}H NMR, 0.506 mmol, 57% yield). **IR** (film from $CDCl_3$, cm^{-1}) υ 2980, 2919, 2889, 2809, 1490, 1107, 756. **^{1}H NMR** (300 MHz, $CDCl_3$) δ 7.45–7.35 (m, 2H), 7.34–7.26 (m, 3H), 3.33 (s, 6H), 3.31–3.26 (m, 4H), 2.46 (s, 2H), 2.34–2.22 (m, 2H), 1.73 (s, 6H), 1.67 (s, 3H). **^{13}C NMR** (75 MHz, $CDCl_3$) δ 131.6, 129.0, 128.4, 128.3, 127.6, 124.4, 88.2, 82.7, 75.2, 59.2, 44.2, 36.5, 24.1, 21.2, 21.1, 20.9. **HRMS** (ESI +) calculated for $[C_{20}H_{28}NaO_2]^+$ $[M+Na]^+$ 323.1982 *m/z*; found 323.1982 *m/z*.

Results on the formal [4+2] cycloaddition of 1,6-enynes

General procedure GP5: enantioselective formal [4 + 2] cycloaddition of 1,6-enynes[90]

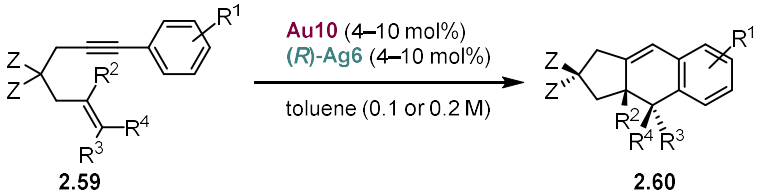

2.59 **2.60**

In the glovebox, under Ar and at room temperature, anhydrous toluene (0.5 or 1.0 mL) was added to a MW-vial containing enyne **2.59** (0.150 mmol, 1 equiv) and complex **Au10** (*e.g.* 6.7 mg, 7.5 µmol, 0.05 equiv) obtaining a white suspension. To it was added a yellow clear solution of *(R)*-**Ag6** (equimolar amount to **Au10**, *e.g.* 7.1 mg, 7.5 µmol, 0.05 equiv) in anhydrous toluene (0.25 or 0.5 mL, final reaction volume 0.75 or 1.5 mL, respectively), obtaining a solution, that generally became cloudy within few minutes. The vial was capped, removed from the glovebox, and placed to stir under inert gas (connected to a N_2 balloon) in the dark (wrapped in Al foil) at the desired temperature for the indicated time. Then, the reaction mixture was quenched by the addition of triethylamine (0.2 mL) and volatiles were removed under reduced pressure. The residue was dissolved in $CDCl_3$, the internal standard (1,1,2,2-tetrachloroethane, 31.7 µL, 0.300 mmol, 2 equiv) added and the ^{1}H NMR spectrum recorded. The crude product was purified by FCC and/or PTLC, obtaining compound **2.60**.

(*R*)-2,2-Bis(methoxymethyl)-3*a*,4,4-trimethyl-2,3,3a,4-tetrahydro-1*H*-cyclopenta[*b*]naphthalene (2.60a)

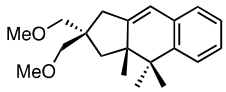

Small scale reaction (0.15 mmol)

Prepared following the general procedure **GP5** using enyne **2.59a** (43.0 mg, 0.150 mmol, 1.0 equiv), gold(I) complex **Au10** (5.3 mg, 6.0 µmol, 0.04 equiv) and chiral salt ***(R)*-Ag6** (5.6 mg, 6.0 µmol, 0.04 equiv) in toluene (1.5 mL, 0.1 M), at –10 ºC for 24 h. The crude product was purified by FCC (silica, dry load, CyH:EtOAc 100:0 to 95:5). Compound **2.60a** was obtained as a colorless oil (40.1 mg, 0.140 mmol, 93% yield) with 98:2 *er*.

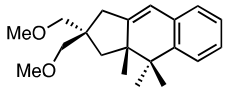

Large scale reaction (2 mmol)

Gold(I) complex **Au10** (17.8 mg, 20.0 µmol, 0.01 equiv) was added under air to a colorless solution of enyne **2.59a** (572.8 mg, 2.000 mmol, 1 equiv) in technical-grade toluene (2 mL, EssentQ® brand), obtaining a cloudy white suspension, that was sonicated for few seconds to remove traces of Au complex from the walls of the vial. The suspension was then cooled to –10 ºC, and a yellow solution of ***(R)*-Ag6** (18.7 mg, 20.0 µmol, 0.01 equiv) in toluene (1.0 mL, final concentration 0.66 M) was added. The resulting cloudy yellow solution was stirred at –10 ºC in the dark under air for 24 h. After 24 h, Et_3N (0.5 mL) was added and the reaction mixture evaporated to dryness. The residue was dissolved in CDCl3 and diphenylmethane (16.8 mg, 16.7 µL, 100 µmol, 0.05 equiv) was added as internal standard. ^{1}H NMR analysis showed mostly product (110% against internal standard) and traces of remaining starting material (no more than 1% against internal standard). The crude product was purified by automated FCC (40-g silica column, silica dry load, CyH:EtOAc 100:0 to 90:10), yielding compound **2.60a** as a colorless oil (565.5 mg, 1.974 mmol, 99% yield) with 98:2 *er*. Spectroscopic data for product **2.60a** matched those reported in the literature.[28e] **^{1}H NMR** (500 MHz, $CDCl_3$): δ

90. Racemic reactions were performed in GCMS vials on a 0.1 mmol scale, using [(JohnPhos)Au(MeCN)]SbF_6 (3 mol%) in DCM (0.1M).

7.31–7.29 (m, 1H), 7.16–7.12 (m, 2H), 7.02–7.00 (m, 1H), 6.30 (br s, 1H), 3.40–3.37 (m, 5H), 3.34 (s, 3H), 3.27 (d, *J* = 14.0 Hz, 1H), 3.24 (d, *J* = 14.0 Hz, 1H), 2.78–2.71 (m, 1H), 2.51 (d, *J* = 17.9 Hz, 1H), 2.35 (d, *J* = 17.9 Hz, 1H), 1.86 (dd, *J* = 12.5, 8.4 Hz, 1H), 1.57 (app t, *J* = 12.2 Hz, 1H), 1.40 (s, 3H), 0.93 (s, 3H). **^{13}C NMR** (126 MHz, $CDCl_3$): δ 146.8, 144.6, 134.6, 126.6, 126.2, 126.0, 123.6, 119.0, 77.4, 75.1, 59.47, 59.45, 48.3, 46.8, 37.9, 36.8, 31.6, 25.7, 22.0. **HPLC** (OD-H (250 × 4.6 mm, 5 µm), 100% *n*-hexane, 1.5 mL/min, 25 ºC, 280 nm): en1 (major, 97.5%) min 5.70, en2 (minor, 2.5%) min 6.19. Since the second peak slightly overlaps with the tail of the first peak (up to 2% *ee underestimation* error assumed), this HPLC method was used only for reaction optimization. For the substrate scope, separation by SFC was employed instead. **SFC** (OJ (150 × 3.0 mm, 3 µm), CO_2:*i*-PrOH 99:1, 2.0 mL/min, 35 ºC, ABRP 2000 psi, 266 nm): en1 (major, 98%) min 1.06, en2 (minor, 2%) min 1.21. **$[\alpha]^{24.7}_D$** +0.15 (c 0.98, $CHCl_3$, sample with 98:2 *er*); lit: [28e] **$[\alpha]^{26.8}_D$** +1.7 (c 1.0, $CHCl_3$, sample with 94:6 *er*).

(*R*)-2,2-Bis((benzyloxy)methyl)-4,4-dimethyl-2,3,3*a*,4-tetrahydro-1*H*-cyclopenta[*b*]naphthalene (2.60b)

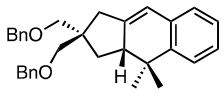

Prepared following the general procedure **GP5** using enyne **2.59b** (65.8 mg, 0.150 mmol, 1.0 equiv), gold(I) complex **Au10** (6.7 mg, 7.5 µmol, 0.05 equiv) and chiral salt ***(R)*-Ag6** (7.1 mg, 7.5 µmol, 0.05 equiv) in toluene (1.5 mL, 0.1 M), at –10 ºC for 24 h. The crude product was purified by FCC (silica, dry load, pentane:EtOAc 100:0 to 97:3) and then by PTLC (silica, pentane:EtOAc 97:3). Compound **2.60b** was obtained as a pale-yellow oil (55.1 mg, 0.126 mmol, 84% yield) with 98:2 *er*. **IR** (film from $CDCl_3$, cm^{-1}) υ 3029, 2960, 2926, 2855, 1478, 1453, 1360, 1096, 1028, 749, 734, 696. **^{1}H NMR** (500 MHz, $CDCl_3$): δ 7.37–7.26 (m, 11H), 7.17–7.12 (m, 2H), 7.02–6.99 (m, 1H), 6.29 (m/app br q, 1H), 4.57 (s, 2H), 4.53 (d, *J* = 12.4 Hz, 1H), 4.49 (d, *J* = 12.4 Hz, 1H), 3.41 (s, 2H), 3.54 (app q, *J* = 8.7 Hz, 2H), 2.72 (m, 1H), 2.56 (d, *J* = 18.0 Hz, 1H), 2.41 (dt, *J* = 17.9, 2.8 Hz, 1H), 1.95 (dd, *J* = 12.5, 8.3 Hz, 1H), 1.57 (app t, *J* = 12.5 Hz, 1H), 1.39 (s, 3H), 0.92 (s, 3H). **^{13}C NMR** (126 MHz, $CDCl_3$): δ 146.9, 144.6, 139.04, 138.97, 134.6, 128.4 (CH × 4), 127.52 (CH × 4), 127.47 (CH × 2), 126.6, 126.2, 126.0, 123.6, 119.0, 77.4, 75.1, 59.47, 59.45, 48.3, 46.8, 37.9, 36.8, 31.6, 25.7, 22.0. **HRMS** (APCI +) calculated for $[C_{31}H_{35}O_2]^+$ $[M + H]^+$ 439.2632 *m/z*; found 439.2630 *m/z*. **SFC** (OJ (100 × 3 mm, 3 µm), CO_2:*i*-PrOH 80:20, 1.2 mL/min, 35 ºC, BPR 150 bar, 280 nm): en1 (major, 98%) min 2.39, en2 (minor, 2%) min 2.70. **$[\alpha]^{25.9}_D$** +7.8. (c 0.99, $CHCl_3$, sample with 98:2 *er*).

(*R*)-2,2-Bis((allyloxy)methyl)-4,4-dimethyl-2,3,3*a*,4-tetrahydro-1*H*-cyclopenta[*b*]naphthalene (2.60c)

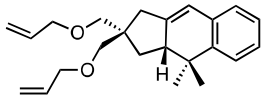

Prepared following the general procedure **GP5** using enyne **2.59c** (50.8 mg, 0.150 mmol, 1.0 equiv), gold(I) complex **Au10** (6.7 mg, 7.5 µmol, 0.05 equiv) and chiral salt ***(R)*-Ag6** (7.1 mg, 7.5 µmol, 0.05 equiv) in toluene (1.5 mL, 0.1 M), at –10 ºC for 25 h. The crude product was purified by FCC (silica, liquid load in CyH, CyH:EtOAc 100:0 to 96:4). Compound **2.60c** was obtained as a pale-yellow oil (48.4 mg, 0.143 mmol, 95% yield) with 95.5:4.5 *er*. **IR** (film from $CDCl_3$, cm^{-1}) υ 2961, 2928, 2851, 1478, 1133, 1094, 989, 921, 750. **^{1}H NMR** (500 MHz, $CDCl_3$): δ 7.30–7.28 (m, 1H), 7.15–7.10 (m, 2H), 7.01–6.98 (m, 1H), 6.28 (m/app br q, 1H), 5.94 (ddt, *J* = 17.2, 10.4, 5.3 Hz, 1H), 5.88 (ddt, *J* = 17.1, 10.4, 5.3 Hz, 1H), 5.29 (dq, *J* = 17.0, 1.5 Hz, 1H), 5.24 (dq, *J* = 17.3, 1.5 Hz, 1H), 5.17 (dq, *J* = 10.4, 1.5 Hz, 1H), 5.14 (dq, *J* = 10.4, 1.5 Hz, 1H), 4.04–4.00 (m, 2H), 3.96–3.94 (m, 2H), 3.46 (d, *J* = 12.1 Hz, 1H), 3.44 (d, *J* = 12.1 Hz, 1H), 3.32 (d, *J* = 12.0 Hz, 1H), 3.30 (d, *J* = 12.0 Hz, 1H), 2.76–2.70 (m, 1H), 2.51 (d, *J* = 18.3 Hz, 1H), 2.37 (dt, *J* = 18.0, 2.7 Hz, 1H), 1.88 (dd, *J* = 12.5, 8.4 Hz, 1H), 1.58 (app t, *J* = 12.2 Hz, 1H), 1.38 (s, 3H), 0.91 (s, 3H). **^{13}C**

NMR (126 MHz, $CDCl_3$): δ 147.0, 144.7, 135.4, 135.3, 134.7, 126.6, 126.2, 126.0, 123.6, 119.0, 116.5, 116.4, 74.8, 72.5, 72.43, 72.38, 48.4, 46.9, 38.1, 36.9, 31.7, 25.7, 22.0. **HRMS** (ESI +) calculated for $[C_{23}H_{30}NaO_2]^+$ $[M + Na]^+$ 361.2138 *m/z*; found 361.2136 *m/z*. **HPLC** (OD-H (250 × 4.6 mm, 5 µm), 99:1 *n*-hexane:*i*-PrOH, 0.5 mL/min, 25 ºC, 280 nm): en1 (major, 95.5%) min 7.25, en2 (minor, 4.5%) min 7.54. **$[\alpha]^{26.1}_D$** +4.5 (c 1.0, $CHCl_3$, sample with 95.5:4.5 *er*).

(*R*)-(4,4-Dimethyl-2,3,3*a*,4-tetrahydro-1*H*-cyclopenta[*b*]naphthalene-2,2-diyl)bis(methylene) diacetate (2.60d)

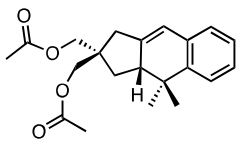

Prepared following the general procedure **GP5** using enyne **2.59d** (51.4 mg, 0.150 mmol, 1.0 equiv), gold(I) complex **Au10** (6.7 mg, 7.5 µmol, 0.05 equiv) and chiral salt ***(R)*-Ag6** (7.1 mg, 7.5 µmol, 0.05 equiv) in toluene (0.75 mL, 0.2 M), at –10 ºC for 48 h. The crude product was purified by FCC (silica, dry load, pentane:EtOAc 95:5 to 85:15). Compound **2.60d** was obtained as a yellow oil (48.5 mg, 0.142 mmol, 94% yield) with 96.5:3.5 *er*. Alternatively, the reaction was performed as described above but in toluene (1.5 mL, 0.1 M) at –10 ºC for 72 h, yielding after purification compound **2.60d** as a yellow oil (51.1 mg, 0.149 mmol, 99% yield) with 96.5:3.5 *er*. Spectroscopic data for product **2-60d** matched those reported in the literature.[28e] **^{1}H NMR** (500 MHz, $CDCl_3$): δ 7.30–7.28 (m, 1H), 7.18–7.11 (m, 2H), 7.01–6.98 (m, 1H), 6.31 (m/app br q, 1H), 4.13 (d, *J* = 11.0 Hz, 1H), 4.09 (d, *J* = 11.0 Hz, 1H), 4.02 (d, *J* = 11.2 Hz, 1H), 3.96 (d, *J* = 11.2 Hz, 1H), 2.80–2.70 (m, 1H), 2.55 (d, *J* = 18.0 Hz, 1H), 2.40 (dt, *J* = 18.3, 3.0 Hz, 1H), 2.09 (s, 3H), 2.07 (s, 3H), 1.87 (dd, *J* = 12.8, 8.9 Hz, 1H), 1.60 (app t, *J* = 12.8 Hz, 1H), 1.39 (s, 3H), 0.91 (s, 3H). **^{13}C NMR** (126 MHz, $CDCl_3$): δ 171.14, 171.08, 144.4, 144.3, 134.2, 127.0, 126.4, 126.3, 123.6, 120.0, 68.1, 65.8, 48.2, 45.0, 37.7, 36.8, 31.9, 25.7, 22.0, 21.0. **SFC** (IB-N (100 × 3 mm, 3 µm), CO_2:MeOH 90:10, 1.2 mL/min, 35 ºC, BPR 150 bar, 280 nm): en1 (minor, 3.5%) min 0.93, en2 (minor, 96.5%) min 1.11. **$[a]^{24.7}_D$** +5.1 (c 1.0, $CHCl_3$, sample with 96.5:3.5 *er*); lit: [28e] $[a]^{23.9}_D$ +3.1 (c 1.0, $CHCl_3$, sample with 79:21 *er*).

(*R*)-(4,4-Dimethyl-2,3,3*a*,4-tetrahydro-1*H*-cyclopenta[*b*]naphthalene-2,2-diyl)bis(methylene) Bis(phenylcarbamate) (2.60e)

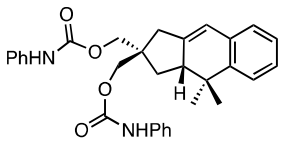

Prepared following the general procedure **GP5** using enyne **2.59e** (74.5 mg, 0.150 mmol, 1.0 equiv), gold(I) complex **Au10** (6.7 mg, 7.5 µmol, 0.05 equiv) and chiral salt ***(R)*-Ag6** (7.1 mg, 7.5 µmol, 0.05 equiv) in toluene (1.5 mL, 0.1 M), at –10 ºC for 25 h. The crude product was purified by FCC (silica, liquid load, CyH:EtOAc 90:10 to 80:20). Compound **2.60e** was obtained as a white fluffy solid (69.5 mg, 0.140 mmol, 93% yield) with 97:3 *er*. **M.p.** 86 °C (sample with 97:3 *er*). **IR** (film from $CDCl_3$, cm^{-1}) υ 339, 2961, 2928, 1707, 1600, 1528, 1501, 1443, 1313, 1213, 1057, 752. **^{1}H NMR** (500 MHz, $CDCl_3$): δ 7.40–7.27 (m, 9H), 7.18–7.12 (m, 2H), 7.09–7.05 (m, 2H), 7.02–6.99 (m, 1H), 6.73 (br s, 1H), 6.70 (br s, 1H), 6.33 (m/app br q, 1H), 4.27 (d, *J* = 10.7 Hz, 1H), 4.24 (d, *J* = 10.7 Hz, 1H), 4.15 (d, *J* = 11.0 Hz, 1H), 4.11 (d, *J* = 11.0 Hz, 1H), 2.86–2.78 (m, 1H), 2.60 (d, *J* = 18.0 Hz, 1H), 2.47 (app dt, *J* = 18.0, 2.6 Hz, 1H), 1.94 (dd, *J* = 12.7, 8.1 Hz, 1H), 1.64 (app t, *J* = 12.2 Hz, 1H), 1.40 (s, 3H), 0.93 (s, 3H). **^{13}C NMR** (101 MHz, $CDCl_3$): δ 153.8, 153.7, 144.3, 144.2, 137.8, 134.1, 129.3, 129.2, 126.9, 126.3, 126.2, 123.7, 123.6, 120.0, 118.9 (br s), 68.9, 66.4, 48.1, 45.3, 37.6, 36.7, 31.8, 25.7, 22.0. **HRMS** (ESI +) calculated for $[C_{31}H_{32}N_2NaO_4]^+$ $[M + Na]^+$ 519.2254 *m/z*; found 519.2260 *m/z*. **SFC** (IC (100 × 3 mm, 3 µm), CO_2:EtOH 70:30, 1.2 mL/min, 35 ºC, BPR 150 bar, 280 nm): en1 (minor, 3%) min 1.57, en2 (major, 97%) min 3.17. **$[\alpha]^{24.8}_D$** +12 (c 0.82, $CHCl_3$, sample with 97:3 *er*).

(*R*)-(4,4-Dimethyl-2,3,3*a*,4-tetrahydro-1*H*-cyclopenta[*b*]naphthalene-2,2-diyl)bis(methylene) Bis(4-methylbenzenesulfonate) (2.60f)

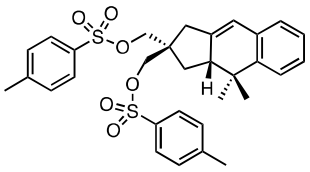

Prepared following the general procedure **GP5** using enyne **2.59f** (85.0 mg, 0.150 mmol, 1.0 equiv), gold(I) complex **Au10** (6.7 mg, 7.5 μmol, 0.05 equiv) and chiral salt ***(R)*-Ag6** (7.1 mg, 7.5 μmol, 0.05 equiv) in toluene (1.5 mL, 0.1 M), at 23 ºC for 48 h. The crude product was purified by automated FCC (silica, dry load, CyH: CH_2Cl_2 80:20). Compound **2.60f** was obtained as a white solid (77.5 mg, 0.137 mmol, 91% yield) with 97.5:2.5 *er*. **M.p.** 73–77 °C (racemic sample). **IR** (film from $CDCl_3$, cm^{-1}) n 2961, 2927, 1361, 1189, 1176, 962, 830, 813, 665, 554. **^{1}H NMR** (300 MHz, $CDCl_3$): δ 7.74 (dd, *J* = 18.4, 8.3 Hz, 4H), 7.34 (dd, *J* = 17.4, 8.0 Hz, 4H), 7.25–7.09 (m, 3H), 7.00–6.88 (m, 1H), 6.21 (d, *J* = 2.3 Hz, 1H), 3.98 (d, *J* = 9.5 Hz, 1H), 3.94 (d, *J* = 9.5 Hz, 1H), 3.83 (d, *J* = 9.9 Hz, 1H), 3.78 (d, *J* = 9.9 Hz, 1H), 2.47–2.44 (m, 4H), 2.42 (s, 3H), 2.41–2.16 (m, 2H), 1.79 (dd, *J* = 13.1, 8.1 Hz, 1H), 1.48–1.35 (m, 1H), 1.28 (s, 3H), 0.80 (s, 3H). **^{13}C NMR** (75 MHz, $CDCl_3$) δ 145.3, 144.0, 142.6, 133.8, 132.5, 132.4, 130.2, 128.1, 128.0, 127.2, 126.4, 126.3, 123.6, 120.6, 72.6, 70.0, 47.6, 45.7, 37.2, 36.7, 31.0, 25.6, 21.9, 21.8. **HRMS** (ESI +) calculated for $[C_{31}H_{34}NaO_6S_2]^+$ $[M+Na]^+$ 589.1689 *m/z*; found 589.1675 *m/z*. **SFC** (OJ (100 × 3 mm, 3 μm), CO_2:MeOH 85:15, 1.2 mL/min, 35 ºC, BRP 150 bar, 280 nm): en1 (major, 97.5%) min 2.86, en2 (minor, 2.5%) min 3.16. **$[\alpha]^{25.0}_D$** + 18 (c 1.0, $CHCl_3$, sample with 97.5:2.5 *er*).

(*R*)-2',2',4,4-Tetramethyl-1,3,3*a*,4-tetrahydrospiro[cyclopenta[*b*]naphthalene-2,5'-[1,3]dioxane] (2.60g)

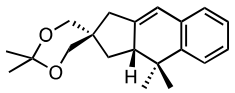

Prepared following the general procedure **GP5** using enyne **2.59g** (44.8 mg, 0.150 mmol, 1.0 equiv), gold(I) complex **Au10** (6.7 mg, 7.5 μmol, 0.05 equiv) and chiral salt ***(R)*-Ag6** (7.1 mg, 7.5 μmol, 0.05 equiv) in toluene (1.5 mL, 0.1 M), at –10 ºC for 26 h. The crude product was purified by FCC (silica, liquid load, CyH:EtOAc 100:0 to 96:4). Compound **2.60g** was obtained as a colorless oil (42.6 mg, 0.143 mmol, 95% yield) with 96:4 *er*. **IR** (film from $CDCl_3$, cm^{-1}) υ 2990, 2961, 2936, 2859, 1383, 1197, 1060. **^{1}H NMR** (500 MHz, $CDCl_3$): δ 7.31–7.29 (m, 1H), 7.18–7.12 (m, 2H), 7.02–6.99 (m, 1H), 6.32 (m/app br q, 1H), 3.78 (d, *J* = 11.6 Hz, 1H), 3.74 (d, *J* = 11.8 Hz, 1H), 3.68 (d, *J* = 11.5 Hz, 1H), 3.60 (d, *J* = 11.5 Hz, 1H), 2.74–2.67 (m, 1H), 2.64 (d, *J* = 18.0 Hz, 1H), 2.29 (app dt, *J* = 18.0, 2.8 Hz, 1H), 2.07 (dd, *J* = 12.5, 8.2 Hz, 1H), 1.47 (s, 3H), 1.46 (s, 3H), 1.46–1.44 (m, 1H), 1.41 (s, 3H), 0.92 (s, 3H). **^{13}C NMR** (126 MHz, $CDCl_3$): δ 145.2, 144.4, 134.4, 126.9, 126.3, 126.2, 123.7, 119.7, 98.2, 69.8, 68.0, 48.0, 40.9, 38.9, 36.7, 33.0, 25.8, 24.1, 23.9, 22.1. **HRMS** (APCI +) calculated for $[C_{20}H_{26}O_2]^+$ $[M]^+$ 298.1927 *m/z*; found 298.1927 *m/z*. **HPLC** (OD-H (250 × 4.6 mm, 5 mm), 99:1 *n*-hexane:*i*-PrOH, 1 mL/min, 25 ºC, 270 nm): en1 (major, 96%) min 5.58, en2 (minor, 4%) min 6.42. **$[\alpha]^{26.1}_D$** –3.3 (c 0.87, $CHCl_3$, sample with 96:4 *er*).

Dimethyl (*R*)-4,4-dimethyl-1,3,3*a*,4-tetrahydro-2*H*-cyclopenta[*b*]naphthalene-2,2-dicarboxylate (2.60h)

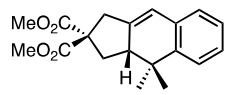

Prepared following the general procedure **GP5** using enyne **2.59h** (47.2 mg, 0.150 mmol, 1.0 equiv), gold(I) complex **Au10** (6.7 mg, 7.5 μmol, 0.05 equiv) and chiral salt ***(R)*-Ag6** (7.1 mg, 7.5 μmol, 0.05 equiv) in toluene (0.75 mL, 0.2 M), at –10 ºC for 48 h. The crude product was purified by FCC (silica, liquid load, CyH:EtOAc 98:2 to 90:10). Compound **2.60h** was obtained as a white solid (44.8 mg, 0.143 mmol, 95% yield) with 96.5:3.5 *er*. Crystals suiTable for X-ray diffraction were grown by slow evaporation of a solution in chloroform at 23 ºC. Spectroscopic data for product **2.60h** matched those reported in the literature.[78] **M.p.** 57–59 °C (racemic sample). **^{1}H NMR** (300 MHz, $CDCl_3$)

δ 7.31–7.28 (m, 1H), 7.18–7.10 (m, 2H), 7.03–6.99 (m, 1H), 6.35 (m/app br q, 1H), 3.77 (s, 3H), 3.72 (s, 3H), 3.31 (dq, *J* = 18.1, 1.7 Hz, 1H), 2.99 (app dt, *J* = 18.1, 3.0 Hz, 1H), 2.75–2.66 (m, 1H), 2.60 (ddd, *J* = 12.2, 7.5, 1.4 Hz, 1H), 2.15 (app t, *J* = 12.2 Hz, 1H), 1.43 (s, 3H), 0.93 (s, 3H). **^{13}C NMR** (75 MHz, $CDCl_3$): δ 172.3, 172.1, 144.1, 143.0, 134.0, 127.0, 126.38, 126.36, 123.6, 119.5, 59.0, 53.01, 52.98, 48.5, 39.3, 36.7, 34.9, 25.7, 22.1. **SFC** (IB-N (100 × 3 mm, 3 μm), CO_2:EtOH 95:5, 1.2 mL/min, 35 ºC, BPR 150 bar, 210 nm): en1 (major, 96.5%) min 1.11, en2 (minor, 3.5%) min 1.32. **[α]$^{24.8}_D$** –15 (c 0.79, $CHCl_3$, sample with 96.5:3.5 *er*); lit: [28e] **[α]$^{26.8}_D$** –14 (c 0.79, $CHCl_3$, sample with 93:7 *er*).

(*R*)-6-Methoxy-2,2-bis(methoxymethyl)-4,4-dimethyl-2,3,3*a*,4-tetrahydro-1*H*-cyclopenta[*b*]naphthalene (2.60i)

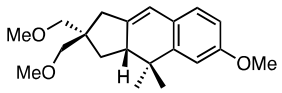

Prepared following the general procedure **GP5** using enyne **2.59i** (47.5 mg, 0.150 mmol, 1.0 equiv), gold(I) complex **Au10** (6.7 mg, 7.5 μmol, 0.05 equiv) and chiral salt ***(R)*-Ag6** (7.1 mg, 7.5 μmol, 0.05 equiv) in toluene (0.75 mL, 0.2 M), at –10 ºC for 48 h. The crude product was purified by FCC (silica, dry load, pentane:EtOAc 98:2 to 95:5). Compound **2.60i** was obtained as a colorless oil (46.5 mg, 0.147 mmol, 98% yield) with 97:3 *er*. Spectroscopic data for product **2.60i** matched those reported in the literature.[28e] **^{1}H NMR** (400 MHz, $CDCl_3$): δ 6.94 (d, *J* = 8.2 Hz, 1H), 6.88 (d, *J* = 2.5 Hz, 1H), 6.66 (dd, *J* = 8.2, 2.6 Hz, 1H), 6.26–6.22 (m/app br q, 1H), 3.80 (s, 3H), 3.38 (s, 3H), 3.37 (s, 2H), 3.32 (s, 3H), 3.26 (d, *J* = 9.1 Hz, 1H), 3.23 (d, *J* = 9.1 Hz, 1H), 2.72–2.63 (m, 1H), 2.51–2.43 (m, 1H), 2.31 (dt, *J* = 17.9, 2.8 Hz, 1H), 1.84 (dd, *J* = 12.6, 8.3 Hz, 1H), 1.53 (t, *J* = 12.2 Hz, 1H), 1.36 (s, 3H), 0.90 (s, 3H). **^{13}C NMR** (101 MHz, $CDCl_3$): δ 158.5, 146.6, 144.0, 128.0, 126.8, 118.4, 110.9, 110.0, 77.4, 75.1, 59.45, 59.43, 55.4, 48.1, 46.8, 37.8, 37.1, 31.7, 25.7, 21.9. **SFC** (OJ (100 × 3 mm, 3 μm), CO_2:MeOH 97:3, 1.2 mL/min, 35 ºC, BPR 150 bar, 280 nm): en1 (major, 97%) min 1.04, en2 (minor, 3%) min 1.24. **[α]$^{24.8}_D$** –22 (c 1.0, $CHCl_3$, sample with 97:3 *er*); lit: [28e] **[α]$^{26.8}_D$** –22 (c 1.0, $CHCl_3$, sample with 96:4 *er*).

(*R*)-6-(*tert*-Butyl)-2,2-bis(methoxymethyl)-4,4-dimethyl-2,3,3*a*,4-tetrahydro-1*H*-cyclopenta[*b*]naphthalene (2.60j)

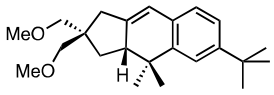

Prepared following the general procedure **GP5** using enyne **2.59j** (51.1 mg, 0.150 mmol, 1.0 equiv), gold(I) complex **Au10** (6.7 mg, 7.5 μmol, 5 mol%) and chiral salt ***(R)*-Ag6** (7.0 mg, 7.5 μmol, 5 mol%) in toluene (1.5 mL, 0.1 M), at −10 ºC for 24 h. The crude product was purified FCC (silica, dry load, CyH:CH_2Cl_2 95:5). Compound **2.60j** was obtained as a colorless oil (44.7 mg, 0.131 mmol, 87% yield) with 97.5:2.5 *er*. Spectroscopic data match those previously reported. [28e] **^{1}H NMR** (300 MHz, $CDCl_3$): δ 7.37 (d, *J* = 1.9 Hz, 1H), 7.19 (dd, *J* = 7.9, 2.0 Hz, 1H), 6.98 (d, *J* = 7.9 Hz, 1H), 6.34–6.27 (m/app br q, 1H), 3.45–3.38 (m, 5H), 3.37–3.33 (m, 2H), 3.28–3.24 (m, 3H), 2.75 (td, *J* = 8.4, 3.6 Hz, 1H), 2.56–2.45 (m, 1H), 2.43–2.29 (m, 1H), 1.88 (dd, *J* = 12.3, 8.4 Hz, 1H), 1.57 (t, *J* = 12.2 Hz, 1H), 1.44 (s, 3H), 1.36 (s, 9H), 0.95 (s, 3H). **^{13}C NMR** (75 MHz, $CDCl_3$): δ 149.4, 145.8, 144.2, 132.1, 125.6, 122.9, 120.5, 118.7, 77.4, 75.1, 59.5, 48.4, 46.8, 37.9, 37.0, 34.9, 31.7, 31.6, 25.7, 22.1. **HPLC** (OD-H (100 × 3 mm, 3 μm) isocratic hexane, 25 °C, 1.0 mL/min, 280 nm): en1 (minor, 2.5%) 6.54 min; en2 (major, 97.5%) 8.59 min. **[α]$^{25.0}_D$** −22 (c 1.0, $CHCl_3$, sample with 97.5:2.5 *er*); lit: [28e] **[α]$^{27.0}_D$** −17 (c 1.0, $CHCl_3$, sample with 91:9 *er*).

(*R*)-2,2-Bis(methoxymethyl)-4,4-dimethyl-6-(trifluoromethyl)-2,3,3*a*,4-tetrahydro-1*H*-cyclopenta[*b*]naphthalene (2.60k)

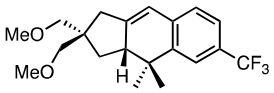

Prepared following the general procedure **GP5** using enyne **2.59k** (53.2 mg, 0.150 mmol, 1.0 equiv), gold(I) complex **Au10** (6.7 mg, 7.5 μmol, 0.05 equiv) and chiral salt ***(R)*-Ag6** (7.1 mg, 7.5 μmol, 0.05 equiv) in toluene (0.75 mL, 0.2 M) at –10 ºC for 48 h. The crude product was purified by FCC (silica, dry load, pentane:EtOAc 98:2 to 95:5). Compound **2.60k** was obtained as a colorless oil (51.8 mg, 0.146 mmol, 97% yield) with 97:3 *er*. Spectroscopic data for product **2.60k** matched those reported in the literature.[28e] **^{1}H NMR** (400 MHz, $CDCl_3$): δ 7.48 (s, 1H), 7.43–7.32 (m, 1H), 7.06 (d, *J* = 7.9 Hz, 1H), 6.37–6.28 (m/app br q, 1H), 3.38 (s, 3H), 3.37 (s, 2H), 3.33 (s, 3H), 3.26 (d, *J* = 9.1 Hz, 1H), 3.23 (d, *J* = 9.1 Hz, 1H), 2.80–2.70 (m, 1H), 2.57–2.48 (m, 1H), 2.41–2.33 (m, 1H), 1.87 (dd, *J* = 12.6, 8.5 Hz, 1H), 1.59 (t, *J* = 12.1 Hz, 1H), 1.42 (s, 3H), 0.93 (s, 3H). **^{13}C NMR** (101 MHz, $CDCl_3$): δ 150.2, 145.2, 137.9 (app d, *J* = 1.3 Hz), 128.2 (q, *J* = 31.8 Hz), 126.0, 124.7 (q, *J* = 272.3 Hz), 123.3 (q, *J* = 4.0 Hz), 120.5 (q, *J* = 3.8 Hz), 118.3, 77.3, 75.2, 59.5, 48.3, 46.8, 38.0, 37.0, 31.5, 25.6, 21.9. **^{19}F NMR** (376 MHz, $CDCl_3$): δ −62.1. **HPLC** (IB (250 × 4.6 mm, 5 μm), 50% hexane, 50% 99.9:0.1:2 hexane:*i*-PrOH:MTBE, 0.5 mL/min, 25 ºC, 220 nm): en1 (minor, 3%) min 11.4, en2 (major, 97%) min 11.7. **$[\alpha]^{24.9}_D$** –2.7 (c 1.0, $CHCl_3$, sample with 97:3 *er*); lit:[28e] **$[\alpha]^{26.8}_D$** –0.9 (c 1.0, $CHCl_3$, sample with 91:9 *er*).

(*R*)-2,2-Bis(methoxymethyl)-4,4-dimethyl-6-nitro-2,3,3*a*,4-tetrahydro-1*H*-cyclopenta[*b*]naphthalene (2.60l)

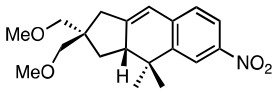

Prepared following the general procedure **GP5** using enyne **2.59l** (49.7 mg, 0.150 mmol, 1.0 equiv), gold(I) complex **Au10** (6.7 mg, 7.5 μmol, 0.05 equiv) and chiral salt ***(R)*-Ag6** (7.1 mg, 7.5 μmol, 0.05 equiv) in toluene (0.75 mL, 0.2 M), at –10 ºC for 48 h. The crude product was purified by PTLC (silica, CyH:EtOAc 95:5). Compound **2.60l** was obtained as a yellow oil (42.2 mg, 0.127 mmol, 85% yield) with 89.5:10.5 *er*. Spectroscopic data for product **2.60l** matched those reported in the literature.[28e] **^{1}H NMR** (400 MHz, $CDCl_3$): δ 8.13 (d, *J* = 2.3 Hz, 1H), 8.00 (dd, *J* = 8.3, 2.3 Hz, 1H), 7.07 (d, *J* = 8.4 Hz, 1H), 6.42–6.34 (m/app br q, 1H), 3.38 (s, 3H), 3.36 (s, 2H), 3.32 (s, 3H), 3.26 (d, *J* = 9.1 Hz, 1H), 3.23 (d, *J* = 9.1 Hz, 1H), 2.82–2.71 (m, 1H), 2.60–2.50 (m, 1H), 2.44–2.35 (m, 1H), 1.88 (dd, *J* = 12.8, 8.6 Hz, 1H), 1.64–1.58 (m, 1H, overlapping with residual H_2O signal), 1.46 (s, 3H), 0.94 (s, 3H). **^{13}C NMR** (101 MHz, $CDCl_3$): δ 153.7, 146.4, 145.9, 141.1, 126.2, 122.2, 119.5, 118.2, 75.3, 59.5, 48.4, 46.9, 38.3, 37.3, 31.4, 25.7, 21.9. **SFC** (IG (100 × 3 mm, 3 μm), CO_2:MeOH 97:3, 1.2 mL/min, 35 ºC, BPR 150 bar, 210 nm): en1 (minor, 10.5%) min 2.51, en2 (major, 89.5%) min 2.79. **$[\alpha]^{24.9}_D$** –76 (c 1.0, $CHCl_3$, sample with 89.5:10.5 *er*); lit:[28e] **$[\alpha]^{26.8}_D$** –69 (c 1.0, $CHCl_3$, sample with 90:10 *er*).

(*R*)-2,2-Bis(methoxymethyl)-4,4,8-trimethyl-2,3,3*a*,4-tetrahydro-1*H*-cyclopenta[*b*]naphthalene (2.60m)

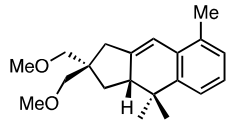

Prepared following the general procedure **GP5** using enyne **2.59m** (45.1 mg, 0.150 mmol, 1.0 equiv), gold(I) complex **Au10** (6.7 mg, 7.5 μmol, 0.05 equiv) and chiral salt ***(R)*-Ag6** (7.1 mg, 7.5 μmol, 0.05 equiv) in toluene (0.75 mL, 0.2 M) at –10 ºC for 48 h. The crude product was purified by FCC (silica, dry load, pentane:EtOAc 100:0 to 95:5). Compound **2.60m** was obtained as a colorless oil (43.9 mg, 0.146 mmol, 97% yield) with 95:5 *er*. Spectroscopic data for product **2m** matched those reported in the literature.[28e] **^{1}H NMR** (400 MHz, $CDCl_3$): δ 7.16 (d, *J* = 7.6 Hz, 1H), 7.05 (t, *J* = 7.6 Hz, 1H), 6.99 (d, *J* = 7.4 Hz, 1H), 6.52–6.47 (m/app br q, 1H), 3.39 (s, 5H), 3.33 (s, 3H), 3.26 (d, *J* = 9.2 Hz, 1H), 3.24 (d, *J* = 9.2 Hz, 1H), 2.74–2.65 (m, 1H), 2.57–2.49 (m,

1H), 2.41–2.31 (m, 4H), 1.85 (dd, *J* = 12.2, 8.5 Hz, 1H), 1.59–1.51 (m, 1H), 1.38 (s, 3H), 0.91 (s, 3H). **^{13}C NMR** (101 MHz, $CDCl_3$): δ 146.8, 144.8, 132.8, 132.8, 128.1, 126.2, 121.4, 115.8, 77.4, 75.1, 59.49, 59.46, 47.7, 46.8, 38.3, 37.1, 31.7, 26.0, 21.7, 19.8. **SFC** (OJ (100 × 3 mm, 3 μm), CO_2:MeOH 98:2, 1.2 mL/min, 35 ºC, BPR 150 bar, 210 nm): en1 (major, 95%) min 1.04, en2 (minor, 5%) min 1.23. **[α]$^{24.9}_D$** –36 (c 1.0, $CHCl_3$, sample with 95:5 *er*); lit:[28e] **[α]$^{23.8}_D$** –35 (c 1.0, $CHCl_3$, sample with 95:5 *er*).

(*R*)-8-Fluoro-2,2-bis(methoxymethyl)-4,4-dimethyl-2,3,3*a*,4-tetrahydro-1*H*-cyclopenta[*b*]naphthalene (2.60n)

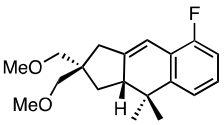

Prepared following the general procedure **GP5** using enyne **2.59n** (45.7 mg, 0.150 mmol, 1.0 equiv), gold(I) complex **Au10** (6.7 mg, 7.5 μmol, 0.05 equiv) and chiral salt ***(R)*-Ag6** (7.1 mg, 7.5 μmol, 0.05 equiv) in toluene (1.5 mL, 0.1 M) at –10 ºC for 48 h. The crude product was purified by FCC (silica, dry load, pentane:EtOAc 98:2 to 96:4). Compound **2.60n** was obtained as a colorless oil (43.4 mg, 0.143 mmol, 95% yield) with 95:5 *er*. Spectroscopic data for product **2.60n** matched those reported in the literature.[28e] **^{1}H NMR** (400 MHz, $CDCl_3$): δ 7.12–7.03 (m, 2H), 6.91–6.80 (m, 1H), 6.59–6.48 (m/app br q, 1H), 3.38 (s, 3H), 3.35 (s, 2H), 3.33 (s, 3H), 3.26 (d, *J* = 9.2 Hz, 1H), 3.23 (d, *J* = 9.1 Hz, 1H), 2.78–2.66 (m, 1H), 2.57–2.49 (m, 1H), 2.41–2.32 (m, 1H), 1.86 (dd, *J* = 12.5, 8.4 Hz, 1H), 1.61–1.52 (m, 1H), 1.38 (s, 3H), 0.91 (s, 3H). **^{13}C NMR** (101 MHz, $CDCl_3$): δ 158.4 (d, *J* = 246.0 Hz), 147.8 (d, *J* = 1.7 Hz), 147.1 (d, *J* = 3.5 Hz), 127.0 (d, *J* = 8.5 Hz), 122.4 (d, *J* = 14.3 Hz), 119.1 (d, *J* = 2.9 Hz), 112.9 (d, *J* = 21.7 Hz), 111.0 (d, *J* = 6.3 Hz), 77.3, 75.1, 59.47, 59.45, 48.0, 46.8, 38.2, 37.1 (d, *J* = 2.5 Hz), 31.5, 25.8, 21.7. **^{19}F NMR** (376 MHz, $CDCl_3$): δ –122.8. **SFC** (IG (100 × 3 mm, 3 μm), CO_2:MeOH 97:3, 1.2 mL/min, 35 ºC, BPR 150 bar, 280 nm): en1 (minor, 5%) min 1.17, en2 (major, 95%) min 1.33. **[α]$^{25.0}_D$** –1.3 (c 1.0, $CHCl_3$, sample with 95:5 *er*); lit:[28e] **[α]$^{26.8}_D$** –2.0 (c 1.0, $CHCl_3$, sample with 93:7 *er*).

(*R*)-5,7-Dibromo-2,2-bis(methoxymethyl)-4,4-dimethyl-2,3,3*a*,4-tetrahydro-1*H*-cyclopenta[*b*]naphthalene (2.60o)

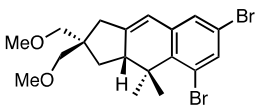

Prepared following the general procedure **GP5** using enyne **2.59o** (66.6 mg, 0.150 mmol, 1.0 equiv), gold(I) complex **Au10** (6.7 mg, 7.5 μmol, 0.05 equiv) and chiral salt ***(R)*-Ag6** (7.1 mg, 7.5 μmol, 0.05 equiv) in toluene (0.75 mL, 0.2 M) at –10 ºC for 48 h. The crude product was purified by FCC (silica, dry load, pentane:EtOAc 100:0 to 95:5). Compound **2.60o** was obtained as a pale-yellow oil (65.3 mg, 0.147 mmol, 98% yield) with 98.5:1.5 *er*. Spectroscopic data for product **2.60o** matched those reported in the literature.[28e] **^{1}H NMR** (400 MHz, $CDCl_3$): δ 7.50 (d, *J* = 2.2 Hz, 1H), 7.03 (d, *J* = 2.2 Hz, 1H), 6.12 (q, *J* = 2.3 Hz, 1H), 3.37 (s, 3H), 3.34 (s, 2H), 3.33 (s, 3H), 3.25 (d, *J* = 8.9 Hz, 1H), 3.22 (d, *J* = 9.1 Hz, 1H), 2.85–2.75 (m, 1H), 2.55–2.45 (m, 1H), 2.41–2.30 (m, 1H), 1.86 (dd, *J* = 12.4, 8.4 Hz, 1H), 1.73 (s, 3H), 1.64–1.56 (m, 1H), 1.03 (s, 3H). **^{13}C NMR** (101 MHz, $CDCl_3$): δ 148.2, 141.3, 139.6, 135.4, 128.7, 122.2, 120.0, 118.5, 75.2, 59.49, 59.46, 49.8, 46.5, 40.0, 38.0, 32.4, 27.4, 18.6. **SFC** (IG (100 × 3 mm, 3 μm), CO_2:EtOH 75:25, 1.2 mL/min, 35 ºC, BPR 150 bar, 280 nm): en1 (major, 98.5%) min 0.85, en2 (minor, 1.5%) min 0.93. **[α]$^{25.0}_D$** –11 (c 1.0, $CHCl_3$, sample with 98.5:1.5 *er*); lit:[28e] **[α]$^{26.8}_D$** –11 (c 1.0, $CHCl_3$, sample with 95:5 *er*).

(*R*)-7-Chloro-2,2-bis(methoxymethyl)-4,4-dimethyl-2,3,3*a*,4-tetrahydro-1*H*-cyclopenta[*b*]naphthalene (2.60p)

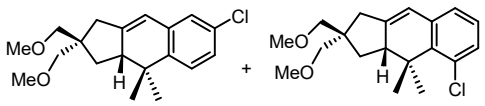

2.60p **2.60p'**

Prepared following the general procedure **GP5** using enyne **2.59p** (48.1 mg, 0.150 mmol, 1.0 equiv), gold(I) complex **Au10** (6.7 mg, 7.5 μmol, 0.05 equiv) and chiral salt ***(R)*-Ag6** (7.1 mg, 7.5 μmol, 0.05 equiv) in toluene (0.75 mL, 0.2 M) at –10 ºC for 48 h. ^{1}H NMR of the crude reaction mixture against internal standard showed 100% product, with a 7:3 **2.60p**:**2.60p'** regioisomeric ratio, and no residual starting material. The crude was purified by FCC (silica, dry load, CyH:EtOAc 100:0 to 95:5). Compound **2.60p** was obtained in a 7:3 mixture with regioisomeric **2.60p'** as a colorless oil (46.8 mg, 0.146 mmol, 97% yield) with 96:4 *er* for the major isomer **2.60p**; enantiomeric peaks for the minor isomer **2.60p'** could not be resolved. **IR** (film from $CDCl_3$, cm^{-1}) υ 2963, 2925,2873, 1475, 1198, 1106. **^{1}H NMR** (400 MHz, $CDCl_3$): δ 7.19 (d, *J* = 8.3 Hz, 1H, **2.60p)**, 7.10 (dd, *J* = 7.9, 1.4 Hz, 1H, **2.60p')**, 7.07 (dd, *J* = 8.2, 2.3 Hz, 1H, **2.60p)**, 7.00 (t, *J* = 7.7 Hz, 1H, **2.60p')**, 6.96 (d, *J* = 2.2 Hz, 1H, **2.60p)**, 6.87 (dd, *J* = 7.4, 1.3 Hz, 1H, **2.60p')**, 6.24–6.16 (m, 1H, **2.60p + 2.60p')**, 3.38 (s, 3H, **2.60p** + **2.60p')**, 3.36 (s, 2H, **2.60p** + **2.60p')**, 3.34 (s, 3H, **2.60p')**, 3.32 (s, 3H, **2.60p)**, 3.27 (d, *J*=8.9 Hz, 1H, **2.60p')**, 3.25 (d, *J* = 8.9 Hz, 1H, **2.60p')**, 3.25 (d, *J* = 9.1, 1H, **2.60p)**, 2.87–2.78 (m, 1H, **2.60p')**, 2.55–2.45 (m, 1H, **2.60p + 2.60p')**, 2.40–2.27 (m, 1H, **2.60p** + **2.60p')**, 1.95–1.81 (m, 1H, **2.60p + 2.60p')**, 1.72 (s, 3H, **2.60p')**, 1.62–1.56 (m, 1H, **2.60p')**, 1.60–1.50 (m, 1H, **2.60p)**, 1.36 (s, 3H, **2.60p)**, 1.05 (s, 3H, **2.60p')**, 0.89 (s, 3H, **2.60p)**. **^{13}C NMR** (101 MHz, $CDCl_3$): δ 148.8 (**2.60p)**, 146.3 (**2.60p')**, 143.0 (**2.60p)**, 140.8 (**2.60p')**, 138.0 (**2.60p')**, 136.4 (**2.60p')**, 133.3 (**2.60p')**, 131.8 (**2.60p)**, 130.1 (**2.60p + 2.60p')**, 127.2 (**2.60p')**, 126.2 (**2.60p)**, 125.7 (**2.60p)**, 125.5 (**2.60p')**, 125.1 (**2.60p)**, 119.3 (**2.60p')**, 118.2 (**2.60p)**, 77.3 (**2.60p + 2.60p')**, 75.21 (**2.60p')**, 75.18 (**2.60p)**, 59.5 (**2.60p** + **2.60p')**, 49.7 (**2.60p')**, 48.4 (**2.60p)**, 46.8 (**2.60p)**, 46.4 (**2.60p')**, 39.7 (**2.60p')**, 38.0 (**2.60p)**, 36.7 (**2.60p')**, 32.3 (**2.60p')**, 31.5 (**2.60p)**, 27.5 (**2.60p')**, 25.7 (**2.60p)**, 22.0 (**2.60p)**, 18.9 (**2.60p')**. **HRMS** (ESI +) calculated for $[C_{19}H_{25}ClNaO_2]^+$ $[M + Na]^+$ 343.1435 *m/z*; found 343.1434 *m/z*. **SFC** (OJ (100 × 3 mm, 3 μm), CO_2:MeOH 98:2, 1.2 mL/min, 35 ºC, BPR 150 bar, 230 nm): **2.60p'** (both enantiomers) min 1.03, **2.60p-**en1 (major, 96%) min 1.19, **2.60p-**en2 (minor, 4%) min 1.38. **[α]$^{26.1}_D$** –16 (c 1.0, $CHCl_3$, sample with 7:3 **2.60p**:**2.60p'** rr, and 96:4 *er* for **2.60p**).

(*R*)-9,9-Bis(methoxymethyl)-7,7-dimethyl-7*a*,8,9,10-tetrahydro-7*H*-cyclopenta[*b*]phenanthrene (2.60q)

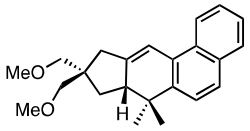

Prepared following the general procedure **GP5** using enyne **2.59q** (50.5 mg, 0.150 mmol, 1.0 equiv), gold(I) complex **Au10** (6.7 mg, 7.5 μmol, 0.05 equiv) and chiral salt ***(R)*-Ag6** (7.1 mg, 7.5 μmol, 0.05 equiv) in toluene (0.75 mL, 0.2 M) at –10 ºC for 48 h. The crude product was purified by FCC (silica, dry load, pentane:EtOAc 98:2 to 92:8). Compound **2.60q** was obtained as a colorless oil (50.0 mg, 0.149 mmol, 99% yield) with 92.5:7.5 *er*. **IR** (film from $CDCl_3$, cm^{-1}) υ 2961, 2924, 2873, 2824, 1459, 1388, 1197, 1105, 813, 745. **^{1}H NMR** (400 MHz, $CDCl_3$): δ 8.14 (d, *J* = 8.5 Hz, 1H), 7.80 (dd, *J* = 8.3, 1.0 Hz, 1H), 7.70 (d, *J* = 8.6 Hz, 1H), 7.54 (d, *J* = 8.6 Hz, 1H), 7.48 (ddd, *J* = 8.4, 6.8, 1.5 Hz, 1H), 7.42 (ddd, *J* = 7.9, 6.8, 1.2 Hz, 1H), 7.15–7.09 (m/app br q, 1H), 3.44 (s, 2H), 3.42 (s, 3H), 3.35 (s, 3H), 3.31 (d, *J* = 9.2 Hz, 1H), 3.28 (d, *J* = 9.1 Hz, 1H), 2.88–2.79 (m, 1H), 2.71–2.62 (m, 1H), 2.48 (dt, *J* = 18.2, 2.9 Hz, 1H), 1.93 (dd, *J* = 11.9, 8.5 Hz, 1H), 1.69–1.60 (m, 1H), 1.50 (s, 3H), 0.99 (s, 3H). **^{13}C NMR** (101 MHz, $CDCl_3$): δ 147.8, 141.6, 132.4, 129.58, 129.57, 128.3, 126.6, 125.8, 125.0, 123.4, 122.7, 114.3, 75.1, 59.51, 59.47, 48.2, 46.9, 38.5, 37.5, 31.7, 26.3, 21.3. **HRMS** (ESI +) calculated for $[C_{23}H_{28}NaO_2]^+$ $[M+Na]^+$ 359.1982 *m/z*; found 359.1976 *m/z*. **SFC** (IB-N (100 × 3 mm, 3 μm), CO_2:MeOH 80:20,

1.2 mL/min, 35 ºC, BPR 150 bar, 210 nm): en1 (major, 92.5%) min 1.25, en2 (minor, 7.5%) min 1.44. **[α]$^{26.1}_{D}$** –37 (c 1.0, $CHCl_3$, sample with 92.5:7.5 *er*).

(*R*)-2,2-Bis(methoxymethyl)-10,10-dimethyl-2,3,10,10*a*-tetrahydro-1*H*-benzo[*b*]indeno[5,6-*d*]thiophene (2.60r)

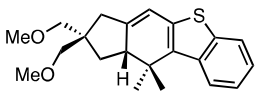

Prepared following the general procedure **GP5** using enyne **2.59r** (51.4 mg, 0.150 mmol, 1.0 equiv), gold(I) complex **Au10** (6.7 mg, 7.5 µmol, 0.05 equiv) and chiral salt ***(R)*-Ag6** (7.1 mg, 7.5 µmol, 0.05 equiv) in toluene (0.75 mL, 0.2 M) at –10 ºC for 48 h. The crude product was purified by FCC (silica, dry load, pentane:EtOAc 100:0 to 95:5). Compound **2.60r** was obtained as a colorless oil (50.3 mg, 0.147 mmol, 98% yield) with 98.5:1.5 *er*. **IR** (film from $CDCl_3$, cm^{-1}) υ 2984, 2956, 2883, 2825, 1452, 1424, 1200, 1098, 962, 729. **^{1}H NMR** (400 MHz, $CDCl_3$): δ 8.00 (d, *J* = 8.2 Hz, 1H), 7.80–7.75 (m, 1H), 7.30 (ddd, *J* = 8.3, 7.1, 1.3 Hz, 1H), 7.21 (ddd, *J* = 8.1, 7.1, 1.1 Hz, 1H), 6.31 (q, *J* = 2.4 Hz, 1H), 3.40 (s, 2H), 3.39 (s, 3H), 3.35 (s, 3H), 3.31 (d, *J* = 9.1 Hz, 1H), 3.28 (d, *J* = 9.1 Hz, 1H), 3.03–2.93 (m, 1H), 2.62–2.51 (m, 1H), 2.46–2.36 (m, 1H), 1.92 (dd, *J* = 12.6, 8.3 Hz, 1H), 1.71 (s, 3H), 1.62 (t, *J* = 12.3 Hz, 1H), 1.01 (s, 3H).**^{13}C NMR** (101 MHz, $CDCl_3$): δ 147.3, 139.4, 138.4, 136.1, 135.8, 124.0, 123.0, 122.9, 122.7, 113.1, 77.3, 75.1, 59.5, 51.4, 46.9, 37.9, 37.8, 31.0, 27.4, 19.8. **HRMS** (ESI +) calculated for $[C_{21}H_{26}NaO_2S]^+$ $[M+Na]^+$ 365.1546 *m/z*; found 365.1546 *m/z*. **SFC** (OJ (100 × 3 mm, 3 µm), CO_2:MeOH 70:30, 1.2 mL/min, 35 ºC, BPR 150 bar, 254 nm): en1 (major, 98.5%) min 0.88, en2 (minor, 1.5%) min 1.11. **[α]$^{26.1}_{D}$** –43 (c 1.0, $CHCl_3$, sample with 98.5:1.5 *er*).

(3a*R*,4*S*)-2,2-Bis(methoxymethyl)-4-methyl-4-(4-methylpent-3-en-1-yl)-2,3,3*a*,4-tetrahydro-1*H*-cyclopenta[*b*]naphthalene (2.60s)

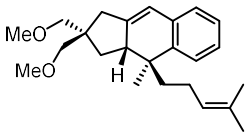

Prepared following the general procedure **GP5** using enyne **2.59s** (53.2 mg, 0.150 mmol, 1.0 equiv), gold(I) complex **Au10** (6.7 mg, 7.5 µmol, 0.05 equiv) and chiral salt ***(R)*-Ag6** (7.0 mg, 7.5 µmol, 0.05 equiv) in toluene (0.75 mL, 0.2 M) at 0 ºC for 48 h. The crude product was purified FCC (silica, dry load, CyH:CH_2Cl_2 95:5). Compound **2.60s** was obtained as a pale-yellow oil (47.7 mg, 0.135 mmol, 90% yield) with 95.5:4.5 *er*. Spectroscopic data match those previously reported.[28e] **^{1}H NMR** (300 MHz, $CDCl_3$) δ 7.24–7.07 (m, 3H), 7.06–6.99 (m, 1H), 6.28−6.23 (m, 1H), 5.25–5.12 (m, 1H), 3.39 (s, 5H), 3.34 (s, 3H), 3.27 (s, 2H), 2.99 (td, *J* = 8.6, 4.0 Hz, 1H), 2.61–2.48 (m, 1H), 2.34 (dt, *J* = 18.1, 2.8 Hz, 1H), 2.12–1.93 (m, 3H), 1.82 (dd, *J* = 12.5, 8.3 Hz, 1H), 1.73 (s, 3H), 1.68–1.45 (m, 5H), 0.91 (s, 3H). **^{13}C NMR** (75 MHz, $CDCl_3$) δ 146.8, 142.0, 135.5, 131.4, 126.5, 126.4, 126.1, 125.0, 124.1, 118.5, 77.4, 75.1, 59.5. 46.8, 43.4, 40.5, 37.9, 36.9, 31.4, 25.9, 23.5, 23.1, 17.8. **SFC** (IG (100 × 3 mm, 3 µm), CO_2:*i*-PrOH 97:3, 1.2 mL/min, 35 ºC, BRP 150 bar, 268 nm): en1 (minor, 4.5%) min 1.12, en2 (major, 95.5%) min 1.31. **[α]$^{25.0}_{D}$** −16 (c 1.0, $CHCl_3$, sample with 95.5:4.5 *er*); lit:[28e] **[α]$^{24.0}_{D}$** −16 (c 1.0, $CHCl_3$, sample with 93:7 *er*).

(3*aS*,4*R*)-2,2-Bis(methoxymethyl)-4-phenyl-2,3,3*a*,4-tetrahydro-1*H*-cyclopenta[*b*]naphthalene (2.60t)

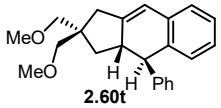

2.60t

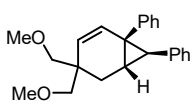

2.60t'

Prepared following the general procedure **GP5** using enyne **2.59t** (100:0 *E:Z*, 50.2 mg, 0.150 mmol, 1.0 equiv), gold(I) complex **Au10** (13.3 mg, 15.0 µmol, 0.10 equiv) and chiral salt ***(R)*-Ag6** (14.1 mg, 15.0 µmol, 0.10 equiv) in toluene (1.5 mL, 0.1 M) at 23 ºC for 48 h. The crude product was purified by FCC (silica, liquid load, CyH:EtOAc 98:2 to 97:3). Compound **2.60t** was obtained as a pale-yellow oil (49.6 mg, 0.148 mmol, 99% yield, including 5

mol % of an inseparable isomeric impurity tentatively identified as compound **2.60t'** arising from 6-*endo*-dig cyclization) with 89:11 *er*. Spectroscopic data for product **2.60t** matched those reported in the literature.[28e] **^{1}H NMR** (500 MHz, CD_2Cl_2): δ 7.42–7.37 (m, 2H), 7.34–7.28 (m, 3H), 7.11 (tt, *J* = 7.4, 1.1 Hz, 1H), 7.04 (dd, *J* = 7.4, 1.2 Hz, 1H), 6.94 (td, *J* = 7.5, 1.4 Hz, 1H), 6.53 (d, *J* = 7.6 Hz, 1H), 6.35 (q, *J* = 2.2 Hz, 1H), 3.72 (d, *J* = 15.1 Hz, 1H), 3.31 (s, 3H), 3.29 (d, *J* = 3.6 Hz, 2H), 3.27 (s, 3H), 3.20 (s, 2H), 3.16–3.07 (m, 1H), 2.51 (q, *J* = 2.1 Hz, 2H), 1.64 (dd, *J* = 13.0, 8.1 Hz, 1H), 1.30 (dd, *J* = 13.0, 10.6 Hz, 1H). **^{13}C NMR** (126 MHz, CD_2Cl_2): δ 149.0, 143.1, 138.7, 136.3, 129.0, 127.2, 127.1, 126.9, 126.3, 125.9, 119.4, 77.4, 76.3, 59.40, 59.38, 53.5, 47.4, 45.4, 38.2, 37.6. **SFC** (IG (150 × 4.6 mm, 3 μm), CO_2:MeOH 95:5, 2 mL/min, 35 ºC, ABPR 2000 psi, 267 nm): en1 (major, 89%) min 4.06, en2 (minor, 11%) min 4.41. **$[\alpha]^{25.1}_D$** –20 (c 1.0, $CHCl_3$, sample with 89:11 *er*); lit:[28e] **$[\alpha]^{26.8}_D$** –16 (c 1.0, $CHCl_3$, sample with 81:19 *er*).

(3*aS*,4*S*)-2,2-Bis(methoxymethyl)-4-phenyl-2,3,3*a*,4-tetrahydro-1*H*-cyclopenta[*b*]naphthalene (2.60u)

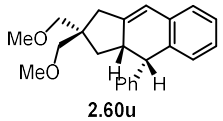

2.60u

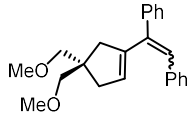

2.60u'

Prepared following the general procedure **GP5** using enyne **2.60u** (95:5 *Z*:*E*, 50.2 mg, 0.150 mmol, 1.0 equiv), gold(I) complex **Au10** (13.3 mg, 15.0 μmol, 0.10 equiv) and chiral salt ***(R)*-Ag6** (14.1 mg, 15.0 μmol, 0.10 equiv) in toluene (1.5 mL, 0.1 M) at 23 ºC for 48 h. ^{1}H NMR of the crude reaction mixture against internal standard showed 55% of *cis* product **2.60u**, 6% of *trans* product **2.60t** (arising from *E*-enyne **2.59t**), 6% of unreacted *Z*-enyne **2.59u**, and 26% of a side product, tentatively identified as diene **2.60u'**. The crude product was purified by PTLC (silica, CyH:EtOAc 94:6, plate eluted twice), obtaining compound **2.60u** as a colorless oil (24.1 mg, 0.072 mmol, 48% yield) with 82:18 *er*. **IR** (film from $CDCl_3$, cm^{-1}) υ 2921, 2891, 2850, 1450, 1106. **^{1}H NMR** (500 MHz, CD_2Cl_2): δ 7.21–7.13 (m, 4H), 7.13–7.10 (m, 1H), 7.08–7.03 (m, 4H), 6.39 (q, *J* = 2.3 Hz, 1H), 4.08 (d, *J* = 8.3 Hz, 1H), 3.39–3.31 (m, 2H), 3.29 (s, 3H), 3.24 (d, *J* = 9.5 Hz, 1H), 3.22 (d, *J* = 9.1 Hz, 1H), 3.16 (s, 2H), 3.03 (d, *J* = 8.8 Hz, 1H), 2.97 (d, *J* = 8.8 Hz, 1H), 2.45–2.38 (m, 1H), 2.18–2.09 (m, 1H), 1.84 (dd, *J* = 12.7, 8.3 Hz, 1H), 1.04 (t, *J* = 12.3 Hz, 1H). **^{13}C NMR** (126 MHz, CD_2Cl_2): δ 146.7, 142.0, 138.5, 135.8, 129.5, 129.4, 128.4, 127.4, 126.75, 126.74, 126.4, 119.6, 77.4, 75.6, 59.4, 59.2, 47.6, 47.1, 43.2, 37.9, 34.1. **HRMS** (ESI +) calculated for $[C_{23}H_{26}NaO_2]^+$ $[M+Na]^+$ 357.1825 *m/z*; found 357.1830 *m/z*. **SFC** (IB-N (100 × 3 mm, 3 μm), CO_2:*i*-PrOH 90:10, 1.2 mL/min, 35 ºC, BPR 150 bar, 210 nm): en1 (minor, 18%) min 1.69, en2 (major, 82%) min 2.00. **$[\alpha]^{26.2}_D$** +38 (c 1.0, $CHCl_3$, sample with 82:18 *er*).

(*R*)-2',2'-Bis(methoxymethyl)-1',2',3',3*a*'-tetrahydrospiro[cyclohexane-1,4'-cyclopenta[*b*]naphthalene] (2.60v)

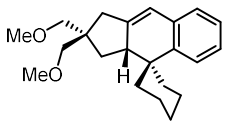

Prepared following the general procedure **GP5** using enyne **2.59v** (49.0 mg, 0.150 mmol, 1.0 equiv), gold(I) complex **Au10** (6.7 mg, 7.5 μmol, 0.05 equiv) and chiral salt ***(R)*-Ag6** (7.0 mg, 7.5 μmol, 0.05 equiv) in toluene (1.5 mL, 0.1 M), at −10 ºC for 96 h. The crude product was purified FCC (silica, dry load, CyH:CH_2Cl_2 95:5). Compound **2.60v** was obtained as a colorless oil (45.7 mg, 0.143 mmol, 95% yield) with 85:15 *er*. **IR** (film from $CDCl_3$, cm^{-1}) υ 2924, 2886, 1475, 1449, 1108, 749. **^{1}H NMR** (300 MHz, $CDCl_3$): δ 7.63–7.52 (m, 1H), 7.18–7.05 (m, 2H), 7.00 (dd, *J* = 6.7, 2.2 Hz, 1H), 6.28 (m/app br q, 1H), 3.39 (s, 5H), 3.30 (s, 3H), 3.20 (d, *J* = 1.1 Hz, 2H), 2.80–2.66 (m, 1H), 2.48 (d, *J* = 17.9 Hz, 1H), 2.30 (dt, *J* = 17.9, 2.8 Hz, 1H), 2.13–1.90 (m, 2H), 1.87–1.61 (m, 6H), 1.48–0.78 (m, 4H, overlapping with residual water signal). **^{13}C NMR** (75 MHz, $CDCl_3$): δ 146.6, 144.2, 135.8, 126.6, 126.1, 126.0, 125.3, 119.4, 77.3, 75.1, 59.5, 59.4, 49.6, 46.7, 39.1, 37.9, 32.9, 31.7, 28.0, 26.6, 24.8, 21.9. **HRMS** (ESI +) calculated for $[C_{22}H_{30}NaO_2]^+$ $[M+Na]^+$

349.2138 *m/z*; found 349.2137 *m/z*. **SFC** (IA (100 × 3 mm, 3 µm) CO_2:ACN 92:8, 1.2 mL/min, 35 ºC, BRP 150 bar, 210 nm): en1 (major, 85%) 1.19 min; en2 (minor, 15%) 1.32 min. **[α]$^{25.3}_D$** −17 (c 1.1, $CHCl_3$, sample with 85:15 *er*).

(*R*)-2,2-Bis(methoxymethyl)-3*a*,4,4-trimethyl-2,3,3*a*,4-tetrahydro-1*H*-cyclopenta[*b*]naphthalene (2.60w)

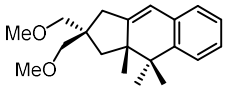

Prepared following the general procedure **GP5** using enyne **2.59w** (27.2 mg, 0.0905 mmol, 1.0 equiv), gold(I) complex **Au10** (4.1 mg, 4.6 µmol, 0.05 equiv) and chiral salt ***(R)*-Ag6** (4.3 mg, 4.6 µmol, 0.05 equiv) in toluene (0.9 mL, 0.1 M) at −10 ºC for 48 h. The crude product was purified by automated FCC (silica, dry load, CyH:EtOAc 9:1). Compound **2.60w** was obtained as a colorless oil (16.7 mg, 0.0556 mmol, 61% yield) with 80.5:19.5 *er*. **IR** (film from $CDCl_3$, cm^{-1}) υ 2964, 2923, 2873, 1479, 1455, 1198, 1104, 747. **^{1}H NMR** (500 MHz, $CDCl_3$): δ 7.24–7.21 (m, 1H), 7.15–7.07 (m, 2H), 6.94 (dd, *J* = 6.9, 1.8 Hz, 1H), 6.15 (d, *J* = 2.4 Hz, 1H), 3.39 (s, 5H), 3.35 (s, 3H), 3.27 (d, *J* = 8.9 Hz, 1H), 3.19 (d, *J* = 8.9 Hz, 1H), 2.56 (dd, *J* = 16.9, 2.7 Hz, 1H), 2.30 (d, *J* = 17.0 Hz, 1H), 2.10 (d, *J* = 14.3 Hz, 1H), 1.40–1.23 (m, 4H), 1.06 (s, 3H), 0.94 (s, 3H). **^{13}C NMR** (75 MHz, $CDCl_3$): δ 152.4, 144.0, 133.4, 126.7, 126.0, 125.6, 124.1, 117.4, 78.1, 75.6, 59.4, 59.3, 49.0, 47.1, 40.4, 39.0, 37.8, 26.2, 23.2, 21.5. **HRMS** (ESI +) calculated for $[C_{20}H_{28}NaO_2]^+$ $[M+Na]^+$ 323.1982 *m/z*; found 323.1975 *m/z*. **SFC** (OJ (100 × 3 mm, 3 µm), CO_2:MeOH 95:5, 1.2 mL/min, 35 °C, BRP 150 bar, 280 nm): en1 (minor, 19.5%) min 0.91, en2 (major, 80.5%) min 0.99. **[α]$^{25.0}_D$** +106 (c 0.55, $CHCl_3$, sample with 80.5:19.5 *er*).

General procedure GP6: enantioselective 6-*endo*-dig cyclizations with nucleophile addition[91]

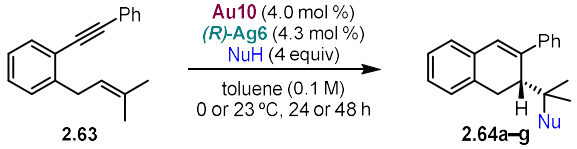

In the glovebox, under Ar and at room temperature, anhydrous toluene (1.0 mL) was added to a MW-vial containing enyne **2.63**[28e] (37.0 mg, 0.150 mmol, 1 equiv) and complex **Au10** (5.3 mg, 6.0 µmol, 0.040 equiv), obtaining a white suspension. Then the desired nucleophile (4.0 equiv) was added, immediately followed by a yellow clear solution of *(R)*-**Ag6** (6.1 mg, 6.5 µmol, 0.043 equiv) in anhydrous toluene (0.5 mL, final reaction volume 1.5 mL), obtaining a pale-yellow solution, that became cloudy after ca 1 minute. The vial was capped, removed from the glovebox, and placed to stir under inert gas (N_2 balloon) at 0 or 23 ºC for 24 or 48 h. Then, the reaction mixture was quenched by the addition of triethylamine (0.2 mL) and volatiles were removed under reduced pressure. The residue was dissolved in acetone-d_6, the internal standard (1,1,2,2-tetrachloroethane, 31.7 µL, 0.300 mmol, 2 equiv) added and the ^{1}H NMR spectrum recorded. The crude product was purified by FCC or PTLC, obtaining compound **2.64**.

(1*S*,6*S*,7*R*)-6,7-Diphenyl-3-oxabicyclo[4.1.0]hept-4-ene (2.62)

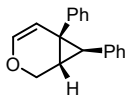

Prepared following the general procedure **GP5** using enyne **2.61**[35a] (37.2 mg, 0.150 mmol, 1.0 equiv), gold(I) complex **Au10** (6.7 mg, 7.5 µmol, 0.05 equiv) and chiral salt ***(R)*-Ag6** (7.0 mg, 7.5 µmol, 0.05 equiv) in toluene (0.2 M) at −20 ºC for 72 h. The crude product was purified FCC (silica, dry load, CyH:CH_2Cl_2 95:5). Compound **2.62** was obtained as a white solid (26.1 mg, 0.105 mmol, 70% yield) with 92.5:7.5 *er*. Spectroscopic data

91. Racemic samples were prepared on a 0.1 mmol scale in GCMS vials, using [(JohnPhos)Au(MeCN)]SbF_6 (3 mol%) in DCM (0.1M) and using 5 equivalents of the corresponding nucleophile.

match those previously reported.[35b] **M.p.** 84 °C (racemic sample, previously reported like an oil). **^{1}H NMR** (300 MHz, $CDCl_3$) δ 7.21–6.98 (m, 8H), 6.81–6.73 (m, 2H), 6.27 (d, *J* = 6.0 Hz, 1H), 5.36 (dd, *J* = 6.0, 1.0 Hz, 1H), 4.42 (dd, *J* = 10.5, 1.1 Hz, 1H), 4.10 (dd, *J* = 10.5, 2.1 Hz, 1H), 2.78 (d, *J* = 6.0 Hz, 1H), 2.46 (d, *J* = 4.7 Hz, 1H). **^{13}C NMR** (75 MHz, $CDCl_3$) δ 140.6, 139.8, 137.6, 129.7, 128.2, 127.72, 127.67, 126.4, 125.6, 111.5, 61.4, 37.3, 31.0, 29.8. **SFC** (IG (100 × 3 mm, 3 µm), CO_2:ACN 96:4, 1.2 mL/min, 35 ºC, BRP 150 bar, 210 nm): en1 (minor, 7.5%) min 1.79, en2 (major, 92.5%) min 2.11. **$[\alpha]^{25.0}_D$** +16 (c 0.51, $CHCl_3$, sample with 92.5:7.5 *er*); lit: **$[\alpha]^{20.0}_D$** −29 (c 0.51, $CHCl_3$, sample with 8.5:91.5 *er*).

(*R*)-2-(3-Phenyl-1,2-dihydronaphthalen-2-yl)propan-2-ol (2.64a)

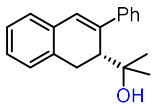

Prepared following the general procedure **GP6** using distilled water (11 µL, 0.61 mmol, 4.1 equiv) as a nucleophile, at 0 ºC for 24 h. The crude product was purified by automated FCC (silica, dry load, CyH:Et_2O 90:10 to 50:50, product eluting in CyH:Et_2O 70:30 to 60:40). Compound **2.64a** was obtained as a white solid (30.7 mg, 0.116 mmol, 77% yield) with 92.5:7.5 *er*. Crystals suiTable for X-ray diffraction were grown by slow evaporation of a solution in acetone at 23 ºC; their Flack parameter value, 0.08(3), corresponds approximately to 84±6% ee. The absolute configuration of the major enantiomer was thus assigned as *R*, and it agrees with the magnitude and positive sign of the specific rotation when compared with the literature (see below). Spectroscopic data for product **2.64a** matched those reported in the literature.[28e,36] **M.p.** 136–139 °C (sample with 92.5:7.5 *er*; lit:[36] 114–116 ºC for a racemic sample; lit:[28e] 138–140 ºC for a sample with 97:3 *er*). **^{1}H NMR** (400 MHz, acetone-d_6): δ 7.60–7.57 (m, 2H), 7.39–7.36 (m, 2H), 7.27 (tt, *J* = 7.3, 1.2 Hz, 1H), 7.18–7.10 (m, 4H), 6.85 (s, 1H), 3.52 (d, *J* = 15.8 Hz, 1H), 3.18 (d, *J* = 8.5 Hz, 1H), 3.17 (s, 1H), 3.13 (dd, *J* = 15.7, 8.3 Hz, 1H), 0.86 (s, 3H), 0.78 (s, 3H). **^{13}C NMR** (101 MHz, acetone-d_6): δ 144.7, 142.0, 136.8, 135.7, 129.2 (CH × 2), 128.3, 128.2, 127.9, 127.8, 127.6 (CH × 2), 127.00, 126.97, 74.5, 46.4, 31.0, 30.8, 26.5. **SFC** (OJ (100 × 3 mm, 3 µm), CO_2:EtOH 65:35, 1.2 mL/min, 35 ºC, BPR 150 bar, 230 nm): en1 (minor, 7.5%) min 0.82, en2 (major, 92.5%) min 1.15. **$[\alpha]^{23.6}_D$** +256 (c 0.80, $CHCl_3$, sample with 92.5:7.5 *er*); lit:[28e] **$[\alpha]^{25.8}_D$** –265 (c 0.83, $CHCl_3$, sample with 3:97 *er*).

(*R*)-2-(2-Methoxypropan-2-yl)-3-phenyl-1,2-dihydronaphthalene (2.64b)

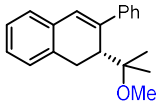

Prepared following the general procedure **GP6** using anhydrous methanol (25 µL, 0.62 mmol, 4.1 equiv) as a nucleophile, at 0 ºC for 24 h. The crude product was purified by PTLC (silica, CyH:Et_2O 95:5). Compound **2.64b** was obtained as a white solid (29.9 mg, 0.107 mmol, 71% yield) with 89:11 *er*. Spectroscopic data for product **6b** matched those reported in the literature.[36] **M.p.** 92 °C. **^{1}H NMR** (400 MHz, acetone-d_6): δ 7.60–7.57 (m, 2H), 7.40–7.36 (m, 2H), 7.28 (tt, *J* = 7.4, 1.3 Hz, 1H), 7.17–7.12 (m, 4H), 6.83 (s, 1H), 3.39–3.34 (m, 2H), 3.13–3.07 (m, 4H), 0.80 (s, 3H), 0.68 (s, 3H). **^{13}C NMR** (101 MHz, acetone-d_6): δ 144.7, 141.7, 136.7, 135.6, 129.2 (CH × 2), 129.0, 128.3, 127.8 (CH × 2), 127.6 (CH × 2), 127.1, 127.0, 79.1, 48.9, 42.3, 30.2 (overlapping with the acetone septet at 29.8 ppm, see attached spectrum), 25.4, 22.8. **SFC** (OJ (100 × 3 mm, 3 µm), CO_2:EtOH 85:15, 1.2 mL/min, 35 ºC, BPR 150 bar, 230 nm): en1 (minor, 11%) min 1.16, en2 (major, 89%) min 1.93. **$[\alpha]^{23.8}_D$** +213 (c 0.72, $CHCl_3$, 23.8 ºC, sample with 89:11 *er*).

(*R*)-2-(2-(Benzyloxy)propan-2-yl)-3-phenyl-1,2-dihydronaphthalene (2.64c)

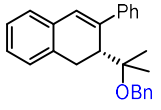

Prepared following the general procedure **GP6** using benzyl alcohol (62 µL, 0.60 mmol, 4.0 equiv) as a nucleophile, at 0 ºC for 24 h. The crude product was purified by PTLC (silica, CyH:Et_2O 95:5). Compound **2.64c** was obtained as a white solid (37.9 mg, 0.107 mmol, 71% yield) with 89:11 *er*. Spectroscopic data for product **2.64c** matched

those reported in the literature.[28e] **M.p.** 82–84 °C (racemic sample; lit: [28e] 79–81 ºC for a sample with 95:5 *er*). **^{1}H NMR** (400 MHz, acetone-d_6): δ 7.63–7.60 (m, 2H), 7.41–7.36 (m, 2H), 7.31–7.26 (m, 3H), 7.23–7.13 (m, 7H), 6.88 (s, 1H), 4.47 (d, *J* = 11.6 Hz, 1H), 4.37 (d, *J* = 11.6 Hz, 1H), 3.52–3.47 (m, 2H), 3.16 (dd, *J* = 16.5, 8.5 Hz, 1H), 0.95 (s, 3H), 0.85 (s, 3H). **^{13}C NMR** (101 MHz, acetone-d_6): δ 144.7, 141.7, 141.0, 136.7, 135.7, 129.3 (CH × 2), 129.0, 128.8 (CH × 2), 128.3, 127.9 (CH × 2), 127.8 (CH × 2), 127.6 (CH × 2), 127.5, 127.09, 127.06, 79.9, 63.8, 43.3, 30.6, 25.7, 23.4. **SFC** (IC (100 × 3 mm, 3 µm), CO_2:EtOH 90:10, 1.2 mL/min, 35 ºC, BPR 150 bar, 230 nm): en1 (minor, 11%) min 1.21, en2 (major, 89%) min 1.51. **$[\alpha]^{23.7}_D$** +102 (c 1.1, $CHCl_3$, sample with 89:11 *er*); lit: [28e] **$[\alpha]^{25.8}_D$** –137 (c 1.19, $CHCl_3$, sample with 5:95 *er*).

(*R*)-2-(2-(Allyloxy)propan-2-yl)-3-phenyl-1,2-dihydronaphthalene (2.64d)

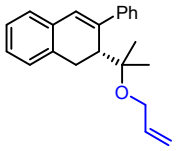

Prepared following the general procedure **GP6** using allyl alcohol (41 µL, 0.60 mmol, 4.0 equiv) as a nucleophile, at 0 ºC for 24 h. The crude product was purified by PTLC (silica, pentane:Et_2O 96:4). Compound **2.64d** was obtained as a white solid (28.5 mg, 0.0936 mmol, 62% yield) with 88.5:11.5 *er*. Spectroscopic data for product **2.64d** matched those reported in the literature. [28e] **M.p.** 83 °C (racemic sample; lit: [28e] 78–80 ºC for a sample with 95:5 *er*). **^{1}H NMR** (400 MHz, acetone-d_6): δ 7.60–7.57 (m, 2H), 7.40–7.36 (m, 2H), 7.27 (tt, *J* = 7.3, 1.3 Hz, 1H), 7.18–7.12 (m, 4H), 6.84 (s, 1H), 5.77 (ddt, *J* = 17.2, 10.4, 5.0 Hz, 1H), 5.15 (app dq, *J* = 17.2, 1.9 Hz, 1H), 4.98 (app dq, *J* = 10.6, 1.8 Hz, 1H), 3.92 (app ddt, *J* = 12.9, 5.0, 1.7 Hz, 1H), 3.81 (app ddt, *J* = 12.9, 4.9, 1.7 Hz, 1H), 3.44–3.39 (m, 2H), 3.12 (dd, *J* = 16.7, 8.7 Hz, 1H), 0.86 (s, 3H), 0.73 (s, 3H). **^{13}C NMR** (101 MHz, acetone-d_6): δ 144.7, 141.7, 137.4, 136.7, 135.6, 129.3 (CH × 2), 129.0, 128.3, 127.8 (CH × 2), 127.6 (CH × 2), 127.1, 127.0, 114.7, 79.5, 62.8, 42.9, 30.5, 25.9, 23.3. **SFC** (OJ (100 × 3 mm, 3 µm), CO_2:EtOH 90:10, 1.2 mL/min, 35 ºC, BPR 150 bar, 230 nm): en1 (minor, 11.5%) min 1.48, en2 (major, 88.5%) min 3.28. **$[\alpha]^{23.9}_D$** +175 (c 0.68, $CHCl_3$, sample with 88.5:11.5 *er*); lit: [28e] **$[\alpha]^{25.8}_D$** –181 (c 0.66, $CHCl_3$, sample with 5:95 *er*).

(*R*)-2-(3-Phenyl-1,2-dihydronaphthalen-2-yl)propan-2-yl acetate (2.64e)

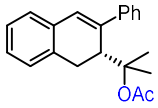

Prepared following the general procedure **GP6** using distilled acetic acid (34 µL, 0.60 mmol, 4.0 equiv) as a nucleophile, at 0 ºC for 48 h. The crude product was purified by PTLC (silica, pentane:Et_2O 96:4). Compound **2.64e** was obtained as a white solid (25.3 mg, 0.0826 mmol, 55% yield) with 89.5:10.5 *er*. Spectroscopic data for product **2.64e** matched those reported in the literature.[28e] **M.p.** 97–103 °C. **^{1}H NMR** (400 MHz, acetone-d_6): δ 7.55–7.52 (m, 2H), 7.41–7.37 (m, 2H), 7.28 (tt, *J* = 7.3, 1.3 Hz, 1H), 7.21–7.15 (m, 4H), 6.89 (s, 1H), 3.92 (dd, *J* = 7.7, 2.0 Hz, 1H), 3.25 (dd, *J* = 16.7, 7.7 Hz, 1H), 3.18 (dd, *J* = 16.7, 1.9 Hz, 1H), 1.39 (s, 3H), 1.32 (s, 3H), 1.01 (s, 3H). **^{13}C NMR** (101 MHz, acetone-d_6): δ 170.4, 144.2, 141.2, 135.8, 135.5, 129.3, 129.2 (CH × 2), 128.4, 127.80, 127.75 (CH × 2), 127.7, 127.3, 127.1, 85.8, 42.0, 31.1, 25.2, 24.9, 21.8. **SFC** (OJ (100 × 3 mm, 3 µm), CO_2:EtOH 80:20, 1.2 mL/min, 35 ºC, BPR 150 bar, 230 nm): en1 (minor, 10.5%) min 0.78, en2 (major, 89.5%) min 1.67. **$[\alpha]^{24.0}_D$** +212 (c 0.47, $CHCl_3$, sample with 89.5:10.5 *er*); lit:[28e] **$[\alpha]^{25.8}_D$** –196 (c 0.46, $CHCl_3$, sample with 10:90 *er*).

(*R*)-2-(2-Azidopropan-2-yl)-3-phenyl-1,2-dihydronaphthalene (2.64f)

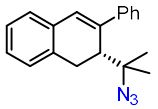

Prepared following the general procedure **GP6** adding azidotrimethylsilane (79 µL, 0.60 mmol, 4.0 equiv), then (*R*)-**Ag6** stock solution (0.5 mL, corresponding to 6.0 mg, 6.4 mmol, 0.043 equiv) and finally anhydrous propan-2-ol (46 µL, 0.60 mmol, 4.0 equiv); stirred at 23 ºC for 24 h. The crude product was purified by PTLC (silica, pentane). Compound **2.64f** was obtained as a white solid (27.0 mg, 0.0933 mmol, 62% yield) with

90:10 *er*. A typical side product in this reaction is the isopropoxycyclization product **2.64l**. The use of other alcohols as TMSazide activators led either to sluggish reaction (*tert*-butanol) or lower *er* (HFIP, **2.64f** isolated in 68% yield with 88:12 *er*). During the extensive reaction optimization, batches of compound **2.64f** with variable enantioenrichment were obtained. **M.p.** 86–89 °C. **IR** (film, cm^{-1}) n 3057, 3022, 2970, 2933, 2099 (strong band, due to asymmetric N≡N stretching, characteristic of organic azides),[92] 1490, 1454, 1260, 1388, 1370, 1130, 765, 696. **^{1}H NMR** (400 MHz, CD_2Cl_2): δ 7.54–7.50 (m, 2H), 7.41–7.37 (m, 2H), 7.30 (tt, *J* = 7.3, 1.3 Hz, 1H), 7.21–7.14 (m, 4H), 6.87 (s, 1H), 3.31–3.21 (m, 2H), 3.12 (dd, *J* = 6.1, 3.2 Hz, 1H), 1.00 (s, 3H), 0.90 (s, 3H). **^{13}C NMR** (101 MHz, CD_2Cl_2): δ 143.4, 139.5, 135.4, 134.8, 129.3, 128.9 (CH × 2), 128.1, 127.6, 127.4, 126.90 (CH × 2), 126.85, 126.7, 66.1, 43.9, 31.2, 26.2, 23.7. **HRMS** (APCI +) calculated for $[C_{19}H_{20}N]^+$ $[M - N_2 + H]^+$ 262.1590 *m/z*; found 262.1585 *m/z*. **HRMS** (ESI +) calculated for $[C_{19}H_{19}N_3Na]^+$ $[M + Na]^+$ 312.1471 *m/z*; found 312.1481 *m/z*. **SFC** (IC (100 × 3 mm, 3 µm), CO_2:MeOH 95:5, 1.2 mL/min, 35 ºC, BPR 150 bar, 230 nm): en1 (minor, 10%) min 1.01, en2 (major, 90%) min 1.19. **$[\alpha]^{26.1}_D$** +200 (c 1.0, CH_2Cl_2, sample with 87:13 *er*).

Note: azidotrimethylsilane with an acid can generate highly explosive, toxic and volatile hydrazoic acid. The reaction mixture was basified with Et_3N (0.2 mL), and a plastic blast shield was placed around the rotary evaporator when concentrating the reaction mixture (T max 38 °C). On this scale, the use of azidotrimethylsilane with alcohol additives was not problematic.

(*R*)-2-(2-Fluoropropan-2-yl)-3-phenyl-1,2-dihydronaphthalene (2.64g)

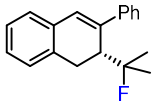

Prepared in a plastic vial following the general procedure **GP6** using hydrogen fluoride pyridine (CAS 62778-11-4, HF ca 70%$_{w/w}$, 77 µL, corresponding to 0.60 mmol, 4.0 equiv of HF) as a nucleophile, at 0 ºC for 24 h. The crude product was purified by PTLC (silica, pentane). Compound **2.64g** was obtained as a white solid (27.6 mg, 0.104 mmol, 69% yield) with 61:39 *er*. Spectroscopic data for product **2.64g** matched those reported in the literature.[28e] **M.p.** 73 °C (racemic sample; lit:[28e] 72–75 ºC for a sample with 96:4 *er*). **^{1}H NMR** (400 MHz, acetone-d_6): δ 7.62–7.60 (m, 2H), 7.41–7.37 (m, 2H), 7.29 (tt, *J* = 7.5, 1.2 Hz, 1H), 7.22–7.14 (m, 4H), 6.94 (d, *J* = 1.1 Hz, 1H), 3.43 (ddd, *J* = 10.4, 7.4, 2.0 Hz, 1H), 3.29 (dd, *J* = 16.7, 2.0 Hz, 1H), 3.23 (dd, *J* = 16.7, 7.4 Hz, 1H), 1.11 (d, *J* = 21.8 Hz, 3H), 0.92 (d, *J* = 22.5 Hz, 3H). **^{13}C NMR** (101 MHz, acetone-d_6): δ 143.6, 140.1 (d, J_{CF} = 6.3 Hz), 135.7, 135.4, 129.3 (CH × 2), 128.8, 128.5, 128.0, 127.9, 127.6 (CH × 2), 127.34, 127.28, 99.7 (d, J^1_{CF} = 171.3 Hz), 44.5 (d, J^2_{CF} = 22.7 Hz), 30.8 (d, J^3_{CF} = 6.3 Hz), 27.2 (d, J^2_{CF} = 24.4 Hz), 24.7 (d, J^2_{CF} = 24.7 Hz). **^{19}F NMR** (376 MHz, acetone-d_6): –133.3. **SFC** (OJ (100 × 3 mm, 3 µm), CO_2:EtOH 80:20, 1.2 mL/min, 35 ºC, BPR 150 bar, 230 nm): en1 (minor, 39%) min 1.41, en2 (major, 61%) min 2.22. **$[\alpha]^{24.1}_D$** +50 (c 1.1, $CHCl_3$, sample with 61:39 *er*); lit:[28e] **$[\alpha]^{25.8}_D$** –165 (c 0.165, $CHCl_3$, sample with 4:96 *er*).

2-(2-Isopropoxypropan-2-yl)-3-phenyl-1,2-dihydronaphthalene (2.64l)

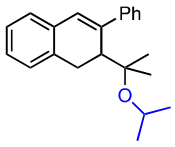

Prepared following general procedure **GP6** using propan-2-ol (46 µL, 0.60 mmol, 4.0 equiv) as a nucleophile, at 0 ºC for 24 h. After purification by FCC (silica, dry load, CyH:Et_2O 100:0 to 90:10), compound **2.64l** was obtained as a white solid in 30% yield (13.9 mg, 0.0454 mmol) and with 87.5:12.5 *er*. The low yield was due to low conversion. **M.p.** 58 °C (racemic sample). **IR** (film from acetone-d_6, cm^{-1}) υ 2971, 2929, 1491, 1453, 1366, 1114, 1015, 766. **^{1}H NMR** (400 MHz, acetone-d_6): δ 7.58 (d, *J* = 7.3 Hz, 2H), 7.38 (t, *J* = 7.7 Hz, 2H), 7.27 (t, *J* = 7.3, 1H), 7.17–7.11 (m, 4H), 6.84 (s, 1H), 3.76 (sept, *J* = 6.1 Hz, 1H), 3.51 (d, *J* = 16.5 Hz, 1H), 3.23 (d, *J* = 8.4 Hz, 1H), 3.09 (dd, *J* = 16.4,

92. Lieber, E.; Rao, C. N. R.; Chao, T. S.; Hoffman, C. W. W. *Anal. Chem.* **1957**, *29*, 916–918.

8.5 Hz, 1H), 1.01 (d, *J* = 6.1 Hz, 3H), 0.99 (d, *J* = 6.1 Hz, 3H), 0.80 (s, 3H), 0.70 (s, 3H). **^{13}C NMR** (101 MHz, acetone-d_6): δ 144.9, 141.7, 137.0, 135.7, 129.2 (CH × 2), 128.8, 128.3, 127.74, 127.70, 127.6 (CH × 2), 127.0, 126.9, 79.8, 63.4, 44.5, 30.7, 26.5, 25.6, 25.3, 23.2. **HRMS** (ESI +) calculated for $[C_{22}H_{26}NaO]^+$ $[M + Na]^+$ 329.1876 *m/z*; found 329.1876 *m/z*. **SFC** (OJ (100 × 3 mm, 3 µm), CO_2:*i*-PrOH 85:15, 1.2 mL/min, 35 ºC, BPR 150 bar, 230 nm): en1 (minor, 12.5%) min 0.90, en2 (major, 87.5%) min 1.88. **$[\alpha]^{24.9}_D$** +148 (c 0.68, $CHCl_3$, sample with 87.5:12.5 *er*).

Derivatization of products of the gold(I)-catalyzed 6-endo-dig cyclization of enyne 2.62

2-(3-Phenyl-1,2-dihydronaphthalen-2-yl)propan-2-yl benzoate (2.64h)

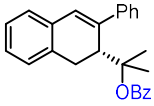

Under Ar, benzoic anhydride (29.4 mg, 130 µmol, 1.3 equiv) and triethylamine (42 µL, 0.30 mmol, 3.0 equiv) were sequentially added to a solution of compound **2.64a** (26.4 mg, 100 µmol, 1.0 equiv, 92.5:7.5 *er*) and 4-(dimethylamino)pyridine (12.2 mg, 100 µmol, 1.0 equiv) in 1,2-DCE (0.1 mL). The reaction mixture was heated to 80 ºC for 66 h. After cooling to room temperature, water (3 mL) was added, layers separated, and the aqueous phase was extracted with CH_2Cl_2 (3 × 5 mL). The combined organic layers were washed with brine, dried over $MgSO_4$, filtered and evaporated. The crude product was purified by FCC (silica, CyH:EtOAc 95:5). Compound **2.64h** was obtained as a colorless oil (25.3 mg, 68.7 µmol, 69% yield) with 93:7 *er*. **IR** (film from $CDCl_3$, cm^{-1}) υ 2924, 1705, 1278, 1106, 753, 710, 695. **^{1}H NMR** (300 MHz, $CDCl_3$) δ 7.62–7.56 (m, 2H), 7.54–7.50 (m, 2H), 7.49–7.42 (m, 1H), 7.32–7.25 (m, 4H), 7.22–7.10 (m, 5H), 6.86 (s, 1H), 4.05 (dd, *J* = 8.0, 1.7 Hz, 1H), 3.34 (dd, *J* = 16.7, 8.0 Hz, 1H), 3.23 (dd, *J* = 16.7, 1.7 Hz, 1H), 1.44 (s, 3H), 1.24 (s, 3H). **^{13}C NMR** (75 MHz, $CDCl_3$) δ 165.9, 143.1, 140.0, 135.04 134.7, 132.4, 131.7, 129.4, 128.9, 128.6, 128.0, 127.8, 127.1, 126.9, 126.6, 126.5, 87.0, 41.7, 30.8, 25.6, 24.7. **HRMS** (ESI +) calculated for $[C_{26}H_{24}NaO_2]^+$ $[M + Na]^+$ 391.1669 *m/z*; found 391.1668 *m/z*. **SFC** (IC (100 × 3 mm, 3 µm), CO_2:MeOH 85:15, 1.2 mL/min, 35 ˚C, BRP 150 bar, 210 nm): en1 (minor, 7%) min 1.22, en2 (major, 93%) min 1.41. **$[\alpha]^{25.2}_D$** +265 (c 1.0, $CHCl_3$, sample with 93:7 *er*).

(*R*)-1-(2-(3-Phenyl-1,2-dihydronaphthalen-2-yl)propan-2-yl)-4-(*p*-tolyl)-1*H*-1,2,3-triazole (2.64i)

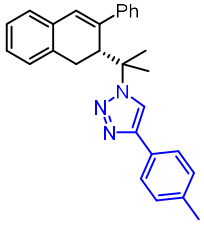

Under Ar, in a V-shaped MW vial equipped with a triangular stir bar, 1-ethnynyl-4-methylbenzene (20 µL, 0.16 mmol, 3.0 equiv) and degassed *tert*-butanol (50 µL) were added in sequence to azide **2.64f** (15.0 mg, 51.8 µmol, 1 equiv, 90:10 *er*), obtaining a beige suspension. A freshly prepared and degassed colorless solution of sodium (L)-ascorbate (20.5 mg in 0.5 mL of H_2O; 50 µL added, corresponding to 2.05 mg, 10.4 µmol, 0.20 equiv of sodium ascorbate) was added. Then, a freshly prepared and degassed blue solution of copper(II) sulphate pentahydrate (6.5 mg in 0.5 mL of H_2O; 50 µL added, corresponding to 0.65 mg, 2.6 µmol, 0.05 equiv of copper(II) sulphate pentahydrate) was added dropwise to the reaction mixture (beige suspension). Upon addition, a strong orange color developed, that gradually faded leaving a bright yellow suspension. The resulting yellow biphasic reaction mixture was vigorously stirred in the sealed MW vial at 90 ºC for 22 h. After 22 h, the reaction mixture was cooled to room temperature, diluted with EtOAc (10 mL), H_2O (5 mL) and brine (5 mL). Phases were separated and the aqueous layer was extracted with EtOAc (3 × 10 mL). Combined organic phases were dried over Na_2SO_4, filtered and evaporated. The crude product was purified by FCC (silica, liquid load in CH_2Cl_2/pentane, eluent pentane:EtOAc 95:5 to 85:15), obtaining compound **2.64i** as a white solid (17.2 mg, 42.4 µmol, 82% yield) with 90:10 *er*. **M.p.** 198–201 °C. **IR** (film from $CDCl_3$, cm^{-1}) υ 3021, 2920, 1495, 1451, 1185, 1035, 815, 761, 691. **^{1}H NMR** (300 MHz, $CDCl_3$) δ 7.59 (d, *J* = 8.1 Hz, 2H), 7.50 (s, 1H), 7.48 (dd, *J* = 8.2, 1.1 Hz, 2H), 7.31 (t, *J* = 7.7 Hz, 2H), 7.22–7.18 (m,

3H), 7.17–7.13 (m, 3H), 7.05 (br d, *J* = 6.7 Hz, 1H), 6.91 (s, 1H), 3.89 (d, *J* = 8.1 Hz, 1H), 3.21 (dd, *J* = 16.7, 8.1 Hz, 1H), 2.67 (d, *J* = 16.7 Hz, 1H), 2.38 (s, 3H), 1.50 (s, 3H), 1.30 (s, 3H). **^{13}C NMR** (75 MHz, $CDCl_3$) δ 146.7, 142.0, 138.9, 137.7, 134.4, 134.3, 129.5 (CH × 2), 129.2, 128.6 (CH × 2), 128.2, 128.0, 127.6, 127.2, 126.9, 126.6 (CH × 2), 126.5, 125.7 (CH × 2), 117.9, 66.0, 44.4, 31.0, 28.1, 24.6, 21.4. **HRMS** (ESI +) calculated for $[C_{28}H_{27}N_3Na]^+$ $[M + Na]^+$ 428.2097 *m/z*; found 428.2094 *m/z*. **SFC** (ID (100 × 3 mm, 3 µm), CO_2:MeOH 75:25, 1.2 mL/min, 35 ºC, BPR 150 bar, 254 nm): en1 (minor, 10%) min 3.08, en2 (major, 90%) min 3.51. **$[\alpha]^{25.9}_D$** +133 (c 0.48, $CHCl_3$, sample with 90:10 *er*).

(*R*)-2-(3-Phenyl-1,2-dihydronaphthalen-2-yl)propan-2-amine (2.64j)

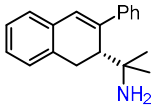

Under Ar, a dark grey suspension of lithium aluminium hydride (5.8 mg, 0.15 mmol, 2.2 equiv) in Et_2O (0.5 mL) was added dropwise to a suspension of azide **2.64f** (20.0 mg, 69.1 µmol, 1 equiv, 93:7 *er*) in Et_2O (0.5 mL) kept at 0 ºC. The resulting dark grey mixture was stirred at 0 ºC for 10 minutes, then at 23 ºC. Mild bubbling was observed upon warming to rt. After 6 h, TLC (CyH, then CH_2Cl_2) indicated complete consumption of the starting material. The reaction mixture was carefully diluted with Et_2O (4 mL) and quenched by dropwise addition of water (5 mL) under a flow of nitrogen, then transferred into a separatory funnel. CH_2Cl_2 (ca 5 mL) was added until the organic phase fell to the bottom of the funnel, layers were separated, and the aqueous one was extracted with CH_2Cl_2 (2 × 5 mL). Combined organic phases were dried over Na_2SO_4, filtered and evaporated. The crude product showed ca 90–95% purity as judged by ^{1}H NMR. It was further purified by a short FCC (silica, liquid load in CH_2Cl_2, eluent CH_2Cl_2:MeOH 100:0 to 90:10), obtaining compound **2.64j** as a pale beige solid (16.4 mg, 62.3 µmol, 90% yield) with 93:7 *er*. **M.p.** 116–120 °C (decomposition). **IR** (film from $CDCl_3$, cm^{-1}) υ 3024, 2952, 2919, 2866, 1564, 1489, 1452, 1363, 875, 845, 771, 765, 694. **^{1}H NMR** (300 MHz, CD_2Cl_2) δ 7.53 (dd, *J* = 7.6 Hz, 2H), 7.38 (t, *J* = 7.7 Hz, 2H), 7.28 (tt, *J* = 7.5, 1.2 Hz, 1H), 7.16–7.10 (m, 4H), 6.85 (s, 1H), 3.31–3.18 (m, 2H), 2.97 (dd, *J* = 6.1, 3.2 Hz, 1H), 1.13 (br s, 2H), 0.84 (s, 3H), 0.80 (s, 3H). **^{13}C NMR** (75 MHz, CD_2Cl_2) δ 144.4, 141.8, 136.0, 135.3, 128.9 (CH × 2), 128.1, 127.8, 127.4, 127.3, 126.9 (CH × 2), 126.7, 126.4, 55.0, 46.2, 31.5, 29.9, 29.5. **HRMS** (APCI +) calculated for $[C_{19}H_{22}N]^+$ $[M + H]^+$ 264.1747 *m/z*; found 264.1740 *m/z*. **SFC** (IF (150 × 3 mm, 3 µm), 70:30 CO_2:(MeOH with 0.3% Et_2NH), 2 mL/min, 35 ºC, 2000 psi, 280 nm): en1 (minor, ca 7%) min 1.51, en2 (major, ca 93%) min 2.27. Due to the basic nature of the compound, the second peak tails and tends to shift, depending on concentration. For a reliable ee determination, see the further derivatization to amide **2.64k** (below). **$[\alpha]^{25.9}_D$** +217 (c 0.68, CH_2Cl_2, sample with 93:7 *er*).

(*R*)-*N*-(2-(3-Phenyl-1,2-dihydronaphthalen-2-yl)propan-2-yl)acetamide (2.64k)

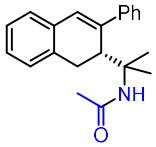

Reduction of azide **2.64f** (20.0 mg, 69.1 µmol, 1 equiv, 90:10 *er*) to amine **2.64j** was performed exactly as described in the section above. After work-up, the compound was carried to the next step without FCC. Thus, under Ar, anhydrous triethylamine (19.3 µL, 138 µmol, 2.0 equiv) was added to a solution of crude amine **2.64j** (assumed to be 69.1 µmol, 1 equiv, 90:10 *er*) and 4-(dimethylamino)pyridine (2.5 mg, 20 µmol, 0.3 equiv) in anhydrous CH_2Cl_2 (0.2 mL). The resulting yellow solution was cooled to 0 ºC, then acetyl chloride (6.9 µL, 97 µmol, 1.4 equiv) was added, obtaining an orange suspension. The reaction mixture was stirred at 23 ºC. After 2 h, TLC (CH_2Cl_2:MeOH 95:5, stained with ninhydrin solution) indicated complete consumption of the starting material. The reaction mixture was quenched by addition of 2.5 M aqueous HCl (4 mL) and CH_2Cl_2 (5 mL). Layers were separated and the aqueous one was extracted with CH_2Cl_2 (2 × 5 mL). Combined organic phases were washed with brine, dried over Na_2SO_4, filtered and evaporated. The crude

product was purified by FCC (silica, liquid load in CH_2Cl_2, eluent CH_2Cl_2:EtOAc 100:0 to 90:10), obtaining compound **2.64k** as an off-white solid (19.4 mg, 63.5 µmol, 92% yield) with 90:10 *er*. **M.p.** 156–157 °C. **IR** (film from $CDCl_3$, cm^{-1}) υ 3632, 3291, 2970, 2928, 1644, 1366, 1180, 755, 693. **^{1}H NMR** (500 MHz, $CDCl_3$) δ 7.51 (dd, *J* = 8.3, 1.2 Hz, 2H), 7.38 (t, *J* = 7.7 Hz, 2H), 7.26 (tt, *J* = 7.4, 1.2 Hz, 1H, overlapping with $CHCl_3$), 7.18–7.10 (m, 4H), 6.83 (s, 1H), 4.84 (br s, NH, 1H), 3.93 (dd, *J* = 8.2, 1.2 Hz, 1H), 3.26 (dd, *J* = 16.6, 8.2 Hz, 1H), 3.10 (d, *J* = 16.5, 1.1 Hz, 1H), 1.31 (s, 6H), 0.89 (s, 3H). **^{13}C NMR** (126 MHz, $CDCl_3$) δ 169.8, 143.5, 141.2, 135.1, 134.7, 128.8 (CH × 2), 128.5, 127.7, 127.3, 127.1, 126.8 (CH × 2), 126.7, 126.3, 57.9, 39.9, 31.2, 26.1, 25.7, 24.0. **HRMS** (ESI +) calculated for $[C_{21}H_{23}NNaO]^+$ $[M + Na]^+$ 328.1672 *m/z*; found 328.1673 *m/z*. **SFC** (OJ (100 × 3 mm, 3 µm), CO_2:*i*-PrOH 80:20, 1.2 mL/min, 35 ºC, BPR 150 bar, 230 nm): en1 (minor, 10%) min 0.94, en2 (major, 90%) min 1.79. **$[\alpha]^{25.9}_D$** +237 (c 0.55, $CHCl_3$, sample with 90:10 *er*).

3-Phenyl-2-(prop-1-en-2-yl)-1,2-dihydronaphthalene (2.65)

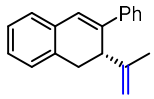

Following a modified literature procedure,[28e] under Ar, to a solution of **2.64a** (26.4 mg, 100 µmol, 1.0 equiv, 92.5:7.5 *er*) in anhydrous THF (1.4 mL) was added the Burgess reagent (1-methoxy-*N*-triethylammoniosulfonylmethanimidate, 33.4 mg, 140 µmol, 1.4 equiv) and the mixture was stirred for 3 h at 23 ºC. Water (5 mL) and EtOAc (5 mL) were then added , layers separated, and the aqueous phase extracted once more with EtOAc (10 mL). The combined organic layers were dried over $MgSO_4$, filtered and evaporated. The crude product was purified by FCC (silica, CyH:EtOAc 95:5). Compound **2.65** was obtained as a white solid (21.6 mg, 87.7 µmol, 88% yield) with 92:8 *er*. **M.p.** 53–55 °C. **IR** (film from $CDCl_3$, cm^{-1}) υ 3358, 3056, 3018, 2917, 2850, 1451, 889, 758, 684. **^{1}H NMR** (300 MHz, acetone-d_6) δ 7.71–7.53 (m, 2H), 7.42–7.32 (m, 2H), 7.30–7.07 (m, 6H), 4.72–4.67 (m, 1H), 4.66–4.60 (m, 1H), 3.55 (d, *J* = 7.6 Hz, 1H), 3.22 (dd, *J* = 15.9, 7.6 Hz, 1H), 3.04 (dd, *J* = 15.9, 2.2 Hz, 1H), 1.73 (s, 3H). **^{13}C NMR** (75 MHz, acetone-d_6) δ 145.0, 141.3, 140.7, 135.4, 134.4, 129.2, 128.5, 128.14, 128.11, 127.4, 127.3, 126.5, 125.9, 112.4, 44.1, 34.2, 21.4. **HRMS** (APCI +) calculated for $[C_{19}H_{19}]^+$ $[M + H]^+$ 247.1841 *m/z*; found 247.1483 *m/z*. **SFC** (OJ (100 × 3 mm, 3 µm), CO_2:EtOH 80:20 1.2 mL/min, 35 °C, BRP 150 bar, 230 nm): en1 (minor, 8%) min 1.63, en2 (major, 92%) min 1.95. **$[\alpha]^{25.0}_D$** +37 (c 1.0, $CHCl_3$, sample with 92:8 *er*).

(*R*)-2-(2-Methoxypropan-2-yl)-1-methylene-2,3-dihydro-1*H*-indene (2.67)

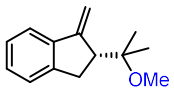

In the glovebox, under Ar, to a MW-vial containing complex **Au10** (4.4 mg, 4.9 µmol, 0.05 equiv) and enyne **2.66**[20] (17.0 mg, 0.100 mmol, 1 equiv) were added toluene (0.5 mL) and MeOH (81 µL, 2.0 mmol, 20 equiv) obtaining a white suspension. The vial was capped, removed from the glovebox, covered from light and cooled to −20 ºC under inert gas (connected to a N_2 balloon). Then *(R)*-**Ag6** (4.7 mg, 5.0 µmol, 0.05 equiv) was added as a solution in toluene (0.5 mL) under N_2. The resulting mixture was stirred at −20 ºC for 18 h in the dark. The reaction mixture was quenched by filtration through a silica-filled glass pipette, eluting with CH_2Cl_2. Volatiles were removed under reduced pressure and the crude product was purified by FCC (silica, CyH:CH_2Cl_2 100:0 to 80:20). Compound **2.67** was obtained as a colorless oil (19.0 mg, 0.094 mmol, 94% yield) with 78.5:21.5 *er*. Spectroscopic data for product **2.67** matched those reported in the literature.[59n] **^{1}H NMR** (400 MHz, $CDCl_3$): δ 7.51–7.40 (m, 1H), 7.25–7.14 (m, 3H), 5.61 (dd, *J* = 2.1, 0.6 Hz, 1H), 5.19 (d, *J* = 1.8 Hz, 1H), 3.27 (s, 3H), 3.22 (ddt, *J* = 7.9, 3.9, 2.0 Hz, 1H), 3.05 (dd, *J* = 16.9, 8.1 Hz, 1H), 2.96 (dd, *J* = 16.9, 3.8 Hz, 1H), 1.22 (s, 3H), 0.96 (s, 3H). **^{13}C NMR** (100 MHz, $CDCl_3$) δ 150.9, 145.3, 142.0, 128.4, 126.5, 125.0, 120.4, 106.3, 77.6, 50.0, 49.2, 33.4, 22.4, 22.1. **HPLC** (OD-H (250 × 4.6 mm, 5

μm), *n*-hexane, 1.0 mL/min, 25 ºC, 270 nm): en1 (major, 78.5%) min 12.52, en2 (minor, 21.5%) min 13.83. **[α]$^{25.0}_{D}$** +17 (c 1.0, $CHCl_3$, sample with 78.5:21.5 *er*).

(1*S*,5*S*,6*R*)-6-Phenyl-3-oxabicyclo[3.1.0]hexane-1-carbaldehyde (2.69)

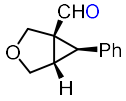

In the glovebox, under Ar, to a GCMS-vial containing complex **Au10** (2.2 mg, 2.5 μmol, 0.05 equiv) and *(R)*-**Ag6** (2.3 mg, 2.5 μmol, 0.05 equiv) at 23 ºC was added a solution of enyne **2.68**[50] (8.6 mg, 50 μmol, 1 equiv) and diphenyl sulfoxide (15.2 mg, 75.0 μmol, 1.5 equiv) in toluene (0.5 mL). The resulting mixture was stirred at 23 ºC for 48 h in the dark, then it was quenched by the addition of triethylamine (0.1 mL) and filtered through a silica-filled glass pipette. Volatiles were removed under reduced pressure and the crude product was purified by PTLC (silica, CyH:EtOAc 70:30). Compound **2.69** was obtained as a colorless oil (4.2 mg, 21 μmol, 42% yield) with 83:17 *er*. The moderate yield is due to the formation of an achiral diene side product, stemming from enyne cycloisomerization without trapping of the Au(I) carbene. Therefore, a higher amount of diphenyl sulfoxide is expected to improve the yield for cyclopropyl aldehyde **2.69**. Spectroscopic data for product **2.69** matched those reported in the literature. [40] The absolute configuration is assigned by comparison with the literature based on both the sign of optical rotation and the order of elution under identical HPLC conditions.[40] **^{1}H NMR** (300 MHz, $CDCl_3$): δ 8.96 (s, 1H), 7.38–7.26 (m, 5H), 4.21 (d, *J* = 9.2 Hz, 1H), 4.09 (d, *J* = 8.8 Hz, 1H), 4.03 (d, *J* = 9.2 Hz, 1H), 3.90 (dd, *J* = 8.8, 3.0 Hz, 1H), 2.99 (dd, *J* = 5.6, 3.0 Hz, 1H), 2.93 (d, *J* = 5.6 Hz, 1H). **^{13}C NMR** (75 MHz, $CDCl_3$): δ 198.4, 134.0, 129.1, 129.0, 127.6, 69.0, 68.2, 47.0, 33.5, 32.0. **HPLC** (AD-H (250 × 4.6 mm, 5 μm), 95:5 *n*-hexane:*i*-PrOH, 0.7 mL/min, 25 ºC, 240 nm): en1 (minor, 17%) min 14.83, en2 (major, 83%) min 19.67. **[α]$^{26.0}_{D}$** +77 (c 0.21, $CHCl_3$, sample with 17:83 *er*); lit: [40] $[\alpha]^{20}_{D}$ +3.6 (c 1.0, $CHCl_3$, sample with 48.5:51.5 *er*).

Enantioselective ynenone tandem cyclization-nucleophile addition

Substrate synthesis

The synthesis of enone **1.40** was reported in Chapter 1. **2.70a–k** were prepared following literature procedures[52a,52b] from the corresponding 2-iodocycloenones *via* Sonogashira cross-coupling reaction.

General procedure GP7: Sonogashira cross-coupling

To an oven dried flask were added 2-iodocyclohex-2-en-1-one (1 equiv), copper(I) iodide (2–6 mol%) and bis(triphenylphosphine)palladium(II) dichloride (1–3 mol%). After purging the system with argon, the corresponding alkynylbenzene (2 equiv) was added, followed by THF (0.15 M). The system was then degassed for 15 min by N_2 sparging with a N_2 balloon while sonicating in an ultrasound bath prior to the addition of diisopropylamine (3 equiv) at 0 °C. The reaction was left stirring at the same temperature until starting material consumption as assessed by TLC and/or GCMS analysis. Quenching was done by addition of saturated NH_4Cl aqueous solution followed by extraction with CH_2Cl_2 (3 times). The combined organic layers were washed with brine, dried over Na_2SO_4, filtered and concentrated. The crude product was purified by FCC (silica, CyH:EtOAc solvent mixtures) affording the desired 2-alkynylenones.

2-((4-Methoxyphenyl)ethynyl)cyclohex-2-en-1-one (2.70a)

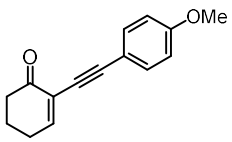

Prepared following general procedure **GP7** using 2-iodocyclohex-2-en-1-one (222 mg, 1.00 mmol, 1 equiv), copper iodide (5.7 mg, 30 μmol, 3 mol%), bis(triphenylphosphine)palladium(II) dichloride (7.0 mg, 10 μmol, 1 mol%), 1-ethynyl-4-methoxybenzene (259 μL, 2.00 mmol, 2.0 equiv) and diisopropylamine (393 μL, 3.00 mmol, 3 equiv) at 0 °C for 1 h. The crude product was purified

by FCC (silica, CyH:EtOAc, 95:5). Compound **2.70a** was obtained as a pale orange solid (200 mg, 0.88 mmol, 88% yield). Spectroscopic data for product **2.70a** matched those reported in the literature. [52a] **^{1}H NMR** (300 MHz, $CDCl_3$): δ 7.47 – 7.39 (m, 2H), 7.34 – 7.29 (m, 1H), 6.87 – 6.77 (m, 2H), 3.81 (s, 3H), 2.58 – 2.37 (m, 4H), 2.16 – 1.95 (m, 2H). **^{13}C NMR** (101 MHz, $CDCl_3$): δ 195.9, 159.9, 153.6, 133.4, 125.7, 115.2, 114.0, 92.3, 82.6, 55.4, 38.3, 26.7, 22.6.

2-(*m*-Tolylethynyl)cyclohex-2-en-1-one (2.70b)

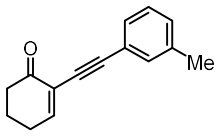

Prepared following general procedure **GP7** using 2-iodocyclohex-2-en-1-one (0.200 g, 0.901 mmol, 1 equiv), copper iodide (3.4 mg, 18 μmol, 2 mol%), bis(triphenylphosphine)palladium(II) dichloride (6.3 mg, 9 μmol, 1 mol%), 3-ethynyltoluene (0.23 mL, 1.80 mmol, 2.0 equiv) and diisopropylamine (0.35 mL, 2.70 mmol, 3 equiv) at 0 °C for 1.5 h. The crude product was purified by FCC (silica, CyH:EtOAc, 97:3). Compound **2.70b** was obtained as a colorless oil (140.2 mg, 0.666 mmol, 74% yield). Spectroscopic data for product **2.70b** matched those reported in the literature. [52a] **^{1}H NMR** (300 MHz, $CDCl_3$): δ 7.36 – 7.27 (m, 3H), 7.20 (t, J = 7.5 Hz, 1H), 7.12 (dtd, J = 7.6, 1.5, 0.7 Hz, 1H), 2.58 – 2.45 (m, 4H), 2.32 (d, J = 0.8 Hz, 3H), 2.12 – 2.01 (m, 2H).

2-(*o*-Tolylethynyl)cyclohex-2-en-1-one (2.70c)

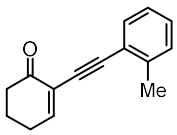

Prepared following general procedure **GP7** using 2-iodocyclohex-2-en-1-one (0.100 g, 0.450 mmol, 1 equiv), copper iodide (8.6 mg, 45 μmol, 10 mol%), bis(triphenylphosphine)palladium(II) dichloride (15.8 mg, 22.5 μmol, 5 mol%), 2-ethynyltoluene (0.11 mL, 0.90 mmol, 2.0 equiv) and diisopropylamine (0.18 mL, 1.37 mmol, 3 equiv) at 0 °C for 1.5 h. The crude product was purified by FCC (silica, CyH:EtOAc, 97:3). Compound **2.70c** was obtained as a pale orange oil (57.6 mg, 0.274 mmol, 61% yield). Spectroscopic data for product **2.70c** matched those reported in the literature. [52a] **^{1}H NMR** (300 MHz, $CDCl_3$): δ 7.44 (d, J = 7.4 Hz, 1H), 7.32 (t, J = 4.5 Hz, 1H), 7.24 – 7.14 (m, 2H), 7.19 – 7.06 (m, 1H), 2.57 – 2.42 (m, 7H), 2.11 – 1.98 (m, 2H).

2-((4-Bromophenyl)ethynyl)cyclohex-2-en-1-one (2.70d)

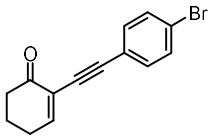

Prepared following general procedure **GP7** using 2-iodocyclohex-2-en-1-one (150 mg, 0.68 mmol, 1 equiv), copper iodide (3.9 mg, 20 μmol, 3 mol%), bis(triphenylphosphine)palladium(II) dichloride (4.7 mg, 6.8 μmol, 1 mol%), 1-bromo-4-ethynylbenzene (227 μL, 2.0 mmol, 2.0 equiv) and diisopropylamine (266 μL, 3.0 mmol, 3 equiv) at 0 °C for 1.5 h. The crude product was purified by FCC (silica, CyH:EtOAc, 95:5). Compound **2.70d** was obtained as a pale orange solid (110 mg, 0.40 mmol, 59% yield). Spectroscopic data for product **2.70d** matched those reported in the literature.[93] **^{1}H NMR** (300 MHz, $CDCl_3$): δ 7.50 (dd, J = 3.0, 1.2 Hz, 1H), 7.34 (t, J = 4.5 Hz, 1H), 7.28 – 7.22 (m, 1H), 7.16 (dd, J = 5.0, 1.2 Hz, 1H), 2.57 – 2.43 (m, 4H), 2.06 (dq, J = 8.1, 6.1 Hz, 2H). **^{13}C NMR** (75 MHz, $CDCl_3$): 195.5, 154.6, 133.3, 131.7, 125.3, 122.8, 122.0, 91.1, 85.1, 38.3, 26.7, 22.5.

2-((4-Fluorophenyl)ethynyl)cyclohex-2-en-1-one (2.70e)

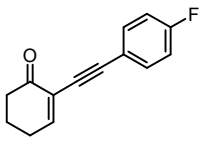

Prepared following general procedure **GP7** using 2-iodocyclohex-2-en-1-one (222 mg, 1.00 mmol, 1 equiv), copper iodide (5.7 mg, 30 μmol, 3 mol%), bis(triphenylphosphine)palladium(II) dichloride (7.0 mg, 10 μmol, 1 mol%),

93. Wang, T.; Shi, S.; Vilhelmsen, M. H.; Zhang, T.; Rudolph, M.; Rominger, F.; Hashmi, A. S. K. *Chem. Eur. J.* **2013**, *19*, 12512–12516.

1-ethynyl-4-fluorobenzene (229 μL, 2.0 mmol, 2.0 equiv) and diisopropylamine (393 μL, 3.0 mmol, 3 equiv) at 0 °C for 1.5 h. The crude product was purified by FCC (silica, CyH:EtOAc, 95:5). Compound **2.70e** was obtained as a pale orange oil (200 mg, 0.93 mmol, 93% yield). Spectroscopic data for product **2.70e** matched those reported in the literature.[93] **^{1}H NMR** (300 MHz, $CDCl_3$): δ 7.51 – 7.42 (m, 2H), 7.33 (t, *J* = 4.5 Hz, 1H), 7.05 – 6.91 (m, 2H), 2.56 – 2.41 (m, 4H), 2.13 – 1.95 (m, 2H). **^{13}C NMR** (101 MHz, $CDCl_3$): δ 195.5, 162.6 (d, *J* = 249.6 Hz), 154.2, 133.7 (d, *J* = 8.4 Hz), 125.2, 119.0 (d, *J* = 3.6 Hz), 115.5 (d, *J* = 22.0 Hz), 91.0, 83.5 (d, *J* = 1.6 Hz), 38.1, 26.5, 22.4. **^{19}F NMR** (282 MHz, $CDCl_3$) δ −110.4.

2-((3-Fluorophenyl)ethynyl)cyclohex-2-en-1-one (2.70f)

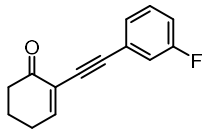

Prepared following general procedure **GP7** using 2-iodocyclohex-2-en-1-one (222 mg, 1.00 mmol, 1 equiv), copper iodide (5.7 mg, 30 μmol, 3 mol%), bis(triphenylphosphine)palladium(II) dichloride (7.0 mg, 10 μmol, 1 mol%), 1-ethynyl-3-fluorobenzene (230 μL, 2.0 mmol, 2.0 equiv) and diisopropylamine (393 μL, 3.0 mmol, 3 equiv) at 0 °C for 1.5 h. The crude product was purified by FCC (silica, CyH:EtOAc, 95:5). Compound **2.70f** was obtained as a pale orange oil (165 mg, 0.77 mmol, 77% yield). **^{1}H NMR** (300 MHz, $CDCl_3$): δ 7.35 (t, J = 4.4 Hz, 1H), 7.29 – 7.20 (m, 2H), 7.19 – 7.13 (m, 1H), 7.05 – 6.93 (m, 1H), 2.56 – 2.42 (m, 4H), 2.10 – 1.98 (m, 2H). **^{13}C NMR** (75 MHz, $CDCl_3$): δ 195.5, 162.4 (d, *J* = 246.3 Hz), 154.5, 129.9 (d, *J* = 8.6 Hz), 127.8 (d, *J* = 3.1 Hz), 125.2, 124.9 (d, *J* = 9.5 Hz), 118.7 (d, *J* = 22.8 Hz), 115.9 (d, *J* = 21.2 Hz), 90.9, 84.8, 38.2, 26.7, 22.5. **^{19}F NMR** (282 MHz, $CDCl_3$) δ −113.1. **HRMS** (APCI +): calculated for $[C_{14}H_{12}FO]^+$ $[M+H]^+$ 215.0867 *m/z*; found 215.0873 *m/z*.

2-((2-Fluorophenyl)ethynyl)cyclohex-2-en-1-one (2.70g)

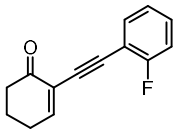

Prepared following general procedure **GP7** using 2-iodocyclohex-2-en-1-one (222 mg, 1.00 mmol, 1 equiv), copper iodide (5.7 mg, 30 μmol, 3 mol%), bis(triphenylphosphine)palladium(II) dichloride (7.0 mg, 10 μmol, 1 mol%), 1-ethynyl-2-fluorobenzene (227 μL, 2.0 mmol, 2.0 equiv) and diisopropylamine (393 μL, 3.0 mmol, 3 equiv) at 0 °C for 1.5 h. The crude product was purified by FCC (silica, CyH:EtOAc, 95:5). Compound **2.70g** was obtained as a pale orange oil (170 mg, 0.79 mmol, 79% yield). **^{1}H NMR** (300 MHz, $CDCl_3$): δ 7.35 (t, J = 4.4 Hz, 1H), 7.29 – 7.20 (m, 2H), 7.19 – 7.13 (m, 1H), 7.05 – 6.93 (m, 1H), 2.56 – 2.42 (m, 4H), 2.10 – 1.98 (m, 2H). **^{13}C NMR** (75 MHz, $CDCl_3$): δ 195.4, 162.8 (d, *J* = 251.9 Hz), 155.0, 133.8, 130.3 (d, *J* = 8.0 Hz), 125.3, 124.0 (d, *J* = 3.8 Hz), 115.6 (d, *J* = 21.0 Hz), 111.7 (d, *J* = 15.5 Hz), 89.0, 85.5, 38.2, 26.7, 22.5. **^{19}F NMR** (282 MHz, $CDCl_3$) δ −109.6. **HRMS** (APCI +): calculated for $[C_{14}H_{12}FO]^+$ $[M+H]^+$ 215.0867 *m/z*; found 215.0872 *m/z*.

2-(Thiophen-3-ylethynyl)cyclohex-2-en-1-one (2.70h)

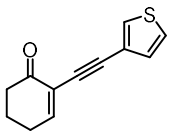

Prepared following general procedure **GP7** using 2-iodocyclohex-2-en-1-one (150 mg, 0.68 mmol, 1 equiv), copper iodide (3.9 mg, 20 μmol, 3 mol%), bis(triphenylphosphine)palladium(II) dichloride (4.7 mg, 6.8 μmol, 1 mol%), 3-ethynylthiophene (133 μL, 1.35 mmol, 2.0 equiv) and diisopropylamine (266 μL, 2.03 mmol, 3 equiv) at 0 °C for 1.5 h. The crude product was purified by FCC (silica, CyH:EtOAc, 95:5). Compound **2.70h** was obtained as a pale orange solid (98 mg, 0.48 mmol, 72% yield). Spectroscopic data for product **2.70h** matched those reported in the literature.[52a] **^{1}H NMR** (300 MHz, $CDCl_3$): δ 7.50 (dd, *J* = 3.0, 1.2 Hz, 1H), 7.34 (t, *J* = 4.5 Hz, 1H), 7.27 – 7.23 (m, 1H), 7.16 (dd, *J* = 5.0, 1.2 Hz, 1H), 2.65 – 2.34 (m, 4H), 2.15 – 1.93 (m, 2H). **^{13}C NMR**

(75 MHz, $CDCl_3$): δ 195.7, 154.2, 130.1, 129.3, 125.4, 125.3, 122.0, 87.3, 83.5, 38.3, 26.7, 22.6.

2-(Cyclohexylethynyl)cyclohex-2-en-1-one (2.70i)

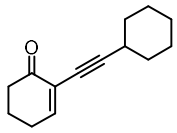

Prepared following general procedure **GP7** using 2-iodocyclohex-2-en-1-one (200 mg, 0.90 mmol, 1 equiv), copper iodide (13.7 mg, 72 μmol, 8 mol%), bis(triphenylphosphine)palladium(II) dichloride (25.3 mg, 36 μmol, 4 mol%), ethynylcyclohexane (235 μL, 1.80 mmol, 2.0 equiv) and diisopropylamine (354 μL, 2.70 mmol, 3 equiv) at 0 °C for 5 h. The crude product was purified by FCC (silica, CyH:EtOAc, 95:5). Compound **2.70i** was obtained as a colorless oil (100 mg, 0.49 mmol, 55% yield). Spectroscopic data for product **2.70i** matched those reported in the literature.[93] **^{1}H NMR** (300 MHz, $CDCl_3$): δ 7.18 (t, *J* = 4.5 Hz, 1H), 2.61 – 2.49 (m, 1H), 2.49 – 2.35 (m, 4H), 2.07 – 1.93 (m, 2H), 1.90 – 1.77 (m, 2H), 1.77 – 1.62 (m, 2H), 1.56 – 1.38 (m, 3H), 1.38 – 1.23 (m, 3H). **^{13}C NMR** (75 MHz, $CDCl_3$): δ 196.2, 153.0, 125.7, 97.5, 75.0, 38.3, 32.7, 29.7, 26.5, 26.0, 25.0, 22.6.

2-(Phenylethynyl)cyclopent-2-en-1-one (2.70j)

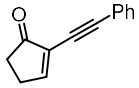

Prepared following general procedure **GP7** using 2-iodocyclopent-2-en-1-one (208 mg, 1.00 mmol, 1 equiv), copper iodide (5.7 mg, 30 μmol, 3 mol%), bis(triphenylphosphine)palladium(II) dichloride (7.0 mg, 10 μmol, 1 mol%), phenylacetylene (220 μL, 2.00 mmol, 2.0 equiv) and diisopropylamine (393 μL, 3.00 mmol, 3 equiv) at 0 °C for 1h. The crude product was purified by FCC (silica, CyH:EtOAc, 95:5). Compound **2.70j** was obtained as a pale orange solid (125 mg, 0.69 mmol, 69% yield). Spectroscopic data for product **2.70j** matched those reported in the literature. [51b] **^{1}H NMR** (400 MHz, $CDCl_3$): δ 7.85 (t, *J* = 3.1 Hz, 1H), 7.53 – 7.48 (m, 2H), 7.35 – 7.29 (m, 3H), 2.79 – 2.72 (m, 2H), 2.55 – 2.49 (m, 2H). **^{13}C NMR** (75 MHz, $CDCl_3$): δ 205.7, 165.1, 132.0, 130.3, 128.9, 128.4, 122.6, 95.1, 80.0, 34.2, 27.6.

2-(Phenylethynyl)cyclohept-2-en-1-one (2.70k)

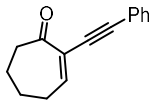

Prepared following general procedure **GP7** using 2-iodocycloheptenone (250 mg, 1.06 mmol, 1 equiv), copper iodide (12.1 mg, 0.064 mmol, 6 mol%), bis(triphenylphosphine)palladium(II) dichloride (22.3 mg, 0.032 mmol, 3 mol%), phenylacetylene (233 μL, 2.12 mmol, 2.0 equiv) and diisopropylamine (416 μL, 3.18 mmol, 3 equiv) at 0 °C for 1 h. The crude product was purified by FCC (silica, CyH:EtOAc, 95:5). Compound **2.70k** was obtained as a pale orange solid (140 mg, 0.67 mmol, 63% yield). Spectroscopic data for product **2.70k** matched those reported in the literature. [51b] **^{1}H NMR** (300 MHz, $CDCl_3$): δ 7.51 – 7.43 (m, 2H), 7.33 – 7.27 (m, 3H), 7.16 (t, *J* = 6.5 Hz, 1H), 2.74 – 2.66 (m, 2H), 2.57 – 2.49 (m, 2H), 1.92 – 1.75 (m, 4H). **^{13}C NMR** (126 MHz, $CDCl_3$): δ 201.1, 150.9, 131.9, 128.8, 128.4, 128.3, 123.2, 90.3, 86.5, 42.5, 28.7, 25.1, 21.6.

General procedure GP8: enantioselective ynenone tandem cyclization-nucleophile addition[91]

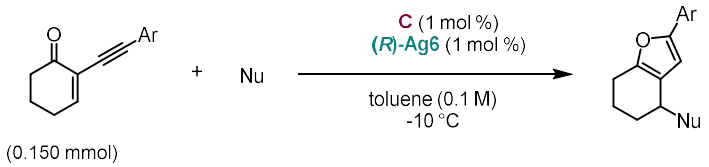

Under N_2, a solution of enone (0.150 mmol, 1 equiv) and nucleophile (1.0–3.0 equiv) in toluene (1.5 mL) cooled to −10 °C was added to a microwave vial containing complex **C** (1.3 mg, 1.5 μmol, 0.01 equiv) and (*R*)-**Ag6** (1.3 mg, 1.5 μmol, 0.01 equiv) kept at −10 ºC. The resulting mixture was stirred at −10 °C under inert atmosphere (N_2 balloon) in the dark, until the enone starting material was consumed, as judged by TLC or GCMS analysis. The reaction was then quenched by addition of triethylamine (0.2 mL) and filtered through a silica-filled glass pipette. Volatiles were removed under reduced pressure and the crude product was purified by FCC or PTLC.

(*S*)-3-(2-Phenyl-4,5,6,7-tetrahydrobenzofuran-4-yl)-1*H*-indole (1.42)

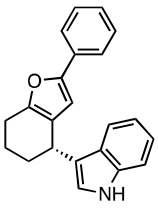

Prepared following general procedure **GP8** using enone **1.40** (29.4 mg, 0.150 mmol, 1.0 equiv) and indole (17.6 mg, 0.150 mmol, 1.0 equiv) as a nucleophile in toluene (1.5 mL, 0.1 M), at −10 ºC for 4 h. The crude product was purified by PTLC (silica, CyH:EtOAc 95:5). Compound **1.42** was obtained as a white solid (35.8 mg, 0.115 mmol, 77% yield) with 91:9 *er*. Spectroscopic data for product **1.42** matched those reported in the literature. [52a] The absolute configuration was assigned by comparison with the literature based on both the sign of optical rotation and the order of elution under identical HPLC conditions.[14a,52a, 52b] **^{1}H NMR** (400 MHz, $CDCl_3$): δ 7.94 (br s, 1H), 7.64–7.55 (m, 3H), 7.38 (dt, *J* = 8.1, 0.9 Hz, 1H), 7.36–7.30 (m, 2H), 7.24–7.16 (m, 2H), 7.15–7.09 (m, 1H), 6.88 (s, 1H), 6.45 (s, 1H), 4.26 (t, *J* = 5.7 Hz, 1H), 2.88–2.64 (m, 2H), 2.25–2.09 (m, 1H), 2.05–1.93 (m, 2H), 1.93–1.76 (m, 1H). **^{13}C NMR** (101 MHz, $CDCl_3$): δ 151.8, 151.4, 136.7, 131.5, 128.7, 126.8, 126.7, 123.4, 122.2, 122.1, 120.4, 119.41, 119.37, 111.3, 106.2, 31.3, 31.1, 23.6, 21.3. **HPLC** (IA (250 × 4.6 mm, 5 μm), 95:5 *n*-hexane:*i*-PrOH, 1.0 mL/min, 25 °C, 280 nm): en1 (major, 91%) min 12.66, en2 (minor, 9%) min 15.68. **$[\alpha]^{26.0}_D$** −27 (c 0.89, $CHCl_3$, sample with 91:9 *er*); lit:[14a] $[\alpha]_D$ +38 (c 0.89, $CHCl_3$, sample with 2:98 *er*); lit: $[\alpha]^{20}_D$ −30 (c 0.5, $CHCl_3$, sample with 93:7 *er*).[52b]

(*S*)-5-Methoxy-3-(2-phenyl-4,5,6,7-tetrahydrobenzofuran-4-yl)-1*H*-indole (2.72a)

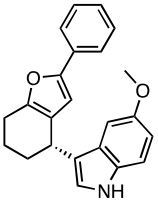

Prepared following general procedure **GP8** using using enone **1.40** (29.4 mg, 0.150 mmol, 1.0 equiv) and 5-methoxyindole (22.1 mg, 0.150 mmol, 1.0 equiv) as a nucleophile in toluene (1.5 mL, 0.1M), at −10 ºC for 2.5 h. The crude product was purified by PTLC (silica, CyH:EtOAc 90:10). Compound **2.72a** was obtained as a white solid (47.2 mg, 0.138 mmol, 92% yield) with 89:11 *er*. Spectroscopic data for product **2.72a** matched those reported in the literature.[14a] The absolute configuration was assigned by comparison with the literature based on both the sign of optical rotation and the order of elution under identical HPLC conditions.[14a] **^{1}H NMR** (300 MHz, $CDCl_3$): δ 7.84 (brs, 1H), 7.61 (dd, *J* = 8.2, 1.0 Hz, 2H), 7.40–7.29 (m, 2H), 7.27 (d, *J* = 8.8 Hz, 1H), 7.24–7.16 (m, 1H), 7.09 (d, *J* = 2.4 Hz, 1H), 6.90 (dd, *J* = 8.8, 2.4 Hz, 1H), 6.85 (d, *J* = 2.3 Hz, 1H), 6.47 (s, 1H), 4.28–4.18 (m, 1H), 3.87 (s, 3H), 2.78 (t, *J* = 5.8 Hz, 2H), 2.24–2.10 (m, 1H), 2.05–1.79 (m, 3H). **^{13}C NMR** (75 MHz, $CDCl_3$): δ 154.0, 151.8, 151.4, 131.9, 131.5, 128.7, 127.2, 126.7, 123.4, 123.1, 122.2, 120.0, 112.1, 112.0, 106.2, 101.3, 56.1, 31.1, 30.9, 23.5, 21.2. **SFC**

(IA (150 × 3.0 mm, 3 μm), CO_2:*i*-PrOH 60:40, 1.2 mL/min, 35 ºC, BPR 150 bar, 280 nm): en1 (major, 89%) min 1.73, en2 (minor, 11%) min 2.10. **[α]$^{26.0}_{D}$** +6.5 (c 0.98, $CHCl_3$, sample with 89:11 *er*); lit:[14a] **[α]$_D$** −7.0 (c 0.98, $CHCl_3$, sample with 1.5:98.5 *er*).

(*S*)-5-Bromo-3-(2-phenyl-4,5,6,7-tetrahydrobenzofuran-4-yl)-1*H*-indole (2.72b)

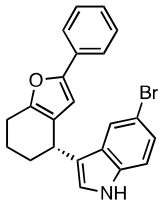

Prepared following general procedure **GP8** using enone **1.40** (29.4 mg, 0.150 mmol, 1.0 equiv) and 5-bromoindole (29.4 mg, 0.150 mmol, 1.0 equiv) as a nucleophile in toluene (1.5 mL, 0.1 M), at −10 ºC for 2.5 h. The crude product was purified by PTLC (silica, CyH:EtOAc 90:10). Compound **2.72b** was obtained as an off-white solid (49.6 mg, 0.126 mmol, 84% yield) with 93:7 *er*. Spectroscopic data for product **2.72b** matched those reported in the literature.[14a] The absolute configuration was assigned by comparison with the literature based on the sign of optical rotation.[14a] **^{1}H NMR** (400 MHz, $CDCl_3$): δ 7.94 (br s, 1H), 7.77 (d, *J* = 1.7 Hz, 1H), 7.61 (dd, *J* = 8.3, 1.1 Hz, 2H), 7.35 (t, *J* = 7.8 Hz, 2H), 7.30 (dd, *J* = 8.6, 1.8 Hz, 1H), 7.25 – 7.17 (m, 2H), 6.86 (d, *J* = 2.2 Hz, 1H), 6.43 (s, 1H), 4.20 (t, *J* = 5.4 Hz, 1H), 2.84 – 2.69 (m, 2H), 2.21 – 2.07 (m, 1H), 2.00 – 1.78 (m, 3H). **^{13}C NMR** (75 MHz, $CDCl_3$): δ 151.9, 151.4, 135.3, 131.4, 128.7, 128.6, 126.8, 125.0, 123.5, 123.4, 121.8, 121.7, 120.2, 112.8, 112.7, 105.9, 31.2, 30.8, 23.5, 21.1. **SFC** (IA (150 × 3.0 mm, 3 μm), CO_2:*i*-PrOH 60:40, 1.2 mL/min, 35 ºC, BPR 150 bar, 230 nm): en1 (major, 93%) min 1.63, en2 (minor, 7%) min 2.17. **[α]$^{26.0}_{D}$** +9.8 (c 1.0, $CHCl_3$, sample with 93:7 *er*); lit:[13] **[α]$_D$** −10 (c 1.0, $CHCl_3$, sample with 1.5:98.5 *er*).

***(S)*-2-Methyl-3-(2-phenyl-4,5,6,7-tetrahydrobenzofuran-4-yl)-1*H*-indole (2.72c)**

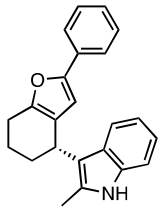

Prepared following the general procedure **GP8** using enone **1.40** (29.4 mg, 0.150 mmol, 1.0 equiv) and 2-methyl-1H-indole (19.7 mg, 0.150 mmol, 1.0 equiv) as a nucleophile in toluene (1.5 mL, 0.1 M), at −10 ºC for 2.5 h. The crude product was purified by PTLC (silica, CyH:EtOAc 90:10). Compound **2.72c** was obtained as a white solid (47.6 mg, 0.147 mmol, 97% yield) with 71.5:28.5 *er*. Spectroscopic data for product **2.72c** matched those reported in the literature.[14a] The absolute configuration was assigned by comparison with the literature based on the sign of optical rotation.[14a] **^{1}H NMR** (400 MHz, $CDCl_3$): δ 7.72 (br s, 1H), 7.57 (d, *J* = 7.7 Hz, 2H), 7.34 – 7.27 (m, 3H), 7.17 (t, *J* = 7.4 Hz, 1H), 7.09 (t, *J* = 7.6 Hz, 1H), 6.96 (t, *J* = 7.5 Hz, 1H), 6.30 (s, 1H), 4.20 – 4.13 (m, 1H), 2.89 – 2.79 (m, 2H), 2.34 (s, 3H), 2.18 – 2.05 (m, 2H), 1.93 (td, *J* = 9.2, 4.9 Hz, 2H).**^{13}C NMR** (75 MHz, $CDCl_3$): δ 151.8, 150.8, 135.3, 131.6, 131.1, 128.6, 128.0, 126.6, 123.4, 122.8, 120.9, 119.3, 119.1, 114.3, 110.2, 106.4, 31.8, 31.3, 23.5, 23.0, 12.3. **SFC** (IA (150 × 3.0 mm, 3 μm), CO_2:MeOH 75:25, 1.2 mL/min, 35 ºC, BPR 150 bar, 210 nm): en1 (major, 71.5%) min 2.05, en2 (minor, 28.5%) min 2.30. **[α]$^{27.2}_{D}$** −16 (c 1.2, $CHCl_3$, sample with 71.5:28.5 *er*); lit: [14a] **[α]$_D$** +26 (c 1.2 $CHCl_3$, sample with 7:93 *er*).

(*S*)-1-Methyl-3-(2-phenyl-4,5,6,7-tetrahydrobenzofuran-4-yl)-1*H*-indol (2.72d)

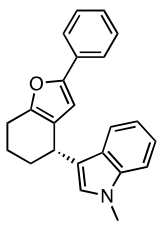

Prepared following general procedure **GP8** using enone **1.40** (29.4 mg, 0.150 mmol, 1.0 equiv) and 1-methyl-1H-indole (19.7 mg, 0.150 mmol, 1.0 equiv) as a nucleophile in toluene (1.5 mL, 0.1 M), at −10 ºC for 2.5 h. The crude product was purified by PTLC (silica, CyH:EtOAc 90:10). Compound **2.72d** was obtained as an off-white solid (34.0 mg, 0.104 mmol, 69% yield) with 84:16 *er*. Spectroscopic data for product **2.72d** matched those reported in the literature.[14a] The absolute configuration was assigned by comparison with the literature based on the sign of optical rotation.[14a] **^{1}H NMR** (400 MHz, $CDCl_3$): δ 7.67 – 7.58 (m, 3H), 7.39 – 7.28 (m, 3H), 7.27 – 7.17 (m, 3H), 7.16 – 7.10 (m, 1H), 6.74 (s, 1H), 6.47 (s, 1H), 4.27 (t, *J* = 5.8 Hz,

1H), 3.74 (s, 3H), 2.84 – 2.68 (m, 2H), 2.23 – 2.12 (m, 1H), 2.04 – 1.93 (m, 2H), 1.91 – 1.81 (m, 1H). **^{13}C NMR** (75 MHz, $CDCl_3$): δ 151.8, 151.3, 137.4, 131.5, 128.7, 127.2, 127.1, 126.7, 123.4, 122.4, 121.6, 119.4, 118.8, 109.4, 106.3, 32.8, 31.5, 30.9, 23.6, 21.2. **SFC** (IG (100 × 3 mm, 3 μm), CO_2:MeOH 70:30, 1.2 mL/min, 35 ºC, BPR 150 bar, 280 nm): en1 (major, 84%) min 1.80, en2 (minor, 16%) min 2.28. **$[\alpha]^{27.2}_D$** +4.1 (c 0.78, $CHCl_3$, sample with 84:16 *er*); lit: [14a] **$[\alpha]_D$** −5 (c 0.78, $CHCl_3$, sample with 7:93 *er*).

(*S*)-3-Methyl-3-(2-phenyl-4,5,6,7-tetrahydrobenzofuran-4-yl)-1*H*-indole (2.72e)

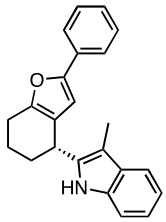

Prepared following general procedure **GP8** using enone **1.40** (29.4 mg, 0.150 mmol, 1.0 equiv) and 3-methyl-1H-indole (19.7 mg, 0.150 mmol, 1.0 equiv) as a nucleophile in toluene (1.5 mL, 0.1 M), at −10 ºC for 2 h. The crude product was purified by PTLC (silica, CyH:EtOAc 95:5). Compound **2.72e** was obtained as an off-white solid (33.0 mg, 0.101 mmol, 67% yield) with 91:9 *er*. Spectroscopic data for product **2.72e** matched those reported in the literature. [14a] The absolute configuration was assigned by comparison with the literature based on the sign of optical rotation. [14a] **^{1}H NMR** (300 MHz, $CDCl_3$): δ 7.67 (br s, 1H), 7.64 – 7.53 (m, 3H), 7.41 – 7.32 (m, 2H), 7.27 – 7.20 (m, 2H), 7.17 – 7.07 (m, 2H), 6.38 (s, 1H), 4.33 – 4.23, (m, 1H), 2.89 – 2.78 (m, 2H), 2.36 (s, 3H), 2.28 – 2.13 (m, 1H), 2.09 – 1.98 (m, 1H), 1.97 – 1.71 (m, 2H). **^{13}C NMR** (75 MHz, $CDCl_3$): δ 152.5, 152.2, 137.1, 135.0, 131.1, 129.6, 128.8, 127.1, 123.4, 121.3, 120.1, 119.2, 118.3, 110.6, 106.9, 105.6, 31.7, 31.3, 23.4, 21.9, 8.6. **SFC** (IB-N (150 × 3.0 mm, 3 μm), CO_2:EtOH 60:40, 1.2 mL/min, 35 ºC, BPR 150 bar, 210 nm): en1 (minor, 9%) min 1.35, en2 (major, 91%) min 1.51. **$[\alpha]^{27.2}_D$** −49 (c 1.2, $CHCl_3$, sample with 91:9 *er*); lit: [14a] **$[\alpha]_D$** +83 (c 1.2 $CHCl_3$, sample with 3.5:96.5 *er*.

(*S*)-3-(2-(4-Methoxyphenyl)-4,5,6,7-tetrahydrobenzofuran-4-yl)-1*H*-indole (2.72f)

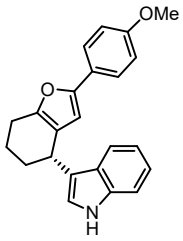

Prepared following general procedure **GP8** using enone **2.70a** (33.9 mg, 0.150 mmol, 1.0 equiv) and indole (17.6 mg, 0.150 mmol, 1.0 equiv) as a nucleophile in toluene (1.5 mL, 0.1 M), at −10 ºC for 1.5 h. The crude product was purified by PTLC (silica, CyH:EtOAc 90:10). Compound **2.72f** was obtained as a yellow oil (39.2 mg, 0.114 mmol, 76% yield) with 85:15 *er*. Spectroscopic data for product **2.72f** matched those reported in the literature. [14a] The absolute configuration was assigned by comparison with the literature based on the sign of optical rotation.[14a] **^{1}H NMR** (400 MHz, $CDCl_3$): δ 7.93 (s, 1H), 7.64 (d, J = 8.0 Hz, 1H), 7.58 – 7.49 (m, 1H), 7.38 (dt, J = 8.1, 0.9 Hz, 1H), 7.21 (ddd, J = 8.2, 7.0, 1.2 Hz, 1H), 7.12 (ddd, J = 8.0, 7.1, 1.1 Hz, 1H), 6.93 – 6.84 (m, 2H), 6.31 (s, 1H), 4.25 (t, J = 5.7 Hz, 1H), 3.82 (s, 2H), 2.85 – 2.66 (m, 2H), 2.21 – 2.09 (m, 1H), 2.03 – 1.91 (m, 2H), 1.91 – 1.79 (m, 1H). **^{13}C NMR** (101 MHz, $CDCl_3$): δ 158.6, 151.8, 150.6, 136.7, 126.9, 124.8, 124.7, 122.2, 122.08, 122.06, 120.45, 119.4, 114.2, 111.3, 104.6, 55.4, 31.4, 31.1, 23.5, 21.3. **SFC** (ID (150 × 3.0 mm, 3 μm), CO_2:MeOH 75:25, 1.2 mL/min, 35 ºC, BPR 150 bar, 210 nm): en1 (major, 85%) min 1.84, en2 (minor, 15%) min 2.55. **$[\alpha]^{26.0}_D$** −8.6 (c 0.65, $CHCl_3$, sample with 85:15 *er*); lit: [14a] $[\alpha]_D$ +11 (c 1.90, $CHCl_3$, sample with 4.5:95.5 *er*).

(*S*)-2-(2-(m-Tolyl)-4,5,6,7-tetrahydrobenzofuran-4-yl)-1*H*-indole (2.72g)

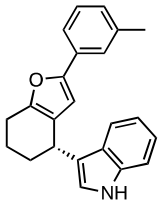

Prepared following general procedure **GP8** using enone **2.70b** (31.5 mg, 0.150 mmol, 1.0 equiv) and indole (17.6 mg, 0.150 mmol, 1.0 equiv) as a nucleophile in toluene (1.5 mL, 0.1 M), at −10 ºC for 3 h. The crude product was purified by FCC (silica, CyH:EtOAc 95:5). Compound **2.72g** was obtained as a white solid (32.3 mg, 0.099 mmol, 66% yield) with 93:7 *er*. The absolute configuration was assigned assuming a uniform stereochemical mechanism. **^{1}H NMR** (300 MHz, $CDCl_3$): δ 7.92 (brs, 1H), 7.63 (d, *J* = 7.7 Hz, 1H), 7.43 (d, *J* = 5.8 Hz, 1H), 7.38 (d, *J* = 8.0 Hz, 2H), 7.25 – 7.18 (m, 2H), 7.17 – 7.09 (m, 1H), 7.02 (d, *J* = 7.5 Hz, 1H), 6.88 (d, *J* = 2.3 Hz, 1H), 6.43 (s, 1H), 4.27 (t, *J* = 5.7 Hz, 1H), 2.78 (t, *J* = 6.0 Hz, 2H), 2.36 (s, 3H), 2.26 – 2.08 (m, 1H), 2.06 – 1.76 (m, 3H). **^{13}C NMR** (75 MHz, $CDCl_3$): δ 151.9, 151.2, 138.3, 136.7, 131.4, 128.6, 127.6, 126.8, 124.0, 122.2, 122.2, 122.1, 120.6, 120.4, 119.4, 111.3, 106.1, 31.4, 31.1, 23.5, 21.6, 21.3. **HPLC** (IA (250 × 4.6 mm, 5 μm), 95:5 *n*-hexane:*i*-PrOH, 1 mL/min, 25 ºC, 240 nm): en1 (major, 93%) min 11.33, en2 (minor, 7%) min 15.50. **$[\alpha]^{27.5}_D$** −23 (c 1.0, $CHCl_3$, sample with 93:7 *er*).

(*S*)-2-(2-(*o*-Tolyl)-4,5,6,7-tetrahydrobenzofuran-4-yl)-1*H*-indole (2.72h)

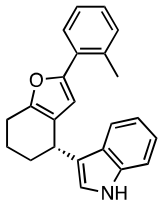

Prepared following general procedure **GP8** using enone **2.70c** (31.5 mg, 0.150 mmol, 1.0 equiv) and indole (17.6 mg, 0.150 mmol, 1.0 equiv) as a nucleophile in toluene (1.5 mL, 0.1 M), at −10 ºC for 3 h. The crude product was purified by FCC (silica, CyH:EtOAc 95:5). Compound **2.72h** was obtained as a white solid (29.8 mg, 0.091 mmol, 61% yield) with 78:22 *er*. The absolute configuration was assigned assuming a uniform stereochemical mechanism. **IR** (film from $CDCl_3$, cm^{-1}) 3419, 3057, 2932, 2854, 1456, 742. **^{1}H NMR** (400 MHz, $CDCl_3$): δ 7.92 (s, 1H), 7.73 (dd, *J* = 7.8, 1.1 Hz, 1H), 7.65 (d, *J* = 8.0 Hz, 1H), 7.38 (d, *J* = 8.1 Hz, 1H), 7.26 – 7.18 (m, 4H), 7.18 – 7.10 (m, 3H), 6.88 (d, *J* = 2.0 Hz, 1H), 6.36 (s, 1H), 4.35 – 4.27 (m, 2H), 2.87 – 2.68 (m, 3H), 2.43 (s, 3H), 2.24 – 2.14 (m, 1H), 2.03 – 1.93 (m, 4H), 1.93 – 1.83 (m, 1H).**^{13}C NMR** (75 MHz, $CDCl_3$): δ 151.9, 151.2, 138.3, 136.7, 131.4, 128.6, 127.6, 126.8, 124.0, 122.2, 122.1, 120.6, 120.4, 119.4, 111.3, 106.1, 31.4, 31.1, 23.5, 21.6, 21.3. **HRMS** (ESI +) calculated for $[C_{23}H_{22}NO]^+$ $[M + H]^+$ 328.1696 *m/z*; found 328.1700 *m/z*. **SFC** (IG (150 × 3.0 mm, 3 μm), CO_2:EtOH 80:20, 1.2 mL/min, 35 ºC, BPR 150 bar, 230 nm): en1 (major, 78%) min 2.05, en2 (minor, 22%) min 2.84. **$[\alpha]^{27.5}_D$** −26 (c 0.92, $CHCl_3$, sample with 78:22 *er*).

(*S*)-3-(2-(4-Bromophenyl)-4,5,6,7-tetrahydrobenzofuran-4-yl)-1*H*-indole (2.72i)

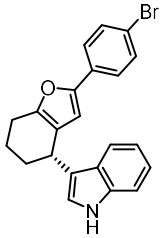

Prepared following general procedure **GP8** using enone **2.70d** (41.3 mg, 0.150 mmol, 1.0 equiv) and indole (17.6 mg, 0.150 mmol, 1.0 equiv) as a nucleophile in toluene (1.5 mL, 0.1 M), at −10 ºC for 7 h. The crude product was purified by FCC (silica, CyH:EtOAc 100:0 to 80:20). Compound **2.72i** was obtained as a pale brown oil (35 mg, 0.89 mmol, 59% yield) with 80:20 *er*. The absolute configuration was assigned assuming a uniform stereochemical mechanism. **IR** (film from CH_2Cl_2, cm^{-1}) 3414, 3057, 2935, 2855, 1592, 1544, 1478, 1456, 743. **^{1}H NMR** (400 MHz, $CDCl_3$) δ 7.93 (s, 1H), 7.64 – 7.59 (m, 1H), 7.45 – 7.41 (m, 4H), 7.40 – 7.37 (m, 1H), 7.22 (ddd, *J* = 8.2, 7.0, 1.2 Hz, 1H), 7.12 (ddd, *J* = 8.0, 7.1, 1.1 Hz, 1H), 6.88 (dd, *J* = 2.4, 0.8 Hz, 1H), 6.44 (s, 1H), 4.25 (t, *J* = 5.9 Hz, 1H), 2.76 (tt, *J* = 6.0, 2.0 Hz, 2H), 2.17 (dddd, *J* = 12.9, 7.6, 5.3, 2.5 Hz, 1H), 2.05 – 1.78 (m, 3H). **^{13}C NMR** (101 MHz, CDCl3) δ 151.8, 150.8, 136.8, 131.8, 130.4, 126.8, 124.9, 122.6, 122.18, 122.15, 120.28, 120.26, 119.5, 119.4, 111.4, 106.8, 31.3, 31.1, 23.6, 21.3. **HRMS** (APCI +): calculated for $[C_{22}H_{19}BrNO]^+$ $[M+H]^+$ 392.0645

m/z; found 392.0655 *m/z*. **SFC** (ID (150 × 3.0 mm, 3 μm), CO_2:MeOH 75:25, 1.2 mL/min, 35 ºC, BPR 150 bar, 210 nm): en1 (major, 80%) min 1.88, en2 (minor, 20%) min 2.23. **[α]$^{26.0}_{D}$** −3.6 (c 0.52, $CHCl_3$, sample with 80:20 *er*).

(*S*)-3-(2-(4-Fluorophenyl)-4,5,6,7-tetrahydrobenzofuran-4-yl)-1*H*-indole (2.72j)

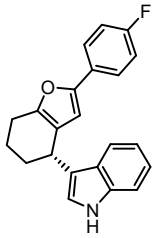

Prepared following general procedure **GP8** using enone **2.70e** (32.1 mg, 0.150 mmol, 1.0 equiv) and indole (17.6 mg, 0.150 mmol, 1.0 equiv) as a nucleophile in toluene (1.5 mL, 0.1 M), at −10 ºC for 1.5 h. The crude product was purified by FCC (silica, CyH:CH_2Cl_2 90:10 to 70:30). Compound **2.72j** was obtained as a brown oil (35.2 mg, 0.115 mmol, 71% yield) with 82:18 *er*. Spectroscopic data for product **2.72j** matched those reported in the literature.[52a] The absolute configuration was assigned assuming a uniform stereochemical mechanism. **IR** (film from CH_2Cl_2, cm^{-1}) 3415, 2935, 2850, 1558, 1496, 1456, 1228, 744. **^{1}H NMR** (500 MHz, $CDCl_3$): δ 7.93 (s, 1H), 7.63 (d, *J* = 7.9 Hz, 1H), 7.55 (ddd, *J* = 9.8, 5.2, 2.5 Hz, 2H), 7.38 (d, *J* = 8.1 Hz, 1H), 7.23 – 7.19 (m, 1H), 7.12 (ddd, *J* = 8.0, 7.1, 1.0 Hz, 1H), 7.06 – 6.98 (m, 2H), 6.89 (d, *J* = 2.3 Hz, 1H), 6.37 (s, 1H), 4.25 (t, *J* = 5.9 Hz, 1H), 2.84 – 2.63 (m, 2H), 2.20 – 2.18 (m, 1H), 2.08 – 1.93 (m, 2H), 1.90 – 1.84 (m 1H). **^{13}C NMR** (126 MHz, $CDCl_3$): δ 161.8 (d, *J* = 245.9 Hz), 151.3, 151.0, 136.8, 127.9 (d, *J* = 3.2 Hz), 126.8, 125.1, 125.0, 122.3, 122.17, 122.15, 120.3, 119.4 (d, *J* = 9.3 Hz), 115.6 (d, *J* = 21.8 Hz), 111.4, 105.8, 31.3, 31.1, 23.5, 21.3. **^{19}F NMR** (471 MHz, $CDCl_3$) δ −115.5. **SFC** (IG (150 × 3.0 mm, 3 μm), CO_2:EtOH 75:25, 1.2 mL/min, 35 ºC, BPR 150 bar, 280 nm): en1 (major, 82%) min 1.51, en2 (minor, 18%) min 1.96. **[α]$^{26.0}_{D}$** −5.2 (c 0.95, $CHCl_3$, sample with 82:18 *er*).

(*S*)-3-(2-(3-Fluorophenyl)-4,5,6,7-tetrahydrobenzofuran-4-yl)-1*H*-indole (2.72k)

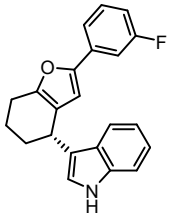

Prepared following general procedure **GP8** using enone **2.70f** (32.1 mg, 0.150 mmol, 1.0 equiv) and indole (17.6 mg, 0.150 mmol, 1.0 equiv) as a nucleophile in toluene (1.5 mL, 0.1 M), at −10 ºC for 6 h. The crude product was purified by PTLC (silica, CyH:EtOAc 90:10). Compound **2.72k** was obtained as a brown oil (35.0 mg, 0.11 mmol, 70% yield) with 83:17 *er*. The absolute configuration was assigned assuming a uniform stereochemical mechanism. **IR** (film from CH_2Cl_2, cm^{-1}) 3416, 2934, 2853, 1612, 1558, 1485, 1455, 1155, 743. **^{1}H NMR** (400 MHz, $CDCl_3$) δ 7.94 (s, 1H), 7.62 (dd, *J* = 7.9, 1.1 Hz, 1H), 7.39 (dt, *J* = 8.1, 0.9 Hz, 1H), 7.35 (dt, *J* = 7.8, 1.3 Hz, 1H), 7.32 – 7.25 (m, 2H), 7.25 – 7.19 (m, 1H), 7.13 (ddd, *J* = 8.0, 7.0, 1.1 Hz, 1H), 6.91 – 6.84 (m, 2H), 6.46 (s, 1H), 4.26 (t, *J* = 6.0 Hz, 1H), 2.78 (tt, *J* = 5.9, 2.0 Hz, 2H), 2.22 – 2.11 (m, 1H), 2.06 – 1.76 (m, 3H). **^{13}C NMR** (101 MHz, $CDCl_3$) δ 163.3 (d, *J* = 244.5 Hz), 151.9, 150.6 (d, *J* = 3.0 Hz), 136.8, 133.6 (d, *J* = 8.5 Hz), 130.2 (d, *J* = 8.6 Hz), 126.8, 122.5, 122.2, 120.2, 119.5, 119.3, 118.98, 118.95, 113.4 (d, *J* = 21.4 Hz), 111.4, 110.2 (d, *J* = 23.5 Hz), 107.3, 31.3, 31.1, 23.5, 21.3. **^{19}F NMR** (376 MHz, $CDCl_3$) δ −113.4. **HRMS** (APCI +): calculated for $[C_{22}H_{19}FNO]^+$ $[M+H]^+$ 332.1445 *m/z*; found 332.1458 *m/z*. **SFC** (ID (150 × 3.0 mm, 3 μm), CO_2:MeOH 80:20, 1.2 mL/min, 35 ºC, BPR 150 bar, 210 nm): en1 (major, 83%) min 1.41, en2 (minor, 17%) min 1.74. **[α]$^{26.0}_{D}$** −15 (c 0.40, $CHCl_3$, sample with 83:17 *er*).

(*S*)-3-(2-(2-Fluorophenyl)-4,5,6,7-tetrahydrobenzofuran-4-yl)-1*H*-indole (2.72l)

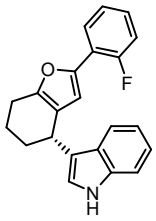

Prepared following general procedure **GP8** using enone **2.70g** (32.1 mg, 0.150 mmol, 1.0 equiv) and indole (17.6 mg, 0.150 mmol, 1.0 equiv) as a nucleophile in toluene (1.5 mL, 0.1 M), at −10 ºC for 7 h. The crude product was purified by PTLC (silica, CyH:EtOAc 90:10). Compound **2.72l** was obtained as a white solid (47 mg, 0.14 mmol, 95% yield) with 92:8 *er*. The absolute configuration was assigned assuming a uniform stereochemical mechanism. **mp:** 50–52 ºC. **IR** (film from CH_2Cl_2, cm^{-1}) 3418, 2935, 2852, 1488, 1455, 1218, 743. **^{1}H NMR** (400 MHz, $CDCl_3$): δ 7.92 (s, 1H), 7.87 – 7.79 (m, 1H), 7.64 (d, *J* = 7.9 Hz, 1H), 7.38 (d, *J* = 8.1 Hz, 1H), 7.24 – 7.00 (m, 5H), 6.87 (d, *J* = 2.4 Hz, 1H), 6.66 (d, *J* = 3.9 Hz, 1H), 4.29 (t, *J* = 6.0 Hz, 1H), 2.88 – 2.68 (m, 2H), 2.24 – 2.12 (m, 1H), 2.08 – 1.78 (m, 3H). **^{13}C NMR** (101 MHz, $CDCl_3$): δ 158.4 (d, *J* = 250.1 Hz), 151.5 (d, *J* = 1.1 Hz), 145.9 (d, *J* = 3.2 Hz), 136.8, 127.5 (d, *J* = 8.3 Hz), 126.8, 125.6 (d, *J* = 3.4 Hz), 124.3 (d, *J* = 3.5 Hz), 122.45 (d, *J* = 1.7 Hz), 122.2 (d, *J* = 21.0 Hz), 120.3, 119.8 (d, *J* = 12.0 Hz), 119.3 (d, *J* = 10.6 Hz), 115.9 (d, *J* = 21.5 Hz), 111.5 (d, *J* = 11.6 Hz), 111.3, 31.3, 31.0, 23.5, 21.1. **^{19}F NMR** (376 MHz, $CDCl_3$) δ −113.8. **HRMS** (APCI +): calculated for $[C_{22}H_{19}FNO]^+$ $[M+H]^+$ 332.1445 *m/z*; found 332.1447 *m/z*. **SFC** (ID (150 × 3.0 mm, 3 μm), CO_2:MeOH 75:25, 1.2 mL/min, 35 ºC, BPR 150 bar, 210 nm): en1 (major, 92%) min 1.06, en2 (minor, 8%) min 1.18. **$[\alpha]^{26.0}_D$** −15 (c 0.40, $CHCl_3$, sample with 92:8 *er*).

(*S*)-3-(2-(Thiophen-3-yl)-4,5,6,7-tetrahydrobenzofuran-4-yl)-1*H*-indole (2.72m)

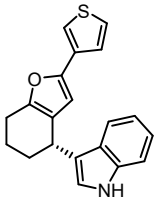

Prepared following general procedure **GP8** using enone **2.70h** (30.3 mg, 0.150 mmol, 1.0 equiv) and indole (17.6 mg, 0.150 mmol, 1.0 equiv) as a nucleophile in toluene (1.5 mL, 0.1 M), at −10 ºC for 7 h. The crude product was purified by PTLC (silica, CyH:EtOAc 90:10). Compound **2.72m** was obtained as a white solid (41 mg, 0.13 mmol, 86% yield) with 84:16 *er*. The absolute configuration was assigned assuming a uniform stereochemical mechanism. **IR** (film from CH_2Cl_2, cm^{-1}) 3416, 2932, 2852, 1456, 777, 743. **^{1}H NMR** (500 MHz, $CDCl_3$): δ 7.93 (s, 1H), 7.62 (d, *J* = 7.9 Hz, 1H), 7.39 – 7.37 (m, 2H), 7.31 – 7.25 (m, 1H), 7.23 – 7.18 (m, 2H), 7.12 (t, *J* = 7.5 Hz, 1H), 6.88 (d, *J* = 2.2 Hz, 1H), 6.26 (s, 1H), 4.25 (t, *J* = 5.6 Hz, 1H), 2.80 – 2.68 (m, 2H), 2.19 – 2.12 (m, 1H), 2.01 – 1.91 (m, 2H), 1.89 – 1.81 (m, 1H). **^{13}C NMR** (126 MHz, $CDCl_3$): δ 150.6, 149.0, 136.7, 133.3, 126.8, 126.0, 124.7, 122.2, 122.1, 121.8, 120.4, 119.41, 119.37, 117.6, 111.3, 105.9, 31.35, 31.05, 23.5, 21.30. **HRMS** (APCI +): calculated for $[C_{20}H_{18}NOS]^+$ $[M+H]^+$ 320.1104 *m/z*; found 320.1114 *m/z*. **SFC** (IG (150 × 3.0 mm, 3 μm), CO_2:EtOH 75:25, 1.2 mL/min, 35 ºC, BPR 150 bar, 210 nm): en1 (major, 84%) min 2.18, en2 (minor, 16%) min 3.58. **$[\alpha]^{26.0}_D$** −8.9 (c 0.29, $CHCl_3$, sample with 84:16 *er*).

(*R*)-3-(2-Cyclohexyl-4,5,6,7-tetrahydrobenzofuran-4-yl)-1*H*-indole (2.72n)

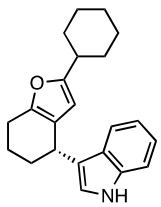

Prepared following general procedure **GP8** using enone **2.70i** (30.3 mg, 0.150 mmol, 1.0 equiv) and indole (17.6 mg, 0.150 mmol, 1.0 equiv) as a nucleophile in toluene (1.5 mL, 0.1 M), at −10 ºC for 20 h. The crude product was purified by PTLC (silica, CyH:EtOAc 90:10). Compound **2.72n** was obtained as a colorless oil (32.0 mg, 0.100 mmol, 67% yield) with 75:25 *er*. The absolute configuration was assigned assuming a uniform stereochemical mechanism. **IR** (film from CDCl3, cm^{-1}) ν 3417, 2926, 2852, 1455, 741. **^{1}H NMR** (300 MHz, $CDCl_3$): δ 7.94 (s, 1H), 7.63 (d, *J* = 7.9 Hz, 1H), 7.44–7.35 (m, 1H), 7.25–7.19 (m, 1H), 7.19–7.09 (m, 1H), 6.87 (d, *J* = 1.8 Hz, 1H), 5.75 (s, 1H), 4.20 (t, *J* = 5.7 Hz, 1H), 2.75–2.62 (m, 2H), 2.61–2.49 (m, 1H), 2.24–2.09 (m, 1H), 2.04 –1.67 (m, 8H), 1.40–1.26 (m, 5H). **^{13}C NMR** (75 MHz, $CDCl_3$): δ 158.9, 148.9,

136.7, 127.0, 122.1, 122.0, 120.8, 120.1, 119.4, 119.3, 111.3, 103.6, 37.6, 31.93, 31.88, 31.5, 31.0, 26.3, 26.2, 23.4, 21.4. **HRMS** (ESI +) calculated for $[C22H26NO]^+$ [M + H]+ 320.2009 *m/z*; found 320.2006 *m/z*. **SFC** (IC (150 × 3.0 mm, 3 μm), CO_2:MeOH 85:15, 1.2 mL/min, 35 ºC, BPR 150 bar, 230 nm): en1 (major, 75%) min 1.23, en2 (minor, 25%) min 1.45. **$[\alpha]^{26.0}_D$** −14 (c 0.34, $CHCl_3$, sample with 75:25 *er*).

(*S*)-3-(2-Phenyl-5,6-dihydro-4*H*-cyclopenta[*b*]furan-4-yl)-1*H*-indole (2.72o)

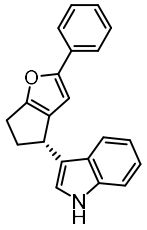

Prepared following modified general procedure **GP8** with 3 mol% catalyst loading complex **C** (3.9 mg, 4.5 μmol, 0.03 equiv) and *(R)*-**Ag6** (4.2 mg, 4.5 μmol, 0.03 equiv)] using enone **2.70j** (27.3 mg, 0.150 mmol, 1.0 equiv) and indole (17.6 mg, 0.150 mmol, 1.0 equiv) as a nucleophile in toluene (1.5 mL, 0.1 M), at −10 ºC for 24 h. The crude product was purified by FCC (silica, CyH:CH_2Cl_2 80:20 to 50:50). Compound **2.72o** was obtained as a yellow oil (32 mg, 0.11 mmol, 71% yield) with 86:14 *er*. Spectroscopic data for product **2.72o** matched those reported in the literature.[14a] The absolute configuration was assigned assuming a uniform stereochemical mechanism. **^{1}H NMR** (500 MHz, $CDCl_3$): δ 7.91 (s, 1H), 7.67 – 7.58 (m, 4H), 7.59 (d, *J* = 7.9 Hz, 1H), 7.39 – 7.32 (m, 3H), 7.24 – 7.16 (m, 2H), 7.14 – 7.06 (m, 1H), 6.96 (d, *J* = 2.2 Hz, 1H), 6.58 (s, 1H), 4.52 – 4.45 (m, 1H), 3.05 (dtd, *J* = 12.8, 8.5, 4.5 Hz, 1H), 2.98 – 2.82 (m, 2H), 2.50 (ddt, *J* = 12.7, 8.8, 5.7 Hz, 1H). **^{13}C NMR** (126 MHz, $CDCl_3$): δ 159.5, 157.9, 136.95, 132.0, 130.25, 128.8, 126.84, 126.78, 123.2, 122.25, 120.8, 120.7, 119.5 (2C), 111.3, 103.7, 37.6, 34.1, 24.9. **SFC** (IG (150 × 3.0 mm, 3 μm), CO_2:EtOH 75:25, 1.2 mL/min, 35 ºC, BPR 150 bar, 280 nm): en1 (major, 86%) min 2.09, en2 (minor, 14%) min 2.54. **$[\alpha]^{26.0}_D$** −53 (c 0.33, $CHCl_3$, sample with 86:14 *er*).

(*S*)-3-(2-Phenyl-5,6,7,8-tetrahydro-4*H*-cyclohepta[*b*]furan-4-yl)-1*H*-indole (2.72p)

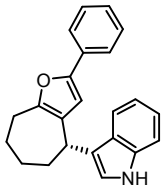

Prepared following general **GP8** using enone **2.70k** (35 mg, 0.150 mmol, 1.0 equiv) and indole (17.6 mg, 0.150 mmol, 1.0 equiv) as a nucleophile in toluene (1.5 mL, 0.1 M), at −10 ºC for 4 h. The crude product was purified by FCC (silica, CyH:EtOAc 100:0 to 80:20). Compound **2.72p** was obtained as a white solid (37 mg, 0.11 mmol, 75% yield) with 85:15 *er*. Spectroscopic data for product **2.72p** matched those reported in the literature. [14a] The absolute configuration was assigned assuming a uniform stereochemical mechanism. **Mp:** 54–56 ºC. **^{1}H NMR** (400 MHz, $CDCl_3$) δ 7.94 (s, 1H), 7.63 (dd, *J* = 7.9, 1.0 Hz, 1H), 7.56 – 7.50 (m, 2H), 7.38 (dt, *J* = 8.2, 0.9 Hz, 1H), 7.29 (dd, *J* = 8.5, 7.1 Hz, 2H), 7.21 (ddd, *J* = 8.2, 7.0, 1.2 Hz, 1H), 7.18 – 7.09 (m, 2H), 6.84 (dd, *J* = 2.4, 0.8 Hz, 1H), 6.26 (s, 1H), 4.29 (dd, *J* = 7.7, 3.2 Hz, 1H), 2.96 (d, *J* = 5.6 Hz, 2H), 2.38 – 2.27 (m, 1H), 2.14 – 2.03 (m, 1H), 1.88 – 1.68 (m, 4H). **^{13}C NMR** (101 MHz, $CDCl_3$) δ 152.8, 149.8, 136.7, 131.2, 128.5, 126.6, 126.45, 126.0, 123.2, 122.4, 121.9, 119.8, 119.6, 119.2, 111.2, 108.9, 35.3, 34.4, 29.1, 27.4, 26.7. **SFC** (ID (150 × 3.0 mm, 3 μm), CO_2:MeOH 75:25, 1.2 mL/min, 35 ºC, BPR 150 bar, 210 nm): en1 (major, 85%) min 1.29, en2 (minor, 15%) min 1.89. **$[\alpha]^{26.0}_D$** +62 (c 0.28, $CHCl_3$, sample with 85:15 *er*).

(*R*)-*N*,2-Diphenyl-4,5,6,7-tetrahydrobenzofuran-4-amine (2.73a)

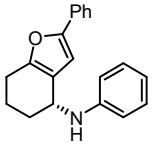

Prepared following general procedure **GP8** using enone **1.40** (29.4 mg, 0.150 mmol, 1.0 equiv) and aniline (13.7 μL , 0.150 mmol, 1.0 equiv) as a nucleophile in toluene (1.5 mL, 0.1 M), at −10 ºC for 24 h. The crude product was purified by PTLC (silica, CyH:EtOAc 95:5). Compound **2.73a** was obtained as a colorless oil (35.0 mg, 0.120mmol, 78% yield) with 62:38 *er*. Spectroscopic data for product **2.73a** matched those reported in the literature.[14a] The absolute configuration was assigned by comparison with the literature based on the sign of optical rotation.[14a] **^{1}H NMR** (300 MHz, $CDCl_3$): δ 7.65 – 7.59

(m, 2H), 7.36 (t, *J* = 7.6 Hz, 2H), 7.23 (t, *J* = 8.0 Hz, 3H), 6.80 – 6.66 (m, 3H), 6.61 (s, 1H), 4.58 (t, *J* = 2.9 Hz, 1H), 3.82 (s, 1H), 2.79 – 2.61 (m, 2H), 2.10 – 1.94 (m, 2H), 1.93 – 1.78 (m, 2H).**^{13}C NMR** (75 MHz, $CDCl_3$): δ 152.5, 152.3, 147.4, 131.1, 129.5, 128.8, 127.1, 123.5, 121.6, 117.5, 113.3, 105.0, 47.0, 29.4, 23.3, 19.8. **HPLC** (IB-N (250 × 4.6 mm, 5 μm), 98:2 *n*-hexane:*i*-PrOH, 1 mL/min, 25 ºC, 240 nm): en1 (minor, 38%) min 11.67, en2 (major, 62%) min 14.38. **$[\alpha]^{27.2}_D$** −1.7 (c 0.95, $CHCl_3$, sample with 62:38 *er*). lit:[13] **$[\alpha]_D$** +4 (c 0.95 $CHCl_3$, sample with 17.5:82.5 *er*).

***tert*-Butyl (*R*)-(2-phenyl-4,5,6,7-tetrahydrobenzofuran-4-yl)carbamate (2.73b)**

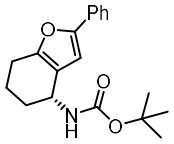

Prepared following general procedure **GP8** using enone **1.40** (29.4 mg, 0.150 mmol, 1.0 equiv) and tert-butyl carbamate (17.6 mg, 0.150 mmol, 1.0 equiv) as a nucleophile in toluene (1.5 mL, 0.1 M), at −10 ºC for 1 h. The crude product was purified by PTLC (silica, CyH:EtOAc 95:5). Compound **2.73b** was obtained as a white solid (41.8 mg, 0.133 mmol, 89% yield) with 95:5 *er*. Spectroscopic data for product **2.73b** matched those reported in the literature.[52b] The absolute configuration was assigned assuming a uniform stereochemical mechanism. **^{1}H NMR** (500 MHz, $CDCl_3$): δ 7.67 – 7.59 (m, 2H), 7.37 (t, *J* = 7.8 Hz, 2H), 7.27 – 7.18 (m, 1H), 6.62 (s, 1H), 4.78 – 4.67 (m, 2H), 2.74 – 2.58 (m, 2H), 2.13 – 1.99 (m, 1H), 1.99 – 1.82 (m, 2H), 1.77 – 1.67 (m, 1H), 1.51 (s, 9H). **^{13}C NMR** (75 MHz, $CDCl_3$): δ 155.5, 152.6, 152.2, 131.1, 128.7, 127.1, 123.5, 120.7, 104.8, 79.5, 44.7, 30.6, 28.6, 23.1, 20.0. **HPLC** (ID (250 × 4.6 mm, 5 μm), 95:5 *n*-hexane:*i*-PrOH, 1 mL/min, 25 ºC, 270 nm): en1 (major, 95%) min 9.73, en2 (minor, 5%) min 11.78. **$[\alpha]^{27.3}_D$** +16.7 (c 0.995, $CHCl_3$, sample with 95:5 *er*).

Benzyl (*R*)-(2-phenyl-4,5,6,7-tetrahydrobenzofuran-4-yl)carbamate (2.73c)

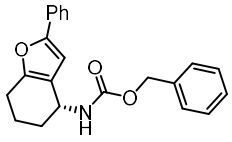

Prepared following general procedure **GP8** using enone **1.40** (29.4 mg, 0.150 mmol, 1.0 equiv) and benzyl carbamate (22.7 mg, 0.150 mmol, 1.0 equiv) as a nucleophile in toluene (1.5 mL, 0.1 M), at −10 ºC for 1 h. The crude product was purified by PTLC (silica, CyH:EtOAc 90:10). Compound **2.73c** was obtained as a white solid (35.8 mg, 0.103 mmol, 69% yield) with 95:5 *er*. Spectroscopic data for product **2.73c** matched those reported in the literature.[14a] The absolute configuration was assigned by comparison with the literature based on the sign of optical rotation.[14a] **^{1}H NMR** (300 MHz, $CDCl_3$): δ 7.60 (d, *J* = 7.6 Hz, 2H), 7.42 – 7.29 (m, 7H), 7.26 – 7.19 (m, 1H), 6.58 (s, 1H), 5.16 (s, 2H), 5.01 – 4.64 (m, 2H), 2.80 – 2.50 (m, 2H), 2.10 – 1.80 (m, 3H), 1.78 – 1.68 (m, 1H).**^{13}C NMR** (75 MHz, $CDCl_3$): δ 155.9, 152.7, 152.3, 136.7, 131.0, 128.7, 128.7, 128.3, 127.2, 123.5, 120.3, 104.7, 66.8, 45.3, 30.6, 23.1, 20.0. **HPLC** (IB-N (250 × 4.6 mm, 5 μm), 95:5 *n*-hexane:*i*-PrOH, 1 mL/min, 25 ºC, 280 nm): en1 (major, 95%) min 17.45, en2 (minor, 5%) min 20.65. **$[\alpha]^{27.3}_D$** +1.6 (c 1.15, $CHCl_3$, sample with 95:5 *er*). lit:[14a] **$[\alpha]_D$** −3 (c 1.15 $CHCl_3$, sample with 3:97 *er*).

(*R*)-4-Methoxy-2-phenyl-4,5,6,7-tetrahydrobenzofuran (2.73d)

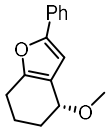

Prepared following general procedure **GP8** using enone **1.40** (29.4 mg, 0.150 mmol, 1.0 equiv) and methanol (6.1 μL, 0.150 mmol, 1.0 equiv) as a nucleophile in toluene (1.5 mL, 0.1 M), at −10 ºC for 1 h. The crude product was purified by PTLC (silica, CyH:EtOAc 90:10). Compound **2.73d** was obtained as a colorless oil (31.9 mg, 0.140 mmol, 93% yield) with 72:28 *er*. Spectroscopic data for product **2.73d** matched those reported in the literature.[52b] The absolute configuration was assigned assuming a uniform stereochemical mechanism. **^{1}H NMR** (300 MHz, $CDCl_3$): δ 7.67 – 7.57 (m, 2H), 7.41 – 7.29 (m, 2H), 7.25 – 7.16 (m, 1H), 6.65 (s, 1H), 4.30 (t, *J* = 4.1 Hz, 1H), 3.45 (s, 3H), 2.81 – 2.53 (m, 2H), 2.11 – 1.90 (m,

2H), 1.90 – 1.75 (m, 2H). **^{13}C NMR** (75 MHz, $CDCl_3$): δ 153.0, 152.4, 131.3, 128.7, 127.0, 123.6, 120.1, 105.5, 72.6, 56.3, 28.6, 23.4, 19.0. **SFC** (IG(150 × 3.0 mm, 3 μm), CO_2:ACN 80:20, 1.2 mL/min, 35 ºC, BPR 150 bar, 280 nm): en1 (major, 72%) min 1.51, en2 (minor, 28%) min 2.12. **$[\alpha]^{26.9}_D$** +12 (c 0.76, $CHCl_3$, sample with 72:28 *er*).

(*R*)-2-Phenyl-4-((3-phenylprop-2-yn-1-yl)oxy)-4,5,6,7-tetrahydrobenzofuran (2.73e)

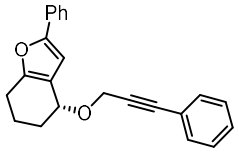

Prepared following general procedure **GP8** using enone **1.40** (29.4 mg, 0.150 mmol, 1.0 equiv) and 3-phenylprop-2yn.-1-ol (19.8 mg, 0.150 mmol, 1.0 equiv) as a nucleophile in toluene (1.5 mL, 0.1 M) at −10 ºC for 1 h. The crude product was purified by PTLC (silica, CyH:EtOAc 98:2). Compound **2.73e** was obtained as a colorless oil (47.2 mg, 0.144 mmol, 96% yield) with 77:23 *er*. Spectroscopic data for product **2.73e** matched those reported in the literature.[51b] The absolute configuration was assigned assuming a uniform stereochemical mechanism. **^{1}H NMR** (300 MHz, $CDCl_3$): δ 7.67 – 7.58 (m, 2H), 7.54 – 7.44 (m, 2H), 7.40 – 7.30 (m, 5H), 7.25 – 7.18 (m, 1H), 6.73 (s, 1H), 4.79 – 4.72 (m, 1H), 4.51 (s, 2H), 2.77 (ddd, *J* = 16.9, 5.5, 3.9 Hz, 1H), 2.70 – 2.54 (m, 1H), 2.18 – 2.01 (m, 2H), 1.93 – 1.78 (m, 2H). **^{13}C NMR** (75 MHz, $CDCl_3$): δ 153.4, 152.5, 131.9, 131.2, 128.7, 128.6, 128.5, 127.1, 123.6, 122.9, 119.5, 105.6, 86.3, 85.9, 69.7, 56.4, 29.0, 23.4, 19.0. **SFC** (IB-N (150 × 3.0 mm, 3 μm), CO_2:EtOH 70:30, 1.2 mL/min, 35 ºC, BPR 150 bar, 280 nm): en1 (major, 77%) min 1.61, en2 (minor, 23%) min 1.96. **$[\alpha]^{26.5}_D$** +120 (c 1.0, $CHCl_3$, sample with 77:23 *er*).

(*R*)-4-(Allyloxy)-2-phenyl-4,5,6,7-tetrahydrobenzofuran (2.73f)

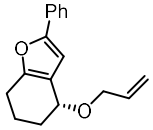

Prepared following general procedure **GP8** using enone **1.40** (29.4 mg, 0.150 mmol, 1.0 equiv) and allyl alcohol (10.2 μL, 0.150 mmol, 1.0 equiv) as a nucleophile in toluene (1.5 mL, 0.1 M) at −10 ºC for 1 h. The crude product was purified by PTLC (silica, CyH:EtOAc 98:2). Compound **2.73f** was obtained as a colorless oil (30.1 mg, 0.118 mmol, 79% yield) with 76:24 *er*. Spectroscopic data for product **2.73f** matched those reported in the literature.[51b] The absolute configuration was assigned assuming a uniform stereochemical mechanism. **^{1}H NMR** (300 MHz, $CDCl_3$): δ 7.68 – 7.59 (m, 2H), 7.40 – 7.31 (m, 2H), 7.25 – 7.17 (m, 1H), 6.64 (s, 1H), 5.99 (ddt, *J* = 17.2, 10.4, 5.6 Hz, 1H), 5.34 (dq, *J* = 17.2, 1.7 Hz, 1H), 5.26 – 5.15 (m, 1H), 4.49 – 4.41 (m, 1H), 4.20 – 4.07 (m, 2H), 2.74 (dt, *J* = 16.8, 5.3 Hz, 1H), 2.68 – 2.51 (m, 1H), 2.23 – 2.02 (m, 1H), 2.02 – 1.90 (m, 1H), 1.90 – 1.75 (m, 2H). **^{13}C NMR** (75 MHz, $CDCl_3$): δ 153.1, 152.4, 135.6, 131.3, 128.7, 127.0, 123.6, 120.3, 116.8, 105.4, 70.6, 69.6, 29.1, 23.4, 19.1. **SFC** (IG (150 × 3.0 mm, 3 μm), CO_2:MeOH 70:30, 1.2 mL/min, 35 ºC, BPR 150 bar, 254 nm): en1 (major, 76%) min 0.87, en2 (minor, 24%) min 1.05. **$[\alpha]^{27.2}_D$** −2.3 (c 0.8, $CHCl_3$, sample with 76:24 *er*).

(*R*)-4-Isopropoxy-2-phenyl-4,5,6,7-tetrahydrobenzofuran (2.73g)

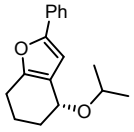

Prepared following general procedure **GP8** using enone **1.40** (29.4 mg, 0.150 mmol, 1.0 equiv) and 2-propanol (11.5 μL, 0.150 mmol, 1.0 equiv) as a nucleophile in toluene (1.5 mL, 0.1 M), at −10 ºC for 2 h. The crude product was purified by PTLC (silica, CyH:EtOAc 90:10). Compound **2.73g** was obtained as a colorless oil (35.4 mg, 0.138 mmol, 92% yield) with 82:18 *er*. Spectroscopic data for product **2.73g** matched those reported in the literature.[51b] The absolute configuration was assigned assuming a uniform stereochemical mechanism. **^{1}H NMR** (300 MHz, $CDCl_3$): δ 7.64 (dd, *J* = 8.4, 1.2 Hz, 2H), 7.37 (td, *J* = 7.0, 1.6 Hz, 2H), 7.28 – 7.19 (m, 1H), 6.62 (s, 1H), 4.48 (t, *J* = 3.8 Hz, 1H), 3.86 (hept, *J* = 6.1 Hz, 1H), 2.81 – 2.69 (m, 1H), 2.67 – 2.55 (m, 1H), 2.19 – 2.00 (m, 1H), 1.87 (qt, *J* = 5.6, 3.3 Hz, 3H), 1.26 (dd, *J* = 6.1, 3.4 Hz, 6H). **^{13}C NMR** (75 MHz, $CDCl_3$): δ 152.7, 152.4, 131.4,

128.7, 126.9, 123.6, 121.1, 105.2, 77.6, 77.2, 76.7, 69.5, 68.6, 29.9, 23.4, 23.3, 22.8, 19.2. **SFC** (IB-N(150 × 3.0 mm, 3 μm), CO_2:*i*-PrOH 98:2, 1.2 mL/min, 35 ºC, BPR 150 bar, 280 nm): en1 (minor, 18%) min 1.93, en2 (major, 82%) min 2.17. **[α]$^{26.9}_{D}$** −46 (c 1.0, $CHCl_3$, sample with 82:18 *er*).

(*R*)-4-(Cyclohexyloxy)-2-phenyl-4,5,6,7-tetrahydrobenzofuran (2.73h)

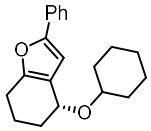

Prepared following general procedure **GP8** using enone **1.40** (29.4 mg, 0.150 mmol, 1.0 equiv) and cyclohexanol (19.8 mg, 0.150 mmol, 1.0 equiv) as a nucleophile in toluene (1.5 mL, 0.1 M), using 3 mol% catalyst, at −10 ºC for 2 h. The crude product was purified by PTLC (silica, CyH:EtOAc 90:10). Compound **2.73h** was obtained as a pale orange oil (32.2 mg, 0.109 mmol, 72% yield) with 81.5:18.5 *er*. The absolute configuration was assigned assuming a uniform stereochemical mechanism. **IR** (film from $CHCl_3$, cm^{-1}) ν 2929, 2854, 1805, 1449, 1069, 758. **^{1}H NMR** (300 MHz, $CDCl_3$): δ 7.70 – 7.59 (m, 2H), 7.37 (ddd, *J* = 7.8, 6.9, 1.1 Hz, 2H), 7.26 – 7.14 (m, 1H), 6.61 (s, 1H), 4.53 (t, *J* = 4.3 Hz, 1H), 3.58 – 3.37 (m, 1H), 2.74 (dt, *J* = 15.9, 5.0 Hz, 1H), 2.68 – 2.52 (m, 1H), 2.15 – 1.92 (m, 3H), 1.90 – 1.72 (m, 5H), 1.47 – 1.12 (m, 6H). **^{13}C NMR** (75 MHz, $CDCl_3$): δ 152.7, 152.5, 131.4, 128.7, 126.9, 123.6, 121.3, 105.2, 75.8, 68.5, 33.7, 33.1, 30.0, 26.0, 24.7, 24.6, 23.4, 19.3. **HRMS** (ESI +) calculated for $[C_{20}H_{24}NaO_2]^+$ $[M + Na]^+$ 319.1669 *m/z*; found 319.1665 *m/z*. **SFC** (IG (150 × 3.0 mm, 3 μm), CO_2:MeOH 80:20, 1.2 mL/min, 35 ºC, BPR 150 bar, 210 nm): en1 (major, 81.5%) min 1.16, en2 (minor, 18.5%) min 1.40. **[α]$^{26.9}_{D}$** +1.2 (c 1.0, $CHCl_3$, sample with 81.5:18.5 *er*).

(*R*)-4-Phenoxy-2-phenyl-4,5,6,7-tetrahydrobenzofuran (2.73i)

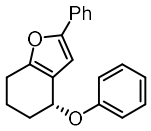

Prepared following general procedure **GP8** using enone **1.40** (29.4 mg, 0.150 mmol, 1.0 equiv) and phenol (14.1 mg, 0.150 mmol, 1.0 equiv) as a nucleophile in toluene (1.5 mL, 0.1 M), at −10 ºC for 2 h. The crude product was purified by PTLC (silica, CyH:EtOAc 90:10). Compound **2.73i** was obtained as a white solid (37.1 mg, 0.127 mmol, 85% yield) with 87:13 *er*. Spectroscopic data for product **2.73i** matched those reported in the literature.[14a] The absolute configuration was assigned by comparison with the literature based on the sign of optical rotation.[14a] **^{1}H NMR** (500 MHz, $CDCl_3$): δ 7.65 – 7.59 (m, 2H), 7.39 – 7.30 (m, 4H), 7.25 – 7.20 (m, 1H), 7.08 – 7.03 (m, 2H), 7.00 (tt, *J* = 7.4, 1.1 Hz, 1H), 6.61 (s, 1H), 5.38 (t, *J* = 4.4 Hz, 1H), 2.82 (dt, *J* = 16.7, 5.3 Hz, 1H), 2.74 – 2.62 (m, 1H), 2.20 – 2.10 (m, 2H), 2.02 – 1.94 (m, 1H), 1.94 – 1.84 (m, 1H). **^{13}C NMR** (126 MHz, $CDCl_3$): δ 158.2, 153.5, 152.7, 131.1, 129.7, 128.7, 127.1, 123.6, 121.1, 119.6, 116.4, 105.1, 69.8, 28.8, 23.3, 19.2. **HPLC** (IB-N (250 × 4.6 mm, 5 μm), 98:2 *n*-hexane:*i*-PrOH, 1 mL/min, 25 ºC, 280 nm): en1 (minor, 13%) min 6.54, en2 (major, 87%) min 9.99. **[α]$^{27.1}_{D}$** +20 (c 0.99, $CHCl_3$, sample with 87:13 *er*). lit:[14a] **[α]$_D$** −21 (c 0.99 $CHCl_3$, sample with 5:95 *er*).

(*R*)-2-(2-Phenyl-4,5,6,7-tetrahydrobenzofuran-4-yl)naphthalen-1-ol (2.73j)

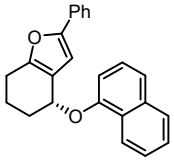

Prepared following general procedure **GP8** using enone **1.40** (29.4 mg, 0.150 mmol, 1.0 equiv) and 1-naphtol (21.6 mg, 0.150 mmol, 1.0 equiv) as a nucleophile in toluene (1.5 mL, 0.1 M), at −10 ºC for 2 h. The crude product was purified by PTLC (silica, CyH:EtOAc 95:5). Compound **2.73j** was obtained as a colorless oil (40.0 mg, 0.120mmol, 78% yield) with 88.5:11.5 *er*. The absolute configuration was assigned assuming a uniform stereochemical mechanism. **IR** (film from $CHCl_3$, cm^{-1}) ν 3053, 2924, 2852, 1595, 1578, 1506, 1461, 1397, 1266, 1235, 1093, 1062, 939, 791, 772, 759. **^{1}H NMR** (300 MHz, $CDCl_3$): δ 8.39 – 8.27 (m, 1H), 7.85 (dd, *J* = 7.4, 1.7 Hz, 1H), 7.70 – 7.60 (m, 2H), 7.55 – 7.43 (m, 4H), 7.43 – 7.33 (m, 2H), 7.28 – 7.22 (m, 1H), 7.11 (dd, *J* = 7.0,

1.3 Hz, 1H), 6.69 (s, 1H), 5.60 (t, J = 4.2 Hz, 1H), 2.91 (dt, J = 16.8, 5.3 Hz, 1H), 2.84 – 2.66 (m, 1H), 2.38 – 2.19 (m, 2H), 2.19 – 2.05 (m, 1H), 2.05 – 1.88 (m, 1H). **^{13}C NMR** (75 MHz, $CDCl_3$): δ 154.1, 153.5, 152.6, 134.9, 131.1, 128.7, 127.6, 127.1, 126.7, 126.5, 125.9, 125.3, 123.6, 122.6, 120.5, 119.9, 106.8, 105.3, 70.3, 29.0, 23.4, 19.5. **HRMS** (ESI +) calculated for $[C_{24}H_{20}NaO_2]^+$ $[M + Na]^+$ 363.1356 *m/z*; found 363.1352 *m/z*. **SFC** (ID (150 × 3.0 mm, 3 µm), CO_2:EtOH 75:25, 1.2 mL/min, 35 ºC, BPR 150 bar, 210 nm): en1 (major, 88.5%) min 1.04, en2 (minor, 11.5%) min 1.15. **[α]$^{27.3}_D$** −87 (c 0.98, $CHCl_3$, sample with 88.5:11.5 *er*).

(4*R*,4'*R*)-4,4'-Oxybis(2-phenyl-4,5,6,7-tetrahydrobenzofuran) (2.73k)

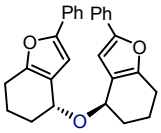

Prepared following general procedure **GP8** using enone **1.40** (29.4 mg, 0.150 mmol, 1.0 equiv) and water (4.0 µL, 0.221 mmol, 1.48 equiv) as a nucleophile in toluene (1.5 mL, 0.1 M), at −10 ºC for 1.5 h. The crude product was purified by PTLC (silica, CyH:EtOAc 90:10). Compound **2.73k** was obtained as a white solid (26.1 mg, 0.064mmol, 85% yield) with 95:5 *er* and as a single diastereomer. Spectroscopic data for product **2.73k** matched those reported in the literature.[14a] The absolute configuration was assigned by comparison with the literature based on the sign of optical rotation.[14a] **^{1}H NMR** (400 MHz, $CDCl_3$): δ 7.63 (d, J = 8.2 Hz, 4H), 7.35 (d, J = 8.4 Hz, 4H), 7.25 – 7.17 (m, 2H), 6.63 (s, 2H), 4.63 (t, J = 4.3 Hz, 2H), 2.75 (dt, J = 16.3, 5.1 Hz, 2H), 2.68 – 2.56 (m, 2H), 2.22 – 2.09 (m, 1H), 2.08 – 1.97 (m, 2H), 1.96 – 1.81 (m, 4H). **^{13}C NMR** (75 MHz, $CDCl_3$): δ 153.0, 152.5, 131.4, 128.7, 127.0, 123.6, 120.8, 105.2, 69.1, 29.7, 23.4, 19.1. **SFC** (ID (150 × 3.0 mm, 3 µm), CO_2:*i*-PrOH 75:25, 1.8 mL/min, 35 ºC, BPR 150 bar, 280 nm): en1 (major, 95%) min 1.08, en2 (minor, 5%) min 1.66. **[α]$^{26.0}_D$** −65 (c 0.95, $CHCl_3$, sample with 95:5 *er*). lit:[14a] **[α]$_D$** + 75 (c 0.95 $CHCl_3$, sample with 1.5:98.5 *er*).

General procedure GP9: phosphite formation

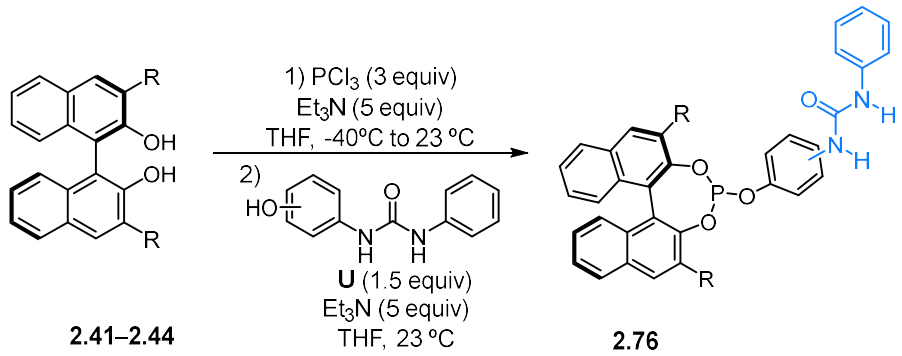

Following a modified literature procedure,[28c] under Ar, a flame-dried Schlenk tube equipped with a stir bar was charged with the desired binaphthol **2.41–2.44** (1 equiv). Anhydrous THF was added and the solid was dissolved before cooling it to -40 °C. A solution of PCl_3 (3 equiv) in THF (0.12 M final concentration) was then added dropwise. After stirring for 10 min, anhydrous Et_3N (5 equiv) was added at the same temperature. The mixture was allowed to warm up to room temperature and stirred for 2 h. The reaction was moved inside the glovebox where it was filtered through a celite pad (rinsing with THF). The filtrate was concentrated under reduced pressure, treated with toluene (1 mL) and evaporated. The obtained crude was redissolved in anhydrous THF (0.04 M) and Et_3N (5 equiv) was added followed by the corresponding hydroxyurea **U** (2 equiv). The resulting mixture was left stirring 18 h at room temperature. Next day, the volatiles were removed under vacuum and the crude was purified by FCC (CyH:EtOAc or pent:EtOAc solvent mixtures) providing the desired phosphite ligand (**2.76**).

Note: phosphites were found to readily oxidize under air. FCC were carried out using N_2. Compounds had to be stored in the glovebox or quickly coordinated to gold.

1-(4-Hydroxyphenyl)-3-phenylurea (U1)

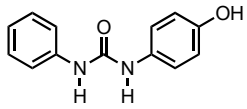

To an oven-dried 50 mL flask was added 4-aminophenol (0.88 mL, 9.16 mmol, 1.0 equiv) and dissolved in anhydrous MeCN (18 mL). The system was cooled to 0 ºC with an ice/water bath and isocyanatobenzene (1.0 mL, 9.16 mmol, 1.0 equiv) was added dropwise and the mixture was left stirring at the same temperature for 2h. The solvent was evaporated obtaining hidroxyurea **U1** as a white solid (2.08g, 9.11 mmol, 99% yield) which was used as it is without further purification. Spectroscopic data matched those reported in the literature.[94] **^{1}H NMR** (500 MHz, $(CD_3)_2SO$) δ 9.06 (s, 1H), 8.52 (s, 1H), 8.31 (s, 1H), 7.43 (dt, J = 8.7, 1.6 Hz, 2H), 7.31 – 7.24 (m, 2H), 7.24 – 7.19 (m, 2H), 6.94 (tt, J = 7.5, 1.1 Hz, 1H), 6.75 – 6.63 (m, 2H).

1-(3-Hydroxyphenyl)-3-phenylurea (U2)

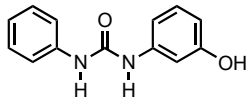

To an oven-dried 50 mL flask was added 3-aminophenol (0.500 g, 4.58 mmol, 1.0 equiv) and dissolved in anhydrous MeCN (9 mL). The system was cooled to 0 ºC with an ice/water bath and isocyanatobenzene (0.50 mL, 4.58 mmol, 1.0 equiv) was added dropwise. The mixture was left stirring at the same temperature for 1h. The solvent was evaporated and the crude was purified by FCC (CyH:EtOAc 70:30 to 50:50) obtaining hidroxyurea **U2** as a white solid (0.982 g, 4.30 mmol, 94% yield). Spectroscopic data matched those reported in the literature.[94] **^{1}H NMR** (500 MHz, $(CD_3)_2SO$) δ 9.31 (s, 1H), 8.56 (d, J = 18.3 Hz, 2H), 7.44 (dd, J = 8.6, 1.1 Hz, 2H), 7.30 – 7.24 (m, 2H), 7.07 – 7.00 (m, 2H), 6.99 – 6.91 (m, 1H), 6.79 (s, 1H), 6.37 (ddd, J = 8.1, 2.3, 0.8 Hz, 1H).

1-(2-Hydroxyphenyl)-3-phenylurea (U3)

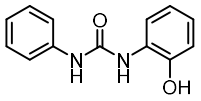

To an oven-dried 50 mL flask was added 2-aminophenol (0.500 g, 4.58 mmol, 1.0 equiv) and dissolved in anhydrous MeCN (9 mL). The system was cooled to 0 ºC with an ice/water bath and isocyanatobenzene (0.50 mL, 4.58 mmol, 1.0 equiv) was added dropwise. The mixture was left stirring at the same temperature for 1h. The solvent was evaporated and the crude was purified by FCC (CyH:EtOAc 70:30 to 50:50) obtaining hidroxyurea **U3** as a white solid (0.963 g, 4.22 mmol, 92% yield). Spectroscopic data matched those reported in the literature.[95] **^{1}H NMR** (500 MHz, $(CD_3)_2SO$) δ 9.93 (s, 1H), 9.29 (s, 1H), 8.16 (s, 1H), 8.03 (dd, *J* = 7.9, 1.7 Hz, 1H), 7.44 (dt, *J* = 8.7, 1.6 Hz, 2H), 7.31 – 7.23 (m, 2H), 6.95 (tt, *J* = 7.5, 1.1 Hz, 1H), 6.84 (dd, *J* = 7.8, 1.6 Hz, 1H), 6.76 (dtd, *J* = 23.8, 7.4, 1.7 Hz, 2H). **^{13}C NMR** (126 MHz, $(CD_3)_2SO$) δ 153.0, 146.1, 140.4, 129.3, 128.3, 122.2, 122.1, 119.6, 119.0, 118.3, 114.8.

94. Velappan, A. B.; Charan Raja, M. R.; Datta, D.; Tsai, Y. T.; Halloum, I.; Wan, B.; Kremer, L.; Gramajo, H.; Franzblau, S. G.; Kar Mahapatra, S.; Debnath, J. *Eur. J. Med. Chem.* **2017**, 125, 825–841.
95. Zou, H.; Supa, K.; Zhang, J. Patent CN109776244, May 21, **2019**.

(*R*)-2.75a

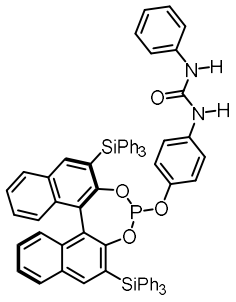

Prepared following general procedure **GP9**, using binaphthol (*R*)-**2.43** (200 mg, 0.250 mmol, 1.0 equiv) and hidroxyurea **U1** (114 mg, 0.500 mmol, 2.0 equiv). (*R*)-**2.75a** was obtained as a white solid) (94 mg, 0.089 mmol, 36% yield) after FCC (CyH:EtOAc dry load, silica, 90:10 to 80:20). **M.p.** 212 °C. **^{1}H NMR** (500 MHz, CD_2Cl_2) δ 8.10 (s, 1H), 7.96 (s, 1H), 7.83 (d, *J* = 8.2 Hz, 1H), 7.78 (d, *J* = 8.2 Hz, 1H), 7.57 (ddd, *J* = 20.0, 8.0, 1.5 Hz, 12H), 7.46 – 7.19 (m, 28H), 7.09 (tt, *J* = 6.8, 1.7 Hz, 1H), 6.79 – 6.69 (m, 2H), 6.46 (brs, 1H), 6.35 (brs, 1H), 5.79 – 5.68 (m, 2H). **^{13}C NMR** (126 MHz, CD_2Cl_2) δ 152.8, 152.5 (d, *J* = 4.4 Hz) 151.9 (d, *J* = 4.4 Hz), 147.3 (d, *J* = 7.4 Hz), 141.1, 141.0, 138.4, 136.7, 136.5, 134.7 (d, *J* = 38.5 Hz) 134.6, 133.7, 133.6, 130.9, 130.4, 129.7, 129.5, 129.2, 128.7 (d, *J* = 6.4 Hz)128.0, 127.8, 127.5, 127.2 (d, *J* = 7.7 Hz)126.8, 126.7, 126.6, 125.1 (d, *J* = 5.7 Hz), 123.8, 123.4 (d, *J* = 4.4 Hz), 122.9 (d, *J* = 4.4 Hz), 121.8, 121.2 (d, *J* = 6.8 Hz), 120.5. **^{31}P NMR** (203 MHz, CD_2Cl_2) δ 149.9. **HRMS (ESI +)** calculated for [$C_{69}H_{51}N_2NaO_4PSi_2$] [M+Na]+ 1081.3017m/z; found 1081.3003 m/z. **$[\alpha]^{26}_D$** −140.5 (c 0.38, acetone).

(*R*)-2.75b

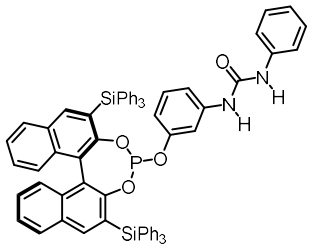

Prepared following general procedure **GP9**, using binaphthol (*R*)-**2.43** (200 mg, 0.250 mmol, 1.0 equiv) and hidroxyurea **U2** (114 mg, 0.500 mmol, 2.0 equiv). (*R*)-**2.75b** was obtained as a white solid (123 mg, 0.116 mmol, 47% yield) after FCC (CyH:EtOAc dry load, silica, 90:10 to 80:20). **M.p.** 215 °C. **^{1}H NMR** (500 MHz, CD_2Cl_2) δ 8.14 (s, 1H), 7.99 (s, 1H), 7.88 (d, *J* = 8.2 Hz, 1H), 7.81 (d, *J* = 8.1 Hz, 1H), 7.67 – 7.55 (m, 12H), 7.53 – 7.22 (m, 29H),7.16 (t, *J* = 7.1 Hz, 1H), 6.78 (t, *J* = 8.2 Hz, 1H), 6.34 (brs, 1H), 5.57 (brs, 1H), 5.56 – 5.53 (m, 1H), 5.50 – 5.47 (m, 1H). **^{13}C NMR** (126 MHz, CD_2Cl_2) δ 152.2 (d, J = 5.0 Hz), 151.7, 151.5 (d, J = 4.1 Hz), 150.7 (d, J = 6.9 Hz), 140.9 (d, J = 21.9 Hz), 138.1 (d, J = 29.0 Hz), 136.4, 136.4, 134.5, 134.2, 134.2, 133.5, 130.7, 130.1, 129.4, 129.2, 129.0, 129.0, 128.5 (d, J = 5.6 Hz), 127.7, 127.5, 126.9 (d, J = 3.6 Hz), 126.6, 126.4, 126.3, 124.8 (d, J = 1.7 Hz), 123.7, 123.1 (d, J = 4.9 Hz), 122.6 (d, J = 3.0 Hz), 120.2, 115.6 (d, J = 7.3 Hz), 115.5, 112.1 (d, J = 6.7 Hz). **^{31}P NMR** (203 MHz, CD_2Cl_2) δ 149.9. **HRMS (ESI +)** calculated for [$C_{69}H_{52}N_2O_4PSi_2$] $^{+\cdot}$ $[M+H]^{+\cdot}$ 1059.3198 m/z; found 1059.3184 m/z. **$[\alpha]^{26}_D$** −159.2 (c 0.43, acetone).

(*R*)-2.75c

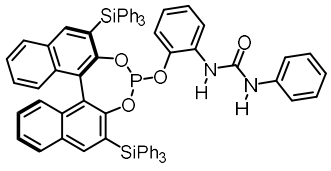

Prepared following general procedure **GP9**, using binaphthol **(*R*)-2.43** (200 mg, 0.250 mmol, 1.0 equiv) and hidroxyurea **U3** (114 mg, 0.500 mmol, 2.0 equiv). **(*R*)-2.75c** was obtained as a white solid (130 mg, 0.129 mmol, 49% yield, 97% pure according to ^{31}P NMR) after FCC (CyH:EtOAc dry load, silica, 90:10 to 80:20). **M.p.** 177 °C. **^{1}H NMR** (500 MHz, CD_2Cl_2) δ 8.06 (d, *J* = 4.6 Hz, 2H), 7.89 – 7.77 (m, 3H), 7.56 – 7.45 (m, 12H), 7.45 – 7.40 (m, 2H), 7.37 – 7.15 (m, 25H), 7.02 (d, *J* = 7.6 Hz, 2H), 6.97 – 6.85 (m, 2H), 6.52 (td, *J* = 7.9, 1.5 Hz, 1H), 5.92 (s, 1H), 5.82 (d, *J* = 8.0 Hz, 1H). **^{13}C NMR** (126 MHz, CD_2Cl_2) δ 152.5 (d, *J* = 5.3 Hz), 151.3, 141.2 (d, *J* = 9.9 Hz), 139.2 (d, *J* = 6.6 Hz), 138.1, 136.4, 136.3, 134.5 (d, *J* = 41.7 Hz), 134.0, 133.4, 131.1, 130.4, 130.3, 129.6 (d, *J* = 16.5 Hz), 128.9 (d, *J* = 2.1 Hz), 128.0, 127.7, 127.4, 127.3, 126.6 (d, *J* = 5.1 Hz), 125.4 (d, *J* = 11.4 Hz), 123.8, 123.4, 122.7, 121.6, 120.6, 119.6, 119.5. **^{31}P NMR** (162 MHz, $CDCl_3$) δ 147.5. **HRMS**

(ESI +) calculated for $[C_{69}H_{52}N_2O_4PSi_2]^{+\cdot}$ $[M+H]^{+\cdot}$ 1059.3198 m/z; found 1059.3178 m/z. $[\alpha]^{26}_D$ −66.5 (c 1.01, acetone).

(*R*)-2.75d

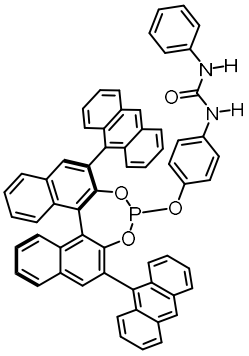

Prepared following general procedure **GP9**, using binaphthol **(*R*)-2.44** (300 mg, 0.470 mmol, 1.0 equiv) and hidroxyurea **U1** (241 mg, 0.940 mmol, 2.0 equiv). **(*R*)-2.75d** was obtained as a beige solid (348 mg, 0.349 mmol, 83% yield) after FCC (CyH:EtOAc dry load, silica, 90:10). **M.p.** 258 °C. **^{1}H NMR** (500 MHz, CD_2Cl_2) δ 8.54 (d, *J* = 13.9 Hz, 2H), 8.21 (s, 1H), 8.16 – 8.03 (m, 5H), 7.97 (dd, *J* = 15.4, 8.5 Hz, 2H), 7.88 – 7.78 (m, 4H), 7.77 – 7.66 (m, 3H), 7.66 – 7.50 (m, 3H), 7.50 – 7.19 (m, 11H), 7.15 – 6.99 (m, 2H), 6.44 (d, *J* = 8.5 Hz, 3H), 6.27 (brs, 1H), 4.75 (d, *J* = 8.4 Hz, 2H. **^{13}C NMR** (126 MHz, CD_2Cl_2) δ 153.1, 147.8, 147.2 (d, *J* = 10.9 Hz), 138.6, 133.8, 133.6 (d, *J* = 9.6 Hz), 133.2, 132.7, 132.1 (d, *J* = 4.9 Hz), 131.9 (d, *J* = 9.1 Hz), 131.8, 131.6, 131.5, 131.4, 131.3, 130.9 (d, *J* = 27.8 Hz), 129.4, 129.1, 128.9 (d, *J* = 5.6 Hz), 128.7 (d, *J* = 6.8 Hz), 128.4, 127.75, 127.68, 127.6, 127.2, 127.1, 127.04 126.9, 126.4 (d, *J* = 10.2 Hz), 126.1, 125.9, 125.7 (d, *J* = 7.3 Hz), 125.5 (d, *J* = 11.2 Hz), 125.4, 124.1, 124.0 (d, *J* = 2.8 Hz), 122.3, 120.8, 119.3 (d, *J* = 9.1 Hz). **^{31}P NMR** (203 MHz, CD_2Cl_2) δ 143.7. **HRMS (ESI +)** calculated for $[C_{61}H_{39}N_2NaO_4P]^{+\cdot}$ $[M+Na]^{+\cdot}$ 917.2540 m/z; found 917.2559 m/z. $[\alpha]^{26}_D$ −56.21 (c 0.49, acetone).

(*R*)-2.75e

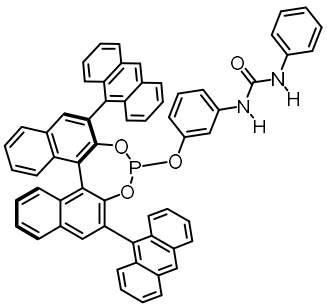

Prepared following general procedure **GP9**, using binaphthol **(*R*)-2.44** (150 mg, 0.235 mmol, 1.0 equiv) and hidroxyurea **U2** (107 mg, 0.470 mmol, 2.0 equiv). **(*R*)-2.75e** was obtained as a beige solid (175 mg, 0.196 mmol, 83% yield) after FCC (CyH:EtOAc dry load silica, 90:10). **M.p.** 254–256 °C. **^{1}H NMR** (500 MHz, $(CD_3)_2CO$) δ 8.61 (s, 1H), 8.49 (s, 1H), 8.24 – 8.09 (m, 5H), 8.06 – 7.92 (m, 3H), 7.78 (dt, *J* = 32.2, 10.5 Hz, 5H), 7.70 – 7.46 (m, 9H), 7.45 – 7.19 (m, 8H), 7.14 (t, *J* = 7.5 Hz, 1H), 7.05 – 6.96 (m, 2H), 6.84 – 6.77 (m, 1H), 6.28 (t, *J* = 8.1 Hz, 1H), 5.20 (s, 1H), 4.60 (dd, *J* = 8.1, 2.0 Hz, 1H). **^{13}C NMR** (126 MHz, $(CD_3)_2CO$) δ 152.6, 151.2 (d, *J* = 11.6 Hz), 148.3 (d, *J* = 5.3 Hz), 147.1, 140.9 (d, *J* = 14.7 Hz), 134.1 (d, *J* = 7.7 Hz), 133.9, 133.6, 132.7, 132.6, 132.42, 132.4, 132.3, 132.1, 132.1 (d, *J* = 12.5 Hz), 131.8, 131.7, 131.5, 131.1, 129.7, 129.7, 129.53, 129.48, 129.4, 129.2, 128.9, 128.3 (d, *J* = 8.9 Hz), 127.9 (d, *J* = 1.9 Hz), 127.8 (d, *J* = 11.4 Hz), 127.4, 127.3 (d, *J* = 3.8 Hz), 127.2, 127.0, 126.9, 124.5, 123.0, 119.5, 114.7, 112.3 (d, *J* = 11.4 Hz), 109.9 (d, *J* = 8.9 Hz). **^{31}P NMR** (203 MHz, $(CD_3)_2CO$) δ 145.2. **HRMS (ESI +)** calculated for $[C_{61}H_{39}N_2NaO_4P]^+$ $[M+Na]^+$ 917.2540 m/z; found 917.2545 m/z. $[\alpha]^{24.6}_D$ −12.6 (c 1.18, acetone).

(*R*)-2.75f

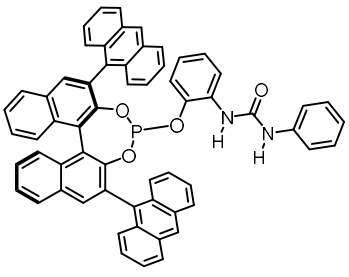

Prepared following general procedure **GP9**, using binaphthol **(*R*)-2.44** (100 mg, 0.157 mmol, 1.0 equiv) and hidroxyurea **U3** (71 mg, 0.313 mmol, 2.0 equiv). **(*R*)-2.75f** was obtained as a beige solid (71 mg, 0.079 mmol, 51% yield) after FCC (CyH:EtOAc dry load, silica, 90:10). **M.p.** 190–194 °C. **^{1}H NMR** (500 MHz, $(CD_3)_2CO$) δ 8.46 (d, *J* = 6.7 Hz, 2H), 8.25 – 8.18 (m, 3H), 8.16 (s, 1H), 8.13 (d, *J* = 8.5 Hz, 1H), 7.92 (dd, *J* = 8.4, 3.2 Hz, 2H), 7.83 (dd, *J* = 21.7, 8.7 Hz, 5H), 7.71 (td, *J* = 9.5, 7.7, 2.3 Hz, 2H), 7.68 – 7.55 (m, 5H), 7.55 –

7.47 (m, 2H), 7.46 – 7.37 (m, 2H), 7.35 – 7.20 (m, 7H), 7.02 – 6.94 (m, 3H), 6.56 – 6.49 (m, 1H), 6.34 (s, 1H), 5.84 (td, *J* = 7.8, 1.4 Hz, 1H), 4.58 (d, *J* = 8.0 Hz, 1H). **^{13}C NMR** (126 MHz, $(CD_3)_2CO$) δ 152.1, 148.1 (d, *J* = 4.9 Hz), 146.7 (d, *J* = 1.8 Hz), 140.7, 139.1 (d, *J* = 11.3 Hz), 134.5 (d, *J* = 6.0 Hz), 133.8, 133.6, 132.8, 132.7, 132.5, 132.4, 132.3, 132.26, 132.10, 132.04, 131.99, 131.84 (d, *J* = 3.4 Hz), 131.60, 131.42, 131.14, 130.95 (d, *J* = 2.9 Hz), 129.70 (d, *J* = 11.8 Hz), 129.5, 129.4, 129.3 (d, *J* = 3.6 Hz), 128.9, 128.5, 128.2, 128.0 (d, *J* = 7.0 Hz), 127.9 (d, *J* = 7.1 Hz), 127.5, 127.3, 127.24, 127.18, 126.9, 126.8 (d, *J* = 10.3 Hz), 126.53 (d, *J* = 5.8 Hz), 126.48, 126.1, 126.02, 125.98, 125.6, 124.5 (d, *J* = 2.3 Hz), 124.2, 122.9, 121.2, 119.5, 119.4, 117.6 (d, *J* = 16.7 Hz). **^{31}P NMR** (203 MHz, $(CD_3)_2CO$) δ 144.6. **HRMS (ESI +)** calculated for $[C_{61}H_{40}N_2O_4P]^{+\cdot}$ $[M+H]^{+\cdot}$ 895.2720 m/z; found 895.2708 m/z. **$[\alpha]^{26}_D$** +150.7 (c 0.45, acetone).

(R)-2.75g

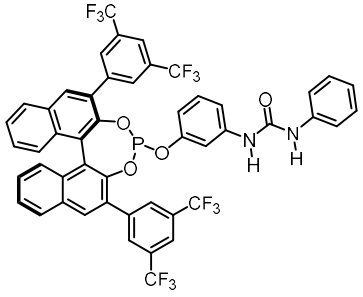

Prepared following general procedure **GP9**, using binaphthol **(*R*)-2.42** (100 mg, 0.141 mmol, 1.0 equiv) and hidroxyurea **U2** (64 mg, 0.248 mmol, 2.0 equiv). **(*R*)-2.75g** was obtained as a white solid (84 mg, 0.087 mmol, 62% yield) after FCC (CyH:EtOAc dry load silica, 90:10). **M.p.** 250 °C. **^{1}H NMR** (500 MHz CD_2Cl_2) δ 8.24 (d, *J* = 1.7 Hz, 2H), 8.17 (s, 1H), 8.12 (d, *J* = 1.7 Hz, 2H), 8.11 – 8.08 (m, 2H), 8.06 (d, *J* = 8.2 Hz, 1H), 7.92 (s, 1H), 7.83 (s, 1H), 7.62 – 7.54 (m, 2H), 7.51 – 7.47 (m, 1H), 7.46 – 7.38 (m, 3H), 7.35 – 7.28 (m, 4H), 7.13 – 7.06 (m, 1H), 7.00 (dd, *J* = 7.8, 2.4 Hz, 1H), 6.91 (td, *J* = 8.2, 1.8 Hz, 1H), 6.56 – 6.44 (m, 1H), 6.41 (d, *J* = 2.4 Hz, 1H), 6.37 (d, *J* = 25.7 Hz, 1H), 5.98 (dd, *J* = 8.1, 2.3 Hz, 1H). **^{13}C NMR** (126 MHz, CD_2Cl_2) δ 152.0, 151.6 (d, *J* = 9.7 Hz), 144.4 (d, *J* = 3.8 Hz), 143.7 (d, *J* = 2.8 Hz), 139.9, 139.7, 139.3, 138.0, 133.0, 132.6, 131.9, 131.8, 131.7, 131.6, 131.5, 131.44, 131.39, 131.33, 131.30, 131.2, 131.13, 131.07, 130.91, 130.87, 130.4 – 129.9 (m), 129.7, 129.1, 128.8 (d, *J* = 4.7 Hz), 127.4 (d, *J* = 13.5 Hz), 126.6 (d, *J* = 12.0 Hz), 126.3, 126.2, 125.6 (d, *J* = 5.5 Hz), 124.3 (d, *J* = 2.4 Hz), 124.0, 123.43 (q, *J* = 272.8), 123.39 (q, *J* = 272.8), 121.6 (hept, *J* = 7.7 Hz), 121.2 (hept, *J* = 7.7 Hz), 120.8. **^{31}P NMR** (203 MHz, CD_2Cl_2) δ 147.0. **^{19}F NMR** (471 MHz, CD_2Cl_2) δ -62.98 (6F), -63.03 (6F). **HRMS (ESI +)** calculated for $[C_{49}H_{27}F_{12}N_2NaO_4P]^{+\cdot}$ $[M+Na]^{+\cdot}$ 989.1409 m/z; found 989.1408 m/z. **$[\alpha]^{26}_D$** −100.5 (c 0.485, acetone).

(*R*)-2.75h

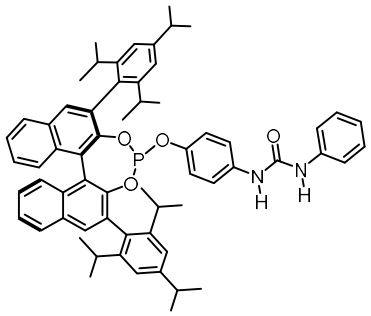

Prepared following general procedure **GP9**, using binaphthol (*R*)-**2.41** (250 mg, 0.361 mmol, 1.0 equiv) and hidroxyurea **U1** (165 mg, 0.723 mmol, 2.0 equiv). **(*R*)-2.75h** was obtained as a white solid (260 mg, 0.274 mmol, 76% yield) after FCC (CyH:EtOAc dry load silica, 90:10). **M.p.** 271 °C. **^{1}H NMR** (500 MHz, CD_2Cl_2) δ 7.96 (dd, *J* = 14.3, 8.2 Hz, 2H), 7.91 (s, 2H), 7.50 (dt, *J* = 14.1, 7.3 Hz, 2H), 7.42 (t, *J* = 8.8 Hz, 2H), 7.36 – 7.23 (m, 6H), 7.17 – 7.11 (m, 3H), 7.10 – 7.04 (m, 2H), 6.98 (d, *J* = 8.8 Hz, 2H), 6.65 (t, *J* = 28.9 Hz, 2H), 6.04 (d, *J* = 8.7 Hz, 2H), 3.04 – 2.92 (m, 2H), 2.92 – 2.83 (m, 1H), 2.84 – 2.74 (m, 1H), 2.73 – 2.64 (m, 1H), 2.59 (hept, *J* = 6.2 Hz, 1H), 1.34 (d, *J* = 6.9 Hz, 6H), 1.31 (d, *J* = 3.1 Hz, 3H), 1.29 (d, *J* = 3.1 Hz, 3H), 1.24 (d, *J* = 6.8 Hz, 3H), 1.21 (d, *J* = 6.8 Hz, 3H), 1.15 (d, *J* = 6.8 Hz, 6H), 1.07 (d, *J* = 6.8 Hz, 3H), 1.02 (d, *J* = 6.8 Hz, 3H), 0.95 (d, *J* = 6.8 Hz, 3H), 0.90 (d, *J* = 6.8 Hz, 3H). **^{13}C NMR** (126 MHz, CD_2Cl_2) δ 153.4, 149.2, 148.9, 148.2, 148.1, 148.0, 147.9 (d, *J* = 8.2 Hz), 147.8 (d, *J* = 11.5 Hz), 147.7, 145.6, 138.6, 134.8, 134.0, 133.0, 132.9, 132.7, 132.4, 132.1, 132.0, 131.7,

130.9, 129.5, 128.7 (d, *J* = 26.4 Hz), 127.7, 126.3 (d, *J* = 23.0 Hz), 126.0, 125.71 (d, *J* = 44.7 Hz), 124.3, 122.9 (d, *J* = 2.3 Hz), 122.3, 121.9 (d, *J* = 7.6 Hz), 121.5 (d, *J* = 19.7 Hz), 121.0, 120.8 (d, *J* = 14.5 Hz), 34.8 (d, *J* = 4.9 Hz), 31.7, 31.6, 31.2 (d, *J* = 4.6 Hz), 31.1, 27.3, 27.0, 26.3, 25.5, 25.1, 24.6, 24.4, 24.4, 23.5, 23.2, 23.0, 22.9. **^{31}P NMR** (203 MHz, CD_2Cl_2) δ 140.4. **HRMS (ESI +)** calculated for $[C_{63}H_{68}N_2O_4P]^{+\cdot}$ $[M+H]^{+\cdot}$ 947.4911 m/z; found 947.4913 m/z. **$[\alpha]^{26}_D$** +16.1 (c 0.86, acetone).

(*R*)-Au16

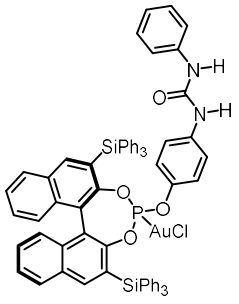

Prepared following general procedure **GP3**, using phosphite **(*R*)-2.75a** (77.5 mg, 0.073 mmol, 1.0 equiv). **(*R*)-Au16** was obtained as a white solid (89 mg, 0.069 mmol, 94% yield) after FCC (CyH:EtOAc dry load silica, 100:0 to 80:20). **M.p.** 200–203 ºC. **^{1}H NMR** (500 MHz, CD_2Cl_2) δ 8.21 (s, 1H), 8.13 (s, 1H), 7.87 (d, *J* = 8.2 Hz, 1H), 7.84 (d, *J* = 8.2 Hz, 1H), 7.62 – 7.57 (m, 6H), 7.56 – 7.46 (m, 8H), 7.35 (t, *J* = 7.5 Hz, 13H), 7.33 – 7.20 (m, 17H), 7.04 (t, *J* = 7.3 Hz, 1H), 6.94 (d, *J* = 8.9 Hz, 4H), 5.90 (d, *J* = 8.7 Hz, 2H). **^{13}C NMR** (126 MHz, CD_2Cl_2) δ 152.7, 151.0 (d, *J* = 13.3 Hz), 149.8 (d, *J* = 7.6 Hz), 144.2, 142.3 (d, *J* = 40.1 Hz), 138.3, 136.6, 136.4, 136.1, 134.2 (d, *J* = 29.9 Hz), 133.5, 133.3, 131.4, 131.1, 130.0 (d, *J* = 2.0 Hz), 129.1, 128.8 (d, *J* = 10.4 Hz), 128.3, 128.1, 127.9 (d, *J* = 8.2 Hz), 126.7 (d, *J* = 30.5 Hz), 126.1 (d, *J* = 11.7 Hz), 125.7, 123.8, 122.5, 122.0, 121.3 (d, *J* = 5.3 Hz), 120.6, 120.5. **^{31}P NMR** (202 MHz, CD_2Cl_2) δ 123.7. **HRMS (ESI +)** calculated for $[C_{69}H_{51}AuClN_2NaO_4PSi_2]^{+\cdot}$ $[M+Na]^{+\cdot}$ 1313.2371 m/z; found 1313.2377 m/z. **$[\alpha]^{24.6}_D$** −55.7 (c 1.22, $CHCl_3$).

(*R*)-Au17

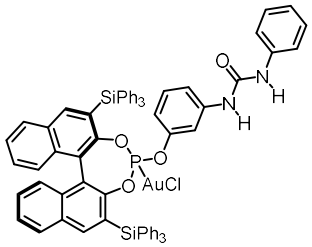

Prepared following general procedure **GP3**, using phosphite (*R*)-**2.75b** (112 mg, 0.106 mmol, 1.0 equiv). (*R*)-**Au17** was obtained as a white solid (132 mg, 0.102 mmol, 97% yield) after FCC (CyH:EtOAc dry load, silica, 100:0 to 80:20). **M.p.** 208–211 °C. **^{1}H NMR** (500 MHz, CD_2Cl_2) δ 8.20 (s, 1H), 8.13 (s, 1H), 7.90 – 7.80 (m, 2H), 7.61 – 7.55 (m, 6H), 7.55 – 7.48 (m, 8H), 7.42 – 7.22 (m, 28H), 7.09 (tt, *J* = 7.3, 1.2 Hz, 1H), 6.83 (t, *J* = 8.2 Hz, 1H), 6.69 (s, 1H), 6.31 (s, 1H), 5.99 – 5.90 (m, 1H), 5.81 – 5.70 (m, 1H). **^{13}C NMR** (126 MHz, CD_2Cl_2) δ 152.4, 151.5 (d, *J* = 13.0 Hz), 150.1 (d, *J* = 7.3 Hz), 149.3 (d, *J* = 5.0 Hz), 142.7 (d, *J* = 38.9 Hz), 139.9, 138.6, 137.0 (d, *J* = 17.0 Hz), 134.6 (d, *J* = 30.2 Hz), 133.8 (d, *J* = 14.1 Hz), 131.8, 131.47, 130.3, 130.2, 129.6, 129.3 (d, *J* = 8.4 Hz), 128.6 (d, *J* = 22.1 Hz), 128.4, 127.1 (d, *J* = 17.6 Hz), 126.5 (d, *J* = 18.0 Hz), 126.3, 126.1 (d, *J* = 3.5 Hz), 124.3, 123.0, 122.4, 120.8, 117.2, 115.7 (d, *J* = 5.7 Hz), 112.2 (d, *J* = 5.6 Hz). **^{31}P NMR** (202 MHz, CD_2Cl_2) δ 123.0. **HRMS (ESI +)** calculated for $[C_{69}H_{51}AuClN_2NaO_4PSi_2]^{+\cdot}$ $[M+Na]^{+\cdot}$ 1313.2371 m/z; found 1313.2371 m/z. **$[\alpha]^{24.6}_D$** −65.7 (c 1.0, $CHCl_3$).

(*R*)-Au18

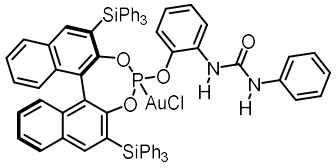

Prepared following general procedure **GP3**, using phosphite (*R*)-**2.75c** (115 mg, 0.109 mmol, 1.0 equiv). (*R*)-**Au18** was obtained as a white solid (139 mg, 0.103 mmol, 95% yield) after FCC (CyH:EtOAc dry load, silica, 100:0 to 90:10). **M.p.** 189–192 °C. **^{1}H NMR** (500 MHz, $CDCl_3$) δ 8.23 (d, *J* = 8.2 Hz, 1H), 8.18 (d, *J* = 14.6 Hz, 2H), 7.90 (dd, *J* = 11.1, 8.5 Hz, 2H), 7.55 (dd, *J* = 12.5, 4.9 Hz, 8H), 7.47 (d, *J* = 7.0 Hz, 7H), 7.39 (dq, *J* = 13.5, 7.8, 7.4 Hz, 7H), 7.30 (t, *J* = 7.3 Hz, 10H), 7.22 (q, *J* = 7.6 Hz, 8H),

7.03 (t, *J* = 7.9 Hz, 1H), 6.97 (t, *J* = 7.3 Hz, 1H), 6.42 – 6.34 (m, 2H), 5.82 (d, *J* = 8.2 Hz, 1H), 5.78 (s, 1H). **^{13}C NMR** (126 MHz, $CDCl_3$) δ 151.6, 150.6 (d, *J* = 13.2 Hz), 149.6 (d, *J* = 7.3 Hz), 142.6, 142.3, 138.0, 137.5 (d, *J* = 10.4 Hz), 136.7, 136.5, 134.0 (d, *J* = 55.2 Hz), 133.2 (d, *J* = 26.3 Hz), 131.4 (d, *J* = 49.6 Hz), 130.3, 130.1 (d, *J* = 2.2 Hz), 129.3, 129.2, 128.4, 128.3, 128.2, 126.8 (d, *J* = 28.0 Hz), 126.6, 126.5, 126.2 (d, *J* = 3.1 Hz), 126.1, 124.1, 122.7 (d, *J* = 2.9 Hz), 122.3 (d, *J* = 3.2 Hz), 122.0, 120.9, 120.3 (d, *J* = 3.9 Hz), 120.2. **^{31}P NMR** (203 MHz, $CDCl_3$) δ 120.8. **HRMS (ESI +)** calculated for $[C_{69}H_{51}AuClN_2NaO_4PSi_2]^{+\cdot}$ $[M+Na]^{+\cdot}$ 1313.2371 m/z; found 1313.2346 m/z. **[α]$^{24.6}_D$** −108 (c 2.09, $CHCl_3$).

(*R*)-Au19

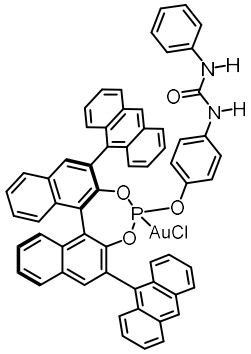

Prepared following general procedure **GP3**, using phosphite (*R*)-**2.75d** (348 mg, 0.389 mmol, 1.0 equiv). (*R*)-**Au19** was obtained as a military green solid (395 mg, 0.350 mmol, 90% yield) after FCC (CyH:EtOAc dry load, silica, 100:0 to 80:20). **M.p.** 253–255 °C. **^{1}H NMR** (500 MHz, CD_2Cl_2) δ 8.58 (s, 1H), 8.45 (s, 1H), 8.34 (s, 1H), 8.20 – 8.13 (m, 2H), 8.08 (d, *J* = 8.3 Hz, 2H), 8.06 – 7.97 (m, 2H), 7.97 – 7.88 (m, 2H), 7.80 (t, *J* = 9.4 Hz, 2H), 7.75 – 7.70 (m, 3H), 7.71 – 7.64 (m, 2H), 7.64 – 7.52 (m, 2H), 7.49 – 7.34 (m, 6H), 7.30 – 7.18 (m, 5H), 7.04 – 6.97 (m, 2H), 6.64 – 6.55 (m, 1H), 6.53 – 6.41 (m, 3H), 4.81 (d, *J* = 8.7 Hz, 2H). **^{13}C NMR** (126 MHz, CD_2Cl_2) δ 152.4, 146.2 (d, *J* = 13.4 Hz), 144.0 (d, *J* = 7.0 Hz), 143.7, 138.2, 135.8, 135.0, 134.5, 132.9, 132.75(d, *J* = 31.5 Hz), 132.6, 132.2, 131.9, 131.7, 131.5, 131.2 (d, *J* = 8.6 Hz), 130.9, 130.8, 130.5 (d, *J* = 5.9 Hz), 130.3, 130.0, 129.8 (d, *J* = 2.8 Hz), 129.6, 129.0, 128.9, 128.7, 128.6 (d, *J* = 7.4 Hz), 128.3, 128.1 (d, *J* = 8.8 Hz), 127.5, 127.4, 127.4, 126.9, 126.8, 126.7, 126.3, 126.2, 126.0, 125.9, 125.6, 125.3, 125.2, 125.1, 124.1, 123.7, 122.8, 120.6, 120.4, 119.6 (d, *J* = 6.9 Hz). **^{31}P NMR** (202 MHz, CD_2Cl_2) δ 125.4. **HRMS (ESI +)** calculated for $[C_{61}H_{39}AuClN_2NaO_4P]^{+\cdot}$ $[M+Na]^{+\cdot}$ 1149.1894 m/z; found 1149.1885 m/z. **[α]$^{24.6}_D$** −36.5 (c 1.0, $CHCl_3$).

(*R*)-Au20

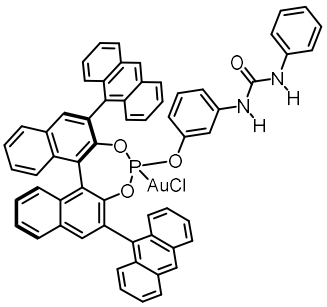

Prepared following general procedure **GP3**, using phosphite **(*R*)-2.75e** (155.7 mg, 0.174 mmol, 1.0 equiv). **(*R*)-Au20** was obtained as a military green solid (182 mg, 0.161 mmol, 93% yield) after FCC (CyH:EtOAc dry load, silica, 100:0 to 80:20). **M.p.** 316 °C. **^{1}H NMR** (500 MHz, CD_2Cl_2) δ 8.55 (d, *J* = 2.6 Hz, 1H), 8.48 (d, *J* = 3.0 Hz, 1H), 8.31 (s, 1H), 8.19 – 8.13 (m, 2H), 8.12 – 7.97 (m, 4H), 7.92 (d, *J* = 8.8 Hz, 1H), 7.87 – 7.76 (m, 3H), 7.76 – 7.65 (m, 4H), 7.65 – 7.53 (m, 3H), 7.52 – 7.37 (m, 6H), 7.36 – 7.24 (m, 4H), 7.18 – 7.09 (m, 2H), 7.02 – 6.96 (m, 1H), 6.96 – 6.86 (m, 1H), 6.46 – 6.35 (m, 2H), 5.95 (s, 1H), 4.76 – 4.61 (m, 2H). **^{13}C NMR** (126 MHz, CD_2Cl_2) δ 152.4, 148.9, 146.7 (d, *J* = 13.5 Hz), 144.6 (d, *J* = 6.8 Hz), 139.6, 138.7, 135.6, 135.2, 133.5 (d, *J* = 1.3 Hz), 133.2 (d, *J* = 1.6 Hz), 132.8, 132.6, 132.4, 132.1, 131.9, 131.7, 131.5, 131.5, 131.1, 131.0, 130.8, 130.7, 130.6 (d, *J* = 2.4 Hz), 130.3, 130.0, 129.81 129.4, 129.3 (d, *J* = 5.5 Hz), 129.2, 129.1, 129.0, 128.8 (d, *J* = 9.8 Hz), 128.7, 128.1, 128.04, 128.02, 127.99, 127.5 (d, *J* = 23.7 Hz), 127.2, 127.0, 126.9, 126.7, 126.6, 126.5, 126.4, 126.0, 125.8, 125.6, 124.8, 124.6, 123.5 (d, *J* = 2.9 Hz), 121.55 – 121.25 (m), 117.7, 114.2, 111.3 (d, *J* = 7.8 Hz). **^{31}P NMR** (202 MHz, CD_2Cl_2) δ 125.5. **HRMS (ESI +)** calculated for $[C_{61}H_{40}AuClN_2O_4P]^{+\cdot}$ $[M+H]^{+\cdot}$1127.2074 m/z; found 1127.2029 m/z. **[α]$^{26}_D$** −37.4 (c 0.32, acetone).

(*R*)-Au21

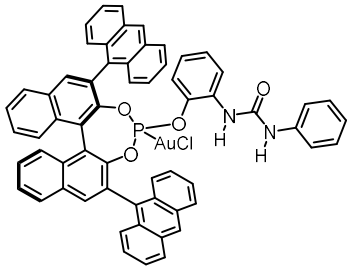

Prepared following general procedure **GP3**, using phosphite (*R*)-**2.75f** (53 mg, 0.059 mmol, 1.0 equiv). (*R*)-**Au21** was obtained as a white solid (66 mg, 0.059 mmol, 99% yield) after FCC (CyH:EtOAc dry load, silica, 100:0 to 80:20). **M.p.** 240–242 °C. **^{1}H NMR** (500 MHz, $CDCl_3$) δ 8.50 (s, 1H), 8.38 (s, 1H), 8.33 (s, 1H), 8.14 (d, *J* = 8.3 Hz, 1H), 8.11 – 8.06 (m, 2H), 8.04 (d, *J* = 8.2 Hz, 2H), 8.00 – 7.97 (m, 1H), 7.92 (d, *J* = 8.4 Hz, 1H), 7.84 – 7.58 (m, 10H), 7.57 – 7.52 (m, 1H), 7.49 – 7.27 (m, 11H), 7.12 (t, *J* = 7.6 Hz, 1H), 7.07 – 7.00 (m, 1H), 6.93 – 6.81 (m, 1H), 6.70 (t, *J* = 7.9 Hz, 1H), 5.98 (td, *J* = 7.8, 1.6 Hz, 1H), 5.63 (s, 1H), 4.98 (d, *J* = 8.2 Hz, 1H), 4.77 (s, 1H). **^{13}C NMR** (126 MHz, $CDCl_3$) δ 150.8, 146.4 (d, *J* = 13.7 Hz), 143.8 (d, *J* = 6.6 Hz), 138.2, 135.2, 134.9, 132.9, 132.7, 132.4, 132.0, 131.8, 131.5, 131.3, 131.1, 130.9, 130.7, 130.55 – 130.33 (m), 130.2 (d, *J* = 2.8 Hz), 130.0, 129.6 (d, *J* = 5.4 Hz), 129.3, 129.2, 129.0 (d, *J* = 3.2 Hz), 128.9 (d, *J* = 2.4 Hz), 128.8 (d, *J* = 4.1 Hz), 128.3, 127.9, 127.8, 127.7, 127.6, 127.3, 127.0, 126.9, 126.3, 126.3, 126.1, 126.05, 125.99, 125.9, 125.7, 125.6, 124.9, 124.3 (d, *J* = 3.2 Hz), 123.6, 122.9 (d, *J* = 3.0 Hz), 122.1, 120.2, 120.0, 118.8, 118.7. **^{31}P NMR** (202 MHz, $CDCl_3$) δ 125.80. **HRMS (ESI +)** calculated for $[C_{61}H_{40}AuClN_2O_4P]^{+\cdot}$ [M+H] $^{+\cdot}$ 1127.2074 m/z; found 1127.2055 m/z. **[α]$^{24.6}_D$** 126.9 (c 0.39, $CHCl_3$).

(*R*)-Au22

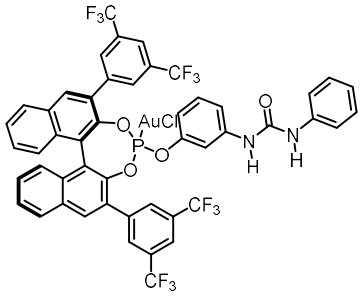

Prepared following general procedure **GP3**, using phosphite **(*R*)-2.75g** (73.1 mg, 0.076 mmol, 1.0 equiv). **(*R*)-Au22** was obtained as a white solid (82 mg, 0.068 mmol, 90% yield) after FCC (CyH:EtOAc dry load, silica, 100:0 to 80:20). **M.p.** 187–189 °C. **^{1}H NMR** (300 MHz, $CDCl_3$) δ 8.23 (s, 1H), 8.18 (s, 2H), 8.16 – 8.08 (m, 2H), 8.07 – 8.00 (m, 3H), 7.98 – 7.85 (m, 2H), 7.74 – 7.58 (m, 2H), 7.57 – 7.47 (m, 4H), 7.37 – 7.27 (m, 4H), 7.17 – 7.02 (m, 2H), 6.93 (t, *J* = 8.2 Hz, 1H), 6.66 – 6.43 (m, 3H), 6.05 – 5.96 (m, 1H). **^{13}C NMR** (126 MHz, $CDCl_3$) δ 152.6, 149.2, 143.5 (d, *J* = 13.2 Hz), 141.3 (d, *J* = 6.7 Hz), 140.7, 138.8, 138.0, 137.7, 132.7 (d, *J* = 11.3 Hz), 132.5, 132.4, 132.2 (d, *J* = 6.8 Hz), 131.9 (d, *J* = 18.5 Hz), 131.1 (d, *J* = 2.5 Hz), 130.6, 130.3, 130.0, 129.3, 129.1, 128.4 (d, *J* = 13.8 Hz), 127.7, 127.5, 127.1 (d, *J* = 6.3 Hz), 125.3 (d, *J* = 3.3 Hz), 124.4, 123.4 (d, *J* = 2.8 Hz), 122.6 – 122.4 (m), 122.4 – 122.2 (m), 121.2, 117.6, 113.3 (d, *J* = 7.3 Hz), 110.8 (d, *J* = 6.6 Hz). **^{31}P NMR** (202 MHz, $CDCl_3$) δ 125.3. **^{19}F NMR** (471 MHz, $CDCl_3$) δ -62.5, -62.6. **HRMS (ESI +)** calculated for $[C_{49}H_{27}AuClF_{12}N_2NaO_4P]^{+\cdot}$ [M+Na] $^{+\cdot}$1221.0763m/z; found 1221.0756 m/z. **[α]$^{24.6}_D$** −18.7 (c 1.95, acetone).

(*R*)-Au23

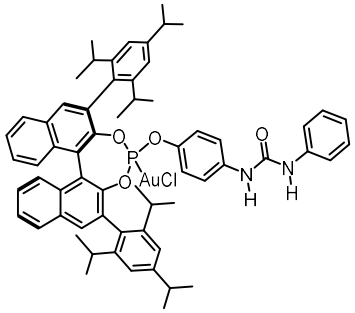

Prepared following general procedure GP2, using phosphite **(*R*)-2.75h** (240 mg, 0.253 mmol, 1.0 equiv). **(*R*)-Au23** was obtained as a white solid (253 mg, 0.214 mmol, 85% yield) after FCC (CyH:EtOAc dry load, silica, 100:0 to 80:20). **M.p.** 250–208 °C. **^{1}H NMR** (500 MHz, CD_2Cl_2) δ 8.04 (s, 2H), 8.03 (d, *J* = 8.2 Hz, 2H), 8.01 – 7.94 (m, 2H), 7.59 (ddd, *J* = 8.1, 5.6, 2.4 Hz, 1H), 7.57 – 7.51 (m, 1H), 7.41 – 7.34 (m, 2H), 7.36 – 7.26 (m, 5H), 7.20 (dd, *J* = 7.6, 1.8 Hz, 2H), 7.16 – 7.10 (m, 2H), 7.13 – 7.04 (m, 5H), 6.59 (s, 2H), 6.15 – 6.07 (m, 2H), 3.10 (hept, *J* = 6.8 Hz, 1H), 2.99 (dh, *J* = 21.0, 6.9 Hz, 2H), 2.88 (h, *J* = 6.8 Hz, 1H), 2.67 – 2.54 (m, *J* = 6.7 Hz, 2H),

1.38 – 1.30 (m, 18H), 1.30 (d, *J* = 7.0 Hz, 11H), 1.20 (d, *J* = 6.7 Hz, 3H), 1.11 (d, *J* = 6.8 Hz, 3H), 1.06 (d, *J* = 6.8 Hz, 3H), 0.91 (d, *J* = 6.8 Hz, 3H), 0.78 (d, *J* = 6.8 Hz, 3H). **^{13}C NMR** (126 MHz, CD_2Cl_2) δ 152.73, 149.73 (d, *J* = 6.1 Hz), 148.27 (d, *J* = 13.7 Hz), 147.91 (d, *J* = 34.8 Hz), 146.37 (d, *J* = 14.2 Hz), 145.46, 138.51, 137.09, 133.65, 133.54, 133.00, 132.61, 131.94, 131.89 (d, *J* = 3.5 Hz), 131.77, 131.15, 130.49, 129.54, 128.82, 127.88, 127.41, 127.14, 126.95, 126.91, 126.55, 124.40, 123.82 (d, *J* = 3.7 Hz), 122.29, 122.16 (d, *J* = 6.6 Hz), 122.01, 121.61, 121.54, 121.19, 121.14, 34.76 (d, *J* = 2.3 Hz), 31.97, 31.55 (d, *J* = 5.2 Hz), 31.05, 27.29 (d, *J* = 9.5 Hz), 26.84, 26.14, 25.54, 25.29, 24.59, 24.33, 24.28, 24.20, 23.75, 23.13, 22.87. **^{31}P NMR** (202 MHz, CD_2Cl_2) δ 124.22. **HRMS (ESI +)** calculated for $[C_{63}H_{67}AuClN_2NaO_4P]^{+\cdot}$ [M+Na] $^{+\cdot}$ 1201.4085 m/z; found 1201.4091 m/z. $[\alpha]^{24.6}_D$ 106 (c 0.81, $CHCl_3$). **$[\alpha]^{24.6}_D$** +106.2 (c 0.84, $CHCl_3$).

Synthesis of 1,6-enynes bearing a terminal alkyne

Enynes **2.77a**–**o** were prepared from the corresponding allyl bromides and commercially available propargyl malonate. Allyl bromides **2.98** were not stable and were prepared from the corresponding allyl alcohols and immediately used or stored in the freezer for a short period of time.

General procedure GP10: 1,6-enyne preparation

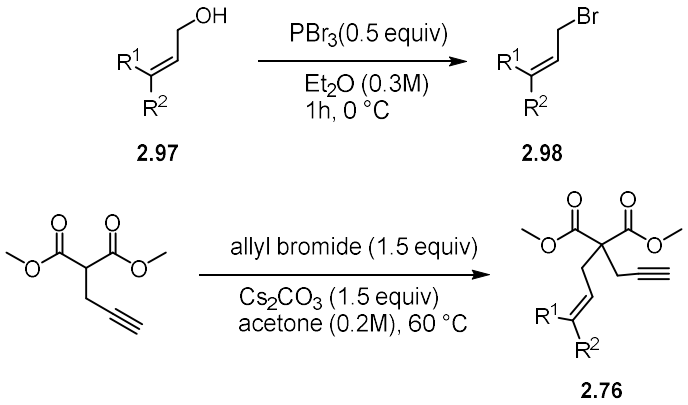

*Allyl bromide **2.98** preparation:* To a flame-dried flask charged with a stirring bar and the corresponding allyl alcohol **2.97** was added anhydrous Et_2O (0.3 M). The solution was cooled to 0 °C with an ice/water bath and PBr_3 (0.5 equiv) was added dropwise. The mixture was allowed to warm up to room temperature and was stirred until starting material consumption (monitored by GC-MS and TLC). The reaction was then quenched by dropwise addition of H_2O, the AP is then extracted with Et_2O (2x). The combined organic layers are washed with brine, dried over Na_2SO_4 or $MgSO_4$, filtered and evaporated. The crude was used as such in the next step without further purification.

Alkylation propargyl malonate: To a flask equipped with a stirring bar and charged with Cs_2CO_3 (1.5 equiv) was added HPLC-grade acetone. Then propargyl malonate was added dropwise (1 equiv) and the system was stirred for 5 min. Finally, all bromide (1.5 equiv) was added as a solution in acetone (0.2 M final concentration). The system was heated to reflux and left stirring until starting material consumption (monitored by GC-MS and TLC). The reaction was filtered, and the solvent evaporated under vacuum. The crude was purified by FCC (CyH:EtOAc, solvent mixtures) affording the corresponding 1,6-enyne.

Dimethyl 2-cinnamyl-2-(prop-2-yn-1-yl)malonate (2.76a)

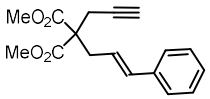

Prepared following general procedure **GP10**, using (*E*)-cinnamyl alcohol (2.69 g, 20.8 mmol). Cinnamyl bromide was obtained as a colorless oil (3.30 g, 16.8 mmol, 83%) and was used in the following step with propargyl malonate (1.70 mL, 11.2 mmol, 1.0 equiv). Enyne **2.76a** was obtained as a white solid (2.90 g, 10.1 mmol, 91% yield) after FCC (CyH:EtOAc dry load, silica, 100:0 to 90:10). Spectroscopic data matched those reported in the literature.[96] **^{1}H NMR** (300 MHz, $CDCl_3$) δ 7.37 – 7.26 (m, 4H), 7.25 – 7.18 (m, 1H), 6.52 (dt, *J* = 15.6, 1.3 Hz, 1H), 6.00 (dt, *J* = 15.5, 7.7 Hz, 1H), 3.76 (s, 6H), 2.97 (dd, *J* = 7.7, 1.3 Hz, 2H), 2.85 (d, *J* = 2.7 Hz, 2H), 2.06 (t, *J* = 5.4 Hz, 1H). **^{13}C NMR** (75 MHz, $CDCl_3$) δ 170.3, 137.1, 134.8, 128.7, 127.7, 126.4, 123.2, 79.0, 71.8, 57.4, 53.0, 36.0, 23.1.

Diisopropyl (*E*)-2-cinnamyl-2-(prop-2-yn-1-yl)malonate (2.76b)

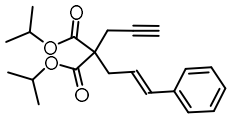

Prepared following a modified literature procedure.[96] Under argon, to a solution of **2.76a** (400 mg, 1.40 mmol) in *i*-PrOH (2.3 mL) was added, at room temperature, Ti(O*i*-Pr)$_4$ (0.83 mL, 2.80 mmol, 2.0 equiv). The mixture was warmed to 80 °C and stirred overnight. After 14 h the reaction was diluted with water (5 mL) and Et_2O (10 mL). The aqueous phase was extracted with Et_2O (3 x 10 mL). The combined organic layers were washed with brine, dried over Na_2SO_4, filtered and evaporated. The crude was purified by FCC (CyH:EtOAc, 100:0 to 98:2) enyne **2.76b** as a colorless oil (306 mg, 0.894 mmol, 64% yield). Spectroscopic data matched those reported in the literature. [97] **^{1}H NMR** (300 MHz, $CDCl_3$) δ 7.38 – 7.25 (m, 4H), 7.27 – 7.16 (m, 2H), 6.51 (d, *J* = 15.7 Hz, 1H), 6.03 (dt, *J* = 15.5, 7.7 Hz, 1H), 5.09 (hept, *J* = 6.3 Hz, 2H), 2.94 (dd, *J* = 7.6, 1.2 Hz, 2H), 2.82 (d, *J* = 2.7 Hz, 2H), 2.04 (t, *J* = 2.7 Hz, 1H), 1.25 (d, *J* = 2.5 Hz, 6H), 1.23 (d, *J* = 2.5 Hz, 6H). **^{13}C NMR** (75 MHz, $CDCl_3$) δ 169.4, 137.2, 134.6, 128.6, 127.6, 126.4, 123.5, 79.2, 71.6, 69.3, 57.0, 35.8, 22.9, 21.8, 21.7.

(*E*)-2-cinnamyl-2-(prop-2-yn-1-yl)propane-1,3-diol (2.96)

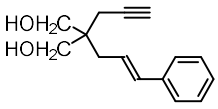

Under argon, to a flame dried 50 mL two-necked flask equipped with a stirring bar and charged with $LiAlH_4$ (159 mg, 4.19 mmol, 4.0 equiv) was added anhydrous Et_2O (15 mL). The suspension was cooled with an ice/water bath and a solution of **2.76a** (300 mg, 1.05 mmol) in Et_2O (6 mL) was added. The mixture was allowed to warm up to room temperature and was left stirring until starting material consumption. After 4 h the reaction was quenched: H_2O (0.15 mL) was added dropwise, then a 15 w% aqueous solution of NaOH (0.15 mL) and H_2O (0.15 mL). The mixture was stirred for 15 min and finally $MgSO_4$ was added allowing it to stir for another 15min. The solution was filtered through a celite pad and washed with Et_2O. The crude was purified by FCC (CyH:EtOAc, 90:10 to 70:30) enyne **2.96** as a white solid (190 mg, 0.825 mmol, 79% yield). Spectroscopic data matched those reported in the literature.[97] **^{1}H NMR** (500 MHz, $CDCl_3$) δ 7.38 – 7.33 (m, 2H), 7.33 – 7.29 (m, 2H), 7.25 – 7.18 (m, 1H), 6.56 – 6.44 (m, 1H), 6.23 (dt, *J* = 15.6, 7.7 Hz, 1H), 3.79 – 3.54 (m, 4H), 2.35 – 2.30 (m, 4H), 2.19 (d, *J* = 16.3 Hz, 2H), 2.07 (t, *J* = 2.7 Hz, 1H). **^{13}C NMR** (126 MHz, $CDCl_3$) δ 137.4, 133.78 128.7, 127.5, 126.3, 125.0, 81.1, 71.2, 67.7, 42.9, 35.4, 21.8.

96. Hungerbühler, E.; Naef, R.; Schnurrenberger, P.; Weidmann, B.; Züger, M.; Seebach, D. *Synthesis,* **1982**, 2, 138 – 141
97. Toullec, P. Y.; Chao, C.-M.; Chen, Q.; Gladiali, S.; Genet, J.-P.; Michelet, V. *Adv. Synth. Catal.* **2008**, 350, 2401−2408

(*E*)-(4,4-bis(methoxymethyl)hept-1-en-6-yn-1-yl)benzene (2.76c)

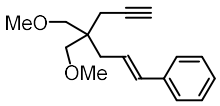

Under argon, to a flame dried 50 mL two-necked flask equipped with a stirring bar and charged with NaH (96.4 mg, 2.41 mmol, 3 equiv) was added anhydrous THF (6 mL). The mixture was cooled to 0 ºC and diol **2.96** (185 mg, 0.803 mmol, 1 equiv) was added dropwise as a solution in THF (2 mL). After 15 min iodomethane (150 µL, 2.41 mmol, 3 equiv) was slowly added at the same temperature. Reaction was allowed to warm up to room temperature and was left stirring overnight. After 16 h, a saturated NH_4Cl aqueous solution was added (10 mL). The aqueous phase was then extracted with Et_2O (3 x 15 mL). The combined organic layers were washed with brine, dried over Na_2SO_4, filtered and evaporated. The crude was purified by FCC (CyH:EtOAc, 99:1) enyne **2.76c** as a colorless oil (202 mg, 0.803 mmol, 98% yield). Spectroscopic data matched those reported in the literature.[98] **^{1}H NMR** (500 MHz, $CDCl_3$) δ 7.38 – 7.35 (m, 2H), 7.33 – 7.29 (m, 2H), 7.24 – 7.19 (m, 1H), 6.46 (d, *J* = 15.8 Hz, 1H), 6.22 (dt, *J* = 15.6, 7.7 Hz, 1H), 3.36 (s, 6H), 3.33 – 3.27 (m, 4H), 2.34 (dd, *J* = 7.7, 1.3 Hz, 2H), 2.27 (d, *J* = 2.7 Hz, 2H), 2.02 (t, *J* = 2.7 Hz, 1H). **^{13}C NMR** (126 MHz, $CDCl_3$) δ 137.9, 133.3, 128.6, 127.2, 126.2, 125.9, 81.4, 74.5, 70.4, 59.5, 42.6, 35.5, 22.4. **HRMS (ESI +)** calculated for $[C_{17}H_{22}NaO_2]^{+\cdot}$ $[M+Na]^{+\cdot}$ 281.1512 m/z; found 281.1523 m/z.

***N*-(*E*)-cinnamyl-4-methyl-*N*-(prop-2-yn-1-yl)benzenesulfonamide (2.76d)**

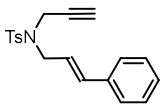

Following a modified literature procedure.[99] To a flame-dried flask equipped with a stirring bar were sequentially added triphenyl phosphine (1.95 g, 7.45 mmol, 2.0 equiv), 4-methyl-N- (prop-2-yn-1-yl)benzenesulfonamide (936 mg, 4.47 mmol, 1.2 equiv), anhydrous THF (12 mL) and cinnamyl alcohol (0.48 mL, 3.37 mmol, 1.0 equiv). The mixture was cooled to 0 °C and diethyl azodicarboxylate (2.9 mL, 7.45 mmol, 2.0 equiv) was added dropwise. Then the reaction was stirred at room temperature for 14h. After complete conversion of the starting material, the solvent was removed under reduced pressure and the residue was redissolved in ethyl acetate, washed with brine, dried over MgSO4, filtered and evaporated under vacuum. The crude was purified by FCC (CyH:EtOAc, 9:1) and the product was obtained as an off-white solid. The columned fraction was then recrystallized from refluxing CyH obtaining enyne **2.76d** as a white solid (762 mg, 2.34 mmol, 63% yield). Spectroscopic data matched those reported in the literature.[99] **^{1}H NMR** (300 MHz, $CDCl_3$) δ 7.83 – 7.72 (m, 2H), 7.37 – 7.22 (m, 7H), 6.58 (d, *J* = 15.8 Hz, 1H), 6.08 (dt, *J* = 15.8, 6.9 Hz, 1H), 4.13 (d, *J* = 2.4 Hz, 2H), 4.00 (dd, *J* = 6.9, 1.1 Hz, 2H), 2.44 (s, 3H), 2.05 (t, *J* = 2.5 Hz, 1H). **^{13}C NMR** (75 MHz, $CDCl_3$) δ 143.6, 136.1, 134.9, 129.5, 128.6, 128.1, 127.8, 126.6, 122.9, 73.8, 48.6, 35.9, 21.6.

Dimethyl (*E*)-2-(prop-2-yn-1-yl)-2-(3-(4-(trifluoromethyl)phenyl)allyl)malonate (2.76e)

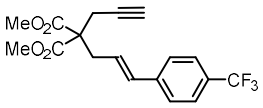

Prepared following general procedure **GP10**, using (*E*)-3-(4-(trifluoromethyl)phenyl)prop-2-en-1-ol (360 mg, 1.73 mmol). Allyl bromide was obtained as a colorless oil (350 mg, 1.32 mmol, 74%) and was used in the following step with propargyl malonate (134 µL, 0.88 mmol, 1.0 equiv). Enyne **2.76e** was obtained as a colorless oil (280 mg, 0.79 mmol, 90% yield) after FCC (CyH:EtOAc dry load, silica, 100:0 to 90:10). Spectroscopic data matched those reported in the literature.[98] **^{1}H NMR** (300 MHz, $CDCl_3$) δ 7.54 (d, *J* = 8.2 Hz, 2H), 7.42 (d, *J* = 8.2 Hz, 2H), 6.55 (d, *J* = 15.7 Hz, 1H), 6.13 (dt, *J* = 15.6, 7.6 Hz, 1H), 3.77 (s, 6H), 2.99 (dd, *J* = 7.6, 1.3 Hz, 2H), 2.85 (d, *J* = 2.7 Hz, 2H), 2.07 (t, *J* = 2.7 Hz, 1H). **^{13}C NMR** (75 MHz, $CDCl_3$) δ 170.2, 140.5, 133.5, 126.6,

98. Wang, G.; Wang, Y.; Li, Z.; Li, H.; Yu, M.; Pang, M.; Zhao, X. *Org. Lett.* **2022**, 24, 9425–9430.
99. Zhao, S.; Zang, Z.-L.; Li, S.; Wen, X.; Wang, C.; Guo, J.; He, Y. *J. Org. Chem.* **2020**, 85, 14, 9321 – 9330.

126.3, 125.6 (q, J = 3.8 Hz), 78.8, 72.0, 57.3, 53.1, 36.1, 23.3. **^{19}F NMR** (282 MHz, $CDCl_3$) δ -62.5.

Dimethyl (*E*)-2-(3-(4-nitrophenyl)allyl)-2-(prop-2-yn-1-yl)malonate (2.76f)

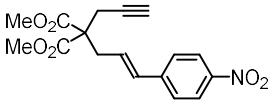

Prepared following general procedure **GP10**, using (*E*)-3-(4-nitrophenyl)prop-2-en-1-ol (400 mg, 2.23 mmol). Allyl bromide was obtained as a yellow oil (410 mg, 1.69 mmol, 76%) and was used in the following step with propargyl malonate (170 µL, 1.11 mmol, 1.0 equiv). Enyne **2.76f** was obtained as a yellow solid (230 mg, 0.69 mmol, 62% yield) after FCC (CyH:EtOAc dry load, silica, 100:0 to 90:10). Spectroscopic data matched those reported in the literature.[59b] **M.p.** 68 ºC **^{1}H NMR** (300 MHz, $CDCl_3$) δ 8.21 – 8.09 (m, 2H), 7.51 – 7.37 (m, 2H), 6.59 (d, J = 15.8 Hz, 1H), 6.33 – 6.14 (m, 1H), 3.77 (s, 6H), 3.01 (dd, J = 7.6, 1.2 Hz, 2H), 2.85 (d, J = 2.7 Hz, 2H), 2.08 (t, J = 2.7 Hz, 1H). **^{13}C NMR** (75 MHz, $CDCl_3$) δ 170.1, 147.1, 143.4, 132.8, 128.8, 127.0, 124.1, 78.6, 72.1, 57.2, 53.1, 36.3, 23.4. **HRMS (ESI +)** calculated for $[C_{17}H_{17}NNaO_6]^+$ $[M+Na]^+$ 354.0948 m/z; found 354.0950 m/z.

Dimethyl (*E*)-2-(3-(4-chlorophenyl)allyl)-2-(prop-2-yn-1-yl) (2.76g)

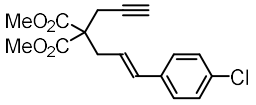

Prepared following general procedure **GP10**, using (*E*)-3-(4-chlorophenyl)prop-2-en-1-ol (200 mg, 1.19 mmol). Allyl bromide was obtained as a colorless oil (200 mg, 0.864 mmol, 76%) and was used in the following step with propargyl malonate (89 µL, 0.588 mmol, 1.0 equiv). Enyne **2.76g** was obtained as a white solid (150 mg, 0.468 mmol, 80% yield) after FCC (CyH:EtOAc dry load, silica, 100:0 to 90:10). Spectroscopic data matched those reported in the literature.[98] **M.p.** 84–86 ºC. **^{1}H NMR** (300 MHz, $CDCl_3$) δ 7.26 – 7.24 (m, 4H), 6.47 (dt, J = 15.7, 1.3 Hz, 1H), 5.99 (dt, J = 15.5, 7.7 Hz, 1H), 3.76 (s, 5H), 2.95 (dd, J = 7.7, 1.3 Hz, 2H), 2.84 (d, J = 2.7 Hz, 2H), 2.06 (t, J = 2.6 Hz, 1H). **^{13}C NMR** (75 MHz, $CDCl_3$) δ 170.2, 135.6, 133.6, 133.3, 128.8, 127.6, 124.1, 78.9, 71.9, 57.3, 53.0, 36.0, 23.2.

Dimethyl (*E*)-2-(3-(4-methoxyphenyl)allyl)-2-(prop-2-yn-1-yl)malonate (2.76h)

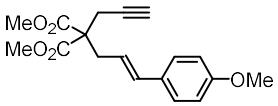

Prepared following general procedure **GP10**, using (*E*)-3-(4-methoxyphenyl)prop-2-en-1-ol (300 mg, 1.83 mmol). Allyl bromide was obtained as a colorless oil (350 mg, 1.54 mmol, 84%) and was used in the following step with propargyl malonate (152 µL, 0.999 mmol, 1.0 equiv). Enyne **2.76h** was obtained as a colorless oil (200 mg, 0.632 mmol, 63% yield) after FCC (CyH:EtOAc dry load, silica, 100:0 to 90:10). Spectroscopic data matched those reported in the literature.[59b] **^{1}H NMR** (300 MHz, $CDCl_3$) δ 7.31 – 7.26 (m, 1H), 7.25 – 7.23 (m, 1H), 6.87 – 6.79 (m, 2H), 6.46 (d, J = 15.7 Hz, 1H), 5.84 (dt, J = 15.5, 7.6 Hz, 1H), 3.80 (s, 3H), 3.76 (s, 6H), 2.94 (dd, J = 7.7, 1.2 Hz, 2H), 2.84 (d, J = 2.7 Hz, 2H), 2.05 (t, J = 2.7 Hz, 1H). **^{13}C NMR** (75 MHz, $CDCl_3$) δ 170.4, 134.2, 127.6, 120.9, 114.1, 79.0, 71.7, 57.44 55.4, 53.0, 36.0, 23.0.

Dimethyl (*E*)-2-(3-(3-methoxyphenyl)allyl)-2-(prop-2-yn-1-yl)malonate (2.76i)

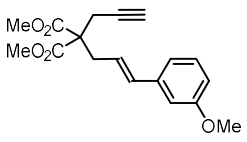

Prepared following general procedure **GP10**, using (*E*)-3-(3-methoxyphenyl)prop-2-en-1-ol (871 mg, 5.30 mmol). Allyl bromide was obtained as a colorless oil (995 mg, 5.30 mmol, 83%) and was used in the following step with propargyl malonate (152 µL, 0.999 mmol, 1.0 equiv). Enyne **2.76i** was obtained as a colorless oil (239 mg, 0.755 mmol, 44% yield) after FCC (CyH:EtOAc dry load, silica, 100:0 to 90:10). **M.p.** 58 ºC. **^{1}H NMR** (500 MHz, $CDCl_3$) δ 7.21 (t, J = 7.9 Hz, 1H), 6.93 (dt, J = 7.6, 1.3 Hz, 1H), 6.86 (dd, J = 2.6, 1.6 Hz, 1H), 6.78 (ddd, J = 8.2,

2.6, 0.9 Hz, 1H), 6.49 (dt, *J* = 15.8, 1.4 Hz, 1H), 6.00 (dt, *J* = 15.5, 7.7 Hz, 1H), 3.81 (s, 3H), 3.76 (s, 6H), 2.96 (dd, *J* = 7.7, 1.3 Hz, 2H), 2.85 (d, *J* = 2.7 Hz, 2H), 2.06 (t, *J* = 2.7 Hz, 1H). **^{13}C NMR** (126 MHz, $CDCl_3$) δ 170.3, 159.9, 138.6, 134.7, 129.6, 123.6, 119.1, 113.2, 112.0, 79.0, 71.8, 57.4, 55.4, 53.0, 36.0, 23.1. **HRMS (ESI +)** calculated for $[C_{18}H_{20}NaO]^{+\cdot}$ $[M+Na]^{+\cdot}$ 339.1203 m/z; found 339.1203 m/z.

Dimethyl (*E*)-2-(3-(3-nitrophenyl)allyl)-2-(prop-2-yn-1-yl)malonate (2.76j)

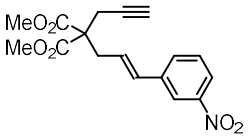

Prepared following general procedure **GP10**, using (*E*)-3-(3-nitrophenyl)prop-2-en-1-ol (432 mg, 2.41 mmol). Allyl bromide was obtained as a yellow solid (350 mg, 1.54 mmol, 84%) and was used in the following step with propargyl malonate (110 µL, 0.723 mmol, 1.0 equiv). Enyne **2.76j** was obtained as pale yellow solid (193 mg, 0.583 mmol, 80% yield) after FCC (CyH:EtOAc dry load, silica, 100:0 to 95:5). **M.p.** 87–90 ºC. **^{1}H NMR** (300 MHz, $CDCl_3$) δ 8.16 (t, *J* = 1.9 Hz, 1H), 8.07 (ddd, *J* = 8.1, 2.2, 1.0 Hz, 1H), 7.63 (d, *J* = 7.8 Hz, 1H), 7.46 (t, *J* = 7.9 Hz, 1H), 6.58 (d, *J* = 15.7 Hz, 1H), 6.18 (dt, *J* = 15.6, 7.6 Hz, 1H), 3.77 (s, 6H), 3.00 (dd, *J* = 7.6, 1.2 Hz, 2H), 2.85 (d, *J* = 2.7 Hz, 2H), 2.09 (t, *J* = 2.7 Hz, 1H).**^{13}C NMR** (75 MHz, $CDCl_3$) δ 170.1, 148.7, 138.8, 132.5, 132.2, 129.6, 127.0, 122.3, 121.1, 78.7, 72.1, 57.2, 53.1, 36.1, 23.3. **HRMS (ESI +)** calculated for $[C_{17}H_{17}NNaO_6]^{+\cdot}$ $[M+Na]^{+\cdot}$ 354.0948 m/z; found 354.0952 m/z.

Dimethyl (*E*)-2-(3-(2-methoxyphenyl)allyl)-2-(prop-2-yn-1-yl)malonate (2.76k)

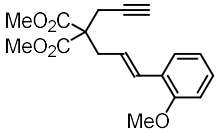

Prepared following general procedure **GP10**, using (*E*)-3-(2-methoxyphenyl)prop-2-en-1-ol (300 mg, 1.83 mmol). Allyl bromide was obtained as a pale-yellow oil (380 mg, 1.67 mmol, 82%) and was used in the following step with propargyl malonate (170 µL, 1.12 mmol, 1.0 equiv). Enyne **2.76k** was obtained as a colorless oil (342 mg, 1.08 mmol, 97% yield) after FCC (CyH:EtOAc dry load, silica, 100:0 to 90:10). **M.p.** 60 ºC. **^{1}H NMR** (300 MHz, $CDCl_3$) δ 7.36 (dd, *J* = 7.6, 1.7 Hz, 1H), 7.24 – 7.16 (m, 1H), 6.93 – 6.77 (m, 3H), 5.99 (dt, *J* = 15.6, 7.7 Hz, 1H), 3.82 (s, 3H), 3.76 (s, 6H), 2.98 (dd, *J* = 7.7, 1.3 Hz, 2H), 2.85 (d, *J* = 2.7 Hz, 2H), 2.05 (t, *J* = 2.7 Hz, 1H). **^{13}C NMR** (75 MHz, $CDCl_3$) δ 170.4, 156.7, 129.8, 128.7, 127.0, 126.4, 123.8, 120.7, 111.0, 79.0, 71.7, 57.6, 55.60, 52.9, 36.4, 23.1. **HRMS (ESI +)** calculated for $[C_{18}H_{20}NaO_5]^{+\cdot}$ $[M+Na]^{+\cdot}$ 339.1203 m/z; found 339.1218 m/z.

Dimethyl (*E*)-2-(3-(2-fluorophenyl)allyl)-2-(prop-2-yn-1-yl)malonate (2.76l)

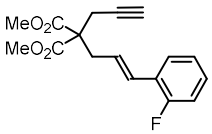

Prepared following general procedure **GP10**, using (*E*)-3-(2-fluorophenyl)prop-2-en-1-ol (191 mg, 1.25 mmol). Allyl bromide was obtained as a colorless oil (250 mg, 1.16 mmol, 93%) and was used in the following step with propargyl malonate (120 µL, 0.789 mmol, 1.0 equiv). Enyne **2.76l** was obtained as a colorless oil (236 mg, 0.775 mmol, 98% yield) after FCC (CyH:EtOAc dry load, silica, 100:0 to 90:10). **^{1}H NMR** (300 MHz, $CDCl_3$) δ 7.41 (td, *J* = 7.7, 1.8 Hz, 1H), 7.25 – 7.18 (m, 1H), 7.09 (td, *J* = 7.5, 1.2 Hz, 1H), 7.03 (ddd, *J* = 10.8, 8.2, 1.2 Hz, 1H), 6.69 (d, *J* = 15.9 Hz, 1H), 6.12 (dt, *J* = 15.7, 7.7 Hz, 1H), 3.79 (s, 6H), 3.01 (dd, *J* = 7.6, 1.3 Hz, 2H), 2.88 (d, *J* = 2.7 Hz, 2H), 2.09 (t, *J* = 2.7 Hz, 1H). **^{13}C NMR** (75 MHz, $CDCl_3$) δ 170.2, 129.0, 127.6, 127.3, 126.1, 124.2, 115.9, 115.6, 78.8, 71.9, 57.4, 53.0, 36.4, 23.1. **^{9}F NMR** (282 MHz, $CDCl_3$) δ -118.4. **HRMS (ESI +)** calculated for $[C_{17}H_{17}FNaO_4]^{+\cdot}$ $[M+Na]^{+\cdot}$ 327.1003 m/z; found 327.1005 m/z.

Dimethyl (*E*)-2-(3-(naphthalen-1-yl)allyl)-2-(prop-2-yn-1-yl)malonate (2.76m)

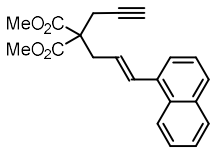

Prepared following general procedure GP3, using (*E*)-3-(naphthalen-1-yl)prop-2-en-1-ol (191 mg, 1.25 mmol). Allyl bromide was obtained as a white solid (250 mg, 1.16 mmol, 93%) and was used in the following step (this time as 1.3 equiv) with propargyl malonate (120 µL, 0.789 mmol, 1.0 equiv). Enyne **2.76m** was obtained as a white solid (261 mg, 0.776 mmol, 98% yield) after FCC (CyH:EtOAc dry load, silica, 100:0 to 90:10). Spectroscopic data matched those reported in the literature.[98] **^{1}H NMR** (300 MHz, $CDCl_3$) δ 8.13 – 8.01 (m, 1H), 7.88 – 7.80 (m, 1H), 7.77 (d, *J* = 8.0 Hz, 1H), 7.56 – 7.37 (m, 5H), 7.34 – 7.26 (m, 1H), 6.02 (dt, *J* = 15.4, 7.7 Hz, 1H), 3.78 (s, 6H), 3.10 (dd, *J* = 7.7, 1.3 Hz, 2H), 2.92 (d, *J* = 2.7 Hz, 2H), 2.12 (t, *J* = 2.7 Hz, 1H). **^{13}C NMR** (75 MHz, $CDCl_3$) δ 170.4, 135.0, 132.5, 128.6, 128.1, 126.6, 126.2, 125.9, 125.7, 124.2, 123.9, 79.0, 71.9, 57.4, 53.0, 36.4, 23.2. **HRMS (ESI +)** calculated for $[C_{17}H_{17}FNaO_4]^{+\cdot}$ [M+Na] $^{+\cdot}$ 327.1003 m/z; found 327.1005 m/z.

Dimethyl (*E*)-2-(3-(naphthalen-1-yl)allyl)-2-(prop-2-yn-1-yl)malonate (2.76n)

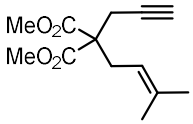

Under argon, to suspension of NaH (170 mg, 60% wt, 4.25 mmol, 1.1 equiv) in anhydrous THF (20mL) at room temperature, was added dropwise propargyl malonate (0.60 mL, 3.95 mmol, 1.0 equiv) and the mixture was left stirring at the same temperature for 15 min. Prenyl bromide (0.58 mL, 95% wt, 4.7 mmol, 1.2 equiv) was then added dropwise at the same temperature and the resulting suspension was stirred for 24 h. The reqction was quenched by slow addition of an aqueous saturated NH4Cl solution (10 mL) and extracted with Et2O (15 mL x 3). The combined organic layers were washed with brine, dried over MgSO4, filtered and the solvent was evaporated. The crude was purified by FCC (CyH:EtOAc, 100:0 slowly to 95:5) enyne **2.76n** as a colorless oil (867 mg, 0.364 mmol, 92% yield). Spectroscopic data matched those reported in the literature. [59b] **^{1}H NMR** (300 MHz, $CDCl_3$) δ 4.94 – 4.84 (m, 1H), 3.75 – 3.70 (m, 6H), 2.82 – 2.73 (m, 4H), 1.99 (td, *J* = 2.7, 0.8 Hz, 1H), 1.69 (s, 3H), 1.64 (s, 3H). **^{13}C NMR** (75 MHz, $CDCl_3$) δ 170.63, 137.11, 117.07, 79.40, 71.32, 57.29, 52.84, 30.90, 26.19, 22.65, 18.06.

Dimethyl (*E*)-2-(3,7-dimethylocta-2,6-dien-1-yl)-2-(prop-2-yn-1-yl)malonate (2.76o)

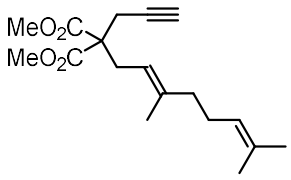

Prepared following general procedure **GP10**, using (*E*)-3,7-dimethylocta-2,6-dien-1-ol (500 mg, 3.25 mmol). Geranyl bromide was obtained as a colorless oil (733 mg, 3.17 mmol, 98%) and was used in the following step (this time as 1.3 equiv) with propargyl malonate (360 µL, 2.35 mmol, 1.0 equiv). Enyne **2.76o** was obtained as a white solid (612 mg,2.00 mmol, 85% yield) after FCC (CyH:EtOAc dry load, silica, 100:0 to 90:10). Spectroscopic data matched those reported in the literature.[59b] **^{1}H NMR** (300 MHz, $CDCl_3$) δ 4.94 – 4.84 (m, 1H), 3.75 – 3.70 (m, 6H), 2.82 – 2.73 (m, 4H), 1.99 (td, *J* = 2.7, 0.8 Hz, 1H), 1.69 (s, 3H), 1.64 (s, 3H). **^{13}C NMR** (75 MHz, $CDCl_3$) δ 170.63, 137.11, 117.07, 79.40, 71.32, 57.29, 52.84, 30.90, 26.19, 22.65, 18.06.

General procedure GP11: enantioselective nucleophile addition to 1,6-enynes[91]

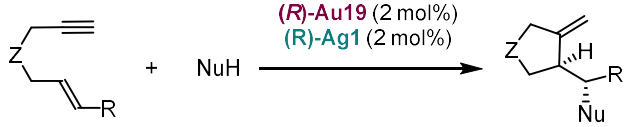

To a GMCS or MW vial containing a solution of enyne (0.100 mmol) and nucleophile (1.0–3.0 equiv) in solvent was added respectively a solution of complex (*R*)-**Au19** (2.3 mg, 2.0 µmol, 2

mol%) and a solution of (*R*)-**Ag1** (2.0mg, 2.0 μmol, 2 mol%) in 1,4-dioxane or toluene (0.1 M final concentration) at the indicated temperature. The resulting mixture was stirred until starting material consumption, determined by TLC or GCMS analysis. The reaction was then quenched by addition of triethylamine (*ca* 0.1 mL) and filtered through a silica-filled glass pipette. Volatiles were removed under reduced pressure and the crude product was purified by FCC or PTLC (silica, CyH:EtOAc or pentane:EtOAc mixtures).

Dimethyl (*R*)-3-((*R*)-(1*H*-indol-3-yl)(phenyl)methyl)-4-methylenecyclopentane-1,1-dicarboxylate (2.77a)

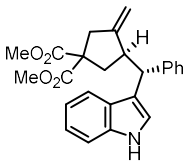

Prepared following general procedure **GP11** using enyne **2.76a** (28.6 mg, 0.100 mmol) and indole (14.1 mg, 0.120 mmol, 1.2 equiv) as a nucleophile in 1,4-dioxane (1.0 mL, 0.1M), at 25 ºC for 6 h. The crude product was purified by FCC (silica, CyH:EtOAc 90:10 to 80:20). Compound **2.77a** was obtained as a white solid (40.1 mg, 0.994 mmol, 99% yield) with >99:1 *er*. Spectroscopic data matched those reported in the literature.[100] The absolute configuration was assigned by comparison to **2.77v**. **^{1}H NMR** (300 MHz, $CDCl_3$) δ 8.06 (brs, 1H), 7.54 (d, *J* = 8.0 Hz, 1H), 7.37 – 7.28 (m, 3H), 7.25 – 7.18 (m, 2H), 7.18 – 7.08 (m, 3H), 7.05 (td, *J* = 7.5, 1.1 Hz, 1H), 4.80 (s, 1H), 4.22 – 4.10 (m, 2H), 3.72 (s, 3H), 3.64 (s, 3H), 3.61 – 3.45 (m, 1H), 3.13 (dq, *J* = 15.9, 2.4 Hz, 1H), 2.97 – 2.85 (m, 1H), 2.76 (ddd, *J* = 13.6, 7.9, 1.5 Hz, 1H), 1.98 (dd, *J* = 13.7, 8.5 Hz, 1H). **^{13}C NMR** (75 MHz, $CDCl_3$) δ 172.4, 172.2, 149.0, 144.5, 136.3, 128.6, 128.2, 127.3, 126.2, 122.1, 121.5, 119.50, 119.47, 118.7, 111.2, 110.2, 58.6, 52.9, 52.8, 48.1, 46.9, 41.9, 40.0. **SFC** (IG (100 × 3 mm, 3 μm), 80:20 CO_2:*i*-PrOH, 1.5 mL/min, 35 ºC, BPR 150 bar, 280 nm): en2 (100%) 1.53 min. **$[\alpha]^{24.6}_D$** +2.8 (c 1.28, $CHCl_3$).

Dimethyl (*R*)-3-((*R*)-(5-Bromo-1*H*-indol-3-yl)(phenyl)methyl)-4-methylenecyclopentane-1,1-dicarboxylate (2.77b)

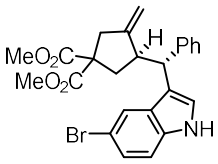

Prepared following general procedure **GP11** using enyne **2.76a** (28.6 mg, 0.100 mmol) and 5-bromoindole (23.5 mg, 0.120 mmol, 1.2 equiv) as a nucleophile in 1,4-dioxane (1.0 mL, 0.1M), at 25 ºC for 6 h. The crude product was purified by FCC (silica, CyH:EtOAc 90:10 to 80:20). Compound **2.77b** was obtained as a white solid (44.8 mg, 0.929 mmol, 93% yield) with >99:1 *er*. The absolute configuration was assigned by comparison to **2.77v**. **1H NMR** (300 MHz, $CDCl_3$) δ 8.16 (s, 1H), 7.65 (dt, J = 1.4, 0.7 Hz, 1H), 7.36 – 7.09 (m, 8H), 4.80 (t, J = 1.7 Hz, 1H), 4.11 (d, J = 2.3 Hz, 1H), 4.08 (d, J = 10.4 Hz, 1H), 3.73 (s, 3H), 3.65 (s, 3H), 3.57 – 3.35 (m, 1H), 3.17 – 2.99 (m, 1H), 2.91 (dd, J = 16.0, 1.5 Hz, 1H), 2.78 – 2.60 (m, 1H), 1.93 (dd, J = 13.7, 8.5 Hz, 1H). **^{13}C NMR** (75 MHz, $CDCl_3$) δ 172.4, 172.2, 148.7, 144.0, 134.8, 129.0, 128.5, 128.4, 126.4, 125.0, 122.7, 121.9, 118.5, 112.84, 112.7, 110.3, 58.5, 53.0, 52.9, 47.9, 46.9, 41.8, 39.9. **HRMS (ESI +)** calculated for $[C_{25}H_{25}BrNO_4]^{+\cdot}$ [M-H] $^{+\cdot}$ 482.0961 m/z; found 482.0959 m/z. SFC (IB-N (100 × 3 mm, 3 μm), 60:40 CO_2:MeOH, 1.2 mL/min, 35 ºC, BPR 150 bar, 210 nm): en1 (major, 100%) 0.99 min. **$[\alpha]^{24.6}_D$** +38.7 (c 1.74, $CHCl_3$).

100.Amijs, C. H. M.; Ferrer, C.; Echavarren, A. M. *Chem. Commun.* **2007**, *7*, 698–700.

Dimethyl (*R*)-3-((*R*)-(5-Methoxy-1*H*-indol-3-yl)(phenyl)methyl)-4-methylenecyclopentane-1,1-dicarboxylate (2.77c)

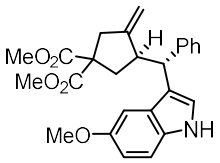

Prepared following general procedure **GP11** using enyne **2.76a** (28.6 mg, 0.100 mmol) and 5-methoxyindole (17.7 mg, 0.120 mmol, 1.2 equiv) as a nucleophile in 1,4-dioxane (1.0 mL, 0.1M), at 25 ºC for 6 h. The crude product was purified by FCC (silica, CyH:EtOAc 90:10 to 80:20). Compound **2.77c** was obtained as a white solid (36.7 mg, 0.837 mmol, 84% yield) with >99:1 *er*. The absolute configuration was assigned by comparison to **2.77v**. **M.p.** 52 ºC. **^{1}H NMR** (300 MHz, $CDCl_3$) δ 7.95 (brs, 1H), 7.34 – 7.28 (m, 2H), 7.26 – 7.07 (m, 5H), 6.95 (d, *J* = 2.4 Hz, 1H), 6.80 (dd, *J* = 8.8, 2.4 Hz, 1H), 4.80 (s, 1H), 4.18 – 4.07 (m, 2H), 3.79 (s, 3H), 3.72 (s, 3H), 3.64 (s, 3H), 3.50 (qd, *J* = 8.3, 1.8 Hz, 1H), 3.11 (dd, *J* = 15.9, 2.1 Hz, 1H), 2.89 (d, *J* = 15.9 Hz, 1H), 2.77 (ddd, *J* = 13.6, 7.9, 1.4 Hz, 1H), 1.98 (dd, *J* = 13.7, 8.5 Hz, 1H). **^{13}C NMR** (75 MHz, $CDCl_3$) δ 172.4, 172.2, 154.0, 149.1, 144.4, 131.5, 128.6, 128.2, 127.8, 126.2, 122.4, 118.5, 112.2, 111.8, 110.1, 101.6, 58.6, 56.0, 52.9, 52.8, 48.1, 46.9, 41.9, 39.9. **HRMS (ESI +)** calculated for $[C_{26}H_{27}NNaO_5]^{+\cdot}$ $[M+Na]^{+\cdot}$ 456.1781 m/z; found 456.1783 m/z**. SFC** (IB-N (100 × 3 mm, 3 μm), 80:30 CO_2:MeOH, 1.2 mL/min, 35 ºC, BPR 150 bar, 210 nm): en2 (major, 100%) min 1.25. **$[\alpha]^{24.6}_D$** +26.7 (c 1.13, $CHCl_3$).

Dimethyl (*R*)-3-((*R*)-(1-Methyl-1*H*-indol-3-yl)(phenyl)methyl)-4-methylenecyclopentane-1,1-dicarboxylate (2.77d)

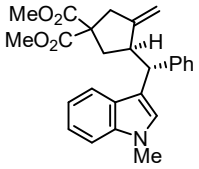

Prepared following general procedure **GP11** using enyne **2.76a** (28.6 mg, 0.100 mmol) and *N*-methylindole (15.7 mg, 0.120 mmol, 1.2 equiv) as a nucleophile in 1,4-dioxane (1.0 mL, 0.1M), at 25 ºC for 6 h. The crude product was purified by FCC (silica, CyH:EtOAc 90:10 to 80:20). Compound **2.77d** was obtained as a white solid (41.1 mg, 0.984 mmol, 98% yield) with 99:1 *er*. Spectroscopic data matched those reported in the literature.[100] The absolute configuration was assigned by comparison to **2.77v**. **^{1}H NMR** (300 MHz, $CDCl_3$) δ 7.60 – 7.53 (m, 1H), 7.38 – 7.29 (m, 2H), 7.25 – 7.03 (m, 5H), 7.03 – 6.97 (m, 1H), 4.79 (s, 1H), 4.19 – 4.07 (m, 2H), 3.76 (s, 3H), 3.73 (s, 3H), 3.65 (s, 3H), 3.60 – 3.47 (m, 1H), 3.14 (dq, *J* = 15.9, 2.4 Hz, 1H), 2.94 – 2.83 (m, 1H), 2.77 (ddd, *J* = 13.6, 7.9, 1.4 Hz, 1H), 1.97 (dd, *J* = 13.7, 8.5 Hz, 1H). **^{13}C NMR** (75 MHz, $CDCl_3$) δ 172.4, 172.2, 149.1, 144.7, 137.0, 128.6, 128.2, 127.7, 126.3, 126.1, 121.7, 119.5, 119.0, 117.3, 110.1, 109.2, 58.5, 52.9, 52.8, 48.2, 46.9, 41.9, 40.1, 32.9. **SFC** (OD (100 × 3 mm, 3 μm), 80:20 CO_2:MeOH, 1.2 mL/min, 35 ºC, BPR 150 bar, 210 nm): en1 (major, 99%) 1.12 min, en2 (minor, 1%) 1.23 min. **$[\alpha]^{24.6}_D$** –7.25 (c 1.49, $CHCl_3$).

Dimethyl (*R*)-3-((*R*)-(2-Methyl-1*H*-indol-3-yl)(phenyl)methyl)-4-methylenecyclopentane-1,1-dicarboxylate (2.77e)

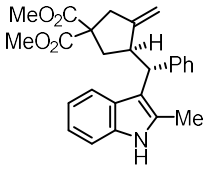

Prepared following general procedure **GP11** enyne **2.76a** (28.6 mg, 0.100 mmol) and 2-methylindole (15.7 mg, 0.120 mmol, 1.2 equiv) as a nucleophile in 1,4-dioxane (1.0 mL, 0.1M), at 25 ºC for 6 h. The crude product was purified by FCC (silica, CyH:EtOAc 90:10 to 80:20). Compound **2.77e** was obtained as a white solid (35.5 mg, 0.85 mmol, 85% yield) with >99:1 *er*. The absolute configuration was assigned by comparison to **2.77v**. **M.p.** 61–66 ºC. **^{1}H NMR** (300 MHz, $CDCl_3$) δ 7.79 – 7.68 (m, 2H), 7.41 (d, *J* = 7.3 Hz, 2H), 7.25 – 7.17 (m, 3H), 7.14 – 7.03 (m, 3H), 4.89 – 4.78 (m, 1H), 4.31 – 4.23 (m, 1H), 4.04 (s, 1H), 3.99 – 3.82 (m, 1H), 3.72 (s, 3H), 3.62 (s, 3H), 3.20 – 3.08 (m, 1H), 3.05 – 2.93 (m, 1H), 2.57 – 2.46 (m, 1H), 2.41 (s, 3H), 1.84 (dd, *J* = 13.5, 9.2 Hz, 1H). **^{13}C NMR** (75 MHz, $CDCl_3$) δ 172.5, 172.4, 150.2, 144.8, 135.4, 131.3, 128.3, 128.2, 127.8, 125.9, 120.9, 119.6, 119.4, 114.5, 110.4, 109.6, 58.0, 52.8, 52.8, 47.9, 45.1, 41.8,

39.9, 12.7. **HRMS (ESI +)** calculated for $[C_{26}H_{27}NNaO_4]^{+\cdot}$ [M+Na] $^{+\cdot}$ 440.1830 m/z; found 440.1830 m/z**. SFC** (IB-N (100 × 3 mm, 3 μm), 80:20 CO_2:*i*-PrOH, 1.2 mL/min, 35 ºC, BPR 150 bar, 210 nm): en2 (major, 100%) 3.33 min. **[α]$^{24.6}_D$** –9.49 (c 1.08, $CHCl_3$).

Dimethyl (*R*)-3-Methylene-4-((*R*)-phenyl(2,4,6-trimethoxyphenyl)methyl)cyclopentane-1,1-dicarboxylate (2.77f)

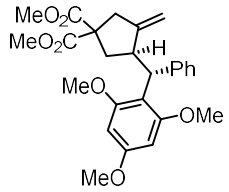

Prepared following general procedure **GP11**, using enyne **2.76a** (28.6 mg, 0.100 mmol) and 1,3,5-trimethoxybenzene (33.6 mg, 0.200 mmol, 2.0 equiv) as a nucleophile in toluene (1.0 mL, 0.1M), at −10 ºC for 6 h. The crude product was purified by FCC (silica, CyH:EtOAc 90:10 to 80:20). Compound **2.77f** was obtained as a white solid (39.4 mg, 0.870 mmol, 87% yield) with 98:2 *er*. Spectroscopic data matched those reported in the literature.[59f] The absolute configuration was assigned by comparison to **2.77v**. **M.p.** 74 ºC. **^{1}H NMR** (500 MHz, $CDCl_3$) δ 7.48 – 7.44 (m, 2H), 7.19 (t, *J* = 7.7 Hz, 2H), 7.09 (t, *J* = 7.3 Hz, 1zH), 6.08 (s, 1H), 4.73 (q, *J* = 2.2 Hz, 1H), 4.50 (d, *J* = 11.0 Hz, 1H), 4.26 (qd, *J* = 2.2, 0.8 Hz, 1H), 3.99 (tdt, *J* = 11.9, 7.5, 2.4 Hz, 1H), 3.81 (s, 6H), 3.76 (s, 3H), 3.74 (s, 3H), 3.66 (s, 3H), 3.09 (dq, *J* = 16.5, 2.2 Hz, 1H), 3.01 (dq, *J* = 16.6, 1.9 Hz, 1H), 2.37 (ddd, *J* = 12.9, 7.5, 1.6 Hz, 1H). **^{13}C NMR** (126 MHz, $CDCl_3$) δ 172.6, 172.5, 159.6, 151.5, 144.7, 128.8, 127.8, 125.6, 113.7, 108.2, 91.1, 57.8, 55.7, 55.3, 52.8, 52.7, 44.3, 43.1, 41.8, 40.1. **SFC** (IG-3 (150 × 4.6 mm, 3 μm), 93:7 CO_2:*i*-PrOH, 2.0 mL/min, 35 ºC, BPR 140 bar, 230 nm): en1 (minor, 2%) 4.33 min, en2 (major, 98%) 4.72 min. **[α]$^{24.6}_D$** +80.9 (c 1.79, $CHCl_3$).

Dimethyl (*R*)-3-Methylene-4-((*R*)-phenyl(2,4-dimethoxyphenyl)methyl)cyclopentane-1,1-dicarboxylate (2.77g)

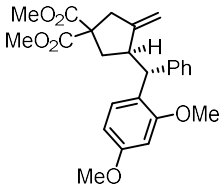

Prepared following general procedure **GP11**, using enyne **2.76a** (28.6 mg, 0.100 mmol) and 1,3-dimethoxybenzene (27.6 mg, 0.200 mmol, 2.0 equiv) as a nucleophile in toluene (1.0 mL, 0.1M), at −10 ºC for 6 h. The crude product was purified by FCC (silica, CyH:EtOAc 90:10 to 80:20). Compound **2.77g** was obtained as a white solid (33.4 mg, 0.790 mmol, 79% yield) with 99:1 *er*. Spectroscopic data matched those reported in the literature. [59f] The absolute configuration was assigned by comparison to **2.77v**. **^{1}H NMR** (300 MHz, $CDCl_3$) δ 7.33 – 7.27 (m, 2H), 7.26 – 7.17 (m, 3H), 7.14 – 7.06 (m, 1H), 6.46 (dd, *J* = 8.4, 2.5 Hz, 1H), 6.38 (d, *J* = 2.5 Hz, 1H), 4.72 (s, 1H), 4.18 (d, *J* = 11.5 Hz, 1H), 4.06 – 4.01 (m, 1H), 3.76 (s, 6H), 3.73 (s, 3H), 3.67 (s, 3H), 3.61 – 3.46 (m, 1H), 3.12 (dq, *J* = 16.0, 2.3 Hz, 1H), 2.90 (dd, *J* = 16.0, 1.5 Hz, 1H), 2.55 (ddd, *J* = 13.4, 7.7, 1.5 Hz, 1H), 1.71 (dd, *J* = 13.4, 9.2 Hz, 1H). **^{13}C NMR** (75 MHz, $CDCl_3$) δ 172.5, 172.2, 159.2, 158.0, 149.5, 144.5, 128.7, 128.1, 126.0, 125.1, 109.7, 104.5, 98.8, 58.2, 55.5, 55.4, 52.9, 52.8, 48.4, 45.3, 41.9, 40.1. **SFC** (IB-N (100 × 3 mm, 3 μm), 90:10 CO_2:MeOH, 1.2 mL/min, 35 ºC, BPR 150 bar, 210 nm): en1 (minor, 1%) 1.20 min, en2 (major, 99%) 1.67 min. **[α]$^{24.6}_D$** +20.03 (c 1.46, $CHCl_3$).

Dimethyl (*R*)-3-((*R*)-(4-(Dimethylamino)phenyl)(phenyl)methyl)-4-methylenecyclopentane-1,1-dicarboxylate (2.77h)

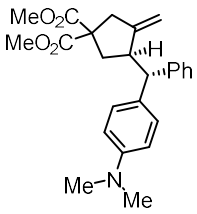

Prepared following general procedure **GP11**, using enyne **2.76a** (28.6 mg, 0.100 mmol) and *N,N*-dimethtlaniline (13.9 μL, 0.110 mmol, 1.1 equiv) as a nucleophile in toluene (1.0 mL, 0.1M), at 25 ºC for 24 h. The crude product was purified by FCC (silica, CyH:EtOAc 90:10). Compound **2.77h** was obtained as a white solid (39.7 mg, 0.977 mmol, 98% yield) with >99:1 *er*. The absolute configuration was assigned by comparison to **2.77v**. **M.p.** 104–107

ºC. **^{1}H NMR** (300 MHz, $CDCl_3$) δ 7.32 – 7.27 (m, 2H), 7.26 – 7.19 (m, 2H), 7.19 – 7.08 (m, 3H), 6.71 – 6.62 (m, 2H), 4.78 – 4.73 (m, 1H), 4.17 – 4.11 (m, 1H), 3.76 – 3.70 (m, 4H), 3.68 (s, 3H), 3.58 – 3.44 (m, 1H), 3.14 – 3.04 (m, 1H), 2.96 – 2.84 (m, 7H), 2.55 (ddd, *J* = 13.4, 7.6, 1.3 Hz, 1H), 1.80 (dd, *J* = 13.5, 9.1 Hz, 1H). **^{13}C NMR** (126 MHz, $CDCl_3$) δ 172.4, 172.3, 149.5, 149.2, 145.1, 132.1, 128.9, 128.4, 128.2, 126.1, 112.9, 109.7, 58.2, 56.0, 52.9, 52.8, 46.1, 41.9, 40.8, 40.0. **HRMS (ESI +)** calculated for $[C_{25}H_{30}NO_4]^{+\cdot}$ $[M+H]^{+\cdot}$ 408.2169 m/z; found 408.2176 m/z. **SFC** (IB-N (100 × 3 mm, 3 μm), 80:20 CO_2:MeOH, 1.2 mL/min, 35 ºC, BPR 150 bar, 210 nm): en1 (minor, 0.5%) 1.11 min, en2 (major, 99.5%) 1.35 min. **$[\alpha]^{24.6}_D$** +17.1 (c 0.56, $CHCl_3$).

Dimethyl (*S*)-3-Methylene-4-((*R*)-phenyl(phenylamino)methyl)cyclopentane-1,1-dicarboxylate (2.77i)

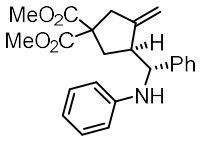

Prepared following general procedure **GP11**, using enyne **2.76a** (28.6 mg, 0.100 mmol) and aniline (10.0 μL, 0.110 mmol, 1.1 equiv) as a nucleophile in toluene (1.0 mL, 0.1M), at 25 ºC for 4 h. The crude product was purified by FCC (silica, CyH:EtOAc 90:10). Compound **2.77i** was obtained as a white solid (32.4 mg, 0.854 mmol, 85% yield) with 99:1 *er*. Spectroscopic data matched those reported in the literature.[59g] The absolute configuration was assigned by comparison to **2.77v**. **^{1}H NMR** (300 MHz, $CDCl_3$) δ 7.41 – 7.28 (m, 4H), 7.26 – 7.14 (m, 1H), 7.12 – 7.02 (m, 2H), 6.69 – 6.58 (m, 1H), 6.50 (dd, *J* = 8.6, 1.0 Hz, 2H), 5.06 (q, *J* = 2.0 Hz, 1H), 4.76 (q, *J* = 2.1 Hz, 1H), 4.54 (d, *J* = 5.0 Hz, 1H), 4.24 (brs, 1H), 3.75 (s, 3H), 3.69 (s, 3H), 3.18 – 2.87 (m, 3H), 2.39 – 2.15 (m, 2H). **^{13}C NMR** (75 MHz, $CDCl_3$) δ 172.6, 172.0, 147.9, 147.3, 142.4, 129.1, 128.7, 127.2, 126.7, 117.64, 113.9, 109.2, 59.2, 57.8, 53.1, 52.9, 49.45 42.2, 35.0. **SFC** (IG (100 × 3 mm, 3 μm), 80:20 CO_2:EtOH, 1.2 mL/min, 35 ºC, BPR 150 bar, 210 nm): en1 (major, 100%) 0.75 min. **$[\alpha]^{24.6}_D$** +39.6 (c 1.27, $CHCl_3$).

Dimethyl (*S*)-3-((*R*)-((2-Bromophenyl)amino)(phenyl)methyl)-4-methylenecyclopentane-1,1-dicarboxylate (2.77j)

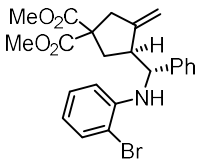

Prepared following general procedure **GP11**, using enyne **2.76a** (28.6 mg, 0.100 mmol) and 2-bromoaniline (18.9 mg, 0.110 mmol, 1.1 equiv) as a nucleophile in toluene (1.0 mL, 0.1M), at 25 ºC for 3 h. The crude product was purified by FCC (silica, CyH:EtOAc 90:10). Compound **2.77j** was obtained as a white solid (42.5 mg, 0.927 mmol, 93% yield) with >99:1 *er*. Spectroscopic data matched those reported in the literature.[59g] The absolute configuration was assigned by comparison to **2.77v**. **^{1}H NMR** (500 MHz, $CDCl_3$) δ 7.40 (dd, *J* = 7.9, 1.5 Hz, 1H), 7.35 – 7.29 (m, 4H), 7.24 (m, 1H), 6.97 (ddd, *J* = 8.5, 7.4, 1.5 Hz, 1H), 6.51 (td, *J* = 7.6, 1.5 Hz, 1H), 6.34 (dd, *J* = 8.2, 1.5 Hz, 1H), 5.07 (d, *J* = 2.3 Hz, 1H), 4.79 (d, *J* = 4.8 Hz, 1H), 4.70 (d, *J* = 2.2 Hz, 1H), 4.51 (t, *J* = 5.3 Hz, 1H), 3.72 (s, 3H), 3.69 (s, 3H), 3.16 (td, *J* = 8.8, 4.7 Hz, 1H), 3.01 (d, *J* = 2.1 Hz, 2H), 2.42 (dd, *J* = 13.7, 8.2 Hz, 1H), 2.27 (dd, *J* = 13.7, 9.9 Hz, 1H). **^{13}C NMR** (126 MHz, $CDCl_3$) δ 171.4, 171.9, 147.1, 144.4, 141.4, 132.3, 128.7, 128.4, 127.5, 127.0, 118.3, 113.1, 110.5, 110.1, 60.4, 58.3, 53.0, 53.0, 49.5, 42.2, 35.6. **HRMS (ESI +)** calculated for $[C_{23}H_{24}BrNNaO_4]^{+\cdot}$ $[M+Na]^{+\cdot}$ 480.0785 m/z; found 480.0781 m/z. **SFC** (IG (100 × 3 mm, 3 μm), 95:5 CO_2:*i*-PrOH, 1.5 mL/min, 35 ºC, BPR 150 bar, 210 nm): en1 (major, 100%) 2.08 min. **$[\alpha]^{24.6}_D$** –11.2 (c 1.27, $CHCl_3$).

Dimethyl (*S*)-3-((*R*)-((2-Iodophenyl)amino)(phenyl)methyl)-4-methylenecyclopentane-1,1-dicarboxylate (2.77k)

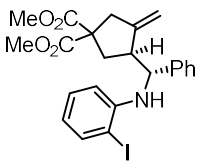

Prepared following general procedure **GP1**, using enyne **2.76a** (28.6 mg, 0.100 mmol) and 2-iodoaniline (24.1 mg, 0.110 mmol, 1.1 equiv) as a nucleophile in toluene (1.0 mL, 0.1M), at 25 ºC for 4 h. The crude product was purified by FCC (silica, CyH:EtOAc 90:10). Compound **2.77k** was obtained as a white sticky solid (44.7 mg, 0.946 mmol, 95% yield) with 98.5:1.5 *er*. Spectroscopic data matched those reported in the literature. [59g] The absolute configuration was assigned by comparison to **2.77v**. **^{1}H NMR** (300 MHz, $CDCl_3$) δ 7.64 (dd, *J* = 7.8, 1.5 Hz, 1H), 7.38 – 7.27 (m, 4H), 7.25 – 7.19 (m, 1H), 6.99 (ddd, *J* = 8.7, 7.4, 1.5 Hz, 1H), 6.39 (td, *J* = 7.7, 1.5 Hz, 1H), 6.27 (dd, *J* = 8.2, 1.3 Hz, 1H), 5.13 – 5.05 (m, 1H), 4.79 – 4.70 (m, 1H), 4.61 (brs, 1H), 4.58 – 4.46 (m, 1H), 3.72 (s, 3H), 3.70 (s, 3H), 3.24 – 3.10 (m, 1H), 3.05 (d, *J* = 2.1 Hz, 2H), 2.42 (dd, *J* = 13.7, 8.0 Hz, 1H), 2.28 (dd, *J* = 13.7, 10.2 Hz, 1H). **^{13}C NMR** (75 MHz, $CDCl_3$) δ 171.9, 171.8, 147.1, 146.6, 141.2, 138.9, 129.3, 128.7, 127.4, 126.9, 119.1, 112.4, 110.2, 86.3, 60.8, 58.3, 53.00, 52.96, 49.6, 42.3, 35.6. **SFC** (OD (100 × 3 mm, 3 μm), 95:5 CO_2:*i*-PrOH, 1.2 mL/min, 35 ºC, BPR 150 bar, 210 nm): en1 (minor, 1.5%) 2.87 min, en2 (major, 98.5%) 3.53 min. **$[\alpha]^{24.6}_D$** – 29.4 (c .90, $CHCl_3$).

Dimethyl (*S*)-3-((*R*)-(((Benzyloxy)carbonyl)amino)(phenyl)methyl)-4-methylenecyclopentane-1,1-dicarboxylate (2.77l)

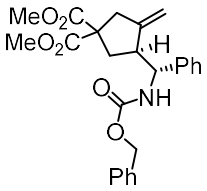

Prepared following general procedure **GP11**, using enyne **2.76a** (28.6 mg, 0.100 mmol) and benzyl carbamate (30.3 mg, 0.200 mmol, 2.0 equiv) as a nucleophile in toluene (1.0 mL, 0.1M), at −10 ºC for 6 h. The crude product was purified by FCC (silica, CH_2Cl_2:EtOAc 99:1). Compound **2.77l** was obtained as a waxy white solid (41.7 mg, 0.953 mmol, 95% yield) with >99:1 *er*. The absolute configuration was assigned by comparison to **2.77v**. **^{1}H NMR** (500 MHz, $CDCl_3$) δ 7.39 – 7.30 (m, 7H), 7.28 (m, 3H), 5.51 (s, 1H), 5.08 (q, *J* = 12.4 Hz, 2H), 4.99 (q, *J* = 2.2 Hz, 2H), 4.69 (s, 1H), 3.72 (s, 3H), 3.69 (s, 3H), 3.14 (s, 1H), 2.99 (dd, *J* = 16.2, 1.7 Hz, 1H), 2.87 (dq, *J* = 16.2, 2.2 Hz, 1H), 2.40 – 2.31 (m, 1H), 2.09 (dd, *J* = 13.8, 9.0 Hz, 1H). **^{13}C NMR** (101 MHz, $CDCl_3$) δ 172.2, 171.8, 156.1, 146.8, 128.6, 128.5, 128.0, 127.4, 126.6, 109.7, 66.8, 57.9, 53.0, 52.9, 47.2, 42.1, 35.5. **HRMS (ESI +)** calculated for $[C_{25}H_{27}NNaO_6]^{+\cdot}$ $[M+Na]^{+\cdot}$ 460.1731 m/z; found 460.1733 m/z. **SFC** (IG (100 × 3 mm, 3 μm), 75:25 CO_2:EtOH, 1.2 mL/min, 35 ºC, BPR 150 bar, 210 nm): en1 (major, 100%) 1.69 min. **$[\alpha]^{24.6}_D$** +47.62 (c 0.61, $CHCl_3$).

Dimethyl (*S*)-3-((*R*)-Hydroxy(phenyl)methyl)-4-methylenecyclopentane-1,1-dicarboxylate (2.77m)

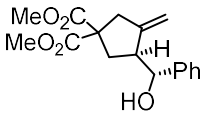

Prepared following general procedure **GP11**, using enyne **2.76a** (28.6 mg, 0.100 mmol) and water (9.0 μL, 0.500 mmol, 5.0 equiv) as a nucleophile in HPLC-grade toluene (1.0 mL, 0.1M), at 25 ºC for 6 h. The crude product was purified by FCC (silica, CyH:EtOAc 90:10 to 80:20). Compound **2.77m** was obtained as a white solid (27.9 mg, 0.917 mmol, 92% yield) with 98:2 *er*. Spectroscopic data matched those reported in the literature.[59f] The absolute configuration was assigned by comparison to **2.77v**. **^{1}H NMR** (300 MHz, $CDCl_3$) δ 7.39 – 7.30 (m, 4H), 7.29 – 7.22 (m, 1H), 5.14 (q, *J* = 2.1 Hz, 1H), 4.98 (d, *J* = 3.9 Hz, 1H), 4.91 (q, *J* = 2.1 Hz, 1H), 3.72 (s, 3H), 3.68 (s, 3H), 3.08 – 2.87 (m, 3H), 2.26 (qd, *J* = 13.6, 9.0 Hz, 3H). **^{13}C NMR** (75 MHz, $CDCl_3$) δ 172.21, 172.16, 149.1, 142.5, 128.4, 127.4, 126.0, 108.5, 74.2, 58.4, 52.92, 52.88, 49.9, 42.2, 33.8. **SFC** (IG (100 × 3 mm, 3 μm), 85:15 CO_2:MeOH, 1.2 mL/min, 35 ºC, BPR 150 bar, 210 nm): en1 (major, 98%) 1.31 min, en2 (minor, 2%) 1.49 min. **$[\alpha]^{24.6}_D$** +70.8 (c 0.70, $CHCl_3$).

Dimethyl (*S*)-3-((*R*)-Methoxy(phenyl)methyl)-4-methylenecyclopentane-1,1-dicarboxylate (2.77n)

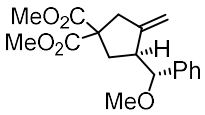

Prepared following general procedure **GP11**, using enyne **2.76a** (28.6 mg, 0.100 mmol) and anhydrous MeOH (20.2 µL, 0.500 mmol, 5.0 equiv) as a nucleophile in 1,4-dioxane (1.0 mL, 0.1M), at 25 ºC for 2 h. The crude product was purified by FCC (silica, CyH:EtOAc 100:0 to 90:10). Compound **2.77n** was obtained as a white solid (28.3 mg, 0.889 mmol, 89% yield) with >99:1 *er*. Spectroscopic data matched those reported in the literature.[59g] The absolute configuration was assigned by comparison to **2.77v**. **^{1}H NMR** (300 MHz, $CDCl_3$) δ 7.39 – 7.26 (m, 5H), 4.97 – 4.89 (m, 1H), 4.56 – 4.47 (m, 1H), 4.17 (d, *J* = 5.9 Hz, 1H), 3.74 (s, 3H), 3.67 (s, 3H), 3.20 (s, 3H), 3.04 – 2.82 (m, 3H), 2.51 – 2.25 (m, 2H). **^{13}C NMR** (75 MHz, $CDCl_3$) δ 172.3, 172.2, 148.6, 140.7, 128.4, 127.7, 127.4, 108.6, 85.8, 58.7, 57.3, 52.8, 49.5, 42.2, 35.5. **HPLC** (OJ-H (250 × 4.6 mm, 5 µm), 99.5:0.5 hexane:*i*-PrOH, 1.0 mL/min, 25 °C, 210 nm): en1 (major, 99.5%) 17.99 min, (minor, 0.5%) 20.25 min. **$[\alpha]^{24.6}_D$** +72.5 (c 1.02, $CHCl_3$).

Dimethyl (*S*)-3-((*R*)-Ethoxy(phenyl)methyl)-4-methylenecyclopentane-1,1-dicarboxylate (2.77o)

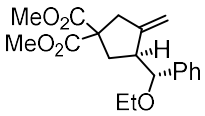

Prepared following general procedure **GP11**, using enyne **2.76a** (28.6 mg, 0.100 mmol) and anhydrous EtOH (29.2 µL, 0.500 mmol, 5.0 equiv) as a nucleophile in 1,4-dioxane (1.0 mL, 0.1M), at 25 ºC for 5 h. The crude product was purified by FCC (silica, CyH:EtOAc 100:0 to 90:10). Compound **2.77o** was obtained as a white solid (32.1 mg, 0.966 mmol, 97% yield) with 98.5:1.5 *er*. Spectroscopic data matched those reported in the literature.[101] The absolute configuration was assigned by comparison to **2.77v**. **^{1}H NMR** (300 MHz, $CDCl_3$) δ 7.39 – 7.26 (m, 5H), 7.26 – 7.19 (m, 1H), 4.93 – 4.87 (m, 1H), 4.47 (s, 1H), 4.25 (d, *J* = 6.1 Hz, 1H), 3.74 (s, 3H), 3.67 (s, 3H), 3.46 – 3.22 (m, 2H), 3.07 – 2.79 (m, 3H), 2.45 (ddd, *J* = 13.5, 8.1, 1.4 Hz, 1H), 2.35 (dd, *J* = 13.5, 8.7 Hz, 1H), 1.13 (t, *J* = 7.0 Hz, 3H). **^{13}C NMR** (75 MHz, $CDCl_3$) δ 172.3, 172.3, 148.7, 141.5, 128.3, 127.6, 127.3, 108.6, 83.9, 64.8, 58.8, 52.8, 49.5, 42.3, 35.5, 15.3. **HPLC** (OJ-H (250 × 4.6 mm, 5 µm), 99:1 hexane:*i*-PrOH, 1.0 mL/min, 25 °C, 210 nm): en1 (major, 98.5%) 20.48 min, en2 (minor, 1.5%) 25.91 min. **$[\alpha]^{24.6}_D$** +74.6 (c 1.12, $CHCl_3$).

Dimethyl (*S*)-3-((*R*)-Isopropoxy(phenyl)methyl)-4-methylenecyclopentane-1,1-dicarboxylate (2.77p)

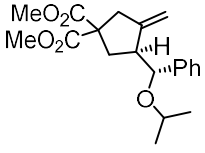

Prepared following general procedure **GP11**, using enyne **2.76a** (28.6 mg, 0.100 mmol) and anhydrous 2-propanol (38.2 µL, 0.500 mmol, 5.0 equiv) as a nucleophile in 1,4-dioxane (1.0 mL, 0.1M), at 25 ºC for 5 h. The crude product was purified by FCC (silica, CyH:EtOAc 100:0 to 90:10). Compound **2.77p** was obtained as a waxy solid (26.0 mg, 0.750 mmol, 75% yield) with >99:1 *er*. The absolute configuration was assigned by comparison to **2.77v**. **^{1}H NMR** (300 MHz, $CDCl_3$) δ 7.37 – 7.24 (m, 7H), 4.91 (s, 1H), 4.49 (s, 1H), 4.38 (d, *J* = 5.8 Hz, 1H), 3.74 (s, 3H), 3.67 (s, 3H), 3.45 (hept, *J* = 6.1 Hz, 1H), 2.99 (dq, *J* = 15.8, 2.7 Hz, 1H), 2.91 – 2.78 (m, 2H), 2.48 – 2.27 (m, 2H), 2.17 (s, 2H), 1.09 (d, *J* = 6.0 Hz, 3H), 1.03 (d, *J* = 6.2 Hz, 3H). **^{13}C NMR** (75 MHz, $CDCl_3$) δ 172.5, 172.30 157.4, 149.4, 136.1, 133.0, 128.8, 127.8, 127.0, 122.0, 121.8, 120.6, 119.6, 119.4, 118.7, 111.0, 110.8, 108.9, 58.8, 55.6, 52.9, 52.8, 46.8, 41.8, 40.2, 39.4. **HPLC** (OJ-H (250 × 4.6 mm, 5

101.Buzas, A. K.; Istrate, F. M.; Gagosz, F. *Angew. Chem. Int. Ed.* **2007**, *46*, 1141–1144.

μm), 99:1 hexane:*i*-PrOH, 1.0 mL/min, 25 °C, 210 nm): en1 (major, 100%) 18.83 min. **[α]$^{24.6}_{D}$** +83.6 (c 1.09, $CHCl_3$).

Dimethyl (*S*)-3-((*R*)-(Benzyloxy)(phenyl)methyl)-4-methylenecyclopentane-1,1-dicarboxylate (2.77q)

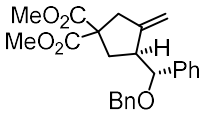

Prepared following general procedure **GP11**, using enyne **2.76a** (28.6 mg, 0.100 mmol) and benzyl alcohol (41.6 μL, 0.400 mmol, 4.0 equiv) as a nucleophile in 1,4-dioxane (1.0 mL, 0.1M), at 25 ºC for 6 h. The crude product was purified by FCC (silica, CyH:EtOAc 90:10 to 80:20). Compound **2.77q** was obtained as a colorless oil (36.0 mg, 0.910 mmol, 91% yield) with 98.5:1.5 *er*. **^{1}H NMR** (300 MHz, $CDCl_3$) δ 7.42 – 7.26 (m, 10H), 4.95 – 4.87 (m, 1H), 4.53 – 4.36 (m, 3H), 4.25 (d, *J* = 11.8 Hz, 1H), 3.71 (s, 3H), 3.68 (s, 3H), 3.04 – 2.81 (m, 3H), 2.59 – 2.32 (m, 2H). **^{13}C NMR** (75 MHz, $CDCl_3$) δ 172.3, 172.2, 148.3, 140.8, 138.6, 128.4, 128.3, 127.8, 127.5, 108.9, 83.5, 70.9, 58.8, 52.8, 49.5, 42.3, 35.6. **HRMS (ESI +)** calculated for $[C_{24}H_{26}NaO_5]^{+\cdot}$ [M+Na] $^{+\cdot}$ 4171672 m/z; found 4171667m/z. **SFC** (OJ (100 × 3 mm, 3 μm), 99:1 CO_2:MeOH, 1.2 mL/min, 35 ºC, BPR 150 bar, 210 nm): en1 (major, 98.5%) 1.76 min, en2 (minor, 1.5%) 2.45 min. **[α]$^{24.6}_{D}$** +78.2 (c 1.43, $CHCl_3$).

Dimethyl (*S*)-3-((*R*)-Allyloxy(phenyl)methyl)-4-methylenecyclopentane-1,1-dicarboxylate (2.77r)

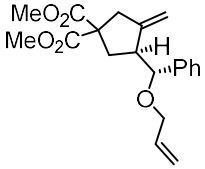

Prepared following general procedure **GP11**, using enyne **2.76a** (28.6 mg, 0.100 mmol) and allyl alcohol (27.1 μL, 0.400 mmol, 4.0 equiv) as a nucleophile in 1,4-dioxane (1.0 mL, 0.1M), at 25 ºC for 6 h. The crude product was purified by FCC (silica, CyH:EtOAc 90:10 to 80:20). Compound **2.77r** was obtained as a colorless oil (34.0 mg, 0.987 mmol, 99% yield) with 98.5:1.5 *er*. Spectroscopic data matched those reported in the literature.[101] The absolute configuration was assigned by comparison to **2.77v**. **^{1}H NMR** (500 MHz, $CDCl_3$) δ 7.35 – 7.26 (m, 5H), 5.91 – 5.78 (m, 1H), 5.21 (dq, *J* = 17.2, 1.7 Hz, 1H), 5.12 (dd, *J* = 10.4, 1.6 Hz, 1H), 4.92 (s, 1H), 4.50 (s, 1H), 4.34 (d, *J* = 5.9 Hz, 1H), 3.92 (ddt, *J* = 12.9, 5.0, 1.5 Hz, 1H), 3.77 – 3.70 (m, 4H), 3.68 (s, 3H), 3.01 – 2.85 (m, 3H), 2.46 (ddd, *J* = 13.4, 8.1, 1.5 Hz, 1H), 2.37 (dd, *J* = 13.5, 8.9 Hz, 1H). **^{13}C NMR** (126 MHz, $CDCl_3$) δ 172.3, 172.2, 148.6, 141.098, 135.1, 128.4, 127.7, 127.4, 116.6, 108.8, 83.2, 70.0, 58.8, 52.8, 49.5, 42.3, 35.5. **HPLC** (OJ-H (250 × 4.6 mm, 5 μm), 99:1 hexane:*i*-PrOH, 1.0 mL/min, 25 °C, 210 nm): en1 (major, 98.5%) 8.59 min, en2 (minor, 1.5%). **[α]$^{24.6}_{D}$** +77.6 (c 1.18, $CHCl_3$).

Dimethyl (*S*)-3-Methylene-4-((*R*)-((3-oxocyclohex-1-en-1-yl)oxy)(phenyl)methyl)cyclopentane-1,1-dicarboxylate (2.77s)

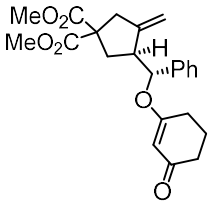

Prepared following general procedure **GP11**, using enyne **2.76a** (28.6 mg, 0.100 mmol) and cyclohexan-1,3-dione (22.4 mg, 0.200 mmol, 2.0 equiv) as a nucleophile in 1,4-dioxane (1.0 mL, 0.1M), at 25 ºC for 6 h. The crude product was purified by FCC (silica, CyH:EtOAc 90:10 to 80:20). Compound **2.77s** was obtained as a colorless oil (35.3 mg, 0.886 mmol, 89% yield) with 97.5:2.5 *er*. Spectroscopic data matched those reported in the literature.[59e] The absolute configuration was assigned by comparison to **2.77v**. **^{1}H NMR** (300 MHz, $CDCl_3$) δ 7.38 – 7.26 (m, 3H), 7.20 (dd, *J* = 7.9, 1.5 Hz, 2H), 5.17 (s, 1H), 5.12 (d, *J* = 5.2 Hz, 1H), 5.04 – 4.97 (m, 1H), 4.66 – 4.57 (m, 1H), 3.73 (s, 3H), 3.68 (s, 3H), 3.07 (d, *J* = 5.1 Hz, 1H), 2.94 (s, 2H), 2.42 (dt, *J* = 14.3, 7.1 Hz, 3H), 2.35 – 2.17 (m, 3H), 1.95 (q, *J* = 6.6 Hz, 2H).**^{13}C NMR** (75 MHz, $CDCl_3$) δ 199.7, 176.7, 171.9, 171.82 147.2, 138.1, 128.8, 128.3, 126.3, 109.4, 105.2, 81.8, 58.6,

53.0, 49.1, 42.1, 36.7, 34.9, 29.1, 21.2. **SFC** (IC (100 × 3 mm, 3 μm), 80:20 CO_2:EtOH, 1.2 mL/min, 35 ºC, BPR 150 bar, 210 nm): en1 (major, 97.5%) 1.55 min, en2 (minor, 2.5%) 1.91 min. **[α]$^{24.6}_{D}$** +59.2 (c 1.4, $CHCl_3$).

Dimethyl (*R*)-3-((*R*)-(1*H*-indol-3-yl)(4-(trifluoromethyl)phenyl)methyl)-4-methylenecyclopentane-1,1-dicarboxylate (2.77t)

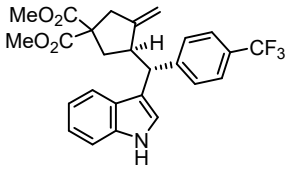

Prepared following general procedure **GP11,** using enyne **2.76e** (35.4 mg, 0.100 mmol) and indole (14.1 mg, 0.120 mmol, 1.2 equiv) as a nucleophile in 1,4-dioxane (1.0 mL, 0.1M), at 25 ºC for 6 h. The crude product was purified by FCC (silica, CyH:EtOAc 90:10 to 80:20). Compound **2.77t** was obtained as a white solid (47.0 mg, 0.997 mmol, >99% yield) with >99:1 *er*. The absolute configuration was assigned by comparison to **2.77v**. **M.p.** 61 ºC. **^{1}H NMR** (300 MHz, $CDCl_3$) δ 8.11 (s, 1H), 7.55 – 7.40 (m, 5H), 7.41 – 7.32 (m, 1H), 7.25 – 7.14 (m, 2H), 7.12 – 7.02 (m, 1H), 4.82 (s, 1H), 4.24 (d, *J* = 10.4 Hz, 1H), 4.16 – 4.06 (m, 1H), 3.74 (d, *J* = 3.7 Hz, 3H), 3.66 (s, 3H), 3.59 – 3.46 (m, 1H), 3.15 (dq, *J* = 16.0, 2.5 Hz, 1H), 2.91 (dd, *J* = 16.0, 1.5 Hz, 1H), 2.78 (ddd, *J* = 13.7, 7.9, 1.6 Hz, 1H), 2.00 (dd, *J* = 13.7, 8.2 Hz, 1H). **^{13}C NMR** (75 MHz, $CDCl_3$) δ 172.3, 172.2, 148.7, 148.5, 136.3, 128.9, 127.1, 125.2 (q, *J* = 3.8 Hz), 122.5, 121.6, 119.8, 119.3, 117.9, 111.3, 110.5, 58.5, 53.0, 52.9, 47.9, 46.9, 41.7, 39.9. **^{19}F NMR** (282 MHz, $CDCl_3$) δ –62.3. **HRMS (ESI +)** calculated for $[C_{26}H_{24}F_3NNaO_4]^{+\cdot}$ $[M+Na]^{+\cdot}$ 494.1550 m/z; found 494.1532 m/z. **SFC** (OD (100 × 3 mm, 3 μm), 85:15 CO_2:*i*-PrOH, 1.2 mL/min, 35 ºC, BPR 150 bar, 210 nm): en2 (major, 100%) 1.74 min. **[α]$^{24.6}_{D}$** –4.6 (c 0.31, $CHCl_3$).

Dimethyl (*R*)-3-((*R*)-(1*H*-Indol-3-yl)(4-nitrophenyl)methyl)-4-methylenecyclopentane-1,1-dicarboxylate (2.77u)

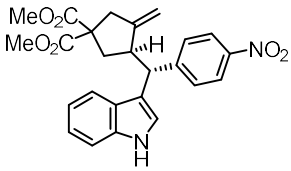

Prepared following general procedure **GP11,** using enyne **2.76f** (33.1 mg, 0.100 mmol) and indole (14.1 mg, 0.120 mmol, 1.2 equiv) as a nucleophile in 1,4-dioxane (1.0 mL, 0.1M), at 25 ºC for 22 h. The crude product was purified by FCC (silica, CyH:EtOAc 90:10 to 80:20). Compound **2.77u** was obtained as a yellow solid (43.0 mg, 0.959 mmol, 96% yield) with >99:1 *er*. The absolute configuration was assigned by comparison to **2.77v**. **M.p.** 75–77 ºC. **^{1}H NMR** (500 MHz, $CDCl_3$) δ 8.14 (s, 1H), 8.11 – 8.05 (m, 2H), 7.46 (d, *J* = 8.7 Hz, 2H), 7.43 (d, *J* = 8.3 Hz, 1H), 7.35 (d, *J* = 8.2 Hz, 1H), 7.20 (d, *J* = 2.5 Hz, 1H), 7.17 (ddd, *J* = 8.2, 7.0, 1.1 Hz, 1H), 7.05 (ddd, *J* = 8.0, 7.0, 1.0 Hz, 1H), 4.80 (d, *J* = 1.6 Hz, 1H), 4.26 (d, *J* = 10.6 Hz, 1H), 4.07 (dt, *J* = 2.8, 1.5 Hz, 1H), 3.72 (s, 3H), 3.64 (s, 3H), 3.51 (dtd, *J* = 9.9, 7.9, 1.8 Hz, 1H), 3.15 (dq, *J* = 15.9, 2.3 Hz, 1H), 2.94 – 2.86 (m, 1H), 2.79 (ddd, *J* = 13.8, 7.9, 1.5 Hz, 1H), 2.00 (dd, *J* = 13.8, 7.9 Hz, 1H). **^{13}C NMR** (126 MHz, $CDCl_3$) δ 172.2, 172.1, 152.2, 148.5, 146.5, 136.4, 129.4, 126.9, 123.6, 122.7, 121.8, 120.0, 119.1, 117.1, 111.4, 110.7, 58.5, 53.0, 53.0, 48.0, 46.9, 41.6, 39.8, 31.1. **HRMS (ESI +)** calculated for $[C_{25}H_{24}N_2NaO_6]^{+\cdot}$ $[M+Na]^{+\cdot}$ 471.1527 m/z; found 471.1527 m/z. **SFC** (IA (100 × 3 mm, 3 μm), 80:20 CO_2:*i*-PrOH, 1.2 mL/min, 35 ºC, BPR 150 bar, 210 nm): en2 (major, 100%) 3.08 min. **[α]$^{24.6}_{D}$** –5.45 (c 0.99, $CHCl_3$).

Dimethyl (*R*)-3-((*R*)-(4-Chlorophenyl)(1H-indol-3-yl)methyl)-4-methylenecyclopentane-1,1-dicarboxylate (2.77v)

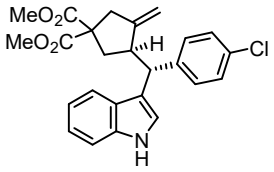

Prepared following general procedure **GP11,** using enyne **2.76g** (32.1 mg, 0.100 mmol) and indole (14.1 mg, 0.120 mmol, 1.2 equiv) as a nucleophile in 1,4-dioxane (1.0 mL, 0.1M), at 25 ºC for 22 h. The crude product was purified by FCC (silica, CyH:EtOAc 90:10 to 80:20). Compound **2.77v** was obtained as a white solid (43.1 mg, 0.984 mmol, 98% yield) with 99:1 *er*. The absolute configuration was assigned by X-Ray crystallography. **M.p.** 129 ºC. **^{1}H NMR** (300 MHz, , $CDCl_3$) δ 8.10 (s, 1H), 7.47 (d, *J* = 8.0 Hz, 1H), 7.32 (d, *J* = 8.1 Hz, 1H), 7.25 – 7.10 (m, 6H), 7.04 (td, *J* = 7.5, 7.1, 1.0 Hz, 1H), 4.81 (s, 1H), 4.28 – 4.01 (m, 2H), 3.72 (s, 3H), 3.63 (s, 3H), 3.53 – 3.36 (m, 1H), 3.12 (dq, *J* = 15.9, 2.4 Hz, 1H), 2.89 (dd, *J* = 15.9, 1.3 Hz, 1H), 2.75 (ddd, *J* = 13.6, 7.9, 1.4 Hz, 1H), 1.97 (dd, *J* = 13.7, 8.2 Hz, 1H). **^{13}C NMR** (75 MHz, $CDCl_3$) δ 172.3, 172.2, 148.7, 143.0, 136.3, 131.8, 130.0, 128.3, 127.1, 122.3, 121.5, 119.6, 119.3, 118.2, 111.3, 110.5, 58.6, 53.0, 52.9, 47.5, 46.9, 41.8, 39.9. **HRMS (ESI +)** calculated for $[C_{25}H_{24}ClNNaO_4]^{+\cdot}$ $[M+Na]^{+\cdot}$ 460.1286 m/z; found 460.1296 m/z. **SFC** (OJ (100 × 3 mm, 3 μm), 80:20 CO_2:EtOH, 1.2 mL/min, 35 ºC, BPR 150 bar, 210 nm): en1 (minor, 1%) 1.93 min, en2 (major, 99%) 2.43 min. **$[\alpha]^{24.6}_D$** +2.41 (c 1.59, $CHCl_3$). **XRD:** Single crystals could be obtained by slow diffusion of pentane into a solution of **2.77v** in CH_2Cl_2 at −20 °C.

Dimethyl (*R*)-3-((*R*)-(1*H*-indol-3-yl)(4-methoxyphenyl)methyl)-4-methylenecyclopentane-1,1-dicarboxylate (2.77w)

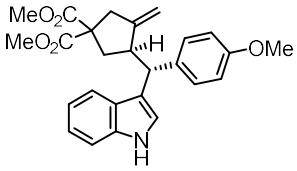

Prepared following general **GP11,** using enyne **2.76h** (31.6 mg, 0.100 mmol) and indole (14.1 mg, 0.120 mmol, 1.2 equiv) as a nucleophile in 1,4-dioxane (1.0 mL, 0.1M), at 25 ºC for 6 h. The crude product was purified by FCC (silica, pentane:EtOAc 90:10 to 80:20). Compound **2.77w** was obtained as a colorless oil (39.0 mg, 0.900 mmol, 90% yield) with 87:13 *er*. The absolute configuration was assigned by comparison to **2.77v**. **M.p.** 50–54 ºC. **^{1}H NMR** (300 MHz, $CDCl_3$) δ 8.07 (brs, 1H), 7.55 (d, *J* = 7.9 Hz, 1H), 7.33 (d, *J* = 8.0 Hz, 1H), 7.27 – 7.20 (m, 2H), 7.19 – 7.10 (m, 2H), 7.10 – 7.03 (m, 1H), 6.84 – 6.72 (m, 2H), 4.83 (s, 1H), 4.19 (s, 1H), 4.14 (d, *J* = 10.3 Hz, 1H), 3.76 (s, 3H), 3.75 (s, 3H), 3.66 (s, 3H), 3.50 (q, *J* = 7.7 Hz, 1H), 3.13 (d, *J* = 15.9 Hz, 1H), 2.91 (d, *J* = 15.9 Hz, 1H), 2.76 (dd, *J* = 13.6, 8.0 Hz, 1H), 1.98 (dd, *J* = 13.6, 8.5 Hz, 1H). **^{13}C NMR** (75 MHz, $CDCl_3$) δ 172.4, 172.2, 157.9, 149.0, 136.7, 136.3, 129.5, 127.3, 122.1, 121.4, 119.5, 119.5, 119.0, 113.6, 111.2, 110.2, 58.6, 55.3, 52.9, 52.8, 47.3, 47.0, 41.9, 40.0. **HRMS (ESI +)** calculated for $[C_{26}H_{27}NNaO_5]^{+\cdot}$ $[M+Na]^{+\cdot}$ 456.1781 m/z; found 434.1794 m/z. **SFC** (IG (100 × 3 mm, 3 μm), 80:20 CO_2:*i*-PrOH, 1.2 mL/min, 35 ºC, BPR 150 bar, 210 nm): en1 (minor, 13%) 1.58 min, en2 (major, 87%) 2.04 min. **$[\alpha]^{24.6}_D$** +3.85 (c 1.28, $CHCl_3$).

Dimethyl (*R*)-3-((*R*)-(1*H*-indol-3-yl)(3-methoxyphenyl)methyl)-4-methylenecyclopentane-1,1-dicarboxylate (2.77x)

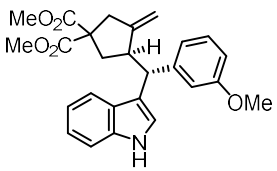

Prepared following general procedure **GP11,** using enyne **2.76i** (31.6 mg, 0.100 mmol) and indole (14.1 mg, 0.120 mmol, 1.2 equiv) as a nucleophile in 1,4-dioxane (1.0 mL, 0.1M), at 25 ºC for 6 h. The crude product was purified by FCC (silica, CyH:EtOAc 90:10 to 85:15). Compound **2.77x** was obtained as a white solid (42.4 mg, 0.978 mmol, 98% yield) with >99:1 *er*. The absolute configuration was assigned by comparison to **2.77v**. **M.p.** 67 ºC. **^{1}H NMR** (500 MHz, $CDCl_3$) δ 8.09 (s, 1H), 7.57 (dq, *J* = 8.0, 0.8 Hz, 1H), 7.30 (dt, *J* = 8.1, 0.9 Hz, 1H), 7.17 – 7.10 (m, 2H), 7.05 (ddd, *J* = 8.0, 7.0, 1.0 Hz, 1H), 6.94 (dt, *J* = 7.7, 1.3

Hz, 1H), 6.89 (dd, *J* = 2.6, 1.6 Hz, 1H), 6.67 (ddd, *J* = 8.2, 2.6, 0.9 Hz, 1H), 4.81 (dt, *J* = 2.5, 1.4 Hz, 1H), 4.20 (h, *J* = 1.0 Hz, 1H), 4.15 – 4.09 (m, 1H), 3.74 (s, 3H), 3.72 (s, 3H), 3.63 (s, 3H), 3.52 (dq, *J* = 8.3, 1.9 Hz, 1H), 3.12 (dq, *J* = 16.0, 2.4 Hz, 1H), 2.90 (dq, *J* = 15.9, 1.5 Hz, 1H), 2.74 (ddd, *J* = 13.7, 7.9, 1.7 Hz, 1H), 1.96 (dd, *J* = 13.7, 8.5 Hz, 1H). **^{13}C NMR** (126 MHz, $CDCl_3$) δ 172.4, 172.2, 159.5, 148.9, 146.2, 136.3, 129.1, 127.3, 122.1, 121.5, 121.2, 119.5, 119.5, 118.6, 114.8, 111.2, 111.1, 110.2, 58.5, 55.2, 52.9, 52.8, 48.1, 46.8, 41.9, 40.0. **HRMS (ESI +)** calculated for $[C_{26}H_{28}NO_5]^{+\cdot}$ $[M+H]^{+\cdot}$ 434.1962 m/z; found 434.1947 m/z. **SFC** (OD (100 × 3 mm, 3 μm), 85:15 CO_2:MeOH, 1.2 mL/min, 35 ºC, BPR 150 bar, 210 nm): en1 (major, 99.5%) 2.67 min, en2 (minor, 0.5%) 3.32 min. **$[\alpha]^{24.6}_D$** +4.64 (c 1.00, $CHCl_3$).

Dimethyl (*R*)-3-((*R*)-(1H-indol-3-yl)(3-nitrophenyl)methyl)-4-methylenecyclopentane-1,1-dicarboxylate (2.77y)

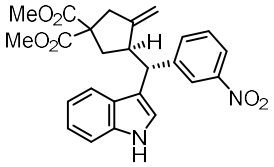

Prepared following general procedure **GP11,** using enyne **2.76j** (33.1 mg, 0.100 mmol) and indole (14.1 mg, 0.120 mmol, 1.2 equiv) as a nucleophile in 1,4-dioxane (1.0 mL, 0.1M), at 25 ºC for 6 h. The crude product was purified by FCC (silica, CyH:EtOAc 90:10 to 80:20). Compound **2.77y** was obtained as a yellow solid (42.7 mg, 0.952 mmol, 95% yield) with >99:1 *er*. absolute configuration was assigned by comparison to **2.77v**. **M.p.** 57–61 ºC. **^{1}H NMR** (300 MHz, $CDCl_3$) δ 8.23 – 8.12 (m, 2H), 7.99 (ddd, *J* = 8.2, 2.3, 1.0 Hz, 1H), 7.68 – 7.60 (m, 1H), 7.45 (d, *J* = 7.9 Hz, 1H), 7.40 (d, *J* = 7.9 Hz, 1H), 7.37 – 7.33 (m, 1H), 7.23 (d, *J* = 2.3 Hz, 1H), 7.20 – 7.11 (m, 1H), 7.10 – 6.98 (m, 1H), 4.80 (s, 1H), 4.26 (d, *J* = 10.6 Hz, 1H), 4.02 (s, 1H), 3.73 (s, 3H), 3.64 (s, 3H), 3.54 – 3.44 (m, 1H), 3.16 (dq, *J* = 15.9, 1.9 Hz, 1H), 2.90 (d, *J* = 16.8 Hz, 1H), 2.85 – 2.76 (m, 1H), 2.00 (dd, *J* = 13.8, 7.7 Hz, 1H). **^{13}C NMR** (75 MHz, $CDCl_3$) δ 172.2, 148.5, 148.2, 146.7, 136.4, 135.0, 129.1, 126.9, 123.4, 122.6, 121.7, 121.5, 119.9, 119.02, 117.3, 111.4, 110.9, 58.6, 53.0, 52.9, 47.8, 47.1, 41.6, 39.8. **HRMS (ESI +)** calculated for $[C_{25}H_{24}N_2NaO_6]^{+\cdot}$ $[M+H]^{+\cdot}$ 471.1527 m/z; found 471.1540 m/z. **SFC** (IB-N (100 × 3 mm, 3 μm), 70:30 CO_2:*i*-PrOH, 1.2 mL/min, 35 ºC, BPR 150 bar, 210 nm): en1 (major, 99.5%) 1.43 min, en2 (minor, 0.5%) 1.95 min. **$[\alpha]^{24.6}_D$** –13.45 (c 1.04, $CHCl_3$).

Dimethyl (*R*)-3-((*R*)-(1*H*-indol-3-yl)(2-methoxyphenyl)methyl)-4-methylenecyclopentane-1,1-dicarboxylate (2.77z)

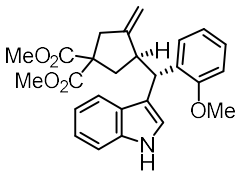

Prepared following general procedure **GP11,** using enyne **2.76k** (31.6 mg, 0.100 mmol) and indole (14.1 mg, 0.120 mmol, 1.2 equiv) as a nucleophile in 1,4-dioxane (1.0 mL, 0.1M), at 25 ºC for 6 h. The crude product was purified by FCC (silica, CyH:EtOAc 90:10 to 85:15). Compound **2.77z** was obtained as a white solid (37.5 mg, 0.865 mmol, 86% yield) with 93:7 *er*. The absolute configuration was assigned by comparison to **2.77v**. **M.p.** 54–60 ºC. **^{1}H NMR** (300 MHz, $CDCl_3$) δ 8.01 (s, 1H), 7.56 (d, *J* = 7.9 Hz, 1H), 7.30 (d, *J* = 8.0 Hz, 1H), 7.23 (dd, *J* = 7.5, 1.6 Hz, 1H), 7.19 – 6.99 (m, 4H), 6.80 (t, *J* = 7.7 Hz, 2H), 4.78 (d, *J* = 10.8 Hz, 1H), 4.69 (s, 1H), 4.04 (s, 1H), 3.85 (s, 3H), 3.72 (s, 3H), 3.64 (s, 3H), 3.45 (q, *J* = 8.1 Hz, 1H), 3.21 (d, *J* = 15.7 Hz, 1H), 2.86 (d, *J* = 15.7 Hz, 1H), 2.77 (dd, *J* = 13.7, 7.9 Hz, 1H), 1.98 (dd, *J* = 13.7, 7.9 Hz, 1H). **^{13}C NMR** (75 MHz, $CDCl_3$) δ 172.6, 172.3, 157.4, 149.4, 136.1, 133.1, 128.8, 127.8, 127.0, 122.0, 121.8, 120.6, 119.7, 119.4, 118.7, 111.0, 110.8, 108.9, 58.85 55.6, 52.9, 52.8, 46.8, 41.8, 40.2, 39.5. **HRMS (ESI +)** calculated for $[C_{26}H_{27}NNaO_5]^{+\cdot}$ $[M+Na]^{+\cdot}$ 456.1781 m/z; found 456.1795 m/z. **SFC** (IC (100 × 3 mm, 3 μm), 90:10 CO_2:EtOH, 1.2 mL/min, 35 ºC, BPR 150 bar, 210 nm): en1 (minor, 7%) 2.13 min, en2 (major, 93%) 2.55 min. **$[\alpha]^{24.6}_D$** –35.60 (c 1.10, $CHCl_3$).

Dimethyl (*R*)-3-((*R*)-(1*H*-indol-3-yl)(2-fluorophenyl)methyl)-4-methylenecyclopentane-1,1-dicarboxylate (2.77aa)

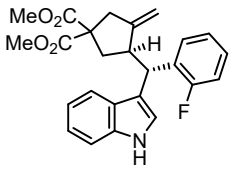

Prepared following general procedure **GP11,** using enyne **2.76l** (30.4 mg, 0.100 mmol) and indole (14.1 mg, 0.120 mmol, 1.2 equiv) as a nucleophile in 1,4-dioxane (1.0 mL, 0.1M), at 25 ºC for 30 h. The crude product was purified by FCC (silica, CyH:EtOAc 90:10 to 80:20). Compound **2.77aa** was obtained as a white solid (31.0 mg, 0.736 mmol, 74% yield) with 98.5:1.5 *er*. The absolute configuration was assigned by comparison to **2.77v**. **M.p.** 54–58 ºC. **^{1}H NMR** (300 MHz, $CDCl_3$) δ 8.07 (s, 1H), 7.56 (d, *J* = 7.7 Hz, 1H), 7.36 – 7.26 (m, 3H), 7.22 (d, *J* = 2.3 Hz, 1H), 7.19 – 7.12 (m, 1H), 7.11 – 7.02 (m, 2H), 7.01 – 6.92 (m, 2H), 4.76 (s, 1H), 4.54 (d, *J* = 11.1 Hz, 1H), 4.07 (s, 1H), 3.72 (s, 3H), 3.64 (s, 3H), 3.54 – 3.43 (m, 1H), 3.26 – 3.13 (m, 1H), 2.92 – 2.83 (m, 1H), 2.82 – 2.73 (m, 1H), 1.97 (dd, *J* = 13.8, 7.6 Hz, 1H). **^{13}C NMR** (75 MHz, $CDCl_3$) δ 172.4, 172.1, 149.0, 136.2, 131.4 (d, *J* = 13.8 Hz), 129.7 (d, *J* = 4.4 Hz), 127.7 (d, *J* = 8.4 Hz), 127.4, 124.0 (d, *J* = 3.4 Hz), 121.89, 121.87, 121.0 (d, *J* = 198.9 Hz), 119.2, 117.6, 115.3 (d, *J* = 23.1 Hz), 111.2, 109.8, 58.8, 52.9 (d, *J* = 5.9 Hz), 46.1, 41.7, 40.2. **^{19}F NMR** (282 MHz, $CDCl_3$) δ -117.8. **HRMS (ESI +)** calculated for $[C_{17}H_{17}FNaO_4]^{+\cdot}$ $[M+Na]^{+\cdot}$ 327.1003 m/z; found 327.1005 m/z. **SFC** (OJ (100 × 3 mm, 3 μm), 80:20 CO_2:*i*-PrOH, 1.2 mL/min, 35 ºC, BPR 150 bar, 210 nm): en1 (minor, 1.5%) 2.28 min, en2 (major, 98.5%) 3.03 min. **$[\alpha]^{24.6}_D$** –23.33 (c 1.01, $CHCl_3$).

Dimethyl (*R*)-3-((*R*)-(1*H*-indol-3-yl)(naphthalen-1-yl)methyl)-4-methylenecyclopentane-1,1-dicarboxylate (2.77ab)

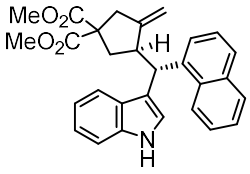

Prepared following general procedure **GP11,** using enyne **2.76m**, 33.1 mg, 0.100 mmol) and indole (14.1 mg, 0.120 mmol, 1.2 equiv) as a nucleophile in 1,4-dioxane (1.0 mL, 0.1M), at 25 ºC for 6 h. The crude product was purified by FCC (silica, CyH:EtOAc 90:10 to 80:20). Compound **2.77ab** was obtained as a white solid (32.3 mg, 0.712 mmol, 70% yield) with 98.5:1.5 *er*. The absolute configuration was assigned by comparison to **2.77v**. **M.p.** 68–71 ºC. **^{1}H NMR** (300 MHz, , $CDCl_3$) δ 8.39 – 8.23 (m, 1H), 7.99 (s, 1H), 7.82 (dd, *J* = 7.7, 1.8 Hz, 1H), 7.68 (d, *J* = 8.1 Hz, 1H), 7.60 (dd, *J* = 7.3, 1.2 Hz, 1H), 7.54 – 7.33 (m, 4H), 7.31 – 7.26 (m, 1H), 7.18 – 7.06 (m, 2H), 6.99 (ddd, *J* = 8.1, 7.0, 1.1 Hz, 1H), 5.19 (d, *J* = 9.4 Hz, 1H), 4.73 – 4.62 (m, 1H), 4.25 – 4.15 (m, 1H), 3.70 (s, 3H), 3.67 (s, 3H), 3.13 (dd, *J* = 16.4, 2.2 Hz, 1H), 2.94 (d, *J* = 16.2 Hz, 1H), 2.69 (dd, *J* = 13.5, 7.7 Hz, 1H), 2.23 (dd, *J* = 13.6, 9.1 Hz, 1H). **^{13}C NMR** (75 MHz, $CDCl_3$) δ 172.5, 172.4, 149.4, 140.5, 136.3, 134.0, 132.3, 129.0, 127.4, 126.8, 126.0, 125.5, 125.3, 125.14, 123.6, 122.4, 122.1, 119.6, 119.6, 118.7, 111.1, 109.6, 58.5, 52.9, 52.9, 47.5, 41.9, 41.6, 39.8. **HRMS (ESI +)** calculated for $[C_{29}H_{27}NNaO_4]^{+\cdot}$ $[M+Na]^{+\cdot}$ 476.1832 m/z; found 476.1840 m/z. **SFC** (IC (100 × 3 mm, 3 μm), 85:15 CO_2:*i*-PrOH, 1.2 mL/min, 35 ºC, BPR 150 bar, 210 nm): en1 (minor, 1.5%) 2.02 min, en2 (major, 98.5%) 2.55 min. **$[\alpha]^{24.6}_D$** –45.81 (c 1.29, $CHCl_3$).

Dimethyl (*S*)-3-(2-(1*H*-indol-3-yl)propan-2-yl)-4-methylenecyclopentane-1,1-dicarboxylate (2.77ac)

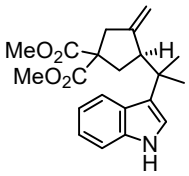

Prepared following general procedure **GP11,** using enyne **2.76n** (23.8 mg, 0.100 mmol) and indole (23.4 mg, 0.200 mmol, 2.0 equiv) as a nucleophile in toluene (1.0 mL, 0.1M), at -10 ºC for 14 h. The crude product was purified by FCC (silica, CyH:EtOAc 90:10 to 85:15). Compound **2.77ac** was obtained as a white solid (32.3 mg, 0.712 mmol, 70% yield) with 99:1 *er*. Spectroscopic data matched those reported in the literature.[35a] The absolute configuration was assigned by comparison to **2.77v**. **M.p.** 114–117 ºC. **^{1}H NMR** (300 MHz, $CDCl_3$) δ 7.94 (s, 1H), 7.84 (d, *J* =

8.0 Hz, 1H), 7.35 (d, *J* = 8.0 Hz, 1H), 7.24 – 7.14 (m, 1H), 7.08 (td, *J* = 7.6, 1.2 Hz, 1H), 6.93 (d, *J* = 2.4 Hz, 1H), 4.93 (s, 1H), 4.45 (s, 1H), 3.67 (s, 6H), 3.45 (t, *J* = 8.7 Hz, 1H), 2.91 – 2.73 (m, 2H), 2.42 (dd, *J* = 13.7, 8.4 Hz, 1H), 1.88 (dd, *J* = 13.7, 9.2 Hz, 1H), 1.45 (s, 3H), 1.36 (s, 3H). **^{13}C NMR** (75 MHz, $CDCl_3$) δ 172.3, 172.1, 149.1, 137.3, 125.8, 124.7, 121.8, 121.3, 121.1, 119.2 111.4, 110.6, 58.8, 52.7, 49.6, 44.2, 38.0, 36.6, 25.7, 24.8. **SFC** (OJ (100 × 3 mm, 3 μm), 80:20 CO_2:MeOH, 1.2 mL/min, 35 ºC, BPR 150 bar, 210 nm): en1 (minor, 1%) 2.35 min, en2 (minor, 99%) 3.11 min. **$[\alpha]^{24.6}_D$** +32.90 (c 0.84, $CHCl_3$).

Dimethyl (*S*)-3-((*S*)-2-Ethoxy-6-methylhept-5-en-2-yl)-4-methylenecyclopentane-1,1-dicarboxylate (2.77ad)

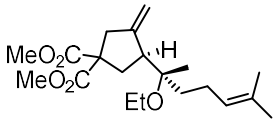

Prepared following general procedure **GP11,** using enyne **2.76o** (30.6 mg, 0.100 mmol) and EtOH (29.2 μL, 0.500 mmol, 5.0 equiv) as a nucleophile in 1,4-dioxane (1.0 mL, 0.1M), at 23 ºC for 14 h. The crude product was purified by FCC (silica, CyH:EtOAc 90:10 to 85:15). Compound **2.77ad** was obtained as a white solid (31.3 mg, 0.925 mmol, 92% yield) with >99:1 *er*. Spectroscopic data matches those reported in the literature.[59n] The absolute configuration was assigned by comparison to **2.77v**. **^{1}H NMR** (300 MHz, $CDCl_3$) δ 5.17 – 5.07 (m, 1H), 5.06 – 4.99 (m, 1H), 4.93 – 4.86 (m, 1H), 3.75 (s, 3H), 3.73 (s, 3H), 3.36 (qd, *J* = 6.9, 1.2 Hz, 2H), 3.03 – 2.87 (m, 2H), 2.87 – 2.77 (m, 1H), 2.56 (ddd, *J* = 13.7, 8.4, 1.7 Hz, 1H), 2.15 (dd, *J* = 13.8, 8.8 Hz, 1H), 2.08 – 1.95 (m, 2H), 1.70 (q, *J* = 1.3 Hz, 3H), 1.69 – 1.51 (m, 6H), 1.15 (t, *J* = 7.0 Hz, 3H), 1.08 (s, 3H). **^{13}C NMR** (75 MHz, $CDCl_3$) δ 172.3, 172.1, 148.8, 131.5, 124.8, 110.6, 78.2, 58.7, 56.2, 52.8, 52.8, 48.4, 44.0, 35.8, 35.4, 25.8, 22.1, 20.1, 17.8, 15.9. **$[\alpha]^{24.6}_D$** +11.7 (c 0.84, $CHCl_3$).

3-((*R*)-((*R*)-4,4-Bis(methoxymethyl)-2-methylenecyclopentyl)(phenyl)methyl)-1*H*-indole (2.77ae)

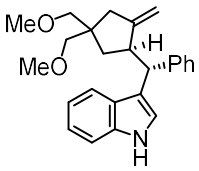

Prepared following general procedure **GP11,** using enyne **2.76c** (25.8 mg, 0.100 mmol) and indole (35.1 mg, 0.300 mmol,3.0 equiv) as a nucleophile in 1,4-dioxane (1.0 mL, 0.1M), at 25 ºC for 6 h. The crude product was purified by FCC (silica, CyH:EtOAc 90:10). Compound **2.77ae** was obtained as a colorless oil (23.5 mg, 0.626 mmol, 63% yield) with 96:4 *er*. The absolute configuration was assigned by comparison to **2.77v**. **HRMS (ESI +)** calculated for $[C_{25}H_{29}NNaO_2]^{+\cdot}$ $[M+Na]^{+\cdot}$ 398.2090 m/z; found 398.2090 m/z. **^{1}H NMR** (300 MHz, $CDCl_3$) δ 8.01 (s, 1H), 7.53 (d, *J* = 8.0 Hz, 1H), 7.38 – 7.30 (m, 3H), 7.27 – 7.20 (m, 2H), 7.18 – 7.09 (m, 3H), 7.04 (ddd, *J* = 8.0, 7.1, 1.1 Hz, 1H), 4.75 (s, 1H), 4.19 (d, *J* = 10.0 Hz, 1H), 4.15 (d, *J* = 0.9 Hz, 1H), 3.45 – 3.32 (m, 4H), 3.29 (s, 3H), 3.25 – 3.20 (m, 4H), 2.39 – 2.20 (m, 2H), 1.91 (dd, *J* = 14.1, 8.1 Hz, 1H), 1.53 (dd, *J* = 13.8, 7.9 Hz, 1H). **^{13}C NMR** (75 MHz, $CDCl_3$) δ 152.2, 144.9, 136.2, 128.6, 127.9, 127.5, 125.8, 121.9, 121.5, 119.5, 119.2, 119.1, 110.9, 108.9, 75.3, 59.3, 59.2, 48.3, 46.9, 45.7, 40.2, 37.9. **SFC** (IB-N (100 × 3 mm, 3 μm), 80:20 CO_2:MeOH, 1.2 mL/min, 35 ºC, BPR 150 bar, 210 nm): en1 (major, 96%) 2.62 min, en2 (minor, 4%) 3.65 min. **$[\alpha]^{24.6}_D$** +45.5 (c 0.27, $CHCl_3$).

Diisopropyl (*R*)-3-((*R*)-(1*H*-Indol-3-yl)(phenyl)methyl)-4-methylenecyclopentane-1,1-dicarboxylate (2.77af)

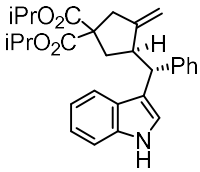

Prepared following general procedure **GP11,** using enyne **2.76b** (34.2 mg, 0.100 mmol) and indole (14.1 mg, 0.120 mmol, 1.2 equiv) as a nucleophile in 1,4-dioxane (1.0 mL, 0.1M), at 25 ºC for 6 h. The crude product was purified by FCC (silica, CyH:EtOAc 90:10). Compound **2.77af** was obtained as a

colorless oil (41.1 mg, 0.916 mmol, 92% yield) with 93:7 *er*. The absolute configuration was assigned by comparison to **2.77v**. **^{1}H NMR** (300 MHz, $CDCl_3$) δ 8.08 (s, 1H), 7.54 (d, *J* = 7.9 Hz, 1H), 7.37 – 7.28 (m, 3H), 7.25 – 7.18 (m, 2H), 7.17 – 7.07 (m, 3H), 7.07 – 6.98 (m, 1H), 5.06 (hept, 1H), 4.95 (hept, *J* = 6.3 Hz, 1H), 4.78 (s, 1H), 4.17 (d, *J* = 10.3 Hz, 1H), 4.13 (s, 1H), 3.60 – 3.44 (m, 1H), 3.17 – 3.00 (m, 1H), 2.86 (dd, *J* = 15.9, 1.3 Hz, 1H), 2.71 (ddd, *J* = 13.5, 7.8, 1.4 Hz, 1H), 1.95 (dd, *J* = 13.6, 8.5 Hz, 1H), 1.21 (d, *J* = 6.3 Hz, 6H), 1.18 (d, *J* = 6.2 Hz, 3H), 1.09 (d, *J* = 6.3 Hz, 3H). **^{13}C NMR** (75 MHz, $CDCl_3$) δ 171.4, 171.3, 149.3, 144.5, 136.2, 128.5, 128.1, 127.23 126.0, 121.9, 121.4, 119.4, 119.3, 118.7, 111.04 109.7, 68.9, 68.8, 58.53, 47.9, 46.8, 41.7, 39.6, 21.6, 21.5, 21.5. **HRMS (ESI +)** calculated for $[C_{29}H_{33}NNaO_4]^{+\cdot}$ $[M+Na]^{+\cdot}$ 482.2302 m/z; found 482.2312 m/z. **SFC** (IB-N (100 × 3 mm, 3 μm), 85:15 CO_2:MeOH, 1.2 mL/min, 35 ºC, BPR 150 bar, 210 nm): en1 (major, 93%) 2.14 min, en2 (minor, 7%) 2.70 min. **$[\alpha]^{24.6}_D$** –0.4 (c 1.14, $CHCl_3$).

3-((*R*)-((*R*)-4-Methylene-1-tosylpyrrolidin-3-yl)(phenyl)methyl)-1*H*-indole (2.77ag)

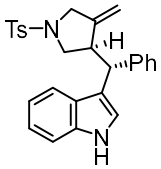

Prepared following general procedure **GP11**, using **Au23** (3.5 mg, 3 mol%), **(*R*)-Ag5** (3.3 mg, 3 mol%), enyne **2.76d** (32.5 mg, 0.100 mmol) and indole (17.6 mg, 0.150 mmol, 1.5 equiv) as a nucleophile in toluene (1.0 mL, 0.1M), at 25 ºC for 24 h. The crude product was purified by FCC (silica, CyH:EtOAc 80:20). Compound **2.77ag** was obtained as an off-white solid (40.3 mg, 0.911 mmol, 91% yield) with 99:1 *er*. Spectroscopic data matched those reported in the literature.[59e] The absolute configuration was assigned by comparison to **2.77ai.** **^{1}H NMR** (300 MHz, $CDCl_3$) δ 8.06 (s, 1H), 7.60 (d, *J* = 8.2 Hz, 2H), 7.33 (d, *J* = 8.2 Hz, 2H), 7.24 (d, *J* = 8.1 Hz, 2H), 7.20 – 6.99 (m, 7H), 4.79 – 4.70 (m, 1H), 4.28 – 4.19 (m, 1H), 3.96 (d, *J* = 10.2 Hz, 1H), 3.91 – 3.79 (m, 2H), 3.50 – 3.30 (m, 3H), 2.43 (s, 3H). **^{13}C NMR** (75 MHz, $CDCl_3$) δ 145.2, 143.7, 143.3, 136.5, 132.9, 129.8, 128.4, 128.3, 127.9, 127.0, 126.4, 122.4, 121.2, 119.6, 119.4, 118.1, 111.3, 110.3, 53.2, 52.5, 47.9, 45.9, 21.7. **SFC** (IC (100 × 3 mm, 3 μm), 80:20 CO_2:EtOH, 1.2 mL/min, 35 ºC, BPR 150 bar, 210 nm): en1 (minor, 1%) 4.66 min, en2 (major, 99%) 5.11 min. **$[\alpha]^{24.6}_D$** –38.4 (c 0.54, $CHCl_3$).

(*R*)-3-((*R*)-Methoxy(phenyl)methyl)-4-methylene-1-tosylpyrrolidine (2.77ah)

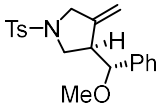

Prepared following general procedure **GP11**, using **Au23** (3.5 mg, 3 mol%), **(*R*)-Ag5** (3.3 mg, 3 mol%), enyne **2.76d** (32.5 mg, 0.100 mmol) and anhydrous MeOH (20.2 μL, 0.500 mmol, 5.0 equiv) as a nucleophile in toluene (1.0 mL, 0.1M), at 25 ºC for 14 h. The crude product was purified by FCC (silica, CyH:EtOAc 80:20). Compound **2.77ah** was obtained as white solid (34.8 mg, 0.974 mmol, 97% yield) with 98:2 *er*. Spectroscopic data matched those reported in the literature.[59e] The absolute configuration was assigned by comparison to **2.77ai**. **^{1}H NMR** (300 MHz, $CDCl_3$) δ 7.77 – 7.69 (m, 2H), 7.38 – 7.26 (m, 6H), 7.16 (dd, *J* = 7.6, 1.8 Hz, 2H), 4.76 (q, *J* = 1.9 Hz, 1H), 4.20 (q, *J* = 2.2 Hz, 1H), 3.91 (d, *J* = 8.3 Hz, 1H), 3.88 – 3.80 (m, 1H), 3.76 – 3.64 (m, 2H), 3.29 – 3.19 (m, 1H), 3.10 (s, 3H), 2.91 – 2.78 (m, 1H), 2.44 (s, 3H). **^{13}C NMR** (75 MHz, $CDCl_3$) δ 143.7, 143.6, 139.5, 133.0, 129.8, 128.4, 128.2, 128.0, 127.7, 110.1, 83.9, 57.0, 52.4, 50.7, 50.6, 21.7. **SFC** (IA (100 × 3 mm, 3 μm), 85:15 CO_2:MeOH, 1.2 mL/min, 35 ºC, BPR 150 bar, 210 nm): en1 (major, 98%) 1.27 min, en2 (minor, 2%) 2.31 min. **$[\alpha]^{24.6}_D$** +63.0 (c 1.62, $CHCl_3$).

(*1R,5R,6S*)-6-Phenyl-3-tosyl-3-azabicyclo[3.1.0]hexane-1-carbaldehyde (2.77ai)

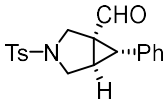

Prepared following general procedure **GP11**, using **Au23** (3.5 mg, 3 mol%), **(*R*)-Ag5** (3.3 mg, 3 mol%), enyne **2.76d** (32.5 mg, 0.100 mmol) and diphenyl sulfoxide (30.3 mg, 0.150 mmol, 1.5 equiv) in toluene (1.0 mL, 0.1M), at 0 ºC for 24 h. The crude product was purified by PTLC (silica, pentane: CH_2Cl_2 30:70). Compound

2.77ai was obtained as white solid (32.1 mg, 0.940 mmol, 94% yield) with 99:1 *er*. Spectroscopic data matched those reported in the literature.[39] The absolute configuration was assigned by X-Ray crystallography. **^{1}H NMR** (300 MHz, $CDCl_3$) δ 8.71 (s, 1H), 7.78 – 7.70 (m, 2H), 7.40 – 7.27 (m, 6H), 7.25 – 7.21 (m, 1H), 3.84 (d, *J* = 9.6 Hz, 1H), 3.73 (d, *J* = 10.0 Hz, 1H), 3.47 (d, *J* = 10.0 Hz, 1H), 3.24 – 3.14 (m, 1H), 3.11 (d, *J* = 5.4 Hz, 1H), 2.83 (dd, *J* = 5.4, 4.0 Hz, 1H), 2.44 (s, 3H). **^{13}C NMR** (75 MHz, $CDCl_3$) δ 197.4, 144.2, 133.4, 132.7, 130.0, 129.05, 129.00, 127.8, 49.2, 48.2, 45.0, 34.2, 29.9, 21.7. **SFC** (OD (100 × 3 mm, 3 μm), 70:30 CO_2:EtOH, 1.2 mL/min, 35 ºC, BPR 150 bar, 210 nm): en1 (minor, 1%) 0.83 min, en2 (minor, 99%) 1.25 min. **$[\alpha]^{24.6}_D$** –63.5 (c 0.40, $CHCl_3$). **XRD:** Single crystals could be obtained by slow diffusion of pentane into a solution of **2.77ai** in CH_2Cl_2 at 0 °C.

Dimethyl (1*R*,8*aS*)-1-Phenyl-4,6,8,8a-tetrahydro-1*H*-cyclopenta[*c*]oxepine-7,7(3*H*)-dicarboxylate (2.77r')

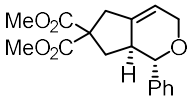

To a solution of **2.77r** (13.8 mg, 40.0 μmol, 98.5:1.5 *er*) in anhydrous CH_2Cl_2 (0.1M) was added Grubbs-II catalyst (1.7 mg, 2 μmol, 5 mol%). The mixture was heated to 50 ºC and left stirring overnight. Next day, after 17h, the reaction was filtered through a silica-filled glass pipette washing with CH_2Cl_2. Compound 2.77r' was obtained as an orange oil (11.8 mg, 37.3 μmol, 93% yield) with 99:1 *er*. Spectroscopic data matched those reported in the literature.[64] The absolute configuration was assigned by comparison of the configuration of the starting material. **^{1}H NMR** (300 MHz, $CDCl_3$) δ 7.39 – 7.27 (m, 5H), 5.77 – 5.65 (m, 1H), 4.98 (d, *J* = 6.2 Hz, 1H), 4.18 (tq, *J* = 4.9, 2.4 Hz, 2H), 3.71 (s, 3H), 3.66 (s, 3H), 3.13 – 2.92 (m, 2H), 2.91 – 2.78 (m, 1H), 2.05 (dd, *J* = 12.8, 7.3 Hz, 1H), 1.64 (t, *J* = 12.9 Hz, 1H). **^{13}C NMR** (75 MHz, $CDCl_3$) δ 172.89, 172.21, 139.62, 138.66, 128.52, 127.61, 126.84, 118.57, 63.76, 56.66, 53.04, 52.91, 41.82, 38.48, 35.66. **SFC** (IG (100 × 3 mm, 3 μm), 95:5 CO_2:MeOH, 1.2 mL/min, 35 ºC, BPR 150 bar, 210 nm): en1 (major, 99%) 2.60 min, en2 (minor, 1%) 3.795 min. **$[\alpha]^{24.6}_D$** +73.1 (c 0.45, $CHCl_3$).

Dimethyl (5*aR*,8*aS*)-5a-Methyl-1-phenyl-4,5,5*a*,6,8,8*a*-hexahydrocyclopenta[*c*]azepine-7,7(3*H*)-dicarboxylate (2.77k')

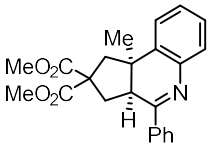

To a MW vial containing $Pd(OAc)_2$ (2.1 mg, 9.5 μmol, 10 mol%), PPh_3 (5.0 mg, 19 μmol, 20 mol%) and K_2CO_3 (26.0 mg, 19.0 μmol, 2 equiv) wad added **2.77k** (48 mg, 95.0 μmol, 98.5:1.5 *er*) as a solution in anhydrous and degassed DMF (0.63 mL). The mixture was heated to 110 ºC and left stirring for 24h. The solvent was evaporated and the crude was purified by PTLC (pentane:Et_2O 90:10). Compounds **2.77k'** was obtained as a white solid (25.6 mg, 65.4 μmol, 69% yield) with 98.5:1.5 *er*. Spectroscopic data matched those reported in the literature.[59g] The absolute configuration was assigned based on the configuration of the starting material. **^{1}H NMR** (300 MHz, $CDCl_3$) δ 8.11 (dd, *J* = 6.7, 3.0 Hz, 2H), 7.50 (ddt, *J* = 9.6, 6.4, 2.7 Hz, 4H), 7.39 (dd, *J* = 7.3, 1.7 Hz, 1H), 7.33 – 7.26 (m, 2H), 7.23 (dd, *J* = 7.3, 1.6 Hz, 1H), 3.80 (s, 3H), 3.51 (s, 3H), 3.43 (d, *J* = 14.1 Hz, 1H), 3.31 (dd, *J* = 12.3, 7.7 Hz, 1H), 2.66 (dd, *J* = 13.7, 7.7 Hz, 1H), 2.55 (d, *J* = 14.2 Hz, 1H), 2.18 (dd, *J* = 13.7, 12.4 Hz, 1H), 1.21 (s, 3H). **^{13}C NMR** (75 MHz, $CDCl_3$) δ 173.37, 171.41, 165.80, 142.44, 138.64, 131.71, 130.79, 128.78, 128.57, 127.90, 127.74, 126.95, 125.66, 58.47, 53.23, 52.90, 46.91, 46.49, 44.51, 38.81, 28.67. **SFC** (IG (100 × 3 mm, 3 μm), 85:15 CO_2:EtOH, 1.2 mL/min, 35 ºC, BPR 150 bar, 210 nm): en1 (major, 98.5%) 1.05 min, en2 (minor, 1.5%) 1.30 min. **$[\alpha]^{24.6}_D$** +217.0 (c 0.87, $CHCl_3$).

(*R*)-4-((*R*)-Methoxy(phenyl)methyl)-3-methylene-1-tosylpyrrolidin-2-one (2.77ah')

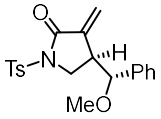

To a white suspension of **2.77ah** (17.9 mg, 50.0 μmol, 98:2 *er*) in HPLC-grade MeCN (0.33 mL) and distilled water (0.17 mL), was added *N*-hydroxyphtalamide (1.6 mg, 10.0 μmol, 20 mol%). Then $NaClO_2$ (17.5 mg, 155 μmol, 3.1 equiv) was added portionwise turning the white suspension into an orange one. The mixture is then warmed up to 50 ºC and left stirring for 24 h (the orange suspension turned into a colorless solution upon warming up). The reaction was worked up by diluting it in EtOAc (2 mL) and an aqueous 0.1 M solution of $Na_2S_2O_3$ (2 mL). The organic phase was then washed with an aqueous saturated $NaHCO_3$ solution (2 mL), water (2 mL) and brine (2 mL), dried over $MgSO_4$, filtered, and evaporated. The crude was purified by PTLC (pentane:Et_2O 60:40). Compound **2.77ah'** was obtained as a colorless oil (9.2 mg, 25.0 μmol, 50% yield) with 98:2 *er*. The absolute configuration was assigned based on the configuration of the starting material. **^{1}H NMR** (500 MHz, $CDCl_3$) δ 7.97 – 7.93 (m, 2H), 7.38 – 7.30 (m, 6H), 7.25 – 7.18 (m, 2H), 5.99 (d, *J* = 2.4 Hz, 1H), 4.68 (d, *J* = 2.0 Hz, 1H), 4.12 (dd, *J* = 10.5, 3.2 Hz, 1H), 4.00 (d, *J* = 7.9 Hz, 1H), 3.83 (dd, *J* = 10.4, 8.1 Hz, 1H), 3.17 (s, 3H), 2.44 (s, 3H). **^{13}C NMR** (126 MHz, $CDCl_3$) δ 165.8, 145.3, 138.4, 138.1, 135.2, 129.8, 128.7, 128.4, 127.8, 123.5, 85.1, 57.1, 46.9, 42.9, 21.8. **HRMS (ESI +)** calculated for $[C_{20}H_{22}NO_4S]^{+\cdot}$ $[M+H]^{+\cdot}$ 372.1264 m/z; found 372.1266 m/z. **SFC** (IC (100 × 3 mm, 3 μm), 80:20 CO_2:ACN, 1.2 mL/min, 35 ºC, BPR 150 bar, 210 nm): en1 (minor, 2%) 2.26 min, en2 (major, 98%) 3.30 min. **$[\alpha]^{24.6}_D$** +93.9 (c 0.33, $CHCl_3$).

Crystallographic Data[102]

Complex Au1 (CCDC2107746)

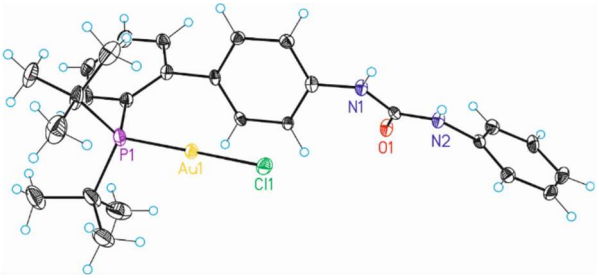

Table 2.21. Crystal data and structure refinement for AF-2-54 **(complex Au1)**

Identification code	AF-2-54	
Empirical formula	$C_{28}H_{35}AuCl_3N_2OP$	
Formula weight	749.86	
Temperature	100(2) K	
Wavelength	0.71073 Å	
Crystal system	orthorhombic	
Space group	P 21 21 21	
Unit cell dimensions	a = 8.9980(5) Å	α = 90°
	b = 15.4500(5) Å	β = 90°
	c = 21.0665(7) Å	γ = 90°
Volume	2928.6(2) $Å^3$	
Z	4	
Density (calculated)	1.701 Mg/m^3	
Absorption coefficient	5.376 mm^{-1}	
F(000)	1480	
Crystal size	0.040 x 0.040 x 0.020 mm^3	
Theta range for data collection	2.340 to 32.120°	
Index ranges	-7<=h<=13,-20<=k<=22,-16<=l<=31	
Reflections collected	16349	
Independent reflections	9009[R(int) = 0.0270]	
Completeness to theta =32.120°	92.5%	
Absorption correction	Multi-scan	
Max. and min. transmission	1.00 and 0.96	
Refinement method	Full-matrix least-squares on F^2	
Data / restraints / parameters	9009/ 0/ 331	
Goodness-of-fit on F2	1.004	
Final R indices [I>2sigma(I)]	R1 = 0.0294, wR2 = 0.0529	
R indices (all data)	R1 = 0.0376, wR2 = 0.0548	
Flack parameter	x = -0.015(3)	
Largest diff. peak and hole	1.256 and -0.739 e.$Å^{-3}$	

102. These data are provided free of charge by the joint Cambridge Crystallographic Data Centre (CCDC) and Fachinformationszentrum Karlsruhe Access Structures service. For more information access www.ccdc.cam.ac.uk/structures with the corresponding CCDC codes provided in this section.

Complex Au4 (CCDC2107749)

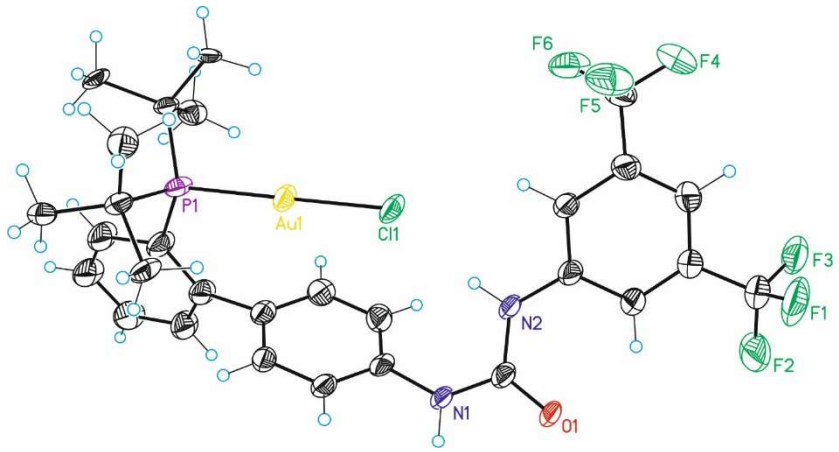

Table 2.22. Crystal data and structure refinement for complex mo_AF2216B-b_0m (Complex **Au4**)

Identification code	mo_AF2216B-b_0m	
Empirical formula	$C_{30.50}H_{34.50}AuClF_6N_2OP$	
Formula weight	822.49	
Temperature	100(2)K	
Wavelength	0.71073 Å	
Crystal system	monoclinic	
Space group	C 2/c	
Unit cell dimensions	a = 24.3608(12) Å	α = 90°
	b = 18.4710(10) Å	β = 123.7947(14)°
	c = 17.9807(9) Å	γ = 90°
Volume	6723.7(6) $Å^3$	
Z	8	
Density (calculated)	1.625 Mg/m^3	
Absorption coefficient	4.562 mm^{-1}	
F(000)	3236	
Crystal size	0.010 x 0.010 x 0.010 mm^3	
Theta range for data collection	1.492 to 25.085°	
Index ranges	-28<=h<=28,-22<=k<=21,-15<=l<=21	
Reflections collected	34695	
Independent reflections	5947[R(int) = 0.0785]	
Completeness to theta =25.085°	99.5%	
Absorption correction	Multi-scan	
Max. and min. transmission	0.74 and 0.60	
Refinement method	Full-matrix least-squares on F^2	
Data / restraints / parameters	5947/ 572/ 558	
Goodness-of-fit on F^2	1.057	
Final R indices [I>2sigma(I)]	R1 = 0.0444, wR2 = 0.1096	
R indices (all data)	R1 = 0.0726, wR2 = 0.1253	
Largest diff. peak and hole	2.879 and -0.646 e.$Å^{-3}$	

Complex Au6 (CCDC2107748)

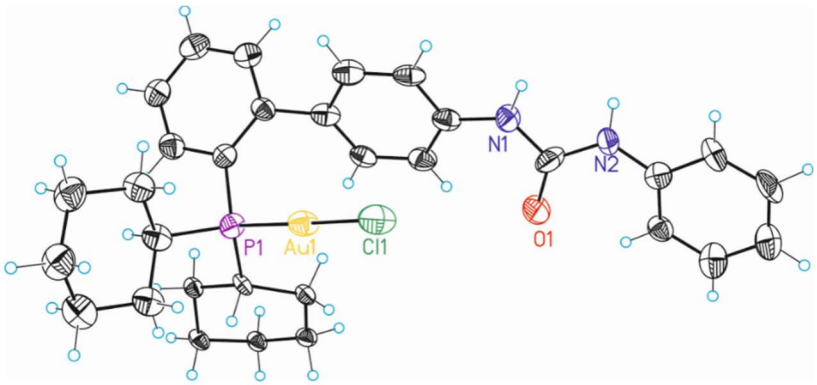

Table 2.23. Crystal data and structure refinement for complex AF-2-92c_hklf5 (Complex **Au6**)

Identification code	AF-2-92c_hklf5	
Empirical formula	$C_{31}H_{37}AuClN_2OP$	
Formula weight	717.01	
Temperature	100(2)K	
Wavelength	0.71073 Å	
Crystal system	monoclinic	
Space group	P 21/n	
Unit cell dimensions	a = 10.0455(6)Å	α= 90°
	b = 17.3190(14)Å	β = 103.737(6)°
	c = 17.1012(10)Å	γ = 90°
Volume	2890.1(3) $Å^3$	
Z	4	
Density (calculated)	1.648 Mg/m^3	
Absorption coefficient	5.265 mm^{-1}	
F(000)	1424	
Crystal size	0.080 x 0.010 x 0.010 mm^3	
Theta range for data collection	2.155 to 27.812°.	
Index ranges	-12<=h<=8,-22<=k<=22,-22<=l<=22	
Reflections collected	9780	
Independent reflections	9780[R(int) = ?]	
Completeness to theta =27.812°	88.9%	
Absorption correction	Multi-scan	
Max. and min. transmission	1.00 and 0.60	
Refinement method	Full-matrix least-squares on F^2	
Data / restraints / parameters	9780/ 357/ 389	
Goodness-of-fit on F^2	1.143	
Final R indices [I>2sigma(I)]	R1 = 0.0852, wR2 = 0.2017	
R indices (all data)	R1 = 0.1595, wR2 = 0.2219	
Largest diff. peak and hole	4.713 and -1.918 $e.Å^{-3}$	

Complex Au7 (CCDC2107750)

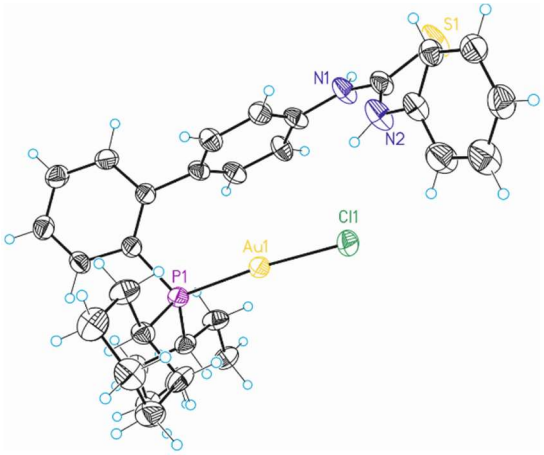

Table 2.24. Crystal data and structure refinement for AF-2-100_crystal1 (complex **Au7)**

Identification code	AF-2-100_crystal1	
Empirical formula	$C_{33}H_{41}AuCl_3N_2PS$	
Formula weight	832.02	
Temperature	100(2)K	
Wavelength	0.71073 Å	
Crystal system	triclinic	
Space group	P -1	
Unit cell dimensions	a = 9.59892(14) Å	α = 94.4905(13)°
	b = 12.6994(2) Å	β = 100.6664(12)°
	c = 14.05405(19) Å	γ = 93.9681(13)°
Volume	1672.29(5) $Å^3$	
Z	2	
Density (calculated)	1.652 Mg/m^3	
Absorption coefficient	4.774 mm^{-1}	
F(000)	828	
Crystal size	0.100 x 0.080 x 0.050 mm^3	
Theta range for data collection	2.087 to 29.431°.	
Index ranges	-13<=h<=13,-16<=k<=17,-19<=l<=19	
Reflections collected	49817	
Independent reflections	8695[R(int) = 0.0640]	
Completeness to theta =29.431°	93.7%	
Absorption correction	Multi-scan	
Max. and min. transmission	1.00 and 0.60	
Refinement method	Full-matrix least-squares on F^2	
Data / restraints / parameters	8695/ 223/ 472	
Goodness-of-fit on F^2	1.275	
Final R indices [I>2sigma(I)]	R1 = 0.0541, wR2 = 0.1596	
R indices (all data)	R1 = 0.0585, wR2 = 0.1621	
Largest diff. peak and hole	2.971 and -2.156 e.$Å^{-3}$	

Complex Au8 (CCDC2107754)

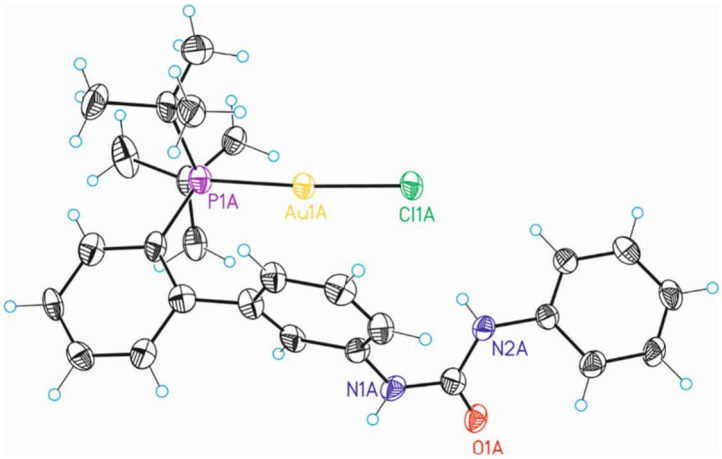

Table 2.25. Crystal data and structure refinement for AF-2-77_060_hklf4 (complex **Au8**).

Identification code	AF-2-77_060_hklf4	
Empirical formula	$C_{113.40}H_{144.20}Au_4Cl_4N_8O_{4.60}P_4$	
Formula weight	2746.50	
Temperature	100(2) K	
Wavelength	0.71073 Å	
Crystal system	triclinic	
Space group	P -1	
Unit cell dimensions	a = 14.2477(3) Å	α = 76.813(2)°
	b = 14.3488(4) Å	β = 65.068(2)°
	c = 15.1942(3) Å	γ = 84.806(2)°
Volume	2742.45(12) $Å^3$	
Z	1	
Density (calculated)	1.663 Mg/m^3	
Absorption coefficient	5.544 mm^{-1}	
F(000)	1361	
Crystal size	0.080 x 0.060 x 0.030 mm^3	
Theta range for data collection	2.007 to 29.829°.	
Index ranges	-19<=h<=19,-19<=k<=19,-21<=l<=20	
Reflections collected	80554	
Independent reflections	14654[R(int) = 0.0963]	
Completeness to theta =29.829°	93.1%	
Absorption correction	Multi-scan	
Max. and min. transmission	1.00 and 0.60	
Refinement method	Full-matrix least-squares on F^2	
Data / restraints / parameters	14654/ 111/ 689	
Goodness-of-fit on F^2	1.041	
Final R indices [I>2sigma(I)]	R1 = 0.0886, wR2 = 0.2394	
R indices (all data)	R1 = 0.1154, wR2 = 0.2566	
Largest diff. peak and hole	10.107 and -3.219 e.$Å^{-3}$	

Complex Au9 (CCDC2107747)

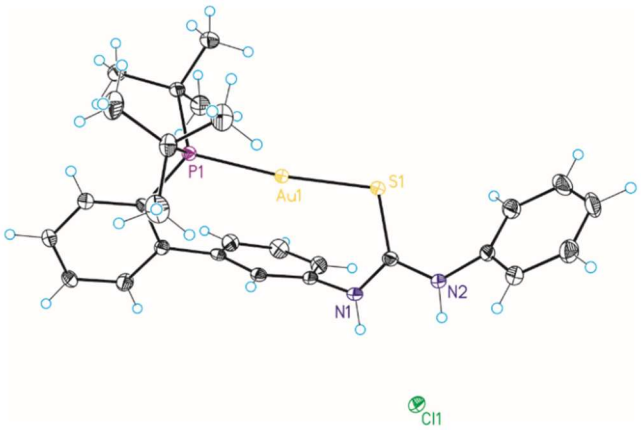

Table 2.26. Crystal data and structure refinement for complex AF-2-78 (Complex **Au9**).

Identification code	AF-2-78	
Empirical formula	$C_{27.50}H_{34}AuCl_2N_2PS$	
Formula weight	723.46	
Temperature	100(2) K	
Wavelength	0.71073 Å	
Crystal system	triclinic	
Space group	P -1	
Unit cell dimensions	a = 9.7623(2) Å	α = 101.2040(10)°
	b = 12.7526(2) Å	β = 103.1730(10)°
	c = 12.7995(2) Å	γ = 108.3070(10)°
Volume	1410.76(4) $Å^3$	
Z	2	
Density (calculated)	1.703 Mg/m^3	
Absorption coefficient	5.554 mm^{-1}	
F(000)	714	
Crystal size	0.100 x 0.060 x 0.020 mm^3	
Theta range for data collection	2.067 to 28.761°.	
Index ranges	-12<=h<=13,-17<=k<=17,-17<=l<=11	
Reflections collected	16367	
Independent reflections	6482[R(int) = 0.0249]	
Completeness to theta =28.761°	88.3%	
Absorption correction	Multi-scan	
Max. and min. transmission	1.00 and 0.72	
Refinement method	Full-matrix least-squares on F^2	
Data / restraints / parameters	6482/ 25/ 340	
Goodness-of-fit on F^2	1.022	
Final R indices [I>2sigma(I)]	R1 = 0.0172, wR2 = 0.0414	
R indices (all data)	R1 = 0.0196, wR2 = 0.0419	
Largest diff. peak and hole	1.001 and -0.525 $e.Å^{-3}$	

Complex Au10 (CCDC2107755)

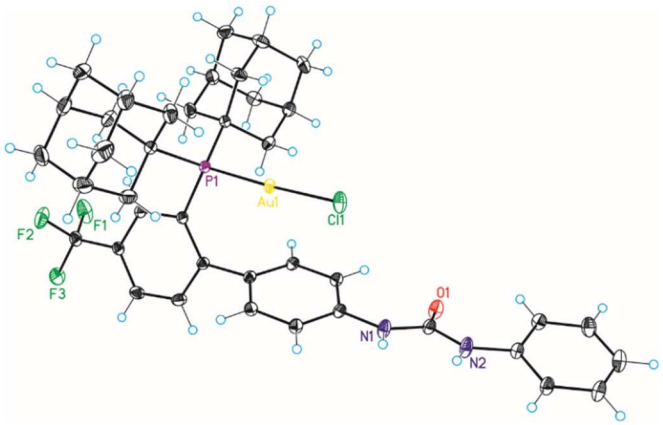

Table 2.27. Crystal data and structure refinement for af-3-10 (complex Au10).

Identification code	af-3-10	
Empirical formula	$C_{40}H_{44}AuClF_3N_2OP$	
Formula weight	889.16	
Temperature	100(2)K	
Wavelength	0.71073 Å	
Crystal system	monoclinic	
Space group	P 21/c	
Unit cell dimensions	a = 16.7400(2) Å	α = 90°
	b = 9.63050(10) Å	β = 95.1940(10)°
	c = 22.2650(2) Å	γ = 90°
Volume	3574.70(7) $Å^3$	
Z	4	
Density (calculated)	1.652 Mg/m^3	
Absorption coefficient	4.286 mm^{-1}	
F(000)	1776	
Crystal size	0.200 x 0.200 x 0.100 mm^3	
Theta range for data collection	2.296 to 37.114°	
Index ranges	-27<=h<=27,-16<=k<=16,-37<=l<=37	
Reflections collected	118305	
Independent reflections	17914[R(int) = 0.0227]	
Completeness to theta =37.114°	97.7%	
Absorption correction	Multi-scan	
Max. and min. transmission	1.00 and 0.64	
Refinement method	Full-matrix least-squares on F^2	
Data / restraints / parameters	17914/ 0/ 442	
Goodness-of-fit on F^2	1.014	
Final R indices [I>2sigma(I)]	R1 = 0.0161, wR2 = 0.0371	
R indices (all data)	R1 = 0.0228, wR2 = 0.0390	
Largest diff. peak and hole	1.057 and -0.831 e.$Å^{-3}$	

Complex Au13 (CCDC2107756)

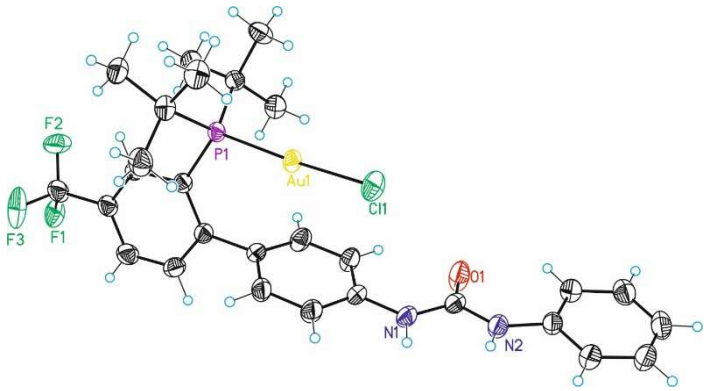

Table 2.28. Crystal data and structure refinement for AF-3-202 (complex **Au13**).

Identification code	AF-3-202	
Empirical formula	$C_{30}H_{38}AuClF_3N_2O_2PS$	
Formula weight	811.07	
Temperature	100(2)K	
Wavelength	0.71073 Å	
Crystal system	monoclinic	
Space group	P 21/c	
Unit cell dimensions	a = 17.8212(2) Å	α = 90°
	b = 9.22438(10) Å	β = 96.4124(11)°
	c = 19.6969(2) Å	γ = 90°
Volume	3217.70(7) $Å^3$	
Z	4	
Density (calculated)	1.674 Mg/m^3	
Absorption coefficient	4.817 mm^{-1}	
F(000)	1608	
Crystal size	0.150 x 0.100 x 0.010 mm^3	
Theta range for data collection	2.262 to 26.370°	
Index ranges	-22<=h<=22,-11<=k<=11,-24<=l<=24	
Reflections collected	98973	
Independent reflections	6587[R(int) = 0.0620]	
Completeness to theta =26.370°	100.0%	
Absorption correction	Multi-scan	
Max. and min. transmission	1.00 and 0.66	
Refinement method	Full-matrix least-squares on F^2	
Data / restraints / parameters	6587/ 42/ 443	
Goodness-of-fit on F^2	1.240	
Final R indices [I>2sigma(I)]	R1 = 0.0232, wR2 = 0.0602	
R indices (all data)	R1 = 0.0255, wR2 = 0.0610	
Largest diff. peak and hole	1.951 and -0.874 $e.Å^{-3}$	

Complex Au15 (CCDC2107753)

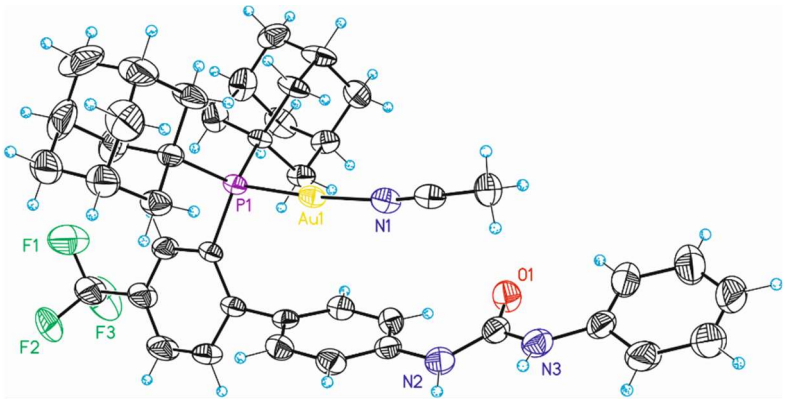

Table 2.29. Crystal data and structure refinement for AF-3-214 (complex **Au15**).

Identification code	AF-3-214	
Empirical formula	$C_{42.50}H_{48}AuClF_9N_3OPSb$	
Formula weight	1172.97	
Temperature	100(2)K	
Wavelength	0.71073 Å	
Crystal system	monoclinic	
Space group	P 21/c	
Unit cell dimensions	a = 9.84181(17) Å	α = 90°
	b = 21.4469(3) Å	β = 102.7073(19)°
	c = 21.4504(4) Å	γ = 90°
Volume	4416.77(13) $Å^3$	
Z	4	
Density (calculated)	1.764 Mg/m^3	
Absorption coefficient	4.101 mm^{-1}	
F(000)	2300	
Crystal size	0.300 x 0.200 x 0.150 mm^3	
Theta range for data collection	2.324 to 28.711°.	
Index ranges	-13<=h<=13,-28<=k<=28,-29<=l<=28	
Reflections collected	73479	
Independent reflections	11411[R(int) = 0.0897]	
Completeness to theta =28.711°	99.9%	
Absorption correction	Multi-scan	
Max. and min. transmission	1.00 and 0.59	
Refinement method	Full-matrix least-squares on F^2	
Data / restraints / parameters	11411/ 223/ 672	
Goodness-of-fit on F^2	1.019	
Final R indices [I>2sigma(I)]	R1 = 0.0393, wR2 = 0.1020	
R indices (all data)	R1 = 0.0532, wR2 = 0.1076	
Largest diff. peak and hole	2.679 and -1.285 $e.Å^{-3}$	

Complex (*R*)-Ag6 (CCDC2107752)

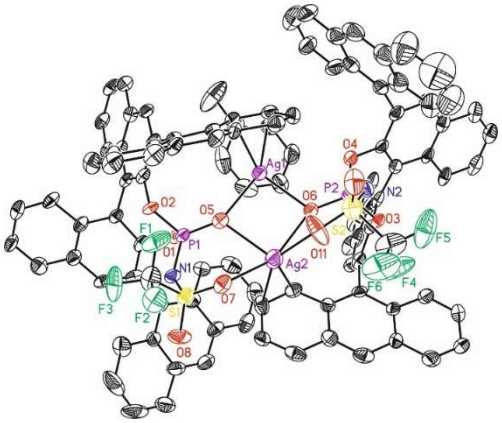

Table 2.30. Crystal data and structure refinement for AF-3-13 ((*R*)-**Ag6**-dimer).

Identification code	AF-3-13	
Empirical formula	$C_{127.25}H_{93.50}Ag_2F_6N_2O_{10}P_2S_2$	
Formula weight	2266.34	
Temperature	100(2)K	
Wavelength	0.71073 Å	
Crystal system	orthorhombic	
Space group	P 21 21 21	
Unit cell dimensions	a = 13.8299(3) Å	α = 90°
	b = 24.8552(6) Å	β = 90°
	c = 33.8903(9) Å	γ = 90°
Volume	11649.6(5) $Å^3$	
Z	4	
Density (calculated)	1.292 Mg/m^3	
Absorption coefficient	0.467 mm^{-1}	
F(000)	4644	
Crystal size	0.150 x 0.030 x 0.020 mm^3	
Theta range for data collection	2.284 to 27.313°.	
Index ranges	-15<=h<=17,-31<=k<=31,-43<=l<=42	
Reflections collected	48392	
Independent reflections	21667[R(int) = 0.0475]	
Completeness to theta =27.313°	90.2%	
Absorption correction	Multi-scan	
Max. and min. transmission	1.00 and 0.83	
Refinement method	Full-matrix least-squares on F^2	
Data / restraints / parameters	21667/ 779/ 1578	
Goodness-of-fit on F^2	1.050	
Final R indices [I>2sigma(I)]	R1 = 0.0680, wR2 = 0.1712	
R indices (all data)	R1 = 0.1121, wR2 = 0.1916	
Flack parameter	x = 0.013(10)	
Largest diff. peak and hole	1.020 and -1.365 e.$Å^{-3}$	

Compound Et_3NH6 (CCDC2107751)[103]

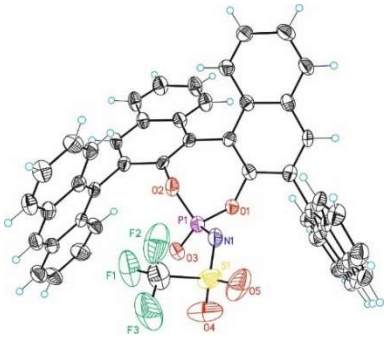

Table 2.31. Crystal data and structure refinement AF-3-135A__hklf5 (**Et_3NH6**).

Identification code	AF-3-135A__hklf5	
Empirical formula	$C_{61}H_{58}F_3N_2O_5PS$	
Formula weight	1019.12	
Temperature	100(2)K	
Wavelength	0.71073 Å	
Crystal system	triclinic	
Space group	P -1	
Unit cell dimensions	a = 10.3632(7) Å	α = 84.304(6)°
	b = 13.2445(12) Å	β = 79.895(5)°
	c = 19.5688(11) Å	γ = 76.852(7)°
Volume	2570.0(3) $Å^3$	
Z	2	
Density (calculated)	1.317 Mg/m^3	
Absorption coefficient	0.158 mm^{-1}	
F(000)	1072	
Crystal size	0.100 x 0.100 x 0.020 mm^3	
Theta range for data collection	2.148 to 27.545°.	
Index ranges	-13<=h<=13,-17<=k<=16,-24<=l<=24	
Reflections collected	15335	
Independent reflections	15335[R(int) = ?]	
Completeness to theta =27.545°	87.8%	
Absorption correction	Multi-scan	
Max. and min. transmission	1.00 and 0.75	
Refinement method	Full-matrix least-squares on F^2	
Data / restraints / parameters	15335/ 885/ 664	
Goodness-of-fit on F^2	1.128	
Final R indices [I>2sigma(I)]	R1 = 0.0897, wR2 = 0.2012	
R indices (all data)	R1 = 0.1773, wR2 = 0.2229	
Largest diff. peak and hole	0.720 and -0.597 $e.Å^{-3}$	

103. Image of the (*R*)-configured anion without the triethylammonium cation. In the crystal, (*R*) and (*S*) anions are present in a 1:1 ratio. The crystals were grown by slow evaporation of a reaction mixture (cycloisomerization of **2.59a**, experiment with 50:50 ratio of **Ag6** enantiomers for the study of non-linear effects) after quenching with Et_3N and diluting with CH_2Cl_2.

Compound (R)-2.60h (CCDC2107757)

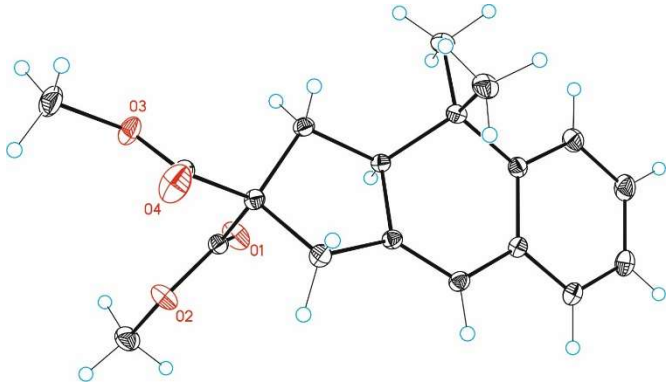

Table 2.32. Crystal data and structure refinement for AF-3-081 (**2.60h**).

Identification code	AF-3-081	
Empirical formula	$C_{19}H_{22}O_4$	
Formula weight	314.36	
Temperature	100(2)K	
Wavelength	0.71073 Å	
Crystal system	monoclinic	
Space group	P 21	
Unit cell dimensions	a = 10.84434(11) Å	α= 90°
	b = 6.16345(4) Å	β = 109.3637(11)°
	c = 13.16108(12) Å	γ = 90°
Volume	829.906(14) $Å^3$	
Z	2	
Density (calculated)	1.258 Mg/m^3	
Absorption coefficient	0.086 mm^{-1}	
F(000)	336	
Crystal size	0.150 x 0.100 x 0.050 mm^3	
Theta range for data collection	2.970 to 42.429°	
Index ranges	-20<=h<=20,-11<=k<=11,-24<=l<=24	
Reflections collected	31525	
Independent reflections	11301[R(int) = 0.0145]	
Completeness to theta =42.429°	98.8%	
Absorption correction	Multi-scan	
Max. and min. transmission	1.00 and 0.86	
Refinement method	Full-matrix least-squares on F^2	
Data / restraints / parameters	11301/ 1/ 212	
Goodness-of-fit on F^2	1.075	
Final R indices [I>2sigma(I)]	R1 = 0.0246, wR2 = 0.0725	
R indices (all data)	R1 = 0.0254, wR2 = 0.0731	
Flack parameter	x = -0.10(8)	
Largest diff. peak and hole	0.466 and -0.203 $e.Å^{-3}$	

Compound (*R*)-2.64a (CCDC2107758)

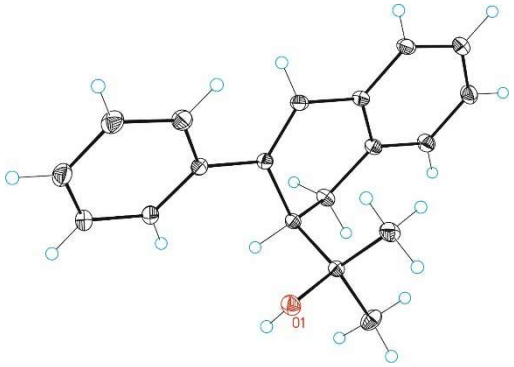

Table 2.33. Crystal data and structure refinement for cu_AF3211_d_0m (compound **2.64a**).

Identification code	cu_AF3211_d_0m	
Empirical formula	$C_{19}H_{20}O$	
Formula weight	264.35	
Temperature	100(2)K	
Wavelength	1.54178 Å	
Crystal system	monoclinic	
Space group	P 21	
Unit cell dimensions	a = 11.0425(4) Å	α = 90°
	b = 5.9014(2) Å	β = 116.8028(9)°
	c = 12.1786(4) Å	γ = 90°
Volume	708.37(4) $Å^3$	
Z	2	
Density (calculated)	1.239 Mg/m^3	
Absorption coefficient	0.572 mm^{-1}	
F(000)	284	
Crystal size	0.10 x 0.15 x 0.30 mm^3	
Theta range for data collection	4.067 to 66.597°.	
Index ranges	-13<=h<=13,-6<=k<=7,-14<=l<=14	
Reflections collected	20279	
Independent reflections	2474[R(int) = 0.0286]	
Completeness to theta =66.597°	99.7%	
Absorption correction	Multi-scan	
Max. and min. transmission	0.75 and 0.62	
Refinement method	Full-matrix least-squares on F^2	
Data / restraints / parameters	2474/ 1/ 187	
Goodness-of-fit on F^2	1.203	
Final R indices [I>2sigma(I)]	R1 = 0.0357, wR2 = 0.0908	
R indices (all data)	R1 = 0.0357, wR2 = 0.0908	
Flack parameter	x = 0.08(3)	
Largest diff. peak and hole	0.271 and -0.397 e.$Å^{-3}$	

Complex Au19 (CCDC2266407)

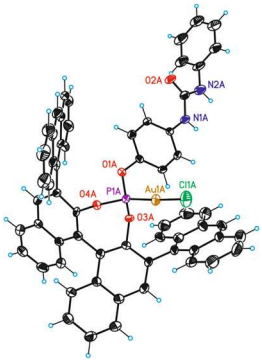

Table 2.34. Crystal data and structure refinement for AMZ-04-067 (complex (R)-**Au19**)

Identification code	AMZ-04-067
Empirical formula	$C_{195.75}H_{130.75}Au_3Cl_{20.25}N_6O_{12}P_3$
Formula weight	4160.48
Temperature	0(2)K
Wavelength	0.71073 Å
Crystal system	triclinic
Space group	P 1
Unit cell dimensions	a = 13.17025(19) Å α = 66.0966(13)° b = 17.6661(2) Å β = 78.2394(12)° c = 20.8530(3) Å γ = 83.1689(12)°
Volume	4338.97(11) $Å^3$
Z	1
Density (calculated)	1.592 Mg/m^3
Absorption coefficient	2.934 mm^{-1}
F(000)	2070
Crystal size	0.700 x 0.020 x 0.020 mm^3
Theta range for data collection	3.455 to 30.414°.
Index ranges	-18<=h<=17,-19<=k<=23,-27<=l<=27
Reflections collected	68959
Independent reflections	34268[R(int) = 0.0547]
Completeness to theta =30.414°	84.1%
Absorption correction	Multi-scan
Max. and min. transmission	1.00 and 0.83
Refinement method	Full-matrix least-squares on F^2
Data / restraints / parameters	34268/ 540/ 2290
Goodness-of-fit on F^2	1.002
Final R indices [I>2sigma(I)]	R1 = 0.0417, wR2 = 0.0944
R indices (all data)	R1 = 0.0522, wR2 = 0.0969
Flack parameter	x =-0.016(2)
Largest diff. peak and hole	1.668 and -3.107 $e.Å^{-3}$

Compound 2.77v (CCDC2266406)

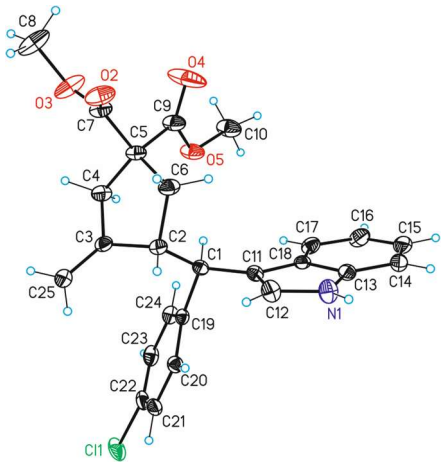

Table 2.35. Crystal data and structure refinement for AMZ-04-364 (**2.77v**)

Identification code	AMZ-04-364	
Empirical formula	$C_{25}H_{24}ClNO_4$	
Formula weight	437.90	
Temperature	100(2)K	
Wavelength	0.71073 Å	
Crystal system	orthorhombic	
Space group	P 21 21 21	
Unit cell dimensions	a = 7.85740(13)Å	α = 90°.
	b = 12.4594(2)Å	β = 90°.
	c = 22.5242(4)Å	γ = 90°.
Volume	2205.07(7) $Å^3$	
Z	4	
Density (calculated)	1.319 Mg/m^3	
Absorption coefficient	0.205 mm^{-1}	
F(000)	920	
Crystal size	0.200 x 0.100 x 0.050 mm^3	
Theta range for data collection	1.808 to 32.372°.	
Index ranges	-11<=h<=11,-18<=k<=18,-33<=l<=32	
Reflections collected	49017	
Independent reflections	7510[R(int) = 0.0301]	
Completeness to theta =32.372°	96.9%	
Absorption correction	Multi-scan	
Max. and min. transmission	1.00 and 0.78	
Refinement method	Full-matrix least-squares on F^2	
Data / restraints / parameters	7510/ 0/ 285	
Goodness-of-fit on F^2	1.060	
Final R indices [I>2sigma(I)]	R1 = 0.0314, wR2 = 0.0824	
R indices (all data)	R1 = 0.0344, wR2 = 0.0840	
Flack parameter	x =-0.008(10)	
Largest diff. peak and hole	0.361 and -0.169 $e.Å^{-3}$	

Compound 2.77ai (CCDC2266405)

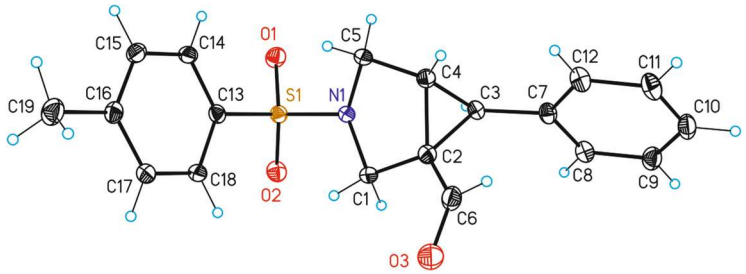

Table 2.36. Crystal data and structure refinement for AMZ-04-453 (**2.77ai**)

Identification code	AMZ-04-453	
Empirical formula	C20 H21 Cl2 N O3 S	
Formula weight	426.34	
Temperature	100(2)K	
Wavelength	0.71073 Å	
Crystal system	monoclinic	
Space group	P 21	
Unit cell dimensions	a = 12.7492(4)Å	α= 90°.
	b = 6.00710(10)Å	β = 113.735(3)°.
	c = 14.1369(4)Å	γ = 90°.
Volume	991.11(5) $Å^3$	
Z	2	
Density (calculated)	1.429 Mg/m^3	
Absorption coefficient	0.454 mm^{-1}	
F(000)	444	
Crystal size	0.400 x 0.200 x 0.200 mm^3	
Theta range for data collection	2.781 to 32.139°.	
Index ranges	-18<=h<=18,-9<=k<=8,-20<=l<=20	
Reflections collected	19275	
Independent reflections	6340[R(int) = 0.0227]	
Completeness to theta =32.139°	95.0%	
Absorption correction	Multi-scan	
Max. and min. transmission	1.00 and 0.86	
Refinement method	Full-matrix least-squares on F^2	
Data / restraints / parameters	6340/ 1/ 245	
Goodness-of-fit on F^2	1.060	
Final R indices [I>2sigma(I)]	R1 = 0.0374, wR2 = 0.0927	
R indices (all data)	R1 = 0.0408, wR2 = 0.0966	
Flack parameter	x =0.009(11)	
Largest diff. peak and hole	0.916 and -0.964 e.Å-3	

DFT Calculations

Computational methods

Calculations were carried out using the Gaussian09 package[104] at the density functional theory (DFT) level by means of the B3LYP[105] functional. Reported geometries and energies were calculated including the corrected dispersion GD3.[106] The 6-31G(d,p)[107] basis set was implemented on all atoms (C, H, N, O, F, P, Cl), except for Au for which the SDD[108] basis set and its corresponding Stuttgart/Dresden Effective Core Potential (ECP) were used. All systems were calculated in toluene whose solvation effects were accounted for using the implicit polarizable continuum model (PCM)[109]. Each stationary point was characterized by vibrational analysis. Transition states (TS) were identified by the presence of a single imaginary frequency while all minima presented only real frequencies. To further confirm the identity of the TS, relaxation experiments of the imaginary frequency were performed connecting reactants and products. Reported energies have been corrected with the thermal and entropic corrections by means of single point calculations at the 6-311G(d,p)[91] level on all atoms (C, H, N, O, F, P, Cl), except for Au for which the SDD basis set and ECP were used. Optimized geometries were visualized using CYLView.[110] NCIPlot was used to obtain the grid data for NCI (non-covalent interactions) analysis[111] and the corresponding results were visualized with the VMD software.[112] Reported energies are potential energies (E) and free energies (G) in solution, computed at 298 K and 1 atm. A dataset collection of computational results of this chapter is available in the ioChem-BD[113] repository and can be accessed through: 10.19061/iochem-bd-1-351 and 10.19061/iochem-bd-1-280.

104. Gaussian 09, Revision D.01, M. J. Frisch, G. W. Trucks, H. B. Schlegel, G. E. Scuseria, M. A. Robb, J. R. Cheeseman, G. Scalmani, V. Barone, B. Mennucci, G. A. Petersson, H. Nakatsuji, M. Caricato, X. Li, H. P. Hratchian, A. F. Izmaylov, J. Bloino, G. Zheng, J. L. Sonnenberg, M. Hada, M. Ehara, K. Toyota, R. Fukuda, J. Hasegawa, M. Ishida, T. Nakajima, Y. Honda, O. Kitao, H. Nakai, T. Vreven, J. A. Montgomery, Jr., J. E. Peralta, F. Ogliaro, M. Bearpark, J. J. Heyd, E. Brothers, K. N. Kudin, V. N. Staroverov, T. Keith, R. Kobayashi, J. Normand, K. Raghavachari, A. Rendell, J. C. Burant, S. S. Iyengar, J. Tomasi, M. Cossi, N. Rega, J. M. Millam, M. Klene, J. E. Knox, J. B. Cross, V. Bakken, C. Adamo, J. Jaramillo, R. Gomperts, R. E. Stratmann, O. Yazyev, A. J. Austin, R. Cammi, C. Pomelli, J. W. Ochterski, R. L. Martin, K. Morokuma, V. G. Zakrzewski, G. A. Voth, P. Salvador, J. J. Dannenberg, S. Dapprich, A. D. Daniels, O. Farkas, J. B. Foresman, J. V. Ortiz, J. Cioslowski, D. J. Fox, Gaussian, Inc., Wallingford CT, **2013**.
105. a) Becke, A. D. *J. Chem. Phys.* **1993**, *98*, 5648–5652. b) Lee, C.; Yang, W.; Parr, R. G. *Phys. Rev. B.* **1988**, *37*, 785–789. c) Vosko, S. H.; Wilk, L.; Nusair, M. *Can. J. Phys.* **1980**, *58*, 1200–1211. d) Stephens, P. J.; Devlin, F. J.; Chabalowsky, C. F.; Frisch, M. J, *J. Phys. Chem.* **1994**, *98*, 11623–11627.
106. S. Grimme, J. Antony, S. Ehrlich, H. Krieg, *J. Chem. Phys.* **2010**, *132*, 154104-1–19.
107. Hehre, E. J.; Ditchfield, R.; Pople, J. A. *J. Chem. Phys.* **1972**, 56, 2257–2261.
108. Andrae, D.; Häussermann, U.; Dolg, M.; Stoll, H.; Preuss, H. *Theor. Chim. Acta* **1990**, 77, 123–141.
109. Cancès, E.; Mennucci, B.; Tomasi, J. *J. Chem. Phys.* **1997**, 107, 3032−3041.
110. Legault, C. Y. CYLview 1.0b; Université de Sherbrooke, 2009; http://www.cylview.org.
111. a) Johnson, E. R.; Keinan, S.; Mori-Sanchez, P.; Contreras-Garcia, J.; Cohen, A. J.; Yang, W. *J. Am. Chem. Soc.* **2010**, *132*, 6498–6506. b) Contreras-Garcia, J.; Johnson, E. R.; Keinan, S.; Chaudret, R.; Piquemal, J. P.; Beratan, D. N.; Yang, W. *J. Chem. Theory Comput.* **2011**, *7*, 625–632.
112. Humphrey, W.; Dalke, A.; Schulten, K. *J. Mol. Graphics.* **1996**, *14*, 33–38.
113. Álvarez-Moreno, M.; De Graaf, C.; López, N.; Maseras, F.; Poblet, J. M.; Bo, C. *J. Chem. Inf. Model.* **2015**, *55*, 95–103.

Computed structures and energies

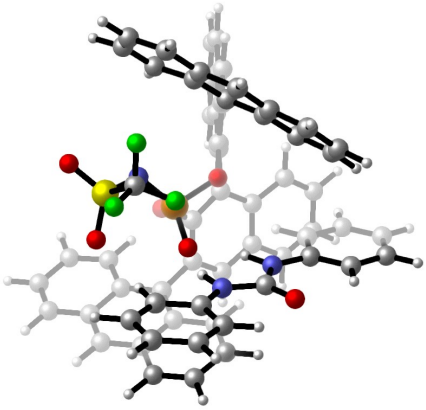

U-I

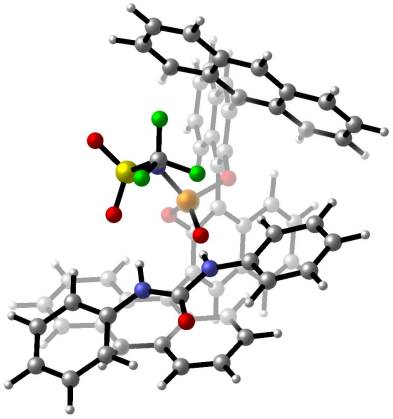

U-II

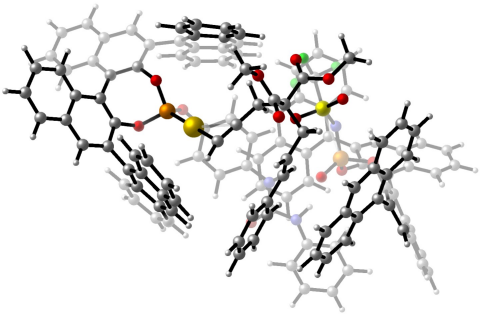

Int1a

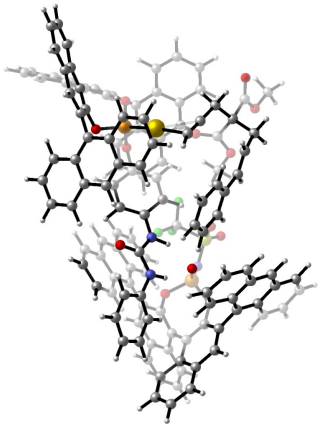

Int1b

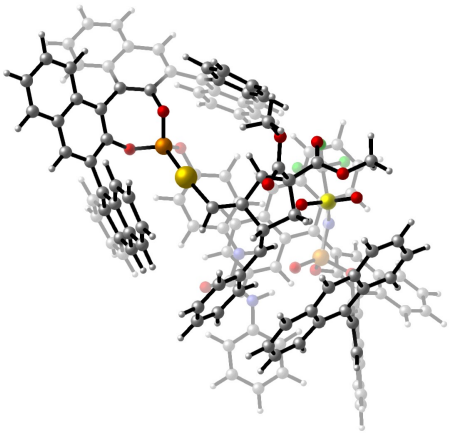

Int2a

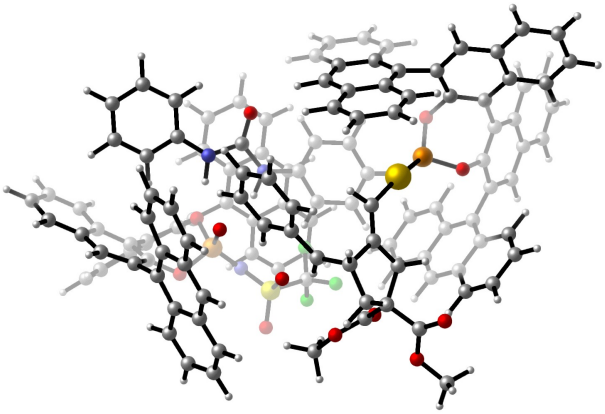

Int2b

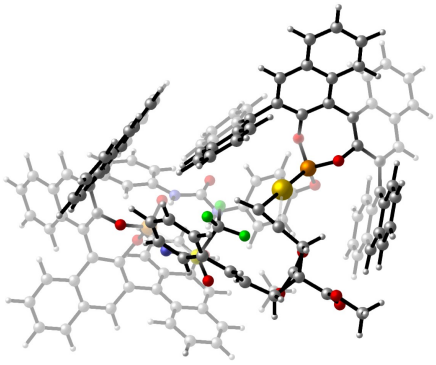

int3a

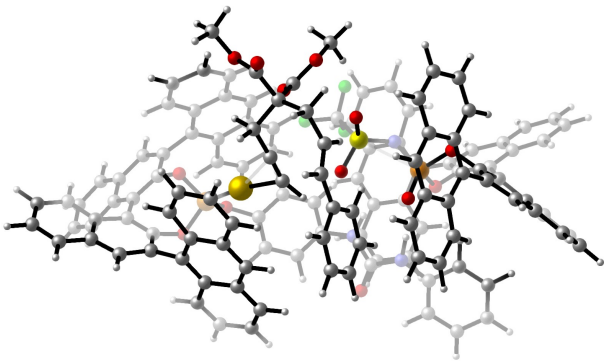

Int3b

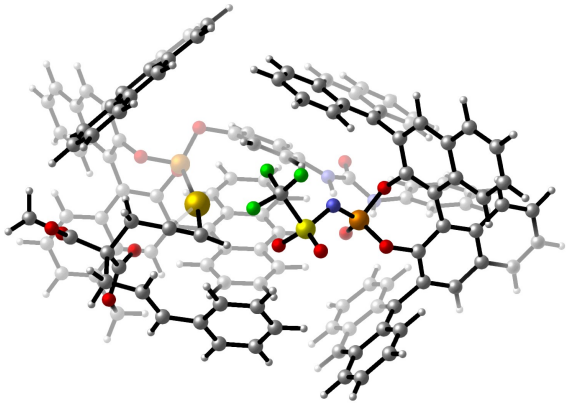

Int3c

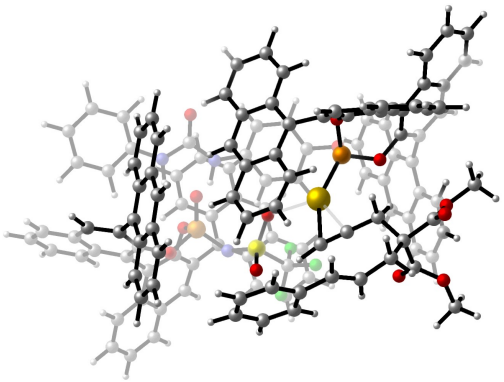

Int3d

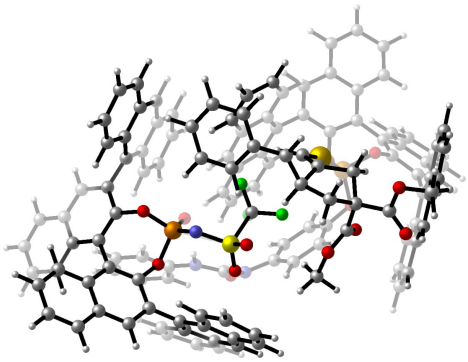

Int4a

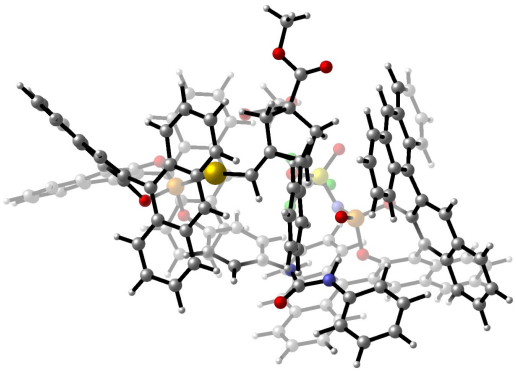

Int4b

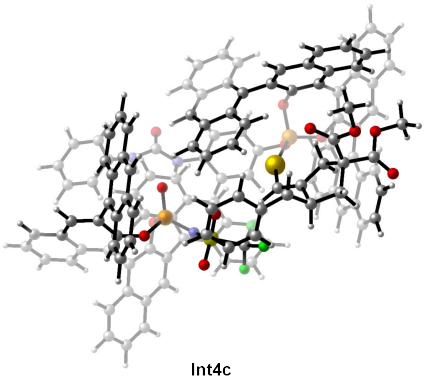

Int4c

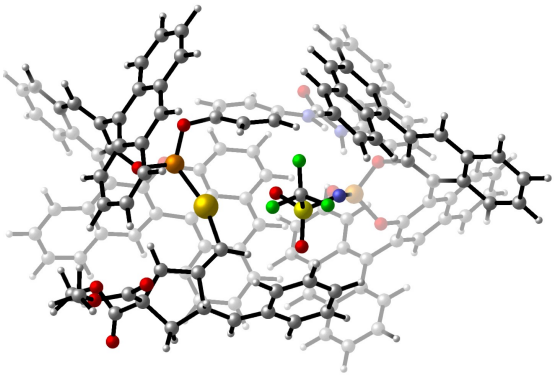

Int4d

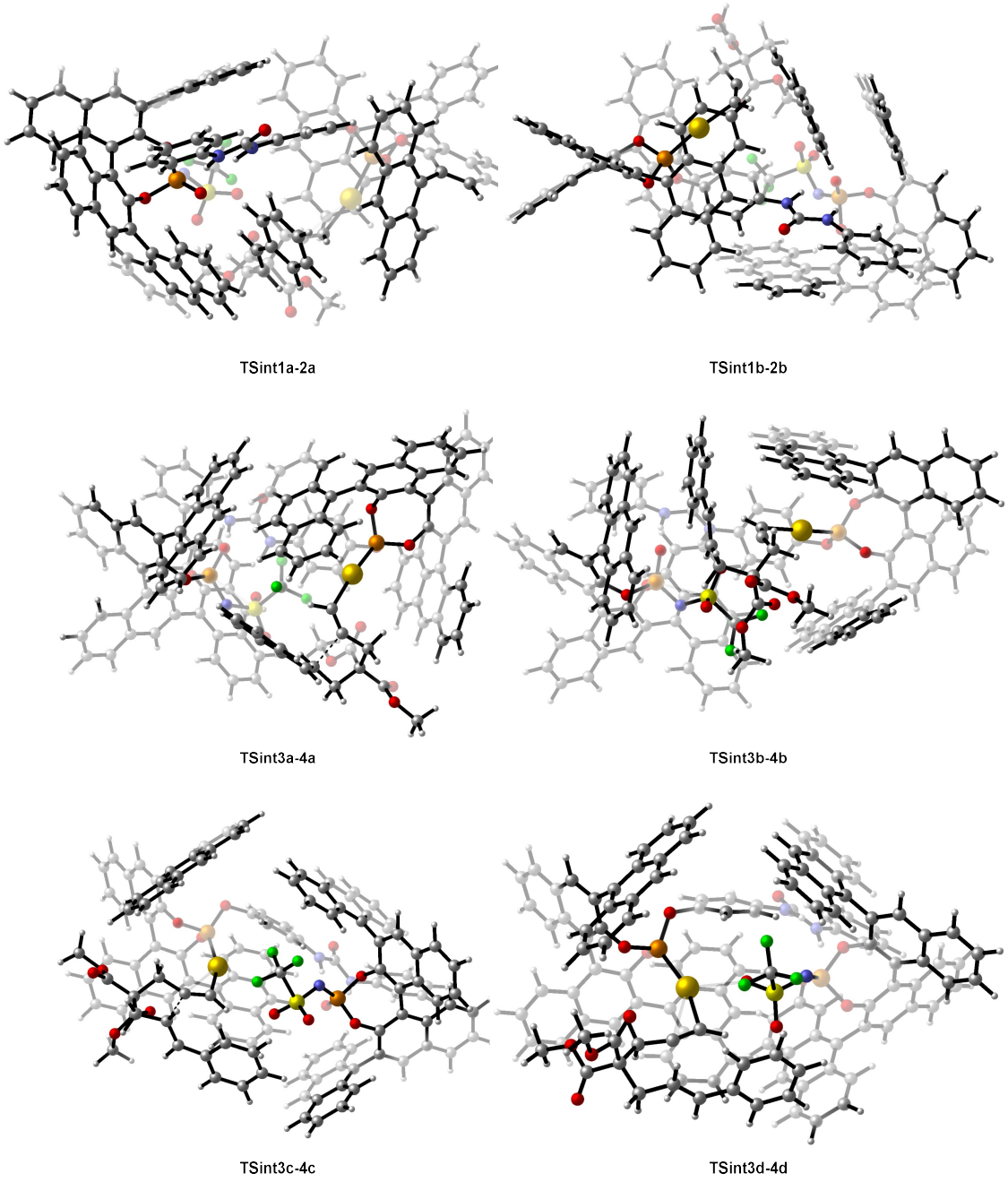

Table 2.37. Potential energies E and free energies in solution (Gsol), of relevant calculated structures of the HCDC with model diphenylurea and counteranion of (*R*)-**Ag6**.

	E (Hartree)	G_{sol}[b] (Hartree)
U-I	−4042.73869	−4041.95919
U-II	−4042.73653	−4041.95795

Table 2.38 Potential energies E and free energies in solution (Gsol), of relevant calculated structures of the gold(I)-catalyzed cyclyzation of enyne **2.76a** with chiral (*R*)-**Au21** and counteranion of (*R*)-**Ag6**.

	E (Hartree)	G_{sol}[b] (Hartree)
Int1a	−7551.29960	−7549.65546
Int1b	−7551.29018	−7549.64434
Int2a	−7551.31111	−7549.66166
Int2b	−7551.29758	−7549.64734
Int3a	−7551.30739	−7549.66033
Int3b	−7551.28746	−7549.64502
Int3c	−7551.29202	−7549.64859
Int3d	−7551.29344	−7549.64971
Int4a	−7551.30247	−7549.65153
Int4b	−7551.30601	−7549.65494
Int4c	−7551.28543	−7549.63976
Int4d	−7551.28307	−7549.63581
TSint1a-2a	−7551.29635	−7549.65253
TSint1b-2b	−7551.27980	−7549.63279
TSint3a-4a	−7551.29473	−7549.64563
TSint3b-4b	−7551.28504	−7549.64110
TSint3c-4c	−7551.27308	−754963095
TSint3d-4d	−7551.27415	−7549.63149

Chapter 3: Total Synthesis of the Daucane Natural Products

Introduction

Daucane Natural Products

The daucane family of sesquiterpenes, also known as carotenes, is a relatively small group of compounds which, for a long time, seemed to be restricted to members isolated from the *Aipaceae* family of plants. All members of this family share a bicyclo[5.3.0]decane core, with the carbon skeleton of daucene **3.1**, with diverse functionality and varied degrees of oxidation and have been shown to exhibit diverse biological activities (Figure 3.1).[1] New natural products with the same hydroazulene structure were later isolated from fungal and marine origins, all of which are formed biosynthetically from the enzymatic cyclization of farnesyl diphosphate (FPP).[2] Other members of this family of natural products include jaeschkeanandiol **(3.2)**,[3] siol acetate (**3.4**)[4] and aspterric acid (**3.5**).[5]

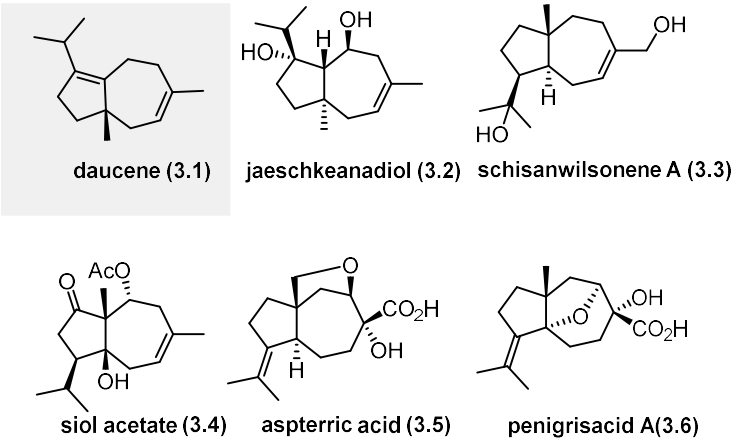

Figure 3.1. Selected members of the Daucane family of natural products.

The first total synthesis of the simplest member (-)-**3.1**, was completed in 1972 by Yamasaki[6] (Scheme 3.1). Starting from enantiopure (*R*)-(+)-limonene **3.7**, epoxidation with peroxybenzoic acid followed by acid hydrolysis afforded diol **3.8** in 66% yield over two steps. Oxidative cleavage of diol **3.8** with $NaIO_4$ and subsequent condensation with piperidine/AcOH of the resulting ketone and aldehyde delivered cyclopentene **3.10** in 40% yield over two steps. Aldol condensation with acetone afforded *α,β*-unsaturated aldehyde **3.11** in 37% yield. Selective reduction of the conjugated double bond was achieved with Ph_3PSnH affording aldehyde **3.12** in 87% yield (attempts with Na in EtOH followed by reoxidation with Jones' reagent led to only 5% yield of the desired product). Hydrogenation of the isoprene group in **3.12** with Pd/C (10%) followed by sodium acetylide addition to the ketone and subsequent partial hydrogenation with Lindlar's

1. a) Foley, D. A.; Maguire, A. R. *Tetrahedron* **2010**, *66*, 1131–1175. b) Galal, A. M.; Abourashed, E. A.; Ross, S. A.; El-Sohly, M. A.; Al-Said, M. S.; El-Feraly, F. S. hermonis *J.* Nat. Prod. **2001**, *64*, 399– 400. c) Y. ang, S.-P.; Cai, Y.-J.; Zhang, B.-L.; Tong, L.-J.; Xie, H.; Wu, Y.; Lin, L.-P.; Ding, J.; Yue, J.-M *J. Med. Chem*. **2008**, *51*, 77– 85.
2. For a review on the biogenesis, isolation and chemistry of the daucane (carotane) sesquiterpenes, see the following: Ghisalberti, E. L. *Phytochemistry* **1994**, *37*, 597–623.
3. Garg, S. N.; Misra, L. N.; Agarwal, S. K.; Mahajan, V. P.; Rastogi, S. N. *Phytochemistry* **1987**, *26*, 449−450
4. Casinovi, C. G.; Cerrini, S.: Motl, O.; Fardella, G.; Fedeli, W.; Gavuzzo, E.: Lamba, D. *Czech. Chem. Comm.* 1**984**, *48*, 2411–2422.
5. Tsuda, Y.; Kaneda, M.; Tada, A.; Nitta, K.; Yamamoto Y.; Iitaka, Y. *J. Chem. Soc. Chem. Commun.* **1978**, 160–161.
6. Yamasaki, M. *J. Chem. Soc., Chem. Commun.* **1972**, *10*, 606b–6607.

catalyst delivered alcohol **3.13**. Finally, acid-catalyzed cyclization of the tertiary alcohol afforded (-)-daucene (3.1) in 42% yield.[7]

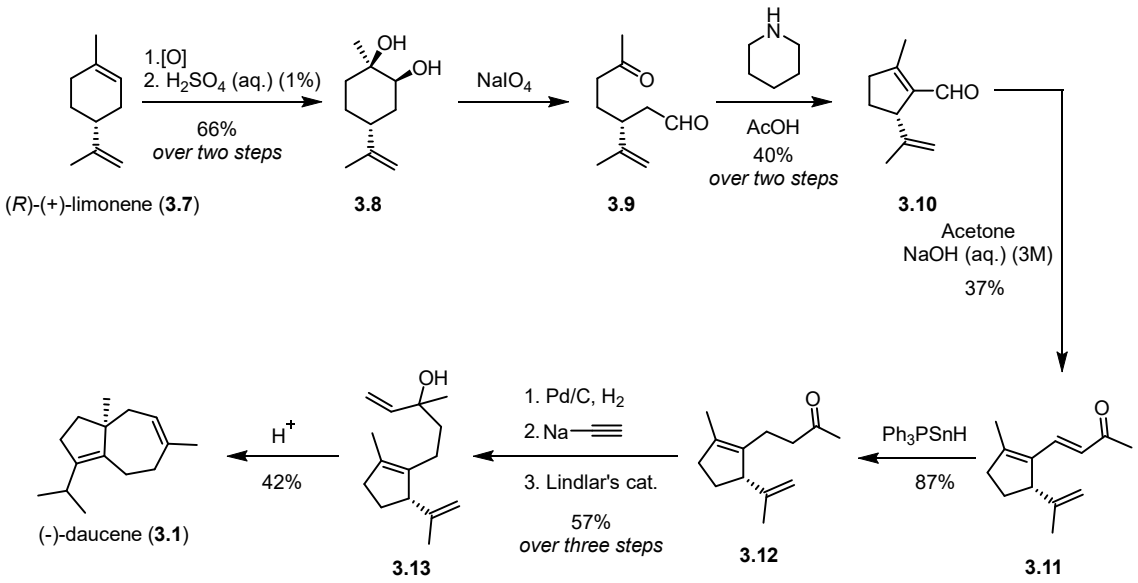

Scheme 3.1. First total synthesis of (-)-daucene (**3.1**), the simplest member of the Daucane family of natural products.

Aspterric Acid

Aspterric acid belongs to the daucane family of natural products and was first isolated in 1978 from the fungus *Aspergillus terreus* IFO-6123, [5] which is commonly found in warm, arable soils. It was the first carotene sesquiterpenoid obtained from fungi and its structure and absolute configuration were determined by X-ray diffraction of a *para*-bromobenzoate derivative **3.14** (Scheme 3.2).[8]

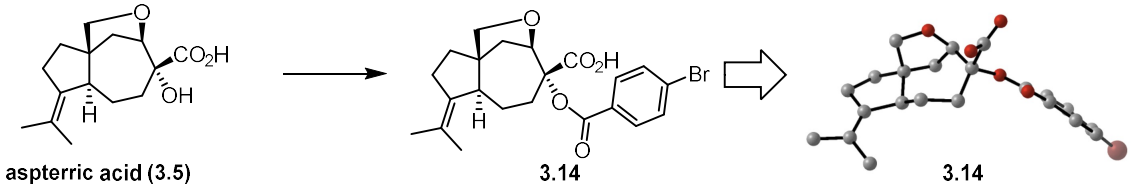

Scheme 3.2. Derivatization of aspterric acid into para bromobenzoate **3.14** and its X-ray structure. H atoms not resolved in the original reported structure.

Recently aspterric acid (**3.5**) has been found to inhibit Arabidopsis pollen development at meiosis.[9] It has also been found to be a natural occurring very potent herbicide inhibiting the branched-chain amino acid (BCAA) biosynthetic pathway, essential for plant growth.[10] Furthermore, as the BCAA is not present in animals it is considered as a validated target for very specific weed-control agents.[11] This biosynthetic pathway is regulated by 3 enzymes: acetolactate

7. Obtained as a mixture that was then further purified with silica treated with 10%-$AgNO_3$. The yield after purification was not provided in the original manuscript.
8. The crystal structure was downloaded from CCDC webpage deposit (**CCDC1103715**) associated to the isolating team of Tsuda *et al.* and represented using the CYLView program.
9. Shimada, A.; Kusano, M.; Takeuchi, S.; Fujioka, S.; Inoku-chi, T.; Kimura, Y. *Naturforsch. C* **2002**, *57*, 459–464.
10. Yan, Y.; Liu, Q.K.; Zang, X.; Yuan, S.G.; Bat-Erdene, U.; Nguyen, C.; Gan, J.H.; Zhou, J.H.; Jacobsen, S.E.; Tang, Y. *Nature* **2018**, *559*, 415–418.
11. Amorim Franco, T. M.; Blanchard, J. S. *Biochemistry* **2017**, *56*, 5849–5865.

synthase (ALS) , dihydroxyacid dehydrase (DHAD) and acetoxyhydroxy acid isomeroreductase (KARI). In contrast to most gene-directed herbicides who target ALS,[12] **3.5** targets the dihydroxyacid dehydrase (DHAD) enzyme, in charge of producing α-keto acids precursor to isoleucine, valine and leucine via β-dehydration (Scheme 3.3A).[13]Aspterric acid **3.5** is the first sub-micromolar DHAD inhibitor, which makes it effective when used as an herbicide in spray applications. Crops resistant to **3.5** have also been prepared to make this herbicide as selective as possible against weed.

In 1978, the isolation team proposed a biosynthetic pathway leading to **3.5**, which was further validated recently by sequential gene expression of genes AstA-C (Scheme 3.3B). After the cyclization of farnesyl diphosphate (**3.20**) by AstA to form (-)-daucane (**3.21**), AstB catalyzes the oxidation of **3.21**, producing the epoxide **3.22**. Subsequent oxidation by AstC at pendant methyl group generates an alcohol, which can undergo intramolecular epoxide opening, leading to the formation of aspterric acid **3.5**.

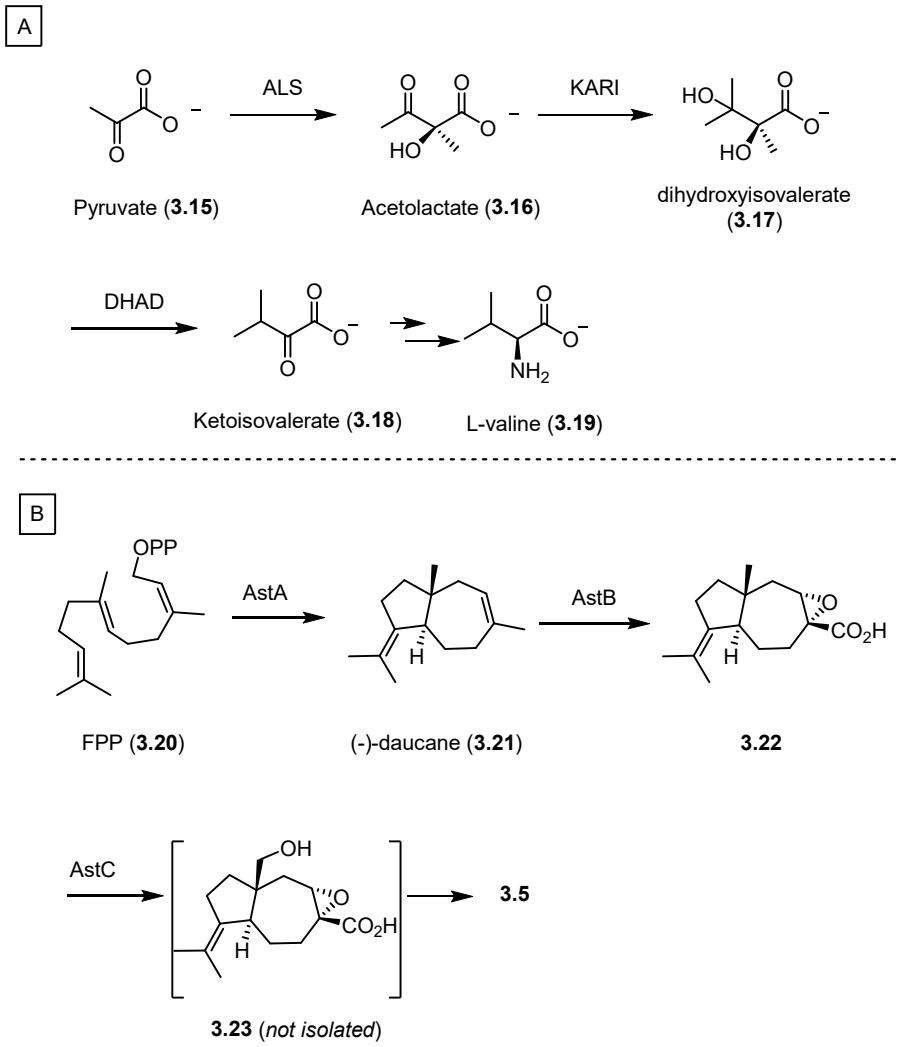

Scheme 3.3. A) BCAA biosynthetic pathway for the synthesis of L-valine. B) Biosynthesis of aspterric acid (**3.5**).

12. Heap, I. *Pest Manag. Sci.* **2014**, *70*, 1306–1315.
13. a) Flint, D. H.; Emptage, M. H. *J. Biol. Chem.* **1988**, *263*, 3558–3564. b) Flint, D. H.; Emptage, M. H.; Finnegan, M. G.; Fu, W.; Johnson, M. K. *J. Biol. Chem.* **1993**, *268*, 14732–14742.

Previous Synthesis of Aspterric Acid

Shortly after its isolation, the group of Inubishi and coworkers reported the total synthesis of aspterric acid (Scheme 3.4).[14] Their synthesis started from cyclooctadienol **3.24** which after 4 steps involving a ring contraction, oxidation and esterification was converted into 7-membered ring *β*-ketoester **3.25**. Robinson annulation of **3.25** with methyl vinyl ketone (MVK) followed by global reduction and allylic reoxidation afforded alcohol **3.27**. Treatment of the alkene with iodine and silver oxide delivered a mixture of **3.28** and **3.29** in 74 and 15% yields, respectively. The former could be converted into the latter in a two-step sequence of acetoxylation of the iodide and hydrolysis of the resulting acetate with an overall 67% yield. Alcohol protection, *α*-dimethylation and ketone reduction afforded protected alcohol **3.30** in 42% yield over three steps.

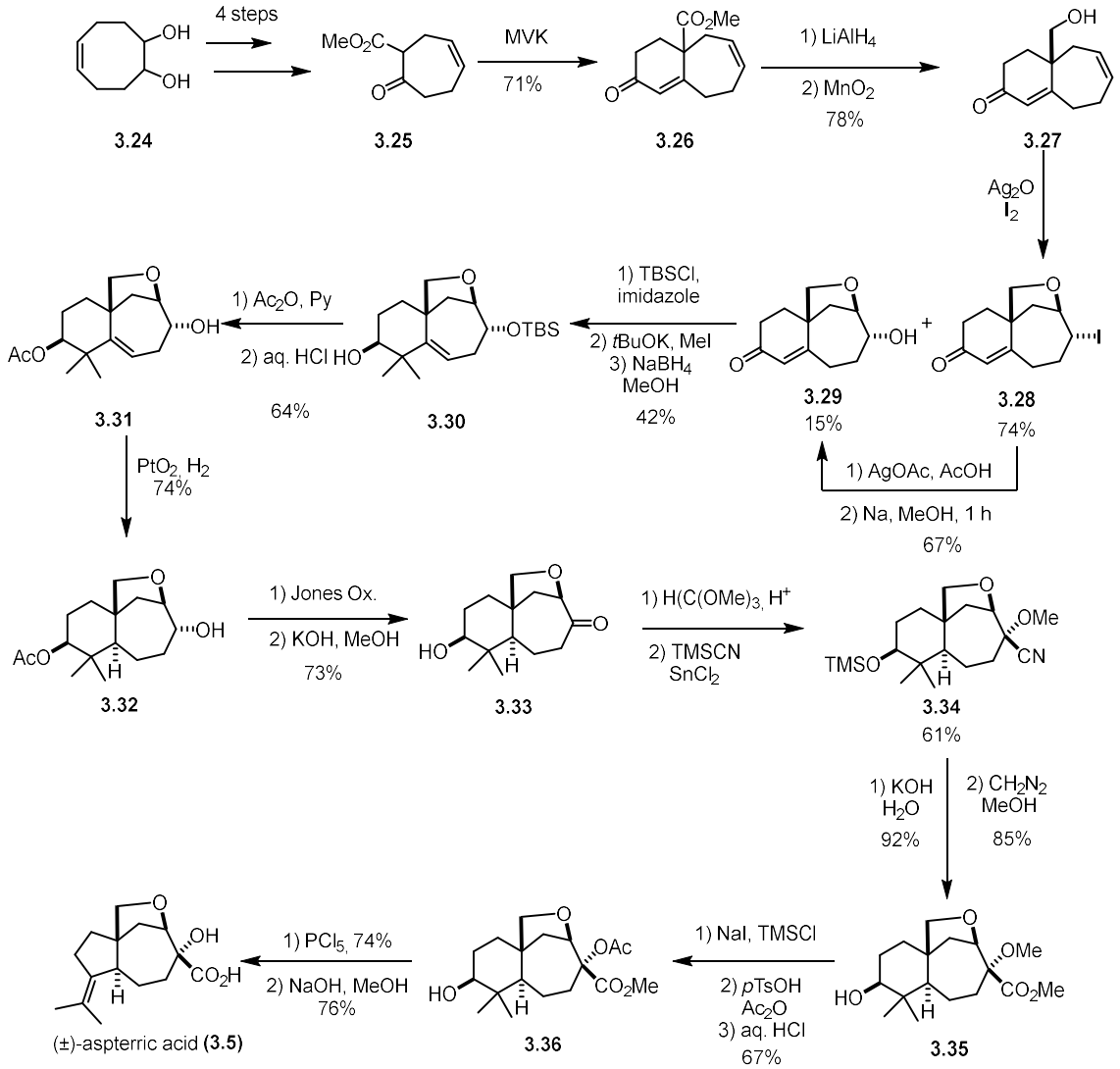

Scheme 3.4. Total synthesis of aspterric acid reported by the Inubishi and Harayama's group in 1987.

To favor hydrogenation to the trans isomer, a three-step sequence of acetylation of the secondary alcohol and deprotection of the bulky neighboring OTBS was performed in 64% yield over the three steps. Then hydrogenation with Adams' catalyst in the presence of catalytic acetic acid was carried out rendering **3.32** with the desired trans configuration in 74% yield. Oxidation and

14. a) Harayama, T.; Shinkai, Y.; Hashimoto, Y.; Fukushi, H.; Inubushi, Y. *Tetrahedron Letters* **1983**, *24*, 5241–5244. b) Harayama, T.; Sakurai, K.; Tanaka, K.; Hashimoto, Y.; Fukushi, H.; Inubushi, Y. *Chem. Pharm. Bull.* **1987**, *35*, 1434–1442.

hydrolysis of **3.32** provided ketone **3.33**, which was converted into **3.34** by acetalyzation and treatment with TMSCN in the presence of catalytic $SnCl_2$, in 65% yield over two steps. Basic hydrolysis of the nitrile in **3.34**, followed by transesterification with diazomethane under mild conditions afforded methyl ester **3.35**. Protection of secondary alcohol with *in situ* generated TMSI followed by acetoxylation and deprotection of the recently introduced TMS group provided product **3.36**. Finally, **3.36** was converted into racemic aspterric acid **3.5** by ring contraction and saponification in 74 and 76% yield respectively.[15]

Penigrisacid A

Penigrisacid A (**3.6**) was isolated in 2019 from deep-sea derived fungi from the Indian Ocean, *Penicillium griseofulvum* (which showed potent anti-food allergic activity), together with other naturally occurring daucanes, including **3.5** (Figure 3.2).[16] These compounds were tested for anti-food allergic activity and subjected to cytotoxicity assays against five different cancer cells, but no significant activity was found in any of the cases. These compounds have only recently been isolated, so their biological testing is scarce. The structure of these compounds was proposed by NMR studies as well as DFT modelling of their circular dichroism (CD).

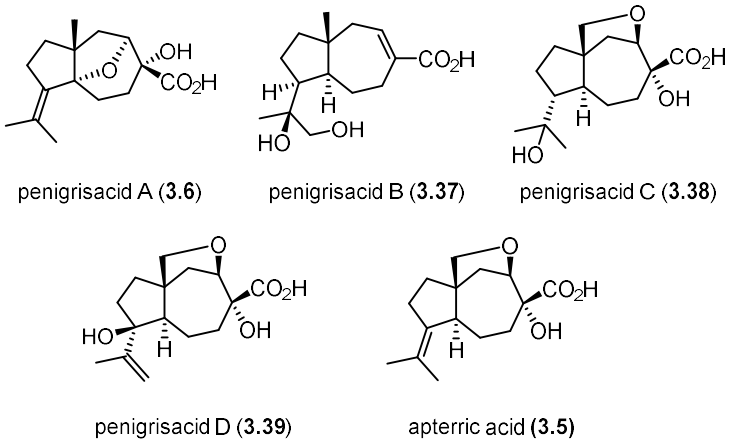

Figure 3.2. Isolated compounds from *Penicillium griseofulvum*.

Among the penigrisacids, we were interested in penigrisacid A (**3.6**), which presented an interesting 5-membered oxygen-bridged skeleton, whose synthesis we envision to be challenging. To date, none of the compounds in Figure 3.2, except aspterric acid, have been synthesized.

Shisanwilsonene A

Among the simpler carotene-like natural products, schisanwilsonene A (**3**) has interesting biological activities. It was first isolated in 2009 from *Schisandra willsoniana* and it presents strong anti-HB (hepatitis B) activity, inhibiting HBsAg and HBeAg secretion, at 50 μg/mL, by 76 and 29% respectively.[17]

15. These two reports are, to the date of this Doctoral thesis, the only total synthesis of Aspterric acid reported in the literature.
16. Xing, C.-P.; Xie, C.-L.; Xia, J.-M.; Liu, Q.-M.; Lin, W.-X.; Ye, D.-Z.; Liu, G.-M.; Yang, X.-W. *Mar. Drugs* **2019**, *17,* 1–8.
17. W.-H. Ma, H. Huang, P. Zhou, D.-F. Chen, *J. Nat. Prod.* **2009**, *72*, 676–678.

Previous Synthesis

In 2013 our group reported the first total synthesis of shisanwilsonene A (**3.3**) relying on a tandem gold(I)-catalyzed cyclization/1,5-OR migration/cyclopropanation as key step (Scheme 3.5),[18] which was later improved in 2016.[19] The synthesis of (+)-schisanwilsonene A was achieved starting from enantioenriched enyne **3.40**. Tandem gold(I)-catalyzed cyclization/1,5-OR migration/cyclopropanation of enyne **3.40** and alkene **3.41** bearing two protected alcohols, afforded cyclopentane **3.42**. After double desilylation with TBAF and monoacetylation with acetic anhydride and pyridine, monoprotected diol **3.43** could be prepared in 81 and 70% yields respectively. Oxidation of the non-protected alcohol and subsequent submission of the product to Witting provided intermediate **3.44**, which underwent a rearrangement under the same reaction conditions to form cycloheptadiene **3.45**. Then a reduction and partial hydrogenation of the double bonds was attempted, but after reduction with $LiAlH_4$, all attempts led to hydrogenation of all unsaturations of **3.46**. Thus, a sequence of oxidations from the alcohol to the ester was carried out to reintroduce the hydrogenated double bond. First, oxidation with TEMPO and PIDA led to the corresponding aldehyde in 55%, which was subjected to Pinnick oxidation conditions and selective methylation of the carboxylic acid with $TMSCHN_2$.

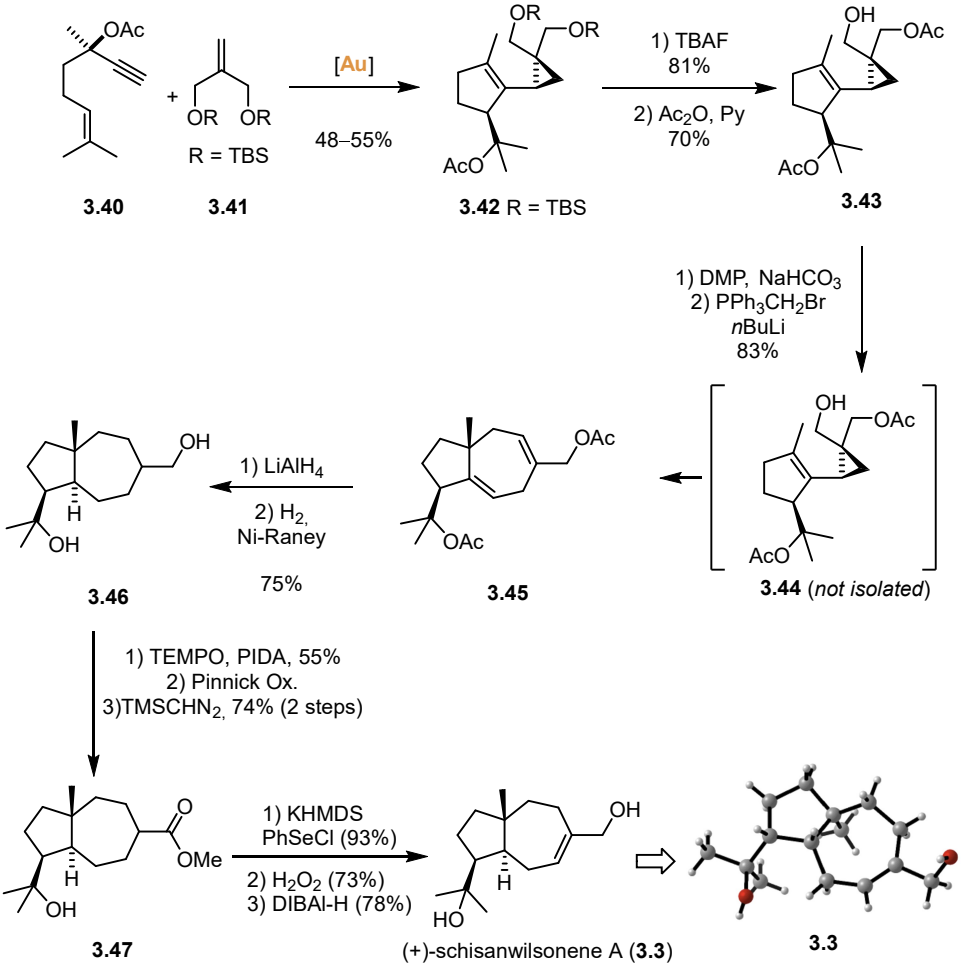

18. M. Gaydou, R. E. Miller, N. Delpont, J. Ceccon, A. M. Echavarren, *Angew. Chem. Int. Ed.* **2013**, *52*, 6396–6399.
19. Calleja, P.; Pablo, Ó.; Ranieri, B.; Gaydou, M.; Pitaval, A.; Moreno, M.; Raducan, M.; Echavarren, A. M. *Chem. Eur. J.* **2016**, *22*, 13613–13618.

Scheme 3.5. First total synthesis of (+)-shisanwilsonene A (**3.3**) by the Echavarren group. [Au] = [JohnPhosAuCl]. Py = pyridine.

Finally, two-step oxidation afforded the corresponding *α,β*-unsaturated ester and selective reduction of the resulting ester with DIBAL-H provided the desired product **3.3** in good yield, whose absolute configuration could be determined by X-ray diffraction.

More recently, an alternative synthesis has been developed by the Xiang group[20] starting from acetylSCoA involving the microbial-promoted synthesis of intermediate **3.49** (through FPP) which after 2 steps involving a Co(II)-catalyzed isomerization of the double bond and allylic oxidation delivered (+)-shisanwilsonene A (**3.3**) in moderate yields (Scheme 3.6).

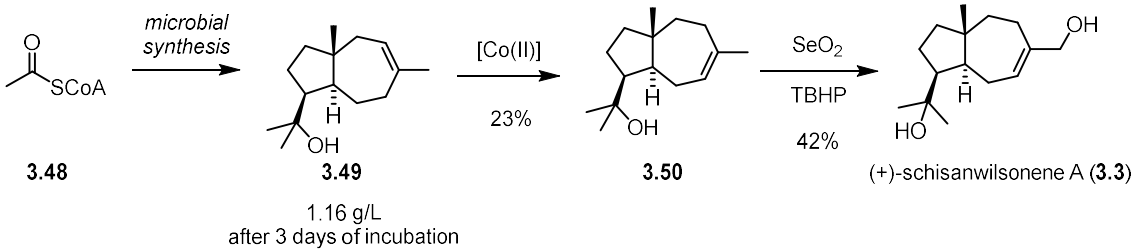

Scheme 3.6. Xiang's total synthesis of shisanwilsonene **3.3**.

20. S.-B Mou, W. Xiao, H.-Q. Wang, K.-Y. Chen, Z. Xiang, *Org. Lett.* **2021**, *23*, 400–404.

Objectives

In recent work by our group we reported the synthesis of hydroazulanes, 5/7 bicyclic compounds, by a gold(I)-catalyzed cycloisomerization / (4+3) cycloaddition of enyne **3.51** and diene **3.52**.[21] The mechanism of the reaction was supported by experimental and computational studies to procced via 5-*exo*-dig gold(I)-catalyzed cyclization to form a gold carbene (**3.54**), which undergoes 1,5-OR-migration and finally a (4+3) cycloaddition with diene **3.52** (Scheme 3.7).

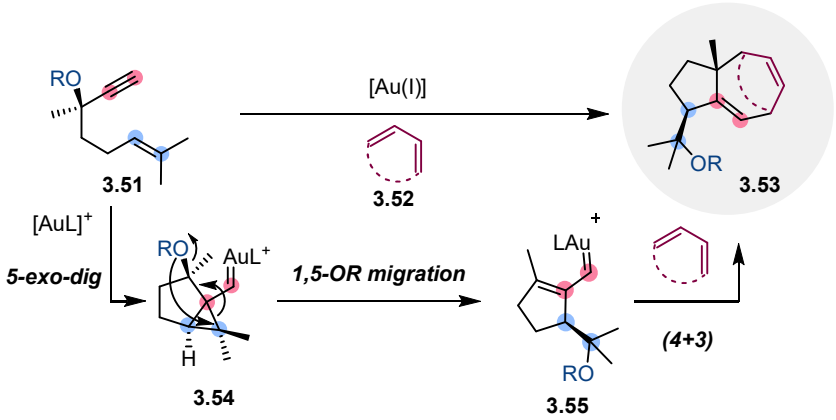

Scheme 3.7. Gold(I)-catalyzed cycloisomerization/formal (4+3) cycloaddition of enyne **3.51** reported by the Echavarren group.

We envisioned that hydroazulane **3.57**, which could be prepared from enyne **3.40** and diene **3.56,** could serve as a good common building block for the divergent total synthesis of several members of the daucane family of natural products, namely schisanwilsonene A, penigrisacid A and aspterric acid. Furthermore, the synthesis of penigrisacid A would be the first reported total synthesis and could serve to elucidate its structure. Finally, the developed route could allow accessing the natural products in an enantioselective manner from the corresponding enantioenriched 1,6-enyne, since the gold(I)-catalyzed reaction is stereospecific, as already demonstrated in our previous synthesis of schisanwilsonene A.[18,19]

21. a) Armengol-Relats, H.; Mato, M.; Echavarren, A. M. *Angew. Chem. Int. Ed.* **2021**, *60*, 1916–1922. b) Armengol-Relats, H.; Mato, M.; Echavarren, A. *Synthesis* **2021**, *53*, 3991–4003.

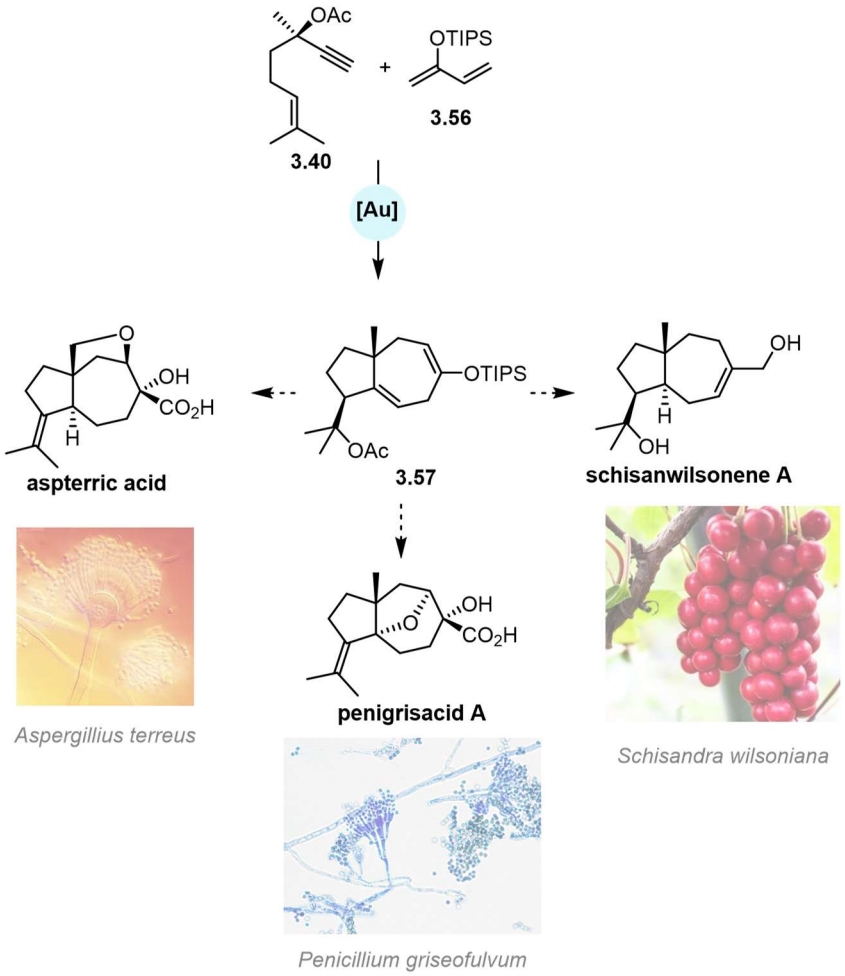

Scheme 3.8. Synthesis of daucane natural products from common building block **3.57**.

Results and Discussion[22]

Retrosynthetic Strategy

Our retrosynthetic plan for penigrisacid A, aspterric acid and schisanwilsonene A is summarized in Scheme 3.9. In the case of penigrisacid A, acetate elimination would render formation of the *exo* alkene in **3.58**. We envision that given the right configuration of the alcohol at C3 we could perform an oxa-Michael addition to double bond C6-7 and then hydration of the resulting double bond conjugated to the ester. Diene **3.59** could arise from Rubottom-type oxidation and further manipulations on silylenol ether **3.57** which could be the product of trapping of the gold(I) carbene intermediate in the gold(I)-catalyzed cyclization of enyne **3.40** with diene **3.56**. On the other hand, for aspterric acid we envision a similar acetate elimination and a hydroxylation alpha to the ester moiety for the formation of intermediate **3.60**. Closing of ring C could arise from a Suárez radical cyclization given the right configuration of the alcohol in intermediate **3.59** and a double hydrogenation would afford the desired *trans*-configuration between rings A and B. Finally, the formal synthesis of schisanwilsonene A could be accomplished by a shorter synthesis of reported intermediate **3.62** of the previous synthesis by our group.[18,19] Methanolysis of the acetate group would render the tertiary alcohol, and hydrogenation of the double bonds in **3.61** would afford the desired *trans*-configuration of the fused rings. Intermediate **3.61** could then come from the deprotection of the TIPS-enol ether and manipulation of the resulting ketone.

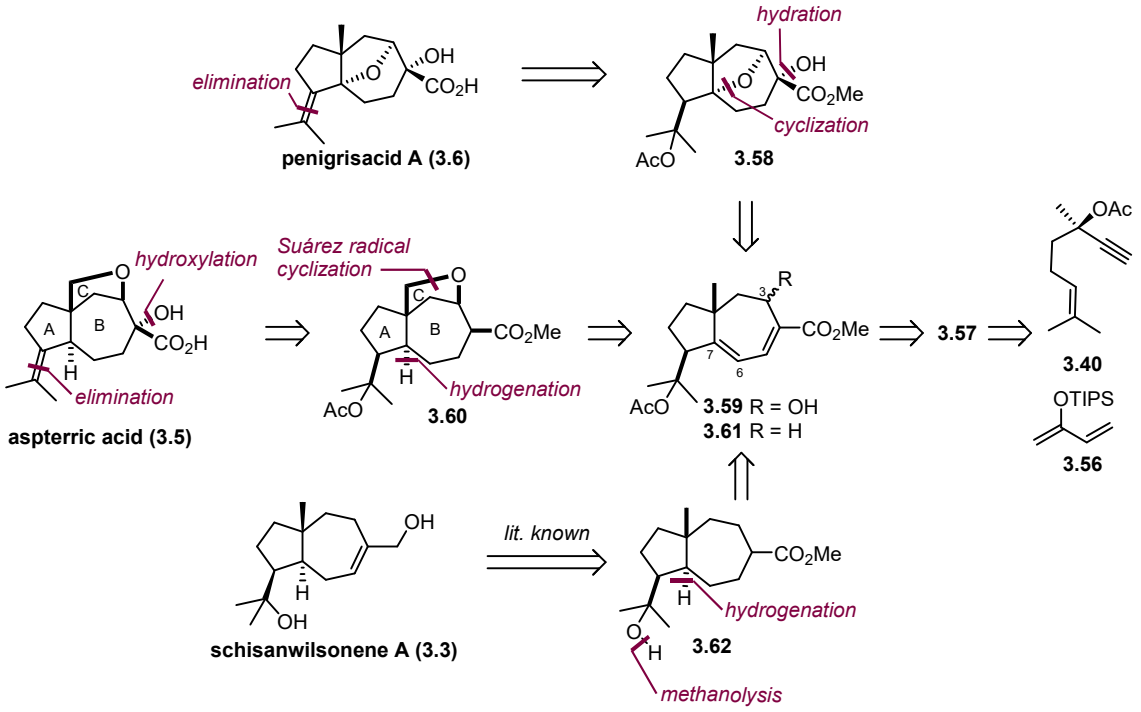

Scheme 3.9. Retrosynthetic analysis to access sesquiterpenes **3.3**, **3.5** and **3.6**.

Synthesis of Common Building Block for Aspterric Acid and Penigrisacid A

We started the synthesis by fine-tuning the conditions for the gold(I)-catalyzed cycloisomerization/formal (4+3) cycloaddition of enyne **3.40** and **3.56**,[23] as the reaction was not

22. Work carried out in collaboration with Dr. Helena Armengol-Relats, Dr. Anna Sadurní and Miquel Àngel Pérez Puigdomènech.
23. Enyne **3.40** and diene **3.56** were prepared in two and one steps, respectively, from commercially available materials.

easily reproducible and required a large excess of 1,3-diene **3.56** (3 equiv). The main side product of the reaction was the cycloisomerization of enyne without trapping of gold(I) carbene intermediate **3.63** with the diene and other side products.[24] The reaction was exothermic, so it was usually cooled to 0 °C with an ice/water bath and the enyne was added dropwise as a stock solution to a solution of diene **3.56** and the corresponding catalyst. On the previous report, the best catalysts were the cationic gold(I) complexes **Au25** and **Au26** (Table 3.1, entries 2 and 3), as adding silver salts as scavengers led to decomposition of the diene. Changing to more coordinating bistriflamide counterion **Au24** or **Au27** led to lower conversion (Table 3.1 entries 1 and 4). Lowering the temperature of the reaction also led to poor conversions even after 48 h (Table 3.1, entry 5). Our hypothesis is that we needed a fast catalytic system that would quickly cyclize the enyne as it enters the reaction mixture and then react with the large excess of diene in solution. Thus, performing a slower addition of the enyne and increasing the concentration of the reaction afforded the desired product in 48 and 40% NMR yield using **Au25** and **Au26**, respectively (Table 3.1, entries 6 and 7). Finally, when performing such a slow addition we could lower the catalyst loading to 0.5 mol%, reduce the amount of diene **3.56** down to 1.05 equiv-and increase the scale of the reaction to up to 12 g of enyne **3.40**, delivering the desired product **3.57** in 42% NMR yield (Table 3.1, entry 8).

Table 3.1. Optimization gold(I)-catalyzed step.

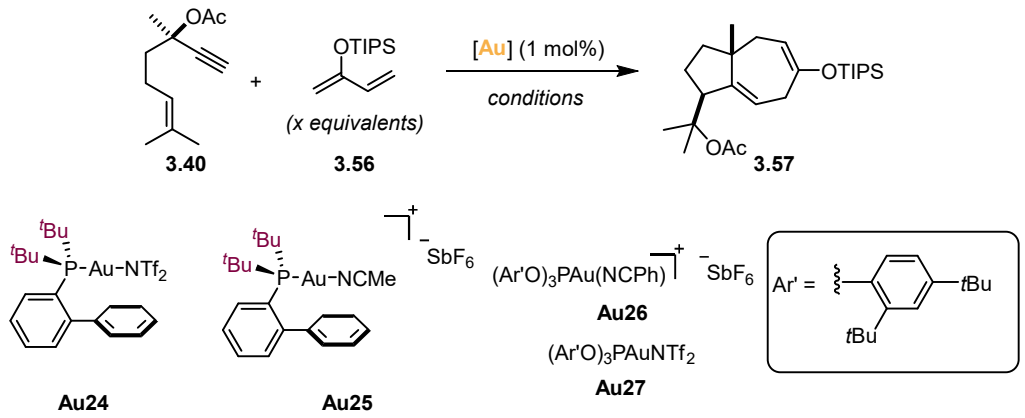

Entry	[Au]	X	Conditions	Yield[a]
1	**Au24**	3	CH_2Cl_2 (0.2M), 0 to 27 °C, 18 h	3%
2	**Au25**	3	CH_2Cl_2 (0.2M), 0 to 27 °C, 10 min	25%
3	**Au26**	3	CH_2Cl_2 (0.2M), 0 to 27 °C, 1 h	19%
4	**Au27**	3	CH_2Cl_2 (0.2M), 0 to 27 °C, 18 h	20%

24. Please see ref. 21 for an in-detail study of the gold(I)-catalyzed reaction.

5[b]	**Au25**	3	CH_2Cl_2 (0.2M), -20 °C, 48 h	6%
6[c]	**Au25**	2	CH_2Cl_2 (0.5M), 0 to 27 °C, 90min	48%
7[c]	**Au26**	2	CH_2Cl_2 (0.5M), 0 to 27 °C, 90 min	40%
8[c,d]	**Au25**	1.05	CH_2Cl_2 (0.5M), 0 to 27 °C	42%

[a] Reactions performed on a 0.3 mmol scale of enyne **3.40**. Yield determined by ^{1}H NMR using diphenyl methane as internal standard. [b] 57% enyne remainig. [c] Addition of a stock solution of enyne **3.40** over a solution of diene **3.56** and catalyst with a syringe pump over 1 h. [d] 12 g of enyne were employed.

Next, we took advantage of the already set silyl enol ether in **3.57** to selectively functionalize the desired α-position via a Rubottom-type oxidation[25] to introduce the hydroxyl group. Intermediate **3.57** was found to be sensitive to acid traces which lead to the isomerization of the double bond into conjugated diene **3.64**. Therefore, the crude mixture of the gold(I)-catalyzed reaction was subjected to the next transformation after quenching with Et_3N and removal of the solvent under reduced pressure.[26]

A screening of conditions for the Rubottom oxidation was performed. The reaction took place with *m*CPBA but the yield was moderate and not easily reproducible (Table 3.2, entry 1). Other epoxidation conditions led to either no reaction or decomposition of the starting material or products. Using milder peroxidation reagent magnesium monoperoxyphtalate (MMPP) led to the desired product with 60% yield (Table 3.2, entry 6). Finally, good yields were obtained when mixing excess *m*CPBA buffered with $NaHCO_3$ in MeOH for 30 min at 23 °C and then cooling to 0 °C and adding a stock solution of the substrate in the minimum amount of CH_2Cl_2.

Table 3.2. Screening of reaction conditions for the Rubottom-type oxidation of **3.57**.

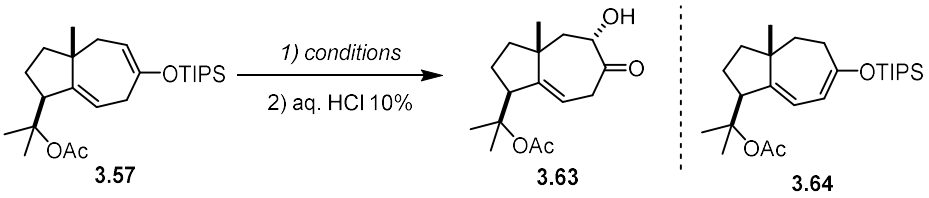

3.57 **3.63** **3.64**

Entry	conditions	NMR yield (3.57)[a]
1	*m*CPBA (1 equiv), MeOH (0.2 M), 0 to 23 °C, 1 h	20–30%
2	H_2O_2 (1.2 equiv), CH_2Cl_2 (0.1M), 0 °C	dec.
3	DMDO (2 equiv), MeOH (0.2M), 0 °C	(90%)
4	Oxone (1 equiv), Acetone (10 equiv), $NaHCO_3$ (5 equiv), 23 °C, EtOAc:Water (1:1, 0.1M)	13%

25. a) Pelegrina, D.R.; Vazquez, M.A.; Rubottom, G.M. *Tetrahedron Lett.* **1974**, *15*,4319–4322. b) Hashiyama, T.; Morikawa, K.; Sharpless, K. B. *J. Org. Chem.* **1992**, *57*, 5067–5068.
26. The crude product could be partially purified by FCC, treating the silica with 1% Et_3N.

5	$MeReO_3$ (6%), UHP (1.5 equiv), pyridine (0.25 equiv), 23 °C, MeCN:AcOH (99:1)	(77%)
6	MMPP (0.55 equiv), $NaHCO_3$ (1.5 equiv), MeCN: CH_2Cl_2 (2:1, 0.1M), 23 °C, 48 h	60% (15)
7[b]	*m*CPBA (1.5 equiv), $NaHCO_3$ (5 equiv), MeOH (0.4M), 0 to 23 °C, 2 h	80%[c]

[a] NMR yield determined by ^1H NMR using diphenylmethane as internal standard, of the crude of epoxidation. In parenthesis remaining starting material. [b] *m*CPBA and $NaHCO_3$ stirred for 30 min at 23 °C before cooling to 0 and adding substrate as a stock solution in the minimum amount of CH_2Cl_2. [c] Yield of isolated material after washing with aq. HCl 10% and FCC. dec. = decomposition.

The relative configuration of **3.63** was determined by Dr. Helena Armengol-Relats by isolation and characterization by X-ray of an *m*CPBA-adduct product, **3.66** (Scheme 3.10). *m*CPBA adducts of this type have been observed before in similar Rubottom-type oxidations, depending on the solvent.[27] Comparison of the coupling constants and NOE experiments confirmed that both **3.63** and **3.66** have the same relative configuration.

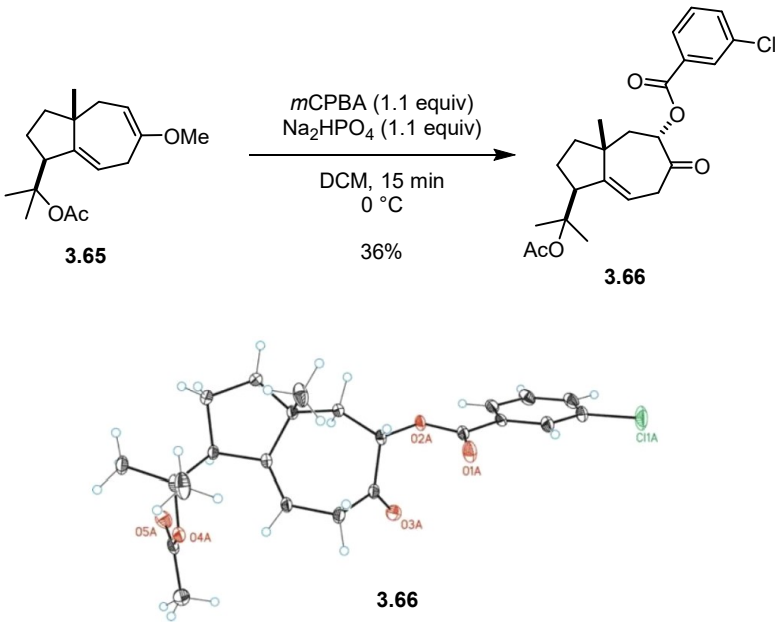

Scheme 3.10. Isolation and characterization of *m*CPBA-adduct **3.66**.

A screening of catalysts and reaction conditions for the hydrogenation of the alkene in **3.63** was performed but either decomposition of the starting material, reduction of the ketone or no reaction were observed. Thus, we decided to introduce the ester in this step by a sequence of alcohol protection, triflation, methoxycarbonylation and deprotection (Scheme 3.11). Protection of the secondary alcohol in **3.63** with TBSCl,[28] followed by triflation using freshly prepared LiHMDS[29] and Comins' reagent allowed the obtention of triflate **3.68**, in 93 and 73% yields respectively. Finally, palladium-catalyzed methoxcarbonylation and subsequent TBS removal afforded common intermediate **3.59** in excellent yields.

27. Boeckman, R. K.; Ramaiah, M. *J. Org. Chem.* **1977**, *42*, 1581–1586.
28. Performing the reaction with a mixture of CH_2Cl_2 and DMF improved the yield compared to when performed only in CH_2Cl_2.
29. Yields were slightly better if LiHMDS was freshly prepared rather than using commercially available solid LiHMDS or NaHMDS.

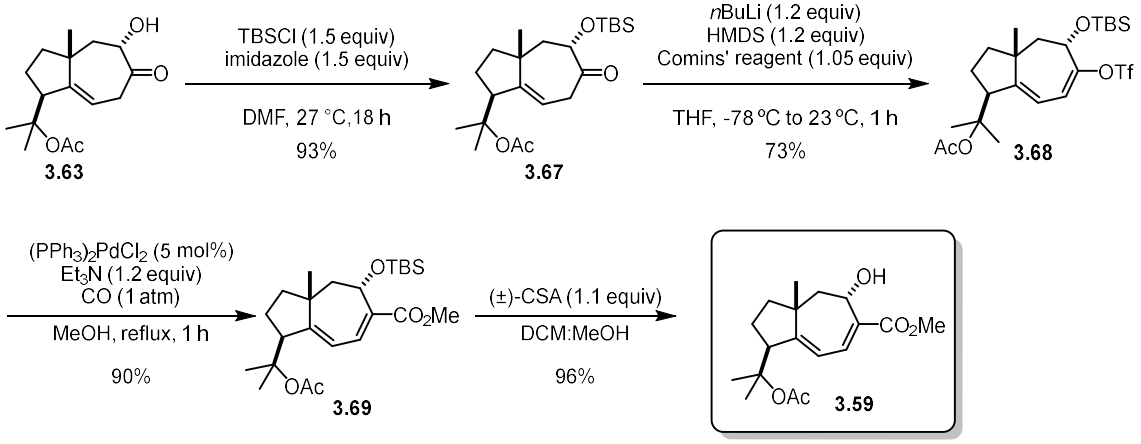

Scheme 3.11. Preparation of common intermediate **3.59** of the total synthesis of aspterric acid and penigrisacid A.

Aspterric acid

With substrate **3.59** in hand, double hydrogenation of the diene was attempted. We were pleased to find that the desired product **3.70** formed in moderate yield at 23 ºC and 20 bar of H_2 with Adams' pre-catalyst (Table 3.3, entry 1). However, when switching to Pd/C or $Pd(OH)_2$ full conversion was observed but only partial hydrogenation of the substrate to **3.71** or decomposition of the starting material, including elimination of the acetate group, could be detected (Table 3.3, entries 2–3). Iridium-based catalysts provided no reaction even after prolonged reaction times (Table 3.3, entries 4–5). To our delight, when the reaction was either performed in MeOH or EtOAc with trace acid and using PtO_2,[30] the product could be obtained reproducibly in good yield (Table 3.3, entries 6–7).

Table 3.3. Hydrogenation of diene in **3.59**.

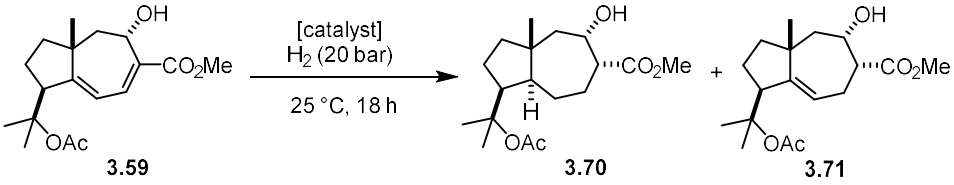

Entry	Catalyst (mol%)	solvent	Conversion	Yield [a]
1	PtO_2 (20)	EtOAc	100%	32%
2	Pd/C	EtOAc	100%	n.d.[b]
3	$Pd(OH)_2$	MeOH	90%	n.d.[b]
4[c]	$[(PCy_3)(COD)(py)Ir]PF_6$	CH_2Cl_2	0%	-
5[c]	$[(PCy_3)(COD)(py)Ir]BAr_4^F$	CH_2Cl_2	0%	-
6	PtO_2 (20)	MeOH	100%	73%
7[d]	PtO_2 (20)	EtOAc	100%	78%

30. Only the batch of catalyst from Sigma Aldrich worked well, while using other batches led to either no reaction or formation of the desired product along with a complex mixture of several unidentified byproducts.

[a]Yield determined by ^{1}H NMR using mesitylene as internal standard. [b] Complex mixture, including partial hydrogenation of the SM. [c] Reaction left for 48 h. [d] One drop of acetic acid was added n.d. = not determined.

The relative *cis* configuration of the two newly formed stereocenters in **3.70** was confirmed by X-ray diffraction of crystalline **3.70'**, prepared by Dr. Helena Armengol by reaction of **3.70** with *para*-nitrobenzoyl chloride (Scheme 3.12).

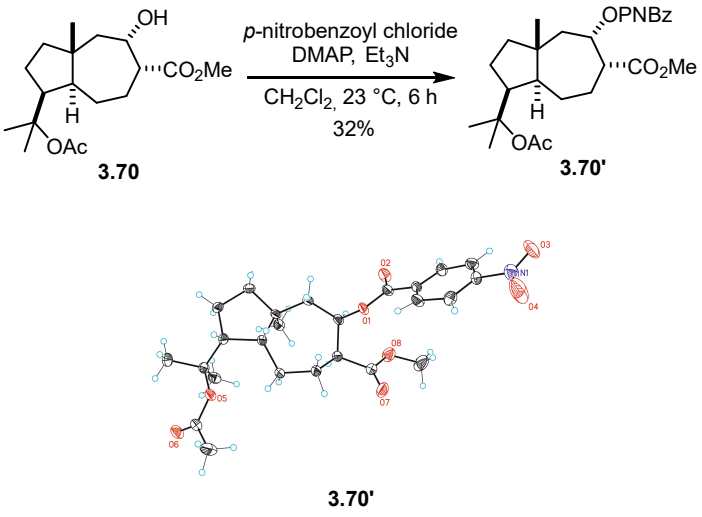

Scheme 3.12 Determination of the relative configuration in **3.70** by preparation of a benzoate derivate.

To close ring C in aspterric acid we need to invert the stereocenter at the secondary alcohol, which would then enable Suárez radical cyclization to forge ring C. Mitsunobu conditions only led to either decomposition of the substrate or no reaction. Thus, we moved to a two-step oxidation/reduction strategy of the alcohol in **3.70**. We also did some tests on the Mitsunobu reaction of substrate **3.59** or the oxidation of the alcohol and then hydrogenation of the resulting enol ether (Scheme 3.13), but no conversion was observed in any of the cases.

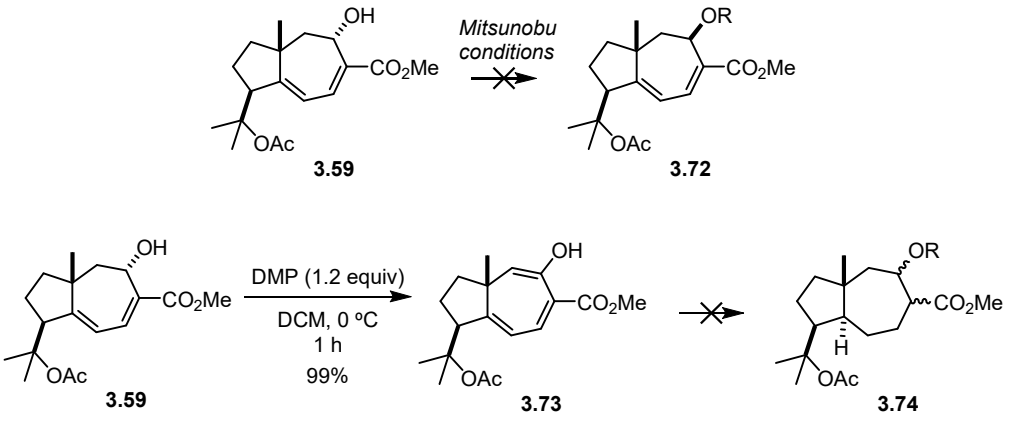

Scheme 3.13. Attempts on the inversion of the configuration of the alcohol in **3.59**.

On the other hand, oxidation of **3.70** with DMP afforded ketoester **3.75**, which was in equilibrium with its enol tautomer, which supposed a loss of the stereochemical information on its α-carbon (Scheme 3.14). After a screening of different reducing agents, we found that performing the reduction in MeOH at 0 ºC and with 1.0 quiv of $NaBH_4$ provided the desired product **3.77** with 70% as well as **3.76** as a 1:1 mixture of diastereomers, which could be converted back into **3.75** in 90% yield (Scheme 3.14).

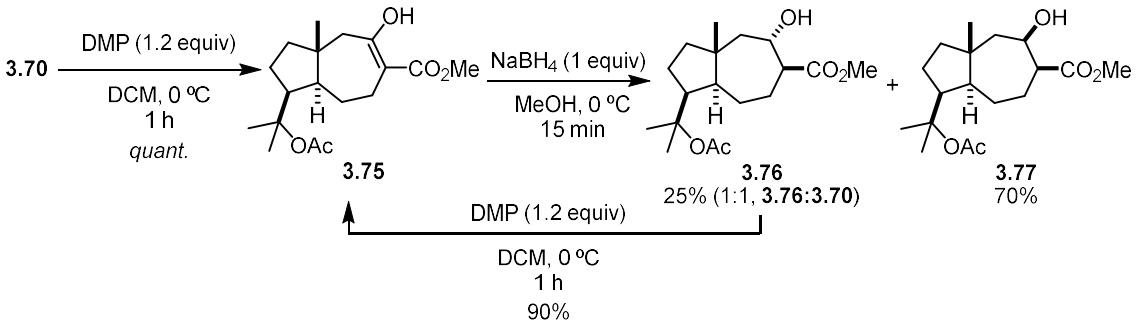

Scheme 3.14. Oxidation/reduction sequence to invert the stereochemistry of the secondary alcohol in **3.70**.

Next, the closing of ring C was performed via a Suárez radical cyclization (Scheme 3.15).[31] Initial attempts by Dr. Helena Armengol led to the formation of the desired product in low yield. The major side product of the reaction was found to be lactone **3.79**, which was detected by UHPLC-MS and isolated when the reaction went to full conversion of the starting material. Its structure was confirmed by X-ray diffraction. Our hypothesis is that this lactone arises from the activation of the other two C–H bonds of the methyl group leading to a triodide intermediate, which undergoes ring closure and then hydrolysis of the resulting cyclic diiodomethylene in the aqueous work up.[32] We observed that the formation of this byproduct was larger if we allowed the reaction to reach completion, thus it was instead stopped at *ca.* 50% conversion of **3.77** (reaction was monitored by UHPLC).

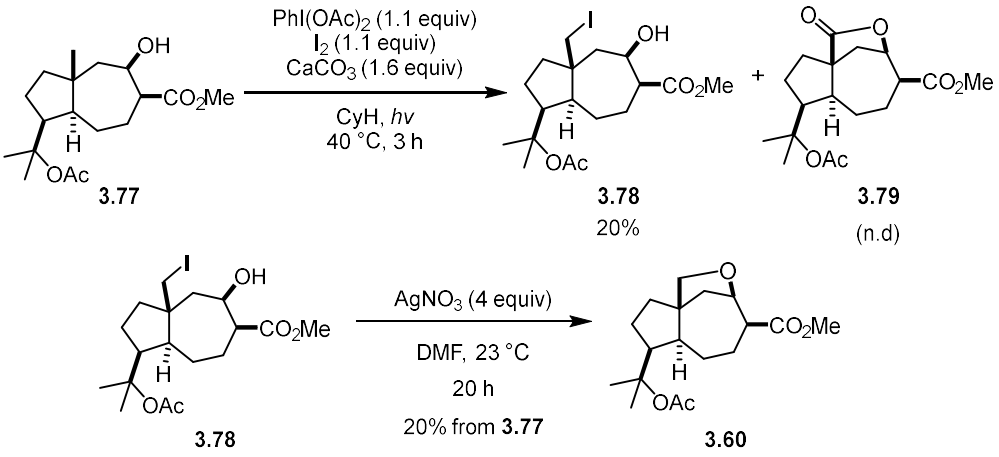

Scheme 3.15. Initial attempts on the Suárez radical cyclization carried out by Dr. Helena Armengol i Relats.

A summary of the screening on the reaction conditions for the Suárez radical cyclization is shown in Table 3.4. Switching from I_2 to perfluorobutyl iodide as iodine source in the presence of excess $CaCO_3$ led to the formation of cyclized **3.60** in comparable yields to the ones previously reported by Dr. Armengol (Table 3.4 entry 1 vs. 2). Using PIFA instead of PIDA led to a slower reaction, only reaching about 50% conversion after more than 10 h (Table 3.4 entry 3). We found out that $CaCO_3$ had no effect on the outcome of the reactivity and that increasing the temperature only provided an increased decomposition of product and starting material (Table 3.4, entries 4–5).

31. a) Concepción, J. I.; Francisco, C. G.; Hernández, R.; Salazar, J. A.; Suárez, E. *Tetrahedron Lett.* **1984**, *25*, 1953–1956; b) Francisco, C. G.; Freire, R.; Herrera, A. J.; Peréz-Martín, I.; Suárez, E. *Org. Lett.* **2002**, *4*, 1959–1961
32. Please check Dr. Helena Armengol i Relats PhD thesis for the proposed mechanism for the formation of **3.79**.

Lowering the temperature led to a slower conversion but better selectivity and reproducibility of the reaction, obtaining the desired primary iodoalkane **3.78** in 40% yield and 30% recovered starting material on a 100 mg scale of **3.77** (Table 3.4, entries 6–7). Importantly, the distance from the light source to the center of the reaction flask had to be about 15 cm, as shortening it led to faster reactions but lower selectivity and increasing it led to very slow reactivity. Finally, increasing the scale of the reaction from 100 to 200 mg delivered the desired product in lower yields (Table 3.4, entry 8). Thus, we chose 100 mg as the optimal scale of the reaction.

Table 3.4. Screening conditions for the C–H activation of **3.77**.

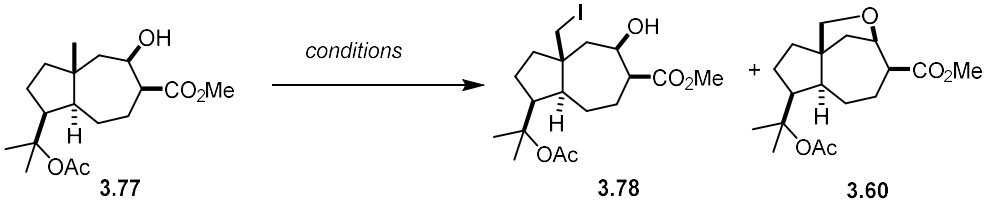

3.77 3.78 3.60

Entry	Conditions	yield (%)[a]
1[b]	PIDA (2 equiv), I_2 (1.0 equiv), $CaCO_3$ (1.6 equiv), CyH, 40 °C, 6 h	20%
2[c]	PIDA (2 equiv), perfluorobutyl iodide (8.0 equiv), $CaCO_3$ (3.0 equiv), CyH, 65 °C, 16 h	20% [28%]
3	PIFA (1.5 equiv), I_2 (1.0 equiv), CyH, 65 °C, 18 h	22% [12%]
4	PIDA (2 equiv), I_2 (1.0 equiv), CyH, 40 °C, 6 h	20% [23%]
5	PIDA (2 equiv), I_2 (1.0 equiv), CyH, 65 °C, 1 h	16% [11%]
6[d]	PIDA (1.5 equiv), I_2 (1.0 equiv), CyH, 25 °C, 6 h	40% [30%]
7[d]	PIDA (1.5 equiv), I_2 (1.0 equiv), CyH, 25 °C, 7 h	39% [28%]
8[e]	PIDA (1.5 equiv), I_2 (1.0 equiv), CyH, 25 °C, 7 h	20% [30%]

[a] Yield determined by ^{1}H NMR using mesitylene as internal standard. In brackets recovered or unreacted starting material. [b] Conditions reported by Dr. Helena Armengol i Relats, yield refers to isolated product **3.60**. [c] The product of ring closing was obtained directly. [d] I_2 was added slowly as a solution in degassed CyH, 100 mg scale, lamp placed 15 cm to the center of the reaction flask. [e] 200 mg scale. CyH = Cyclohexane.

Finally, the configuration of the enol tautomer of **3.75**, alcohol **3.76** and cyclized product **3.60** was confirmed by X-ray diffraction (Figure 3.3) of crystals obtained by slow evaporation of CH_2Cl_2 solutions and pentane at 23 °C.

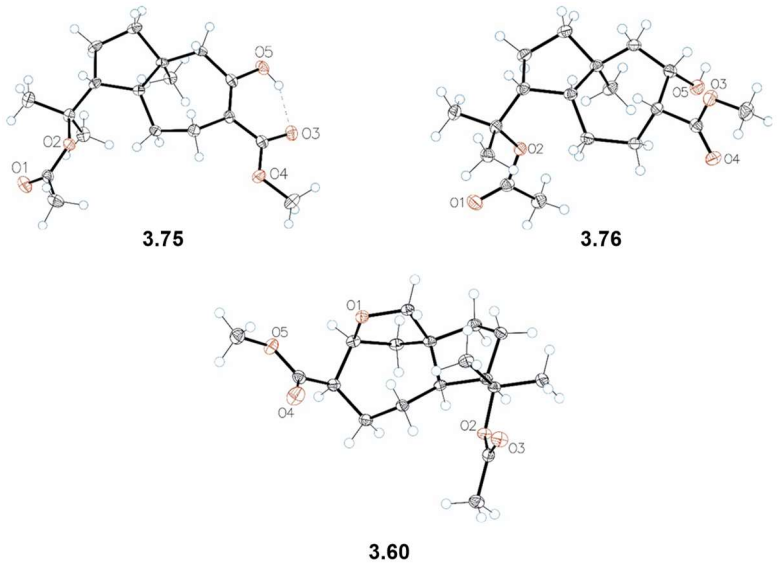

Figure 3.3. Determination of the relative configuration of products **3.75**, **3.76** and **3.60** by X-ray diffraction analysis.

Alpha-hydroxylation of the ester was performed by trapping the corresponding potassium enolate with oxygen and reducing the resulting hydroperoxide with triethylphosphite[33] obtaining product **3.80** as a single diastereomer in 90% yield (Scheme 3.16).

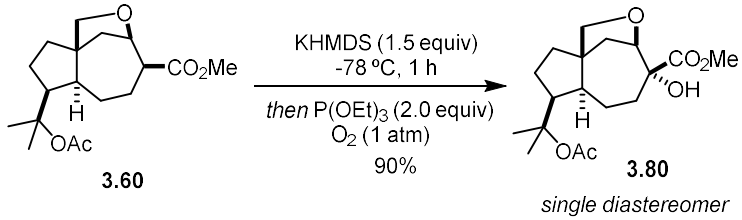

Scheme 3.16. Alpha-hydroxylation of ester **3.60** to form **3.80**.

Screening of basic and acid conditions for the acetate elimination led to either decomposition of the starting material or elimination and isomerization of the double bond into a more stable quaternary endocyclic double bond. While monitoring the acid-promoted acetate elimination by GCMS analysis it was discovered that the reaction was proceeding by first formation of *exo*-alkene **3.81**, which then undergoes isomerization to form the desired product **3.82**. If the reaction was left for too long or the acid employed was too strong, the latter would isomerize to more stable *endo*-alkene **3.83**. While **3.83** could be purified by FCC from **3.81** and **3.82**, none of the purification conditions by FCC provided any separation of either of the *exo*-alkenes. We determined by DFT calculations the relative energies of the three isomers and found that **3.83** is the thermodynamic product in the equilibrium (Scheme 3.17). This explains-why the alkene tends to isomerize to the endo position of **3.83**.

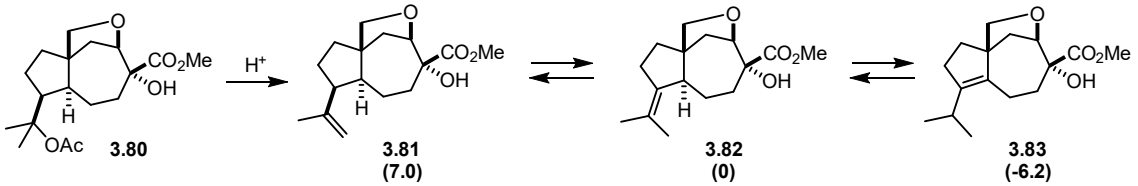

33. a) Liang, Y.-F.; Jiao, N. *Angewandte Chemie International Edition* **2014**, *53*, 548–552. b) Nicolaou, K. C.; Harrison, S. T. *J. Am. Chem. Soc.* **2007**, *129*, 429–440.

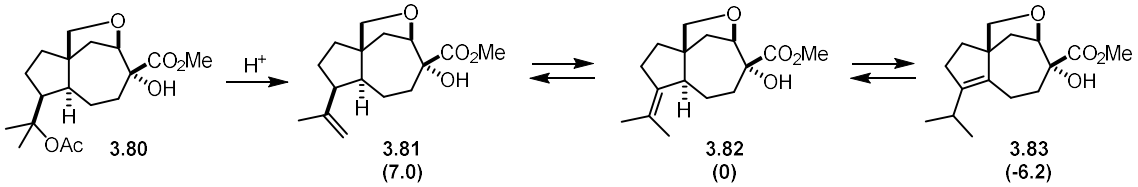

Scheme 3.17. DFT calculations on the acid-promoted acetate elimination, in parenthesis the relative energies in Kcal/mol, using **3.82** as the zero point.

Performing the reaction in acetone in the presence of I_2 as catalyst, the product could be obtained in moderate yield,[34] though as an inseparable 4:1 mixture of **3.82** with the *exo*-alkene isomer **3.81** (Scheme 3.18). Finally, basic hydrolysis of the ester afforded aspterric acid (**3.5**) in excellent yields as a 4:1 mixture with the *exo*-alkene isomer **3.84**.

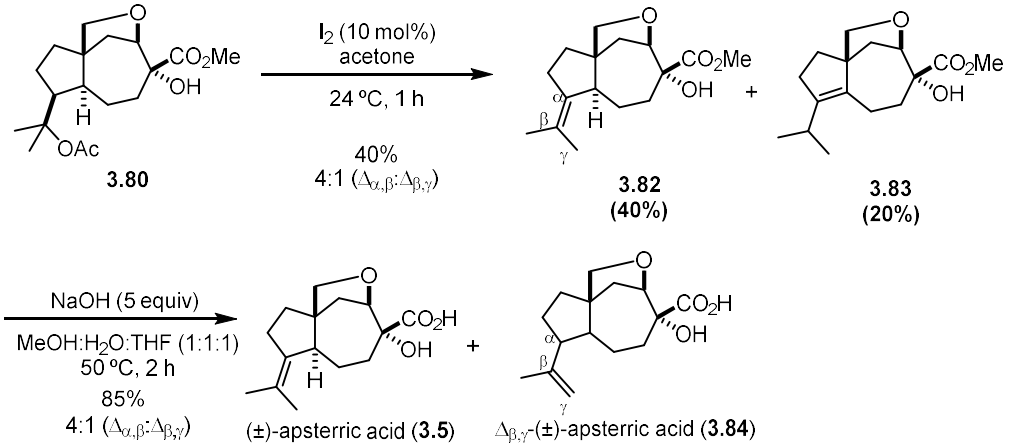

Scheme 3.18. Synthesis of aspterric acid (**3.5**).

The ^{1}H and ^{13}C NMR spectra of synthesized **3.5** agreed with an authentic sample of the commercially available natural product. In Table 3.5 we can see a comparison of the signals of synthetic **3.5** and an authentic sample.[35]

Table 3.5. Comparison of the ^{1}H NMR of synthetically prepared **3.5** and an authentic sample.

Experimental ^{1}H NMR	Authentic sample ^{1}H NMR	Δδ (ppm)[a]
4.30 (d, *J* = 8.7 Hz, 1H)	4.31 (d, *J* = 8.6 Hz, 1H)	−0.01
3.95 (d, *J* = 8.3 Hz, 1H)	3.96 (d, *J* = 8.3 Hz, 1H)	−0.01
3.51 (d, *J* = 8.4 Hz, 1H)	3.52 (dd, *J* = 8.5, 1.5 Hz, 1H)	−0.01
2.47 – 2.40 (m, 1H)	2.47 – 2.40 (m, 1H)	0
2.40 – 2.23 (m, 2H)	2.40 – 2.23 (m, 2H)	0
2.21 – 2.12 (m, 2H)	2.21 – 2.12 (m, 2H)	0

34. Athe, S.; Ghosh, S.; Mehta, G. *Tetrahedron Lett.* **2019**, *24*, 1570–1573.
35. Commercially available aspterric acid (5 mg) was bought from Tebubio Spain. Catalogue number: 10-3489.

2.09 – 2.00 (m, 1H)	2.09 – 2.00 (m, 1H)	0
1.83 – 1.73 (m, 2H)	1.83 – 1.73 (m, 2H)	0
1.72 (brs, 3H)	1.72 (brs, 3H)	0
1.62 (brs, 3H)	1.62 (brs, 3H)	0
1.58 – 1.48 (m, 2H)	1.58 – 1.48 (m, 2H)	0

[a] $\Delta\delta$ (ppm) = $\delta_{experimental}$ - $\delta_{authentic\ sample}$.

Table 3.6. Comparison of the ^{13}C NMR of synthetically prepared **3.5** and an authentic sample.

Experimental ^{13}C NMR	**Authentic sample ^{13}C NMR**	**Δδ (ppm)[a]**
178.3	178.1	+0.2
134.5	134.5	0
125.5	125.5	0
82.7	82.7	0
76.5	76.5	0
75.1	75.1	0
55.6	55.6	0
53.2	53.2	0
37.6	37.6	0
36.4	36.4	0
33.9	33.9	0
32.3	32.3	0
23.8	23.8	0
23.5	23.5	0
21.0	21.0	0

[a] $\Delta\delta$ (ppm) = $\delta_{experimental}$ - $\delta_{authentic\ sample}$.

In 2020, peniterester (**3.85)**, a carotene-type sesquiterpene, was isolated from an artificial mutant *Penicillium sp.* T2-M20, which was obtained from the parental strain *Penicillium sp.* T2-8.[36] Peniterester exhibited antibacterial activities against *Bacillus subtilis*, *Escherichia coli* and *Staphylococcus aureus* with minimum inhibitory concentrations (MICs) of 8.0, 8.0 and 4.0 μg/mL, respectively. The development of isomers of natural products is an active field in medicinal chemistry for the study and discovery of new potentially useful drugs. Thus, we performed the methanolysis of intermediate **3.80** of the total synthesis of aspterric acidd, obtaining **3.86**, a diastereomer of peniterester (Scheme 3.19).

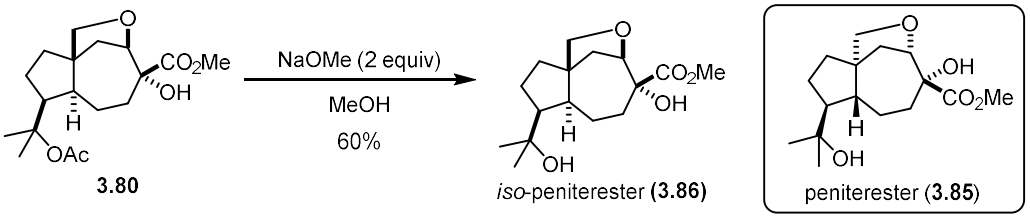

Scheme 3.19. Synthesis of *iso*-peniterester (**3.86)** from **3.80**.

Penigrisacid A

For the synthesis of penigrisacid A we started from common intermediate **3.59** of the total synthesis of aspterric acid. For the formation of the oxygen-bridged cycle we envisioned a one-pot tandem epoxidation/S_N2' sequence that would allow simultaneous formation of the 5-membered ring by 6-*endo*-dig cyclization and the introduction of a hydroxy group in alpha to methyl ester (Scheme 3.20).

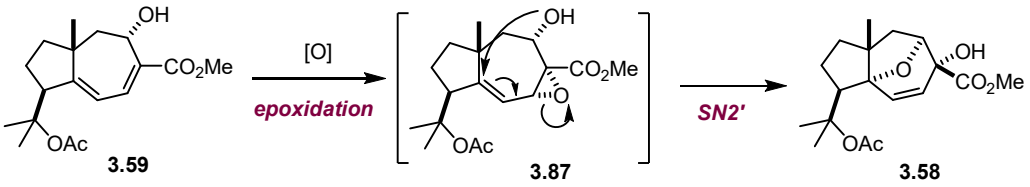

Scheme 3.20. Proposed mechanism for the tandem epoxidation/S_N2' reaction sequence to form oxygen-bridge cycle in **3.58**.

Initial studies using *m*CPBA led to the formation of the desired product **3.58** in moderate yields. However, the reaction was not easily reproducible and in some cases the reaction stopped at epoxide intermediate **3.87** which decomposed during purification. Treating the intermediate with acids such as PPTS, *p*TSOH or CSA led to product **3.58**, albeit in low yields. When switching to a vanadium catalyzed alcohol-directed epoxidation we observed the formation of the desired product with recovered starting material in moderate yields (Table 3.7, entry 1). We found that the source of TBHP was very important, using THBP in alkanes (decane or nonane) provided better yields than using aqueous TBHP (Tab 3.7, entries 1–3), and among them nonane provided the best results. We wondered whether the problem was the stability of the product, so we subjected the product to reaction conditions and observed 49% decomposition after 16 h. To accelerate the rate of the reaction, to reduce product decomposition, we tried increasing the catalyst loading while reducing the reaction time, but only 16% of product was detected with 35% unreacted starting material after 4 h. Lowering the catalyst loading did not increase the yield either (Table 3.7, entries 4–5). Better results were obtained when lowering the concentration of the reaction (Table 3.7, entries 6–7), reaching a 74% yield over the two steps. Under these conditions

36. Duan, R.-T.; Yang, R.-N.; Li, H.-T.; Tang, L.-H.; Liu, T.; Yang, Y.-B.; Zhou, H.; Ding, Z.-T. *Fitoterapia* **2020**, *140*, 104422.

using the $VO(acac)_2$, intermediate **3.87** was not detected by ^1H NMR. Given that there was still starting material after 19 h, we decided to allow it to react for longer reaction times, but the yield dropped (Table 3.7, entry 8).

Table 3.7. Screening of the reaction conditions for the tandem epoxidation/SN2' reaction of **3.59**.

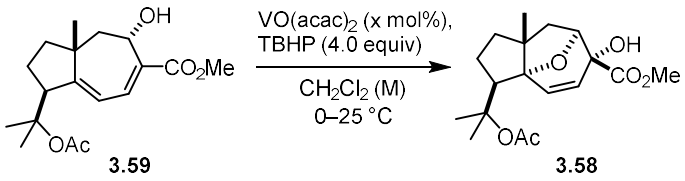

Entry	x mol%	Molarity (M)	TBHP source	Time (h)	Yield [a]
1[b]	7.5	0.1M	5M in decane	16	32% (34%)
2[c]	7.5	0.1M	70% in water	16	2% (47%)
3	7.5	0.1M	5M in nonane	16	45% (13%)
4	15	0.1M	5M in nonane	4	16% (35%)
5	5	0.1M	5M in nonane	4	44% (13%)
6	7.5	0.05M	5M in nonane	16	55% (17%)
7[b]	7.5	0.01M	5M in nonane	19	74% (26%)
8[b]	7.5	0.01M	5M in nonane	40	53%

[a] Yield determined by ^1H NMR using diphenylmethane as internal standard, dry CH_2Cl_2 was employed unless stated otherwise. In brackets remaining starting material **3.59**. [b] Isolated yield, 200 mg scale. [c] HPLC grade CH_2Cl_2 employed.

After some tests on the hydrogenation of the alkene in **3.58**, we discovered that performing the hydrogenation in MeOH at 60 bars of H_2 and using $Pd(OH)_2$[37] led to the desired hydrogenated product **3.88** in good yields (Scheme 3.21).

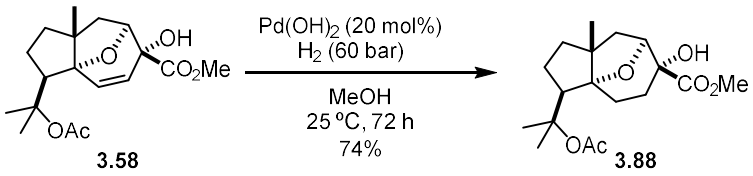

Scheme 3.21. Hydrogenation of **3.58**.

In contrast, to the acid-promoted acetate elimination in the synthesis of aspterric acid, where we observed a preference for the endocyclic alkene (**3.83)**, we obtained the desired product **3.89** in excellent yields by treating **3.88** with excess MsOH (Scheme 3.22). Isomerization of the double bond into endocyclic isomers was only observed when the reaction was heated to >50 °C for prolonged reaction times. This is most likely because in this case the internal alkenes formed upon isomerization are thermodynamically less stable.

37. PtO_2, Pd/C or Crabtree's catalyst were also tested but either partial or no conversion of the starting material was observed.

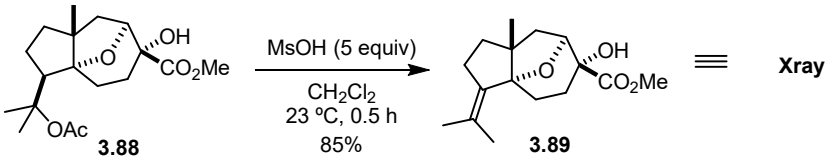

Scheme 3.22. Acid-promoted acetate elimination.

We confirmed by X-ray diffraction the relative *trans* configuration between the 5-membered O-bridged cycle and C15 in both **3.58** and **3.89** (Figure 3.4).

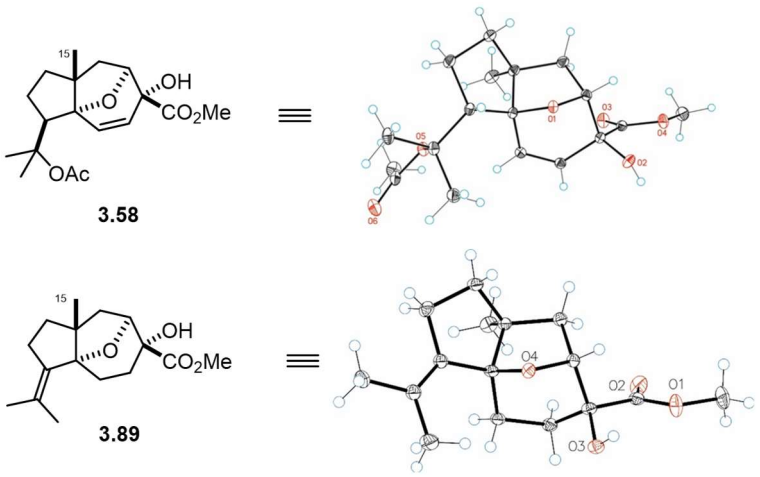

Figure 3.4 X-ray diffraction of intermediates **3.58** and **3.89** of the total synthesis of penigrisacid A (**3.6**).

Finally, ester hydrolysis with NaOH[38] allowed the obtention of the target molecule **3.6** (Scheme 3.23). However, there were small differences between our ^{1}H NMR (Table 3.7) and ^{13}C NMR (Table 3.8) data and those reported for the natural product.[16] However, comparing the coupling constants in the ^{1}H NMR were very similar, suggesting that the relative configuration of most of the stereocenters of our synthetic compound are very similar to that of the natural product.

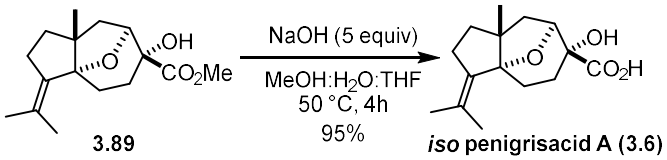

Scheme 3.23. Basic hydrolysis of ester to form target molecule **3.6**.

Table 3.8. Comparison of the ^{1}H NMR natural penigrisacid A with the NMR of synthetic **3.6**.

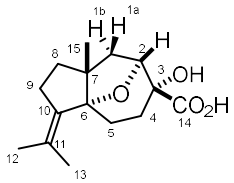

Proton assignment	Penigrisacid A	3.6	Δδ (ppm)[a]
H2	4.48 (d, *J* = 7.5Hz, 1H)	4.30 (d, *J* = 7.8 Hz, 1H)	+0.18

38. Hydrolysis could also be performed with LiOH, delivering the desired product in 90% yield.

H5	2.74 (dt, *J* = 12.6, 6.2 Hz, 1H)	2.65 (ddd, *J* = 14.3, 12.8, 6.3 Hz, 1H)	+0.09
H9	2.38 (m, 2H)	2.47 – 2.27 (m, 3H)	-
H4	2.18 (dd, *J* =13.8, 7.6 Hz, 2H)	2.47 – 2.27 (m, 3H) overlap	-
H1b	2.01 (dd, *J* = 13.2, 7.6 Hz, 1H)	2.05 (dd, *J* = 13.3, 7.8 Hz, 1H)	-0.04
H1a	1.90 (d, *J* =13.2 Hz, 1H)	1.78 (d, *J* = 13.3 Hz, 1H)	+0.12
H13	1.82 (broad s, 3H)	1.93 – 1.90 (m, 3H)	-0.09
H8, H12	1.63 (m, 5H)	1.72 – 1.61 (m, 5H)	-0.03
H5, H8	1.55 (m, 2H)	1.58 – 1.46 (m, 2H)	+0.03
H15	1.18 (s, 3H)	1.19 (s, 3H)	-0.01

[a] For the difference in the multiplets we took the δ(ppm) in the center of the interval.

Table 3.9. Comparison ^{13}C NMR isolation team with the NMR of our synthesised target molecule.

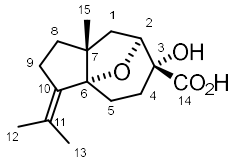

^{13}C signal	Penigrisacid A[a]	3.6	Δδ (ppm)
14	178.0	176.9	+1.1
10	135.6	136.2	-0.6
11	131.6	131.7	-0.1
6	93.9	93.4	+0.5
2	82.6	83.1	-0.5
3	74.4	75.1	-0.7
7	54.0	53.4	+0.6
8	41.6	42.2	-0.6
1	40.4	41.8	-1.4
9	33.3	33.3	0
4	28.5	27.7	+0.8
5	27.7	25.6	-2.1
13	23.5	23.6	-0.1
12	21.3	21.5	-0.2
15	20.1	20.6	-0.5

[a] Data taken from ref. 16.

The isolation team[16] provided us with the raw 1D NMR data which we used to directly compare with our data. In Figure 3.6 we compared the ^{1}H NMR of A) our synthetic sample of **3.6**, B) the

same sample treated with K_2CO_3[39] B) and C) the raw data provided for penigrisacid A by the isolation team.

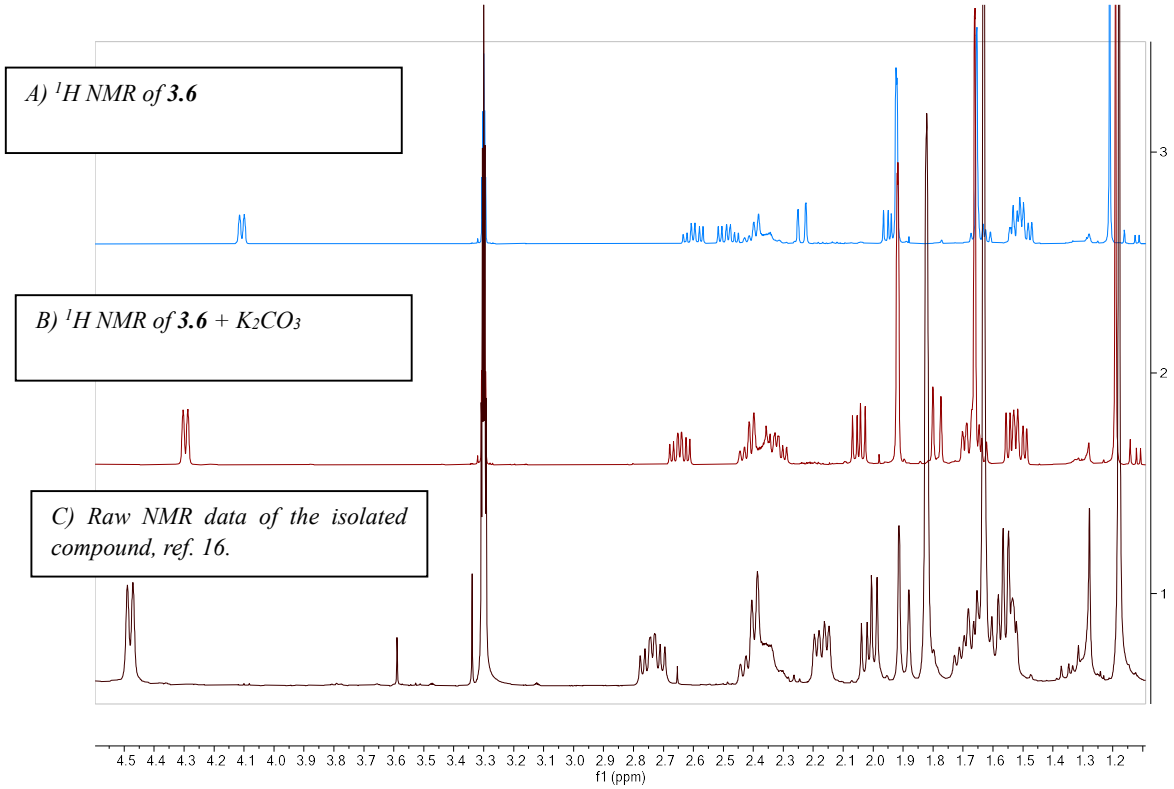

Figure 3.5. Comparison of our ^{1}H NMR data for **3.6** with that of penigrisacid A.

NOESY NMR experiments (Figure 3.7) confirmed close contacts between H2-H1b, H1a-b, H1b-H15, and H15 and the multiplet containing signals from H4, 5 and 8, similar to the ones reported by the isolation team for penigrisacid A.

39. In separate experiments, like acids, NaCl, $CaCl_2$, were added, but no change in the ^{1}H NMR could be observed. Measuring the NMR at different concentrations was also tested.

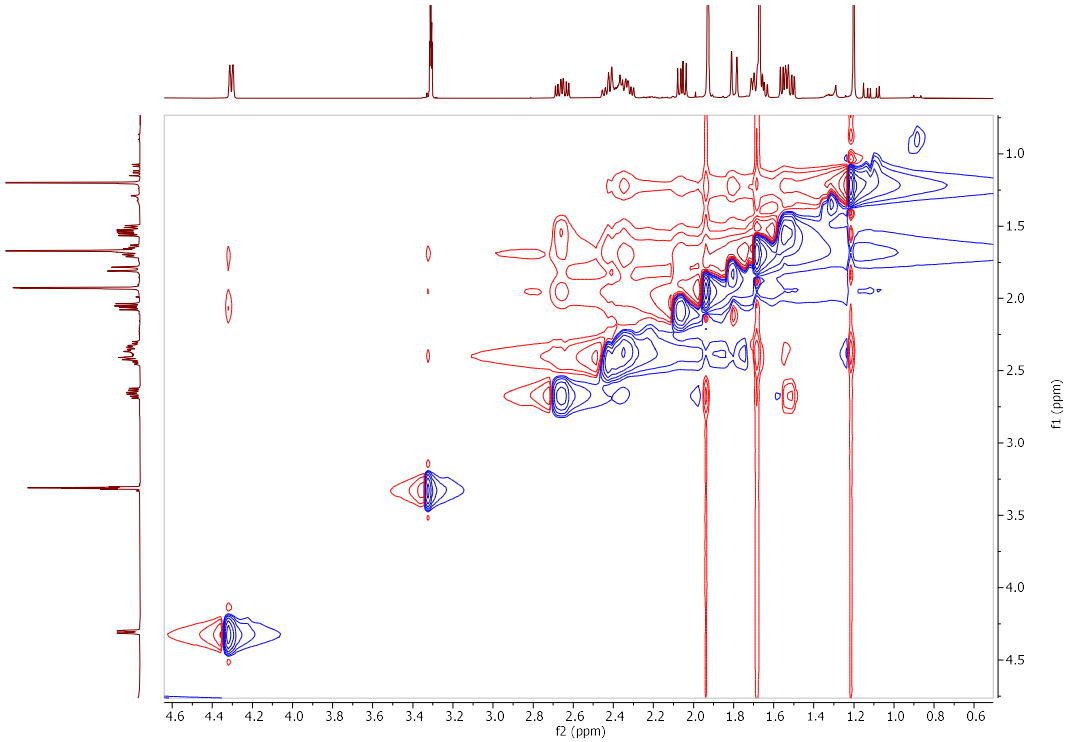

Figure 3.6. NOESY ^{1}H-^{1}H NMR spectrum of **3.6**.

Comparing our experimental data with the one reported for penigrisacid A,[16] our hypothesis is that the penigrisacid A might be a stereoisomer of the molecule that we have synthesized. For instance, it could be the epimer **3.90,** with the opposite configuration at C3 (Figure 3.5), which we presume would present almost no difference in the NOESY NMR and little effect on the ^{1}H and ^{13}C NMR.

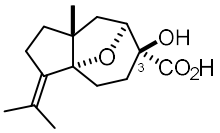

3.90

Figure 3.7. Proposed new structure for penigrisacid A.

We carried out DFT NMR calculations[40] to assist in determining the correct structure of the natural compound.[16] Table 3.10 presents a comparison between the calculated and experimental NMR data for both the proposed structure **3.90** for penigrisacid A and the synthetic compound **3.6**. In both cases a reasonable correlation is observed, considering that the calculations were made in the gas phase. The greatest discrepancies in the ^{1}H NMR are in the H1 and H2 signals, where we

[40] Calculations carried out with Spartan'24, no solvation methods were employed.

can observe a difference of about 0.5ppm in both cases. As for the ^{13}C NMR, as expected, the relative differences are smaller.

Table 3.10. Comparison of the isolated and synthetic NMR spectra with their corresponding calculated ones.

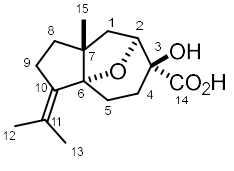

penigrisacid A (3.90)

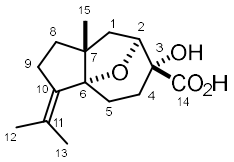

3-*epi*-penigrisacid A (3.6)

	^{13}C NMR				^{1}H NMR				
	3.90[a]	**3.90$_{calc}$**	**3.6**	**3.6$_{calc}$**	**mult.**	**3.90[a]**	**3.90$_{calc}$**	**3.6**	**3.6$_{calc}$**
1	40.4	39.1	41.8	40.1	CH_2	2.01 (13.2, 7.6)	2.06 (13.8, 8.0)	2.05 (13.3, 7.8)	2.07 (13.6, 8.1)
						1.90 (13.2)	2.21 (13.8, 1.2)	1.78 (13.3)	2.23 (13.6, 1.2)
2	82.6	82.9	83.1	83.9	CH	4.48 (7.5)	4.0 (8.0, 1.6)	4.30 (7.8)	3.88 (7.9, 2.0)
3	74.4	72.4	75.1	74.6	C				
4	28.5	27.3	27.7	27.0	CH_2	1.69 m	1.92 (12.7, 7.7)	2.47-2.27 m	2.44 (14.4, 12.8, 7.3)
						2.18 (13.8, 7.6)	1.97 (7.3, 1.6)		1.74 (14.4, 7.2, 2.0)
5	27.7	28.0	25.6	25.8	CH_2	1.55 m	1.60 (15.0, 7.7)	1.58-1.46 m	1.47 (14.7, 7.3)
						2.74 (12.6, 6.2)	2.76 (15.0, 12.7, 7.3)	2.65 (14.3, 12.8, 6.3)	2.55 (14.7, 12.8, 7.2)
6	93.9	93.6	93.4	92.4	C				
7	54.0	53.1	53.4	52.7	C				
8	41.6	39.7	42.2	40.1	CH_2	1.55 m	1.45 (11.5, 7.1)	1.58-1.46 m	1.45 (11.4, 6.9

						1.63 m	1.94 (13.7, 11.5, 7.2)	1.72-1.61 m	1.92 (13.7, 11.7, 7.0)
9	33.3	32.9	33.3	32.8	CH_2	2.38 m		2.47-2.27 m	2.46 (13.7, 6.9, 3.3, 2.7)
							2.44 (7.0)		2.44 (7.0)
10	135.6	138.4	136.2	138.4	C				
11	131.6	134.0	131.7	134.8	C				
12	23.5	22.4	21.5	19.9	CH_3	1.63 s	1.56	1.72-1.61 m	1.63
13	21.3	19.8	23.6	22.3	CH_3	1.82 m	2.07	1.93-1.90 m	1.85
14	178.0	181.7	176.9	179.6	C				
15	20.1	19.8	20.6	20.5	CH_3	1.18	1.19	1.19	1.22

[a] Data taken from ref. 16. Mult. = multiplicity of the signal.

The resemblance observed in the calculated spectroscopic data as well as our experience with this compound leads us to think that the actual compound obtained by Yang *et al.* is **3.90**.[16]

Enantioselective synthesis of 3.6

We demonstrated that the total synthesis of **3.6** could be performed enantioselectively by preparing enantioenriched enyne **3.40** from commercially available geraniol (**3.91**) following a previously reported procedure.[41] We can see how none of the steps lead to any erosion of the diastereomeric ratio achieved in the gold(I)-catalyzed reaction, which is stereospecific (Scheme 3.24).

41. a) Mohapatra, D. K.; Pramanik, C.; Chorghade, M. S.; Gurjar, M. K. *Eur. J. Org. Chem*. **2007**, 5059-5063; b) M. J. Ardolino, J. P. Morken, *J. Am. Chem. Soc.* **2012**, *134,* 8770- 8773.

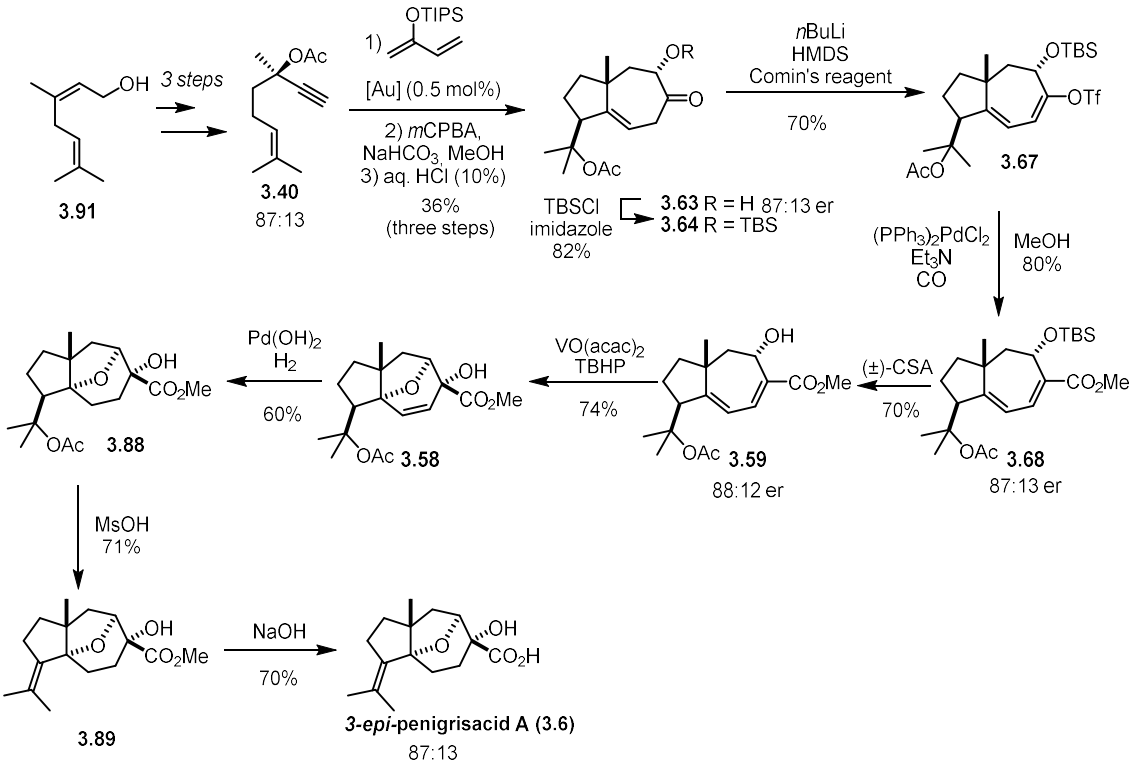

Scheme 3.24. Enantioselective total synthesis of enantioenriched **3.6**.[42]

Schisanwilsonene A

As already mentioned in the objectives, we envisioned that we could also benefit from the hydroazulane core built in the gold(I)-catalyzed tandem cyclization/1,5-OR-migration/formal 4+3 cycloaddition, for the synthesis of the intermediate **3.62** of the previous total synthesis reported by our group (Scheme 3.9)[18,19]. We started by the optimization of the deprotection of TIPS-enol ether **3.57** to form ketone **3.92**. Standard TBAF or acid silyl-enol ether deprotection conditions led to a mixture of **3.92** with varying amounts of isomerized alkene **3.64** (Table 3.11, entry 1–2), which after several attempts we could not deprotected in good yields.[43] Previous tests on the purification of **3.57** revealed that some **3.64** formed after silica-gel FCC. Thus, purifications had to be done using triethylamine-treated silica gel. Our hypothesis is that TBAF was too acidic and led to the isomerization and decomposition of the substrate. Finally, HF·py and HF·3Et$_3$N were found to be the best deprotection conditions for substrate **3.57**, delivering the desired product in excellent yields.

Table 3.11. Screening reaction conditions for the deprotection of TIPS-enol ether **3.58**.

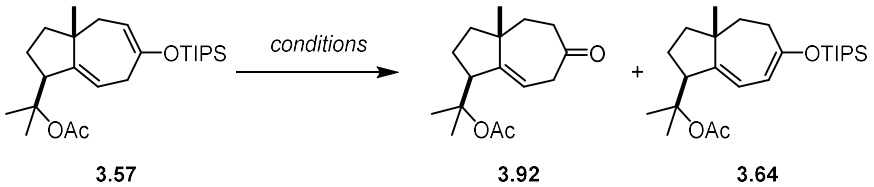

42. Performed in collaboration with Miquel Àngel Pérez Puigdomènech.
43. We discovered that TFA could deprotect **3.65** delivering the desired ketone **3.94**, but decomposition of the product was also observed.

entry	conditions	Ratio 3.94:3.65	NMR yield
1	TBAF (1.5 equiv), THF (0.05M), 10 min, 0 °C	n.d	16–25%
2	1M HCl, 1,4-dioxane (0.1M), 23 h, 23 °C	1:1.8	20%
3	HF·py (10 equiv), THF (0.1M), 23 h, 23 °C	1:0	70%
4	HF·py (10 equiv), THF:py (4:1) (0.1M), 23 h, 23 °C	1:0	88%
5	HF·3Et$_3$N (10 equiv), THF (0.1M), 48 h, 23 °C	1:0	100%

[a] Yield determined by ^{1}H NMR using diphenylmethane as internal standard. N.d = not determined, n.r = no reaction.

Thus, starting from enyne **3.40**, ketone was obtained in 49% yield over two steps. Next, we followed the same 2-step sequence of triflation/Pd-catalyzed methoxycarbonylation as for **3.59**, allowed the obtention of methylester **3.61** (which is a dehydroxy analogue of compound **3.59**). The relatively unstable triflate **3.93** could be crystalized in the glovebox by slow diffusion of pentane into a solution in CH_2Cl_2 and its structure was confirmed by X-ray diffraction (Scheme 3.25).

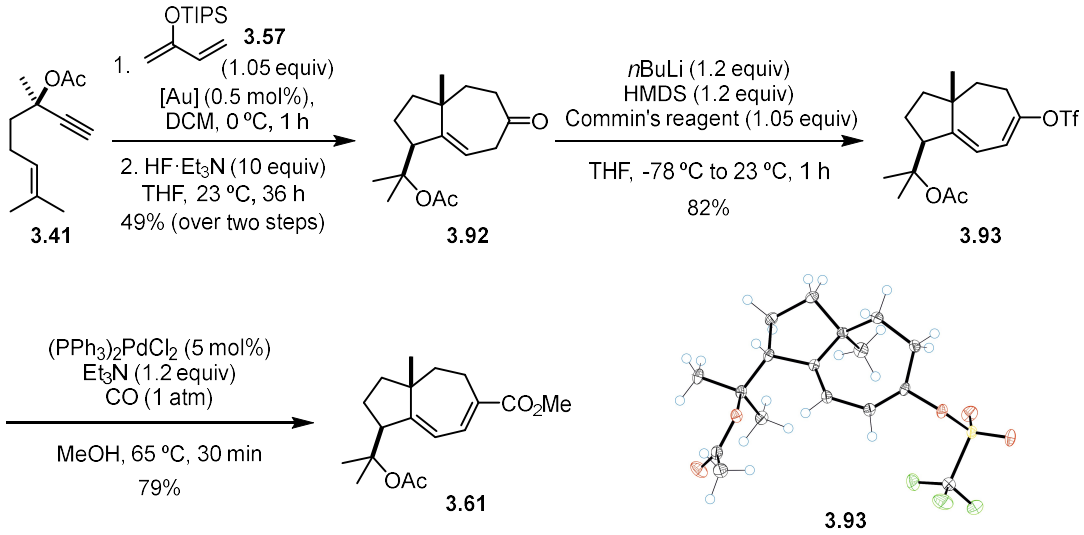

Scheme 3.25. Initial steps towards the formal synthesis of schisanwilsonene A (**3.3**).

Finally, methanolysis of the acetate group and Pd/C catalyzed hydrogenation of the diene rendered product **3.94** and **3.62** in 73% and 80% yields, respectively (Scheme 3.26).[44] Product **3.63** was obtained as a 1:2 *dr* mixture[45] and is a late intermediate of the total synthesis previously reported

44. Attempts on performing first the hydrogenation of the diene led to decomposition of the starting material.
45. The *dr* obtained was not reproducible, usually it varied from 1:2 to 1:4. Nevertheless that stereocenter is then not maintained in the following steps.

by our group, rendering the formal synthesis of schisanwilsonene A in 11 steps using the longest linear sequence (LLS) and an *ca* overall 10% yield.

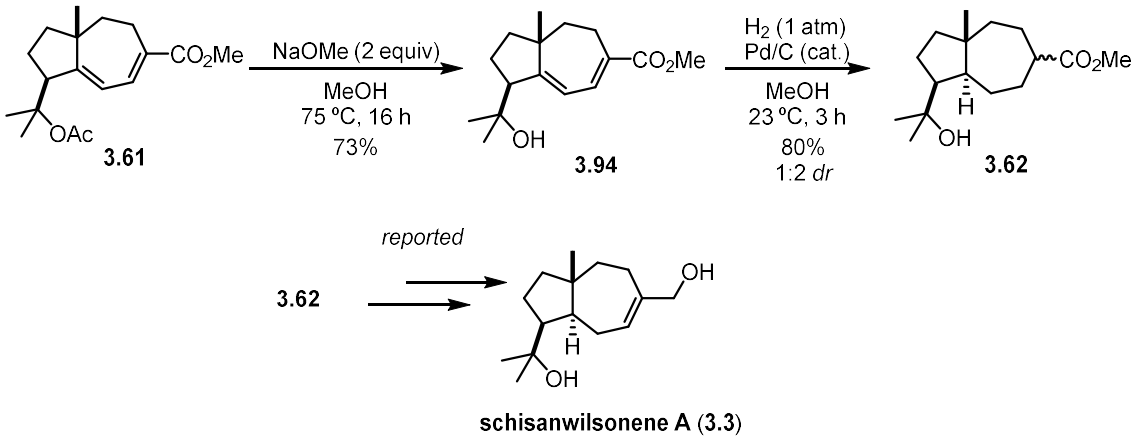

Scheme 3.26. Synthesis of intermediate **3.63** of the total synthesis of schisanwilsonene A (**3.3**).

The biological properties of some intermediates of the synthesis of aspterric acid, penigrisacid A, schisanwilsonene A and *iso*-peniterester (**3.86**) were studied in the drug discovery program CO-AAD (Community for Open Antimicrobial Drug Discovery) from the University of Queensland (Australia).[46] Samples of **3.70**, **3.75** and **3.77** were a hit for two fungi (*Cryptococcus neoformans* and *Candida albicans*) with MIC ≤0.25 μg/mL. More biological studies on other intermediates are currently being carried out.

46. Blaskovich, M. A. T.; Zuegg, J.; Elliott, A. G.; Cooper, M. A. *ACS Infect. Dis*. **2015**, *1*, 285–287.

Conclusion

In this Chapter, we summarized our successful application of the tandem gold(I)-catalyzed cycloisomerization/ 1,5-OR migration/ (4+3) cycloaddition for the total synthesis of two members of the daucane family of natural products, aspterric acid and schisanwilsonene A, as well as the synthesis of two isomers of other members of the same family, *iso*-peniterester and 3-*epi*-penigrisacid A. The synthesis of the proposed structure of penigrisacid A by the isolation team, demonstrated that there was a misassignment on its structure (Scheme 3.27).

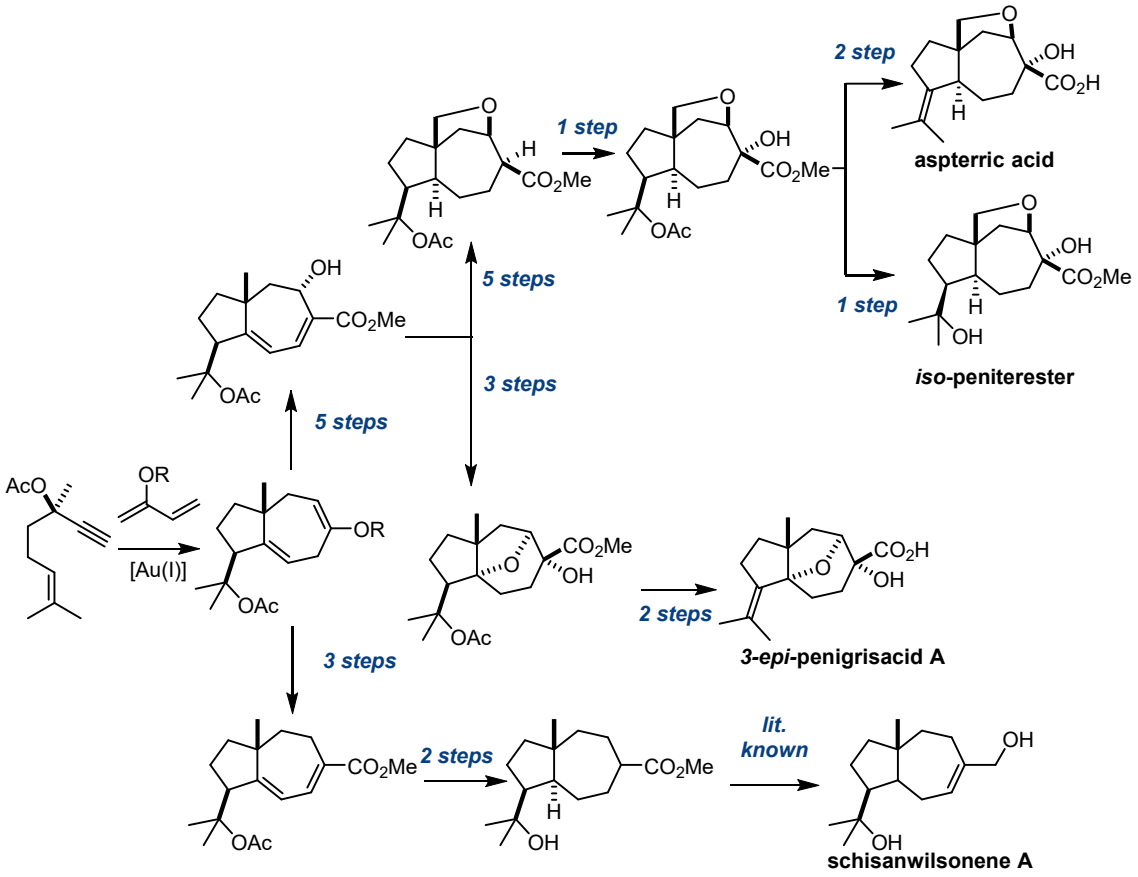

Scheme 3.27. Summary of the divergent synthesis of the daucane family of natural products.

Experimental Part

General Remarks

General information has been provided in the experimental section of Chapter 1.

Synthetic Procedures and Analytical Data

3.40, **3.56**, **3.57** and **3.65** have been prepared following previously described procedures. Spectroscopic data matched those reported in the literature.[21]

2-((1*S*,3*aR*,5*S*)-5-Hydroxy-3*a*-methyl-6-oxo-1,2,3,3*a*,4,5,6,7-octahydroazulen-1-yl)propan-2-yl acetate (3.63)

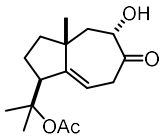

To a solution of cationic [JohnPhosAu(MeCN)]SbF_6 (238 mg, 0.309 mmol, 0.5 mol%) and diene **3.56** (14.7 g, 64.7 mmol, 1.05 equiv) in HPLC-grade CH_2Cl_2 (100 mL) at 0 ºC, was added enyne **3.40** (12.0 g, 61.8 mmol) as a solution in CH_2Cl_2 (20.0 mL), over ca 60 minutes with a syringe pump. After the addition finished, it was warmed up to room temperature and stirred until full consumption of enyne **3.40** (monitored by GCMS or ^{1}H NMR), quenched with Et_3N (1.5 mL) and concentrated under reduced pressure to obtain crude **3.58** (26.0 g, ca 50% pure by ^{1}H NMR). Spectroscopic data matched those reported in the literature.[21] **^{1}H NMR** (500 MHz, CD_2Cl_2) δ 5.48 (ddd, *J* = 6.1, 4.1, 2.3 Hz, 1H), 4.95 (ddd, *J* = 8.9, 3.5, 1.5 Hz, 1H), 3.25 (t, *J* = 8.4 Hz, 1H), 3.10 – 2.91 (m, 2H), 2.24 – 2.16 (m, 1H), 1.94 (s, 3H), 1.89 (dd, *J* = 15.1, 8.9 Hz, 1H), 1.72 – 1.64 (m, 2H), 1.51 – 1.48 (m, 2H), 1.47 (s, 3H), 1.40 (s, 3H), 1.20 – 1.12 (m, 3H), 1.10 – 1.07 (m, 18H), 0.08 (s, 3H).

To a 500 mL flask equipped with a stirring bar were sequentially added *m*CPBA (16.0 g, 92.7 mmol, 70% pure, 1.5 equiv based on **3.40**), MeOH (150 mL) and $NaHCO_3$ (26.0 g, 309 mmol, 5 equiv based on **3.40**). The mixture was stirred for 30 min at room temperature. Then the reaction was cooled down to 0 °C and a solution of **3.57** (26.0 g, ca 50% pure) in the minimum ammount of CH_2Cl_2 was added dropwise. The resulting solution was stirred for 1 h at 0 °Cand then moved to room temperature where it was stirred for an additional 1 h (or until consumption of **3.57**, assessed by ^{1}H NMR). The reaction was quenched by addition of saturated aqueous $Na_2S_2O_3$ (200 mL) and the organic phase was was extracted with Et_2O (x3). The combined organic layers were treated with aqueous 10% HCl followed by saturated aqueous $NaHCO_3$ (x2) or aqueous 10% NaOH (the last basic washings are to remove the excess of *meta*-chlorobenzoic acid present in the crude mixture). Finally the combined organic layers were washed with brine, dried over $MgSO_4$, filtered and concentrated under reduced pressure. The crude reaction mixture was purified by FCC (silica gel, CyH/EtOAc 4:1 to 7:3) obtaining **3.63** (7.10 g, 25.0 mmol, 40% yield) as a pale-yellow oil. **^{1}H NMR** (500 MHz, $CDCl_3$) δ 5.72 (dt, *J* = 10.0, 2.9 Hz, 1H), 4.52 (dd, *J* = 12.3, 5.6 Hz, 1H), 3.76 – 3.55 (m, 1H), 3.42 (dddd, *J* = 13.5, 4.0, 3.2, 0.7 Hz, 1H), 3.35 (s, 1H), 3.06 (dd, *J* = 13.5, 10.0 Hz, 1H), 2.16 (dd, *J* = 13.3, 5.6 Hz, 1H), 2.06 – 1.99 (m, 1H), 1.98 (s, 3H), 1.81 – 1.72 (m, 1H), 1.71 – 1.62 (m, 1H), 1.51 (s, 3H), 1.50 – 1.40 (m, 2H), 1.39 (s, 3H), 1.29 (s, 3H). **^{13}C NMR** (126 MHz, $CDCl_3$) δ 207.2, 170.4, 153.7, 112.5, 85.0, 75.1, 53.4, 48.5, 43.8, 42.0, 39.7, 29.8, 26.0, 25.8, 21.7, 20.6. **HRMS** (ESI+) calculated for $[C_{16}H_{24}NaO_4]^+$ [M + Na] $^+$ 303.1567 *m/z*; found 303.1580 *m/z*.

For the asymmetric synthesis of **3.63** the same procedure was followed, using instead: **3.40** (8.00 g, 41.8 mmol, 87:13 er), [JohnPhosAu(MeCN)]SbF_6 (159 mg, 0.205 mmol, 0.5 mol%), diene **3.56** (9.79 g, 43.2 mmol, 1.05 equiv) and CH_2Cl_2 (80 mL, HPLC grade). Then in the Rubottom-type oxidation were used: *m*CPBA (14.9 g, 60.6 mmol, 1.5 equiv), $NaHCO_3$ (17.0 g, 202 mmol, 5 equiv) and MeOH (100 mL, HPLC grade). Product **3.63** (4.1 g, 15.0 mmol, 36% yield over three

steps, 87:13 er) was obtained as an orange oil. Spectroscopic data matched that of the racemic sample. **[α]$^{24.6}_{D}$** +43.4 (c 0.14, CH_2Cl_2, sample with 87:13 er).

(1*S*,3a*R*,5*S*)-1-(2-Acetoxypropan-2-yl)-3*a*-methyl-6-oxo-1,2,3,3a,4,5,6,7-octahydroazulen-5-yl 3-chlorobenzoate (3.66)

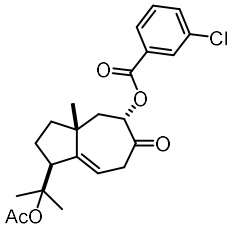

To a suspension of Na_2HPO_4 (48 mg, 0.34 mmol, 1.1 equiv) and methyl enol ether **3.65** (100 mg, 0.31 mmol, 85% pure) in CH_2Cl_2 (0.5 mL, HPLC grade) at 0 °C, was added dropwise a solution of *m*CPBA (58 mg, 0.34 mmol, 1.1 equiv, >77% pure) in CH_2Cl_2 (0.3 mL). The resulting solution was stirred for 15 min allowing it to warm to room temperature. The reaction was quenched by addition of aqueous 10% NaOH and the layers were separated. The aqueous phase was extracted with EtOAc (x 3) and the organic extracts were combined, dried over $MgSO_4$, filtered, and concentrated under reduced pressure. The crude reaction mixture was purified by FCC (silica, CyH/EtOAc 10:1). Compound **3.66** (46 mg, 0.11 mmol, 36% yield) was obtained as a white solid. **^{1}H NMR** (500 MHz, $CDCl_3$) δ 8.05 (t, *J* = 1.9 Hz, 1H), 7.96 (dt, *J* = 7.8, 1.3 Hz, 1H), 7.54 (ddd, *J* = 8.0, 2.2, 1.1 Hz, 1H), 7.39 (t, *J* = 7.9 Hz, 1H), 5.80 (dt, *J* = 10.1, 3.0 Hz, 1H), 5.65 (dd, *J* = 12.9, 4.8 Hz, 1H), 3.51 (dt, *J* = 13.3, 3.8 Hz, 1H), 3.44 – 3.35 (m, 1H), 3.03 (dd, *J* = 13.4, 10.0 Hz, 1H), 2.19 (dd, *J* = 13.0, 4.7 Hz, 1H), 1.98 (s, 3H), 1.96 (d, *J* = 13.0 Hz, 1H), 1.84 – 1.77 (m, 1H), 1.75 – 1.69 (m, 1H), 1.61 – 1.54 (m, 1H), 1.52 (s, 3H), 1.51 – 1.46 (m, 1H), 1.40 (s, 3H), 1.36 (s, 3H). **^{13}C NMR** (126 MHz, $CDCl_3$) δ 200.6, 170.4, 164.6, 152.5, 134.7, 133.4, 131.5, 130.0, 129.9, 128.2, 113.6, 84.9, 77.6, 53.3, 44.4, 43.8, 42.1, 40.2, 26.1, 25.8, 22.9, 21.7, 21.1. **HRMS** (ESI+) calculated for $[C_{23}H_{27}ClNaO_5]^+$ $[M + Na]^+$ 441.1439 *m/z*; found 441.1447 *m/z*. **XRD:** Single crystals suitable for X-ray diffraction analysis were obtained by slow evaporation on CH_2Cl_2/hexane, at 4 ºC.

2-((1*S*,3*aR*,5*S*)-5-((*tert*-Butyldimethylsilyl)oxy)-3*a*-methyl-6-oxo-1,2,3,3a,4,5,6,7-octahydroazulen-1-yl)propan-2-yl acetate (3.67)

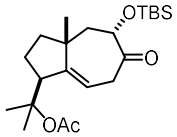

To a solution of **3.63** (6.5 g, 23.2 mmol) in a mixture of anhydrous CH_2Cl_2 (100 mL) and DMF (10 mL) at 0 ºC, under argon, was added imidazole (2.37g, 34.8 mmol, 1.5 equiv) and TBSCl (5.24 g, 34.8 mmol, 1.5 equiv), both as solids. The resulting mixture was allowed to warm up to room temperature and it was stirred for 16 h. The reaction was quenched by addition of saturated aqueous NH_4Cl and extracted with CH_2Cl_2 (x3). The combined organic layers were washed with water, dried over Na_2SO_4, filtered and concentrated under reduced pressure. The crude reaction mixture was purified by FCC (silica, CyH/EtOAc 20:1). Compound **3.67** (8.5 g, 22 mmol, 93% yield) was obtained as a colorless oil. **^{1}H NMR** (400 MHz, $CDCl_3$) δ 5.69 (ddd, *J* = 7.6, 5.1, 2.5 Hz, 1H), 4.45 (dd, *J* = 11.4, 5.6 Hz, 1H), 3.33 – 3.21 (m, 1H), 3.20 – 3.05 (m, 2H), 2.00 (dd, *J* = 13.5, 5.6 Hz, 1H), 1.97 (s, 3H), 1.79 – 1.67 (m, 2H), 1.64 – 1.55 (m, 1H), 1.48 (s, 3H), 1.47 – 1.44 (m, 2H), 1.39 (s, 3H), 1.17 (s, 3H), 0.89 (s, 9H), 0.10 (s, 3H), 0.05 (s, 3H). **^{13}C NMR** (101 MHz, $CDCl_3$) δ 206.3, 170.4, 151.9, 115.0, 85.0, 76.7, 53.3, 48.3, 44.4, 42.1, 40.0, 25.9 (x3*C*), 25.7, 25.5, 22.9, 22.1, 21.3, 18.6, -4.5, -5.0. **HRMS** (ESI+) calculated for $[C_{22}H_{38}NaO_4Si]^+$ $[M + Na]^+$ 417.2432 *m/z*; found 417.2428 *m/z*.

For the asymmetric synthesis of **3.67** the same procedure was followed, using instead: **3.63** (2.40 g, 8.56 mmol, 87:13 er), imidazole (0.874 g, 12.8 mmol, 1.5 equiv), TBSCl (1.935 g, 12.8 mmol, 1.5 equiv), CH_2Cl_2 (40 mL) and DMF (4 mL). Product **3.67** (2.77 g, 7.01 mmol, 82% yield, 87:13 er) was obtained as an orange oil. Spectroscopic data matched that of the racemic sample. **[α]$^{24.6}_{D}$** -61.8 (c 0.105, CH_2Cl_2, sample with 87:13 er).

2-((1*S*,3*aR*,5*S*)-5-((*tert*-Butyldimethylsilyl)oxy)-3a-methyl-6-(((trifluoromethyl)sulfonyl)oxy)-1,2,3,3a,4,5-hexahydroazulen-1-yl)propan-2-yl acetate (3.68)

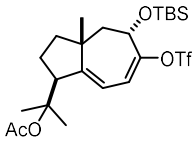

To a solution of HMDS (3.2 mL, 15.2 mmol, 1.2 equiv) in anhydrous THF (200.0 mL), under argon, at 0 ºC, was added *n*BuLi (6.1 mL, 2.3 M, 13.9 mmol, 1.1 equiv) and the mixture was stirred for 10 min. at this temperature. Then it was cooled down to −78 ºC and a solution of **3.67** (5.0 g, 12.7 mmol) in anhydrous THF (20.0 mL) was added dropwise. The resulting solution was stirred for 30 min at −78 ºC, after this time a solution of Comins' reagent (5.22 g, 13.3 mmol, 1.05 equiv) in THF (20 mL) was added dropwise. The mixture was stirred for 15 min at −78 ºC then slowly warmed up to 23 ºC over 1 h. The reaction was quenched with a mixture of water/brine (1:14) and extracted with Et_2O (x3). The combined organic layers were dried over $MgSO_4$, filtered and concentrated under reduced pressure. The crude was purified by FCC (silica, CyH/EtOAc 50:1). Compound **3.68** (4.9 g, 9.3 mmol, 73% yield) was obtained as a white solid. **M.p.** = 50 °C (dec). **^{1}H NMR** (400 MHz, $CDCl_3$) δ 5.95 (d, *J* = 8.5 Hz, 1H), 5.76 (dd, *J* = 8.5, 2.6 Hz, 1H), 4.59 (dd, *J* = 10.9, 7.1 Hz, 1H), 3.47 (br t, *J* = 9.1 Hz, 1H), 2.00 (s, 3H), 1.94 – 1.77 (m, 3H), 1.62 – 1.58 (m, 1H), 1.51 (s, 3H), 1.49 – 1.43 (m, 2H), 1.37 (s, 3H), 1.03 (s, 3H), 0.90 (s, 9H), 0.15 (s, 3H), 0.11 (s, 3H). **^{19}F NMR** (376 MHz, $CDCl_3$) δ -73.5. **^{13}C NMR** (101 MHz, $CDCl_3$) δ 170.4, 160.9, 151.1, 118.1 (q, *J* = 320.5 Hz), 112.4, 84.8, 69.2, 53.0, 44.0, 43.8, 40.7, 26.0, 25.9, 25.6, 22.8, 22.1, 19.2, 18.2, -4.3, -4.4. **HRMS** (ESI+) calculated for $[C_{23}H_{37}F_3NaO_6SSi]^+$ $[M + Na]^+$ 549.1924 *m/z*; found: 549.1940 *m/z*.

For the asymmetric synthesis of **3.68** the same procedure was followed, using instead: **3.67** (1.48 g, 3.74 mmol, 87:13 er), *n*BuLi (2.5 mL, 1.7 M, 4.11 mmol, 1.1 equiv), HMDS (0.94 mL, 4.49 mmol, 1.2 equiv), Comins' reagent (1.54 g, 3.92 mmol, 1.05 equiv) and anhydrous THF (67 mL). Product **3.68** (1.38 g, 2.626 mmol, 70% yield, *er* not determined) was obtained as an orange oil. Spectroscopic data matched that of the racemic sample. Due to the instability of the product, the **$[\alpha]^{24.6}_D$** was not measured.

Methyl (1*S*,3*aR*,5*S*)-1-(2-Acetoxypropan-2-yl)-5-((*tert*-butyldimethylsilyl)oxy)-3a-methyl-1,2,3,3a,4,5-hexahydroazulene-6-carboxylate (3.69)

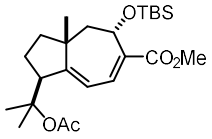

Trifluoromethanesulfonate **3.68** (1.80 g, 3.42 mmol) was dissolved in methanol (17 mL, HPLC grade), under air, at room temperature. Triethylamine (0.57 mL, 4.1 mmol, 1.2 equiv) and $PdCl_2(PPh_3)_2$ (120.0 mg, 0.170 mmol, 5 mol%) were added and the atmosphere was changed to CO (1 atm, balloon). The resulting solution was refluxed for 30 min (usually when the solution turns black it is an indication that it is finished), then it was cooled to room temperature and concentrated under reduced pressure. The crude was purified by FCC (silica, CyH/EtOAc 30:1). Compound **3.69** (1.45 g, 3.32 mmol, 97% yield) was obtained as a pale-yellow solid. **M.p.** (EtOAc): 87-89 ºC. **^{1}H NMR** (400 MHz, $CDCl_3$) δ 6.69 (dt, *J* = 8.0, 1.2 Hz, 1H), 5.91 (dd, *J* = 8.0, 2.5 Hz, 1H), 4.91 (dd, *J* = 11.3, 6.7 Hz, 1H), 3.72 (s, 3H), 3.48 (t, *J* = 8.9 Hz, 1H), 2.05 – 1.95 (m, 1H), 1.99 (s, 3H), 1.90 (dd, *J* = 13.4, 6.8 Hz, 1H), 1.56 – 1.42 (m, 4H), 1.50 (s, 3H), 1.36 (s, 3H), 1.02 (s, 3H), 0.84 (s, 9H), 0.09 (s, 3H), 0.07 (s, 3H). **^{13}C NMR** (101 MHz, $CDCl_3$) δ 170.4, 169.5, 163.3, 136.1, 130.6, 116.3, 84.8, 68.2, 53.2, 51.8, 46.4, 43.9, 40.8, 26.3, 26.0, 25.5, 22.8, 22.2, 19.3, 18.2, -4.1, -4.6. **HRMS** (ESI+) calculated for $[C_{24}H_{40}NaO_5Si]^+$ $[M + Na]^+$ 459.2537 *m/z*; found 459.2540 *m/z*.

For the asymmetric synthesis of **3.69** the same procedure was followed, using instead: **3.68** (1.33 g, 2.55 mmol, 87:13 er), Et_3N (0.57 mL, 4.1 mmol, 1.2 equiv) and $PdCl_2(PPh_3)_2$ (88.6 mg, 0.126

mmol, 5 mol%) and MeOH (67 mL). Product **3.69** (884 mg, 2.03 mmol, 80%, 87:13 *er*) was obtained as an off-white solid. Spectroscopic data matched that of the racemic sample. **[α]$^{24.6}_{D}$** +2.5 (c 0.16, CH_2Cl_2, sample with 87:13 *er*).

Methyl (1*S*,3*aR*,5*S*)-1-(2-Acetoxypropan-2-yl)-5-hydroxy-3*a*-methyl-1,2,3,3*a*,4,5-hexahydroazulene-6-carboxylate (3.59)

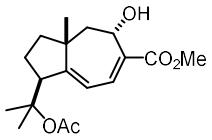

Silyl ether **3.69** (4.1 g, 9.4 mmol) was dissolved in a mixture of CH_2Cl_2/methanol (184 mL, 1:1, both HPLC grade), at room temperature, under air. CSA (2.4 g, 10.0 mmol, 1.1 equiv) was added as a solid and the mixture was stirred for 1.5 h at this temperature. The progress was monitored by TLC (5:1 CyH/EtOAc). After this time, the reaction was quenched by addition of a saturated solution of $NaHCO_3$ and extracted with CH_2Cl_2 (x3). The combined organic layers were combined, dried over Na_2SO_4, filtered and concentrated under reduced pressure. The crude product was purified by FCC (silica, CyH/EtOAc 4:1). Compound **3.59** was obtained compound (150.9 mg, 97% yield) as a colorless oil. **^{1}H NMR** (500 MHz, $CDCl_3$) δ 7.10 (d, *J* = 8.3 Hz, 1H), 5.99 (dd, *J* = 8.3, 2.4 Hz, 1H), 4.78 (dd, *J* = 11.7, 6.1 Hz, 1H), 3.79 (s, 3H), 3.51 (t, *J* = 9.1 Hz, 1H), 2.04 (dd, *J* = 13.4, 6.1 Hz, 1H), 2.01 (s, 3H), 1.93 (dd, *J* = 13.4, 11.7 Hz, 1H), 1.88 – 1.81 (m, 1H), 1.59 (dt, *J* = 8.6, 4.1 Hz, 1H), 1.53 – 1.48 (m, 2H), 1.51 (s, 3H), 1.38 (s, 3H), 1.00 (s, 3H). **^{13}C NMR** (126 MHz, $CDCl_3$) δ 170.4, 169.6, 166.6, 133.9, 132.1, 116.4, 84.8, 66.9, 53.6, 52.2, 44.5, 43.8, 40.5, 26.2, 25.5, 22.8, 22.3, 20.2. **HRMS** (ESI+) calculated for $[C_{18}H_{26}NaO_5]^+$ $[M + Na]^+$ 345.1672 m/z; found 345.1681 m/z.

For the asymmetric synthesis of **3.59** the same procedure was followed, using instead: **3.69** (0.66 g, 1.5 mmol, 87:13 er), CSA (0.39 g, 1.70 mmol, 1.1 equiv) and CH_2Cl_2:MeOH (1:1 ratio, 30 mL, HPLC grade). Product **3.59** (432 mg, 1.343 mmol, 90%, 88:12 er) was obtained a pale-yellow oil. Spectroscopic data matched that of the racemic sample. **[α]$^{24.6}_{D}$** +4.9 (c 0.15, CH_2Cl_2, sample with 88:12 er).

Aspterric acid

Methyl (1*S*,3a*R*,5*S*,6*R*)-1-(2-Acetoxypropan-2-yl)-5-hydroxy-3*a*-methyldecahydroazulene-6-carboxylate (3.70)

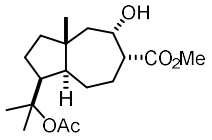

An autoclave reactor was charged with a solution of diene **3.59** (700 mg, 2.12 mmol) in EtOAc (22 mL, HPLC grade), PtO_2 (98.6 mg, 0. 434 mmol, 20 mol%) and AcOH (100 µL), under air. The reactor was sealed, the atmosphere was changed to 20 bar of hydrogen and the mixture was stirred at 800 rpm, at 25 ºC, during 48 h. After this time, the solution was filtered through Celite to remove the catalyst, washing with EtOAc. The filtered solution was quenched with a saturated aqueous $NaHCO_3$ solution, and the aqueous phase was extracted with EtOAc (x3). The combined organic layers were dried over $MgSO_4$, filtered and concentrated under reduced pressure. The crude product was purified by FCC (silica, CyH:EtOAc 9:1 to 4:1). Compound **3.70** was obtained (578 mg, 1.77 mmol, 82%) as a gummy oil. **^{1}H NMR** (500 MHz, $CDCl_3$) δ 3.97 (ddd, *J* = 10.5, 5.7, 3.9 Hz, 1H), 3.74 (s, 3H), 2.98 – 2.90 (m, 1H), 2.60 (td, *J* = 11.1, 8.4 Hz, 1H), 2.20 – 2.02 (m, 3H), 1.97 (s, 3H), 1.88 – 1.73 (m, 2H), 1.71 – 1.60 (m, 2H), 1.58 – 1.50 (m, 5H), 1.46 (s, 3H), 1.45 – 1.42 (m, 1H), 1.30 (td, *J* = 12.7, 6.8 Hz, 1H), 0.97 (s, 3H). **^{13}C NMR** (126 MHz, $CDCl_3$) δ 175.6, 170.4, 85.1, 71.3, 52.0, 51.8, 49.5, 49.3, 48.6, 43.0, 42.9, 27.5, 26.9, 25.5, 24.8, 24.6, 22.9, 20.0. **HRMS** (ESI+) calculated for$[C_{18}H_{30}NaO_5]^+$ $[M + Na]^+$ 349.1985 m/z; found 349.1970 m/z.

Methyl (1*S*,3*aR*,5*S*,6*R*)-1-(2-Acetoxypropan-2-yl)-3*a*-methyl-5-((4-nitrobenzoyl)oxy)decahydroazulene-6-carboxylat (3.70')

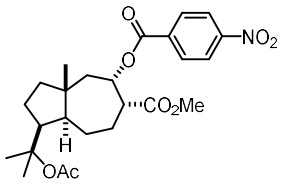

To a solution of **3.70** (7.0 mg, 0.021 mmol), DMAP (0.8 mg, 0.006 mmol, 0.3 equiv.) and TEA (8.7 mg, 0.086 mmol, 4.0 equiv.) in anhydrous CH_2Cl_2 (0.42 mL), under argon, at room temperature, was added 4-nitrobenzoyl chloride (8.0 mg, 0.043 mmol, 2.0 equiv.). The reaction was stirred at room temperature for 6 h and quenched by addition of water. The layers were separated, and the aqueous phase was extracted with CH_2Cl_2 (x2). The combined organic extracts were collected, dried over Na_2SO_4, filtered and concentrated under reduced pressure. Purification by flash column chromatography on silica gel (CyH/EtOAc 4:1 to 3:1) delivered the title compound (3.2 mg, 32% yield) as a yellow solid**.** **^{1}H NMR** (500 MHz, $CDCl_3$) δ 8.30 – 8.24 (m, 2H), 8.18 – 8.13 (m, 2H), 5.59 (ddd, J = 9.8, 6.7, 4.8 Hz, 1H), 3.58 (s, 3H), 3.09 (ddd, J = 10.1, 4.8, 1.7 Hz, 1H), 2.66 (q, J = 10.1 Hz, 1H), 2.37 (dd, J = 13.8, 6.7 Hz, 1H), 2.29 – 2.21 (m, 1H), 2.19 – 2.11 (m, 1H), 1.99 (s, 3H), 1.98 – 1.91 (m, 2H), 1.79 – 1.68 (m, 2H), 1.65 – 1.56 (m, 2H), 1.54 (s, 3H), 1.52 – 1.42 (m, 2H), 1.48 (s, 3H), 1.08 (s, 3H). **^{13}C NMR** (126 MHz, $CDCl_3$) δ 173.1, 170.4, 163.8, 150.8, 135.9, 130.9, 123.7, 85.2, 74.7, 52.9, 51.9, 51.4, 48.1, 45.3, 43.1, 42.6, 27.3, 26.7, 26.1, 25.7, 25.3, 22.9, 19.7. **XRD:** Slow evaporation from CyH/MeCN afforded crystals suitable for single crystal X-ray diffraction analysis.

Methyl (3*S*,3*aS*,8*aR*)-3-(2-Acetoxypropan-2-yl)-7-hydroxy-8*a*-methyl-1,2,3,3*a*,4,5,8,8*a*-octahydroazulene-6-carboxylate (3.75) and tautomers (3.75a and 3.75b)

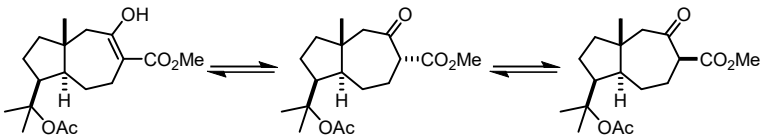

3.75 **3.75a** **3.75b**

To a solution of alcohol **3.70** (580 mg, 1.78 mmol) in CH_2Cl_2 (18 mL, HPLC grade), under air, at 0 ºC, was added DMP (904 mg, 2.13 mmol, 1.2 equiv). The mixture was stirred at this temperature for 30 minutes and the reaction was quenched by addition of an aqueous solution of 10% NaOH. The layers were separated, and the aqueous phase was extracted with CH_2Cl_2 (x2). The combined organic layers were dried over $MgSO_4$, filtered and concentrated under reduced pressure to yield compound **3.75** (576 mg, 1.78 mmol, 100% yield) as a white solid. The product was used in latter steps without further purification nor characterization. In $CDCl_3$, at 25 ºC, it was a mixture of tautomers of varying ratio, being enol **3.75** the main component and ketones **3.75a** and **3.75b** the other isomers, according to some ^{1}H NMR signals of the different isomers, which could be assigned. **M.p.**(CH_2Cl_2): 77–79 ºC. **^{1}H NMR** (500 MHz, $CDCl_3$) δ 12.82 (s, 1H, **enol**), 3.76 (s, 3H, **enol**), 3.71 (s, 3H **3.75a** or **3.75b** minor isomer), 3.71 (s, 3H, **3.75a** or **3.75b**, major isomer), 3.49 (dd, *J* = 9.8, 3.4 Hz, 1H, **3.75a** or **3.75b**, minor isomer), 3.43 (dd, *J* = 12.4, 3.1 Hz, 1H, **3.75a** or **3.75b**, major isomer), 2.95 (ddd, *J* = 15.4, 6.7, 1.7 Hz, 1H, **enol**), 2.77 – 2.68 (m, 1H, overlap), 2.64 – 2.57 (m, 1H, overlap), 2.42 – 2.33 (m, 2H, overlap), 2.17 (dt, *J* = 6.6, 2.5 Hz, 1H, , **3.75a** or **3.75b**, minor isomer), 2.16 – 2.13 (m, 1H, , **3.75a** or **3.75b**, minor isomer), 2.09 (ddd, *J* = 7.0, 3.0, 1.9 Hz, 1H, **3.75a** or **3.75b**, major isomer), 2.06 (dt, *J* = 4.5, 2.0 Hz, 1H, **3.75a** or **3.75b**, major isomer), 2.05 – 2.00 (m, 2H, overlap), 1.98 (s, 3H, **3.75a** or **3.75b**, minor isomer), 1.97 (s, 3H, **3.75a** or **3.75b**, major isomer), 1.96 (s, 3H, **enol**), 1.88 – 1.80 (m, 2H, overlap), 1.80 – 1.74 (m, 2H, overlap), 1.72 – 1.63 (m, 1H, overlap), 1.55 (s, 3H, **3.75a** or **3.75b**, minor isomer), 1.54 (s, 3H, **3.75a** or **3.75b**, major isomer), 1.50 (s, 3H, **enol**), 1.48 (s, 3H, **3.75a** or **3.75b**, minor isomer), 1.47 (s, 3H, **3.75a** or **3.75b**, major isomer), 1.43 (s, 3H, **enol**), 1.42 – 1.35 (m, 2H, overlap), 1.03 (s, 3H, **3.75a** or **3.75b**, minor isomer), 0.97 (s, 3H, **3.75a** or **3.75b**, major isomer),

0.90 (s, 3H, **enol**). **^{13}C NMR** (126 MHz, $CDCl_3$) δ 208.1, 207.1, 177.3, 173.6, 171.4, 170.5, 170.4, 100.3, 85.5, 85.2, 84.8, 59.9, 57.6, 57.5, 56.7, 56.4, 54.9, 52.4, 52.4, 51.7, 51.1, 51.0, 49.7, 48.9, 42.7, 41.7, 41.6, 41.6, 40.9, 40.5, 29.8, 27.2, 27.0, 27.0, 26.9, 26.3, 26.2, 26.1, 25.2, 25.2, 24.9, 23.4, 23.0, 22.9, 22.9, 20.8, 20.5, 18.2. **HRMS** (ESI+) calculated for$[C_{18}H_{28}NaO_5]^+$ [M + Na]$^+$ 347.1829 m/z; found 347.1829m/z. **XRD**: Single crystals of the enol form **3.75** suitable for X-ray diffraction analysis were obtained by slow evaporation on CH_2Cl_2/pentane, at 23 ºC.

Note: enol **3.75** could also be prepared in an analogous methodology to the one presented above from a **3.76:3.70** 1:1 mixture obtained from the reduction of **3.75** with $NaBH_4$ in MeOH.

Methyl (1*S*,3a*R*,5*R*,6*S*,8a*S*)-1-(2-Acetoxypropan-2-yl)-5-hydroxy-3*a*-methyldecahydroazulene-6-carboxylate (3.77)

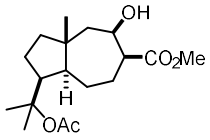

To a solution of **3.75** (252 mg, 0.777 mmol) in MeOH (15.5 mL, HPLC grade), at 0 ºC, under air, was added $NaBH_4$ (29.4 mg, 0.777mmol, 1.0 equiv). The mixture was stirred for 15 min at 0 ºC. After this time, the reaction was diluted with water, quenched with a drop of acetone and extracted with CH_2Cl_2 (x3). The combined organic layers were dried over $MgSO_4$, filtered and concentrated under reduced pressure. The crude product was purified by FCC (silica, CyH:EtOAc, 9:1 to 7:3). Compound **3.77** (178 mg, 0.545 mmol, 70% yield) was obtained as a white solid. The relative configuration of the title compound was assigned by analysis of the crystal structure. **M.p.** (CH_2Cl_2): 95–97 ºC. **^{1}H NMR** (400 MHz, $CDCl_3$) δ 4.29 (br s, 1H), 3.70 (s, 3H), 2.70 (dt, *J* = 11.2, 1.3 Hz, 1H), 2.61 (tt, *J* = 10.8, 8.6 Hz, 1H), 2.46 – 2.30 (m, 1H), 2.10 (dd, *J* = 14.7, 3.1 Hz, 1H), 2.07 – 2.00 (m, 1H), 1.99 (s, 3H), 1.92 – 1.79 (m, 1H), 1.74 – 1.57 (m, 4H), 1.56 (s, 3H), 1.49 (s, 3H), 1.45 (dd, *J* = 10.9, 4.8 Hz, 1H), 1.27 (dd, *J* = 14.4, 4.5 Hz, 1H), 1.22 (s, 1H), 1.13 (s, 3H). **HRMS** (ESI+) calculated for$[C_{18}H_{30}NaO_5]^+$ [M + Na]$^+$ 349.1985 m/z; found 349.1998 m/z. **XRD:** Single crystals suitable for X-ray diffraction analysis were obtained by slow evaporation on CH_2Cl_2/pentane, at 23 ºC.

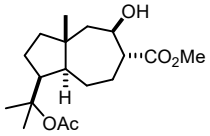

Compound **3.76** could also be obtained (63 mg, 0.19 mmol, 25% yield) as a colorless oil that was a 1:1 unseparable mixture with **3.70** which was used without further purification to prepare **3.75**. **^{1}H NMR** (500 MHz, $CDCl_3$) for **3.76**: δ 4.24 (td, *J* = 10.0, 3.9 Hz, 1H), 3.72 (s, 3H), 3.08 (d, *J* = 9.2 Hz, 1H), 2.82 – 2.74 (m, 1H), 2.70 – 2.54 (m, 2H, overlap with **3.70**), 2.35 (d, *J* = 3.9 Hz, 1H), 2.24 – 2.18 (m, 1H), 2.17 – 2.00 (m, 5H, overlap with **3.70**), 1.97 (s, 3H), 1.90 (dd, *J* = 15.2, 4.0 Hz, 1H), 1.87 – 1.81 (m, 2H, overlap with **3.70**), 1.81 – 1.59 (m, 8H, overlap with **3.70**), 1.51 (s, 3H), 1.46 (s, 7H, overlap with **3.70**), 1.42 (s, 2H, overlap with **3.70**), 1.35 – 1.23 (m, 4H, overlap with **3.70**), 1.10 (s, 3H).

Methyl (3*R*,4*S*,6a*S*,7*S*,9a*S*)-7-(2-Acetoxypropan-2-yl)-1-oxooctahydro-1*H*-3,9a-methanocyclopenta[*c*]oxocine-4-carboxylate (3.79)

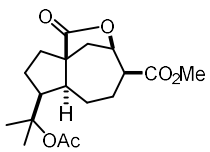

To a degassed solution of **3.77** (4.0 mg, 0.012 mmol) in CyH (1.2 mL, HPLC grade) under argon, at room temperature, were added iodine (3.3 mg, 0.013 mmol, 1.1 equiv) and PIDA (4.3 mg, 0.013 mmol, 1.1 equiv) as solids. The mixture was irradiated with a desk lamp, warmed up to 40 ºC in a water bath and stirred for 1 h. After this time, the progress was checked by NMR, showing <20% conversion. Thus, the crude product was resubmitted to the same reaction conditions with additional iodine

(6.6 mg, 0.026 mmol, 2.2 equiv) and PIDA (8.6 mg, 0.026 mmol, 2.2 equiv). Again, the mixture was irradiated with a desk lamp, warmed up to 40 ºC in a water bath and stirred for 3 h. The reaction was diluted with Et_2O, quenched with a saturated aqueous solution of Na_2SO_3, extracted with Et_2O (x3) and concentrated under reduced pressure. NMR of the crude reaction mixture revealed full conversion. The reaction can also be monitored by UHPLC-MS. The crude product was purified by FCC (silica, CyH/EtOAc 1:1). Compound **3.79** (yield not determined) was obtained as a colorless gummy solid. **^{1}H NMR** (500 MHz, $CDCl_3$) δ 5.10 (dd, *J* = 8.6, 4.9 Hz, 1H), 3.75 (s, 3H), 3.09 (td, *J* = 11.3, 8.5 Hz, 1H), 2.88 (t, *J* = 5.8 Hz, 1H), 2.62 (dd, *J* = 13.0, 8.5 Hz, 1H), 2.51 (ddd, *J* = 15.3, 7.6, 1.2 Hz, 1H), 2.31 (dd, *J* = 14.6, 7.6 Hz, 1H), 2.28 – 2.18 (m, 1H), 2.17 – 2.11 (m, 1H), 1.97 (s, 3H), 1.97 (d, *J* = 13.0 Hz, 1H), 1.92 (dd, *J* = 12.4, 6.8 Hz, 1H), 1.84 (dt, *J* = 12.7, 7.9 Hz, 1H), 1.75 – 1.66 (m, 1H), 1.63 (td, *J* = 12.8, 7.3 Hz, 1H), 1.54 – 1.49 (m, 1H), 1.46 (s, 3H), 1.41 (s, 3H). **^{13}C NMR** (126 MHz, $CDCl_3$) δ 179.3, 172.4, 170.6, 86.2, 77.2 (overlapping with *C*DCl_3 signal), 57.5, 53.8, 52.3, 49.7, 47.2, 37.8, 33.5, 28.3, 27.4, 27.2, 24.2, 24.0, 23.1. **HRMS** (ESI+) calculated for$[C_{18}H_{26}NaO_6]^+$ $[M + Na]^+$ 361.1622 m/z; found 361.1626 m/z. **XRD:** Single crystals suitable for X-ray diffraction analysis could be obtained by slow evaporation in CH_2Cl_2/heptane at room temperature.

Methyl (1*S*,3a*S*,5*R*,6*S*,8a*S*)-1-(2-Acetoxypropan-2-yl)-5-hydroxy-3*a*-(iodomethyl)decahydroazulene-6-carboxylate (3.78)

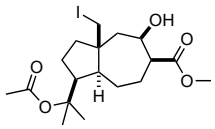

To a degassed solution of **3.77** (125.0 mg, 0.383 mmol) and PIDA (185.0 mg, 0.574 mmol, 1.5 equiv) in CyH (30.0 mL, HPLC grade) at room temperature was added iodine (97.2 mg, 0.383 mmol, 1.0 equiv) as a solution in degassed CyH (8 mL, HPLC grade). The mixture was irradiated with a white light desk lamp, placed 15 cm from the reaction center, at 25 ºC and stirred until a1:1 ratio of product and **3.77** could be observed by UHPLC (EC-C18 column, 50% acetonitrile in water, APCI), usually it took 3–4 h. (starting material **3.77** appears at 1.37 minutes, while **3.78** comes out at 1.96 min). Thus, the reaction was diluted with Et_2O, quenched with a saturated aqueous solution of Na_2SO_3, extracted with Et_2O (x3) and concentrated under reduced pressure. The NMR of the crude reaction mixture confirmed *ca* 50% conversion and the presence of a characteristic C_qCH_2I signal: **^{1}H NMR** (300 MHz, $CDCl_3$) δ 4.01 (dd, *J* = 9.6, 1.9 Hz, 1H), 3.56 (dd, *J* = 9.7, 2.2 Hz, 1H). **UHPLC-MS** (APCI+) *m/z* calc. for $[C_{16}H_{26}IO_3]^+ = [M - AcO^-]^+$: 393.09, found: 393.1.

Compounds **3.77** and **3.78** had the same R_f by TLC so we submitted the crude material to the next step without separating them.

Methyl (3*R*,4*S*,6a*S*,7*S*,9a*S*)-7-(2-Acetoxypropan-2-yl)octahydro-1*H*-3,9*a*-methanocyclopenta[*c*]oxocine-4-carboxylate (3.60)

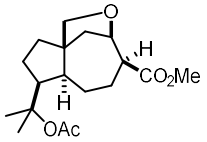

The crude mixture of **3.77** and **3.78** obtained in the previous step was dissolved in DMF (17 mL, HPLC grade) and $AgNO_3$ (113 mg, 0.663 mmol, 4.0 equiv based on calculated **3.78**) was added. The slurry mixture was stirred at room temperature, protected from the light with aluminum foil. After 20 h, the reaction was cooled to 0 °C and quenched by addition of brine and Et_2O. The aqueous phase was extracted with Et_2O (x3). The combined organic layers were washed with water, dried over $MgSO_4$, filtered and concentrated under reduced pressure. The crude product was purified by FCC (silica, CyH/EtOAc 4:1 to 1:1). Compound **3.60** (50.1 mg, 0.153 mmol, 40% from **3.77**) was isolated as a white solid, and **3.77** (37.5 mg, 0.115 mmol, 30%) in a separate fraction. **M.p.**(CH_2Cl_2): 138–141 ºC. **^{1}H NMR** (400 MHz, CD_2Cl_2) δ 4.71 (dd, *J* = 8.8, 4.3 Hz, 1H), 4.00 (dd, *J* = 8.2, 0.9 Hz, 1H), 3.65 (s, 3H), 3.26 (dd, *J* = 8.2, 1.4 Hz, 1H), 2.69 (td, *J* = 10.9, 8.2 Hz, 1H), 2.62 (ddd, *J* = 6.8, 4.1, 1.2 Hz, 1H), 2.31 – 2.26 (m, 1H), 2.25 – 2.17 (m, 1H), 2.17 – 2.08

(m, 1H), 1.96 (s, 3H), 1.91 – 1.75 (m, 3H), 1.70 – 1.57 (m, 2H), 1.52 (s, 3H), 1.47 (d, *J* = 6.4 Hz, 1H), 1.46 (s, 3H), 1.38 – 1.28 (m, 1H), 1.25 – 1.13 (m, 1H). **^{13}C NMR** (101 MHz, CD_2Cl_2) δ 174.4, 170.5, 85.2, 78.8, 74.7, 54.7, 51.6, 51.3, 49.1, 39.6, 35.8, 29.8, 27.4, 27.2, 25.0, 23.5, 23.0. **HRMS** (ESI+) calculated for $[C_{18}H_{28}NaO_5]^+$ [M + Na]$^+$ 347.1829 m/z; found 347.1830 m/z. **XRD:** Single crystals suitable for X-ray diffraction analysis could be obtained by slow evaporation in CH_2Cl_2/pentane at room temperature.

Methyl (3*R*,4*R*,6*aS*,7*S*,9*aS*)-7-(2-Acetoxypropan-2-yl)-4-hydroxyoctahydro-1*H*-3,9*a*-methanocyclopenta[*c*]oxocine-4-carboxylate (3.80)

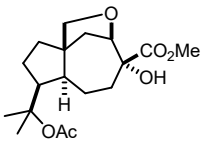

To a solution of ester **3.60** (38.0 mg, 0.12 mmol) in anhydrous THF (4 mL) at −78 °C under argon was added KHMDS (0.1 mL of a 1.75M solution in THF, 0.462 mmol, 1.5 equiv) dropwise. After stirring for 60 min at the same temperature, $P(OEt)_3$ (41 µL, 0.616 mmol, 2 equiv) was added in one portion before O_2 gas was bubbled into the reaction vessel. After complete consumption of the starting material (monitored by TLC), aqueous 2 M HCl (50 mL) was added, and the mixture was allowed to warm up to room temperature. The aqueous phase was extracted with EtOAc (x3) and the combined organics were washed with saturated aqueous $NaHCO_3$, dried over $MgSO_4$, filtered and concentrated under reduced pressure. The crude product was purified by FCC (silica, CyH/EtOAc 4:1 to 7:3). Compound **3.80** (36 mg, 0.11 mmol, 90%) as a white solid. **M.p.**(CH_2Cl_2): 104–106 ºC. **^{1}H NMR** (400 MHz, $CDCl_3$) δ 4.12 (t, *J* = 8.8 Hz, 2H), 3.79 (s, 3H), 3.34 (d, *J* = 8.2 Hz, 1H), 2.63 (q, *J* = 6.5 Hz, 1H, overlap with O*H* signal: s, 1H), 2.36 (dd, *J* = 14.7, 7.7 Hz, 1H), 2.18 (td, *J* = 13.6, 8.0 Hz, 2H), 2.00 (s, 3H), 1.98 – 1.91 (m, 2H), 1.82 (dt, *J* = 12.6, 7.4 Hz, 1H), 1.75 – 1.64 (m, 1H), 1.57 (s, 3H), 1.48 (s, 3H), 1.43 – 1.31 (m, 2H), 1.31 – 1.15 (m, 2H). **^{13}C NMR** (101 MHz, $CDCl_3$) δ 176.0, 170.4, 84.9, 84.6, 78.7, 75.4, 54.3, 52.7, 52.6, 51.1, 37.3, 35.4, 34.9, 29.7, 27.2, 25.1, 22.9, 22.5. **HRMS** (ESI+) calculated for $[C_{18}H_{28}NaO_6]^+$ [M + Na]$^+$ 363.1778 m/z; found 363.1796 m/z.

Methyl (3*R*,4*R*,6*aS*,9*aS*)-4-Hydroxy-7-(propan-2-ylidene)octahydro-1*H*-3,9*a*-methanocyclopenta[*c*]oxocine-4-carboxylate (3.82)

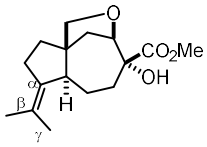

To a flask containing a solution of **3.80** (20.0 mg, 0.059 mmol) in acetone (1.2 mL, HPLC grade) at 0 °C was added iodine (1.5 mg, 5.9 µmol, 10 mol%) as a stock solution in acetone (0.2 mL, HPLC grade). The reaction mixture was removed from the cooling bath and stirred until we can observe by GCMS the consumption of **3.80** and the isomerization of most of *exo*-alkene **3.81** (If the reaction is left for too long it isomerized to **3.83**). Then the solution was quenched with a saturated aqueous $Na_2S_2O_3$, and the aqueous phase was extracted with CH_2Cl_2 (x3). The combined organic layers were dried over $MgSO_4$, filtered and concentrated under reduced pressure. The crude product was purified by FCC (silica, CyH:EtOAc 4:1). Compound **3.82** (6 mg, 21µmol, 40%, obtained as a 85:15 mixture with $\Delta_{\beta,\gamma}$-isomer **3.81**) as a white gummy solid and was used as such in the next step without further purification. ^{1}H NMR (400 MHz, $CDCl_3$) δ 4.17 (d, *J* = 8.3 Hz, 1H), 3.79 (s, 3H), 3.37 (d, *J* = 8.2 Hz, 1H), 2.62 (s, 1H), 2.50 – 2.39 (m, 1H), 2.38 – 2.26 (m, 2H, overlap with **3.81**), 2.23 – 2.14 (m, 1H), 2.04 (d, *J* = 13.2 Hz, 1H), 1.98 – 1.79 (m, 1H, overlap with **3.81**), 1.75 (s, 3H), 1.73 – 1.64 (m, 1H), 1.59 (s, 3H), 1.54 – 1.44 (m, 2H), 1.25 (s, 3H). **HRMS** (ESI+) calculated for $[C_{16}H_{24}NaO_4]^+$ [M + Na]$^+$ 303.1567m/z; found 303.1577 m/z.

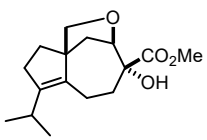

Compound **3.83** (3 mg, 10 µmol, 20 %) could also be obtained as a white solid. **^{1}H NMR** (400 MHz, $CDCl_3$) 4.21 (d, *J* = 8.3 Hz, 1H), 3.82 (s, 3H), 3.76 (d, *J* = 7.9 Hz, 1H), 3.66 (d, *J* = 7.9 Hz, 1H), 2.76 – 2.60 (m, 2H), 2.48 (dd, *J* = 15.2, 9.0 Hz, 1H), 2.41 – 2.31 (m, 1H), 2.29 – 2.17 (m, 4H), 2.00

(dd, *J* = 13.0, 8.4 Hz, 1H), 1.86 – 1.69 (m, 2H), 0.97 (d, *J* = 5.5 Hz, 3H), 0.95 (d, *J* = 5.4 Hz, 3H). **^{13}C NMR** (101 MHz, $CDCl_3$) δ 176.4, 139.7, 138.8, 84.3, 79.4, 77.9, 57.3, 52.9, 38.7, 32.3, 31.5, 28.8, 26.7, 21.6, 21.4, 20.3. **HRMS** (ESI+) calculated for $[C_{16}H_{24}NaO_4]^+$ [M + Na]$^+$ 303.1567m/z; found 303.1568 m/z.

Aspterric acid (3.5)

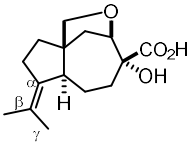

A flask containing a solution of ester **3.82** (5.0 mg, 18 μmol, 85:15 mixture with $\Delta_{\beta,\gamma}$-isomer **3.81**) and NaOH (2.9 mg, 71 μmol, 4.0 equiv) in THF:MeOH:H_2O (0.33 mL, at a 1:1:1 ratio, HPLC grade) at 50 ºC was stirred for 2 h. After this time, the reaction was diluted in water and aqueous 1 M HCl. The aqueous phase was extracted with EtOAc (x3). The combined organic layers were dried over $MgSO_4$, filtered and concentrated under reduced pressure. The crude product was purified by FCC (silica, CH_2Cl_2, MeOH, AcOH 98:2:1). Compound **3.5** (4.0 mg, 15 μmol, 85%, obtained as a 85:15 mixture with $\Delta_{\beta,\gamma}$-isomer **3.85**) was obtained as a white solid. Spectroscopic data matched those of an authentic sample. **^{1}H NMR** (500 MHz, $CDCl_3$) δ 4.30 (d, *J* = 8.7 Hz, 1H), 3.95 (d, *J* = 8.3 Hz, 1H), 3.51 (d, *J* = 8.4 Hz, 1H), 2.47 – 2.40 (m, 1H), 2.40 – 2.23 (m, 2H), 2.21 – 2.12 (m, 2H), 2.09 – 2.00 (m, 1H), 1.83 – 1.73 (m, 2H), 1.72 (q, *J* = 1.8 Hz, 3H), 1.62 (d, *J* = 2.0 Hz, 3H), 1.56 – 1.48 (m, 2H), 0.96 (dd, *J* = 8.1, 6.8 Hz, 1H).**^{13}C NMR** (126 MHz, $CDCl_3$) δ 178.3, 134.5, 125.5, 82.7, 76.5, 75.1, 55.6, 53.2, 37.6, 36.4, 33.9, 32.3, 23.8, 23.5, 21.0. **HRMS** (ESI+) calculated for $[C_{15}H_{22}NaO_4]^+$ [M + Na]$^+$ 289.1415 m/z; found 289.1410 m/z.

(O*H* and CO_2H signals are not visible because they exchange with the deuterated solvent, in this case methanol)

***Iso*-peniterester (3.86)**

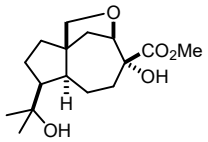

To a microwave vial containing a solution of acetate **3.80** (10 mg, 29 μmol) in anhydrous MeOH (0.30 mL) at 23 ºC, was added a freshly prepared NaOMe solution (42 μL of a 1.4 M solution in MeOH, 59 μmol, 2.1 equiv). The resulting yellow solution was stirred at 70 ºC for 2 h (after prolonged times the product decomposes under the reaction conditions, so the reaction is stopped before full consumption of the starting material). After this time, the reaction was quenched with NH_4Cl and the aqueous phase was extracted with CH_2Cl_2 (x3). The combined organic layers were dried over $MgSO_4$, filtered and concentrated under reduced pressure. The crude product was purified by FCC (silica, CyH/EtOAc 4:1 to 1:1). Compound **3.86** (5.3 mg, 18 μmol, 60% yield) was obtained as a white solid. **M.p. (**CH_2Cl_2**):** 113–115 ºC. **^{1}H NMR** (500 MHz, MeOD) δ 4.28 (d, *J* = 9.3 Hz, 1H), 4.08 (d, *J* = 8.1 Hz, 1H), 3.72 (s, 3H), 3.35 (s, 1H), 3.28 (dd, *J* = 8.1, 1.3 Hz, 1H), 2.45 (dd, *J* = 14.4, 8.4 Hz, 1H), 2.41 – 2.29 (m, 2H), 2.16 (dd, *J* = 13.1, 8.6 Hz, 1H), 2.02 – 1.87 (m, 3H), 1.81 (dt, *J* = 12.6, 7.6 Hz, 1H), 1.71 (ddd, *J* = 13.4, 11.9, 6.9 Hz, 1H), 1.47 (dd, *J* = 11.8, 6.5 Hz, 1H), 1.36 – 1.31 (m, 2H), 1.27 – 1.23 (m, 1H), 1.22 (s, 3H), 1.20 (s, 3H). **^{13}C NMR** (126 MHz, $CDCl_3$) δ ^{13}C NMR (126 MHz, MeOD) δ 176.2, 84.6, 80.0, 76.0, 74.1, 56.0, 53.7, 53.0, 52.4, 37.8, 36.8, 36.4, 31.8, 30.8, 28.1, 23.5. **HRMS** (ESI+) calculated for $[C_{16}H_{27}O_5]^+$ [M + H]$^+$ 299.1853 m/z; found 299.1854 m/z.

Penigrisacid A

Methyl (3*R*,3*aR*,6*R*,7*S*,8*aR*)-3-(2-Acetoxypropan-2-yl)-6-hydroxy-8*a*-methyl-2,3,6,7,8,8*a*-hexahydro-1*H*-3*a*,7-epoxyazulene-6-carboxylate (3.58)

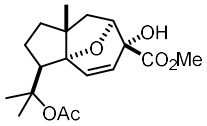

To a flask containing a solution of **3.59** (320 mg, 0.993 mmol) and $VO(acac)_2$ (19.7 mg, 0.074 mmol, 7.5 mol%) in anhydrous CH_2Cl_2 (100 mL) at 0 ºC, was added TBHP (0.8 mL of a 5.3 M solution in nonane, 4.27 mmol, 4.3 equiv) dropwise. The resulting red-brown solution was stirred under argon for 1 h at 0 ºC and then it was allowed to slowly warm up to room temperature overnight. After 20 h, the reaction was quenched by addition of saturated aqueous $Na_2S_2O_3$ (100 mL) and stirred for 30 min. The phases were separated, and the aqueous phase was extracted with CH_2Cl_2 (x3). The combined organic layers were dried over $MgSO_4$, filtered and concentrated under reduced pressure. The crude product was purified by FCC (silica, CyH:EtOAc, 4:1). Compound **3.58** (240 mg, 0.709 mmol, 71%) was obtained as a white solid. **M.p.(**CH_2Cl_2**):** 102–104 ºC. **^{1}H NMR** (500 MHz, $CDCl_3$) δ 6.46 (d, *J* = 10.3 Hz, 1H), 5.91 (dd, *J* = 10.2, 1.9 Hz, 1H), 4.44 (dt, *J* = 8.2, 1.9 Hz, 1H), 3.78 (s, 3H), 2.86 (s, 1H), 2.23 (t, *J* = 9.5 Hz, 1H), 2.14 (dd, *J* = 13.4, 8.2 Hz, 1H), 1.99 (s, 3H), 1.99 – 1.92 (m, 2H), 1.79 (dd, *J* = 12.3, 8.4 Hz, 1H), 1.68 (s, 3H), 1.61 – 1.56 (m, 1H), 1.50 (s, 3H), 1.47 – 1.43 (m, 1H), 1.06 (s, 3H). **^{13}C NMR** (126 MHz, $CDCl_3$) δ 171.8, 170.2, 136.1, 123.6, 92.6, 82.6, 82.0, 74.2, 58.1, 56.2, 52.7, 39.1, 38.8, 29.1, 25.7, 25.6, 22.6, 21.0. **HRMS** (ESI+) calculated for $[C_{18}H_{26}NaO_6]^+$ $[M + Na]^+$ 361.1622 m/z; found: 361.1617 m/z. **XRD:** Single crystals suitable for X-ray diffraction analysis could be obtained by slow evaporation in CH_2Cl_2/heptane at 23 ºC.

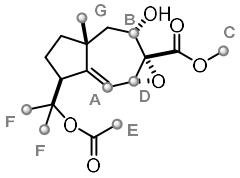

As mentioned in the main text of this Chapter, this procedure was not reproducible using *m*CPBA. In some batches we could obtain the intermediate epoxide **3.87**. This was partially characterized by NMR and it could not be isolated clean because it converted into **3.88** during chromatography on silica gel. **^{1}H NMR** (400 MHz, $CDCl_3$) δ 5.81 (dd, *J* = 5.2, 2.4 Hz, 1H, **A**), 5.02 (dd, *J* = 11.9, 4.7 Hz, 1H, **B**), 3.82 (s, 3H, **C**), 3.52 (d, *J* = 5.1 Hz, 1H, **D**), 2.00 (s, 3H, **E**), 1.51 (s, 3H, **F**), 1.39 (s, 3H, **F**), 1.09 (s, 3H, **G**).

For the asymmetric synthesis of **3.58** the same procedure was followed, using instead: **3.59** (216.5 mg, 0.671 mmol, 87:13 er), $VO(acac)_2$ (13.3 mg, 50.4 µmol, 7.5 mol%), TBHP (0.54 mL of a 5.3 M solution in nonane, 2.89 mmol, 4.3 equiv) and anhydrous CH_2Cl_2 (67 mL). Product **3.58** (135.5 mg, 0.400 mmol, 71%) was obtained as a white solid. Spectroscopic data matched that of the racemic sample. **$[\alpha]^{24.6}_D$** +33.0 (c 0.085, CH_2Cl_2, sample with 87:13 er).

Methyl (3*R*,3*aR*,6*R*,7*S*,8*aR*)-3-(2-Acetoxypropan-2-yl)-6-hydroxy-8*a*-methyloctahydro-1*H*-3*a*,7-epoxyazulene-6-carboxylate (3.88)

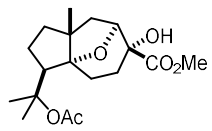

An autoclave reactor was charged with a solution of alkene **3.58** (206 mg, 0.609 mmol) in MeOH (6.1 mL, HPLC grade) and $Pd(OH)_2/C$ (85.5 mg, 20 wt.% loading, 0. 122 mmol, 20 mol%), under air. The reactor was sealed, the atmosphere was changed to 60 bar of hydrogen and the mixture was stirred at 800 rpm, at 25 ºC, during 72 h. After this time, the solution was filtered through Celite to remove the catalyst, washing with MeOH and the combined filtered fractions were concentrated under reduced pressure. The crude product was purified by FCC (silica, CyH:EtOAc 4:1). Compound **3.88** was obtained (153 mg, 0.449 mmol, 74%) as a white solid. **M.p.**(CH_2Cl_2): 138–140 ºC. **^{1}H NMR** (400 MHz, $CDCl_3$) δ 4.21 (d, *J* = 8.0 Hz, 1H), 3.74 (s, 3H), 3.40 (s, 1H, O*H*), 2.42 (t, *J* = 9.3 Hz, 1H), 2.37 – 2.16 (m, 2H), 2.09 (dd, *J* = 13.4, 7.9 Hz, 1H), 1.99 (s, 3H), 1.93 – 1.80 (m, 2H), 1.78 – 1.66 (m, 4H), 1.63 (s, 3H), 1.53 (q, *J* = 4.5 Hz, 1H), 1.49 (s, 3H), 1.17 (s, 3H). **^{13}C NMR** (101 MHz, $CDCl_3$) δ 172.9, 170.2, 94.9, 83.5, 80.8, 74.4, 58.3, 52.6, 51.8, 41.6, 40.9, 29.1, 27.4, 27.0, 25.0, 24.5, 22.8, 19.6. **HRMS** (ESI+) calculated for $[C_{18}H_{28}NaO_6]^+$ $[M + Na]^+$ 363.1778 m/z; found: 363.1769 m/z.

For the asymmetric synthesis of **3.88** the same procedure was followed, using instead: **3.58** (130 mg, 0.384 mmol, 87:13 er), $Pd(OH)_2/C$ (53.9 mg, 20 wt.% loading, 76.8 μmol, 20 mol%) and MeOH (3.8 mL, HPLC grade). Product **3.88** (42.8 mg, 0.236 mmol, 71%) was obtained as a white solid. Spectroscopic data matched that of the racemic sample. $[\alpha]^{24.6}_D$ +33.0 (c 0.085, CH_2Cl_2, sample with 87:13 er).

Methyl (3*aS*,6*R*,7*S*,8*aR*)-6-Hydroxy-8*a*-methyl-3-(propan-2-ylidene)octahydro-1*H*-3*a*,7-epoxyazulene-6-carboxylate (3.89)

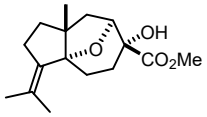

To a flask containing a solution of **3.88** (80.0 mg, 0.240 mmol) in CH_2Cl_2 (4.8 mL, HPLC grade) at 0 °C was added methanesulfonic acid (77 μL, 1.2 mmol, 5 equiv) dropwise. The reaction mixture was removed from the cooling bath and stirred until we can observe by GCMS the consumption of **3.88** and the isomerization of exo-alkene **3.95**. Then the solution was quenched with a saturated aqueous $NaHCO_3$, and the aqueous phase was extracted with CH_2Cl_2 (x3). The combined organic layers were dried over $MgSO_4$, filtered and concentrated under reduced pressure. The crude product was purified by FCC (silica, CyH:EtOAc 9:1 to 4:1). Compound **3.89** was obtained (56 mg, 0.20 mmol, 80%) as a white solid. **M.p.**(CH_2Cl_2): 77–80 ºC. **^{1}H NMR** (500 MHz, $CDCl_3$) δ 4.36 – 4.28 (m, 1H), 3.76 (s, 3H), 3.36 (s, 1H, O*H*), 2.58 (ddd, *J* = 14.7, 12.7, 6.3 Hz, 1H), 2.47 (dd, *J* = 15.7, 7.4 Hz, 1H), 2.40 – 2.21 (m, 2H), 2.13 – 2.05 (m, 1H), 1.94 – 1.89 (m, 3H), 1.84 – 1.75 (m, 2H), 1.73 – 1.65 (m, 4H), 1.61 – 1.52 (m, 2H), 1.19 (d, *J* = 0.9 Hz, 3H). **^{13}C NMR** (126 MHz, $CDCl_3$) δ 173.1, 134.8, 131.3, 92.6, 82.4, 74.6, 52.6, 52.5, 40.8, 40.7, 32.6, 27.2, 24.5, 23.7, 21.6, 20.5. **HRMS** (ESI+) calculated for $[C_{16}H_{24}NaO_4]^+$ $[M + Na]^+$ 303.1567 m/z; found: 303.1576 m/z. **XRD:** Single crystals suitable for X-ray diffraction analysis were obtained by evaporation of a CyH/EtOAc solution, at 40 ºC.

For the asymmetric synthesis of **3.89** the same procedure was followed, using instead: **3.88** (72.7 mg, 0.215 mmol, 87:13 er), MsOH (70 μL, 1.07 mmol, 5.0 equiv) and 1,2-DCE (4.3 mL, HPLC grade). Product **3.89** (42.8 mg, 0.153 mmol, 71%) was obtained as a white solid. Spectroscopic data matched that of the racemic sample. $[\alpha]^{24.6}_D$ +210.2 (c 0.10, CH_2Cl_2, sample with 87:13 er).

3-*epi*-Penigrisacid A (3.6)

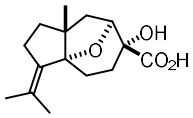

A flask containing a solution of ester **3.89** (56.0 mg, 0.200 mmol) and NaOH (32.0 mg, 0.8 mmol, 4.0 equiv) in THF:MeOH:H_2O (3.9 mL, 1:1:1 ratio of each HPLC grade solvent) at 40 ºC was stirred for 4 h. After this time, the reaction was diluted in water and 1 M aqueous HCl. The aqueous phase was extracted with EtOAc (x3). The combined organic layers were dried over $MgSO_4$, filtered and concentrated under reduced pressure. The crude product was purified by FCC (silica, CH_2Cl_2, MeOH, AcOH 98:2:1). Compound **3.6** (50.5 mg, 0.019 mmol, 95%) was obtained as a white solid. **M.p.**(CH_2Cl_2): 124–130 ºC. **^{1}H NMR** (500 MHz, MeOD) δ 4.31 (dt, *J* = 7.8, 1.7 Hz, 1H), 2.66 (ddd, *J* = 14.3, 12.8, 6.3 Hz, 1H), 2.47 – 2.41 (m, 1H), 2.41 – 2.26 (m, 2H), 2.06 (dd, *J* = 13.3, 7.8 Hz, 1H), 1.95 – 1.90 (m, 3H), 1.79 (dd, *J* = 13.3, 1.4 Hz, 1H), 1.73 – 1.62 (m, 5H), 1.59 – 1.47 (m, 2H), 1.20 (s, 3H) (O*H* and CO_2H signals are not visible because they exchange with the deuterated solvent, in this case methanol). **^{13}C NMR** (126 MHz, MeOD) δ 176.9, 136.2, 131.7, 93.4, 83.1, 75.1, 53.4, 42.2, 41.8, 33.3, 27.7, 25.6, 23.6, 21.5, 20.6. **HRMS** (ESI+) calculated for $[C_{15}H_{22}NaO_4]^+$ $[M + Na]^+$ 289.1410 m/z; found: 289.1414 m/z.

For the asymmetric synthesis of 3-*epi*-Penigrisacid A(**3.6**) the same procedure was followed, using instead: **3.90** (19.5 mg, 69.6 μmol, 87:13 er), NaOH (11.1 mg, 0.278 mmol) and THF:MeOH:H_2O (0.45 mL, 1:1:1 ratio of each HPLC grade solvent). Product **3.6** (13.4 mg, 50.3

μmol, 72%, 87:13) was obtained as a white solid. Spectroscopic data matched that of the racemic sample. **$[\alpha]^{24.6}_D$** +79.4 (c 0.140, ethanol, sample with 87:13 er).

Formal synthesis Schisanwilsonene A

2-((1*S*,3a*R*)-3*a*-Methyl-6-oxo-1,2,3,3a,4,5,6,7-octahydroazulen-1-yl)propan-2-yl Acetate (3.92)

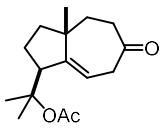

To a solution of cationic [JohnPhosAu(MeCN)]SbF_6 (39.7 mg, 0.051 mmol, 0.5 mol%) and diene **3.56** (4.66 g, 20.6 mmol, 2.0 equiv) in CH_2Cl_2 (15 mL, HPLC-grade) at 0 ºC, was added enyne **3.40** (628 mg, 3.23 mmol) as a solution in CH_2Cl_2 (5.0 mL, HPLC-grade), over ca 20 minutes with a syringe pump (0.25 mL/min). After the addition finished, it was warmed up to room temperature and stirred until full consumption of enyne **3.40** (monitored by GCMS or ^{1}H NMR) quenched with Et_3N (1.5 mL) and concentrated under reduced. The crude material was transferred into a 100 mL Teflon-coated round bottom flask, redissolved in dry THF (25 mL), and cooled to 0 ºC. Finally, $Et_3N{\cdot}3HF$ (8.2 mL, 50.5 mmol, 10 equiv) was added dropwise and the reaction was allowed to warm up to 25 ºC and stirred for 48 h. After 48 h the reaction was very carefully quenched by slow addition of a saturated aqueous $NaHCO_3$ (60 mL) and the aqueous phase was extracted with EtOAc (x3). The combined organic layers were washed with water, and brine, dried over $MgSO_4$, filtered and concentrated under reduced pressure. The crude product was purified by FCC (silica, CyH:EtOAc 95:5 to 90:10). Compound **3.92**(1.35 g, 5.11 mmol, 49% yield over two steps) was obtained as a pale-yellow oil. **^{1}H NMR** (500 MHz, $CDCl_3$) δ 5.58 (td, *J* = 6.1, 2.3 Hz, 1H), 3.32 – 3.19 (m, 2H), 3.11 – 3.03 (m, 1H), 2.67 – 2.53 (m, 2H), 1.97 (s, 3H), 1.93 – 1.80 (m, 2H), 1.79 – 1.72 (m, 1H), 1.52 – 1.48 (m, 3H), 1.48 (s, 3H), 1.41 (s, 3H), 1.08 (s, 3H). **^{13}C NMR** (126 MHz, $CDCl_3$) δ 210.2, 170.6, 151.7, 115.4, 85.1, 53.2, 46.3, 43.4, 40.9, 40.8, 35.8, 25.5, 25.2, 22.8 (2C), 22.7. **HRMS** (ESI+) calculated for $[C_{16}H_{24}NaO_3]^+$ [M + Na] $^+$ 287.1618 m/z; found 287.1616 m/z.

2-((1*S*,3a*R*)-3*a*-Methyl-6-(((trifluoromethyl)sulfonyl)oxy)-1,2,3,3*a*,4,5-hexahydroazulen-1-yl)propan-2-yl Acetate (3.93)

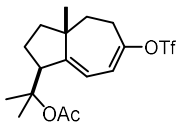

To a solution of HMDS (0.95 mL, 4.53 mmol, 1.2 equiv) in dry THF (60.0 mL), under argon, at 0 ºC, was added *n*BuLi (2.0 mL, 2.05 M, 4.16 mmol, 1.10 equiv) and the mixture was stirred for 10 minutes at this temperature. Then it was cooled to -78 ºC and a solution of **3.92** (1.0 g, 3.78 mmol) in anhydrous THF (4.0 mL) was added dropwise. The resulting solution was stirred for 40 min at -78ºC, after which time a solution of Comins' reagent (1.56 g, 3.97 mmol, 1.05 equiv) in THF (4 mL) was added dropwise. The mixture was stirred for 15 min at -78ºC then slowly warmed up to 23 ºC over 2 h. The reaction was quenched with a mixture of water/brine (1:14) and extracted with Et_2O (x3). The combined organic layers were dried over $MgSO_4$, filtered and concentrated under reduced pressure. The crude was purified by FCC (silica, CyH/EtOAc 50:1). Compound **3.93** (1.23 g, 3.10 mmol, 82% yield) was obtained as a colorless oil. **^{1}H NMR** (400 MHz, $CDCl_3$) δ 5.98 (dd, *J* = 8.8, 2.0 Hz, 1H), 5.79 (dd, *J* = 8.6, 2.6 Hz, 1H), 3.53 – 3.41 (m, 1H), 2.83 – 2.67 (m, 1H), 2.62 (d, *J* = 19.4 Hz, 1H), 2.01 (s, 3H), 1.86 – 1.75 (m, 1H), 1.68 (ddd, *J* = 13.9, 5.9, 3.0 Hz, 1H), 1.61 – 1.55 (m, 2H), 1.55 – 1.48 (m, 5H), 1.39 (s, 3H), 0.94 (s, 3H). **^{19}F NMR** (376 MHz, $CDCl_3$) δ -73.80. **^{13}C NMR** (101 MHz, $CDCl_3$) δ 170.5, 159.8, 151.4, 117.8, 112.2, 85.1, 53.3, 46.4, 40.5, 33.1, 30.2, 26.3, 25.6, 22.9, 22.1, 20.1, (missing *C*F_3). **HRMS** (ESI+) calculated for $[C_{17}H_{23}F_3NaO_5S]^+$ [M + Na] $^+$ 419.1112; found 419.1111 m/z. XRD: Single crystals suitable for X-ray diffraction analysis were obtained by slow diffusion of pentane into a solution of **3.92** in the minimum amount of CH_2Cl_2, at −20 ºC.

Methyl (1*S*,3a*R*)-1-(2-Acetoxypropan-2-yl)-3*a*-methyl-1,2,3,3*a*,4,5-hexahydroazulene-6-carboxylate (3.61)

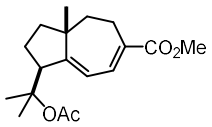

Trifluoromethanesulfonate **3.93** (0.950 g, 2.40 mmol) was dissolved in methanol (24 mL, HPLC grade), under air, at room temperature. Triethylamine (0.40 mL, 2.88 mmol, 1.2 equiv) and $PdCl_2(PPh_3)_2$ (168.0 mg, 0.240 mmol, 10 mol%) were added and the atmosphere was changed to CO (1 atm, balloon). The resulting solution was refluxed for 60 min (usually when the solution turns black it is an indication that it is finished), then it was cooled to room temperature and concentrated under reduced pressure. The crude product was purified by FCC (silica, CyH/EtOAc 50:1). Compound **3.61** (580 mg, 1.89 mmol, 79% yield) was obtained as an orange oil. **^{1}H NMR** (500 MHz, $CDCl_3$) δ 7.12 (ddt, *J* = 8.3, 2.8, 0.9 Hz, 1H), 6.04 (dd, *J* = 8.4, 2.4 Hz, 1H), 3.74 (s, 3H), 3.50 (t, *J* = 9.6 Hz, 1H), 2.77 (d, *J* = 20.4 Hz, 1H), 2.58 – 2.43 (m, 1H), 2.00 (s, 3H), 1.85 – 1.76 (m, 1H), 1.73 (ddd, *J* = 13.6, 5.2, 3.3 Hz, 1H), 1.61 – 1.53 (m, 2H), 1.51 (s, 3H), 1.50 – 1.41 (m, 2H), 1.39 (s, 3H), 0.90 (s, 3H). **^{13}C NMR** (126 MHz, $CDCl_3$) δ 170.5, 169.5, 164.4, 133.2, 131.5, 116.6, 85.1, 53.6, 52.0, 47.5, 40.5, 35.1, 26.6, 26.6, 25.5, 22.9, 22.4, 21.4. **HRMS** (ESI+) calculated for $[C_{18}H_{26}NaO_4]^+$ $[M+Na]^+$ 329.1723 m/z; found 329.1716 m/z.

Methyl (1*S*,3*aR*)-1-(2-Hydroxypropan-2-yl)-3*a*-methyl-1,2,3,3*a*,4,5-hexahydroazulene-6-carboxylate (3.94)

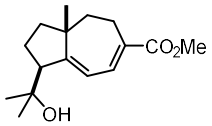

To a microwave vial containing a solution of diene **3.61** (50 mg, 0.163 mmol, 1.0 equiv) in dry MeOH (0.80 mL) at 23 ºC, was added a freshly prepared NaOMe solution (0.23 mL of a 1.4M solution in MeOH, 0.326 mmol, 2.0 equiv). The resulting yellow solution was stirred overnight at 75 ºC. After 18 h, the reaction was quenched with saturated aqueous solution of NH_4Cl and the aqueous phase was extracted with CH_2Cl_2 (x 3). The combined organic layers were dried over $MgSO_4$, filtered and concentrated under reduced pressure. The crude product was purified by FCC (silica, CyH/EtOAc 4:1 to 7:3). Compound **3.94** (34 mg, 0.13 mmol, 79% yield) was obtained as a white solid. **M.p.**(CH_2Cl_2): 67–70 ºC. **^{1}H NMR** (500 MHz, $CDCl_3$) δ 7.13 (ddt, *J* = 8.4, 2.8, 0.9 Hz, 1H), 6.34 (dd, *J* = 8.4, 2.3 Hz, 1H), 3.74 (s, 3H), 2.86 – 2.73 (m, 2H), 2.57 – 2.44 (m, 1H), 1.87 – 1.78 (m, 1H), 1.74 (ddd, *J* = 13.6, 5.1, 3.4 Hz, 1H), 1.64 – 1.52 (m, 2H), 1.52 – 1.43 (m, 2H), 1.35 (br s, 1H), 1.27 (s, 3H), 1.18 (s, 3H), 0.91 (s, 3H). **^{13}C NMR** (126 MHz, $CDCl_3$) δ 169.6, 165.0, 133.4, 131.4, 117.1, 73.8, 57.2, 51.9, 47.4, 40.9, 35.3, 30.8, 27.1, 26.6, 24.8, 21.5. **HRMS** (ESI+): m/z calc. for $[C_{16}H_{25}O_3]^+$: 265.1798; found: 265.1795.

Methyl (1*S*,3*aR*,8*aS*)-1-(2-Hydroxypropan-2-yl)-3*a*-methyldecahydroazulene-6-carboxylate (3.62)

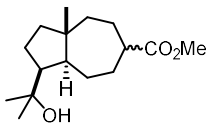

To a flask containing a solution of diene **3.94** (10 mg, 38 µmol) was added Pd/C (8 mg, 10w%, 7.6 µmol, 20 mol%) and dissolved in MeOH (0.4 mL, HPLC grade). Three quick cycles Vac/Ar were done and finally the atmosphere was replaced to hydrogen using a hydrogen balloon. The reaction was stirred for 5 h and the atmosphere was replaced again to argon atmosphere before opening it to air. The mixture was filtered through a celite to remove the catalyst, and the solvents were concentrated under reduced pressure. The crude product was purified by FCC (silica, CyH/EtOAc 4:1). Compound **3.62** (8 mg, 30 µmol, 80%, 2:1 dr) was obtained as a colorless oil. Spectroscopic data match those previously reported.[19] **^{1}H NMR** (500 MHz, $CDCl_3$) signals of the major isomer δ 3.66 (s, 3H), 2.67 (dtd, *J* = 9.9, 7.6, 2.2 Hz, 1H), 2.40 (ddd, *J* = 13.8, 6.8, 3.5 Hz, 1H), 2.33 – 2.24 (m, 1H), 1.89 – 1.84 (m, 2H), 1.81 (ddd, *J* = 12.7, 11.3, 3.6 Hz, 1H), 1.76 – 1.69 (m, 1H), 1.69 – 1.60 (m, 1H), 1.51 – 1.41 (m, 2H), 1.37 (dd, *J* = 11.6, 6.7 Hz, 1H), 1.33 – 1.28 (m, 1H),

1.23 (s, 3H), 1.21 (s, 3H), 1.18 (dd, *J* = 8.1, 2.2 Hz, 2H), 0.92 (s, 3H). **^{13}C NMR** (126 MHz, $CDCl_3$), signals of the major isomer δ 177.3, 74.2, 53.2, 52.9, 51.2, 44.5, 43.9, 42.7, 39.4, 31.9, 30.3, 27.8, 27.1, 26.5, 19.9.

Crystalographic Data

Compound 3.66

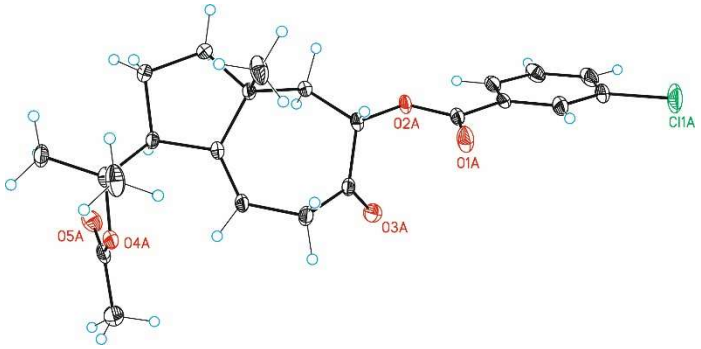

Table 3.12. Crystal data and structure refinement for mo_HA6091_0m. (**3.66**).

Identification code	mo_HA6091_0m	
Empirical formula	$C_{23}H_{27}ClO_5$	
Formula weight	418.89	
Temperature	100(2)K	
Wavelength	0.71073 Å	
Crystal system	monoclinic	
Space group	P 21/c	
Unit cell dimensions	a = 14.9969(4) Å	α = 90°.
	b = 20.7903(5) Å	β = 118.4791(7)°.
	c = 15.4962(4) Å	γ = 90°.
Volume	4246.90(19) $Å^3$	
Z	8	
Density (calculated)	1.310 Mg/m^3	
Absorption coefficient	0.211 mm^{-1}	
F(000)	1776	
Crystal size	0.200 x 0.200 x 0.200 mm^3	
Theta range for data collection	1.787 to 31.594°.	
Index ranges	-20<=h<=22,-30<=k<=30,-18<=l<=22	
Reflections collected	56067	
Independent reflections	14136[R(int) = 0.0363]	
Completeness to theta =31.594°	99.2%	
Absorption correction	Multi-scan	
Max. and min. transmission	0.74 and 0.69	
Refinement method	Full-matrix least-squares on F^2	
Data / restraints / parameters	14136/ 0/ 531	
Goodness-of-fit on F^2	1.025	
Final R indices [I>2sigma(I)]	R1 = 0.0453, wR2 = 0.1110	
R indices (all data)	R1 = 0.0648, wR2 = 0.1221	
Largest diff. peak and hole	0.794 and -0.634 $e.Å^{-3}$	

Compound 3.70'

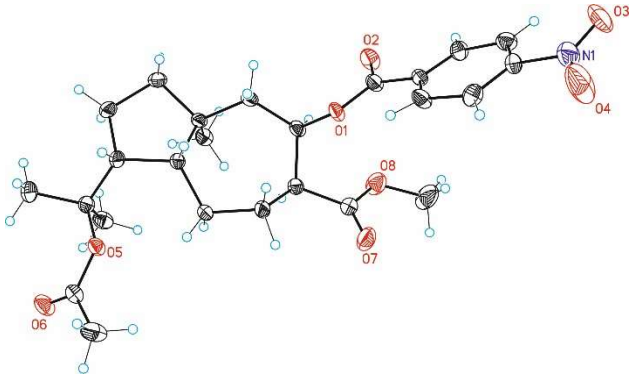

Table 3.13. Crystal data and structure refinement for ha-6-189 (**3.70**).

Identification code	ha-6-189	
Empirical formula	$C_{25}H_{33}NO_8$	
Formula weight	475.52	
Temperature	100(2)K	
Wavelength	0.71073 Å	
Crystal system	monoclinic	
Space group	P 21/n	
Unit cell dimensions	a = 12.4021(2) Å	α = 90°.
	b = 10.9094(2) Å	β = 93.8260(10)°.
	c = 17.7814(3) Å	γ = 90°.
Volume	2400.45(7) $Å^3$	
Z	4	
Density (calculated)	1.316 Mg/m^3	
Absorption coefficient	0.098 mm^{-1}	
F(000)	1016	
Crystal size	0.250 x 0.150 x 0.120 mm^3	
Theta range for data collection	2.296 to 29.896°.	
Index ranges	-17<=h<=16,-15<=k<=15,-24<=l<=24	
Reflections collected	68018	
Independent reflections	6501[R(int) = 0.0323]	
Completeness to theta =29.896°	93.8%	
Absorption correction	Multi-scan	
Max. and min. transmission	1.00 and 0.89	
Refinement method	Full-matrix least-squares on F^2	
Data / restraints / parameters	6501/ 317/ 427	
Goodness-of-fit on F^2	1.014	
Final R indices [I>2sigma(I)]	R1 = 0.0462, wR2 = 0.1195	
R indices (all data)	R1 = 0.0580, wR2 = 0.1257	
Largest diff. peak and hole	0.474 and -0.216 $e.Å^{-3}$	

Compound 3.75

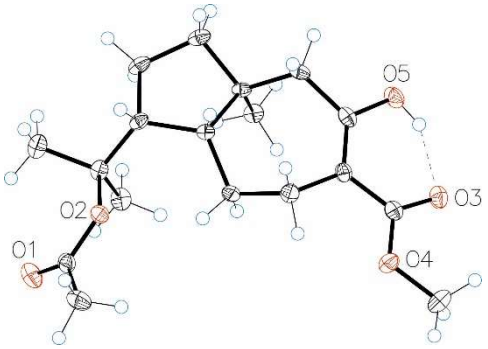

Table 3.14. Crystal data and structure refinement for mo_AMZ06211_0m_a (**3.75**).

Identification code	mo_AMZ06211_0m_a	
Empirical formula	$C_{18}H_{28}O_5$	
Formula weight	324.40	
Temperature/K	99.91	
Crystal system	monoclinic	
Space group	$P2_1/c$	
	a = 9.787(4) Å	α = 90°
	b = 7.187(3) Å	β = 96.91(2) °
	c = 24.370(11) Å	γ = 90°
Volume	1701.8(12) $Å^3$	
Z	4	
ρ_{calc}	1.266 Mg/m^3	
Absorption coefficient	0.091 mm^{-1}	
F(000)	704.0	
Crystal size	0.2 × 0.1 × 0.1 mm^3	
Radiation	MoKα (λ = 0.71073)	
2Θ range for data collection/	3.366 to 54.572 °	
Index ranges	$-12 \leq h \leq 11$, $-9 \leq k \leq 7$, $-31 \leq l \leq 27$	
Reflections collected	16076	
Independent reflections	3769 [R_{int} = 0.0811, R_{sigma} = 0.0726]	
Data/restraints/parameters	3769/0/214	
Goodness-of-fit on F^2	1.081	
Final R indexes [I>=2σ (I)]	R_1 = 0.0569, wR_2 = 0.1328	
Final R indexes [all data]	R_1 = 0.0808, wR_2 = 0.1437	
Largest diff. peak and hole	0.28 and -0.30 $e.Å^{-3}$	

Compound 3.77

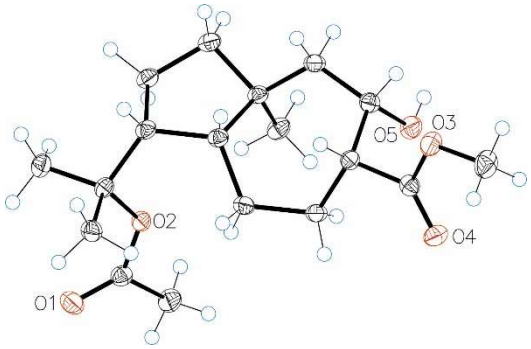

Table 3.15. Crystal data and structure refinement for AMZ-06-230_auto (**3.77**).

Identification code	AMZ-06-230_auto	
Empirical formula	$C_{18}H_{30}O_5$	
Formula weight	326.436	
Temperature	100.0(5) K	
Crystal system	monoclinic	
Space group	P2/c	
	a = 12.5828(4) Å	α = 90 °
	b = 10.0021(3) Å	β = 97.362(3) °
	c = 14.2081(4) Å	γ = 90 °
Volume	1773.41(9) $Å^3$	
Z	4	
ρ_{calc}	1.223 Mg/m^3	
Absortion coeficient	0.088 mm^{-1}	
F(000)	712.5	
Crystal size	0.6 × 0.15 × 0.05 mm^3	
Radiation	Mo Kα (λ = 0.71073)	
2Θ range for data collection	5 to 59.16 °	
Index ranges	-17 ≤ h ≤ 17, -13 ≤ k ≤ 13, -19 ≤ l ≤ 19	
Reflections collected	30498	
Independent reflections	4686 [R_{int} = 0.0409, R_{sigma} = 0.0329]	
Data/restraints/parameters	4686/0/214	
Goodness-of-fit on F^2	1.042	
Final R indexes [I>=2σ (I)]	R_1 = 0.0418, wR_2 = 0.1027	
Final R indexes [all data]	R_1 = 0.0673, wR_2 = 0.1162	
Largest diff. peak and hole	0.59 and -0.38 e.$Å^{-3}$	

Compound 3.79

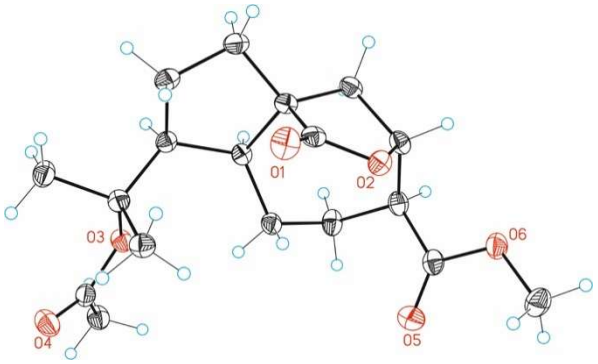

Table 3.16. Crystal data and structure refinement for mo_HA3493 (**3.79**).

Identification code	mo_HA3493	
Empirical formula	$C_{18}H_{26}O_6$	
Formula weight	338.39	
Temperature	99(2)K	
Wavelength	0.71073 Å	
Crystal system	monoclinic	
Space group	P 21/c	
Unit cell dimensions	a = 21.3340(16) Å	α = 90°.
	b = 6.1120(4) Å	β = 105.126(3)°.
	c = 13.2811(11) Å	γ = 90°.
Volume	1671.8(2) $Å^3$	
Z	4	
Density (calculated)	1.344 Mg/m^3	
Absorption coefficient	0.100 mm^{-1}	
F(000)	728	
Crystal size	0.300 x 0.200 x 0.010 mm^3	
Theta range for data collection	1.978 to 27.127°.	
Index ranges	-26<=h<=27,-5<=k<=7,-16<=l<=17	
Reflections collected	18145	
Independent reflections	3685[R(int) = 0.0318]	
Completeness to theta =27.127°	99.7%	
Absorption correction	Multi-scan	
Max. and min. transmission	0.74 and 0.69	
Refinement method	Full-matrix least-squares on F^2	
Data / restraints / parameters	3685/ 0/ 221	
Goodness-of-fit on F^2	1.044	
Final R indices [I>2sigma(I)]	R1 = 0.0433, wR2 = 0.1081	
R indices (all data)	R1 = 0.0582, wR2 = 0.1169	
Largest diff. peak and hole	0.623 and -0.248 $e.Å^{-3}$	

Compound 3.60

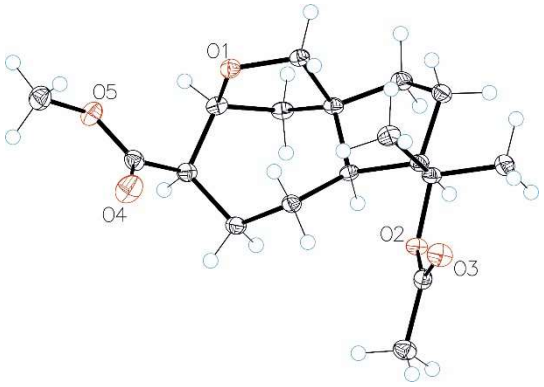

Table 3.17. Crystal data and structure refinement for mo_AMZ06238_a (**3.60**).

Identification code	mo_AMZ06238_a	
Empirical formula	$C_{18}H_{28}O_5$	
Formula weight	324.40	
Temperature	100.07 K	
Crystal system	monoclinic	
Space group	$P2_1/c$	
	a = 21.493(4) Å	α = 90 °
	b = 5.8444(10) Å	β =107.022(5) °
	c = 13.747(2) Å	γ = 90 °
Volume	1651.2(5) $Å^3$	
Z	4	
ρ_{calc}	1.305 Mg/m^3	
absorption coefficient	0.094 mm^{-1}	
F(000)	704.0	
Crystal size	0.2 × 0.1 × 0.05 mm^3	
Radiation	MoKα (λ = 0.71073)	
2Θ range for data collection	3.964 to 56.048 °	
Index ranges	$-28 \leq h \leq 27$, $-5 \leq k \leq 7$, $-18 \leq l \leq 18$	
Reflections collected	22061	
Independent reflections	3979 [R_{int} = 0.0738, R_{sigma} = 0.0518]	
Data/restraints/parameters	3979/0/212	
Goodness-of-fit on F^2	1.033	
Final R indexes [I>=2σ (I)]	R_1 = 0.0428, wR_2 = 0.1021	
Final R indexes [all data]	R_1 = 0.0631, wR_2 = 0.1130	
Largest diff. peak and hole	0.30 and -0.25 e.$Å^{-3}$	

Compound 3.58

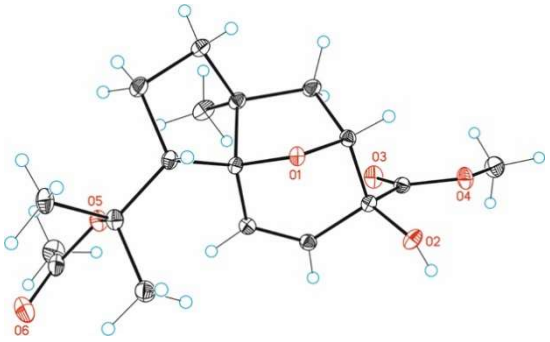

Table 3.18 Crystal data and structure refinement for HA-6-461 (**3.58**).

Identification code	HA-6-461
Empirical formula	$C_{18}H_{26}O_6$
Formula weight	338.39
Temperature	100(2) K
Wavelength	0.71073 Å
Crystal system	orthorhombic
Space group	P 21 21 21
Unit cell dimensions	a = 7.52365(10) Å α = 90°. b = 11.23121(16) Å β = 90°. c = 20.1534(3) Å γ = 90°.
Volume	1702.96(4) $Å^3$
Z	4
Density (calculated)	1.320 Mg/m^3
Absorption coefficient	0.098 mm^{-1}
F(000)	728
Crystal size	0.200 x 0.150 x 0.100 mm^3
Theta range for data collection	2.716 to 31.983°.
Index ranges	-11<=h<=11,-16<=k<=16,-29<=l<=29
Reflections collected	28494
Independent reflections	5592[R(int) = 0.0176]
Completeness to theta =31.983°	96.8%
Absorption correction	Multi-scan
Max. and min. transmission	1.00 and 0.70
Refinement method	Full-matrix least-squares on F^2
Data / restraints / parameters	5592/ 0/ 223
Goodness-of-fit on F^2	1.060
Final R indices [I>2sigma(I)]	R1 = 0.0259, wR2 = 0.0720
R indices (all data)	R1 = 0.0266, wR2 = 0.0726
Flack parameter	x =0.33(10)
Largest diff. peak and hole	0.365 and -0.157 $e.Å^{-3}$

Compound 3.89

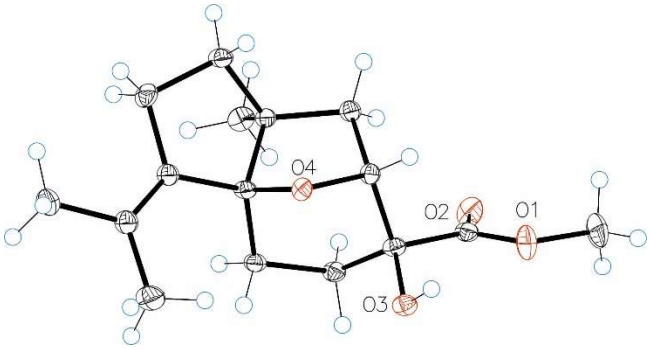

Table 3.19. Crystal data and structure refinement for mo_AMZ06209-b_0m (**3.89**).

Identification code	mo_AMZ06209-b_0m	
Empirical formula	$C_{16}H_{24}O_4$	
Formula weight	280.35	
Temperature	99.27 K	
Crystal system	triclinic	
Space group	P-1	
	a = 7.410(3) Å	α = 113.544(10) °
	b = 9.916(3) Å	β = 91.711(15) °
	c = 11.681(4) Å	γ = 111.096(12) °
Volume	718.9(5) $Å^3$	
Z	2	
ρcalc	1.295 Mg/m^3	
μ	0.092 mm^{-1}	
F(000)	304.0	
Crystal size	0.3 × 0.15 × 0.05 mm^3	
Radiation	MoKα (λ = 0.71073)	
2Θ range for data collection	3.884 to 55.402 °	
Index ranges	$-9 \leq h \leq 9$, $-12 \leq k \leq 7$, $-13 \leq l \leq 15$	
Reflections collected	7110	
Independent reflections	3281 [Rint = 0.0721, Rsigma = 0.0999]	
Data/restraints/parameters	3281/0/187	
Goodness-of-fit on F^2	1.036	
Final R indexes [I>=2σ (I)]	R_1 = 0.0818, wR_2 = 0.2229	
Final R indexes [all data]	R_1 = 0.1021, wR_2 = 0.2466	
Largest diff. peak and hole	0.42 and -0.64 e.$Å^{-3}$	

Compound 3.93

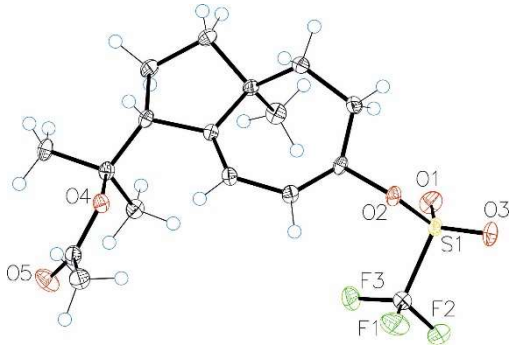

Table 3.20 Crystal data and structure refinement for mo_AMZ06185_a (**3.93**).

Identification code	mo_AMZ06185_a	
Empirical formula	$C_{17}H_{23}F_3O_5S$	
Formula weight	396.430	
Temperature	99.62	
Crystal system	triclinic	
Space group	P-1	
Unit cell dimensions	a = 10.011(4)	α= 71.260(9).
	b = 10.021(4)	β= 72.628(10)
	c = 10.170(4)	γ = 77.378(10).
Volume	913.7(6) $Å^3$	
Z	2	
Density (calculated)	1.441 g/cm^3	
Absorption coefficient	0.232 mm^{-1}	
F(000)	416.6	
Crystal size	0.3 × 0.1 × 0.1mm^3	
Radiation	Mo Kα (λ = 0.71073)	
Theta range for data collection	4.3 to 55.66°.	
Index ranges	-13 ≤ h ≤ 11, -13 ≤ k ≤ 13, -13 ≤ l ≤ 7	
Reflections collected	8839	
Independent reflections	4178 [R_{int} = 0.0886, R_{sigma} = 0.0859]	
Absorption correction	Multi-scan	
Max. and min. transmission	1.00 and 0.70	
Refinement method	Full-matrix least-squares on F^2	
Data / restraints / parameters	4178/0/239	
Goodness-of-fit on F^2	1.042	
Final R indices [I>2sigma(I)]	R1 = 0.0596, wR2 = 0.1652	
R indices (all data)	R1 = 0.0623, wR2 = 0.1691	
Largest diff. peak and hole	0.49 and -0.59 e.$Å^{-3}$	

DFT Calculations

Computational methods

Calculations for the isomerisation of **3.81** to **3.82** and **3.83** were carried out using the Gaussian09 package[47] at the density functional theory (DFT) level by means of the B3LYP[48] functional. Reported geometries and energies were calculated including the corrected dispersion GD3.[49] The 6-31G(d,p)[50] basis set was implemented on all atoms (C, H, N, O, F, P, Cl), except for Au for which the SDD[51] basis set and its corresponding Stuttgart/Dresden Effective Core Potential (ECP) were used. Solvation effects were accounted for CH_2Cl_2 using the implicit polarizable continuum model (PCM)[52]. Each stationary point was characterized by vibrational analysis. Reported energies have been corrected with the thermal and entropic corrections by means of single point calculations at the 6-311G(d,p)[53] level on all atoms (C, H, N, O, F, P, Cl), except for Au for which the SDD basis set and ECP were used. Reported energies are potential energies (E) and free energies (G) in solution, computed at 298 K and 1 atm. NMR calculations were performed by Prof. Antonio Echavarren using Spartan'24 at the density functional theory (DFT) level and employing B3LYP and 6-31G(d) as functional and basis set respectively. All optimized geometries were visualized with the CYLView program.[54]

47. Gaussian 09, Revision D.01, M. J. Frisch, G. W. Trucks, H. B. Schlegel, G. E. Scuseria, M. A. Robb, J. R. Cheeseman, G. Scalmani, V. Barone, B. Mennucci, G. A. Petersson, H. Nakatsuji, M. Caricato, X. Li, H. P. Hratchian, A. F. Izmaylov, J. Bloino, G. Zheng, J. L. Sonnenberg, M. Hada, M. Ehara, K. Toyota, R. Fukuda, J. Hasegawa, M. Ishida, T. Nakajima, Y. Honda, O. Kitao, H. Nakai, T. Vreven, J. A. Montgomery, Jr., J. E. Peralta, F. Ogliaro, M. Bearpark, J. J. Heyd, E. Brothers, K. N. Kudin, V. N. Staroverov, T. Keith, R. Kobayashi, J. Normand, K. Raghavachari, A. Rendell, J. C. Burant, S. S. Iyengar, J. Tomasi, M. Cossi, N. Rega, J. M. Millam, M. Klene, J. E. Knox, J. B. Cross, V. Bakken, C. Adamo, J. Jaramillo, R. Gomperts, R. E. Stratmann, O. Yazyev, A. J. Austin, R. Cammi, C. Pomelli, J. W. Ochterski, R. L. Martin, K. Morokuma, V. G. Zakrzewski, G. A. Voth, P. Salvador, J. J. Dannenberg, S. Dapprich, A. D. Daniels, O. Farkas, J. B. Foresman, J. V. Ortiz, J. Cioslowski, D. J. Fox, Gaussian, Inc., Wallingford CT, **2013**.
48. a) Becke, A. D. *J. Chem. Phys.* **1993**, *98*, 5648–5652. b) Lee, C.; Yang, W.; Parr, R. G. *Phys. Rev. B.* **1988**, *37*, 785–789. c) Vosko, S. H.; Wilk, L.; Nusair, M. *Can. J. Phys.* **1980**, *58*, 1200–1211. d) Stephens, P. J.; Devlin, F. J.; Chabalowsky, C. F.; Frisch, M. J, *J. Phys. Chem.* **1994**, *98*, 11623–11627.
49. S. Grimme, J. Antony, S. Ehrlich, H. Krieg, *J. Chem. Phys.* **2010**, *132*, 154104-1–19.
50. Hehre, E. J.; Ditchfield, R.; Pople, J. A. *J. Chem. Phys.* **1972**, 56, 2257–2261.
51. Andrae, D.; Häussermann, U.; Dolg, M.; Stoll, H.; Preuss, H. *Theor. Chim. Acta* **1990**, 77, 123–141.
52. Cancès, E.; Mennucci, B.; Tomasi, J. *J. Chem. Phys.* **1997**, 107, 3032−3041.
53. W. J. Hehre, R. Ditchfield, J. A. Pople, *J. Chem. Phys.* **1972**, 56, 2257–2261.
54. Legault, C. Y. CYLview 1.0b; Université de Sherbrooke, 2009; http://www.cylview.org.

Computed structures and energies for acetate elimination products of compound 3.80

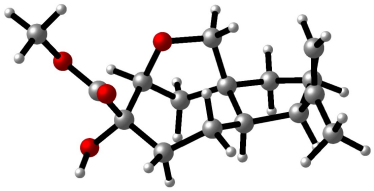

3.81

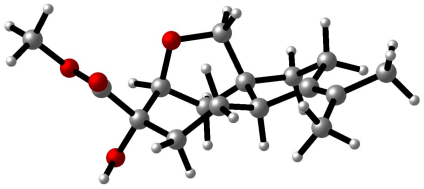

3.82

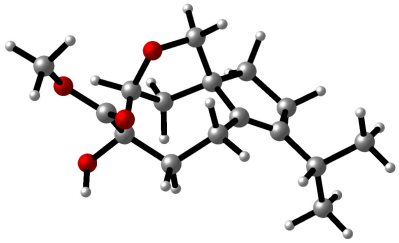

3.83

Table 3.21. Potential energies E and free energies in solution (Gsol), of relevant calculated structures of the isomerization of the products of the acid-catalyzed acetate elimination of compound **3.80**.

	E (Hartree)	**G_{sol}[b] (Hartree)**
3.81	−913.36426	−913.00159
3.82	−913.37462	−913.01277
3.83	−913.38416	−913.02266

Computed structures with Spartan'24

Compound 3.6

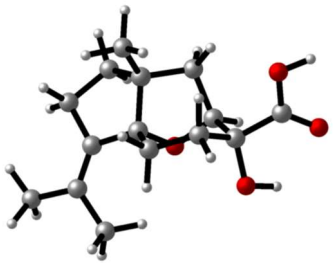

C -0.409088 1.479863 -2.065936
C -0.698585 -0.842041 -1.022850
H -0.370752 -1.880867 -1.147297
H -1.781565 -0.866951 -0.893276
C -0.060609 -0.234587 0.242233
C 1.509348 -0.115971 0.185275
C 1.721641 1.248917 -0.532716
H 2.320174 1.928371 0.083455
H 2.236716 1.140898 -1.491118
C 2.245083 -1.278111 -0.502773
H 2.034068 -2.237258 -0.016357

H	3.328254	-1.115950	-0.447699
C	1.871100	-0.107690	1.690913
H	1.655614	0.879618	2.114147
H	2.930074	-0.328677	1.868947
C	0.919308	-1.143833	2.315662
H	0.827030	-1.016856	3.398224
H	1.301268	-2.162056	2.148784
C	-0.391833	-0.898966	1.576971
C	-1.622660	-1.093841	2.082103
C	-1.848605	-1.775940	3.412475
H	-2.265913	-1.073870	4.148529
H	-0.942506	-2.215082	3.836175
H	-2.588151	-2.581702	3.303619
C	-2.901829	-0.625840	1.422038
H	-2.729914	0.142966	0.668027
H	-3.567387	-0.196901	2.183183
H	-3.454466	-1.460493	0.967021
O	-1.769190	1.872536	-2.000423
H	-1.794535	2.817357	-2.236574
C	0.243972	2.308045	-3.172040
O	-0.172841	3.403189	-3.494987
O	1.350895	1.765899	-3.723897
H	1.681809	2.422127	-4.367260
H	1.985777	-1.381884	-1.559965
O	-0.466481	1.159112	0.316234
C	0.284748	1.808975	-0.695054
H	0.209782	2.887372	-0.519286
C	-0.363998	-0.039826	-2.302368
H	-1.081439	-0.282210	-3.093778
H	0.625688	-0.307842	-2.678364

Compound 2.90

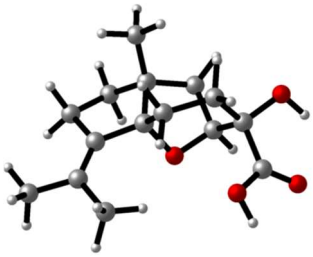

C	0.171073	-1.494619	-2.211273
C	0.515434	0.827142	-1.107624
H	0.173956	1.861394	-1.232388
H	1.593508	0.870146	-0.950001
C	-0.147140	0.201358	0.134506
C	-1.715809	0.088693	0.038057
C	-1.920739	-1.252233	-0.719292
H	-2.559712	-1.935220	-0.149631
H	-2.378194	-1.125501	-1.704295

C	-2.425127	1.274370	-0.636889
H	-2.211925	2.221358	-0.127780
H	-3.510687	1.123145	-0.605195
C	-2.113267	0.036418	1.533008
H	-1.905894	-0.963238	1.930545
H	-3.176860	0.249239	1.691360
C	-1.179632	1.053753	2.211085
H	-1.101745	0.884003	3.289040
H	-1.566169	2.075446	2.080542
C	0.148086	0.850321	1.486856
C	1.360405	1.086708	2.018631
C	1.528855	1.764507	3.360155
H	1.935330	1.066666	4.106518
H	0.600197	2.182121	3.755122
H	2.254956	2.585717	3.280174
C	2.673251	0.675841	1.388581
H	2.551999	-0.088737	0.621106
H	3.334104	0.265110	2.164036
H	3.205106	1.536517	0.957503
H	-2.145006	1.394487	-1.687335
O	0.258731	-1.197958	0.192760
C	-0.492369	-1.830042	-0.838917
H	-0.447676	-2.911801	-0.675187
C	0.222756	0.032396	-2.403216
H	0.956223	0.286615	-3.175936
H	-0.753860	0.307350	-2.812380
O	-0.590038	-2.047282	-3.276975
H	-0.278912	-2.965886	-3.378662
C	1.536849	-2.186113	-2.244285
O	1.664074	-3.335298	-2.622811
O	2.574609	-1.444620	-1.818474
H	3.361259	-2.022271	-1.861039

General Conclusions

General Conclusions

This Doctoral Thesis presents the design, synthesis and characterization of a new family of gold(I) complexes bearing hydrogen bond donors and their application in the catalytic transformation of alkyne-containing substrates. Through detailed experimental and theoretical studies, this work contributes to the development of effective catalytic systems that hold potential for application in organic synthesis and broader areas of chemistry.

In particular, in chapter one we introduced a new family of self-activating achiral gold(I) complexes, containing (thio)urea or squaramide motifs. The structure to activity relationship was established via experimental and theoretical studies. Kinetic and DFT studies supported the role of the hydrogen bond donor in activating the gold(I) complex without the need of external activators. The system was applied to the cycloisomerization of *N*-propargylbenzamides, the hydrohydrazination of alkynes and the cycloisomerization of enynes with and without the addition of exogenous nucleophiles.

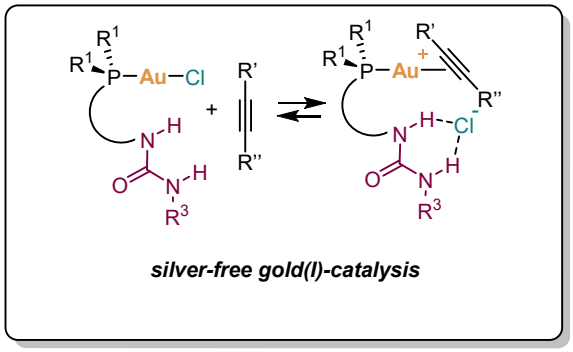

Scheme 1. Self-activating ligands via hydrogen bond interactions.

In chapter two, we presented a novel approach for asymmetric gold(I) catalysis, the Hydrogen-bonded Counterion-Directed Catalysis (HCDC). A new family of achiral JohnPhos-type gold(I) complexes, bearing urea hydrogen bond donors, was combined with chiral counterion for the transformation of alkyne-containing substrates. Mechanistic studies pointed to the role of the urea in anchoring the chiral counterion close to the reaction center. The methodology was applied to the formal [4+2] cycloaddition, the tandem 6-*endo*-dig cyclization/nucleophile addition of 1,6 enynes and the 2-alkynylenone cyclization/nucleophile addition with excellent yields and enantioselectivities. The combination of a chiral gold(I)-phosphitourea with a chiral counterion allowed the application of HCDC to terminal alkynes, in the tandem 5-*exo*-dig cyclization/nucleophile addition of 1,6-enynes with very high yields and enantioselectivities.

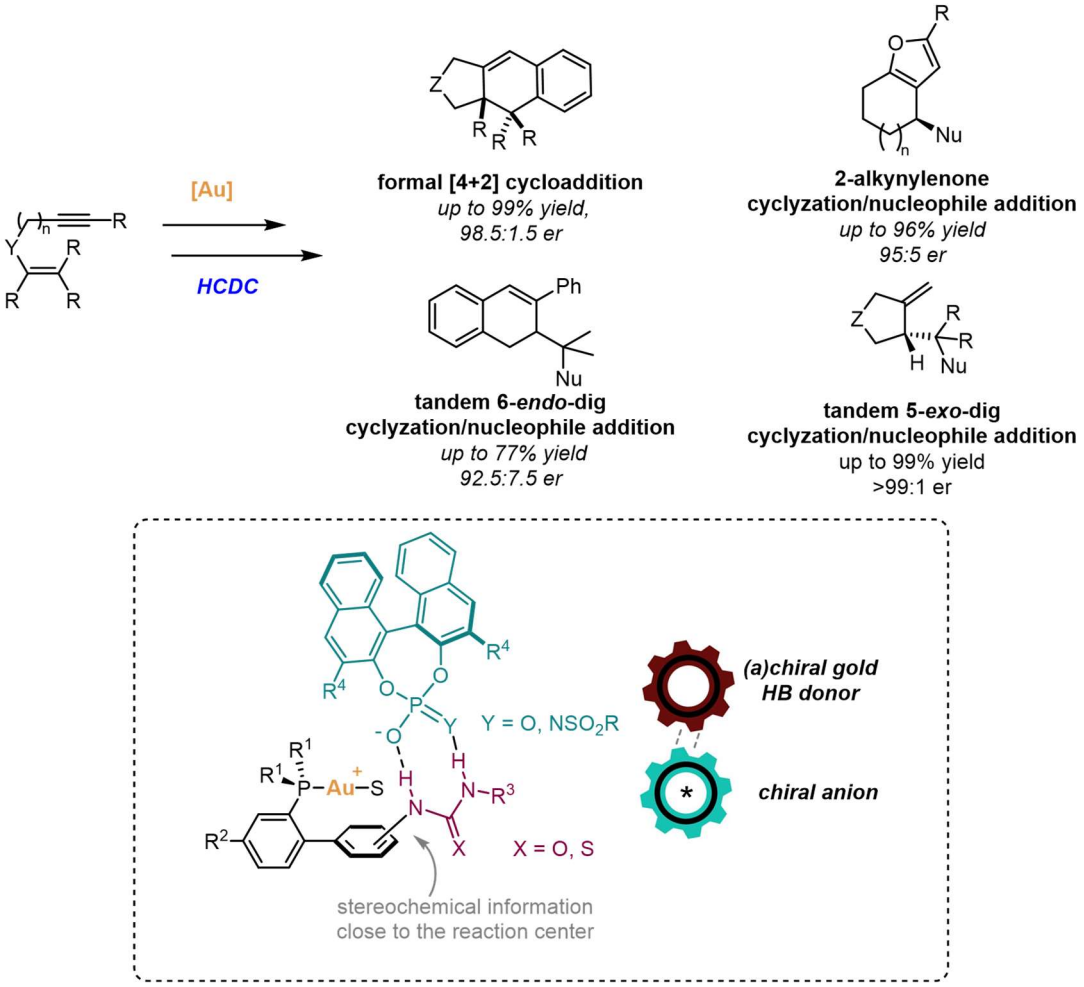

Scheme 2. Application of the gold(I)-catalyzed HCDC in the enantioselective transformation of 1,*n*-enynes.

Finally, the total synthesis of two members of the daucane family of natural products, aspterric acid and shisanwilsonene A, featuring a gold(I)-catalyzed reaction as key step in the construction of the hydroazulane common framework. Furthermore, we synthesized the proposed structure of penigrisacid A by the isolation team and, since the spectroscopic data did not match, we propose an alternative structure for this natural product based on DFT calculations and the data provided in the literature.

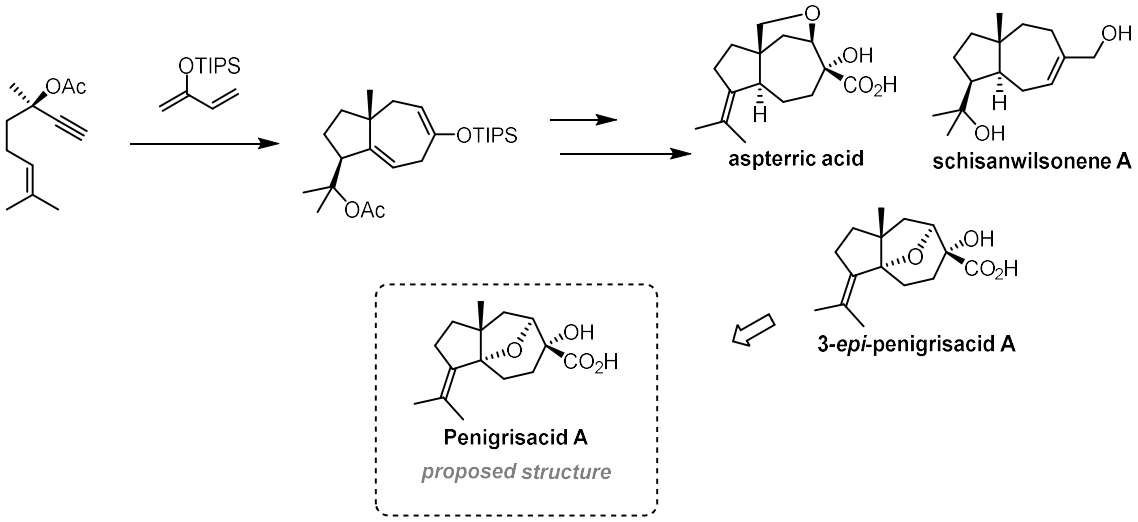

Scheme 16. Gold(I)-enabled total synthesis of members of the daucane family of natural products.


UNIVERSITAT
ROVIRA i VIRGILI


ICIQ
Institut Català
d'Investigació Química